

*17<sup>th</sup> International*  
**North Sea Flow  
Measurement Workshop**



Proceedings

25–28 October 1999

Clarion Oslo Airport Hotel, Gardermoen,  
Norway



**Norwegian  
Society of Chartered  
Engineers**



**NATIONAL ENGINEERING  
LABORATORY**



**NORWEGIAN SOCIETY FOR OIL AND GAS MEASUREMENT  
NORSK FORENING FOR OLJE OG GASSMÅLING**

THE NSFMW '99 IS SPONSORED BY:

**DANIEL**

**KELTON**

FLOW MEASUREMENT CONSULTANTS



**roxar**



**KOS KONGSBERG OFFSHORE a.s**



**MULTI-FLUID**



**FRAMO ENGINEERING AS**

**AUTEK**



PANAMETRICS

**F FAGERBERG**

**HITEC**

**ISA**  
ISA CONTROLS LTD



HYDRO

**JISKOOT**



**Instromet®**

**ABLE**  
Instruments & Controls

**Imtech Systems**



**METCO**

<b>Opening Address</b>	<b>6</b>
<i>Bob Peters, Daniel Industries Europe, UK</i>	

## **Practical Experience – New Concepts**

**Chairman: Steinar Fosse, Norwegian Petroleum Directorate, Norway**

<b>1</b>	<b>Multiphase Flow Measurement System for High GOR Applications</b>	<b>15</b>
	<i>A. Wee, Multi-Fluid ASA, Norway, H. Celios, ARCO Alaska,</i>	
<b>2</b>	<b>Turnkey Well Testing Services: A Successful Modality of Multiphase</b>	<b>24</b>
	<i>M.I.N. Santamaria Guevara, Mexican Petroleum Institute, Mexico</i>	

## **Practical Experience – Ultrasonic Liquid**

**Chairman: Frank Svendsen, Saga Petroleum ASA, Norway**

<b>3</b>	<b>Experience with Ultrasonic Flowmeters in Fiscal Applications for Oil (-products)</b>	<b>35</b>
	<i>A. Boer, Krohne Altometer, The Netherlands</i>	
<b>4</b>	<b>Development and Installation of the ABLE CTM Ultrasonic Cargo Transfer Metering Systems on the BP ABP Amoco "Schiehallion FPSO"</b>	<b>42</b>
	<i>P. Baldwin, J. Spalding, ABLE instruments and Controls Ltd, UK</i>	
<b>5</b>	<b>Two Years of Fiscal Performance by the Krohne Altosonic V liquid 5 Path Ultrasonic Meter at the Vigdis/Snorre Crossover Oil Measurement Station</b>	<b>59</b>
	<i>M. Dahlstrøm, Saga Petroleum ASA, Norway</i>	

## **Venturi Meters**

**Chairman: Reidar Sakariassen, Statoil, Norway**

<b>6</b>	<b>Behaviour of Venturi Meter in Two – Phase Flows</b>	<b>71</b>
	<i>J. P. Couput, Elf Exploration Production, V. de Laharpe, Gaz de FRANCE, A. Strzelecki and P. Gajan, ONERA, France</i>	
<b>7</b>	<b>Use of Venturi Meters in Multiphase Flow Measurement</b>	<b>85</b>
	<i>A.R.W. Hall and M.J. Readers-Harris, National Engineering Laboratory, UK</i>	

## **Installation Effects**

**Chairman: Reidar Sakariassen**

<b>8</b>	<b>Installation Effects on Liquid Ultrasonic Flowmeters</b>	
	<b>G.J. Brown, National Engineering Laboratory – NEL, UK</b>	
		<b>PAPER NOT AVAILABLE</b>
<b>9</b>	<b>Upstream Pipe Wall Roughness Influence on Ultrasonic Flow Measurement</b>	<b>106</b>
	<i>H.J. Dane, Consulting Engineer UK, R. Wilsack, Trans Canada Calibrations, Canada</i>	

- |    |  |     |
|----|--|-----|
| 10 | <b>The Effect of Reynolds Number, Wall Roughness and Profile Asymmetry on Single- and Multi-Path Ultrasonic Meters</b><br><i>K.J. Zanker, Daniel Industries Inc, USA</i> | 117 |
| 11 | <b>Proving a Fiscal 5 Path Ultrasonic Liquid Meter with a Small Volume Prover. Can it be done?</b><br><i>T.Folkestad, Norsk Hydro ASA, Norway</i>                        | 130 |

## Multiphase Meter – New Development

**Chairman: Eivind Dykesteen, Fluenta AS, Norway**

- |    |  |     |
|----|--|-----|
| 12 | <b>A New Generation Multiphase Flow Meters from Schlumberger and Framo</b><br><i>G. Segeal, Schlumberger, Wireline &amp; Testing, France, B.Velle-Hansen, 3-Phase Measurement AS, Norway, K. Eide, Framo Engineerig AS, Norway,</i>  | 154 |
| 13 | <b>A High –Accuracy, Calibration-Free Multiphase Meter</b><br><i>G. Miller, Daniel Industries, UK, C. Alexander, F. Lynch, D. Thompson and W. Letton, Daniel Industries, UK, A.M.Scheers, Shell International E&amp;P, The Netherlands</i>   | 166 |
| 14 | <b>Compact Cyclone Multiphase Meter (CCM) – Discussion of Metering Principle, Slug Handling Capacities and Flow Measurement Results</b><br><i>A.Myrvang Gulbraar, B.Svingen and D. Kvamsdal, B. Christiansen Kværner Process Systems a.s, Norway</i>   | 178 |
| 15 | <b>The Effects of Salinity Variation on Dual Energy Multiphase Flow Measurements and Mixmeter Homogeniser Performance in High Gas and High Viscosity Operation</b><br><i>P.S. Harrison, Melverly Consultants Ltd, G.L. Shires, Imperial College London and S.J. Parry, Imperial College (CARE), UK</i> | 193 |
| 16 | <b>Water-in-Liquid Probe</b><br><i>Chr. Dreyer Skre, Christian Michelsens Research AS, Norway</i>  | 212 |

## Ultrasonic Measurement

**Chairman: Svein Neumann, Phillips Petroleum Co. Norway**

- |    |   |                            |
|----|---|----------------------------|
| 17 | <b>BWT and OKS (Hokey Stick) – Transducers Associated with Ultrasonic Meters</b><br><i>R. McMahon, M. Bragg, Panametrics, UK</i>  | <b>PAPER NOT AVAILABLE</b> |
| 18 | <b>Functional Enhancements within Ultrasonic Gas Flow Measurement</b><br><i>P.Lunde, K.-E. Frøysa, Christian Michelsens Research AS, Norway J.B.Fossdal and T.Heistad, Kongsberg Offshore a.s, Norway</i> | 228                        |
| 19 | <b>Investigations Regarding Installation Effects for Small Ultrasonic Metering Packages</b><br><i>G.de Boer, Instromet Ultrasonics, The Netherlands, M. Kurth, Instromet International, Belgium</i>       | 259                        |

- 20 **Bi-Directional Fiscal Metering by Means of Ultrasonic Meters** 262  
*G.H.Sloet, Gasunie Research, The Netherlands*

## **Standards for Uncertainty Determination**

Chairman: Trond Folkestad, Norsk Hydro ASA, Norway

- 21 **How to Optimize Allocation Systems by using Modelling Using Monte Carlo Simulation** 271  
*M. Basil and P.Cox, FLOW Ltd, UK, L. Coughlan, Shell UK Expl and Production*
- 22 **Presentation of the "Handbook of Uncertainty Calculations – Fiscal Metering Stations"** 283  
*E. O. Dahl, Christian Michelsens Research AS, Norway*

## **Practical Experiences**

Chairman: Richard Paton, National Engineering Laboratory, UK

- 23 **Experience of Ultrasonic Oil/Water Content Monitoring in Two Phase Separator Streams**  
*I.Basoni, University of Miskolc, K.Bauer and S. Puskas, MOL Hungarian Oil & Gas Co, Hungary* **PAPER NOT AVAILABLE**
- 24 **Meter Tube Pulsation Experienced at CATS Terminal "Real or Imagined"** 315  
*M. Donoghue, Amoco CATS Terminal, UK, B.Peters, Daniel Industries Europe Ltd, UK, R.J. McKee, Southwest Research Institute, USA*
- 25 **Multiphase Measurements System With Fully Redundant Measurements to Improve Accuracy and Simplify Maintenance** 346  
*A.Wee, Multi-Fluid, ASA, Norway*
- 26 **Enhanced Performance Multiphase Metering: Optimal Matching of Separation and Metering Facilities for Performance, Cost and Size. Practical Examples from Indonesia Duri Area 10 Expansion Project**  
*J.D. Marelli, Texaco Humble Multiphase Flow Facility, USA* **PAPER NOT AVAILABLE**
- 27 **Operational Experience with Multiphase Meters at Vigdis** 362  
*E. Dykesteen, O.P. Kalsaas, Fluenta a.s, Norway, E.Egner, Saga Petroleum ASA, Norway*



# NORTH SEA FLOW MEASUREMENT WORKSHOP IN OSLO ON THE 25 - 28TH OCTOBER, 1999

OPENING ADDRESS BY DR BOB PETERS - DANIEL EUROPE LTD

---

*"You are young my son, and, as the years go by, time will change, and even reverse many of your present opinions. Refrain therefore awhile from setting yourself up as a judge of the highest matters"*  
Plato

## 1. INTRODUCTION

At the end of the millennium and at the start of the 21st Century, I believe it is forgivable to look back at what has been achieved in the North Sea, since the first joint meeting in 1982 in Stavanger. However it would be quite unforgivable if we did not look forward into the millennium and try to envision what may be achieved in flow measurement in the next century.

In this period of change, when we move from the 20th Century to the 21st Century and when the Crine initiative and cost reduction is the name of the game, it has been necessary for companies to amalgamate e.g. BP/Amoco and Arco; Statoil and Saga; Kongsberg and FMC; Daniel and Fisher-Rosemount.

We even changed the site of the North Sea Flow Measurement Workshop this year to this wonderful facility here in Gardermoen.

Those of us in the flow measurement world must also be prepared for change in the way we do business. However it is to be hoped that, as engineers, it will not be simply change for change sake, but rather technical change, carefully assessed and tested, resulting in improved techniques.

## 2. THE FIRST MEETING ON "MEASUREMENT OF GAS AND LIQUIDS"

It was held in the Atlantic Hotel in Stavanger from the 7th to the 10th June 1982. The meeting was organised by Norwegian Society of Chartered Engineers and the Rogland Regional College, in conjunction with N.P.D., Norwegian Service of Legal Metrology, Gas Metering Department Netherlands. The Registration Fee in 1982 was 3,300 NOK compared to 6,200 NOK for this year. For the 1st year of the North Sea Flow Metering Workshop in 1983 the cost was 4,500NOK so it appears that we have a bargain this year.

The length of the conference was virtually the same - two and a half days with about 14 papers compared to 27 this year. However we work much harder now, starting at 8.30 am, whereas in the early days it was 9.00am.

They also knew how to enjoy themselves 17 years ago with a shellfish party on the beach - but it was in early June. These were the "good old days" as recently we have been exposed to wolves in a dark October night in Kristiansand.

At that Seminar there were 33 delegates plus 9 lecturers and a committee of 5. It is interesting to look at the names and to see how many are still active in the metering world

### 1982 Attendance List

GRO AKSNES	STATOIL
LEIF INGE ANDERSEN	A/S NORSKE SHELL
BJARNE BANG	DANISH ENERGY AGENCY
MARON DAHLSTRØM	PHILLIPS PET.
NUSTRAL DANIR	PETRONAS CARRIAGLI
BILLY GRANT	PHILLIPS PET.
LARS OLAV HOLEN	SUPERIOR OIL NORGE
PER HÆGSTAD	A/S NEBB
PETTER INGEBERRG	SIVILING HELGE INGEBERG
EDGAR B JOHANNESSEN	NILS A. STANG
NILS BJØRN JORDAL	SAGA PET.
ALF R.KLUGE	STATOIL
KARL MARTIN KRISTIANSEN	STATOIL
OLAF KRISTIANSEN	NORSKE HYDRO
SVEINUNG MYHR,	NORSKE HYDO
SVEINUNG NILSEN	STATOIL
FINN PAULSEN	OLJEDIREKTORATET
ROBERT PETERS	DANIEL
ARNE ROALD	NORSK A/S PHILIPS
ROLF RØNNING	PETRONAS CARRIAGALI

ISMAIL SAID  
MORTEN SAXVIK  
OLAV SELVIGVÅG  
SIGBJØRN SOLBAKKEN  
E.A SPENCER  
SVERRE STENVÅG

PETRONAS CARRIAGALI  
STATOIL  
OLJEDIREKTORATET  
OLJEDIREKTORATET  
NEL  
ELF AQUITAINE NORGE A.S.

DAG THOMASSEN  
TOR ARNE THORSEN  
ØYSTEIN B.TUNTLAND

INST. FOR ENERGITEKNIKK  
KVAERNER  
ROGLAND DISTR.HØGSKOLE

REIDAR VIK

NORPIPE PET.

GUNNAR WEDVICH  
KARSTEIN WERGELAND

CHR. MICHESENS INST.  
OLJEDIREKTORATET

TORE ØGLÆND

OLJEDIREKTORATET

**COMMITTEE:**

ARILD BØE  
HARALD DANIELSEN  
KRISTEN HELLERUD  
CP HOEKS

ROGLAND DISTR.HØGSKOLE  
OLJEDIREKTORATET  
JUSTERDIREKTORATET  
NORSK HYDRO

**LECTURERS:**

H BELLINGA  
KNUT BIRKELAND  
PETER A.M.JELLS  
GEIR M.NESBAKKEN  
HALLVARD TUNHEIM  
OLAV VIKANE  
PAULWILCOX

GASUNIE  
JUSTERVESENET  
MOORE, BARRETT & REDWOOD  
NORSK HYDRO  
ELF AQUITAINE NORGE A.S.  
ROGLAND DISTR.HØGSKOLE  
TOTAL OIL MARINE

**ADMINISTRATION:**

JOHAN ASMUNDVAAG  
MERETE JACOBSEN

NORSKE SIVILINGENIØRERS FORENING  
NORSKE SIVILINGENIØRERS FORENING

It is also sad to note that one or two have died, for example Dr Tony Spencer who was so keen to continue from this first meeting to having an annual meeting, alternating between Norway and Scotland.

The International flavour of the Meeting was obvious even then, with delegates from Norway, Denmark, the U.K. and the Netherlands but in addition there was 2 from Malaysia. With the meeting resulting in the first Flow Metering Workshop in 1983. Although the majority continues to be Scandinavian and U.K. personnel, there has been an increasing International representation and now we have a significant number from North America.

The North Sea Flow Measurement Workshop has come of age and has contributed greatly to the effective flow measurement in this environment. It has stimulated ideas, encouraged the exchange of views as well as forming business and friendship ties which have been maintained over the intervening period.

### **3. PAPERS PRESENTED AT THE MEETING IN 1982**

The opening address was entitled "Planning under harder Economic Conditions" by Mr Arne Rettedal, Minister, in the Ministry of Local Government and Labour. - Some things never change, if he was giving the same paper today I wonder if the title would remain the same?

Papers followed this, from Harald Danielsen and Knut Birkeland, which highlighted the economic advantages of accurate metering. A similar paper could be given today. There were papers on orifice metering, vortex meters, turbine meters, provers, computers, LPG Measurement and ultrasonic metering, finally Jan Bosio presented a paper on sonic nozzles.

It was interesting to note that Ultrasonic Meters were being considered in 1982, but it took until fairly recently for Daniel and British Gas to introduce their ultrasonic gas meter onto the market, and more recently to have the ultrasonic liquid meter used for Fiscal purposes.

NOTE: there was no mention of Multi-Phase Meters in these days but Coriolis Meters were being considered. In a paper on initial tests on the Coriolis Meter it was reported that the tube broke after 4 days operation in the laboratory. Early findings like this set the Coriolis Meter back for a number of years but these problems have been overcome and one of the meter manufacturers can claim a "Mean Time Between Failure" of greater than 1.0 million hours

### **4. DEVELOPMENTS FROM THE FIRST WORKSHOP IN 1983**

This year there are 12 Multi-Phase Meter presentations and 12 ultrasonic presentations with 2 uncertainty papers and we still have managed to keep one orifice meter paper which shows the old orifice is still pulsing away.

Remember the tremendous rate of change in technology over this period. In 1983 we did not have PC's and if nothing else you only have to look at the quality improvement of the papers and the presentations to see the effect of that development.

In the field of process control Halvard Tunheim presented a paper in 1982 for the Elf Frigg Flow Measurement System where he used intelligent stream flow computers. These systems have dramatically reduced the computational error in flow measurement.

Technology has advanced at a significant rate over this period. It should be remembered that in these early days the driving force in the North Sea was to develop the technology to extract the hydrocarbons as rapidly as possible to enable the operating companies to get a quick return on investment.

This had the effect that metering costs were not as closely examined as they are today. Today there is in an atmosphere of cost cutting, CRINE Initiatives etc. It must be remembered that, the uncertainty of measurement is the invisible cost of metering.

However, more visible costs include cost of ownership (CAPEX and OPEX etc) and there has been big changes in this area with the concept in Norway of "Conditioned Based Maintenance".

This appears to be the perfectly logical conclusion for the desired goal of unmanned platforms and it does appear that the Norwegian sector has taken a much longer-term view with their philosophy, which foresees the effect of unmanned platforms in the future.

The workshops have reflected the changes through the years.

In 1988 Nolan, O'Hare and Peters presented the first practical gas ultrasonic paper.

10 years ago in 1989 flare as papers were still being presented using turbine meters and there was one paper on wet gas measurement and one on water in oil sampling.

1990 was the year where we started to see a dramatic change in emphasis. There were a number of Coriolis papers including gas measurement. There were 7 Multi-Phase metering papers - it had taken off on the road to the 12 this year.

## **5.ASSESSMENT OF METERING DEVELOPMENT IN THE PAST 17 YEARS**

It has been an exciting time in flow measurement terms since the North Sea Workshop was established. We have seen the Coriolis Meter and the Ultrasonic Gas Meter grow from virtually nothing to very major contributors to metering. Now we see the ultrasonic liquid meter develop into a possible fiscal meter.

Other meters' popularity has risen and fallen e.g. Orifice, Liquid and Gas Turbine Meters, vortex meters have fallen and now Venturi Meters, which were declining in use, are apparently enjoying a resurgence in the field of wet gas metering and are also being incorporated into Multi-Phase Meters.

It is a case of "horses for courses" and the appropriate meter must be supplied:

- for the prevailing flow conditions,
- for the technical expertise available
- for the local economic situation.

I have questioned the extensive application of gas turbine meters in countries where there are no gas calibration facilities present!

However, in my opinion, there have been two major exciting developments over the period in question, namely:

- a) The diagnostic capability of the ultrasonic meter has been a major advancement. The traditional meters give a reading but we have had no mechanism to tell if the reading is significant or not unless it is checked by a Prover. The Ultrasonic Meter tells us a lot about what is taking place in the pipe.

Unfortunately the operators do not always like to know that there is unaccounted for liquid in gas streams and so a meter that simply gives a number (albeit a wrong number) is sometimes preferred.

This diagnostic capability can permit the fiscal authorities to consider these meters for marginal fields where the cost and the weight of a Prover could simply be the "last straw" in deciding if a field can be developed.

- b) The rise of the Multi-Phase Meter over the years has been a fascinating exercise. We have seen, at these workshops, the meters grow from:
- fairly sketchy design concepts,
  - to experimental results,
  - to the current stage where we have operational data from the field.

Some of the extravagant claims have been shown to be false but to be fair there have not been too many over-optimistic promises.

Until we understand the physics and the physical chemistry of the multi-phase systems, I will continue to be very sceptical about the claims that 1% accuracy for flow for the different fractions can be achieved.

Incidentally as some meters popularity has waxed and waned, I believe that the decline in the usage of Provers is one of these transient phases and the use of Provers will be seen to be a necessity for accurate measurement. I venture to suggest that gas Provers will be used regularly in the next century.

## 6. YEAR 2000 AND BEYOND

At the meeting in 1982 Harald Danielsen presented a paper in which he said " In accordance with good and accepted principles of teaching, I will use part of the opening lecture to motivate you for this course. One of the ways to do this, may be to quantify the effects of metering errors in terms of money."

He went on to show that a gas and oil system might be passing 36 Billion NOK's (i.e. approximately £3,600M) per annum. If we saved 0.1% in flow metering per station that would have been 36M NOK/annum or £3.6M.

Harald Danielsen gave me the national figure for Norway for 1997/8 of oil, gas and condensate production and this amounted to approximately 163 billion NOK (approx. £14,000M) or 38% of the total Norwegian export value. If we could save 0.1% in metering that would amount to 163 Million NOK or £14M.

This value may sound a great deal, if that is about the total annual turnover of your company or perhaps very little if you are building a new production platform.

However, if we start to talk in terms of 1% saving then we would all agree that we are talking big money i.e. 1.6 Billion NOK or £140M. Some may argue that with the current sophistication in metering in the North Sea it is impractical to expect a 1% saving. However if we have listened to papers over the years we know that there have been a number of instances where greater than 1% errors have been experienced by bad design, poor maintenance, inaccurate meters, errors in calculations etc.

Furthermore if we think in terms of multiphase and in terms of 10% uncertainty, one could argue that the oil companies and governments should make large sums of money available for research and development.

## **6.1 BEYOND 2000**

But let us stop for a moment!! Until now the paper has been based on current thinking. If we are looking into the next Century what will the Financial arrangements be?

Will it be necessary to separate the liquid/gas/solids offshore and try to measure the components in that difficult environment? Or will we simply bring the total product onshore and then separate it and measure the components? If we did that would there be the requirement for Multi-Phase Meters?

*Note: this is all a flight of fancy and not "Having a go at Multi-Phase Meters"*

Currently I understand that the purpose of offshore measurement is to give the government a value on which tax can be based, or a method of allocation to allow commingling in a pipeline - in very simplistic terms. This is the argument for the adoption of the Multi-Phase Meter.

Is it not conceivable that with all the amalgamations taking place and the adoption of a philosophy similar to that now used in the U.K. railways, where we have one operator responsible for the track, we could have one company/government responsible for bringing all the fluid ashore? The fluids would be then separated, accurate measurement of the separated fractions made and the value divided up on an agreed basis, giving a share to the developer and to the government for Tax purposes? This appears to be the basis of much of the pipeline operation at present, with the exception that just now the operators and the governments are trying to agree the financial split based on offshore metering. This then requires either separation of the fluids or the use of Multi-Phase Meters offshore.

Already we are seeing the situation where companies are offering to take responsibility for all the offshore flow measurement and simply supplying the oil and gas companies with the data they require for accountancy purposes. As the oil and gas companies continue to withdraw into their core business it can be envisaged that they will be content to rely on a sub-supplier to take total responsibility for their metering and simply give them numbers for the daily/hourly production

However, if we can foresee a situation where the fluids produced offshore are simply brought ashore and then separated then it could be argued that there was no need for meters offshore, not even Multi-Phase Meters.

I have no idea how this could be done, or even if it could be done, or even if it is already happening? It certainly would require a completely different accountancy procedure to avoid the allocation question at the very least.

## **6.2 NEW IDEAS FOR THE WORKSHOP**

The North Sea Workshop for the next 16 years must continue to provide the vision for flow measurement. To do this, the delegates need information to let them plan their metering strategy for the future. The Workshop has always had an element of training in it.

It seems to be timely for the Workshop committees to review the Workshop programme. Let us invite production engineers to the workshop to describe to the metering fraternity the options for bringing the product ashore.

Let us include the petroleum accountants and the government officials, responsible for the offshore tax regime, into the Workshop to explain the possible financial models for the future.

In addition we seem to have become too Multi-Phase and Ultrasonic Meter focussed at present. Let us broaden our scope again and include the process industry into our discussions to see the total role of the flow meter into the 21st century.

## **7. CONCLUSIONS**

7.1 The 21st century is going to be one of ever accelerating change and the flow measurement engineer must be well informed to programme the developments in flow measurement for the future.

7.2 The methodology of conducting business will change and again the engineers must keep themselves aware of the changing environment.

7.3 However, certain fundamentals of flow measurement which stay the same and must be remembered.

I suggest that these are:

- You do not get anything worthwhile for nothing and good flow measurement will continue to be costly.
- You do not get good flow measurement without very good service and maintenance
- The technology used for a particular application will depend on the available technical expertise and the local environment

7.4 Flow meters for the future will increasingly provide diagnostic capabilities as an "added value" feature.

7.5 Finally 16 years of Flow Measurement Workshops has taught me that there is something even more important than flow measurement.

It is the friends we make in this world.

I am pleased to say that thanks to the kindness of the Norwegians, the Workshop has been a place of friendship, and kindly rivalry, and I trust that this will continue to be the case this year and throughout the next century.

We trust that this will be a Workshop where we will learn a great deal and also renew old friendships and make new friends.



# Multiphase Flow Measurement System of High-GOR Applications

*Harry Cellos, ARCO Alaska Inc. and Arnstein Wee, Roxar ASA*

---

## 1. Abstract

This paper presents the findings from an installation at Prudhoe Bay which was started up on October 22, 1998. This system consists of a MFI Multiphase Meter, a partial separation separator and a coriolis effect flow meter. The separator is used to widen the operating envelope of the multiphase meter. The control of the separator, data acquisition and final calculations are done by the MFI Meter.

Since the system has a very wide operating envelope it can be used on groups of wells with widely divergent flow rates. This particular system is designed for accurate flow measurements with GOR's up to 80 000 scf/bbl and it can handle liquid flow rates in the range 100–15 000 bbl/d. The accuracy of the oil flowrate is typical within 5% and the gas flow rate is measured within 2-3%.

The key element of the system is the MFI multiphase flow meter which is used to measure the multiphase flow in the “liquid leg” of the compact separator. Unlike most well test systems, the measurements of the liquid line are not adversely affected by gas carry under. In fact, it works best with gas flowing in the liquid line.

Operation and control of the system is greatly simplified by the fact that the primary goal of the separator is to remove the liquid from the gas. The separator is designed to remove down to 5 ppm over the full range of flow rates. The excitation voltage of the coriolis meter is used to detect carryover down to 2-3 ppm. This variable is also used in the control logic and changes the vapor leg flow rate to eliminate carryover.

## 2. MFI MultiPhase Meter

The MFI Multiphase Meter uses a unique, patented microwave technology. However, the fundamental physical principals involved are simple. Multi-Fluid's technological platform is based on the ability to adopt and apply these fundamental principals to the challenging technological task of measuring fractions and flow rates of different components flowing simultaneously in a pipe, without any prior separation of the phases.

The sensor is a compact, straight spool piece with no moving parts and no pressure drop as shown in figure 1. The MFI Multiphase Meters perform all measurements and calculations in a field mounted electronics, consequently, only final results are transmitted from the

field using simple analogue or digital outputs. With this architecture, the MFI Meters can be used as stand-alone, remotely operated devices without the need for support facilities. This can dramatically reduce the cost of installing and using multiphase meters in remote or unmanned facilities.

Instantaneous oil, water and gas fractions are measured using a patented microwave measurement device for measuring mixture dielectric properties and a commercial Cs 137 gamma densitometer for measuring mixture density.

The meter functions over the full 0 - 100% water cut range. Separate sensors are not required for low and high water cut measurements. The microwave measurement system has unparalleled sensitivity. The microwave sensor works by measuring a characteristic microwave frequency that is inversely proportional to the square root of the mixture dielectric constant. A change from 100% gas to 100% water can result in a change in the measured microwave frequency of over 100 to 1. As a result, the meter can measure the water cut, oil flow rate, and water flow rate of multiphase mixtures with superior accuracy, particularly at high GVF. The composition meter accurately measures component volume fractions several times per second. Thus, it is possible for it to function with any flow regime in the line, even intermittent plug flow. Another benefit of 'real-time' measurement is that the meter can be used to determine which flow regime is present in the line. Many other multiphase technologies integrate raw data over tens of seconds to get meaningful results, thereby losing useful real-time information.

The primary element for measuring multiphase flow velocity is a microwave based Cross-Correlation Meter. This device uses two identical microwave sensors (such as used in the composition sensor) separated by a known distance in the pipe to measure velocity. By statistically comparing measurements from the upstream sensor with those of the downstream sensor using cross-correlation methods, one can determine the mean transit time for the mixture to move between the sensors. The sensor spacing and the measured transit time give velocity. Roxar has developed a slip flow model to determine respectively the gas and liquid velocities from the measured velocity using, among other inputs, the statistical data from the composition meter to characterise the flow regime. These two velocities are combined with the readings from the composition meter to obtain the actual oil, water and gas flow rates. The Cross-Correlation Meter has a number of advantages compared to other multiphase velocity meters (including Venturi Tubes):

- Turn-down ratio of up to 35:1
- No moving parts
- High sensitivity.
- It also functions with zero water cut and fine bubble flow such as might be present during early production.
- No differential pressure taps and tubing that can foul, partially fill or leak, or dP transmitters that can drift
- Easily used in high pressure systems without sacrificing accuracy

An optional element for measuring multiphase flow velocity is a Venturi meter. The suitability of a Venturi is assessed on a case-by-case basis. The beta ratio for the Venturi meter is tailored for each application to maximize the turndown ratio and thus improve accuracy. It is

possible to achieve a turndown ratio up towards 10: 1 in mass flow terms. Combining the X-Correlation Meter with a Venturi gives some redundancy. The MFI Meter can continue functioning even if either the Venturi Meter or the X-Correlation Meter should fail. Either velocity meter can be used to measure liquid and gas velocities. The venturi can also be used as an element within the MMS (MultiPhase Management System) as a part of preventive maintenance routines.

### 3. MFI High Gas System

The MFI High Gas System has been developed in cooperation with ARCO Alaska, Inc. This system consists of a partial separation separator with downstream instrumentation containing a MFI MultiPhase Meter and a coriolis effect gas flow meter. The separator is used to widen the operating envelope of the multiphase meter and increase the accuracy of the measurements at conditions with wells having high GORs. The control of the separator, data acquisition and final calculations are done by the MFI Multiphase Meter. A drawing of the complete system is shown in figure 2.

The system consist of the following components:

- A cyclone with one inlet and two outlets, one for gas and one for gassy liquid.
- A MFI Multiphase Meter to measure oil, water and gas in the multiphase outlet line.
- A coriolis meter to measure the separate gas flow and detect liquid carry over.
- Two control valves, one in each of the outlet lines, to control the flow rates in the respective outlets.
- A differential pressure transmitter attached between the liquid and gas outlet of the separator to detect excessive liquid levels in the separator.

#### 3.1 Cyclone Separator

A standard cyclone can be used as the inlet separator. For the systems installed at Prudhoe Bay, a two-stage separator as shown in figure 3 is used. The separator is a two-stage cyclone with an inner and outer gravity spin. Most of the liquid is separated out at the outer gravity spin defined by the total diameter of the separator. The gas with some remaining liquid is then sucked into the inner cyclone thus spinning at a higher velocity. The remaining liquid in the gas evacuates from the inner cyclone through a small slot in the wall of the inner cyclone. The liquid and some gas from the second stage is sucked through the “liquid carry over” pipe section which is terminated near the low pressure area in the first stage vortex.

#### 3.2 Control Algorithm

Unlike most separator systems for which level control is the object of the system control algorithm, the MFI High Gas System controls the flow rates in the liquid line and gas line to ensure best possible accuracy of the total measurement. The system is specifically designed to operate with significant volumes of gas carry under in the liquid line. Consequently, the liquid level in the separator is effectively zero under most normal operating conditions.

Instead of controlling level, the system controls the relative volume of gas flowing in the liquid and gas lines respectively by adjusting one of the control valves to alter the differential pressure balance in the two flowing lines. In this manner, it ensures that the multiphase

flow conditions in the liquid line are such that the MFI Meter delivers optimal accuracy. Similarly, it ensures that sufficient gas volumes are flowing through the gas meter to ensure that it achieves best possible measurement accuracy. In summary, the MFI High Gas System achieves optimum accuracy for any given inlet flowing condition by controlling the flow rate of the gas in the respective flow lines.

Liquid carry over in the gas leg can be detected by two means. When two phase flow is present in the coriolis meter, the amount of energy required to resonate the tubes increases. Consequently, the tube excitation voltage is a good measure of liquid carry-over in the system. Second, the system can be set up with a predefined separator level or dP for which liquid carry over will occur. In the event of “liquid carry over detection”, the system will automatically increase the velocity in the multiphase line of the system to improve the quality of separation. It is important to note that liquid carry-over in the gas leg of conventional test separator operation is something that is usually not monitored and is largely ignored. To a lesser extent gas carry-under in the liquid is also frequently missed.

### **3.3 Operator Interface**

The operator interface for the system is a Graphical User Interface (GUI) running on a Windows 95/NT platform. One GUI can be connected to several systems. The GUI communicates with the system using Modbus RTU protocol and allows the operator to configure and calibrate the system. The GUI has a powerful built-in trending function of all measurement data, and the data can also be stored in a database. Typical tuning parameters such as response time, control gain and liquid carry over threshold for the coriolis excitation voltage and separator level limits can be configured from the GUI. Figure 4 shows a picture of a typical Graphical User Interface (GUI) display.

## **4. Field Experience at Prudhoe Bay**

The MFI High Gas System was commissioned at the end of October 1998, and there have been no operational problems after commissioning.

The control algorithm of the system was able to stabilize the flow within a few minutes as shown in figure 5. The system was operating very reliably and no fault conditions have been observed during operation. Both the coriolis tube excitation voltage and separator level proved to be reliable measurements of any liquid carry over. The coriolis excitation voltage was normally between 2.5 – 2.7 volts. Even for a small amount of liquid carry-over, the excitation voltage instantly increased by several volts. For excess amounts of liquid carry-over (> 1%), the coriolis excitation voltage was saturated at 14.5 volts. The control algorithm is robust enough to correct for any “liquid carry-over” events within seconds from detection by the coriolis excitation voltage. During normal operation, there is no liquid level in the separator as measured by the differential pressure across the separator. For the conditions at Prudhoe-Bay, liquid carry over was detected by the differential pressure measurement with approximately 10 inches of liquid level in the separator. Consequently, any liquid carry-over could reliably be detected by measuring the differential pressure across the separator. The MFI High Gas System was also operating reliably at severe slugging conditions as shown in figure 6.

The well in figure 6 was slugging at a rate of approx. two slugs pr. hour. The system was able to control the valves in order to obtain the desired conditions of the system. This graph also demonstrates one of the great advantages of such a system compared to a conventional test separator. Whereas the measurements from a test separator would be averaged out for several hours filtering out any real time data, the MFI High Gas System gives valuable information of the dynamic behavior of the well. For this particular well, the liquid and gas slugs are in phase indicating a lift gas problem as opposed to just a high GOR. Hence, by optimizing the lift gas rate based on the real-time measurement from the MFI High Gas System, the production rate from the well could be increased. Also the real-time data can be helpful in diagnosing sub-surface equipment or reservoir problems. The first three months of operation as shown in figure 7 reflect results consistent with expected well performance and metering repeatability.

## 5. Acknowledgments

The authors are indebted to Jim Abel the ARCO Alaska, Inc. Project Manager for support in applying this technology. Also, we would like to thank Stuart Parks for his efforts in coordinating the design, construction and start up of these systems. The views in this paper are those of its authors and do not necessarily reflect the views of the Prudhoe Bay Co-Owners.

Appendix – Tables and Figures

## Appendix – Figures



Fig. 1 - 2" MFI Multiphase Meter. The sensor is a compact, straight spool piece with no moving parts and no pressure drop. A two inch, 1500 lb. sensor with ANSI flanges is less than 450mm (18 inches) long. All measurements and calculations are done in the electronics box.

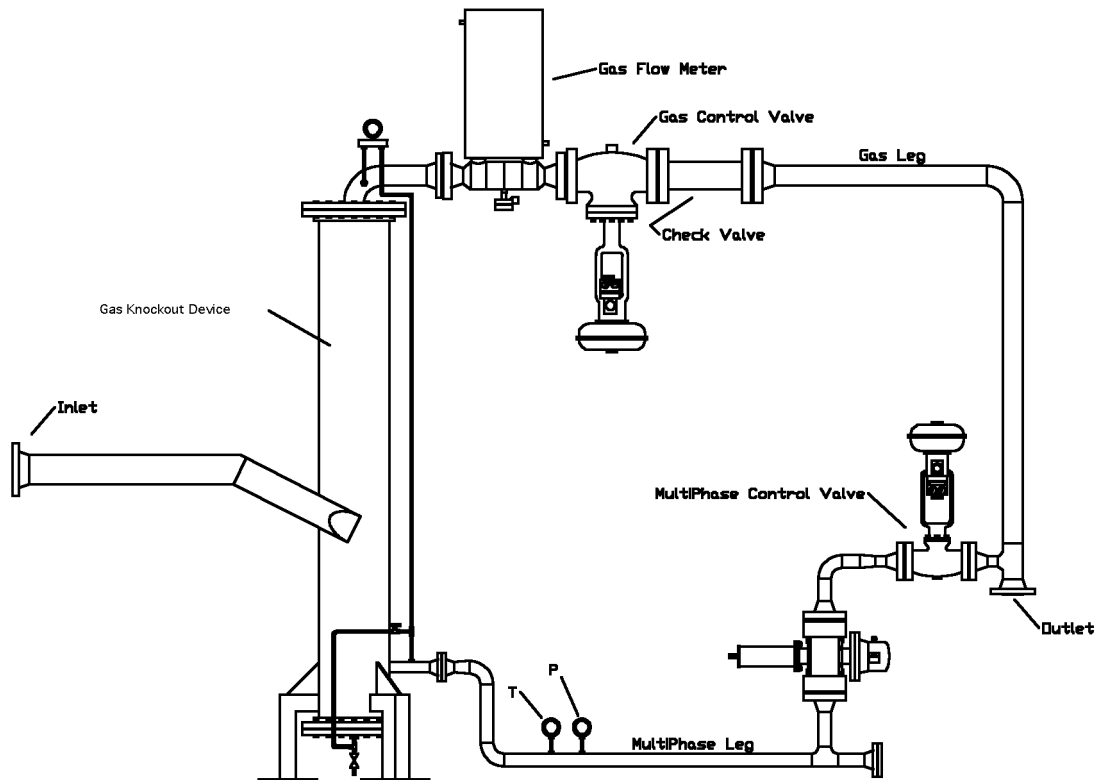


Fig 2. - MFI High Gas System. This system consists of a partial separation separator with downstream instrumentation containing a MFI multiphase flow meter and a coriolis based gas flow meter. The separator is used to widen the operating envelope of the multiphase meter and increase the accuracy of the measurements at conditions with wells having high GORs. The control of the separator, data acquisition and final calculations are done by the MFI Multiphase meter.

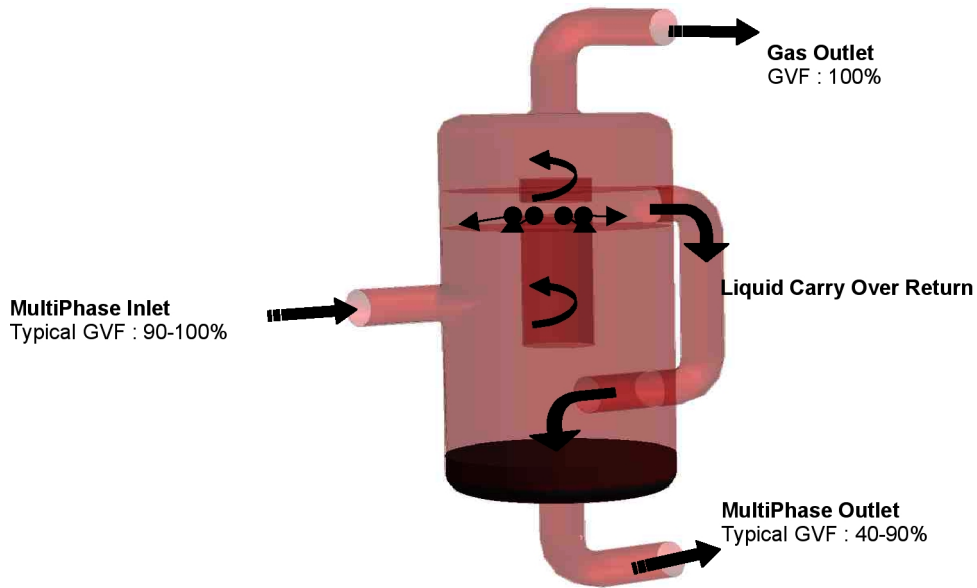


Fig 3. - The separator is a two-stage cyclone with an inner and outer gravity spin. Most of the liquid is separated out at the outer gravity spin defined by the total diameter of the separator. The gas with some remaining liquid is then sucked into the inner cyclone thus spinning at a higher velocity. Remaining liquid in the gas evacuates from the inner cyclone through a small opening at the end of the inner cyclone. Then, since the bottom of the separator is at a lower pressure, liquid from the second stage is sucked through the “liquid carry over” pipe section which is terminated near the low pressure area in the first stage vortex.

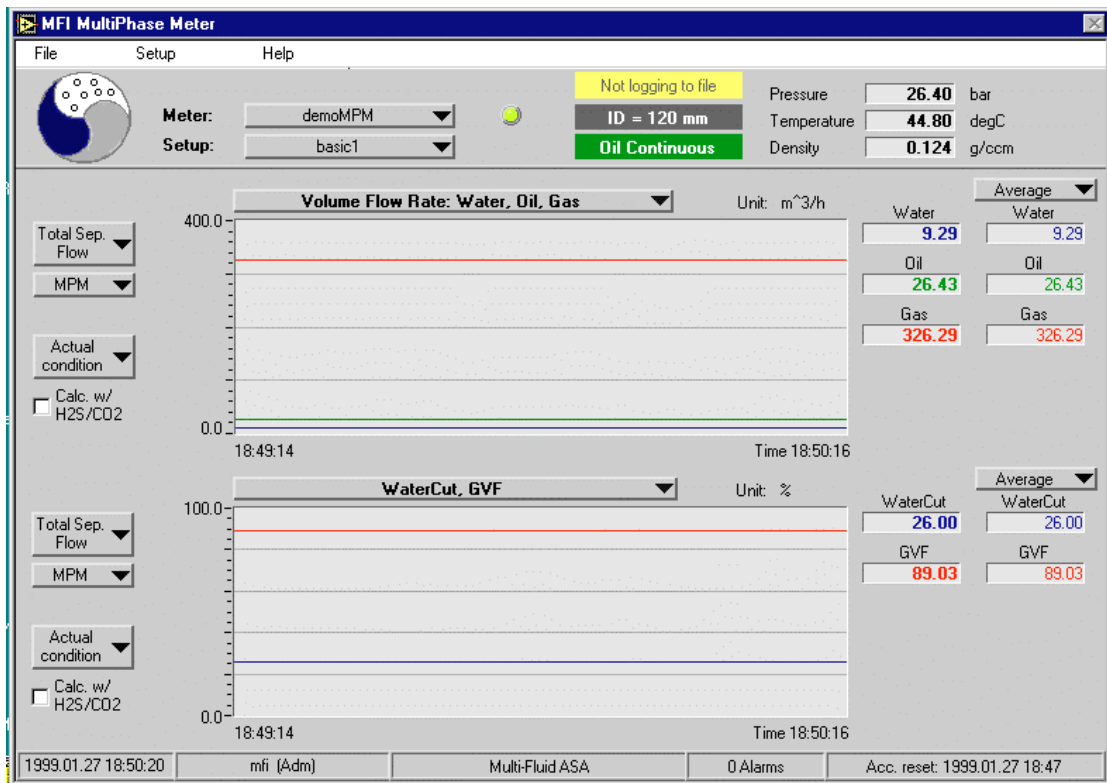


Fig. 4 - The operator interface for the system is a Graphical User Interface (GUI) running on a Windows 95/NT platform. One GUI can be connected to several systems.

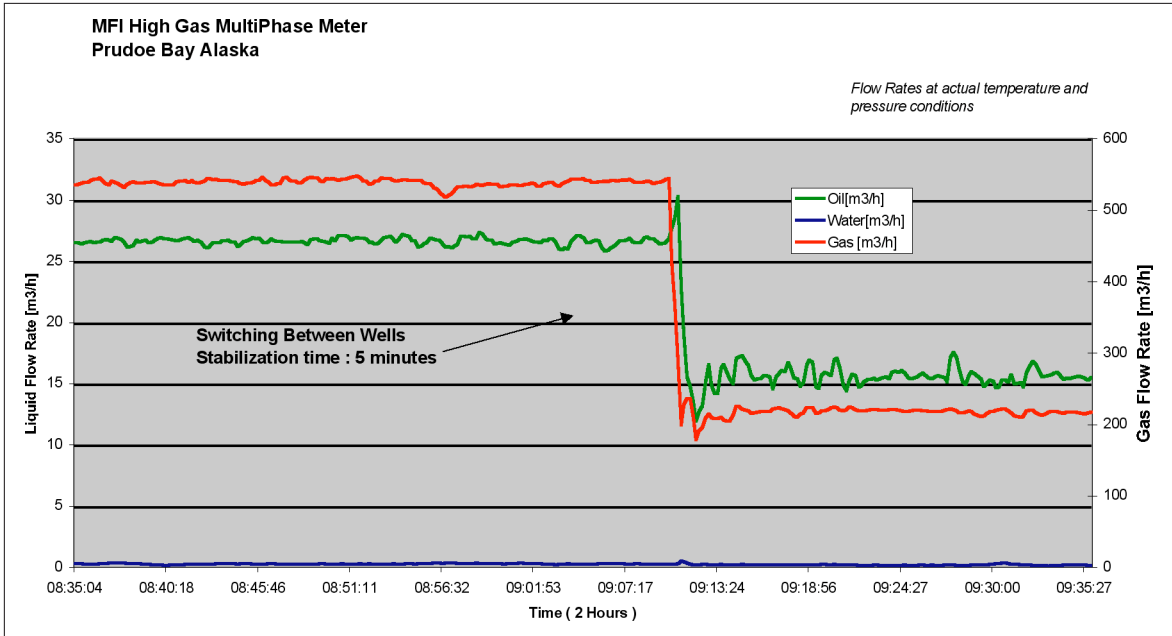


Fig 5. – The control algorithm of the system was able to stabilize the flow within a few minutes as shown in the graph.

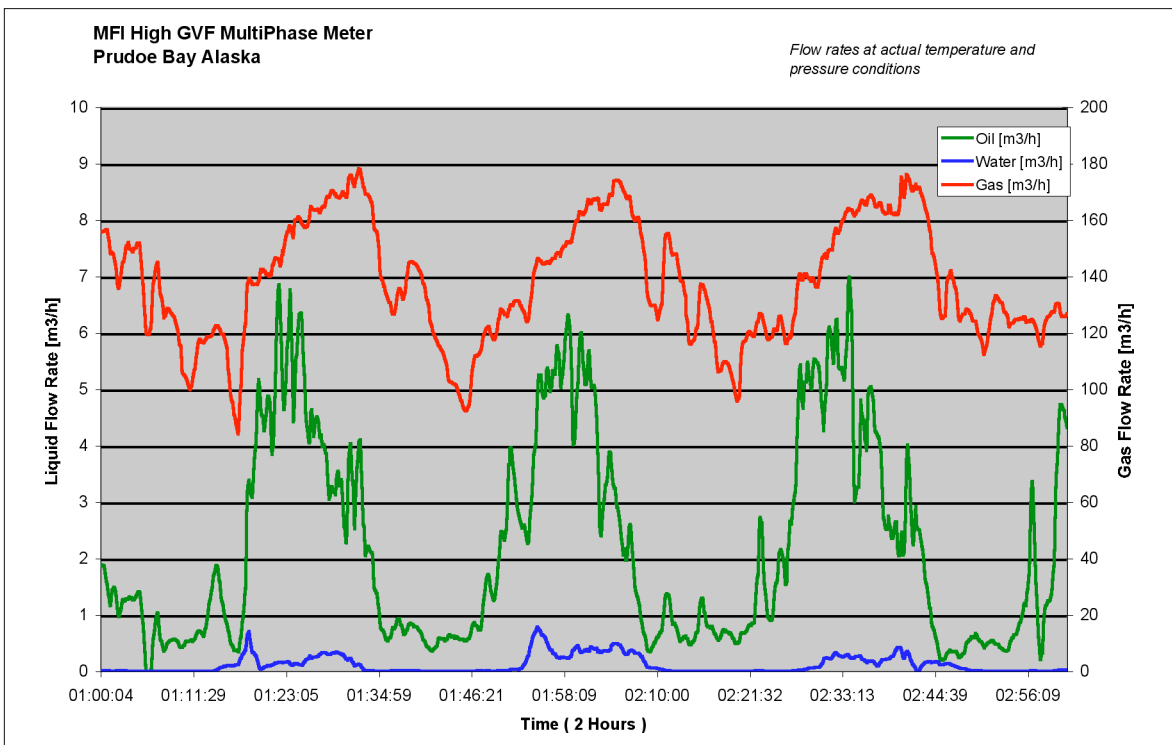


FIG. 6 – The well was slugging at a rate of approx. two slugs pr. hour as seen from the graph above. The system was able to control the valves in order to obtain the desired conditions of the system. This graph also demonstrates one of the great advantages of such a system compared towards a conventional test separator. Whereas the measurements from a test separator would be averaged out for several hours smearing out any real time data, the MFI High Gas System gives valuable information of the behavior of the well. For this particular well, the liquid and gas slugs are in phase indicating a lift gas problem. Hence, by optimizing the lift gas rate based on the real-time measurement from the MFI High Gas System, the production rate from the well could be increased. Also the real-time data can be helpful in diagnosing sub-surface equipment or reservoir problems.

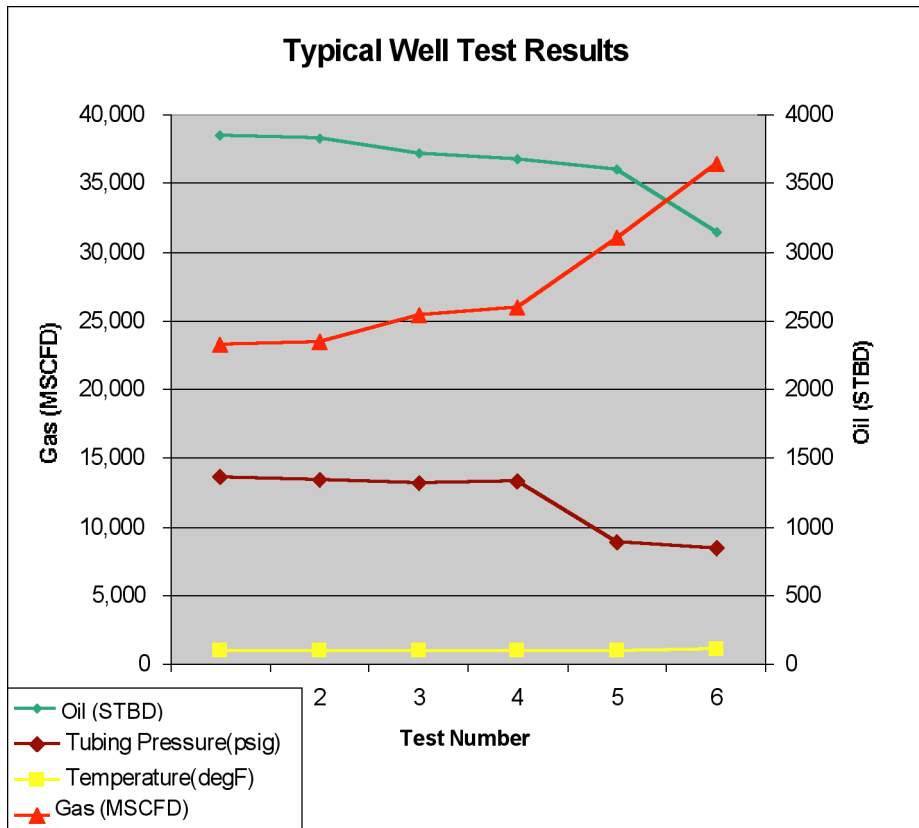
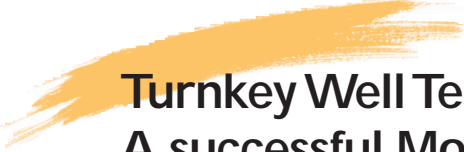


FIG. 7 – This is chart of test results between November 1, 1998 an February 1, 1999. The trend indicates that the results are repeatable and agrees with expected liquid production decline.



# Turnkey Well Testing Services: A successful Modality Measurement in Mexico

*Noel E. Santamaria, Instituto Mexicano del Petróleo, México*

---

## SUMMARY

As part of the program to modernize the surface production facilities, many oil companies have implemented the use of new technologies such as the multiphase flow measurement systems among others. These technological advancements have allowed companies to automate and simplify the operations required to measure flow in oil wells.

In most cases, the implementation of this technology has been achieved by acquisition of the necessary equipment and in some cases through leasing. However, in Mexico after throughout studies had proven its feasibility, it was decided to apply a totally new concept for an specific application. It consists in contracting an integrated well measurement service directly from a company equipped and qualified to provide it efficiently. The company then follows a measurement activity program prepared by Pemex Exploration and Production.

The project scope included 1,656 measurements in 2 years (69 per month) to be performed at 2 separation batteries and 5 individual well collection manifolds located in the Comalcalco District of the Pemex Exploration and Production Southern Region which did not have the necessary infrastructure to adequately measure the flow of oil, gas and water. For this purpose, 2 mobile autonomous measurement units were used, each one equipped with 2 multiphase flow meters, which were designed specifically to cover the flow rates handled in the above mentioned facilities.

This paper discusses the Mexican experience; the details involved in a typical mobile measurement operation; the way information is handled and results reported; the usefulness of the measurement results; and the numerous advantages of implementing the multiphase metering through this new modality as well as recommendations for future applications.

## INTRODUCTION

One of the multiple services that the Instituto Mexicano del Petróleo (IMP), offers to Petróleos Mexicanos is the technical support in optimizing and modernizing its production facilities; particularly those used for well testing, by means of the testing, evaluation and adaptation of new technologies, as the multiphase flow meters

The traditional approach to measure the produced fluids has required separation and independent measurements of the oil, water, and gas. These systems are bulky and require of big spaces for their installation; their operation imply risks of accident for the operative personnel, and contamination of the environment. It is not possible to measure the produced fluids by two or more wells that arrive in a single stream from a remote manifold to the process facilities.

Because of the above facts, the multiphase flow meters were considered a viable alternative to measure the produced fluids, since also they present additional advantages as the immediate readiness, its remote handling, as well as the automation of the well testing operations.

This technology was introduced in Mexico by means of a project developed at the Instituto Mexicano del Petróleo [1] whose scope includes a feasibility study and the acquisition of a multiphase flow meter manufactured especially for a gathering battery located in the southern region of México, where it was installed at the end of 1993.. The functionality of this meter was evaluated by comparing its results with those obtained with the traditional measurement system used in that battery, and the satisfactory results marked the beginning of an era of multiphase flow measurement in México

## **PRODUCTION FACILITIES CONSIDERED TO IMPLANT THE USE OF MULTIPHASE FLOW METERS**

The production facilities considered to implant the use of multiphase flow meter for well testing operations are located in the Comalcalco district, (See Figure 1). Their distances from the monitoring and supervisory center located in the city of Comalcalco are shown in Figure 2. These facilities include the following gathering batteries and remote manifolds, those in which the framework to carry out well testing operations with conventional measurement systems is very limited.

### **Manifolds:**

Sen Norte  
Chinchorro  
Mora  
Bellota 114  
Yagual

### **Batteries**

Pijije  
Luna Modular

The gathering batteries are facilities where the produced fluids are separated, measured, stored and pumped . The produced fluids arrive to these batteries in flow lines that may contain the production from individual wells, or the production from two or more wells. In this last case, it is not possible to measure the individual production of each well.

The remote manifolds are collectors that are located at long distances from the gathering batteries. The fluids produced by several wells are collected in these manifolds and they are sent from here to the gathering batteries. In some cases a flow line for the purpose of measuring the production from an individual well connects the manifold with a battery. One of the manifolds has the arrangements to install portable meters, and others are lacking of any installation for metering purposes. None of them has neither electric power nor phone line.

**Operation conditions and fluids properties.** The operation conditions and the ranges of oil, gas, and water flow rates, as well as the percentage of water in the liquid handled in each one of the facilities are shown in Table 1. The values of the properties of the fluids are shown in Table 2.

## ALTERNATIVES TO IMPLANT THE USE OF MULTIPHASE FLOW METERS

In order to define the best way to implant the use of multiphase flow meters in the Comalcalco district, a project was developed whose scope included the feasibility study to define the convenience of contracting the turnkey well testing services. The following ones were the analyzed alternatives:

**Purchase of multiphase flow meters.** In this modality the meters are the user's property, and they are operated with qualified own personnel. The manufacturer generally provides a lot of spare parts and he is responsibly for assuring operation of the meters during the period of guarantee.

**Rent of multiphase flow meters.** In this case the user operates the multiphase meters with their own personnel, but the manufacturer is the owner of the equipment and has the obligation of providing the appropriate maintenance that guarantees the good operation of the system

**Turnkey well testing services.** In this modality, the user defines a measurement program, the information and parameters required as a result of such measurements, as well as the way and place in that this information should be available. The manufacturer is the owner of the equipment, and is the responsible for its operation. He has the commitment of providing the user the aged reports in the established formats.

## ACTIVITIES CARRIED OUT BEFORE BEGINNING THE WELL TEST SERVICE

Before beginning the well test service, it was necessary to carry out the following activities:

**Bases for bidding and technical specifications.** In these documents the PEP requirements were captured, to carry out the well test operations by using multiphase flow meters in the previously defined facilities; the properties of the produced fluids and the operation conditions were also described.

**Call for bid.** The international public bid SRS-CO-PR-TLC-052/96 was published in april 30, 1996. In this publication were made of the public knowledge the dates for purchase of the bases, technical visits, and reception of offers, among others.

**Evaluation of offers and assignment of the contract.** To make the technical evaluations, 86 concepts of the characteristics of the offered meters were considered; after this evaluation, a technical opinion was elaborated. From those that qualified technically, their economic offers were then revised, selecting that of smaller cost to assign the contract.

**Manufacture of the meters and trucks.** The multiphase flow meters were built in Norway and the trucks for their transportation were manufactured in Houston, USA.

**Adaptation of the facilities.** The adaptations to the facilities to install the multiphase flow meters were in charge of the PEP personnel. These consisted basically on building pipe lines for feeding and discharging the flow, and to condition the place for the access of the mobile units.

**Factory acceptance tests.** The multiphase flow meters were evaluated in the factory, prior to be shipped to México for their test and field evaluation. The factory acceptance tests included hydrostatic tests and the simulation of the measurement process.

**Tests of functionality in field.** The field tests were carried out from June 10 to July 16, 1997, and they consisted on measuring three times the oil, water and gas flow rates from 8 wells whose productions converge to the gathering batteries Mora y Luna Modular. These tests were covered satisfactorily since when comparing the measurement results obtained with multiphase meters and with conventional meters, the deviation obtained were smaller than the specified tolerances.

## SCOPE OF THE SERVICES

The turnkey well testing service included the measurement of the produced fluids, oil, water and gas, of the wells and stream that arrive to the following facilities:

Facilities	Number of wells	Number of stream
Sen Norte	7	
Chinchorro	3	
Mora	11	
Bellota 114	9	
Yagual	2	
Pijije	11	
Luna Modular	11	1

According to the contract they were carried out 1656 measurements during a two year period, 69 monthly, according to a program established by the PEP personnel.

**Duration.** The established duration for the service was 880 days, with date of beginning September 1, 1996 and finishing January 28, 1999, including 150 days for the manufacture of the meters. However, for accidental causes, the measurement service began in August 1997 and it finished in June 1999.

**Deliverables.** According to the contract, the supplier of the service provided the transmission of data and measurement parameters, via cellular phone, from the measurement point to the Monitoring and Control Center located in the city of Comalcalco. This Center was also given and installed by the supplier of the service.

During the operations the supplier delivered the results obtained from the measurement, in digital electronic way, in real time, in a computer of the Monitoring and Control Center , in Comalcalco. Additionally, the supplier deliver to the operative personnel the printed reports with the following information:

- \*Well name
- \*Date and time
- \*Oil flow rate (m3/d)
- \*Gas flow rate (m3/m3)
- \*Water flow rate (m3/m3)
- \*Liquid flow rate (M3/d)
- \*Test duration (hr)
- \*Gas oil ratio (m3/m3)
- \*Water cut (%)
- \*Pressure (kg/cm2)
- \*Temperature (oC)

**Tolerances.** For the batteries Pijje and Luna Modular, as well as for the manifolds Sen Norte, Yagual, and Chinchorro, it was established that the deviations between the volumes measured with the multiphase flow meter and with the conventional test separator use traditionally in PEP, than should not be greater 10%. For the manifolds Mora and Bellota 114 the deviations should not be greater than 5%.

## DESCRIPTION OF THE MULTIPHASE FLOW METERING SYSTEM

**Mobile units.** The measurements were carried out using two completely equipped trucks which operate as autonomous unit; in each one of them it was istalled a control room, an electric power generator, computation and remote communication system, two multiphase flow meters, security equipment, drainages and containers of liquid. In the control room there was a small laboratory to determine the content of water in liquid phase.

**Meters.** The meters were designed to measure the produced fluids at extreme operation conditions, and they should be able to manage any fraction of free gas and any pattern of flow that it could be present during the well testing operations.

During the service, four Fluenta 1900V multiphase flow meters were used, two 1” meter and two 3” meter, to allow a wide range of flowrates to be covered. Each meter was placed in a skid with flange in the ends , to allow a quick connection with the test system, by means of flexible hoses. These meters are non intrusive, they don´t contain mobile parts, and they don´t require to separate the phases to estimate the oil, gas, and water flowrates.

In each truck there were installed two meters, one 1” meter and one 3” meter, in such a way that any one of the units could manage a broad range of flowrates.

**Remote communication equipment.** Each one of the mobile units had a communication system integrated by a cellular modem coupled to a computer. This modem was connected to a cellular phone with a directional antenna that allowed the transmission of information in less than one minute.

**Monitoring and Control Center.** This Center was used for storing the information and integrating a data base for its statistical handling. A computer, a cellular phone, a modem, and a printer were the main components. From this Center it was possible to have access, in real time, to the generated information in any production facility.

**Auxiliary services.** Since the measurement system should operate in an autonomous way, the mobile units had the following services:

- \*Electric power generation
- \*Water for diverse use
- \*Security an against fire equipment
- \*Drainages and collectors
- \*Containers for liquids

## PRINCIPLE OF OPERATION OF MULTIPHASE FLOW METERS

A multiphase flow consists of the three components oil, gas and water. In the process of determining the individual volumetric flow rates of these phases, the fractions and velocities of each of the components are found.

To determine the three fractions, three independent equations are needed. These equations are obtained by 1) measuring the permittivity of the mixture, 2) measuring the density of the mixture, and 3) the fact that the sum of the three fractions always will be one.

A venturimeter is used to determine the velocity of the multiphase mixture. The venturimeter measures the differential pressure before and after a slight narrowing down of the pipe diameter, a technology which has been used with single phase flows for decades. Cross-correlation is used to determine two velocities for the multiphase mixture. Simplified, the velocity of the large gas bubbles gives the velocity of the gas phase, and the velocity of the small gas bubbles gives the velocity of the liquid phase. These two velocities are found by utilizing two different cross-correlation techniques.

### **Determination of oil, water and gas fractions**

The permittivity and density is different for each of the three components of an oil/gas/water mixture. If these permittivities and densities are known, and the total permittivity and density of the mixture can be accurately measured, the fractions of each of the three components can be determined. If the mixture is employed as the dielectric medium between two electrode plates, the electrical field between the plates will be a function of the permittivity of the mixture. If the same medium is positioned in a gamma radiation path, the measured absorption of gamma particles will be a function of the density of the mixture. The Capacitance sensor thus provides the permittivity, and the gamma densitometer the density, of the mixture.

This principle, which relates the fractions of the different components to the mean permittivity and mean density of the mixture, is used by the multiphase flow meter to obtain two independent equations describing the dependency of the three components. The third, and last, equation is the obvious fact that the sum of the three fractions always will be one.

### **Determination of liquid and gas flowrates**

The multiphase flow meter system determines the velocities of the large and the small gas bubbles. Simplified, these indicate the gas and liquid velocities. The sensor contains a number of electrodes with different sizes and patterns, and the two velocities are determined by cross-correlating signals obtained from pairs of electrodes.

When the two flow velocities are determined, these are combined with information from the fraction measurements in a process based model in order to determine the individual flowrates of oil, gas and water.

Even though cross-correlation of signals is a well-defined mathematical method, its use in multiphase flow requires careful selection of a large number of parameters for the results to be satisfactory. Through systematic testing, the parameters are chosen, and the complete algorithm is implemented on an industrial PC.

## **OPERATION**

For carrying out the operations, the PEP personnel provided in advance to the supplier of the service, a monthly program with the list of the wells or stream to be measured. The measurement process began once the trucks were transferred to the production facilities and the system were connected. The procedure carried out for making the measurement was the next.

- - Connect the measurement system to the feeding and discharge pipelines.
- - Start up the electric power generator  
(both communication and computation equipments must be energized)
- - Align the flow to the multiphase meter for their stabilization
- - Select the meter to use, depending on the flowrate to be handled
- - Begin the measurement process.
- - Register, store, and transmit the measurement parameters.

The generated information, operation parameters and flowrates were sent to the Control Center in Comalcalco using a portable computer Notebook, modem and cellular telephone.

In order for the PEP personnel to verify the usefulness of the above activities, it was established that a PEP representative could supervise, in any time, the execution of all those works, and also to supervise the materials used during operations. The system was totally operated by the supplier of the service.

Once the operations were finished, the liquids contained into the metering system were pumped to the process pipes, in such a way that the equipment was cleaned and ready for transferring it to another place.

A diagram of the installation of the mobile unit for realizing the measurement is shown in **Figure 3**.

## CONCLUSIONS

The use of multiphase flow meters in the Comalcalco District, through a turnkey well testing service, demostred to be a successful option for well testing operations in México.

The portable multiphase flow meters allow the measurement of oil, gas and water produced from wells in production facilities where it is not feasible to use convencional systems, because the lack of infrastructure and auxiliary services, or in production facilities with few wells, where the investment in fixed installations are not justified..

Since multiphase flow meters use technical principles that are in a constant evolution and improvement, the turnkey well testing service modality allows the use of this technology, without the need to acquire models that in a little time will be obsolete.

When the multiphase flow meters are used, the time for well testing operations is at least 50% smaller than the time required when using conventional system.

## REFERENCES

1. Santamaria N. E. Ramirez F. y otros  
Prueba y evaluación de Sistemas de Medición Multifásica  
Proyecto CDB-3197, Instituto Mexicano del Petróleo., Septiembre,1994
2. Hernandez M.A., Jofre E.R., Santamaria N.E.  
Implantación de Sistemas de Medición Multifásica, Región Sur.  
Proyecto CDB-6313, Instituto Mexicano del Petróleo, 1995.

Table 1. Operations Conditions

	Qo(m3/d)		Wcut (%)	Qg(m3/d)		GOR (m3/m3)		P(Kg/cm2)		T (°C)	
	Max	Min		Max	Min	Max	Min	Max	Min	Max	Min
<u>GATHERING</u>											
<u>BATTERIES</u>											
<u>PIIJE</u>	7.989	67	54.1	1.034.883	14.405	519	215	82	6	70	30
<u>LUNA MODULAR</u>	626	9	70	802.280	8.856	1.318	646	84	5.5	70	55
<u>MANIFOLDS</u>											
<u>SEN NORTE</u>	1.269	228	1.3	565.974	104.196	457	446	395	81	100	65
<u>BELLOTA 114</u>	361	24	4.2	91.800	7.416	412	179	38	12	38	
<u>YAGUAL</u>	988	71	10.13	219.336	17.324	244	222	106	12	80	
<u>MORA</u>	341	71	2.6	85.932	10.947	312	123	120	12	43	

Table 2 Fluid Properties

	SGo			mo (cp@37 °C)			SGw		SGg(air=1)	
	Max	Min	Avg	Max	Min	Avg	Max	Avg	Max	Avg
<u>GATHERING</u>										
<u>BATTERIES</u>										
<u>PIIJE</u>	0.836	0.822		3.84	2.1		1.114	0.71		
<u>LUNA MODULAR</u>			0.802			2	1.113	0.7074		
<u>MANIFOLDS</u>										
<u>SEN NORTE</u>			0.823			3.05	1.057	0.72		
<u>BELLOTA 114</u>	0.9	0.83				3.4	1.006	0.779		
<u>CHINCHORRO</u>	0.84	0.862		4.6	8.6		1.008	0.912		
<u>YAGUAL</u>			0.84			4.6	1.008			
<u>MORA</u>			0.832			3.7	1.002	0.855		



Fig. 1. Mexico and Comalcalco District

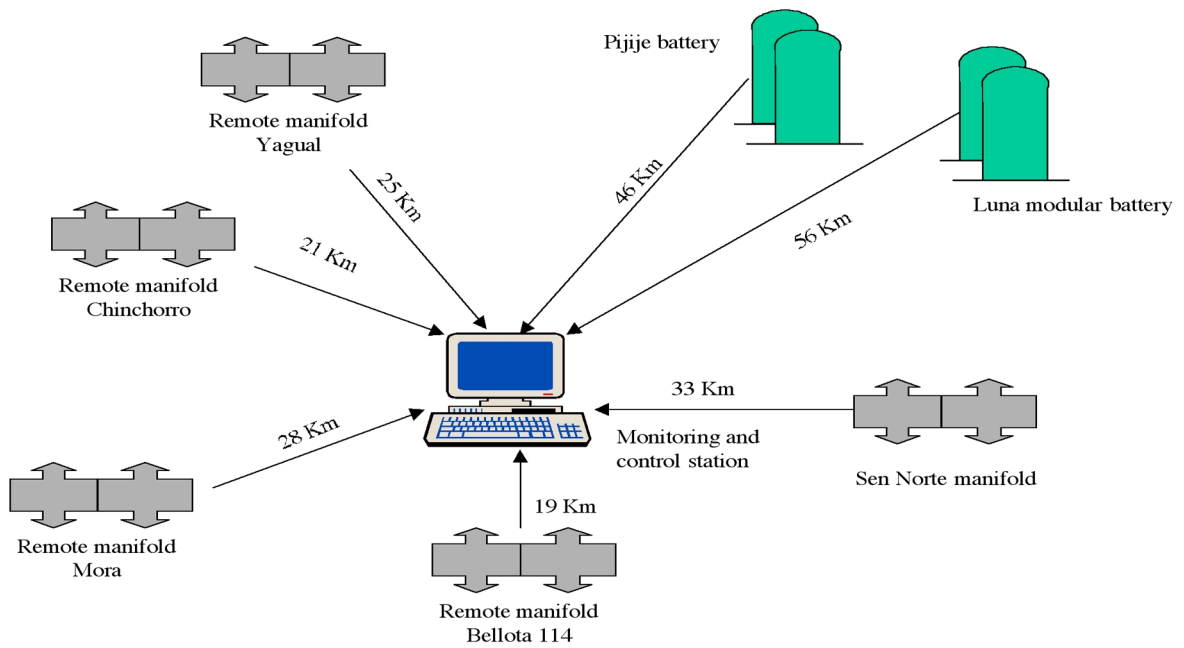
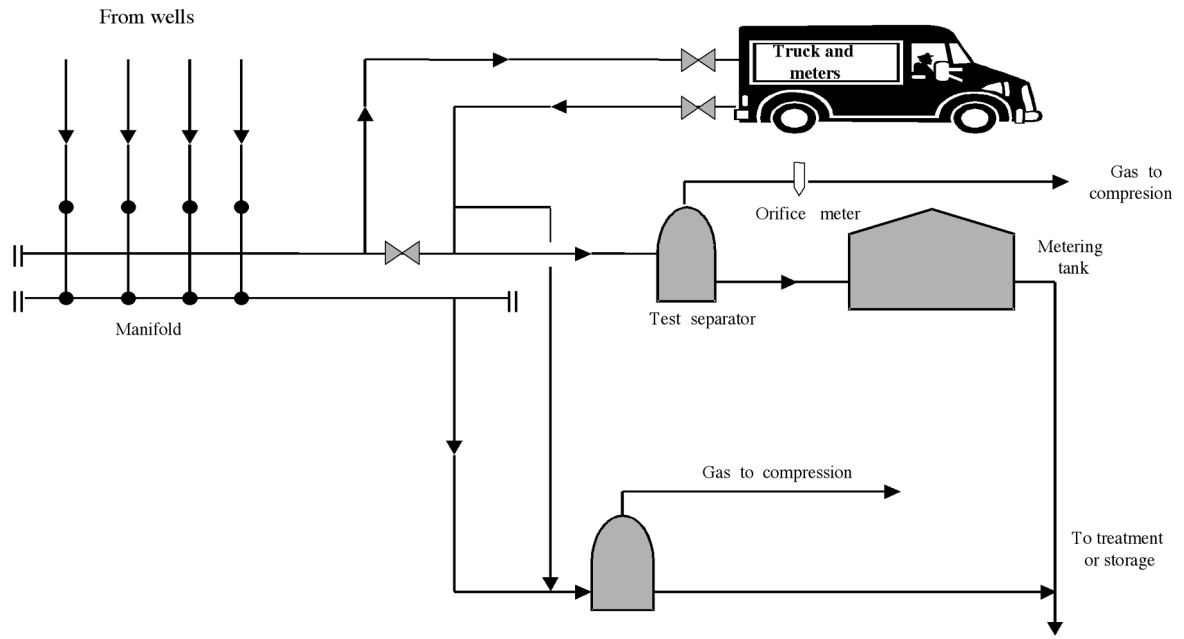


Fig. 2. Gathering batteries and manifolds



*Fig. 3. Configuration in gathering battery*

# Experience with Ultrasonic Flowmeters in Fiscal Applications for Oil (-products)

*C.J. Hogendoorn and A. Boer – Krohne Altometer*

---

## Introduction

Last years the number of applications for fiscal metering of oil (-products) with a multi beam ultrasonic flowmeters has been increased significantly. The growing interest for this type of fiscal metering is mainly due to specific advantages.

Besides the high accuracy and complete independence of viscosity, the long-term stability is very good. These attractive properties are a result of an essentially different measuring principle. Multi beam ultrasonic flowmeters can be smoothly used in installations on the continent. In limited spaced offshore applications some specific features of an ultrasonic flowmeter must be taken into account, in the system design, to stay within the NPD repeatability requirements for turbine meters.

This article explains how to realise a successful application of a multi beam ultrasonic flowmeter in situations with a small prover volume. This is explained starting from the fundamental measuring principle of an ultrasonic flowmeter. The paper is finished with a consideration of the future developments and some conclusions.

## Effects of velocity disturbances and changing viscosity on a multi beam ultrasonic flowmeter

Since several years a multi beam Ultrasonic Flowmeter (UFM) is available on the market which performs very well in custody transfer measurements on oil and oil-products (Figure 1 and Figure 2).



Figure 1: A calibration of a 16" Altosonic V on oil at SPSE in France.



Figure 2: Application of an 8" Altosonic V on oil.

This meter has been made highly independent of disturbed velocity profile by the application of an integrated confusor in the meter body. This confusor homogenises the flow as illustrated in Figure 3.

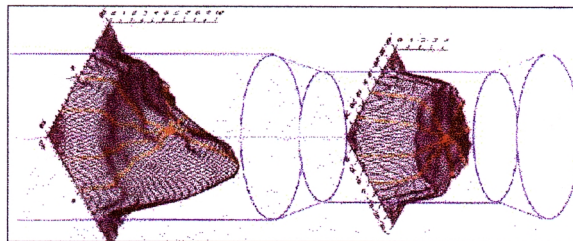


Figure 3: An illustrative example of the effect of a confusor on a disturbance in the velocity profile. The confusor stretches the flow and makes it more homogeneous. Laser Doppler Anemometry (LDA) has been used in this example to measure the velocity.

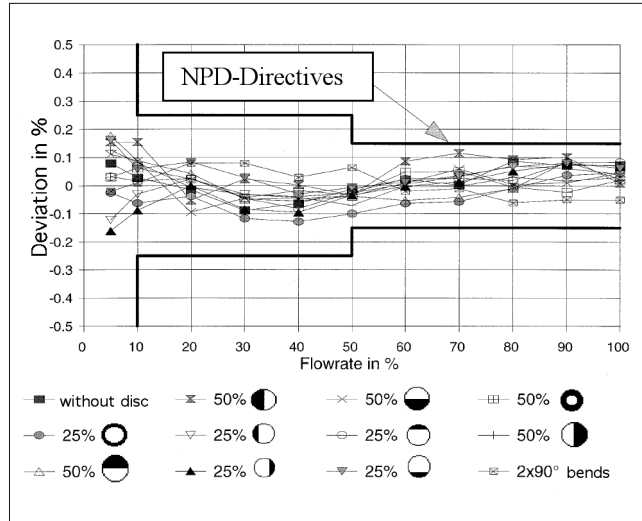


Figure 4: Measurements at Krohne Altometer with a DN200 multi-channel ultrasonic custody transfer flowmeter with naphtha and gas oil. The deviation remains well within the NPD directives at the dynamic range of 1:10. The disturbance is generated 20D upstream.

The effect is apparent from figure 4. This figure shows the sensitivity to different profile disturbances generated 20D upstream the UFM. The contraction stretches the flow and makes the velocity profile more uniform.

Although the disturbances on the velocity profile are diminished the profile is still Reynolds or viscosity dependent. Therefore, the velocity is measured at five different heights in the tube. The shape of the velocity profile is directly related to the Reynolds number or viscosity. This information is taken into account in the measuring algorithm. In this way the linearity and meter factor of the multi beam UFM has been made completely independent of viscosity. The multi beam UFM of Krohne has been officially certified for the viscosity range from 0.1cSt to 150cSt. The linearity and repeatability for three different viscosities is shown in Figure 5 and Figure 6.

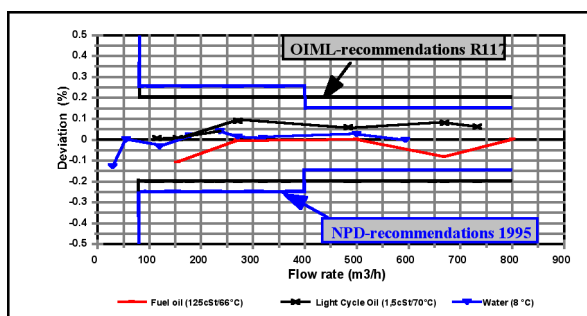


Figure 5: Linearity of an UFM for three different viscosities. All the measurements stay within the NPD directives for turbine meters.

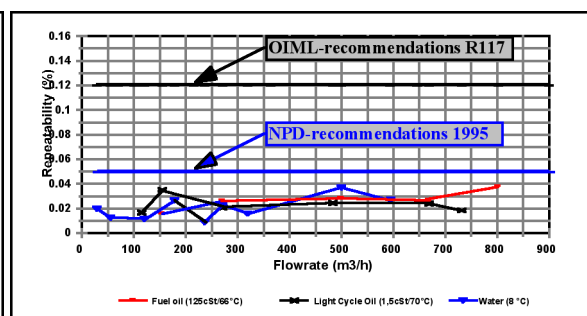


Figure 6: Repeatability of an UFM for three different viscosities. The blue lines indicate the NPD and OIML requirements for turbine meters. Prover volume 8 m3.

A multi beam UFM can handle liquids with changing viscosity without loss of accuracy or need for intermediate calibration.

### 3. Ultrasonic flowmeter and repeatability

To guarantee a successful operating UFM, meeting the NPD repeatability requirements for turbine meters, the nature of the ultrasonic instrument must be taken into account in the early stage of system design. The physical principle demands some requirements with respect to the calibration system. It will be explained why.

The multi beam UFM uses the so-called run-time method. The difference in up and downstream sonic run time is a measure for the fluid velocity along the sonic beam. The method is very fast and doesn't affect the flow by the measurement itself. Furthermore, purely the velocity along the sound beam is measured. It is not a mixture between velocity and momentum as it is the case with a turbine meter. In addition, all the fluctuations in the flow are being measured without filtering by inertia due to moving parts.

The UFM measures the flow including turbulence and characteristics of the overall system. This is illustrated in the next figures. shows an on-line signal measured by a multi beam UFM during a steady flow in an offshore installation (not during a prover run). represents the frequency spectrum of obtained by means of a Fast Fourier Transformation.

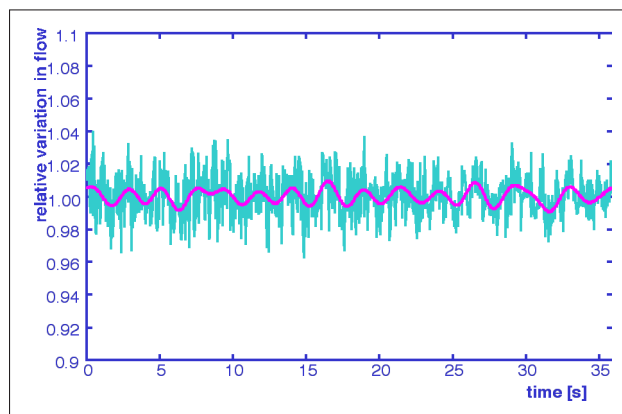


Figure 7: The steady real-time velocity signal measured by the multi beam UFM. The red line is the low frequency variation present in the flow.

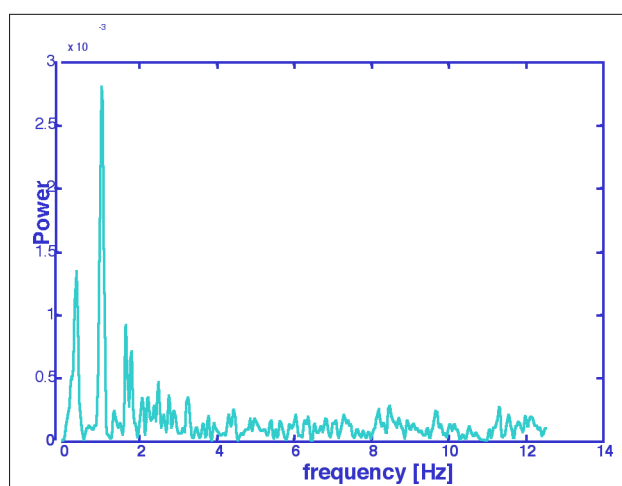


Figure 8: The Fast Fourier Transform of the signal in the left figure. Some strong low frequency components are present.

Some strong peaks are observed in the lower frequency range, whereas this is not obvious from the signal in the time domain. In fact, low frequency peaks are always present as a result of turbulence. However, in a poor system design some dominating low frequency oscillations can be generated additionally.

Precisely the presence of low frequency peaks has an important impact on the calibration of the UFM. Due to the fast response of the UFM these frequencies are fully measured. In order to obtain a good repeatability, a number of periods of these low frequency components must be acquired to eliminate its effect on the mean value. Up to certain limits can be stated that the smaller the oscillations are, the smaller the required prover volume is. The lower natural limit is generated by the turbulence present in the flow.

In several systems the flow conditions change when the ball prover is placed on-line. The flow significantly decreases and becomes unstable as a result of transients in the prover behaviour. These phenomena are accurately measured by the UFM. Because a turbine meter has some inertia, this has a positive consequence for the repeatability but may have a negative effect on the meter factor.

As a matter of fact, the repeatability proof is an excellent way of proving the mechanical condition of a turbine meter. The final goal is to control the overall uncertainty of the meter.

From the ultrasonic point of view, the mechanical proof is not concentrated in the repeatability because it has no moving parts. The less accurate short-term repeatability does not mean that the meter is not in order, but reflects the quality of the measuring principle. Therefore, the UFM is better characterised by the overall uncertainty. Of course, the repeatability should stay within certain limits.

## 4. Recommended calibration procedure

### 4.1 Larger prover volumes

Excellent linearities and repeatabilities have been obtained with larger prover volumes (e.g. in France with 8 and 10m<sup>3</sup> and in the USA with 5.4m<sup>3</sup>). In these applications the UFM can be applied smoothly even with the presence of strongly dominating low frequency components in the flow.

### 4.2 Small volume provers

In the situation that a compact prover is the one and only solution, another calibration procedure is required to satisfy the NPD requirements for turbine meters. A successful working calibration system in this case is a combination of a small volume ball prover, a turbine meter and a multi beam UFM. One of the features of a turbine meter is that it has a good repeatability even when a small prover volume is available. This feature is used. This leads to a three-step method:

- The turbine meter is calibrated with the small volume prover.
- Then the turbine meter is placed in series with the UFM. With a calibration time of e.g. 2 minutes per point the UFM is calibrated.
- After the calibration of the UFM the turbine is put out of operation.

Next, the UFM is being used as the duty meter, which is very stable, constant and independent on viscosity. The turbine meter that is sensitive to wearing and viscosity effects is secluded.

This method has been successfully applied by Saga Petroleum ASA for already two years. They will use the same method for Snorre B platform. Statoil has utilised this approach for Vslefrikk too. The intention is to save calibration costs by reducing the frequency of calibration. The extension of calibration interval will be discussed in chapter 6 too.

A combination of a small prover volume and an UFM may be possible with a well-designed prover (generating a stable flow) using several added runs. Furthermore, a shift towards the accent on uncertainty instead of repeatability may lead to a better characterising treatment of the UFM. This leads to a decrease in required prover volume.

## 5. Advantages of an instrument without moving parts

With the application of a multi beam UFM, the measuring system has become independent of viscosity effects caused by temperature variations or changes in composition of the oil. A recalibration after the velocity has been changed is not necessary. These are important aspects. Another important point is the long-term stability.

Experiments have been performed to investigate the stability of the multi beam UFM on the longer term. shows the stability over a period of 2<sup>1</sup>/<sub>2</sub> years. This multi beam UFM has been externally used and two times recalibrated.

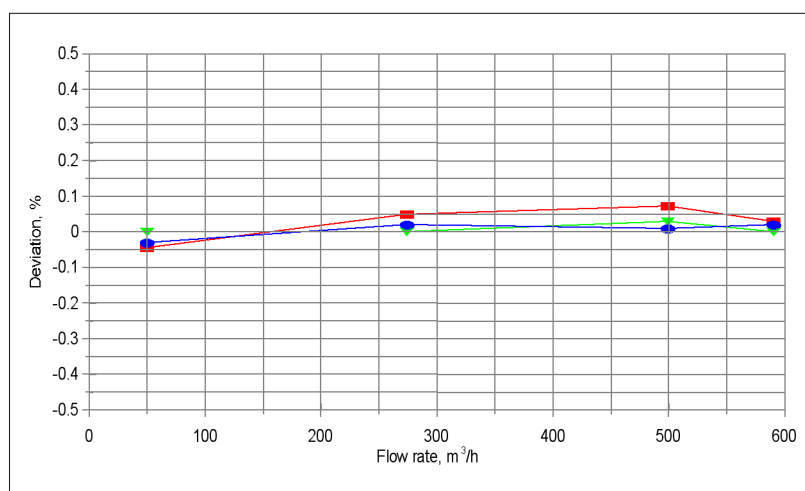


Figure 9: Long-term stability of a multi beam UFM (Altosonic V). Uncertainty of the calibration rig is (0.03%. The results include installation effects. The recalibration is performed on water.

The differences displayed include the uncertainty of the calibration rig (0.03% and installation effects. The shift in meter factor is in the order of a few hundredth of a percent. Similar results have been obtained in offshore applications. There has been no measurable effect of scaling. This shows that the stability on longer term is very good.

## 6. Perception of future developments

With growing confidence in the long term stability of the multi beam UFM the calibration interval of this type of meter may be extended. It is no longer necessary to perform a calibration at each separate viscosity or velocity. This leads to another view on the calibration procedure.

With a move from frequent calibration nowadays towards a calibration e.g. each year in the future, a fixed prover system may be no longer the best solution. It may be replaced by a mobile prover system. The duty UFM may generate a kind of health or confidence factor, which is a measure for the quality of the measurement. A second UFM duty meter eventually checks the first one. This system is sketched in .

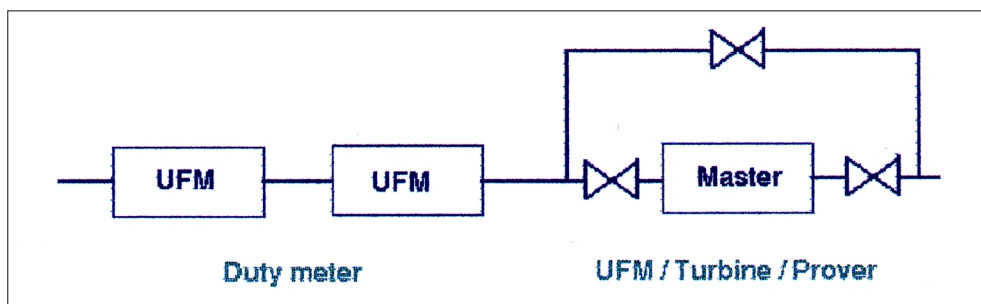


Figure 10: An offshore measuring system as it may become in future. One or two multi beam UFM's run as the duty meter. The master meter can either be an UFM, a turbine or a (mobile) prover. The UFM duty meter generates a kind of quality factor to indicate its health or reliability.

## 7. Conclusions

A multi beam UFM has many advantages when compared to a turbine meter. Since the measuring principle is basically different from the principle of a turbine meter, the nature of an UFM has to be taken into account in the system design. The UFM must be applied as an UFM. This requires a somewhat longer period of a stable flow during calibration to meet the current NPD requirements with respect to the repeatability. In continental applications the prover volume is sufficiently large. A prover volume of about 6 m<sup>3</sup> has been demonstrated to be sufficient.

In some situations the space of a larger prover volume is not available. In these cases a very practical and guaranteed successful method to meet the current NPD requirements is the application of a turbine meter, calibrated with a compact prover, that serves as an intermediate reference. The turbine meter is taken out of service after calibration.

This does not mean that a multi beam UFM can not be combined with a small prover volume. Special attention and ongoing developments makes it presumably possible to meet the NPD requirements in the next future.

A multi beam UFM can be applied as the duty meter. This instrument is completely independent of viscosity and has a proven high long-term stability in the field. The results of the current development show the potential to change the vision on the system design with respect to calibration.



# Development and Installation of the ABLE CTM Ultrasonic Cargo Transfer Metering System on the BP Amoco Schiehallion FPSO

*Peter Baldwin*

---

## Table of Contents

1. Introduction
2. Why the CTM System for Offload?
3. BP Amoco's Commitment to the CTMsystem™
4. System Development
5. Commissioning of the CTMsystem™
6. The Development of OpCon
7. CTMsystem™ Control Methodology
8. Conclusion
9. Subsequent Systems and the Future
10. Glossary of Terms
11. Appendix 1 - CTMflowstation™ 1 Calibration Average
12. Appendix 2 - CTMflowstation™ 2 Calibration Average
13. Appendix 3 - CTMmcvs™ Calibration Average
14. Appendix 4 - Accuracy Data for Offloads 11 through 50
15. Appendix 5 - CTMsystem™ & Shuttle Tanker Offloads
16. Appendix 6 - Shuttle Tanker Offloads
17. Appendix 7 - CTMsystem™ Offloads
18. Appendix 8 - CTMflowstation™ 2 Calibration Average
19. Appendix 9 - CTMflowstation™ 2 Calibration Average
20. Appendix 10 - CTMmcvs™ Calibration Average

## 1. Introduction

Late in 1993 whilst exploring the deep waters to the west of the Shetland Isles the semi-submersible drilling rig, the Ocean Alliance, discovered the Schiehallion oilfield. The Schiehallion field is located beneath 400M of some of the most hostile sea in the UK Continental Shelf. Field reserves were estimated at 425 million barrels and it was anticipated that as many as 29 subsea wells in 4 producing clusters could be required for recovery. It was decided that use of the emerging FPSO technology would be most suited to the task and the world's then largest new build FPSO vessel Schiehallion was commissioned.

## 2. Why the CTM System for Offload?

Discussion between BP Amoco and the DTI, revealed ABLE's pioneering work with the North Sea Operator Kerr McGee Oil (UK) Plc on the Gryphon A. A clamp-on ultrasonic system had been specifically developed to address the unique nuances of FPSO offloading, a system which operated dependably despite the non-stable flow conditions experienced through backwash and tank stripping conditions. A system that delivered significant CAPEX and OPEX advantages.

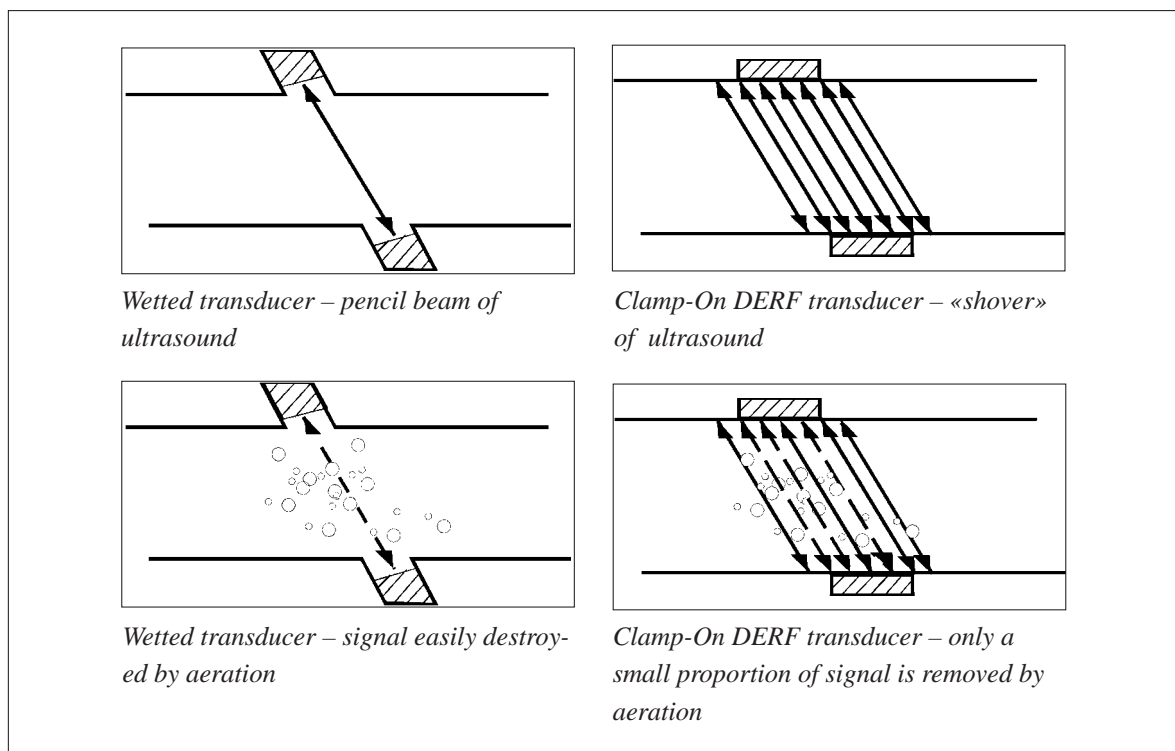


Figure 1 - The advantages of the clamp-on system developed for FPSO offloading

On the Gryphon A a single **CTMflowstation™** had been placed on the export line, before the existing metering point, where its performance had been verified against the DTI accepted calibrated turbine flowmeter skid. Over a period of several months data had been acquired which showed deviations from the reference volume export values to be well within the limits acceptable by the DTI for stand alone offshore loaders. It is worth noting that the Gryphon, like the Schiehallion, was not a strict custody transfer point and as such the normal requirement for 0.25% accuracy was relaxed in favour of 1%.

The live tests on Gryphon A had resulted in a submission being made to the DTI for moth balling of the conventional metering skid, on the basis of the significant operational and cost benefits of the clamp-on **CTMsystem™**. Extracts from the findings of Kerr McGee showed that:-

- \_ Tanker export times reduced from 24 to 18 hours for a typical 66000 tonne export.
- \_ Benefits of faster export of cargo proven during poor weather conditions where slower metering would have resulted in the need for export to have been interrupted and the shuttle tanker to have returned to complete loading.
- \_ Cost savings, taking maintenance and re-calibration of conventional skid in to account as well as reduced transport charges in the region of £200,000 p.a.

BP Amoco having satisfied themselves of the benefits a clamp-on system with no moving or wetted parts could provide with regards to minimum maintenance, manning and intervention, proceeded with purchase.

### **3. BP Amoco's Commitment to the CTMsystem™**

The initial scope of supply was for a master and slave flowstation configuration which utilised an off the shelf comparator / flow computer. Essentially this meant one flow station would take the role of primary measurement - master meter, with measurements from the second or slave meter, being used to determine any undefined shift in the readings of the master meter.

Extensive system testing at the Danfoss calibration facility in Stonehouse, Gloucestershire was witnessed by a core of flow experts who were to become central to the initial development of the **CTMsystem™** (see appendices 1 through 3).

Bill Strang BP Amoco - Schiehallion E & I Project Engineer  
Vincent Withers BP Amoco - Metering Specialist  
Lewis Philp DTI - Head of Gas and Oil Measuring Branch  
Brian Bowers Brown & Root - Lead Instrument Engineer

Whilst testing and calibration proved highly successful it also revealed a number of system limitations which ABLE, BP Amoco and the DTI discussed in depth with a view to improving performance. The master / slave system configuration meant the points of incidence between the flow stations were not identical, therefore the decision as to which station was providing the better performance could not be made with certainty. Furthermore BP Amoco could see the value of individual path interrogation, as it would allow not only the optimisation of the flow measurement, but also allow information relating to the condition of the process to be obtained.

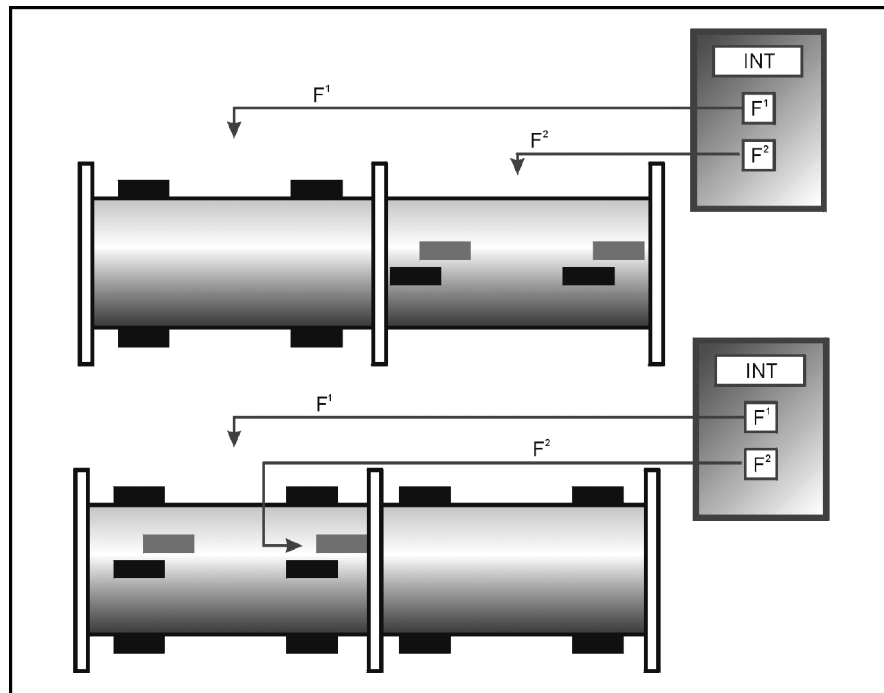


Figure 2 - Original system design is shown in the upper portion, lower diagram shows the current configuration of Schiehallion's Offload Metering System

## 4. System Development

This resulted in a redesign of the existing Schiehallion CTM cargo offload metering system and the deployment of a single spool system with both flowstations measuring at the same cross sectional point, therefore allowing a true comparison of individual transducer signal conditions to be achieved. To maximise the advantage gained by improved transducer location, extensive product development of the process interrogation system was required. It was recognised that a lot of diagnostic data was available and a facility to combine this in a simple Operator Confidence figure was proposed. This resulted in the development of OpCon, a unique feature allowing access to process detail and incorporating a degree of automated diagnostic capability. OpCon constantly verifies multiple parameters received by each transducer, whilst simultaneously providing a real time register of parameters including temperature, pressure, aeration and sonic velocity.

## 5. Commissioning of the CTMsystem™

Successful commissioning of the CTMsystem™ highlighted a number of issues. In the calibration laboratory the CTMsystem™ had performed exceptionally, however it soon became clear that process conditions varied enormously for differing installations and that the Schiehallion offload process bears no resemblance to the «clean» and stable conditions associated with a calibration rig or indeed an export terminal.

Operational experience indicated that during an offload there are numerous events, which can have a detrimental effect on achievable metering accuracy including: -

- 1) Weather Windows - The onset of bad weather is always a possibility, particularly when it is considered that an offload can take up to 18 hours to complete. During extreme conditions it is not unknown for a tanker to have to re-engage five times.
- 2) Tank Stripping - Completely draining the cargo tanks aboard the FPSO.
- 3) Backwashing - To ensure all the available oil is removed from a cargo tank, high pressure oil is sprayed on to the walls and ceiling washing off valuable congealed oil (often referred to as «clingage»)
- 4) Start Up Procedure - Priming of pipes and pumps.
- 5) Offload End Procedure - Long slow decline in pressure induces aeration.

The periods at either end of an offload provide unique challenges for accurate metering. High aeration levels and low pressure are characteristic plus an increase in entrained solids make metering difficult. The ability of an offload metering system to perform at all under these circumstances is vital as during these periods, of up to an hour, acceptable offload figures are won or lost. These problems are amplified when poor weather conditions require a tanker to disengage and then reengage to resume offload.

Similar problems during tank stripping and backwashing procedures occur, as excess air, sediment and congealed solids are drawn into the export line. Once again these conditions are not ideal for metering.

Discussions between ABLE and BP Amoco concluded that no matter how intrinsically accurate an offload metering system, the only process for achieving acceptable live offload results was to increase metering up time. As a result BP Amoco redefined offload procedures to incorporate suggestions from ABLE including priming of pumps and pipes where possible.

## 6. The Development of OpCon

The movement of the oil from the storage facility on the Schiehallion via pipeline to the Shuttle tanker Loch Rannoch periodically suffered from problems such as gas outbreak, tank stripping and slugging. Without OpCon little information would have been available about the condition of the process during an offload. A metering skid would have «masked» potential problems since turbines would continue to spin regardless of whether metering gas or crude, whilst a wetted transducer ultrasonic system would have been unlikely to continue operation due to signal failure through breaks in the narrow ultrasonic beam caused by gas breakout. Information available through OpCon was logged via the **CTMgatherer™**, this allowed operators to rerun individual offloads and build an accurate profile of the offload procedure. Using this information, thresholds within OpCon could be adjusted to maximise metering up time.

The introduction of OpCon effectively freed the Schiehallion cargo offload metering system from depending upon a Master / Slave relationship, where only one flowstation supplies the recorded data. BP Amoco's drive for improved offloads resulted in OpCon intelligence

giving «weight» to the return signals from the flow paths of favourable measurement signals. As an extension of this philosophy OpCon was actually designed to disregard data from any flow path producing outside acceptable thresholds.

The ability of OpCon to allow greater functionality plus the DTI's requirement for guaranteed availability under all offload conditions culminated in the development of a purpose built central brain, the MCVS. The MCVS was developed since conventional flow computers are not designed to interface at the path level of ultrasonic flowmeters. At best a flow computer can manipulate the outputs from ultrasonic meters, however even this requires special programming. The MCVS incorporates two autonomous flow stations, which can be used independently or simultaneously via use of the MCVS depending upon process conditions. The MCVS can mix and match up to eight measurement paths across the two spools if necessary, depending on process and hardware diagnostic OpCon thresholds.

## 7. CTMsystem™ Control Methodology

In order to comply with the ever-changing demands of each individual offload BP Amoco implemented several changes in the recording of offload data. BP Amoco required that the CTMsystem™ be flexible enough to accommodate both start / stop metering and also continuous batch metering. Ultimately this ensured compatibility with whichever offload regime was required. The development of a continuous batch measurement process provides total accountability and ensures that no cargo is lost. The period between batch runs also allows the CTMsystem™ to run a complete routine of self-checks, from auto zeroing through to cabling integrity.

## 8. Conclusion

Successful system enhancement was achieved by a combination of operational experience and fuller knowledge of the process conditions gained by the implementation of an intelligent metering system (see appendices 4 through 7).

## 9. Subsequent Systems and the Future

The first full redundancy system governed by a dual MCVS was purchased by Enterprise Oil late in 1997, with successful commissioning taking place in the spring of 1999. This system provides the ultimate in security, as should the operation of either MCVS be found to be inadequate or be producing unusual results, the second fully functional MCVS system will automatically be brought on line without the loss of any data.

The flow computers are now in their second generation and use a digital encoded signal technique (DERF), removing any uncertainty regarding transmit / receive ultrasonic signal detection times. New High Precision Transducers have evolved which provide the greatest possible signal amplitude and have no sonic signal distortion. This combination of new flow computers and transducers is providing greater accuracy and superior stability, which ultimately extends metering «up time» during adverse conditions (see appendices 8 through 10).

The MCVS is being developed to interrogate up to sixteen different paths simultaneously. This we see as a natural extension of our capability to solve the most difficult flow applications that we are likely to encounter.

Continued development of software and hardware has pushed the **CTMsystem**<sup>TM</sup> further toward the definitive goal of providing similar cost and operational advantages for a fully fiscally approved custody transfer system.

## 10. Glossary of Terms

CTM - Cargo Transfer Metering

DERF - Digitally Encoded Resonant Frequency

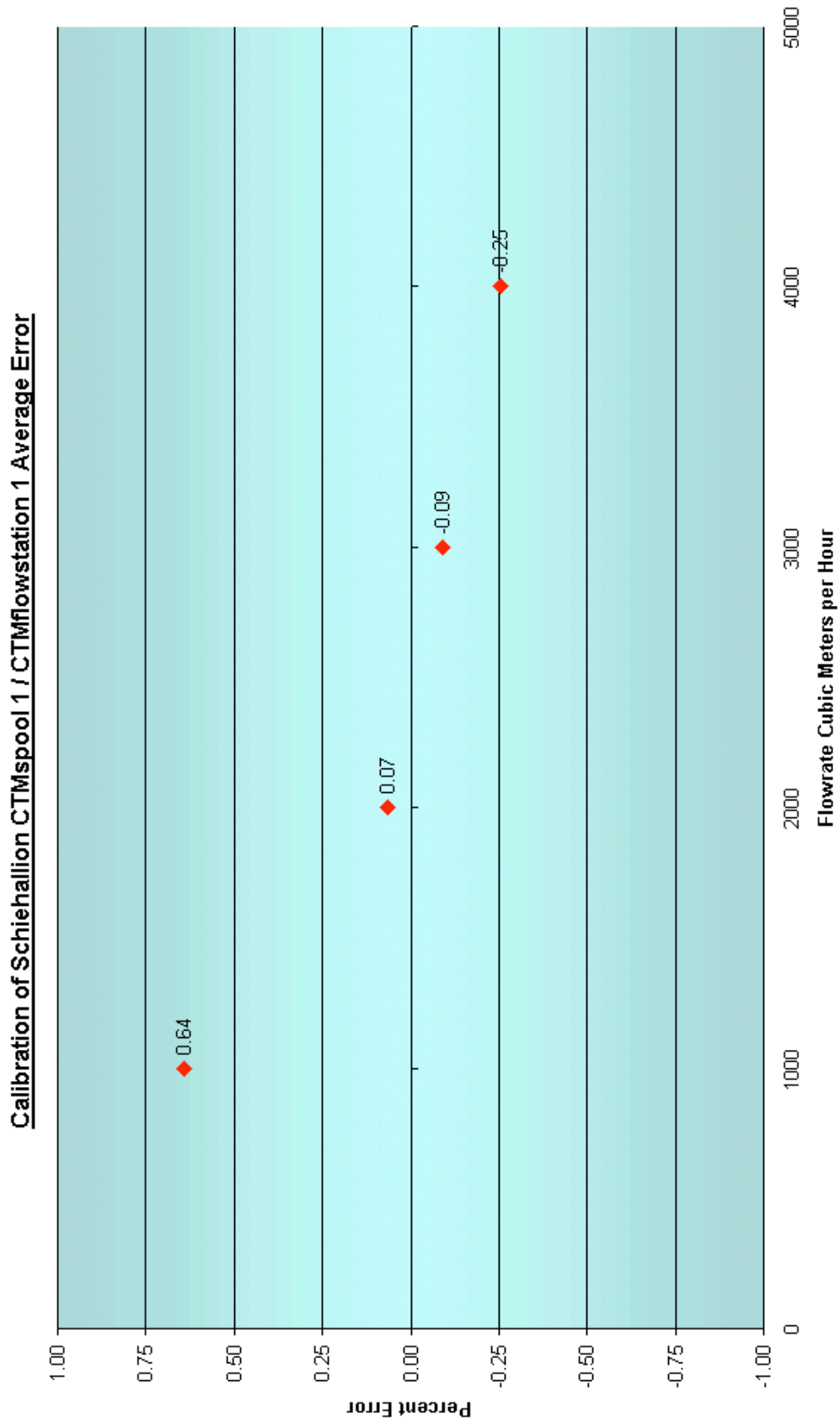
DTI - Department Of Trade and Industry

FPSO - Floating Production, Storage and Offloading

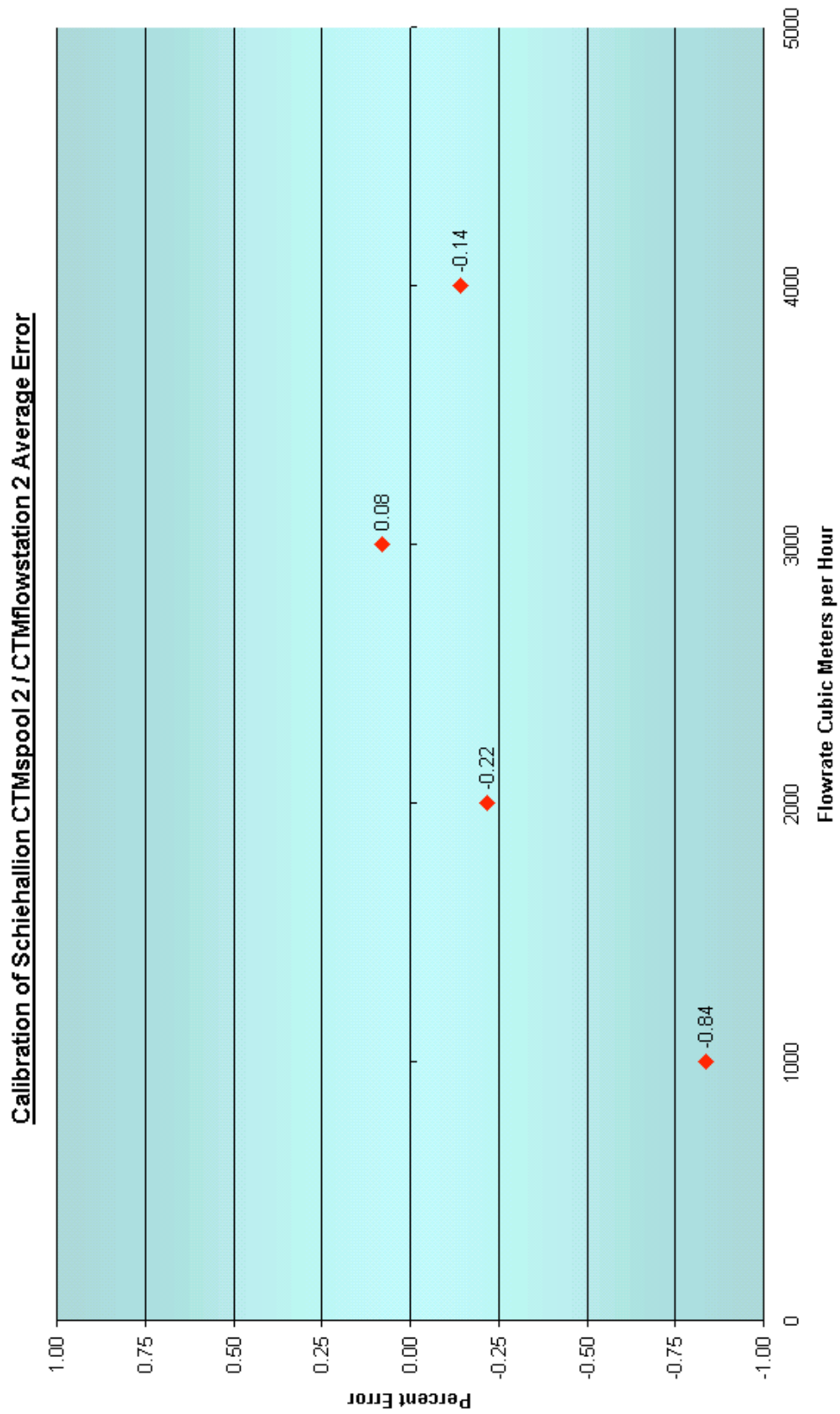
MCVS - Master Control & Verification System

OpCon - Operational Confidence

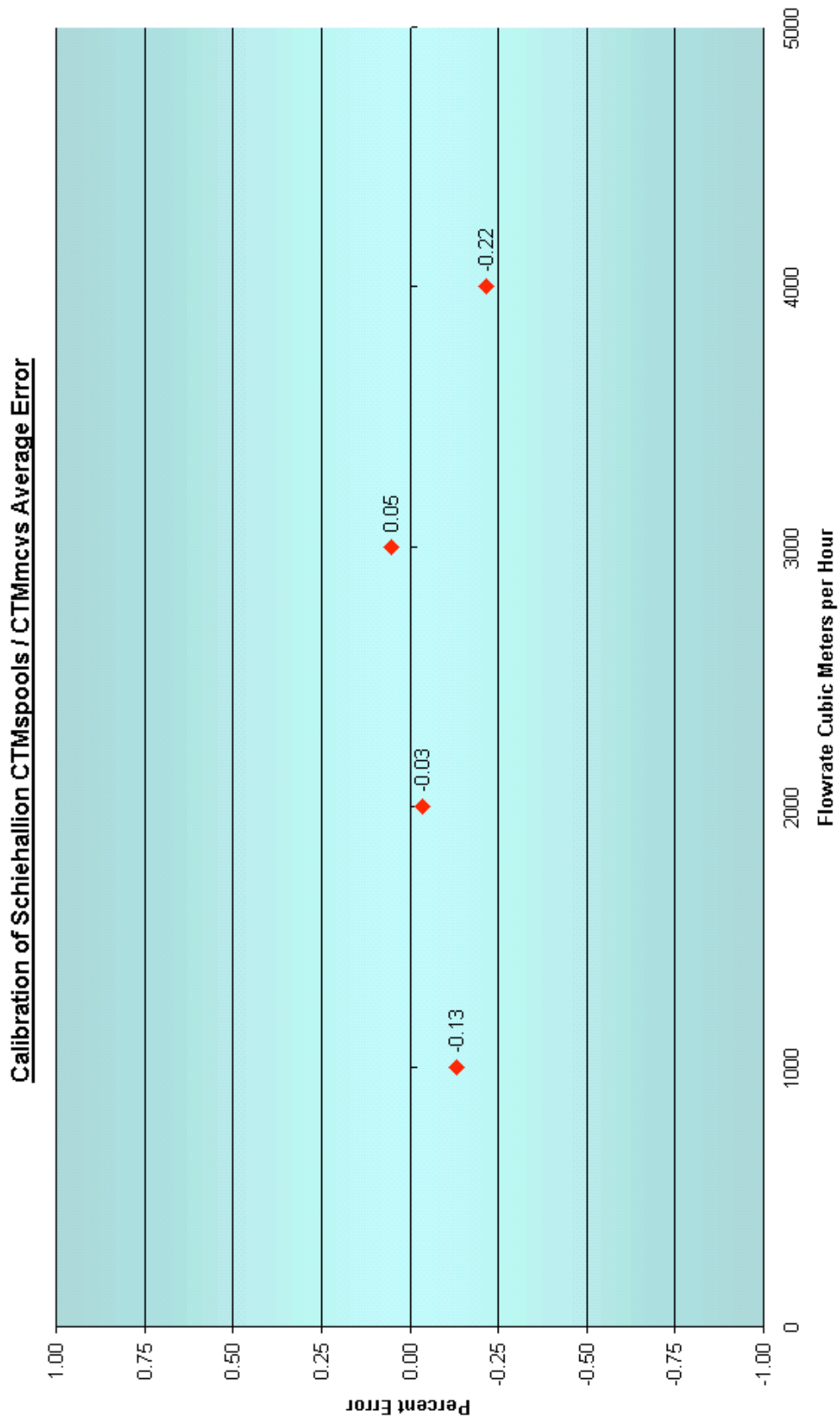
# 11. Appendix 1 - CTMflowstation(tm) 1 Calibration Average



## 12. Appendix 2 - CTMflowstation(tm) 2 Calibration Average



### 13. Appendix 3 - CTMmcvs(tm) Calibration Average



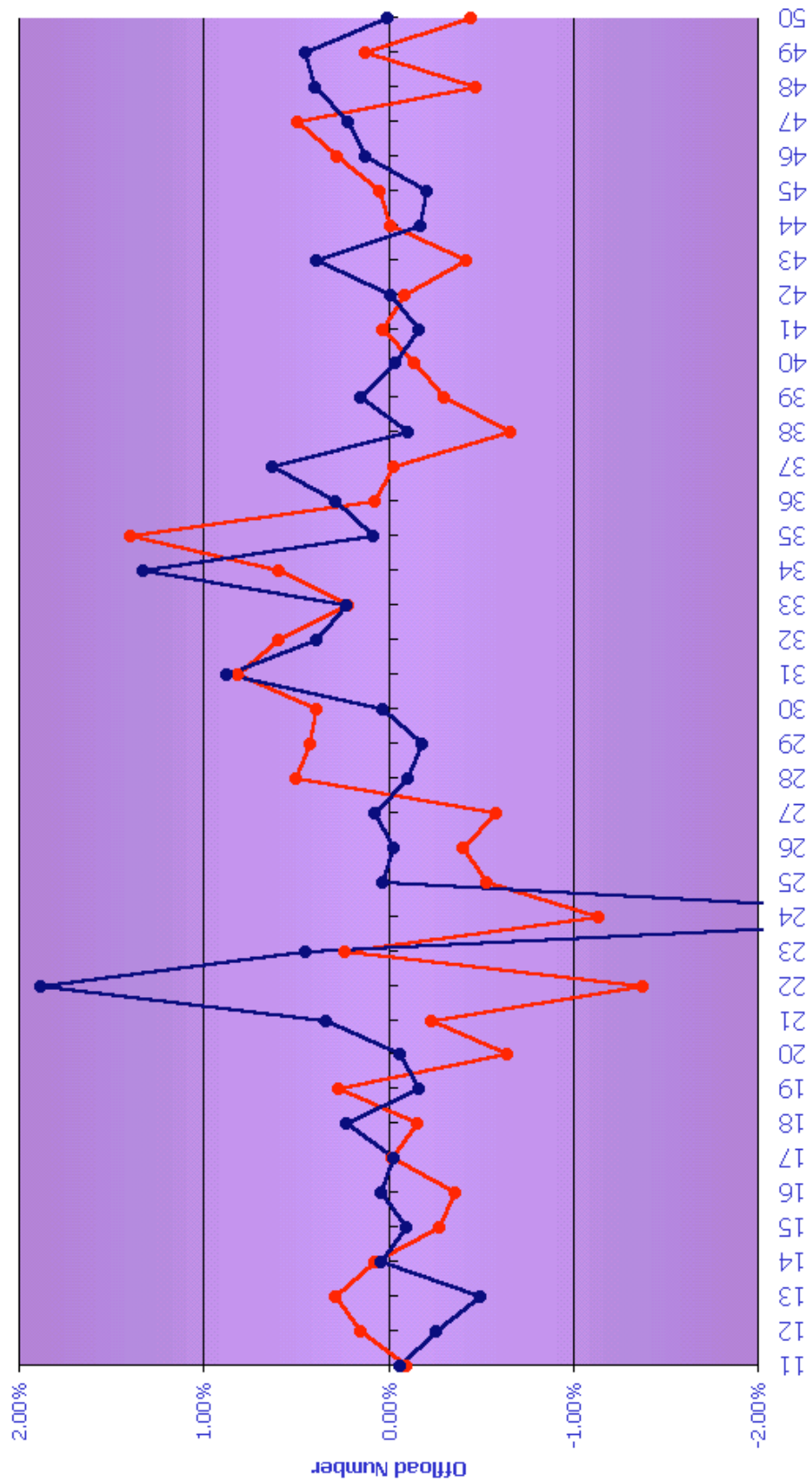
## 14. Appendix 4 - Accuracy Data for Offloads 11 through 50

Offload	FPSO Less SVT	Shuttle Less SVT	Shuttle Less FPSO
11	-0.10%	-0.06%	0.03%
12	0.15%	-0.26%	-0.41%
13	0.29%	-0.50%	-0.78%
14	0.07%	0.04%	-0.03%
15	-0.27%	-0.10%	0.18%
16	-0.36%	0.04%	0.41%
17	-0.02%	-0.03%	-0.01%
18	-0.16%	0.23%	0.39%
19	0.27%	-0.17%	-0.44%
20	-0.64%	-0.06%	0.58%
21	-0.24%	0.34%	0.58%
22	-1.38%	1.88%	3.31%
23	0.23%	0.45%	0.22%
24	-1.14%	-3.36%	-2.24%
25	-0.53%	0.03%	0.56%
26	-0.41%	-0.03%	0.37%
27	-0.58%	0.07%	0.66%
28	0.50%	-0.11%	-0.60%
29	0.42%	-0.19%	-0.61%
30	0.38%	0.03%	-0.35%
31	0.82%	0.87%	0.06%
32	0.60%	0.39%	-0.20%
33	0.22%	0.22%	0.00%
34	0.59%	1.32%	0.73%
35	1.39%	0.08%	-1.29%
36	0.07%	0.29%	0.21%
37	-0.03%	0.63%	0.66%
38	-0.66%	-0.11%	0.56%
39	-0.30%	0.15%	0.45%
40	-0.14%	-0.04%	0.11%
41	0.03%	-0.17%	-0.20%
42	-0.09%	-0.01%	0.07%
43	-0.43%	0.39%	0.82%
44	-0.01%	-0.18%	-0.16%
45	0.05%	-0.21%	-0.26%
46	0.28%	0.13%	-0.15%
47	0.49%	0.21%	-0.27%
48	-0.48%	0.39%	0.87%
49	0.13%	0.45%	0.32%
50	-0.45%	0.00%	0.45%
Average Offloads 11 to 50	-0.04%	0.08%	0.11%
Standard Deviation Offloads 11 to 50	0.51%	0.70%	0.79%

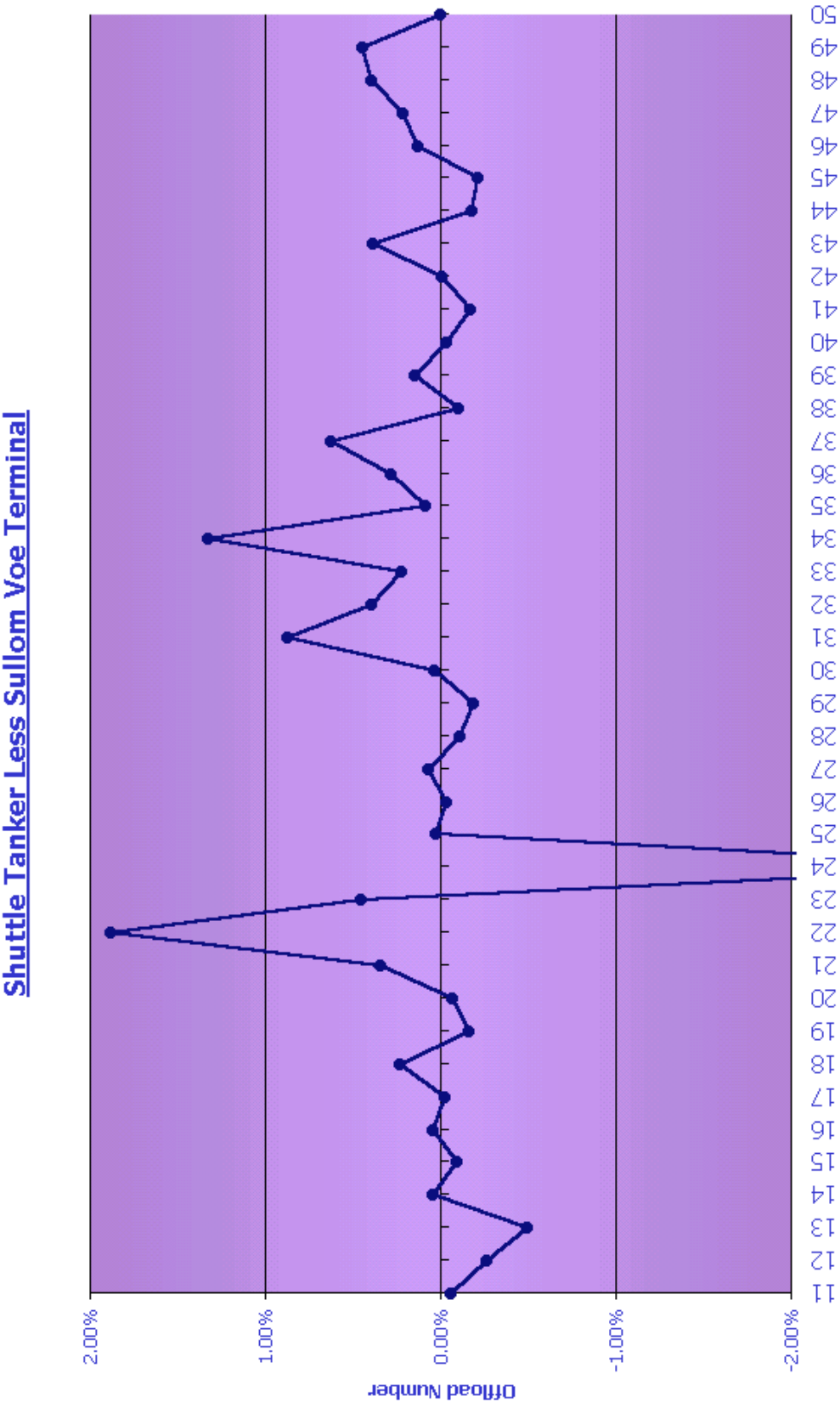
- Offload 22  Poor start to offload OpCon 67%
- Offload 24  Shutdown in middle of Offload OpCon 84%
- Offload 35  Slow pumping for 15 hours OpCon 62%

# 15. Appendix 5 - CTMsystem(tm) & Shuttle Tanker Offloads

Schiehallion CTMsystem & Shuttle Tanker Less Sullom Voe Terminal

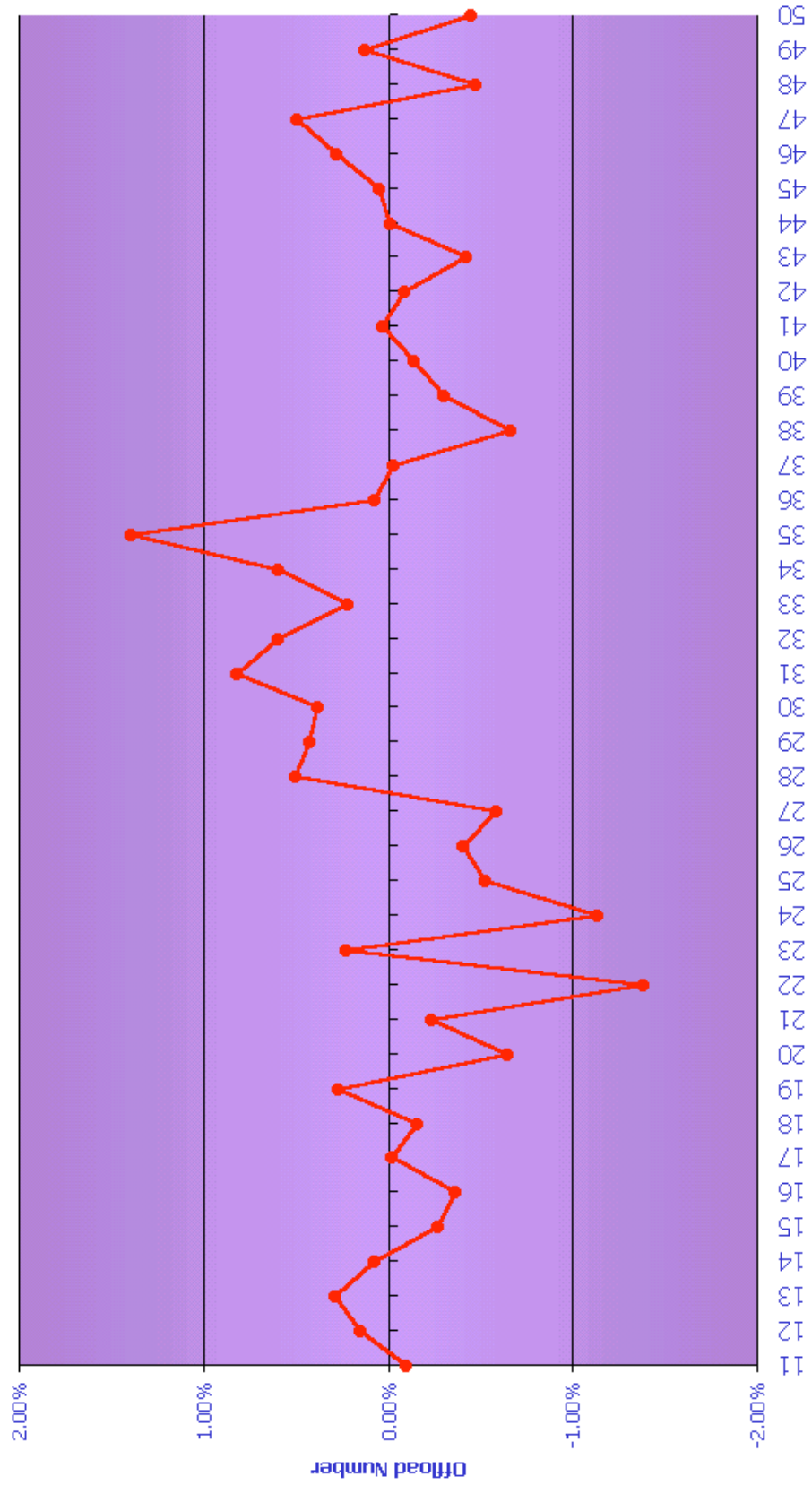


# 16. Appendix 6 - Shuttle Tanker Offloads

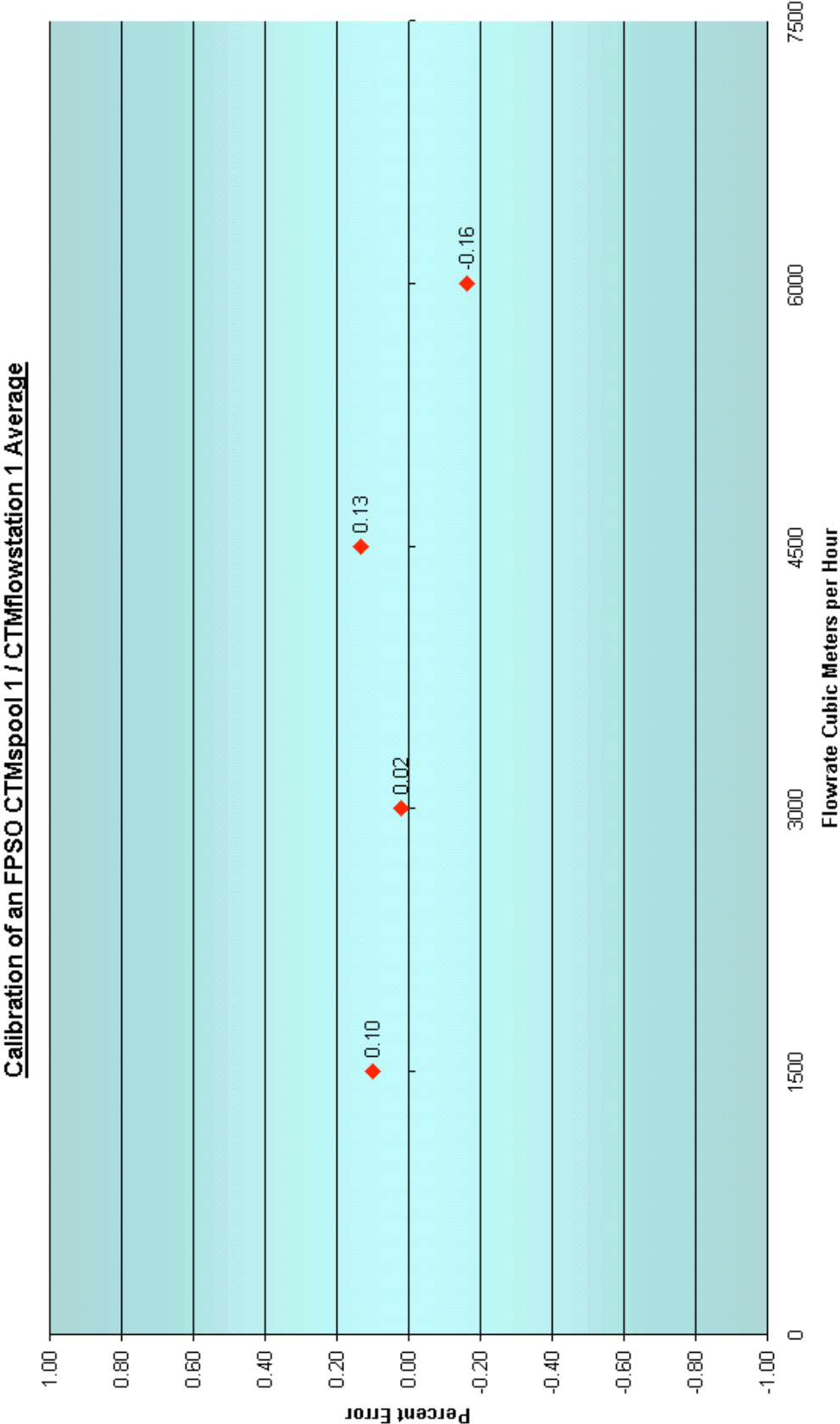


# 17.Appendix 7 - CTMsystem(tm) Offloads

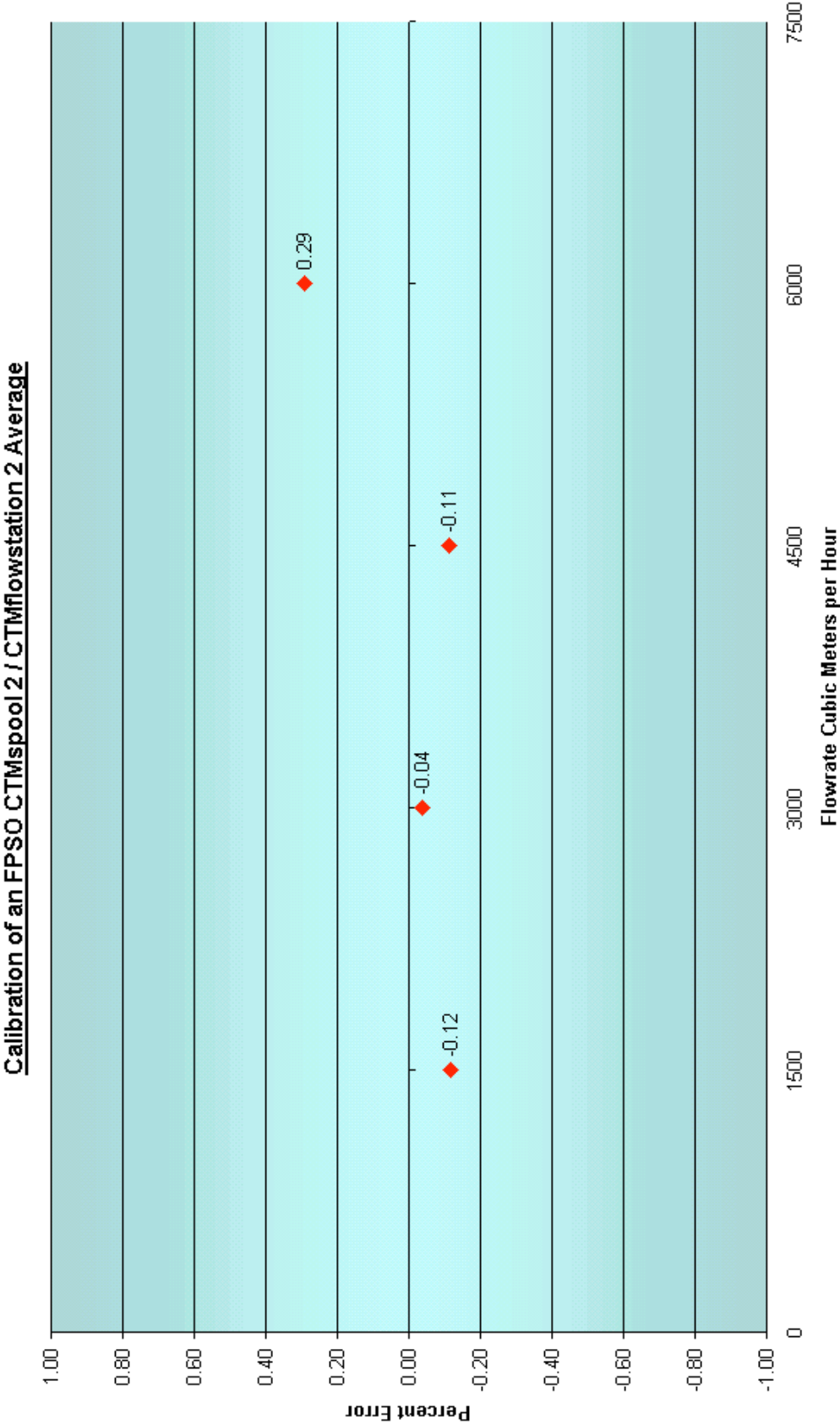
Schiehallion CTMsystem Less Sullom Voe Terminal



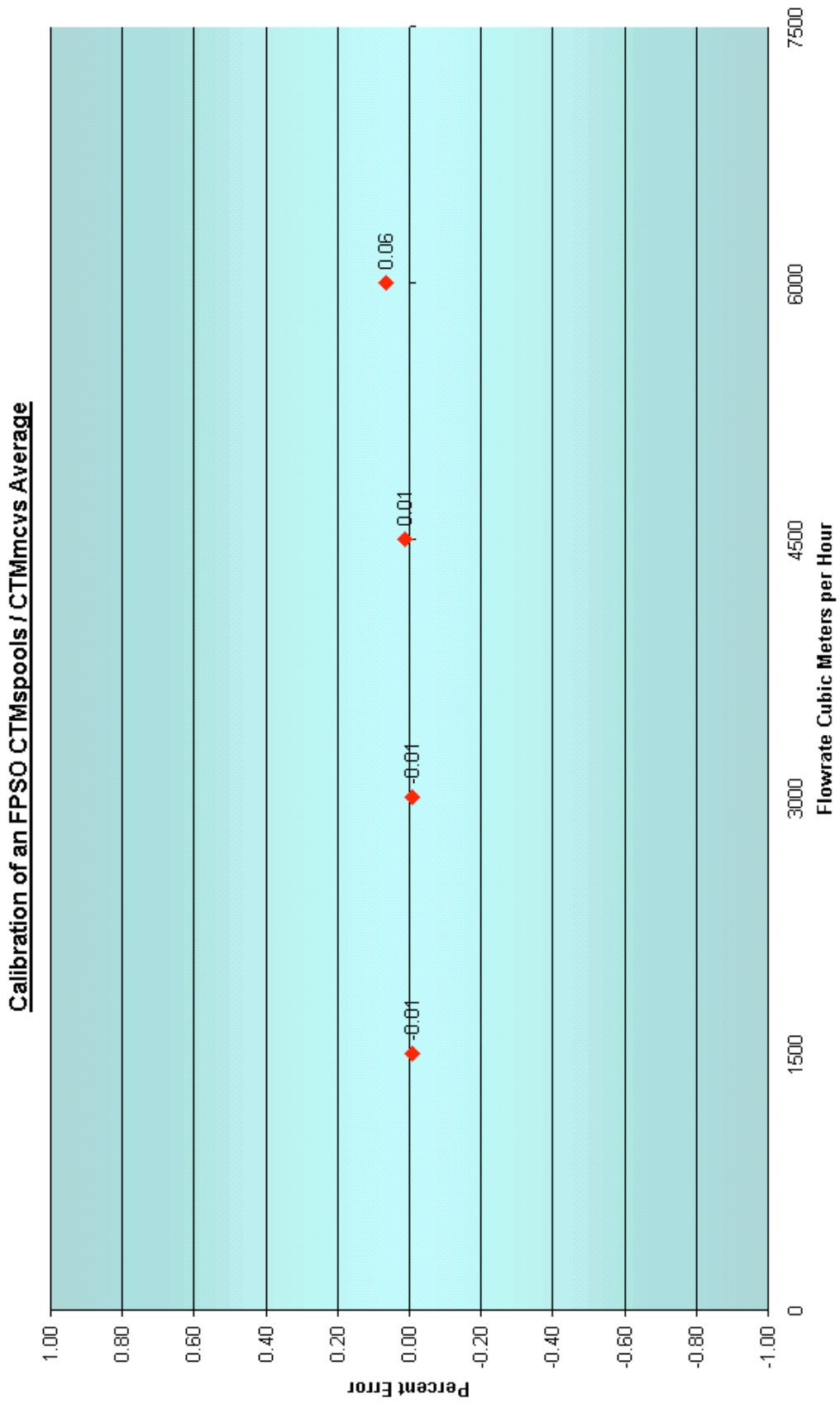
18.Appendix 8 - CTMflowstation(tm) 2 Calibration Average

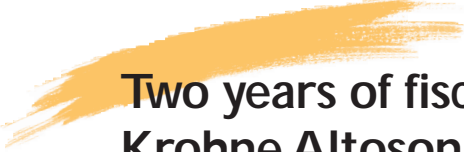


19. Appendix 9 - CTMflowstation(tm) 2 Calibration Average.



## 20. Appendix 10 - CTMmcvs(tm) Calibration Average





# Two years of fiscal performance by the liquid 5 path Krohne Altosonic-V ultrasonic meter at the Vigdis/Snorre Crossover oil measurement station

*Maron J. Dahlstrøm, Saga Petroleum ASA*

---

# Two years of fiscal performance

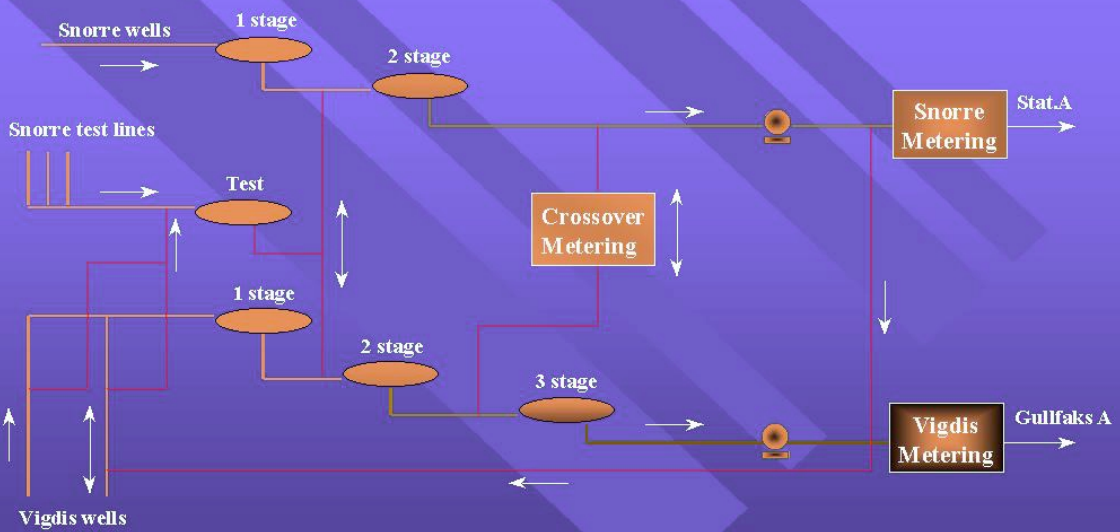
by the liquid 5 path Krohne Altosonic-V ultrasonic meter  
at the Vigdis/Snorre Crossover oil measurement station

NSFMW -99  
Paper 5  
25-28 October 1999  
Maron J. Dahlström



Saga Petroleum ASA

## Snorre/Vigdis oil process outline



Saga Petroleum ASA

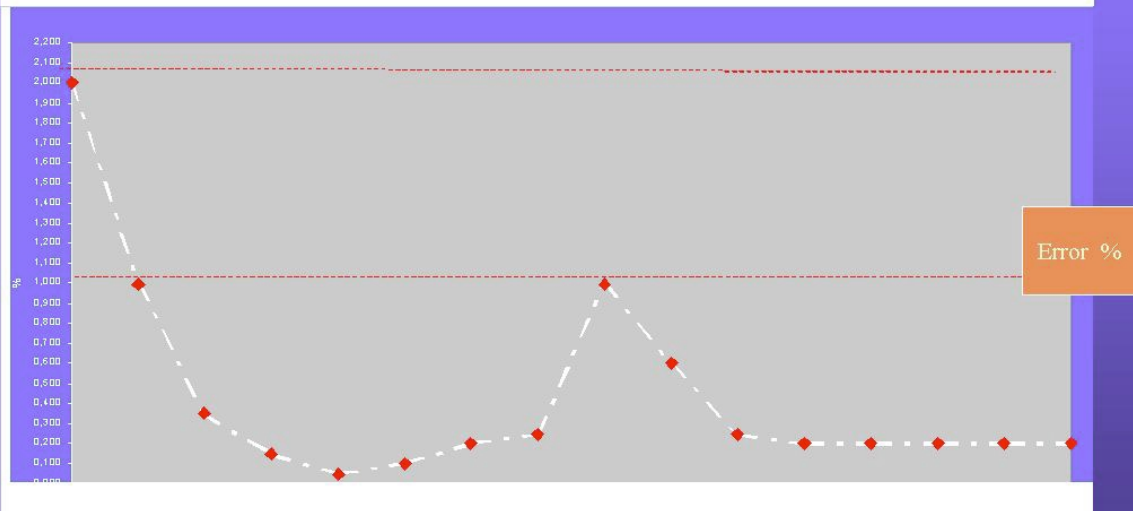
## Use liquid ultrasonic meter correctly ! <sup>3</sup>

- The ultrasonic liquid meter can output a flow modulated frequency similar to the turbine meter. But, the USM can not be calibrated the same way as a turbine meter : Long time and large volume is required to establish Meter Factor or K-factor. Used directly with a regular prover, hundreds of trials are required for stochastic methods. We now use 1 hour synchronized pulse count.
- In-situ calibration connection ; 4 " 90 degree T 10 D upstream of USM Master resulted in +/- 7% variation in reading, at constant flow. USM need natural profile.
- Master meter installed 10 D after 90 degree bend resulted in some swirl and unwanted offset in flow !

Saga Petroleum ASA

## Ultrasonic liquid meter basic nonlinearity <sup>4</sup>

**Never activate Reynolds number compensation, with Reynolds number calculated from entered faulty viscosity ! This mistake resulted in approximate 1 % offset. Note that Snorre/Vigdis Crossover operates in the almost constant effect region.**



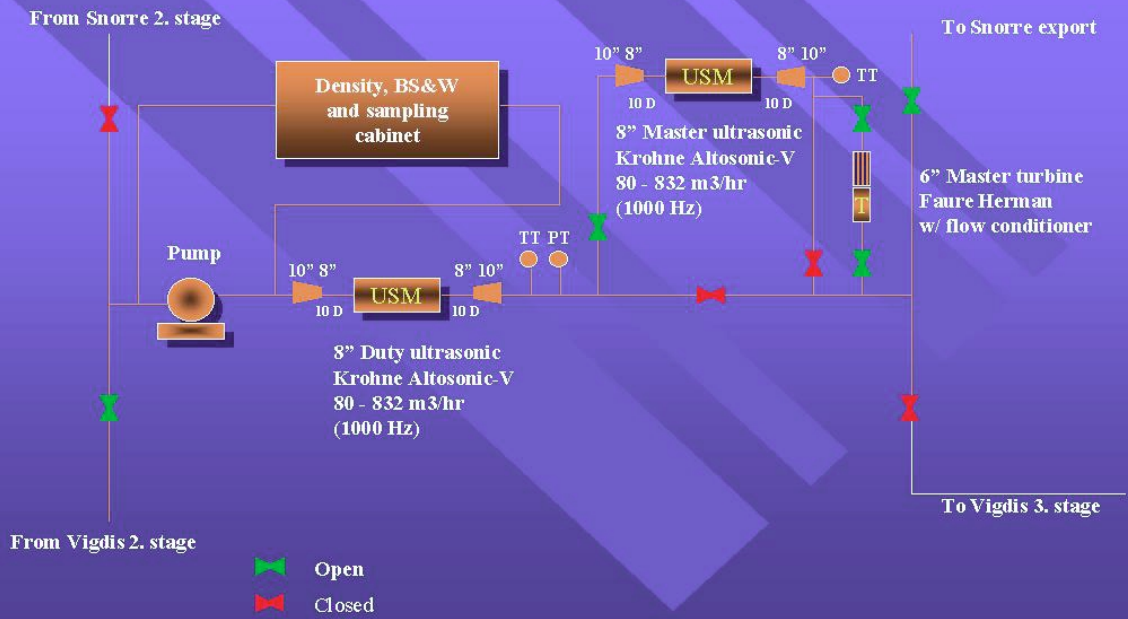
*Typical error compensation curve, with significant error compensation in lower Reynolds number region*

Saga Petroleum ASA

## Crossover Metering connections

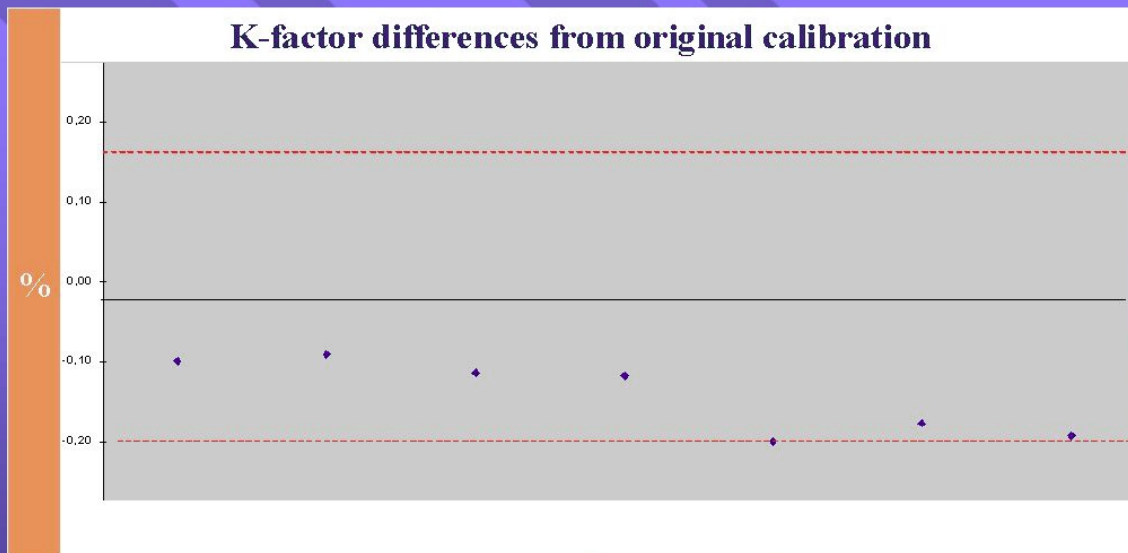
5

Modified with new connection for reference turbine downstream USM



Saga Petroleum ASA

## Duty ultrasonic meter calibrated with Master turbine meter 1998 <sup>6</sup>



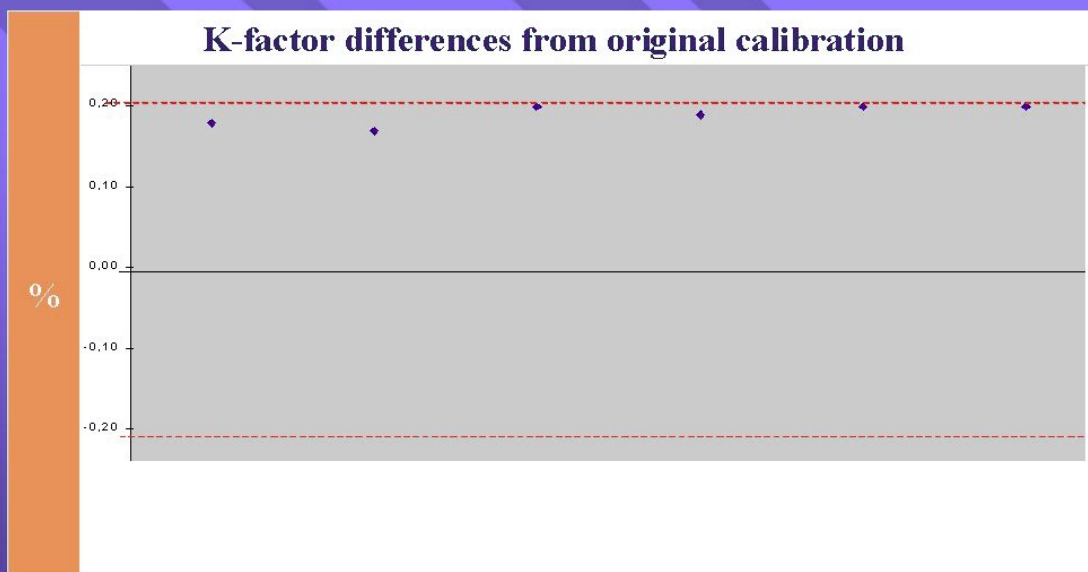
Flowrate approx 220 m<sup>3</sup>/hr; difference -0,12 % from original K-factor ( 4326.9 )

Flowrate approx 260 m<sup>3</sup>/hr; difference -0,19% from original K-factor

Hourly results repeats within 0,025 % band

Saga Petroleum ASA

### *Duty ultrasonic meter calibrated with Master ultrasonic meter 1998*



*Flowrate approx. 216 to 260 m<sup>3</sup>/hr; difference + 0,19 % from original  
K-factor ( 4326,9 )                      Hourly repeats inside 0.03 % band*

Saga Petroleum ASA

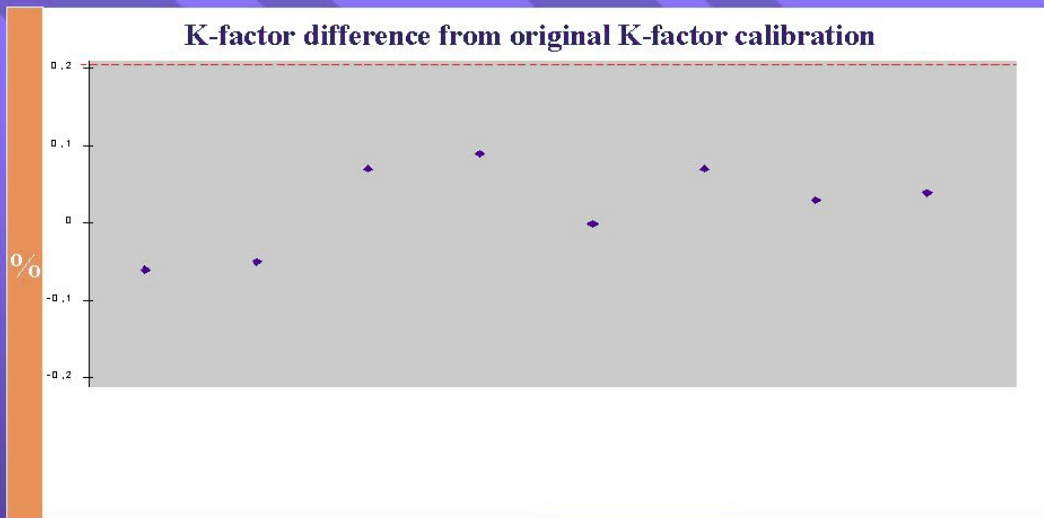
### *Improvements in 1998*

- The swirl measurement for the Master ultrasonic meter showed more swirl than expected. Krohne therefore activated a swirl effect compensation, based on the swirl factor measurement. This improved the uncertainty, however with some consequences for repeatability.
- Based on the NMI certificate, Krohne removed the meter material temperature compensation.
- Verification was carried out with Master turbine meter as in the previous tests.

Saga Petroleum ASA

***New results after swirl compensation 1998***  
***Duty ultrasonic calibrated with Master turbine meter***

9

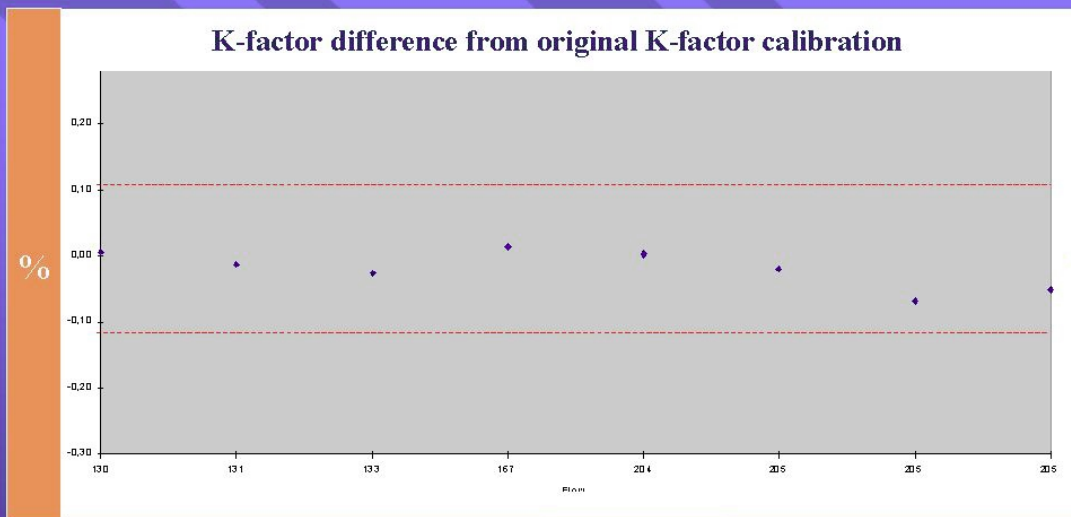


*Flowrate approx. 130 m<sup>3</sup>/hour; difference -0,06 %*  
*Flowrate approx. 270 m<sup>3</sup>/hour; difference +0,04 %*  
*Flowrate approx. 200 m<sup>3</sup>/hour; difference +0,09 %*

Saga Petroleum ASA

***New results after swirl compensation 1998***  
***Duty ultrasonic meter calibrated with Master ultrasonic meter***

10



*Flowrate approx. 130 m<sup>3</sup>/hour; difference -0,03 %*  
*Flowrate approx. 170 m<sup>3</sup>/hour; difference +0,01 %*  
*Flowrate approx. 200 m<sup>3</sup>/hour; difference -0,07 %*

Saga Petroleum ASA

## Master turbine meter verification 1998

11

- Examination of the possible bias for the Faure Herman helical rotor turbine meter (linearity  $\pm 0.01\%$ ) from change in flow profile, indicates that this shift normally will be less than 0.2 % .
- Since the K-factor curve for the master turbine meter with upstream section and flow conditioner, still can shift in a new location, the master turbine meter was therefore verified in-situ.

Saga Petroleum ASA

## Crossover Metering calibration 1998

12

Compact Prover downstream USM and with turbine meter afterwards



Saga Petroleum ASA

## *In-Situ calibration performed with Compact Prover & Master turbine meter 1998*

13

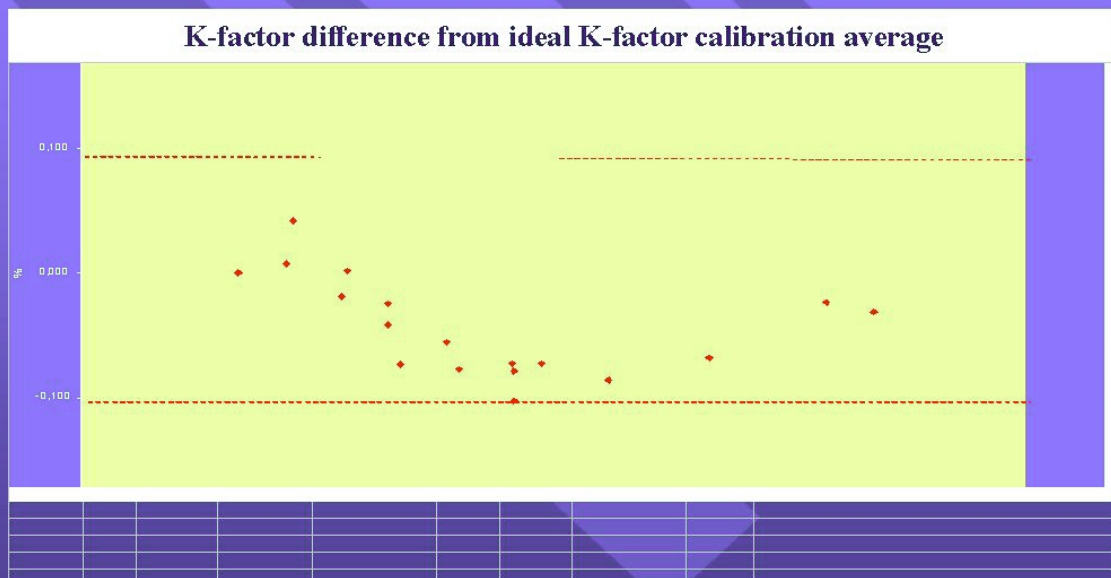
- Con-Tech Compact Prover with downstream master turbine meter temporarily installed with flexihoses between the master turbine meter run connections.
- Master and Duty ultrasonic meter was calibrated with the master turbine meter. Both ultrasonic meters showed a shift in K-factor curve. The master meter position for this purpose is therefore questioned.
- 1999 performance still show all results for the Duty meter inside 0,10 % from the calibration. All results for Duty meter K-factor is well inside 0,10 % from previous K-factor.

Saga Petroleum ASA

## *1999 performance*

14

### *Duty ultrasonic meter calibrated with Master ultrasonic meter*



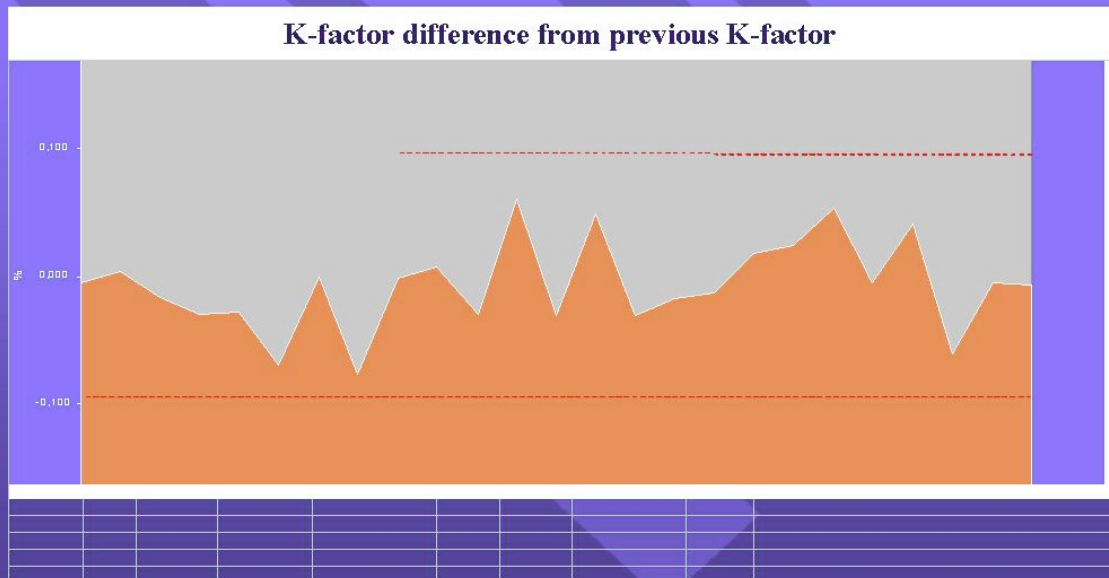
*All Duty USM K-factors inside +/- 0,10 from 1998 calibration average*

Saga Petroleum ASA

## Performance

15

*Duty ultrasonic meter calibrated with Master ultrasonic meter*



*All Duty USM K-factors inside +/- 0,10 from previous K-factor*

Saga Petroleum ASA

## *In-Situ calibration to be performed with Compact Prover & master turbine meter run 1999*

16

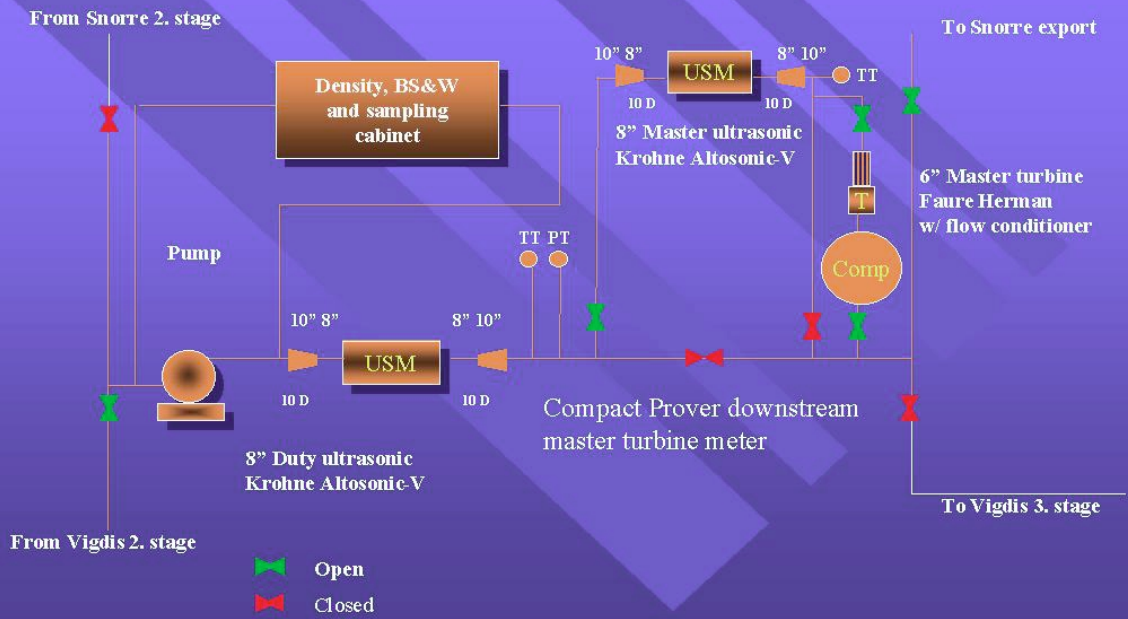
- A turbine meter run is calibrated at the Snorre export oil metering station and moved to the position downstream of the Master USM. This turbine will then be in-situ calibrated with the Con-Tech Compact Prover, temporarily installed between the master turbine meter and the return connection.
- Synchronized pulse count for the Master ultrasonic meter and the master turbine meter over one hour will be repeated for each flow point, while the average turbine meter K-factor is determined with the Compact Prover.

Saga Petroleum ASA

# Crossover Metering calibration 1999

17

Reference turbine downstream USM and with Compact Prover afterwards

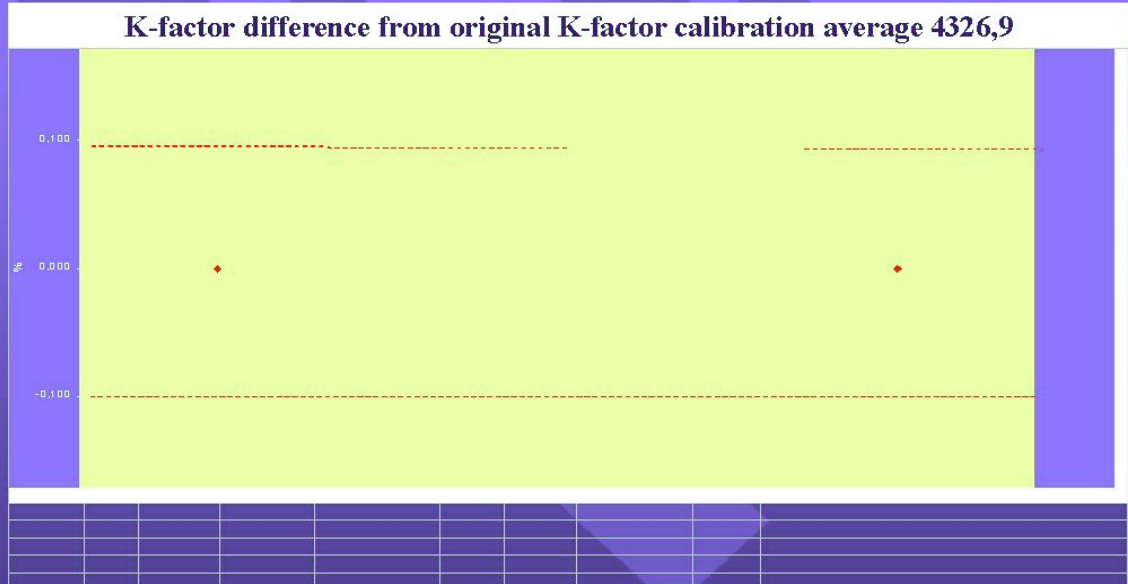


Saga Petroleum ASA

# 1999 Prover calibration

18

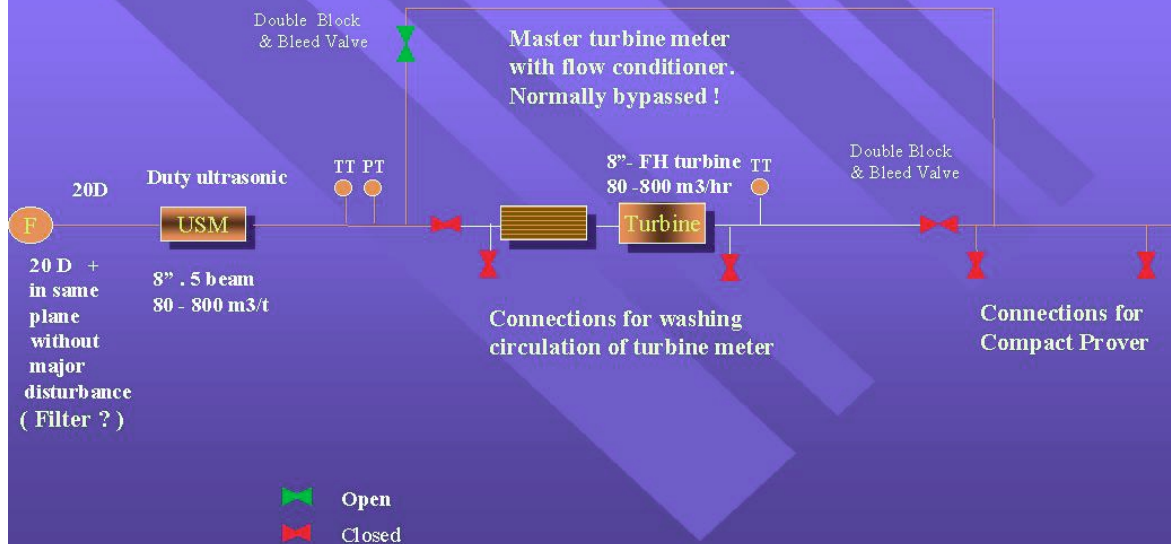
Master ultrasonic meter calibrated with master turbine meter



Comparison data available in November -99

Saga Petroleum ASA

## *Snorre B configuration : Fiscal measurement station for oil with USM*



Saga Petroleum ASA

## *Snorre B calibration philosophy*

- The Faure Herman master turbine meter will be calibrated in-situ with regular intervals ( initially every 2nd month with Compact Prover temporarily installed into the fixed piping arrangement. The master turbine meter K-factor curve is entered into the Snorre B calibration flowcomputer
- Duty ultrasonic meter is calibrated with the master turbine meter, while verified with the Compact Prover, in a synchronized count of pulses over longer time. Duty USM K-factor curve is entered into the Duty flowcomputer.

Saga Petroleum ASA

## *Snorre B calibration philosophy*

21

- In the operational period between Compact Prover calibration, the Duty USM meter factor will be verified with the turbine meter in a synchronized count of pulses.
- We are considering to use the Duty USM meter factor determination for Compact Prover calibration period alert only, since data indicates that the USM is more reliable than a turbine meter !

Saga Petroleum ASA



# Behaviour of Venturi meters in two-phase flows

*J.P. Couput\*, V. de Laharpe\*\*, P. Gajan\*\*\*, A. Strzelecki\*\*\**

*\*ELF-Exploration Production - France*

*\*\* Gaz de France*

*\*\*\* Office National d'Etudes et de Recherches Aérospatiales (ONERA)- France*

---

## ABSTRACT

Needs for accurate and reliable on line metering of two-phase flows (gas and/or liquids) are arising for fiscal and allocation reasons when subsea or topside installations are shared by several partners.

This paper describes the work carried out by ELF EXPLORATION PRODUCTION and GAZ DE FRANCE in collaboration with the ONERA research centre to assess and develop accurate methods applicable for gas metering with condensate ("wet gas").

After a review of allocation metering requirements and available techniques for flow rate measurements in high gas fraction conditions ( $GVF > 95\%$ ), this paper deals with the behaviour of Venturi flow meters in similar two-phase flows.

The applied methodology, which combines experimental laboratory testing in ONERA, numerical simulation and field evaluation is described. The preliminary results obtained on the Venturi meter in different two-phase flow configurations (annular, mist) are presented. The influence of some flow parameters (liquid content, flow pattern) on the Venturi behaviour is discussed.

## INTRODUCTION

In oil & gas production, there is a need to meter well and field productions for reservoir management but also for allocation or fiscal purposes. This has been classically performed using conventional meters with test or production separators.

For the last few years, operators and manufacturers have started research and development to come up with cost effective metering solutions using multiphase metering. One of the target was, in the early days, to develop multiphase meters to replace test separators in a large range of water cuts and gas volume fractions. Accuracy in the range of  $\pm 10\%$  for each phase (oil, gas and water) has been generally accepted by operators for such a service and there are now several examples of multiphase meters in operation, especially on some ELF developments in the Middle East and West Africa.

Where several owners are involved, multiphase meters with higher accuracy will be required: this will be the case of marginal fields developed through existing installations or in subsea applications where several joint ventures will share common pipelines for CAPEX reduction.

This paper describes some work carried out by ELF EXPLORATION PRODUCTION, GAZ DE FRANCE and ONERA to improve accuracy and reliability of metering systems usable on gas/condensate fields where well effluents are composed of gas mixed with liquid condensate or water.

In this first phase, the work has been focused on the use of Venturi meters in two-phase flows, because they are already used by operators for wet gas metering in third-party allocation and there are several designs already available for topside, subsea, high pressure and high temperature applications.

This paper covers our current field applications, the improvement requirements, the study methodology, the experimental and numerical results obtained so far and the future work.

## 1 METERING and ALLOCATION

### **a/Allocation requirements**

Due to economic reasons, more and more wells and fields are sharing a common processing platform or common gas transportation system. In that case, allocation metering systems have to be defined and implemented to measure gas and liquid productions with an acceptable accuracy. Based on these figures, allocation calculation will determine final sales products attributed to the different owners.

For allocation purposes, typical accuracy of 1% to 2% on the main stream component (gas or liquid hydrocarbons) quantities will be required. These figures are significantly higher than figures generally accepted for reservoir monitoring purposes which are in the 10% range.

### **b/Metering schemes for allocation**

Due to multiple ownerships, well or field metering can require independent inlet separators just for metering purposes.

Alternative solutions based on two-phase or three-phase flow measurements have already been implemented because the cost reduction is very significant compared to solutions with separation.

In some cases, they allow the platform design to be simplified and can avoid specific well head platforms to be installed.

The figure 1 gives as an example an ELF case in which gas wells connected to a mother platform are metered without separation before being commingled and processed with other streams. In this situation, the owners of these wells and of the other fields are different, thus accurate gas measurements are required for allocation.

Typical figures for such wells are condensate mass fraction of about 5% with a pressure of 60 bar a, and a temperature of 30°C.

### c/ Two phase-flow meters for allocation purposes

Standard multiphase meters have been designed to give a medium accuracy in a large range of flow regimes and gas volume fractions, but for the time being, they do not necessarily match our requirements for allocation purposes.

As there is no evidence that accurate multiphase flow meters covering the whole range of flow regimes and fractions can be available before a few years, we are first investigating the possibility of achieving accurate flow measurements in two-phase flows on some specific applications such as gas with low liquid content (wet gas).

As a first step, we have focused on Venturi meters because their performances for gas flow rate measurements are claimed to be in the +/-4% range for gas volume fractions higher than 95%, and also because such meters are already in use on some of ELF operational installations.

## 2.VENTURI FOR GAS CONDENSATE FLOW MEASUREMENTS

### a/ Flow regimes in wet gas applications

Practically, we handle "wet gas" applications in which the effluent is gas with an entrained liquid phase. The gas volume fraction GVF at line conditions is generally higher than 95%.

$$GVF = \frac{Q_{vg}}{Q_{vg} + Q_{vl}} * 100$$

In two-phase flow problems, flow regimes are described by classifying the most obvious types of interfacial distribution. This classification depends on the pipe orientation. As an example, these regimes are represented in figures 2 for horizontal flow.

The flow regime can be predicted in the pipe from flow patterns maps or numerical simulation tools. Liquid volume fraction in some wells does not exceed 1 or 2% and in this case the flow regimes vary from annular flow to dispersed flow.

Two-phase flows<sup>1,2</sup>, (figure 3) can be described using the Froude numbers  $Fr_g$  and  $Fr_l$ , defined below, as

$$Fr_g = \frac{U_g}{\sqrt{gD}} \sqrt{\frac{\rho_g}{\rho_l - \rho_g}} \quad \text{and} \quad Fr_l = \frac{U_l}{\sqrt{gD}} \sqrt{\frac{\rho_l}{\rho_l - \rho_g}}$$

where  $U_l$  and  $U_g$  are the superficial velocity of the liquid and gas phases.

### b/ Two-phase flow metering with differential pressure systems

For the measurement of two-phase flows by means of Venturi systems, the main approach is to define a correction factor depending on the flow characteristics in order to calculate the actual flow rate of gas and liquid in the pipe. These corrections use empirical correlations derived from orifice or Venturi measurements.

The mass flow ratio  $x$  is defined by :

$$x = \frac{Q_{mg}}{Q_{mg} + Q_{ml}}$$

where  $Q_{mg}$  and  $Q_{ml}$  are the mass flow rates of the gas phase and the liquid phase. If we suppose that  $\Delta P_t$  is the actual differential pressure measured on the flow meter with a two-phase flow, then the total mass flow rate  $Q_{mt}$  will be :

$$Q_{mt} = C_D \frac{\pi d^2}{4} \varepsilon \frac{1}{\sqrt{1 - \beta^4}} \sqrt{2\rho_t \Delta P_t} = Z \sqrt{2\rho_t \Delta P_t}$$

The apparent mass flow rate of gas and liquid will be :

$$Q_{mgs} = Z \sqrt{2\rho_g \Delta P_t}$$
$$Q_{mls} = Z \sqrt{2\rho_l \Delta P_t}$$

In fact, the actual mass flow rates of gas and liquid are :

$$Q_{mg} = Z \sqrt{2\rho_g \Delta P_g} = x \cdot Q_{mt}$$
$$Q_{ml} = Z \sqrt{2\rho_l \Delta P_l} = (1 - x) \cdot Q_{mt}$$

Thus, we can define the multipliers :

$$\Phi_g = \frac{Q_{mgs}}{Q_{mg}} = \sqrt{\frac{\Delta P_t}{\Delta P_g}} \text{ i.e. } Q_{mg} = \frac{Q_{mgs}}{\Phi_g}$$
$$\Phi_l = \frac{Q_{mls}}{Q_{ml}} = \sqrt{\frac{\Delta P_t}{\Delta P_l}} \text{ i.e. } Q_{ml} = \frac{Q_{mls}}{\Phi_l}$$

For an orifice plate in a horizontal pipe, Murdock obtained the following correlation :

$$\Phi_g = 1.26X + 1$$

where  $X$  is the Lockhart-Martinelli parameter defined by :

$$X = \frac{\Phi_g}{\Phi_l} = \frac{1 - x}{x} \sqrt{\frac{\rho_g}{\rho_l}}$$

Chisholm<sup>4</sup> gives another expression obtained from wet steam measurements with orifice :

$$\Phi_g^2 = 1 + 2.66X + X^2$$

More recently, De Leeuw<sup>2</sup> has developed a new expression derived from the analysis of data collected in a full-scale multiphase flow test facility with Venturi meters. In these tests, the pressure varied from 15 bar to 90 bar and the GVF from 90% to 100%. In these conditions, the Lockhart-Martinelli parameter varies from 0 to 0.3. He observed that the correlation depends on the Froude number  $Fr_g$  and he proposed the following expression for the multiplier parameter, derived from the Chisholm expression.

$$\Phi_g^2 = 1 + C \cdot X + X^2$$

$$\text{With : } C = \left( \frac{\rho_l}{\rho_g} \right)^n + \left( \frac{\rho_g}{\rho_l} \right)^n$$

In this expression :

$$n = 0.41 \text{ for Froude number between } 0.5 \text{ to } 1.5$$

$$n = 0.606 \cdot \left( 1 - e^{-0.746 Fr_g} \right) \text{ for Froude number above } 1.5$$

### 3. STUDY METHODOLOGY

Though the flow regimes encountered in industrial application are well defined, the flow characteristics (liquid phase distribution, droplet size, liquid film thickness) are not easily available and we do not know in detail their influence on the meters (errors) and on the correlations.

An overall approach based on experiments and numerical simulation has been developed using ONERA facilities. This was organised in three steps :

- Low pressure investigations (experiments and simulation)
- Extrapolation to field conditions by numerical simulation
- Validation of simulation results through tests on industrial site or high pressure loops.

The first step is aimed at having a more refined understanding of the physical phenomena which implies a precise measurement of the flow characteristics. In parallel, these experimental results allow validation of the flow simulation approach.

In the second step, the numerical approach allows the prediction of the behaviour of the meter submitted to the actual flow conditions.

In the last step, experiments performed at high pressure conditions will validate the results obtained during the second step.

In the following section we present the experimental and numerical tools used during the study.

## a/ Experimental program

### ONERA wet gas test facility

The wet gas tests are carried out at low pressure on the ONERA experimental flow loop (figure 4). The gas flow (air) is generated by means of high pressure tanks. The gas flow rate is controlled by a sonic nozzle located upstream the test section in a range of 0 to 650 Sm<sup>3</sup>/h. The mass flow rate of liquid (water) can be varied from 0 to 250 l/h. This loop can be used from atmospheric pressure to 5 bar.

The flow loop is composed of :

- an horizontal section (25 pipe diameters long ( $D = 100$  mm)),
- a flow conditioner,
- a liquid injector which can produce different types of two-phase flows,
- a test section where the device under test (Venturi meter or other systems) is located
- a separator to recover the liquid.

The test section can be placed following three different pipe work orientations, i.e. horizontal, vertical upwards or vertical downwards.

### Tested Venturi under test

A Venturi meter with a beta ratio equal to 0.6 has been tested. The upstream internal diameter is equal to 138 mm and the throat diameter to 101.1 mm. Two models have been designed, one in metal for pressure measurements, and the other in perpeX for flow visualization or optical measurements.

### Test conditions

The results presented in this paper are obtained for two pressure values (1 bar and 1.5 bar) and gas flow rates between 350 m<sup>3</sup>/h and 630 m<sup>3</sup>/h. In these conditions the gas Froude number varies from 0.442 to 0.825. The liquid flow rate ranges from 0. to 250 l/h.

## b/ Numerical simulation

### Computational code

The calculations are performed with a code developed at ONERA in order to predict flow phenomenon in combustion chambers. It uses an *Eulerian-Lagrangian* approach because this permits an easy introduction of various physical models for the liquid phase behaviour. The method refers to Eulerian gas phase modelling, and *Lagrangian* liquid phase modelling. Details of the numerical technics can be found in Bissières et al<sup>5</sup>.

### Computational grid and flow conditions

These flow calculations are performed on a Venturi flow meter with a 2D body-fitted grid. The grid contains 153 meshes in the longitudinal direction and 31 in the transverse one (figure 5).

At the inlet of this domain, we consider that the gas phase is composed with air at ambient pressure and temperature. The inlet velocity profile is uniform with a bulk velocity equal to 25 m/s. The turbulence level is set to 5% and the length scale 1 to 3 mm. The liquid phase is simulated by water. Two values of the mass flow ratio of gas are considered (91% and 66%). The distribution of the liquid flow rate along the inlet pipe radius is set constant.

Three droplet sizes are considered successively (10  $\mu$ m, 20  $\mu$ m, 100  $\mu$ m).

## 4. SUMMARY OF RESULTS

All the results obtained during this study are plotted in figure 6 in the form of  $\Phi_g$  distribution versus the Lockhart Martinelli parameter. They are compared to the Murdock and De Leeuw correlation. In the latter, the variation of the Froude number taken into account in the experiments implies a unique curve correlation ( $0.5 < Fr_g < 1.5$  which imposes a constant value of  $n$  in the De Leeuw correlation). Note that the Chisholm and Murdock correlations are equivalent.

### a/ Experimental results

Globally we can note that all the experimental results are located between the Murdock and De Leeuw correlations. We also observe that when the air flow rate increases, the result tends to the De Leeuw prediction.

When we look at the results obtained at atmospheric pressure for which the Froude number varies from 0.442 to 0.825, we observe that the slope of the correction curve increases with the gas Froude number. This tendency has been already noticed by De Leeuw<sup>2</sup>.

Nevertheless, if we compare results obtained at two different pressures, this tendency is not verified. This discrepancy can be explained by a flow regime modification obtained during the tests. As a matter of fact, the first flow visualizations show that when the air flow rate increases, the number of droplets increases what means that the flow tends to a dispersed flow regime.

This influence of the flow regime can also be deduced from the De Leeuw results from which we can note that the correction diminishes with the Froude number and that, in parallel, the flow changes from annular dispersed regime to stratified regime.

This explanation will be verified by a characterization of the two-phase flow.

## b/ Simulation results

In figure 7, the droplets pathes are plotted for the three droplet sizes and for a x value equal to 91%.

We observe that, the larger their diameter is, the less they follow the gas flow. This phenomenon is due to the variation of the relaxation time of the droplets with respect to their diameters. In particular we note an increase of the number of wall impacts. Nevertheless, the results obtained with the 100  $\mu\text{m}$  droplets must be analysed carefully. As a matter of fact, the interaction taken into account between the wall and the droplets is, for this work, simplified.

Though, in this simulation, the larger droplets, which do not follow the gas flow, impact the wall on the converging parts of the Venturi and rebound against it like a ball. This explains why, in figure 7, all the particules are located in the centre of the pipe downstream the flow meter. In the real world, these droplets would form a liquid film, which would be transported downstream and, certainly, would be disintegrated downstream the throat. These phenomena must be studied in more details in the future.

The pressure distribution on the wall is plotted in figure 8. The influence of the mass flow rate ratio and of the droplet size is enhanced on this figure. For the smaller droplet sizes with a mass flow ratio of gas x equal to 66%, a large effect is obtained. In this case, the droplets, which are small enough to follow the gas flow particules fall in a separate zone that appears in this flow configuration downstream the Venturi.

Based on the pressure fields, it is possible to calculate the factor of correction used to take into account the influence of the liquid phase on the measured differential pressure. These results can be compared with experimental correlation obtained in the present study or published in the literature (figure 6).

We can note that, for the smallest droplets, the corrections obtained are well above the De Leeuw correlation and that for the highest ones, the correction is close to those measured in our experiment.

In order to explain this tendency, we have plotted, in figure 6, a new correlation that only takes into account the variation of density of the fluid due to the presence of liquid. As a matter of fact, if we consider that the droplets follow the air flow with no slip, we can calculate an equivalent density  $\rho_t$  from a momentum conservation point of view . If we consider that the slip velocity ratio between the two phases is equal to 1, the equivalent density can be calculated from the following expression :

$$\rho_t = \frac{\rho_g}{x + (1 - x) \frac{\rho_g}{\rho_l}}$$

In the case of water droplets in air flow at atmospheric pressure this expression can be reduced to :

$$\rho_t = \frac{\rho_g}{x}$$

From the general formulation given in section 2b), we obtain the following equation for the correlation parameter plotted in figure 6 (Equivalent density correction):

For the smaller droplets which verified this hypothesis, the flow calculations are in a good agreement to this law. For bigger droplets, slip and wall interaction phenomena appear and this correction is no longer verified and numerical results tend to the classical laws. It is interesting to note that two-phase flow characterizations performed with the same type of injector than those used in our experiments give a mean droplet size around 100  $\mu\text{m}$ .

$$\Phi_g = \sqrt{1 + X \sqrt{\frac{\rho_l}{\rho_g}}}$$

## 5. CONCLUSIONS AND FUTURE WORK

The first results we have obtained are in some cases in accordance with published results. Experimental results and numerical simulation demonstrate that correlation are to some extent sensitive to Froude numbers, to changes in flow regimes (from dispersed to annular dispersed) and to droplet size effects. They indicate that there is no reliable correlation to correct Venturi measurements in wet gas flows with a good accuracy.

For the time being Venturi meters can obviously be used for allocation purposes, but they will still require frequent calibration using test separator until a robust correlation is proposed and accepted.

The work in progress and the methodology in use (experiments and simulation) will allow to quantify effects of fluid composition and flow morphology on wet gas measurements using Venturi.

We expect to come up in the next future with additional information on magnitude of errors due to different parameters and with improved correlation or guidelines for choosing the best correlation to match the allocation requirements.

Wet gas measurements for allocation purposes really corresponds to a common need from different users and manufacturers. This has been clearly understood by International Standardisation Organisation and a specific Sub-Committee SC3 - Upstream Area has recently be created in ISO TC 193 - Natural gas to address questions like upstream measurements (wet gas or raw gas for instance) and allocation procedures.

## REFERENCES

- 1 DeLeeuw H. : Wet gas flow measurement by means of a Venturi and a tracer technique, *North sea Flow measurement Workshop, 1994*
- 2 DeLeeuw H. : Venturi meter performances in wet gas flow, *B.H.R. Group 1997 multiphase*, pp.. 567-582, 1997
- 3 Murdock J.W. : Two-phase flow measurements with orifices, *Journal of basic engineering, Trans. of ASME*, pp. 567-582, 1962.
- 4 Chisholm D. : Two-phase flow through sharp edged orifices, *Journal of Mechanic Engineering Sciences*, vol. 19, N°3, pp. 128-130, 1977.
- 5 Bissieres D., Couput J.P., Estivalezes J.L., Gajan P., Lavergne G., Strzelecki A., Numerical investigation of wet gas in a Venturi meter, *Flomeko'98*, Lund, 19986
- 6 Mottram R.C., Owen I., Turner J.T. : Wet steam/wet gas flow measurement, *Flomic report N°13*, 1991.

## ACKNOWLEDGEMENTS

The authors wish to thank ELF PETROLAND which has helped in the work presented herein.

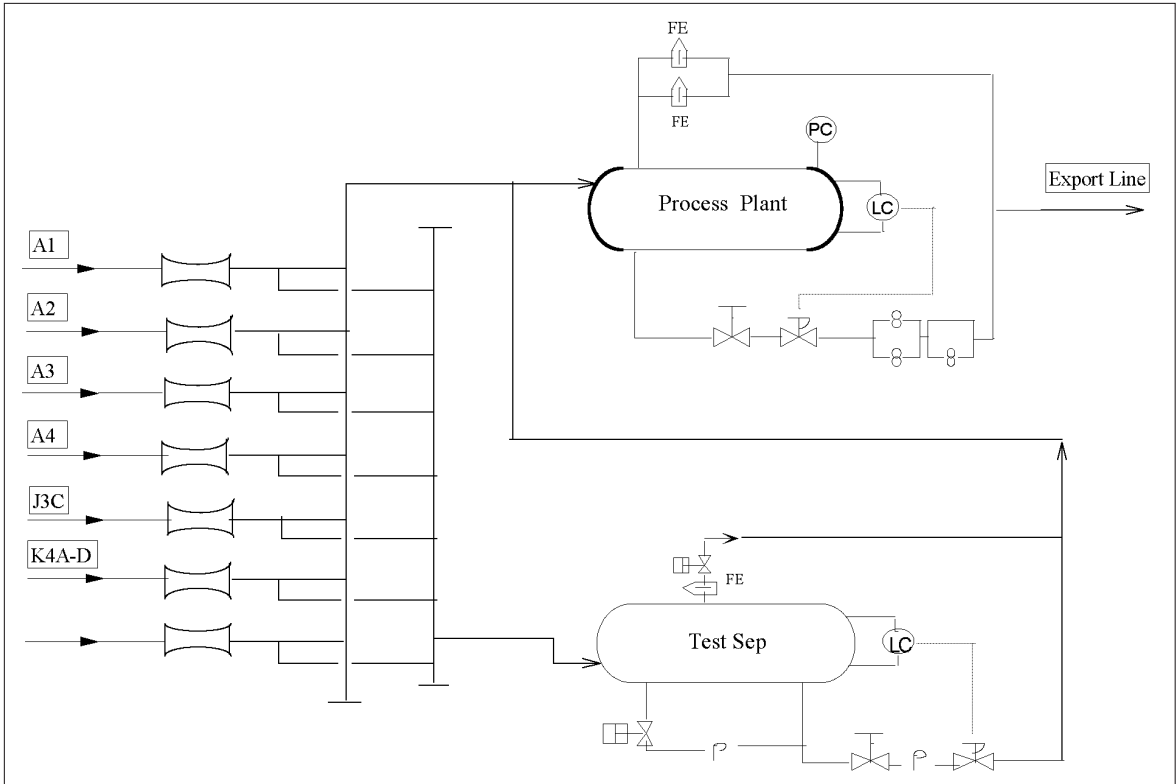


Figure 1 : Metering scheme

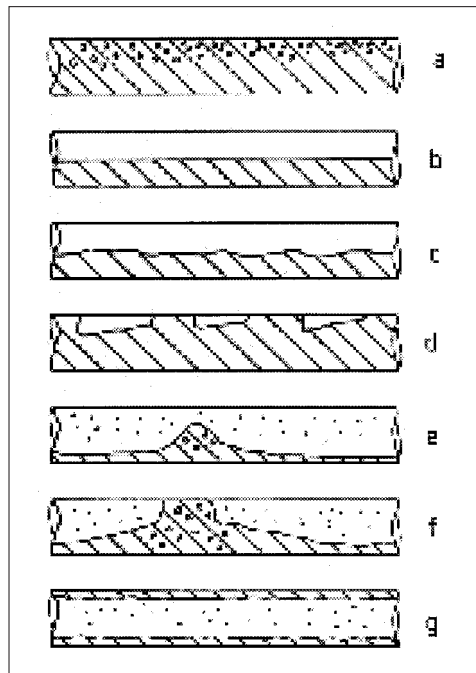


Figure 2 : Gas-liquid flow regimes in horizontal ( a : bubbly, b : stratified, c : wavy, d : plug, e : semi-plug, f : slug, g : annular )

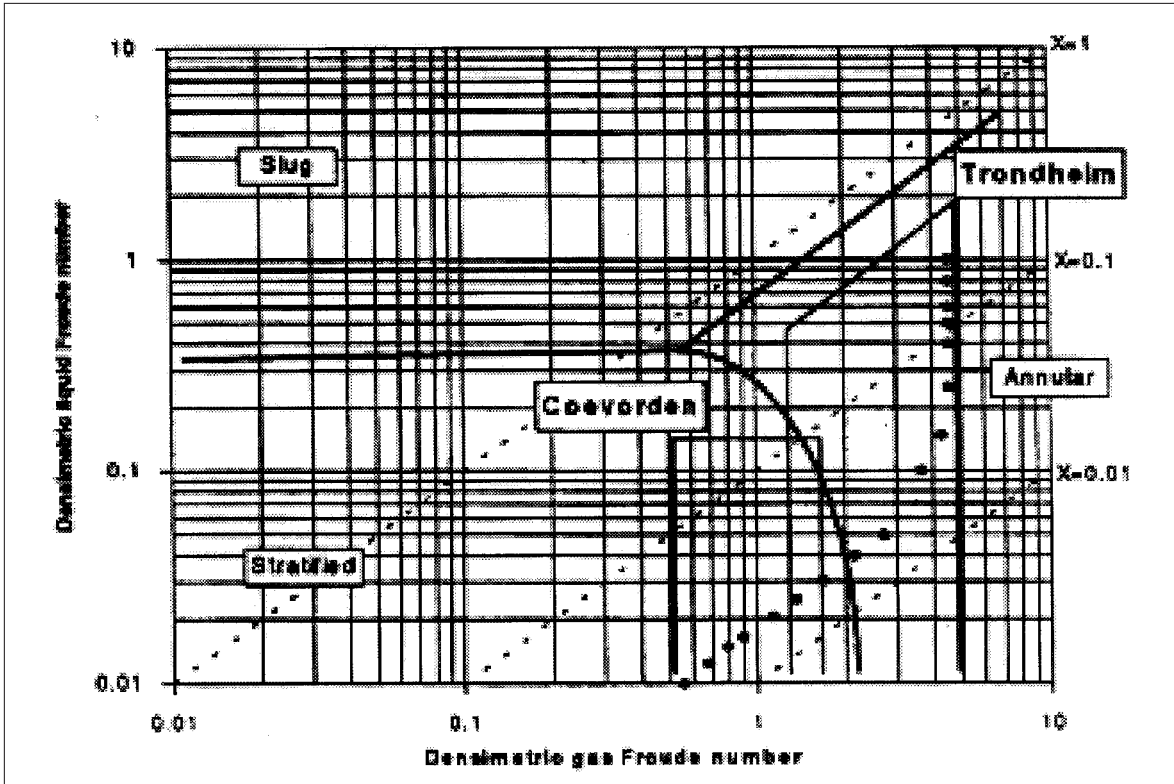


Figure 3 : Flow map obtained by De Leeuw\_

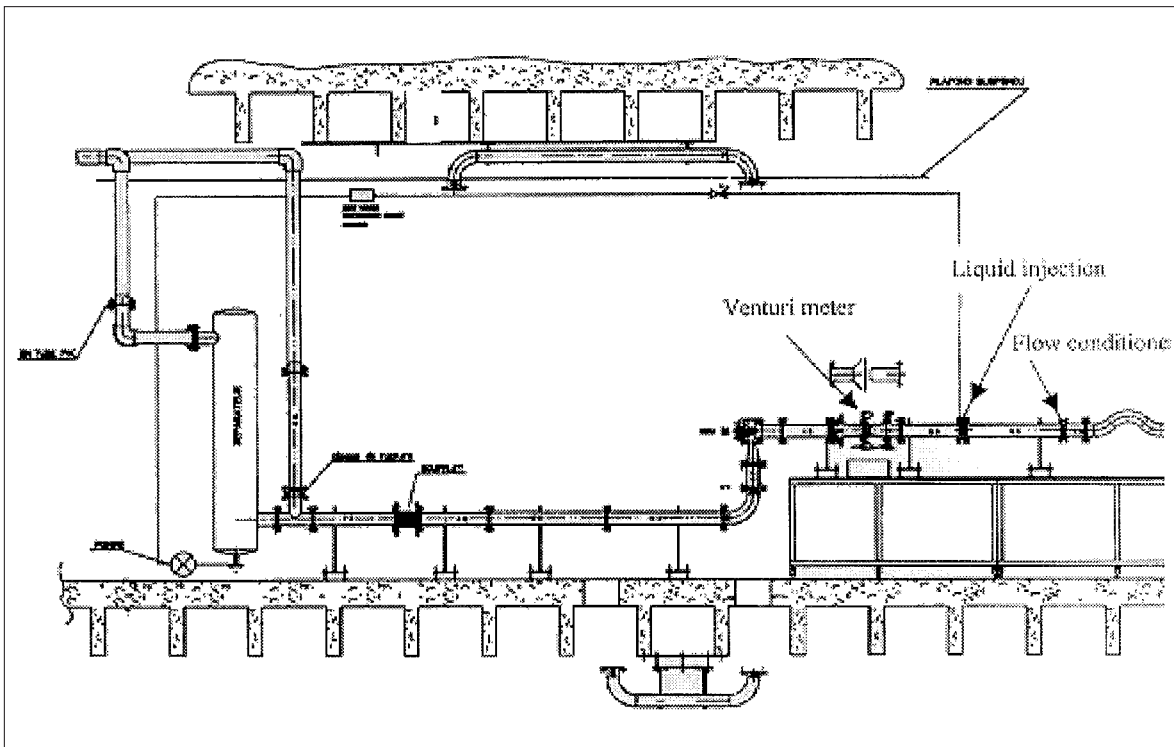


Figure 4 : Experimental test set-up

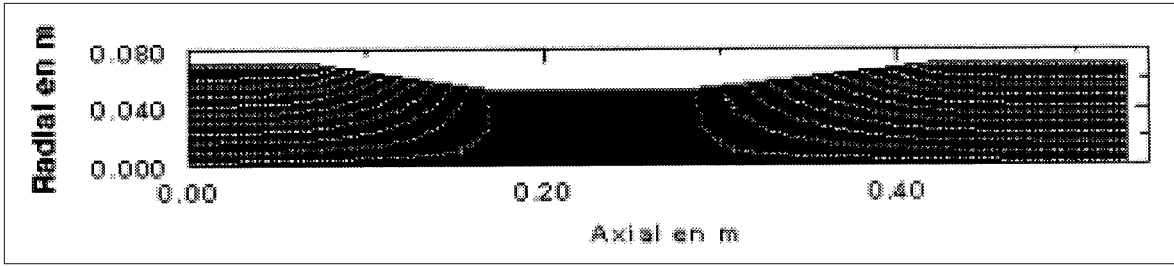


Figure 5 : Venturi mesh

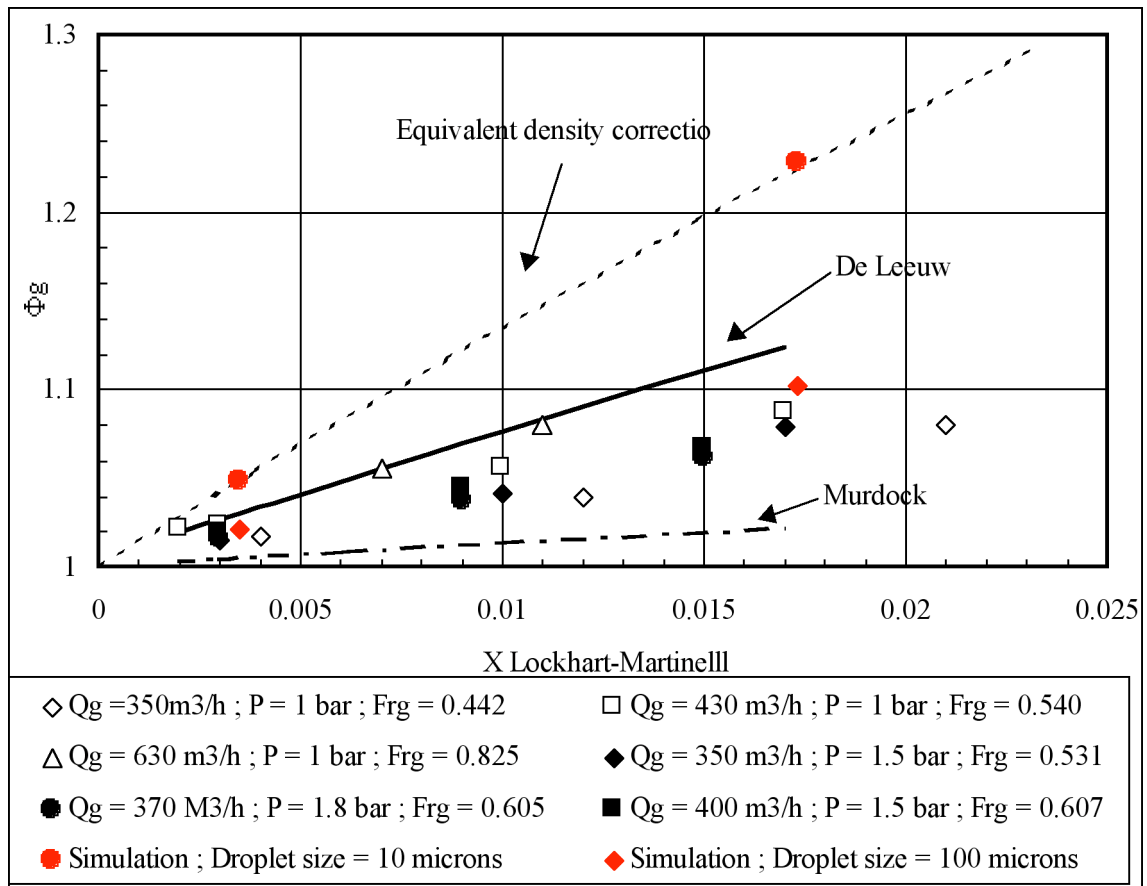


Figure 6 : Correlation parameter versus Lockhart Martinelli coefficient

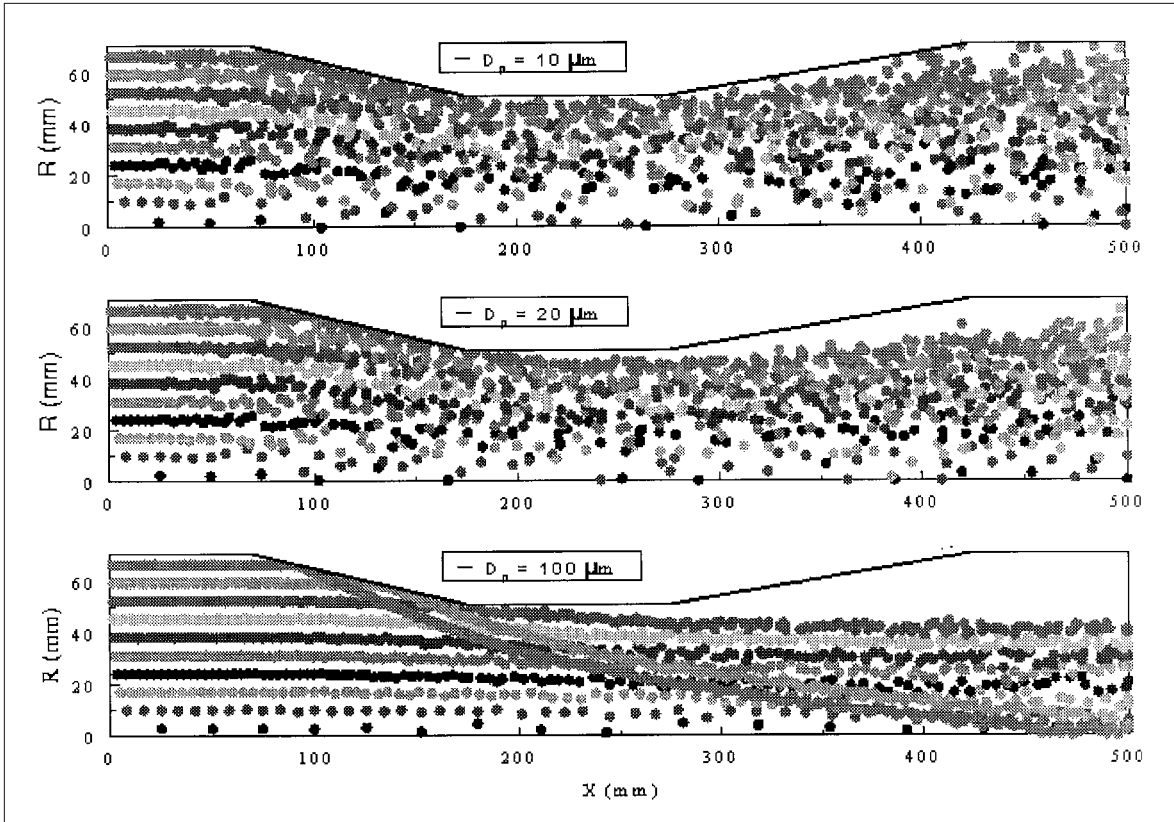


Figure 7 : Droplet paths for  $x = 91 \%$

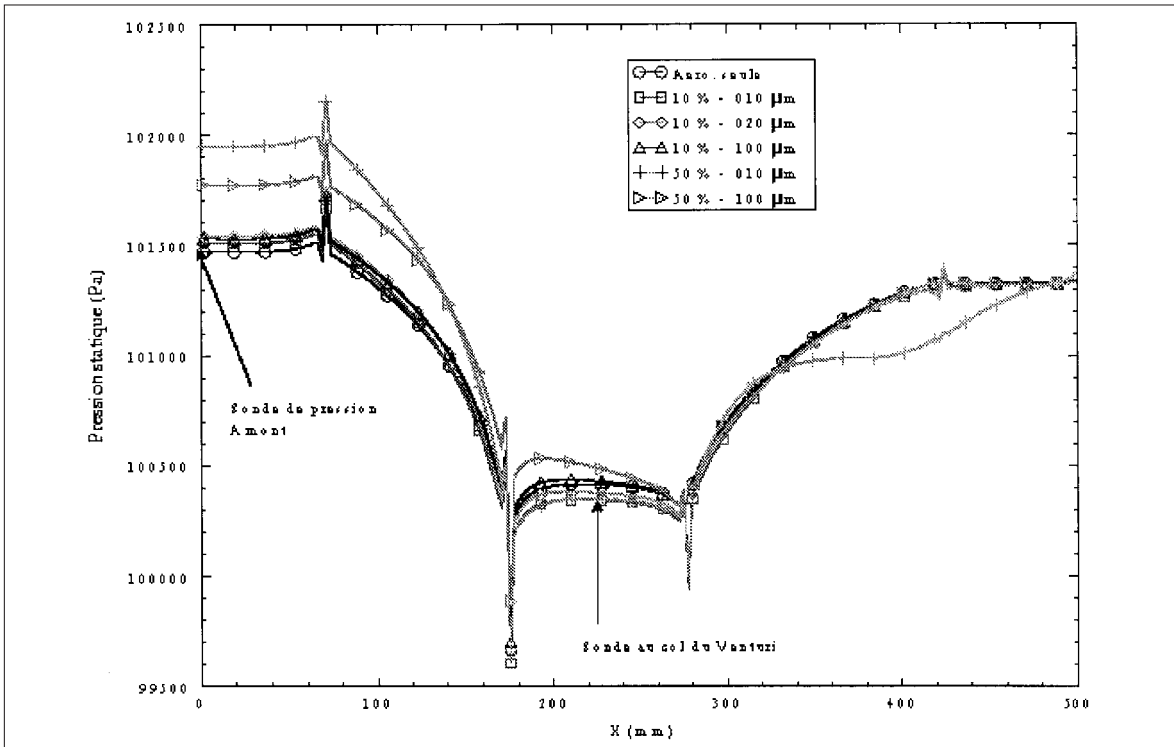


Figure 8 : Wall pressure distribution . The different liquid rates are represented with the ratio

$$\frac{Q_m - \text{liquide}}{Q_m - \text{gas}}$$



# Use of Venturi Meters in Multiphase Flow Measurement

*A R W Hall and M J Reader-Harris*

*Flow Measurement Centre  
National Engineering Laboratory  
Glasgow, UK*

---

## SUMMARY

This paper describes a project to investigate the performance of Venturi meters in multiphase flows. A range of Venturi meters spanning three diameter ratios and three inlet convergent angles was evaluated across a comprehensive range of multiphase flow conditions in the multiphase flow measurement facility at NEL.

The Venturi meters were evaluated in an uninterrupted 4-inch horizontal pipe run, without any mixing. The first stage of the project focused on development of appropriate instrumentation, using standard differential pressure transmitters and a clamp-on gamma densitometer, followed by the full evaluation of the meters.

Based on the results of this programme, one Venturi meter was selected for final evaluation using further refined instrumentation to collect data at a higher frequency. Evaluation of this final meter together with more detailed analysis of the data completes this paper.

## 1 INTRODUCTION

A range of Venturi meters spanning three diameter ratios and three inlet convergent angles was evaluated in the multiphase flow measurement facility at NEL. The multiphase flows used for the tests consisted of mixtures of stabilised crude oil, magnesium sulphate solution and nitrogen gas, across a range of test conditions. Multiphase test conditions are normally specified in terms of liquid flowrate, gas volume fraction (GVF) and the fraction of water in the liquid (water cut); the ranges of these conditions spanned the operating envelope of the multiphase test facility and correspond closely to the conditions used for evaluation of commercial multiphase meters in separate tests carried out by NEL.

The first stage of the project focused on development of appropriate instrumentation to meet the needs of the research programme. This included differential pressure measurement, density measurement, data sampling method and correct averaging of the measurements to give the Venturi discharge coefficients. Flow measurements in multiphase flow are strongly affected by the highly unsteady nature of the flow over much of the test

envelope. For example the Venturi differential pressure can have peaks registering an instantaneous differential pressure more than 5 times the average value during a slug flow. To achieve a reliable discharge coefficient measurement requires a large number of data samples.

All the Venturi meters were tested using a mixture of stabilised Forties crude oil and kerosine as the oil phase. The water phase used for all but two of the Venturi meters was 50 g/litre magnesium sulphate solution, and for the remaining two was 100 g/litre magnesium sulphate solution (the water phase was changed for a separate project). Two Venturi meters were additionally tested using stabilised Oseberg crude oil.

The results of these tests are summarised in this paper. Based on these results one Venturi meter was selected for final evaluation using further developed instrumentation to allow higher frequency data acquisition and the results of this final evaluation together with more detailed analysis of the data completes this paper.

## 2 EXPERIMENTAL PROGRAMME

### 2.1 Venturi Meter Theory

The volumetric flowrate through a Venturi meter is given by the following expression:

$$Q = CA \sqrt{\frac{2\Delta P}{\rho(1-\beta^4)}} \quad (1)$$

In a multiphase flow, where the measurements of differential pressure and density both fluctuate it is not satisfactory to use the ratio of  $\Delta P/\rho$  in this expression. This may be avoided by calculating the mass flowrate

$$M = \rho Q \quad (2)$$

from which it follows that

$$M = CA \sqrt{\frac{2\rho\Delta P}{(1-\beta^4)}} \quad (3)$$

In practice, the mass flowrate is an average value over the measurement period. Equation (3) becomes, by correct summation over the measurement period:

$$\bar{M} = CA \sqrt{\frac{2}{(1-\beta^4)}} \overline{\sqrt{\rho\Delta P}} \quad (4)$$

Therefore the correct quantity to calculate from the measured parameters of density,  $\rho$ , and differential pressure across the Venturi,  $\Delta P$ , is the average of the square root of  $\rho\Delta P$  evaluated for each individual measurement sample.

In this situation we have reference volumetric flowrates for each of the individual streams of oil, water and gas and, knowing their densities at measured pressure and temperature, the reference total mass flowrate may be calculated from

$$M = \rho_{oil} Q_{oil} + \rho_{water} Q_{water} + \rho_{gas} Q_{gas} \quad (5)$$

Having the average reference mass flowrate,  $\bar{M}$ , and the measured value of rDP from the Venturi meter enables calculation of the discharge coefficient from:

$$C = \frac{\bar{M}}{A} \sqrt{\frac{(1 - \beta^4)}{2}} \left( \sqrt{\rho \Delta P} \right)^{-1} \quad (6)$$

where A is the throat area and b is the ratio of throat diameter to full pipe diameter, which will be specific to each Venturi meter tested.

## 2.2 Instrumentation

In a single phase flow the density of the fluid will be known and therefore it is only necessary to measure the differential pressure in order to be able to calculate the flowrate. In multiphase flow, however, although the densities of the individual component phases are known, the density of the multiphase mixture is not known. Therefore it is necessary to measure the density of the fluid mixture entering the Venturi meter. This was done using a gamma densitometer containing a  $^{137}\text{Cs}$  gamma source, clamped onto the pipe upstream of the Venturi meter.

Differential pressure was measured between tappings located upstream and at the Venturi throat, using a Rosemount differential pressure transmitter. These devices are used in the multiphase measurement laboratory and were available in a number of calibrated pressure ranges, enabling the selection of appropriate transmitters for each Venturi, since often two pressure ranges were required to span the range of differential pressures which could be encountered across the whole test programme. There was always a need to balance accuracy of measurement with the total range which could be experienced in a multiphase flow. The Rosemount transmitters have proved to be very robust in multiphase flow, but have signal output which is damped, giving a maximum frequency response of 5 Hz.

Pressure and density measurements were collected using a high speed A to D conversion board in a PC, at the maximum frequency of the pressure transmitters (ie 5 Hz). A much higher data logging frequency was planned for the final stage of the project.

Each test condition was recorded for 10 minutes, giving a total number of 3000 measurements per test point.

## 2.3 Orientation

Typically multiphase flowmeters may be arranged in a vertical or a horizontal flow configuration. Most multiphase flowmeters using Venturi meters are arranged with a vertically upward flow through the Venturi meter. In nearly all cases the multiphase flow mixture passes from horizontal to vertical through a blinded tee just upstream of the metering section. Mixing is beneficial in distributing the gas and liquid across the pipe cross-section such that density measurement is reasonably reliable. This is more easily achieved in vertical flow since gravity does not act to separate the gas and liquid. So for density measurement, a vertical flow orientation is preferred.

For differential pressure measurement, however, vertical flow is less satisfactory. Unless the tapping lines to the pressure transmitters contain a fluid of the same density as the multiphase mixture in the flow conduit, there will be a hydrostatic pressure differential to consider in addition to the Venturi pressure differential. In the case of a large diameter ratio Venturi meter at low flowrate, the hydrostatic pressure differential may be significant compared with the Venturi differential pressure. If the impulse lines were always liquid or gas filled the hydrostatic differential can be calculated, knowing the mixture density, but it is unsatisfactory to correct one measurement with another in this way. Furthermore, it is difficult to ensure that the impulse lines remain filled with a particular fluid phase and so the applied correction itself may be in error. It is easy to obtain Venturi differential pressure measurements with errors higher than  $\pm 50\%$  for low Venturi differential pressure. Therefore, for differential pressure measurement, a horizontal flow orientation is preferred.

In practical tests it was found that a horizontal configuration gave much more satisfactory results than a vertical configuration, since the errors in differential pressure measurement in vertical flow vastly outweigh the difficulties of making a reliable density measurement in horizontal flow. The most satisfactory horizontal flow results were obtained in a long straight horizontal pipe where the density at the gamma densitometer was consistent with the density at the Venturi throat, with the densitometer arranged to give a vertical measurement through the pipe cross-section.

#### 2.4 Data Collection Frequency and Averaging

A typical example of density and differential pressure measurement is shown in Figure 1, where signals from the instruments, in mV, are plotted against time in msec.

Calculating in mV, the average and standard deviations of the measurements are:

	Average	Standard deviation
Venturi differential pressure, $\Delta P$	1046.4	102.0
Density	1863.7	515.9
Density $\times \Delta P$	1987768	807047

The 95% confidence interval of the measurements will depend on the number of samples taken according to the equation

$$\text{confidence interval} = t_{95} \frac{\sigma}{\sqrt{n}} \quad (7)$$

The confidence interval for density  $\times$  Venturi  $\Delta P$  is shown below and as a proportion of the average measurement.

Number of samples	Confidence interval	Confidence interval / average
100	159795	8.0%
1000	50072	2.5%
3000	28880	1.5%
10000	15818	0.80%
30000	9133	0.46%

This is an extreme example, and in many cases the signals are unlikely to vary quite so much. However it is clear from this example that typically 3000 data samples are required to give an acceptable uncertainty in the value of the Venturi discharge coefficient (ie less than  $\pm 1\%$ ), where the uncertainty is half that of the density  $\times \Delta P$  value because of the square root. 3000 samples may be collected by recording at 5 Hz for 10 minutes. To achieve an uncertainty of  $\pm 0.25\%$  would require a further 10-fold increase in the number of samples collected and this was considered in the final stage of the project.

## 2.5 Installation

The Venturi meters were all installed in a similar horizontal orientation consisting of:

- an adaptor from class 150 to class 600 flanges 0.6 m
- a spool piece with bore machined to match the Venturi tube 1.0 m
- the Venturi meter 1.0 m
- a pressure recovery spool piece 1.0 m
- an adaptor from class 600 to class 150 flanges 0.6 m

The whole assembly was then installed in the 4-inch horizontal line of the NEL multiphase flow facility. The clamp-on gamma ray densitometer was located on the conditioning spool piece upstream of the Venturi meter. The installation is illustrated in Figure 2 and the exact measurements of each Venturi meter are given in the table below.

Venturi meter	Nominal diameter ratio	Inlet cone angle (degrees)	Full bore diameter (mm)	Throat diameter (mm)	Diameter ratio
1	0.40	21	102.20	40.86	0.3998
2	0.60	21	102.21	61.33	0.6000
3	0.75	21	102.19	76.73	0.7509
4	0.40	31.5	102.23	40.94	0.4005
5	0.60	31.5	102.26	61.36	0.6000
6	0.75	31.5	102.31	76.76	0.7503
7	0.40	10.5	102.22	40.91	0.4002
8	0.60	10.5	102.20	61.31	0.5999
9	0.75	10.5	102.26	76.76	0.7506
10	0.40	21	102.26	40.88	0.3998
11	0.75	21	102.31	76.74	0.7501

## 2.6 Test Matrix

The typical minimum test matrix for each meter is shown in the table below. This covered the full range of liquid flowrates and gas volume fractions at 4 water cuts (less than 10% water, 40% water, 75% water and 100% water). Some meters were tested over a wider range of test conditions including some additional water cuts (25% water, 60% water and 90% water). The matrix for Venturi meters of diameter ratio 0.40 was reduced to remove points of excessively high Venturi differential pressure since the maximum differential pressure measurement range available was 50 psi (3.45 bar).

Liquid (m <sup>3</sup> /hr)	GVF (%)											
	10	25	40	50	60	70	80	85	90	92.5	95	97.5
14						(X)	(X)	X	X	X	X	X
22						X	X	(X)	X	X	X	
32			X	(X)	X	(X)	(X)	X	(X)	X		
43			(X)	X	(X)	X	X	X				
65		X	(X)	(X)	X	(X)	X					
86	X	(X)	(X)	X	X							
108	(X)	X	X									

Repeated at water cuts of 5, (25), 40, (60), 75 and 90%.

Bracketed values tested for only selected meters, other values for all meters.

## 2.7 Test Fluids

The combination of fluids used for the tests were as follows:

Venturi meter	Diameter ratio ( $\beta$ )	Inlet cone angle ( $^{\circ}$ )	Oil phase	Water phase
1	0.4	21	Forties	50 g/litre
2	0.6	21	Forties	50 g/litre
"	"	"	Oseberg	50 g/litre
"	"	"	Oseberg	100 g/litre
3	0.75	21	Forties	50 g/litre
4	0.4	31.5	Forties	50 g/litre
5	0.6	31.5	Forties	50 g/litre
6	0.75	31.5	Forties	50 g/litre
7	0.4	10.5	Forties	100 g/litre
8	0.6	10.5	Forties	100 g/litre
"	"	"	Oseberg	100 g/litre
9	0.75	10.5	Forties	50 g/litre
10	0.4	21	Forties	50 g/litre
11	0.75	21	Forties	50 g/litre

The properties of the single-phase fluids were typically (at 20°C):

Forties crude oil:	Density = 862.8 kg/m <sup>3</sup> Viscosity = 14.65 cP
Oseberg crude oil:	Density = 878.2 kg/m <sup>3</sup> Viscosity = 31.25 cP
50 g/litre MgSO <sub>4</sub> solution:	Density = 1029.3 kg/m <sup>3</sup> Viscosity = 1.178μ <sub>w</sub> Concentration = 62.4 g/litre
100 g/litre MgSO <sub>4</sub> solution:	Density = 1051.6 kg/m <sup>3</sup> Viscosity = 1.340μ <sub>w</sub> Concentration = 106.2 g/litre

The exact density for each fluid was evaluated as a function of temperature for each test.

### 3 RESULTS FOR INITIAL EVALUATION

#### 3.1 Results for all meters

Figure 2 shows the discharge coefficient plotted against reference gas volume fraction (GVF) for all the meters together. Each group of Venturi meters of similar diameter ratio gave a similar curve of discharge coefficient against GVF although there is quite a marked difference between the curves. The discharge coefficient apparently increases as the diameter ratio is increased, although it is not clear why this should occur.

#### 3.2 Results for meters of $\beta = 0.40$

Figure 3 shows the discharge coefficient against GVF for the Venturi meters of diameter ratio 0.40. The values of discharge coefficient show a consistent behaviour for all three Venturi meters having different inlet cone angles, with the discharge coefficient for the meter with the shallow inlet angle (Venturi No 7) slightly lower than for the other meters. This is expected since the longer inlet length leads to a higher irreversible (frictional) pressure loss between the upstream and throat tappings, than for a standard Venturi operating at the same flowrate. Venturi No 10 was similar to No 1 but without the diffuser section, and this is seen to give similar results to Venturi No 1.

Figures 4, 5 and 6 show discharge coefficient against GVF for the Venturi meters with inlet angles of 21°, 31.5° and 10.5° respectively, shown by water cut. There is a small, but noticeable effect of water cut on the discharge coefficients. This is most apparent in Figure 5 where the discharge coefficient for 60% water cut can be seen to be lower than the other values, but also in Figures 4 and 6 for 40% water cut. It is known that in this intermediate water cut zone between oil continuous and water continuous mixtures, the apparent viscosity, and hence frictional pressure loss is greater than it would be for a single liquid phase. For the test fluids used at NEL it is known that the peak in viscosity occurs at around

60% water cut and so this would be expected to give the lowest discharge coefficient. The effect is largest at high gas fraction and this is consistent with the expectation that liquid viscosity will have the largest effect in the thin liquid films which occur in annular flow.

Above 80% GVF, the difference in discharge coefficient between liquid phases of 60% water cut and of oil can be 5%, with a consequent similar magnitude of error in the calculated value of mass flowrate if a Venturi were used in this flow without compensation for the viscosity enhancement effect.

### 3.3 Results for meters of $\beta = 0.60$

Figure 7 shows the discharge coefficient against GVF for the Venturi meters of diameter ratio 0.60. The values of discharge coefficient show a consistent behaviour for all three Venturi meters with different inlet cone angles. Once again the discharge coefficient for the meter with the shallow inlet angle (Venturi No 8) is slightly lower than for the other meters. There is more scatter in the measurements from these three Venturi meters compared with those of diameter ratio 0.4. This is due to two effects. Firstly the differential pressures were significantly lower, and even using pressure transmitters of lower range to cover the points at the lowest differential pressures, the uncertainties in measuring differential pressure in a multiphase mixture increase at low differential pressure. Secondly, a greater range of test conditions could be covered than for the smaller diameter ratio meters, particularly at high gas fractions, since the overall pressure loss was significantly smaller. There is typically more fluctuation observed in multiphase flows at high gas fractions and greater scatter in the measurements is to be expected.

Figures 8, 9 and 10 show discharge coefficient against GVF for the Venturi meters with inlet angles of  $21^\circ$ ,  $31.5^\circ$  and  $10.5^\circ$  respectively, shown by water cut. Similarly to the smaller diameter ratio meters there is a clear influence of water cut on the discharge coefficients, particularly at 40% and 60% water cut (60% water cut tested for Venturi 2 only).

### 3.4 Results for meters of $\beta = 0.75$

Figure 11 shows the discharge coefficient against GVF for the Venturi meters of diameter ratio 0.75. The values of discharge coefficient show a similar behaviour for all three Venturi meters having different inlet cone angles. The values of discharge coefficient are more scattered still than was observed for the meters of diameter ratio 0.6, although the tests covered similar ranges of flow conditions. In these three Venturi meters the differential pressure measurements are often extremely small which lead to large uncertainties in the measurements.

Figures 12, 13 and 14 show discharge coefficient against GVF for the Venturi meters with inlet cone angles of  $21^\circ$ ,  $31.5^\circ$  and  $10.5^\circ$  respectively, shown by water cut. Even with the greater scatter in the measurements, it is still possible to distinguish the effect of water cut. This is most clearly shown for Venturi No 6, in Figure 13, where approximately 10% difference in discharge coefficient is demonstrated between 5%/40% water cut and 75%/100% water cut.

## 4 RESULTS FOR FINAL EVALUATION

### 4.1 Experimental Tests

The final Venturi meter, Venturi No 2, was assembled in the same configuration described in Section 2.5, but using undamped Gulton-Statham differential pressure transmitters. The full test matrix shown in Table 2 was used for the evaluation of this meter. The test matrix was sorted by the maximum differential pressure observed in the original tests at 5 Hz data collection frequency so that pressure transmitters of differential pressure range 0 to 20 psi and 0 to 50 psi could be used. This allowed more accurate measurement of low differential pressure than would have been possible using a single 0 to 50 psi transmitter range.

The response time of these transmitters was less than 7 msec, which is equivalent to 142 Hz. To achieve the 30,000 data samples as discussed in Section 2.4 therefore required data to be collected over a period of 3\_ minutes for each data point. The discharge coefficient against GVF is shown in Figure 15.

### 4.2 Modelled Data

The behaviour of the Venturi meter in its evaluation described in the previous section has been modelled according to the following process.

The mass flowrate is calculated from equation (4) where the discharge coefficient has been fitted as a function of the reference gas volume fraction (GVF) and liquid Reynolds number ( $Re_L$ ) with different polynomial fits obtained for each water cut. The combination of GVF and  $Re_L$  which yielded the best fit was  $GVF/Re_L$ . This was used since the discharge coefficient depends on both GVF and  $Re_L$ , but it must be emphasised that this is an empirical relationship. The GVF dependence of (apparent) discharge coefficient is most likely related to the use of a live density measurement in place of a volume or area density measurement. If the multiphase flow were fully homogenised it is likely that the discharge coefficient would be close to 1. It should be noted that in practice the GVF and liquid Reynolds number will be outputs from the measurement model and therefore an iterative situation will be required.

Having evaluated the total mass flowrate,  $\dot{M}_{TP}$ , the next stage is to calculate the quality (= gas mass fraction) in order to calculate the  $\dot{M}_{gas}$  and liquid flowrates. The quality,  $\chi$ , is calculated from:

$$\chi = \left\{ 1 + \frac{\rho_L (\rho_{TP} - \rho_G)}{S_{\rho G} (\rho_L - \rho_{TP})} \right\}^{-1} \quad (8)$$

where  $\rho_{TP}$  is the measured two-phase (line) density for consistency with the experimental data set and  $S$  is the slip ratio, defined by

$$S = \frac{Q_G}{Q_L} \left( \frac{1 - \varepsilon}{\varepsilon} \right) \quad (9)$$

The slip ratio represents the ratio between the in situ gas velocity and the in situ liquid velocity. The void fraction,  $\epsilon$ , is calculated from

$$\epsilon = \frac{\rho_{TP} - \rho_L}{\rho_G - \rho_L} \quad (10)$$

Using the reference volumetric flowrates  $Q_G$  and  $Q_L$ , the known single phase densities and the measured density,  $\rho_{TP}$ , the void fraction,  $\epsilon$ , and slip ratio,  $S$ , can be calculated. The best correlation of  $S$  was found to be against the parameter  $GVF/Re_L^{0.25}$  for which all the slip ratio values at different water cut collapse on to one curve for oil-continuous flow and another for water-continuous flow.

The Reynolds number is calculated by the following method. Since in all cases the mass flowrate is dominated by the liquid phase the liquid Reynolds number is used. This is evaluated based on the full pipe diameter,  $D$ :

$$Re_L = \frac{Q_L \rho_L D}{1000 A \mu_L} \quad (11)$$

where  $Q_L$  is the reference liquid flowrate in litre/sec,  $\rho_L$  is the liquid density in  $kg/m^3$  and  $\mu_L$  is the liquid viscosity in Pa.s. The viscosity of the liquid phase is determined according to the methodology developed by Corlett (1998). For oil-continuous flow ( $\phi$  = percentage water cut < 64):

$$\mu_L = \frac{\mu_{oil}}{(1 - \phi/1000)^{1.2}} \quad (12)$$

For water-continuous flow ( $f$  = percentage water cut > 64):

$$\mu_L = \mu_{water} \quad (13)$$

The best results are obtained in the water cut range  $0 < \phi < \sim 50$  where the liquids are oil-continuous and reasonably well mixed. As the inversion point is reached, around 64% water in these tests, the liquid phase distribution can switch between oil-continuous and water-continuous and so the viscosity, and hence the liquid Reynolds number can vary over a wide range.

For water-continuous mixtures, viscosity, and hence liquid Reynolds number can usually be less well characterised. The oil and water can either give temporary mixtures and liquid films with high viscosity or can separate and give an effective viscosity even lower than that of the water phase. Therefore characterisation of the rheological properties of the liquid phases in the three-phase mixture flowing through the Venturi meter is of key importance in the modelling of the meter.

Finally, the liquid and gas volumetric flowrates are calculated from:

$$\text{liquid volume flowrate} = Q_L = \frac{M(1 - \chi)}{\rho_L} \quad (14)$$

$$\text{gas volume flowrate} = Q_G = \frac{M\chi}{\rho_G} \quad (15)$$

The errors in liquid and gas volumetric flowrates are calculated from:

$$\% \text{liquid volume flowrate error} = \frac{100 \times (Q_{L, \text{measured}} - Q_{L, \text{reference}})}{Q_{L, \text{reference}}} \quad (16)$$

$$\% \text{gas volume flowrate error} = \frac{100 \times (Q_{G, \text{measured}} - Q_{G, \text{reference}})}{Q_{G, \text{reference}}} \quad (17)$$

The errors in modelled liquid volume flowrate are shown in Figures 16 and 17, and the overall results of the modelling of the Venturi performance data are shown below. The arithmetical average error (showing the bias) and standard deviation of the errors (showing scatter)

Water cut	Liquid		Gas	
	Average error	Standard deviation of errors	Average error	Standard deviation of errors
5	0.09	3.05	0.71	9.11
25	0.18	3.52	-0.35	7.29
40	0.10	4.46	3.20	7.61
60	-0.05	5.73	6.32	7.87
75	0.06	2.82	1.28	12.05
90	-0.31	2.72	4.76	13.38

are calculated for both liquid and gas flowrates.

## 5 CONCLUSIONS

Eleven Venturi meters have been characterised in multiphase flows across the whole test envelope available in the NEL multiphase flow facility. These conditions spanned the range 10% to 95% gas volume fraction and 5% to 100% water cut, with liquid volumetric flowrate ranging from 14 to 108 m<sup>3</sup>/hr.

The discharge coefficient was evaluated for each test condition based on the mass flowrate from the reference metering system (the sum of mass flowrates of the individually metered single phase flows of oil, water and gas). Measurements of differential pressure between the Venturi meter throat and the upstream tapping and of the density from a gamma ray densitometer were made to complete this calculation.

Discharge coefficient calculated by this method showed a significant variation with reference gas volume fraction and a smaller effect with reference water cut. This latter effect was most significant at water cuts close to the inversion between oil-continuous and water-continuous dispersion (40% to 60% water cut). A small difference was also observed in discharge coefficient between the Venturi meters with shallow inlet cone angle and the other Venturi meters, except at the largest diameter ratio, where scatter in the measurements obscured any difference.

For measurements in multiphase flows across the studied range of conditions, the most appropriate choice of diameter ratio is 0.60. The smaller diameter ratio gave too high a pressure drop and thus restricted the useful operating range, while the larger diameter ratio gave too small a pressure differential for reliably accurate measurements to be made.

There does not appear to be any advantage in varying the inlet cone angle from the standard value of 21°. No significant difference was observed between the Venturi meters with 21° inlet angle and those with 31.5°. The shallow inlet angle led to increased pressure loss without improvement in measurement accuracy. The diffuser section was shown to be essential in mitigating permanent pressure loss over the Venturi measuring system, except in conditions of gas volume fraction above 90% where there was little pressure recovery, with or without the diffuser section.

The standard Venturi meter No 2 with diameter ratio 0.60 and inlet cone angle of 21° was selected for the final evaluation using instrumentation which was revised to allow data recording at a significantly increased frequency. The results of this evaluation were modelled empirically: there was good agreement between modelled and reference volume flowrates.

## REFERENCE

1 Viscosity of oil and water mixtures. A. E. Corlett, NEL Report No 263/97, 1998.

## NOMENCLATURE

A	Venturi meter throat area	m <sup>2</sup>
C	Venturi discharge coefficient	-
D	Pipe diameter	m
M	Mass flowrate	kg/s
n	Number of samples	-
Q	Volume flowrate	m <sup>3</sup> /s
Re	Reynolds number	-
S	Slip ratio	-
t <sub>95</sub>	Student's t-distribution for 95% confidence interval	-
β	Venturi diameter ratio (throat diameter/upstream diameter)	-
ΔP	Differential pressure	Pa
ε	Void fraction	-
μ	Viscosity	Pa.s
ρ	Density	kg/m <sup>3</sup>
σ	Standard deviation	-
φ	Water cut (percentage water in liquid)	-
χ	Quality (gas mass fraction)	-

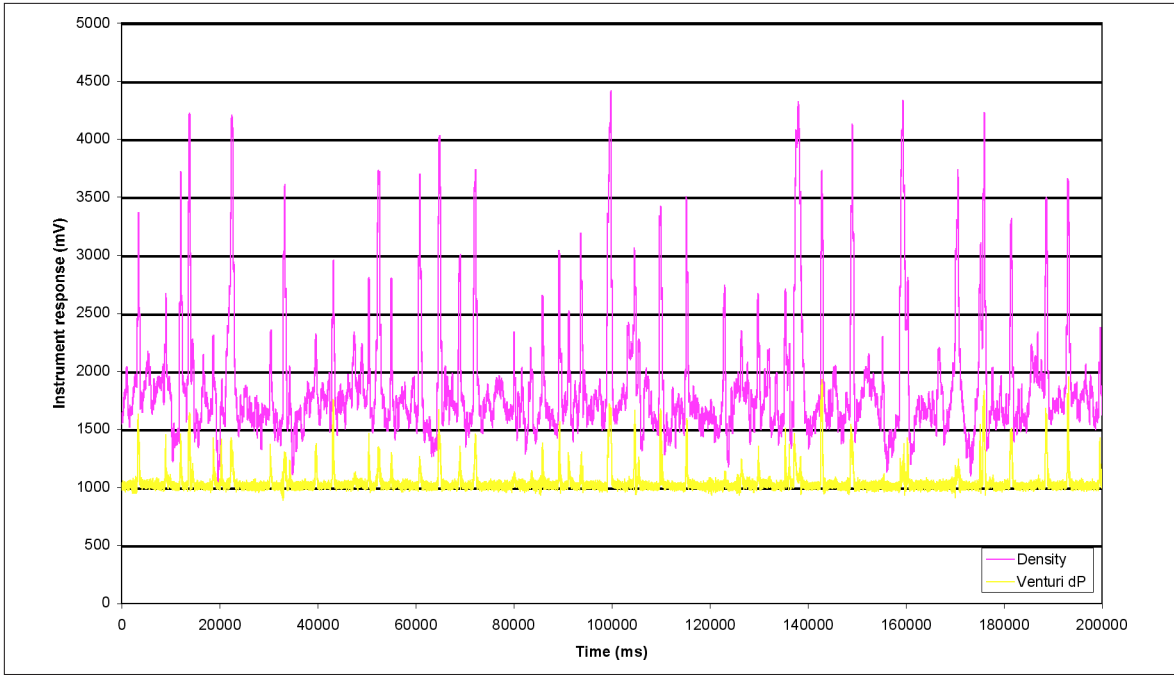


Figure 1: Typical density and Venturi differential pressure signals

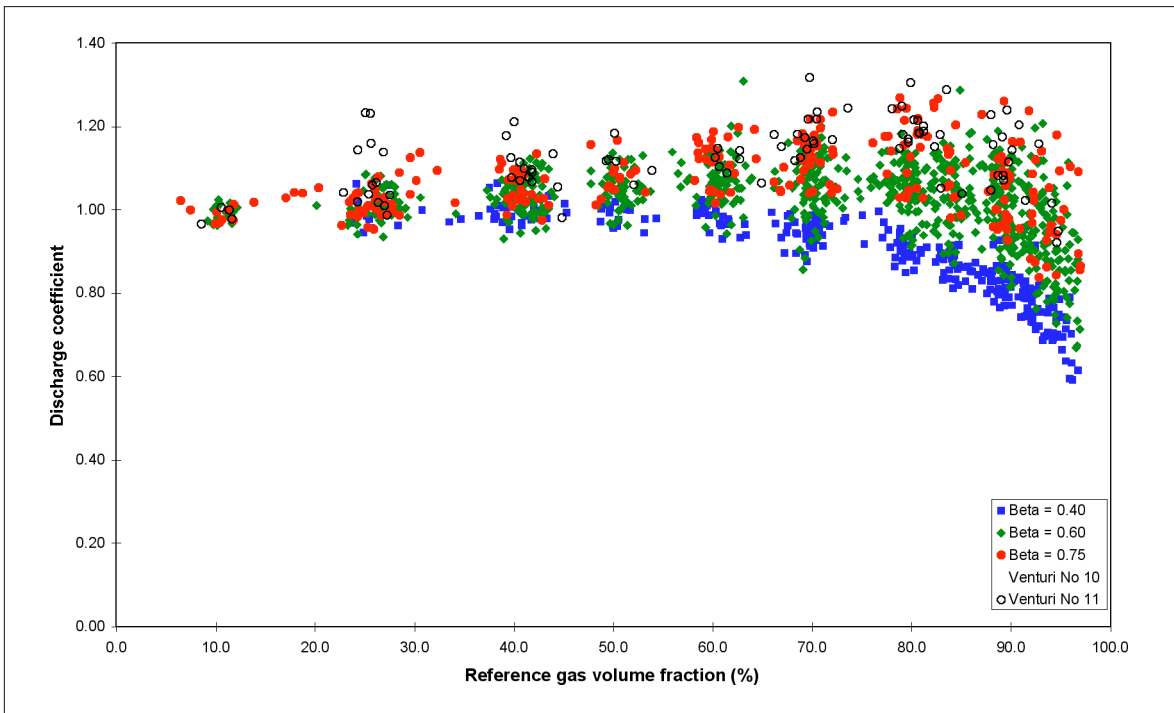


Figure 2: Discharge coefficient vs GVF for all Venturi meters in multiphase flow

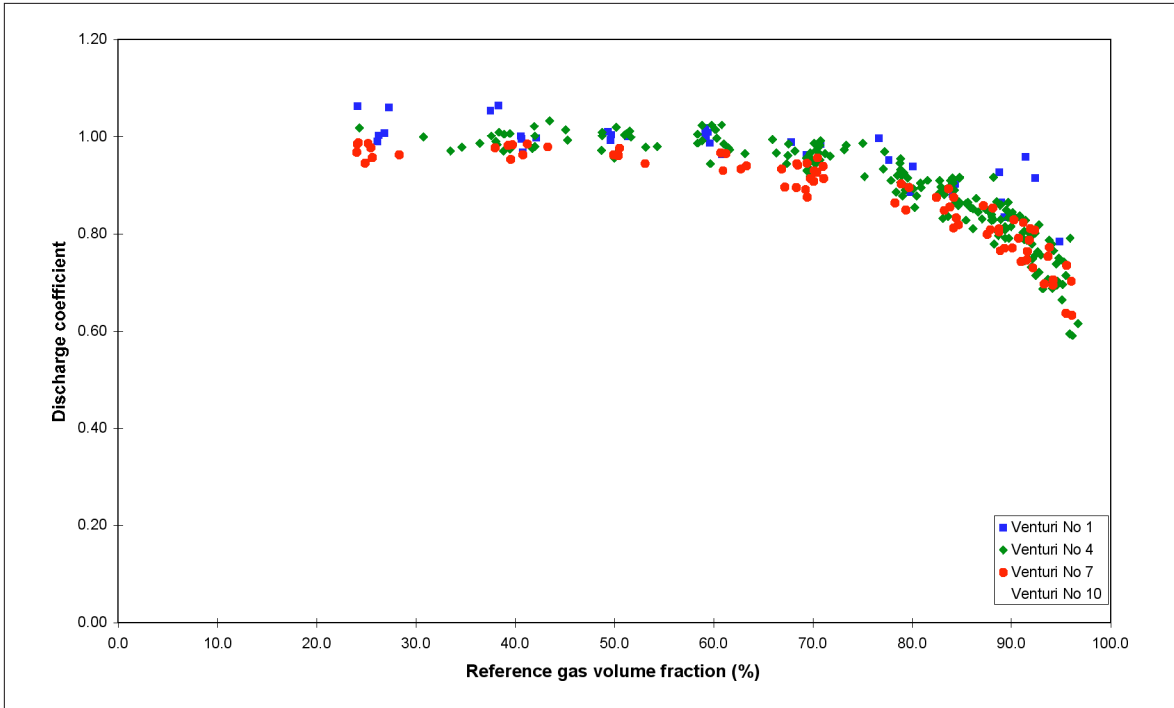


Figure 3: Discharge coefficient vs GVF for all Venturi meters of  $b = 0.40$  in multiphase flow

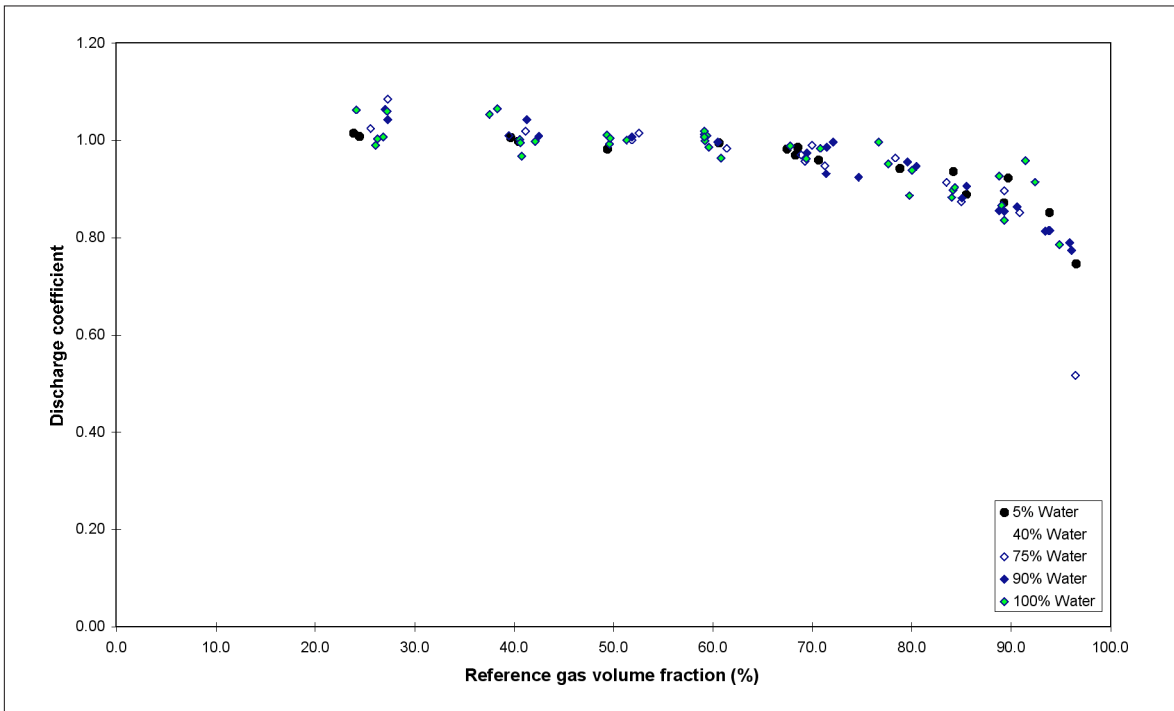


Figure 4: Discharge coefficient vs GVF for Venturi meter 1 in multiphase flow, showing effect of water cut

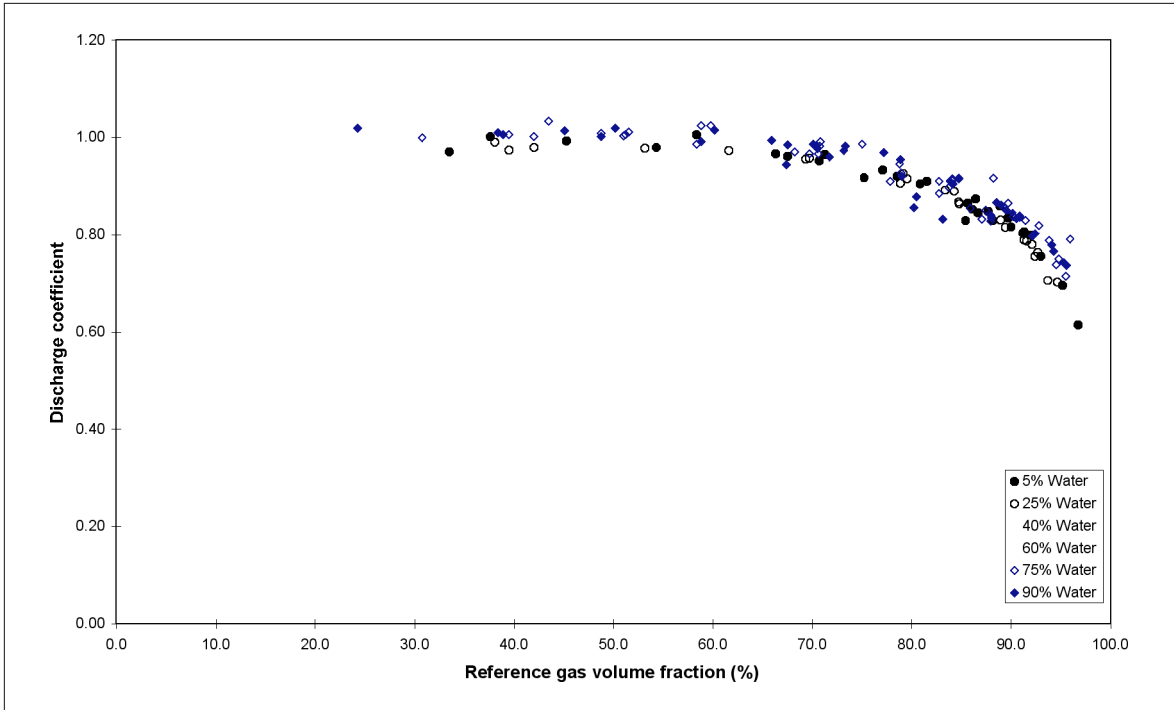


Figure 5: Discharge coefficient vs GVF for Venturi meter 4 in multiphase flow, showing effect of water cut

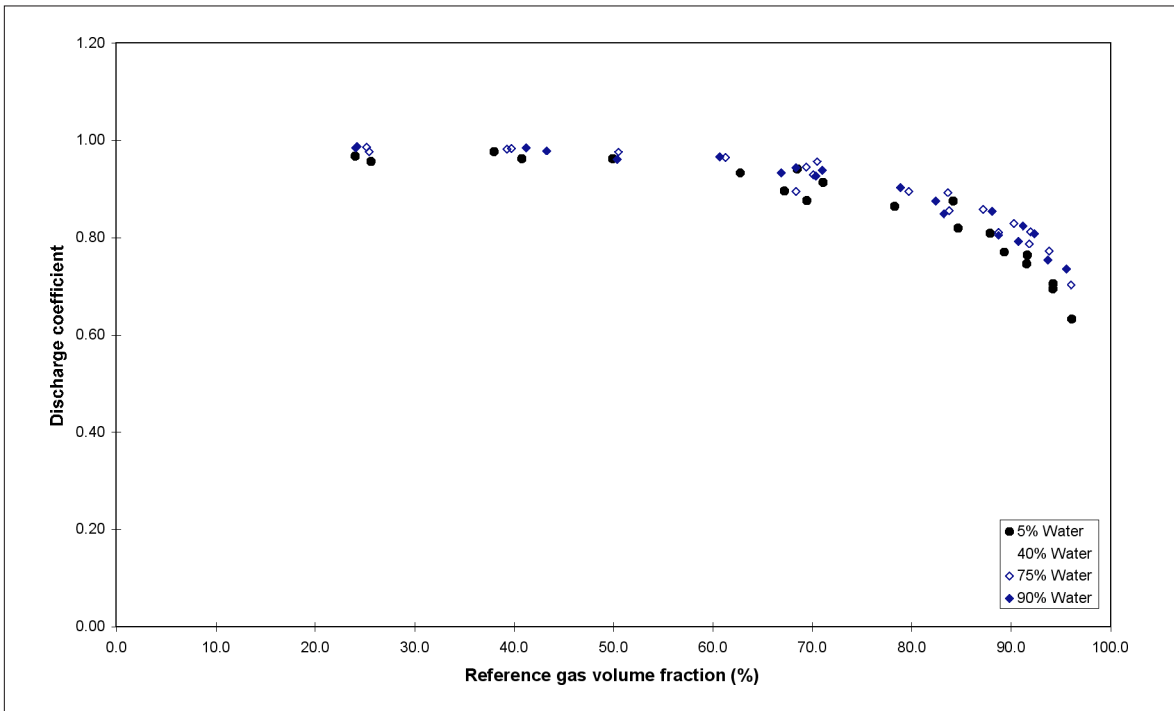


Figure 6: Discharge coefficient vs GVF for Venturi meter 7 in multiphase flow, showing effect of water cut

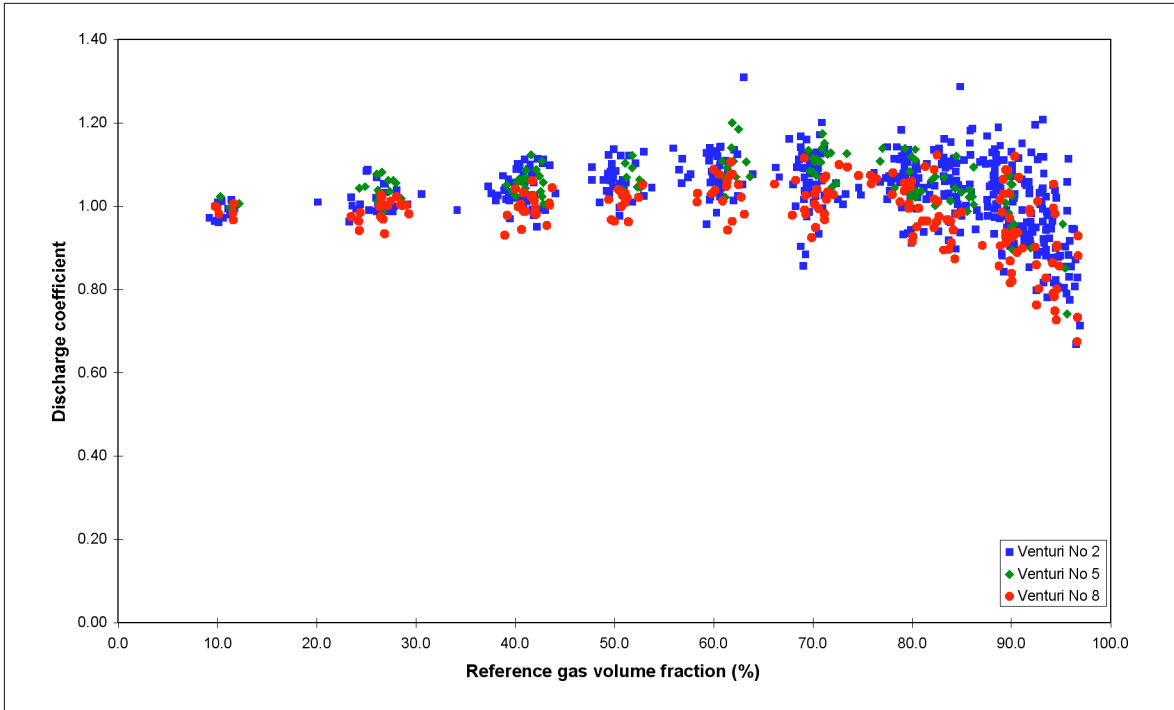


Figure 7: Discharge coefficient vs GVF for all Venturi meters of  $b = 0.60$  in multiphase flow

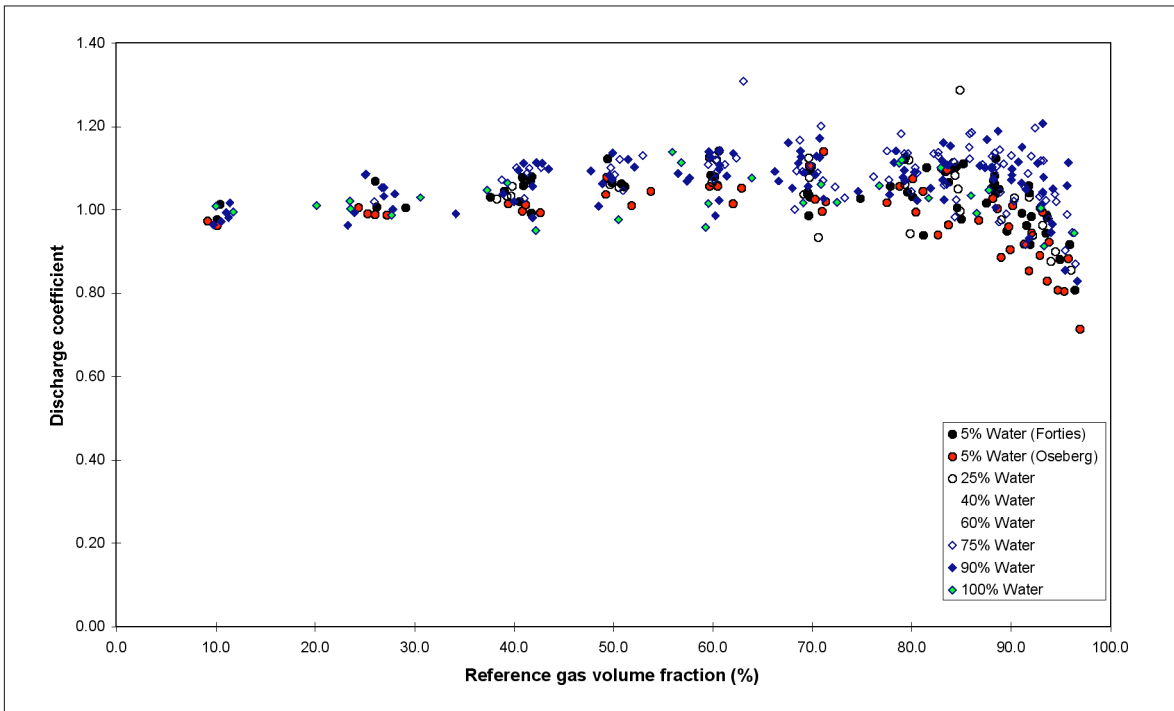


Figure 8: Discharge coefficient vs GVF for Venturi meter 2 in multiphase flow, showing effect of water cut

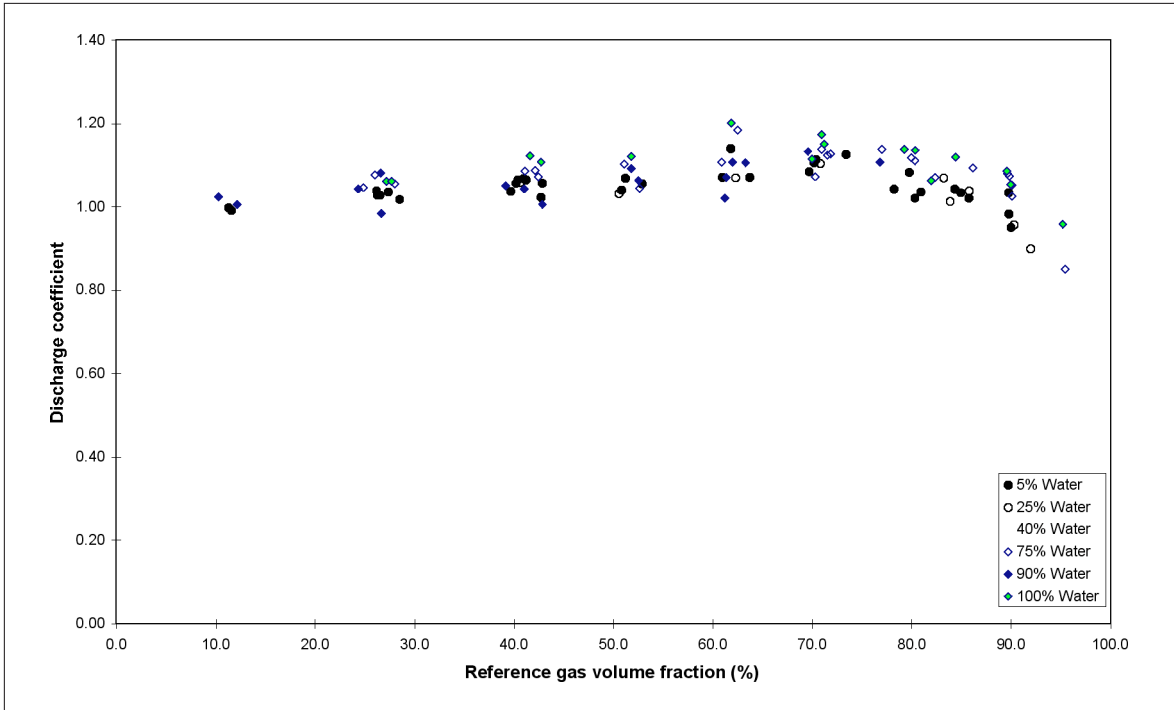


Figure 9: Discharge coefficient vs GVF for Venturi meter 5 in multiphase flow, showing effect of water cut

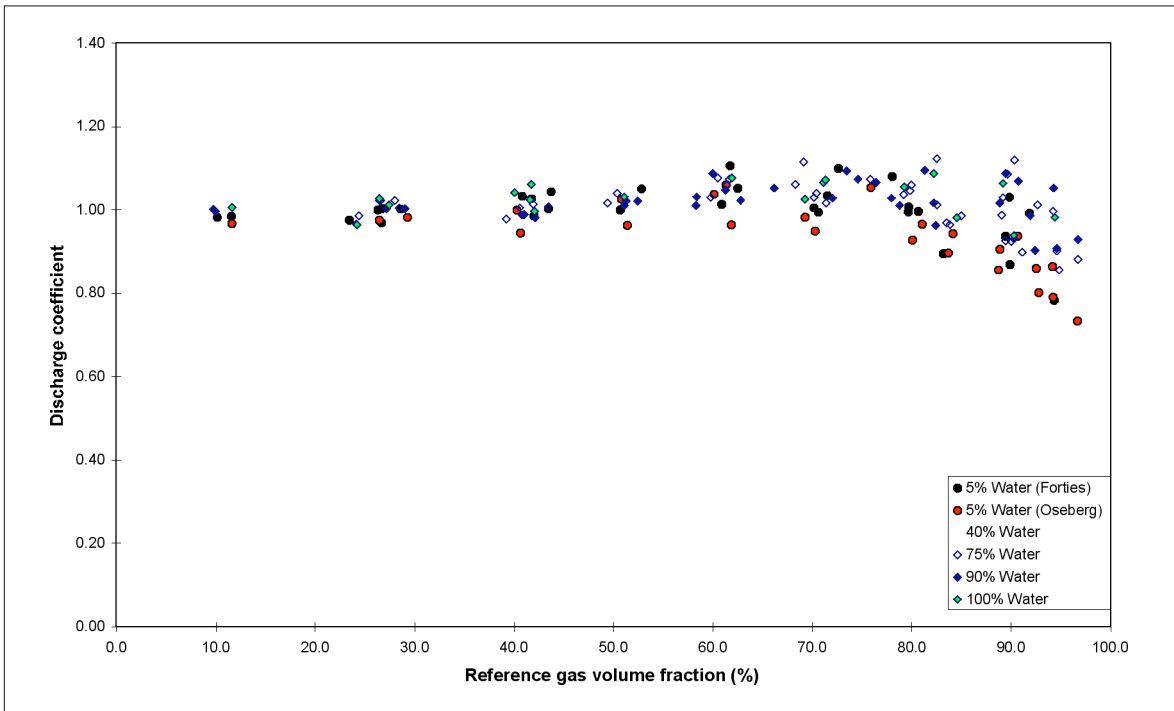


Figure 10: Discharge coefficient vs GVF for Venturi meter 8 in multiphase flow, showing effect of water cut

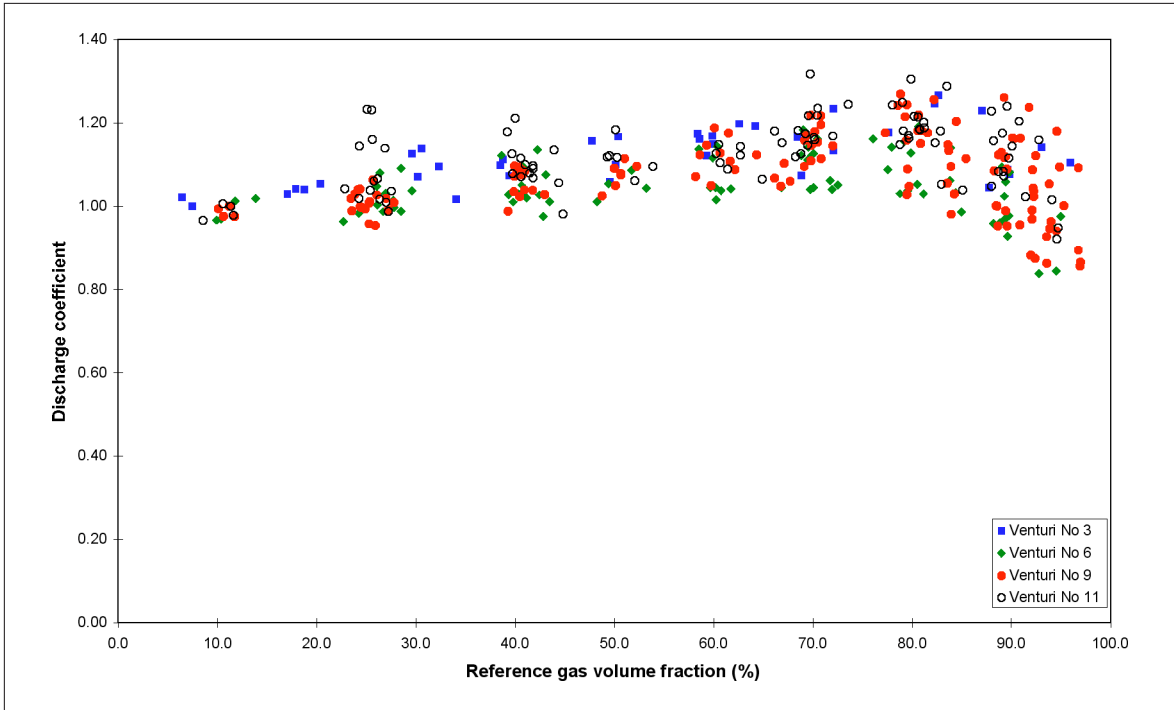


Figure 11: Discharge coefficient vs GVF for all Venturi meters of  $b = 0.75$  in multiphase flow

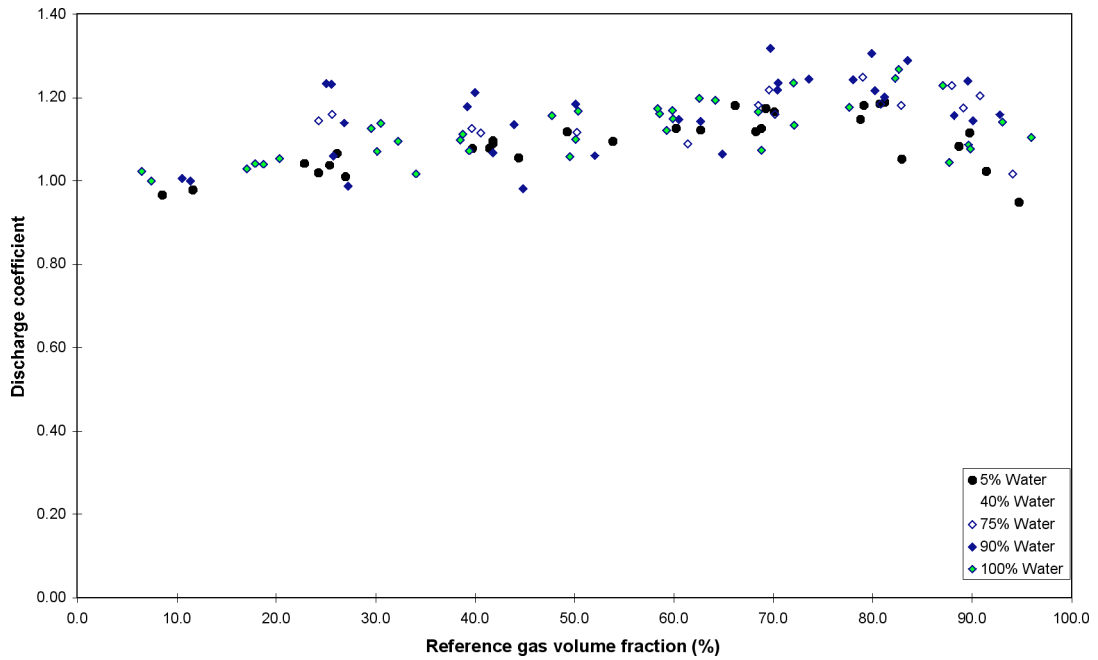


Figure 12: Discharge coefficient vs GVF for Venturi meter 3 in multiphase flow, showing effect of water cut

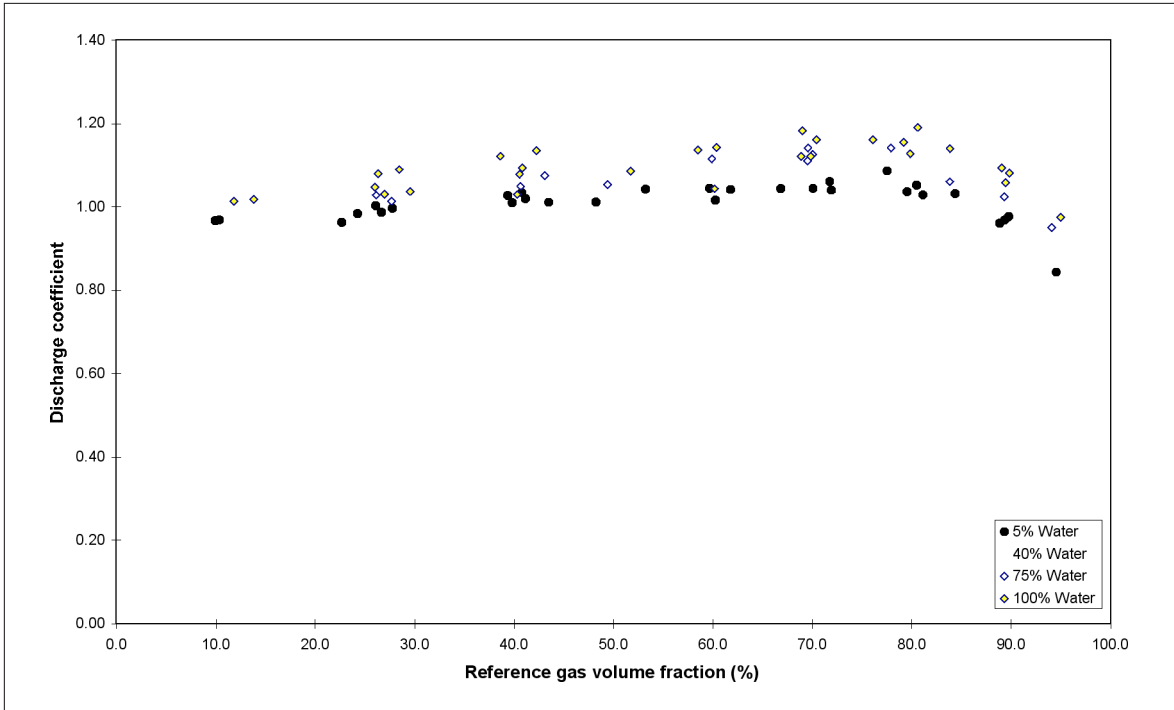


Figure 13: Discharge coefficient vs GVF for Venturi meter 6 in multiphase flow, showing effect of water cut

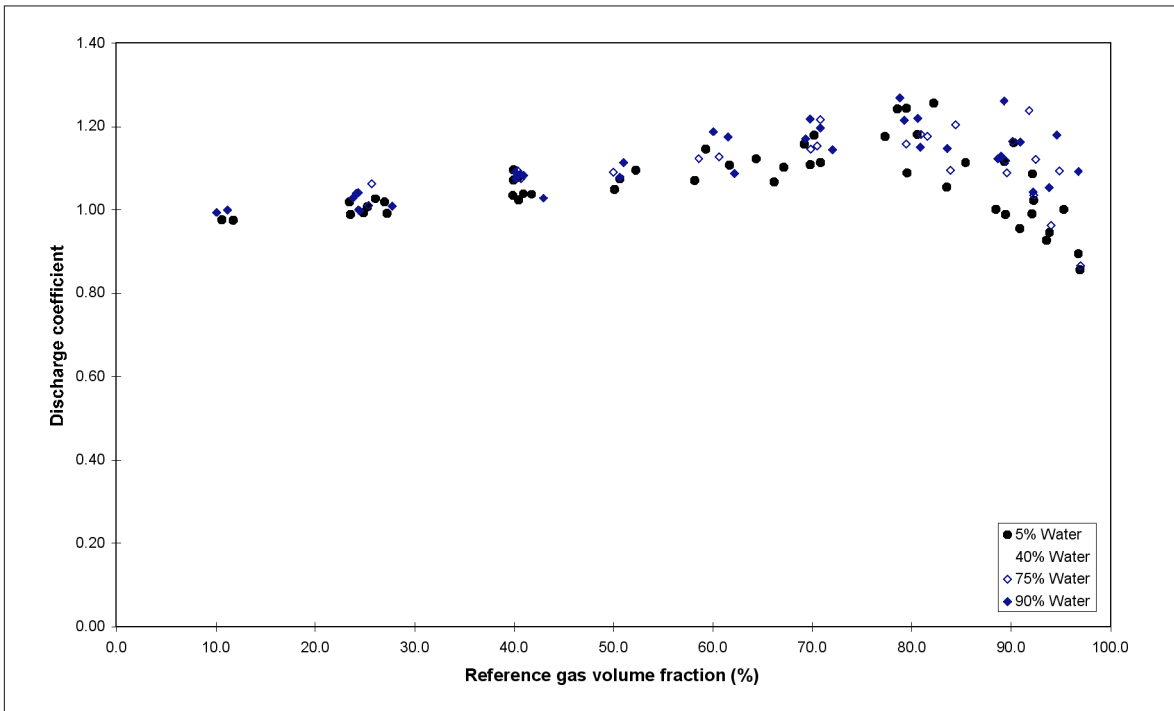


Figure 14: Discharge coefficient vs GVF for Venturi meter 9 in multiphase flow, showing effect of water cut

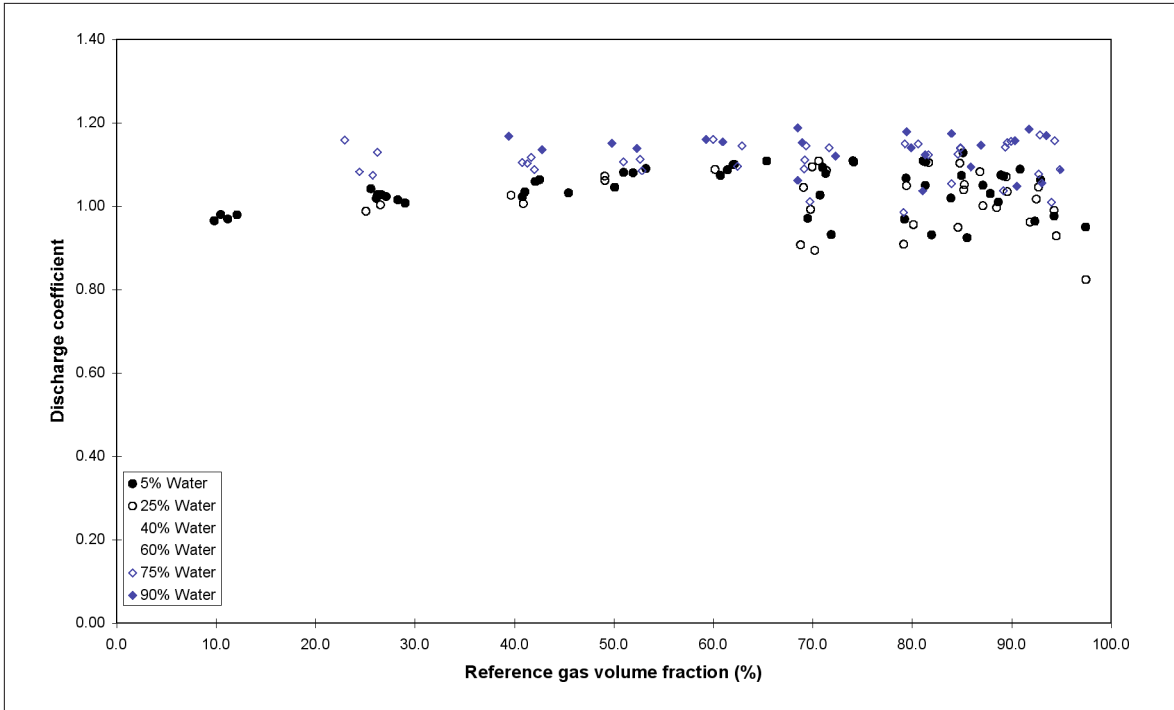


Figure 15: Discharge coefficient vs GVF for Venturi meter 2 in multiphase flow using 142 Hz instrumentation

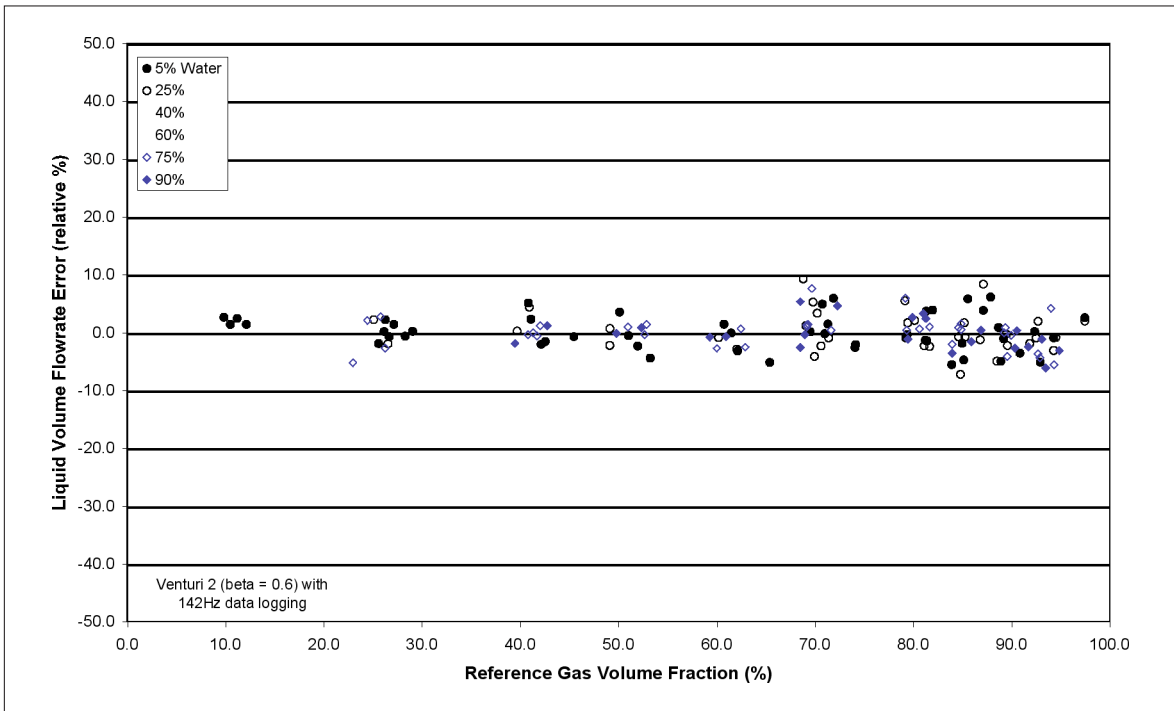


Figure 16: Error in modelled liquid volume flowrate vs reference GVF

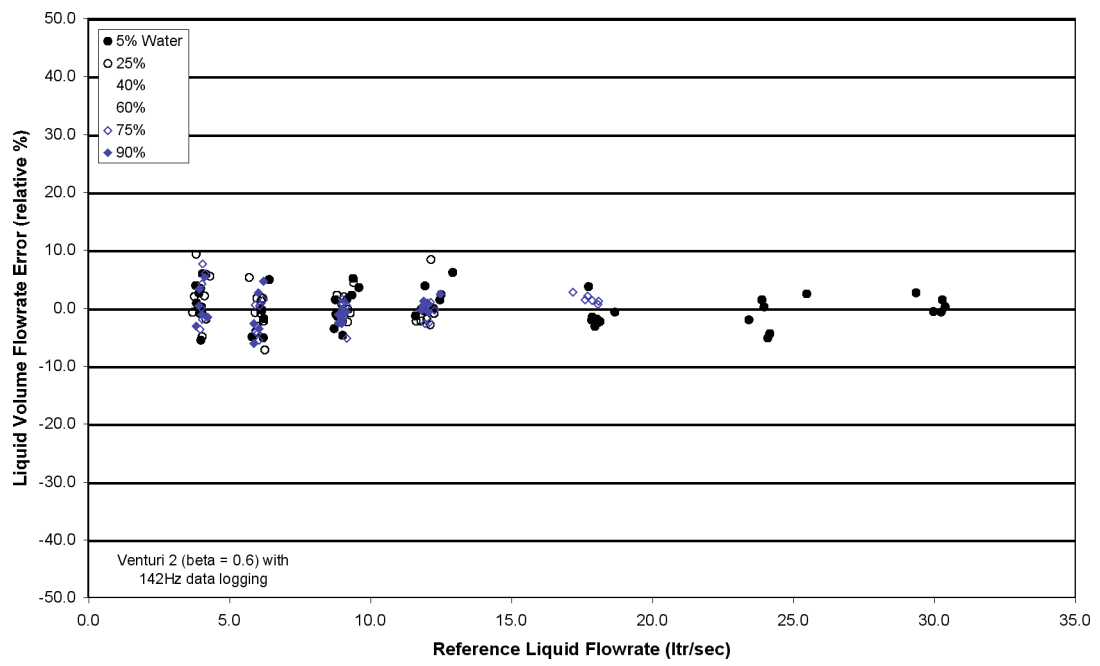
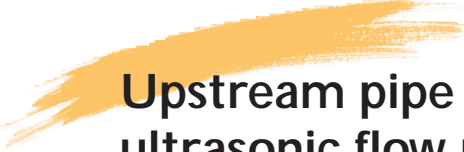


Figure 17: Error in modelled liquid volume flowrate vs reference liquid flowrate



# Upstream pipe wall roughness influence on ultrasonic flow measurement

*H.J. Dane, Consulting Engineer, Dordrecht, The Netherlands*

*R.Wilsack, Technical Manager, TransCanada Calibrations, Canada*

---

## Abstract

In high-pressure natural gas pipelines, installation requirements of modern ultrasonic flow meters usually only specify an upstream pipe length, without mentioning wall roughness. Since no data were available to support a specification, Measurement Canada and TransCanada PipeLines decided to conduct a series of tests under well-defined conditions. This document reports the results. The tests were carried out at the Ruhrgas test facility Pigsar in Germany, where two 12» Q.Sonic® 3-path ultrasonic flow meters (Instromet®) were repeatedly calibrated at about 45 bar, while various pipes of different roughness were mounted upstream. Two Ruhrgas engineers measured the wall roughness of the pipes using ISO 9001 certified standard methods. Over the range of conditions investigated, an increase of the roughness  $R_a$  from about 5  $\mu\text{m}$  to probably 20  $\mu\text{m}$  appears to increase the meter reading by about 0.1 - 0.2 %.

## 1 Introduction

In high-pressure natural gas pipelines, installation requirements of modern ultrasonic flow meters usually only specify an upstream pipe length, without mentioning wall roughness. The reason for this requirement is to make sure, at least to some extent, that the flow meter is presented with a reasonably well-behaved velocity profile. The velocity profile, however, not only depends on upstream conditions and Reynolds number, but on wall roughness also. Since no data were available to support a specification for wall roughness, Measurement Canada and TransCanada PipeLines decided to conduct a series of tests under well-defined conditions. Two 12» Q.Sonic® 3-path ultrasonic flow meters (Instromet®) were repeatedly calibrated at about 45 bar, while various pipes of known and different roughness were mounted upstream. This paper presents the results. Its outline is as follows: In chapter 2 the concept of wall roughness will be discussed, its various measures will be explained, and its influence on the velocity profile. The next chapter will present the main results of the roughness measurements on the pipes used in the tests. The details are described in an official Ruhrgas report (in German). Chapter 4 contains the results of the flow calibrations at the Pigsar facility. Finally the results are summarized in a conclusion.

## 2 Roughness

Every practical surface of a solid state material is like a microscopic landscape, with mountains and valleys. It has a finite roughness: only mathematical surfaces are perfectly smooth. The surface of even the best straight pipe is not an exact mathematical cylinder, the cylinder is just an approximate description of its shape. The roughness is part of the difference between the real shape and the ideal one. The roughness results not only from the internal structure of the material, its atomic or molecular nature, but from the processes that created and influenced the surface, such as machining, polishing, coating, corrosion and the like. Various measures exist to characterize the microscopic landscape, each is a particular compromise between local and more global features of the surface. The most widely used are  $R_a$  and  $R_z$ . The first is defined as the arithmetical mean of the absolute values of the profile departures within the measuring length  $L$ . shows an illustration.

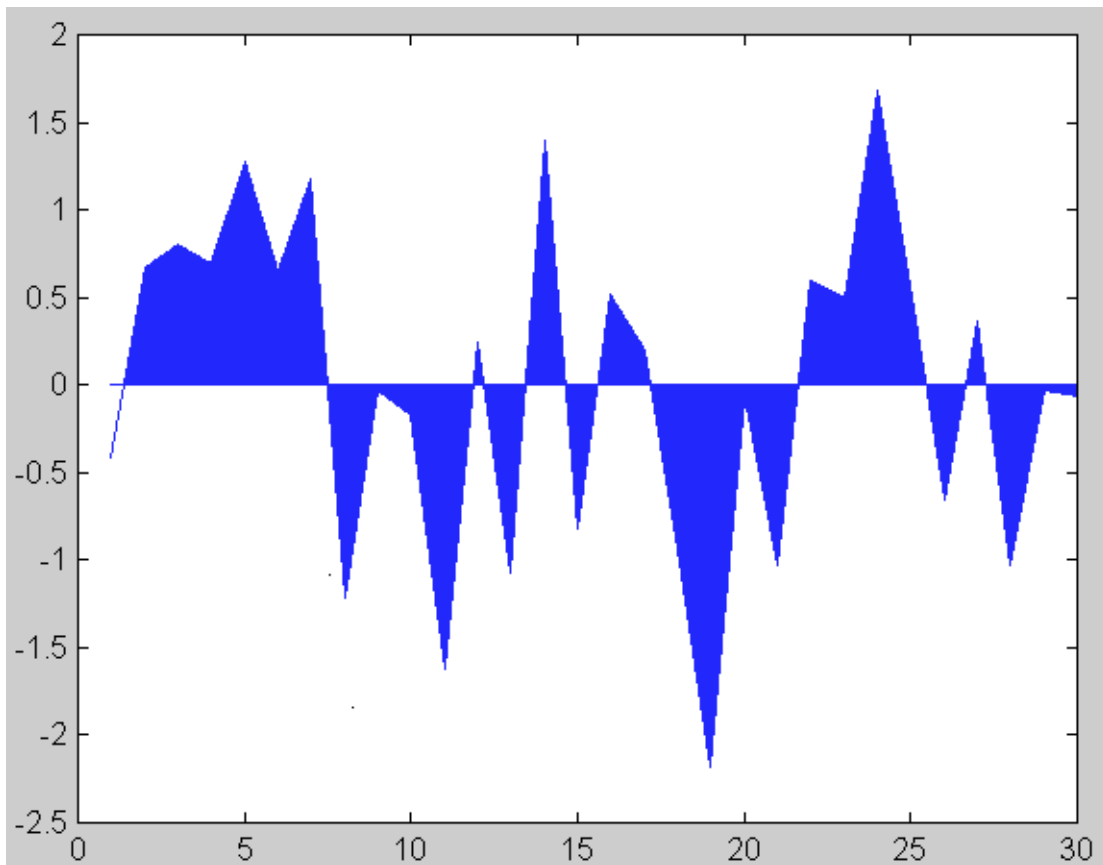


Figure 1, Definition of  $R_a$

$R_z$  is defined as the average value of the absolute values of the heights of five highest profile peaks and the depths of five deepest profile valleys within the measuring length

$$R_a = \frac{1}{L} \int_0^L |y(x)| dx \quad (1)$$

$$R_z = \frac{l}{5} \sum_{i=1}^5 \{ |y_i^+| + |y_i^-| \} \quad (2)$$

where  $y_i^+$  denotes the highest peaks and  $y_i^-$  the deepest valleys on the measuring interval. illustrates this definition

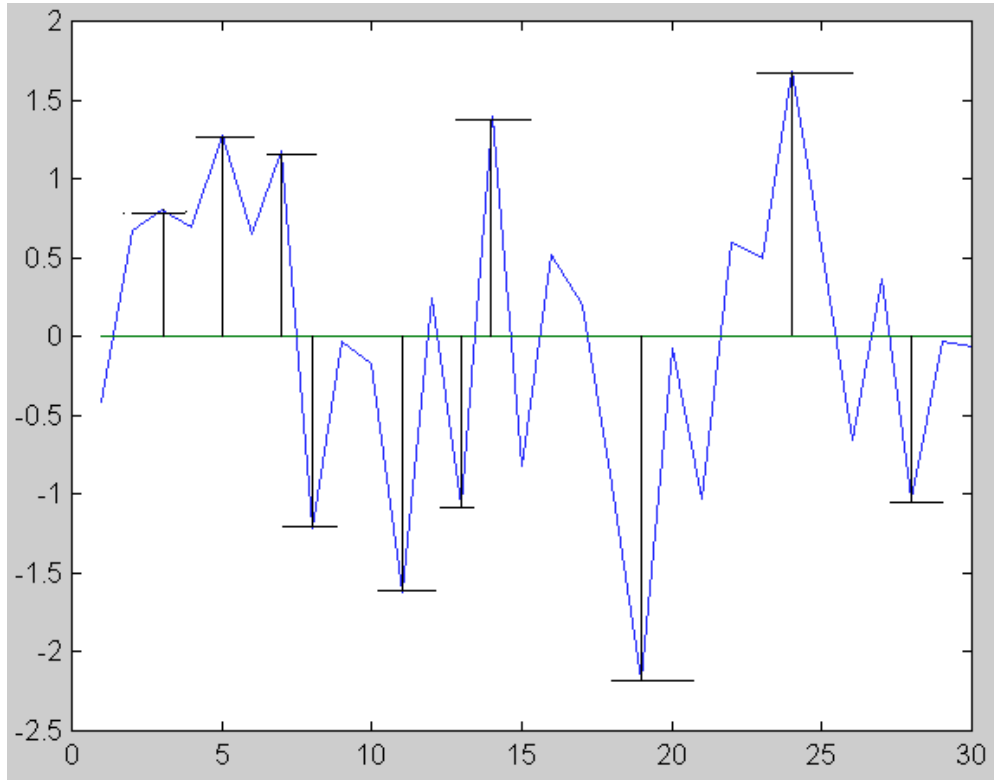


Figure 2, Definition of  $R_z$

In many practical situations the value of  $R_z$  appears to be about five times that of  $R_a$ . According to Van der Kam (1993) in new gas pipes  $R_a$  ( 5  $\mu\text{m}$ , whereas in old pipes it may increase to about 30  $\mu\text{m}$ .

In swirl-free flow through long straight cylindrical tubes with radius  $R$ , the only non-zero time-averaged velocity component will be in the axial direction, and it will be a function of radial position  $r / R$  only. According to Schlichting(1968) the semi-empirical relation

$$v(r) = v_{max} \left( 1 - \frac{r}{R} \right)^n \quad (3)$$

approximately describes this function, which is usually called the fully developed velocity profile. In this relation  $n$ , and therefore the velocity profile  $v(r)$ , is a function of the Reynolds number  $Re$  and the pipe roughness. Colebrook (1939) uses the concept of 'equivalent sand roughness' rather than  $R_a$  or  $R_z$ , probably because the latter were not yet defined at that time. If we equate  $R_a$  with his 'equivalent sand roughness' Colebrook's implicit relation for  $n$  can be written as

$$n = 1.74 - 2 \log_{10} \left( \frac{R_a}{R} + 18.57 \frac{n}{Re} \right) \quad (4)$$

Note that roughness relative to pipe radius rather than roughness proper is the determining factor. As an example, for a 12» pipe the following table lists the value of  $n$  for two values of  $R_a$  and Reynolds number

	Re = 1 M	Re = 10 M
Ra = 5 $\mu\text{m}$	9.13	10.3
Ra = 30 $\mu\text{m}$	8.63	9.07

Figure 3 shows that a smaller value of  $n$  indicates a more peaked velocity profile; a higher value flattens the profile. This change of the velocity profile could conceivably influence the reading of an ultrasonic flow meter, which is the reason for the investigation reported here.

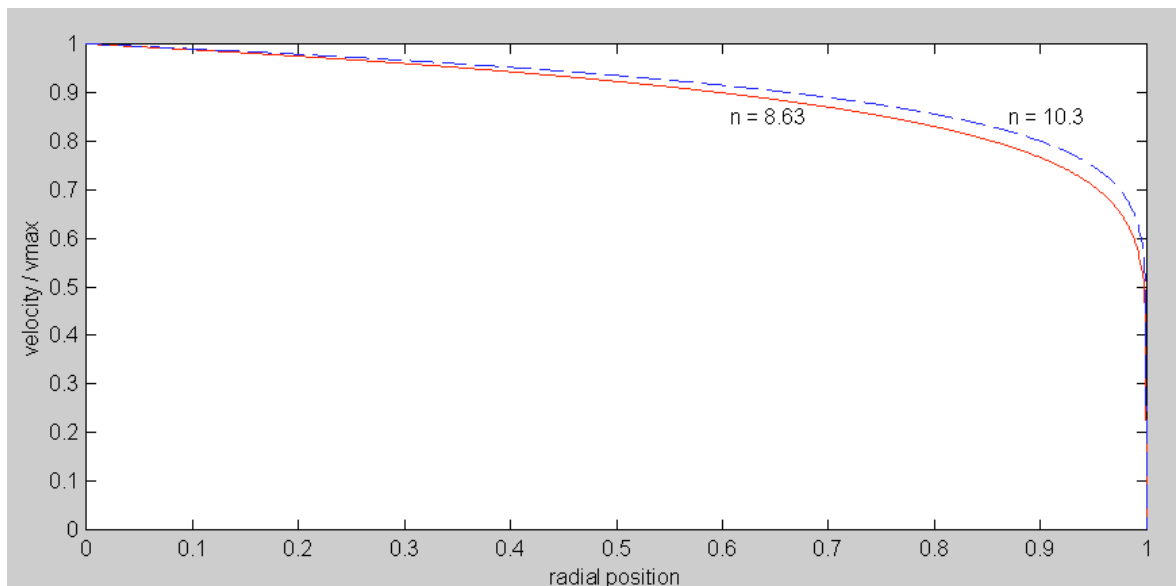


Figure 3, Velocity profile as a function of  $n$

### 3 Roughness Measurements

The inner wall roughness of four 12» pipes was measured using the stylus method, which uses a mechanical pick-up (Hommel, type T500) moving at constant speed across the surface. A linear voltage differential transformer (LVDT) generates an electrical signal that corresponds to the shape of the surface, like a magneto-dynamic cartridge of a gramophone record player. The measuring range is 160  $\mu\text{m}$  (+60/-100  $\mu\text{m}$ ). A measuring length of 15 mm was chosen, and a cut-off length of 2.5 mm. The purpose of the cut-off length is to eliminate unwanted components from the signal. Apart from  $R_a$  and  $R_z$  two other quantities were determined:  $R_{\text{max}}$  which is the depth between the highest peak and the deepest valley, and  $R_k$  which measures the middle part of the roughness distribution and does not look at the highest peaks or deepest valleys.  $R_k$  is illustrated in the next figure, taken from DIN 4776.

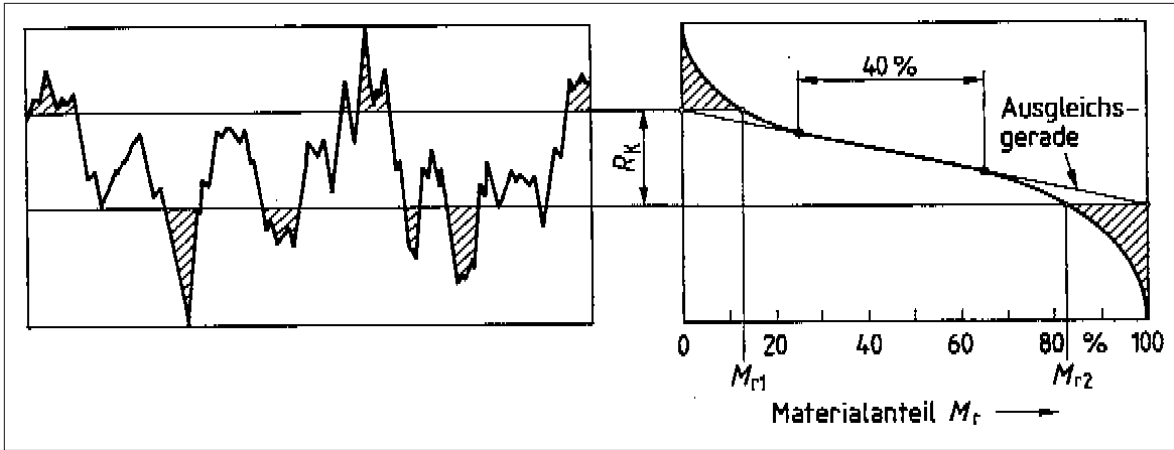


Figure 4, Definition of  $R_k$

The engineers who conducted the measurements were J. Laimmer and E. Reinhard, both from the Ruhrgas research laboratory TBZQ-Metallkunde, and specialists in roughness measurement. The laboratory is ISO 9001 certified, the measurements were carried out according to DIN standards 4768 and 4776. The roughness tests were labeled 1974.1 through 1974.4 and they were all done at the Ruhrgas test facility Pigsar in Dorsten, Germany.

Daniel Industries Canada manufactured the pipe used in test nr 1974.1 on April 29, 1998, and labeled it DCM 98 - 529. The length of the pipe is about 3.1 m and its inner diameter equals 303 mm. On May 7, 1998 its inner wall roughness was measured at 24 positions along the pipe, these tests were witnessed by the author of this report. Visual inspection showed the distribution of the roughness to be regular over the circumference of the pipe, so all 24 test positions were taken on the bottom of the pipe, documented as 600 (6 o'clock).  $R_a$  was found as  $5.1 \pm 1.6 \mu\text{m}$  mean and standard deviation, whereas for  $R_z$  a value of  $33.3 \pm 9.6 \mu\text{m}$  was obtained.  $R_m$  is  $45.6 \pm 13.7 \mu\text{m}$  and  $R_k$  is  $14.9 \pm 6.2 \mu\text{m}$ . Figure 5 shows the data.

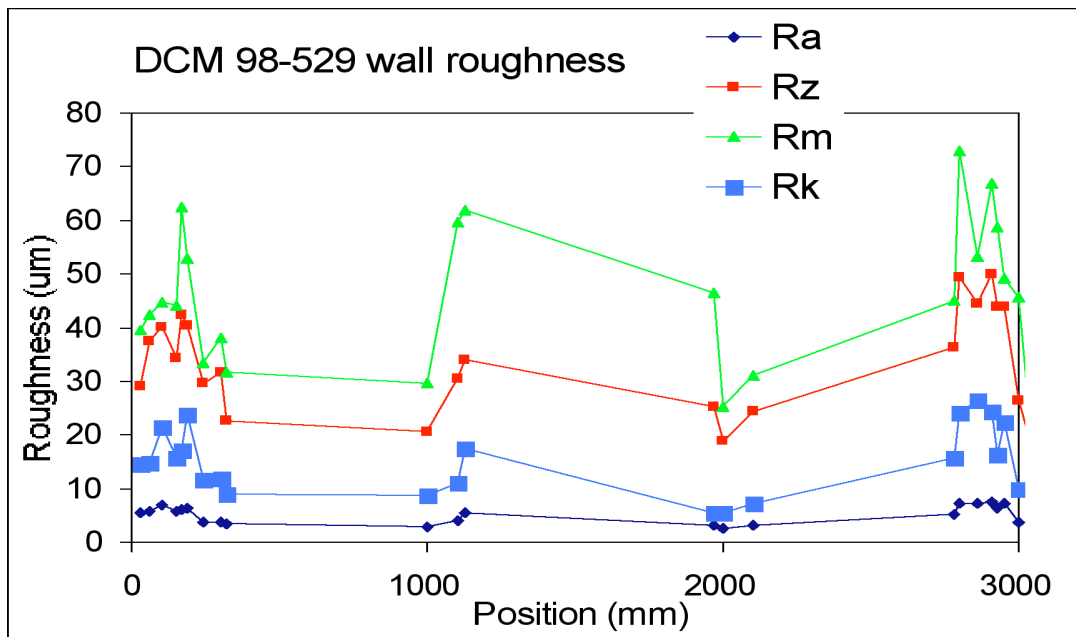


Figure 5, Wall roughness of pipe DCM 98-529

The pipe in test nr 1974.2 was manufactured by Daniel on June 15, 1998, and labeled DCM 98 - 636. It has similar dimensions as DCM 98 - 529. On August 28, 1998 its inner wall roughness was measured at 16 points along the pipe, all at 6 o'clock position.  $R_a$  was found as  $5.2 \pm 2.3 \mu\text{m}$  mean and standard deviation, whereas for  $R_z$  a value of  $36.6 \pm 13.2 \mu\text{m}$  was obtained. Figure 6 shows the data. It is clear that the two Daniel pipes have about equal roughness. A further observation is that for these pipes the standard deviations of  $R_a$  and  $R_z$  are about 30 to 40 % of their mean values, respectively. Figures 5 and 6 are graphical representations of tables 1974.1 and 1974.2 in the Ruhrgas report (Laimmer and Reinhard, 1998). As expected there is a good correlation between the various roughness measures. The next figure shows the scatter diagram of  $R_z$  versus  $R_a$ , the correlation coefficient is about 0.9 for the two DCM pipes.

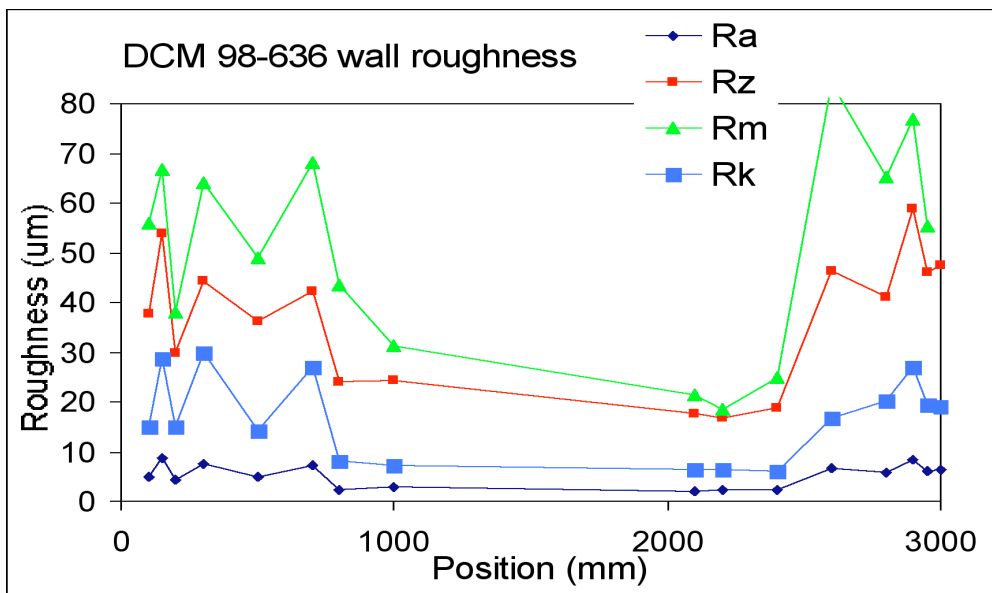


Figure 6, Wall roughness of pipe DCM 98-636

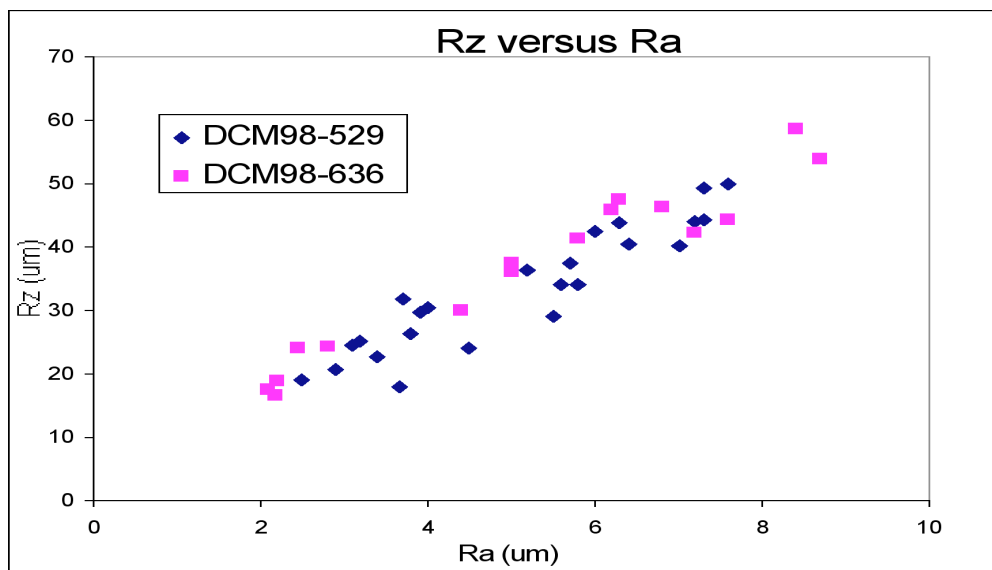


Figure 7, Correlation between  $R_z$   $R_a$

The pipe in test nr 1974.3 on August 28, 1998, belongs to the standard set of upstream pipes used during flow meter calibrations in the Pigsar facility. Its identification number is 218, and its date of manufacturing is unknown. It has a length of 5.10 m and its inner diameter is 310 mm. Like all the pipes in the Pigsar facility its inner surface has been sand blasted, in order to obtain a uniform wall roughness. Most of the surface is corroded, and therefore the wall roughness is considerably higher than that of the two Daniel tubes. At only one point, 50 cm from the flange, the roughness was within in the measuring range.  $R_a$  was found as  $8.7 \mu\text{m}$ ,  $R_z$  as  $58.3 \mu\text{m}$ ,  $R_m$  as  $64.9 \mu\text{m}$  and  $R_k$  as  $26 \mu\text{m}$ . At all the other locations the roughness was outside the measuring range of  $+60$  to  $-100 \mu\text{m}$ . This means that  $R_a$  is definitely greater than  $10 \mu\text{m}$ , probably  $20 \mu\text{m}$ , according to Mr Laimmer.

Finally, test nr 1974.4 on August 28, 1998, concerned a very old pipe, manufactured in May 1978 by Barber Engineering, labeled 11.947, with a length of about 3.4 m and an inner diameter of 304 mm. Due to the heavy corrosion, the inner wall roughness exceeded the measuring range over the entire length of the pipe. No measured data could be obtained, so  $R_a$  far exceeds  $10 \mu\text{m}$ , probably  $20 \mu\text{m}$ , according to Mr Laimmer.

## 4 Flow Calibrations

All flow calibrations reported here were conducted at the Pigsar test facility in Dorsten, Germany, at an absolute gas pressure of about 45 bar. The first calibration took place on May 7, 1998. A 3-path Q.Sonic® ultrasonic flow meter (Instromet®), was mounted in line nr 2, directly downstream of pipe nr 218. The diameter of the flow meter is 0.3033 m, its serial number is 98Q06017, the spoolpiece was manufactured in the USA. The Final Factor of the meter was set exactly equal to one. The gas temperature was 16 C and the pressure was 45 bara. At each flowrate (given in actual m<sup>3</sup>/hr) three consecutive measurements were done of 100 seconds each, at the highest flowrate of 50 seconds each. The table lists the results.

Flow m <sup>3</sup> /hr	Velocity m/s	1 <sup>st</sup> point %	2 <sup>nd</sup> point %	3 <sup>rd</sup> point %
6100	23	0.160	0.110	0.172
5200	19.5	0.114	0.140	0.095
4000	15	0.048	0.121	0.057
2400	9	0.133	0.062	0.086
1600	6	0.078	0.027	0.042
800	3	0.174	0.183	0.121
400	1.5	0.577	0.538	0.523

The OIML weighted mean error equals 0.121 %.

Then the pipe nr 218 was removed and the DCM 98-529 pipe was mounted directly upstream of the ultrasonic flow meter. The calibration was repeated with this new upstream pipe, again at a pressure of 45 bara, but at a gas temperature of 14 C. This time the OIML error appeared to be -0.008 %. The next table presents the results.

Flow m <sup>3</sup> /hr	Velocity m/s	1 <sup>st</sup> point %	2 <sup>nd</sup> point %	3 <sup>rd</sup> point %
6000	23	0.016	0.038	0.024
5100	19	-0.021	-0.112	-0.109
4000	15	0.028	0.044	-0.020
2400	9	-0.020	0.005	-0.047
1600	6	-0.055	-0.071	-0.046
800	3	0.048	0.036	0.065
400	1.5	0.516	0.376	0.392

Figure 8 shows the results, the graph is based on the Excel file from the Pigsar facility.

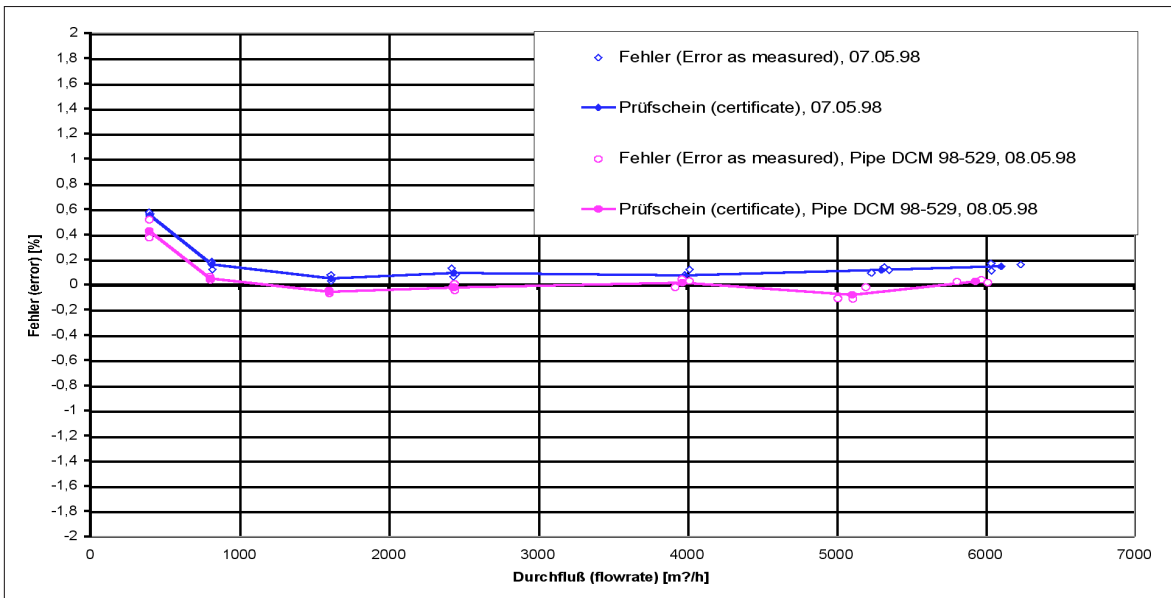


Figure 8, Calibration results of pipes 218 and DCM 98-529

The next series of tests started on August 25, 1998. A similar 3-path ultrasonic meter, serial number 98Q06104 was mounted on line nr 2, directly downstream of pipe DCM 98-636. The diameter of the flow meter is 0.3030 m, the spoolpiece was manufactured in the USA. The Final Factor of the meter was set exactly equal to one. The gas temperature was 11 C and the pressure was 45 bara, during the first calibration of the meter.

Based on the results shown in the table above, the Final Factor of the meter was adjusted by 0.2 % to 0.9980, after which the resulting OIML weighted error equals 0.0005 %. So the remaining errors can be found by subtracting 0.2 % from the entries in the above table. After this adjustment one more point at 400 m<sup>3</sup>/hr was measured as a verification that no errors had been made in the adjustment. The adjusted unweighted average over the flowrates of 5400, 2400 and 800 m<sup>3</sup>/hr equals -0.030 %. This value is important as a reference for the tests on September 1. First the base line of August 25 was checked with the DCM 98-636 pipe upstream of the meter. The gas temperature was 15 C and the pressure 45 bara. The next table lists the results.

Flow m <sup>3</sup> /hr	Velocity m/s	1 <sup>st</sup> point %	2 <sup>nd</sup> point %	3 <sup>rd</sup> point %
6100	23	0.245	0.175	0.220
5400	20	0.211	0.237	0.264
4000	15	0.223	0.146	0.262
2400	9	0.138	0.120	0.136
1600	6	0.064	0.081	0.092
800	3	0.149	0.160	0.119
400	1.5	0.131	0.057	0.007

The unweighted average is -0.086 %, which is an indication of the repeatability of both the meter and the facility. Then the old and dirty pipe, Barber Engineering labeled 11.947, was mounted directly upstream of the ultrasonic meter. The gas temperature was 14 C and the pressure was 43 bara, when the meter was calibrated at 5500, 2400 and 800 actual m<sup>3</sup>/hr. In this case the unweighted average is 0.041 %, which means an unweighted average shift of 0.127 %, the largest difference occurs at the highest flowrate.

Flow m <sup>3</sup> /hr	Velocity m/s	1 <sup>st</sup> point %	2 <sup>nd</sup> point %	3 <sup>rd</sup> point %	4 <sup>th</sup> point %
5500	21	0.069	0.056	0.035	
2400	9	-0.100	-0.056	-0.096	
800	3	-0.230	-0.210	-0.148	-0.181

Then the DCM 98-636 was put back in place, to once more verify the stability of the meter reading, the results are shown below. Pressure was 46 bara, temperature 13 C. This time the unweighted average equals -0.096 %, which

Flow m <sup>3</sup> /hr	Velocity m/s	1 <sup>st</sup> point %	2 <sup>nd</sup> point %	3 <sup>rd</sup> point %	4 <sup>th</sup> point %
5500	21	0.210	0.185	0.177	
2400	9	0.060	0.131	0.060	
800	3	-0.101	-0.091	-0.183	-0.030

again verifies that the meter and the facility are stable. The dirty Barber 11.947 pipe shifts the meter curve by about 0.1 to 0.2 % in upward direction. The graph below summarizes all results obtained on September 1, 1998.

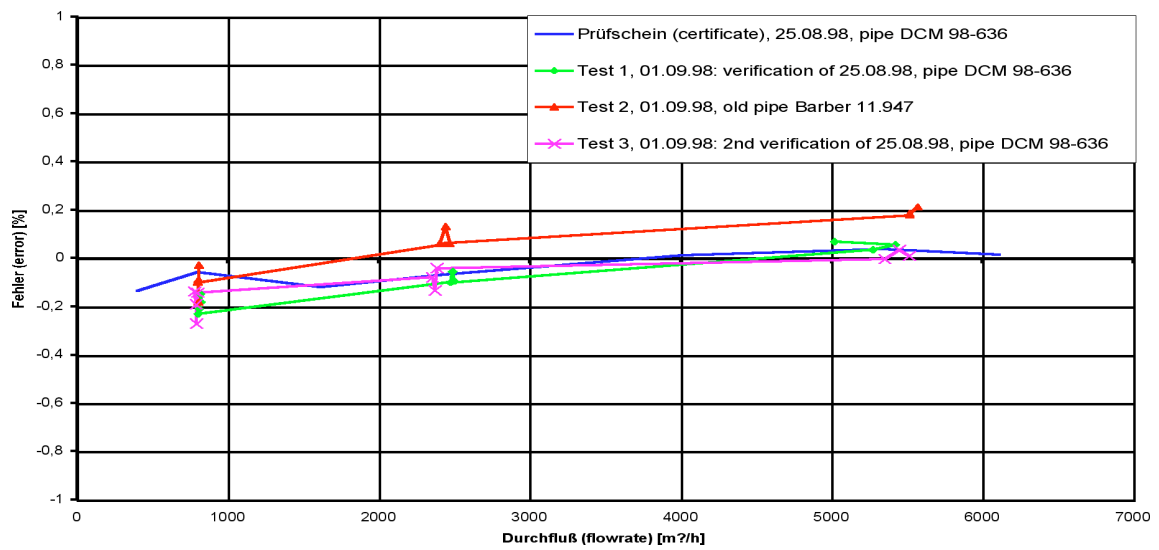


Figure 9, Test results of pipes DCM 98-636 and Barber 11.947

## 5 Conclusion

The results of the roughness measurements and the flow calibrations are summarized in the following table

Date	Pipe s/n	Pipe Ø (m)	Ra µm	Rz µm	Meter s/n	Error %	Mean
May 7	218	0.310	≥ 8.7	≥ 58.3	6017	0.121	OIML
May 7	529	0.303	5.1	33.3	6017	-0.008	OIML
Aug 25	636	0.303	5.2	36.6	6104	0.0005	OIML
Aug 25	636	0.303	5.2	36.6	6104	-0.030	3 pts
Sept 1	636	0.303	5.2	36.6	6104	-0.086	3 pts
Sept 1	947	0.304	20?	100?	6104	0.042	3 pts
Sept 1	636	0.303	5.2	36.6	6104	-0.096	3 pts

The date refers to the flow calibration, the roughness measurements were done on different dates. For August 25 the two rows differ in the way the error is calculated: in the first row it is the OIML weighted error based on all flow rates from 6100 to 400 m<sup>3</sup>/hr, in the second row it is an unweighted average over the three flowrates of 5400, 2400 and 800 m<sup>3</sup>/hr which are similar to those used on September 1.

The two pipes used on May 7 differ in two aspects: wall roughness and inner diameter. Recall that the diameter of the 98Q06017 flow meter itself equals 0.3033 m. It can not be excluded with complete certainty that the observed difference in meter reading of 0.129 % to some extent might be caused by the change of diameter rather than wall roughness. The effect of upstream pipe diameter is outside the scope of the present study, just like the possible interaction between upstream diameter and wall roughness.

In the second series of tests the two pipes have virtually equal diameter, so the observed difference of 0.128 % or 0.138 % quite likely is the result of wall roughness only. Now that we have reached this conclusion, we may take a second look at the May 7 data. Then it seems not unlikely that, whatever the interaction between diameter and roughness, the effect of a two percent change in upstream pipe diameter is of the same order of magnitude as the observed difference in meter reading, that is 0.1 to 0.2 %.

From the data obtained in the present investigation, the roughness of a 10 D pipe directly upstream of a 12» meter appears to have some influence on the reading of a 3-path ultrasonic meter. Over the range of conditions investigated, an increase of the roughness  $R_a$  from about 5  $\mu\text{m}$  to probably 20  $\mu\text{m}$  appears to increase the meter reading by about 0.1 - 0.2 %.

## 6 References

Colebrook, C.F. (1939) Turbulent flow in Pipes, with particular reference to the transition region between the smooth and rough pipe laws. Journal Inst. Civ. Eng., pp 133 - 156

Kam, P.M.A. van der (1993) Personal Communication

Laimmer, J. and Reinhard E. (1998) Rauheitsmessung an Einlaufrohren, Pigsar Dorsten. Untersuchungsbericht 1974 / 98. Ruhrgas AG, TBZQ-Metallkunde

Schlichting, H. (1968) Boundary-Layer Theory, 6th ed., McGraw Hill, New York



# THE EFFECTS OF REYNOLDS NUMBER, WALL ROUGHNESS, AND PROFILE ASYMMETRY ON SINGLE- AND MULTI- PATH ULTRASONIC METERS

*Klaus J. Zanker, Daniel Industries*

---

## 1. ABSTRACT

A simple “power law” velocity profile is used to study the effects of pipe roughness and Reynolds Number ( $Re$ ) on ultrasonic meter performance. Considered here are two measurement methods. The first utilize a single bounce path through the pipe center, and is common to multipath as well as single path meters. The second employs four parallel chordal paths, (e.g. Daniel SeniorSonic).

The single path centerline measurement requires typical corrections from 4% to 8% for changes in velocity profile due to variations in pipe roughness and  $Re$ . A correction for  $Re$  can be calculated from additional information on fluid density and viscosity, but changes of roughness with time cannot be measured, and hence cannot be corrected. It will be shown that the four path meter does an excellent job of integrating the velocity profile to give the correct flow rate over a wide range of both  $Re$  and roughness.

A mathematically generated profile similar to that from a single bend is used to study the effects of asymmetry on the performance of both measurements. The centerline measurement varies over about 1.5%, depending on the path orientation relative to the asymmetry. Unfortunately applying a typical  $Re$  correction then creates a bias error of about 4%. In contrast, the four path meter accurately integrates the velocity profile to give an answer within 0.2% of the flow irrespective of orientation. Furthermore the four-path meter is capable of recognizing the changes in operating conditions.

## 2. EFFECTS OF REYNOLDS NUMBER AND WALL ROUGHNESS ON SINGLE PATH CENTER LINE ULTRASONIC METERS

### Power Law Velocity Profile

The velocity profile in pipe flow is quite complex, but a simple power law is a good approximation everywhere except at the pipe center, where the velocity gradient  $(dv/dy)_R$  exhibits a discontinuity. This is not too serious because there is no flow through the exact center of the pipe, since the area is zero.

The power law profile is defined by

$$\frac{v}{V_{\max}} = \left[ \frac{y}{R} \right]^{\frac{1}{n}}$$

where

- $V_{\max}$  = the velocity at the meter axis
- $y$  = the distance from the meter wall
- $n$  = the 'power'
- $v$  = the velocity at  $y$
- $R$  = the meter radius

By integrating over the pipe area, one obtains the average flow velocity  $V_{\text{avg}}$  from

$$Q = \pi R^2 V_{\text{avg}} = \int_0^R v 2\pi r dr = 2\pi \int_0^R V_{\max} \left( \frac{y}{R} \right)^{\frac{1}{n}} (R - y) dy$$

where

- $Q$  = the volumetric flow rate
- $r$  = the radial location of  $v$  ( $r = R - y$ )

After integration this yields

$$V_{\text{avg}} = V_{\max} \frac{2n^2}{(n+1)(2n+1)}$$

By integrating along the pipe diameter, one obtains the average center chord velocity  $V_{\text{chd}}$  from

$$V_{\text{chd}} R = \int_0^R v dy = \int_0^R V_{\max} \left( \frac{y}{R} \right)^{\frac{1}{n}} dy$$

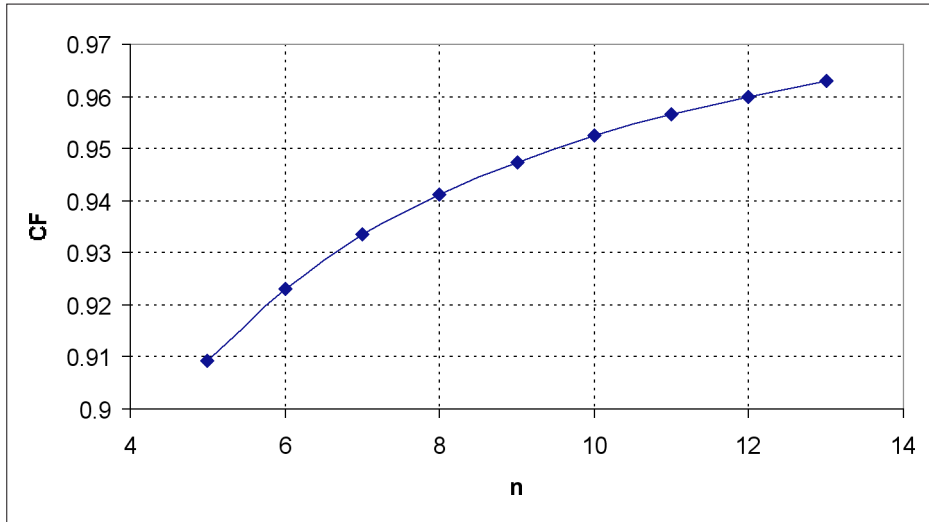
which after integration yields

$$V_{\text{chd}} = V_{\max} \frac{n}{n+1}$$

A correction factor CF can then be defined as the factor used to bring the center chordal velocity to the true average velocity.

$$CF = \frac{V_{avg}}{V_{chd}} = \frac{2n}{2n+1}$$

It is plotted in Figure 1 as a function of the power law exponent.



### Wall Roughness, Reynolds Number, and the Power Law Profile

To be able to use this correction factor one needs to find a way of expressing  $n$  in real world terms of  $Re$  and Wall Roughness  $WR$ . Fortunately, Prandtl and Nikuradse [Ref.1] sorted this out in the 1930's when considering the friction loss in pipe flow. The friction factor ( $f$ ) depends upon  $Re$  and the relative Wall Roughness  $WR/d$  (to the pipe diameter  $d$ ), but can also be related to the velocity profile through the shear stress at the pipe wall. The friction loss is proportional to the wall shear stress, which in turn is proportional to the velocity gradient at the pipe wall.

$$n = 1.74 - 2 \text{LOG} \left( \frac{2WR}{d} + 18.7 \frac{n}{Re} \right) \quad \text{and} \quad n = \frac{1}{\sqrt{f}}$$

The relationship is given by:

$$n = 1.74 - 2 \text{LOG} \left( \frac{2WR}{d} \right)$$

This simplifies for the two special cases. For hydraulically smooth pipe flow with  $WR = 0$ , This is shown in Figure 2

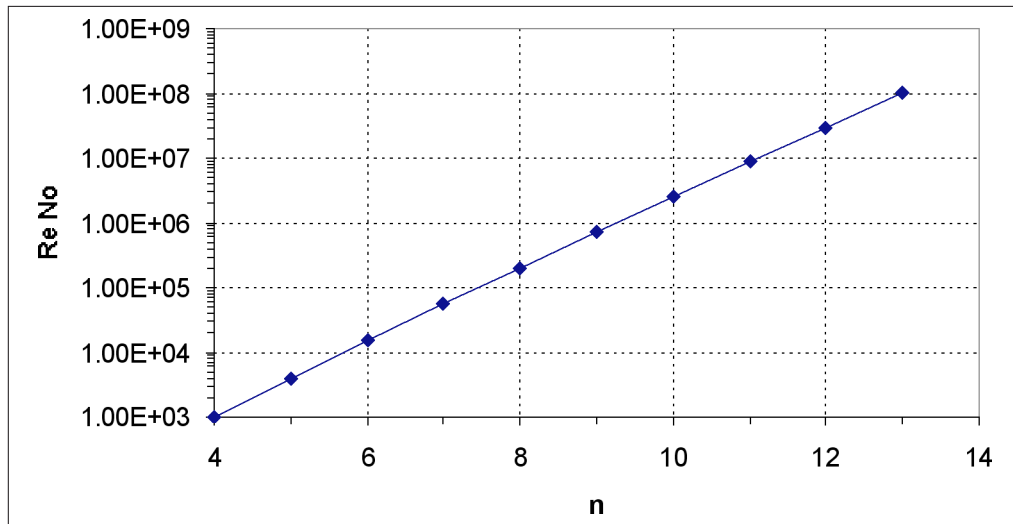


Figure 2. Relation of  $n$  to Reynolds number in smooth pipe flow.

Then for fully turbulent rough pipe flow, as  $Re \rightarrow \infty$

$$n = 1.74 - 2 \text{LOG} \left( \frac{2WR}{d} \right)$$

This is shown in Figure 3.

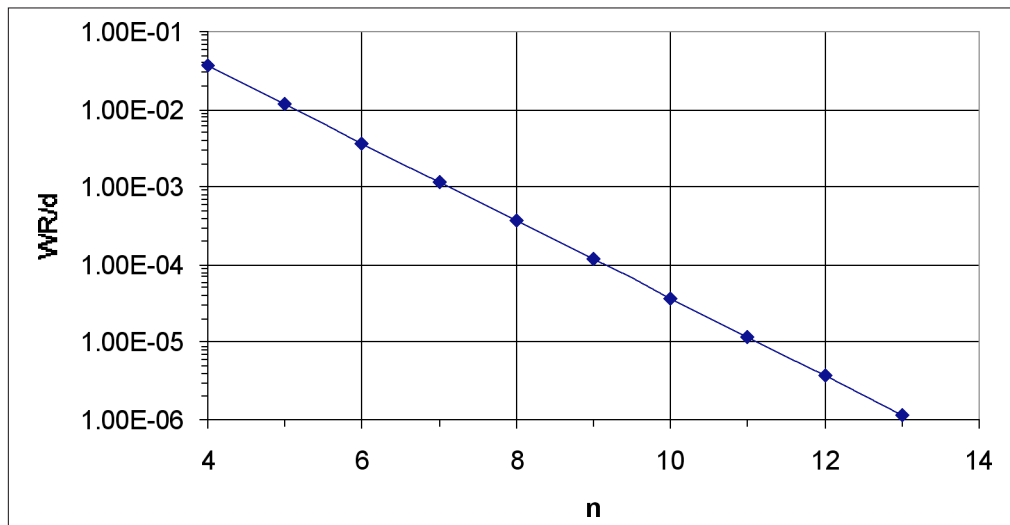


Figure 3. Relation of  $n$  to wall roughness in fully turbulent flow.

### Practical Implications

This work shows that a meter using a single path through the center of the pipe will overestimate the flow by between 4% and 9% if no correction factor is applied. The overestimate is due to the high velocity in the center of the pipe affecting the line integral disproportionately to the small area represented.

It is quite straightforward to calculate the Reynolds Number ( $Re$ ) from:

$$Re = \frac{vd\rho}{\mu}$$

Measuring the pressure and temperature allow reasonable estimates of the density  $r$  and viscosity  $m$ . Then the correction factor CF can be calculated from this live value of  $Re$ . If the relative Wall Roughness  $WR/d$  is known it is easy to calculate a correction factor. Although  $WR/d$  might be known for a new pipe, there is no measure of how it changes with time. Hence it is not possible to make a real-time profile correction for  $WR/d$ . The effects of changing roughness are shown in Figure 4.

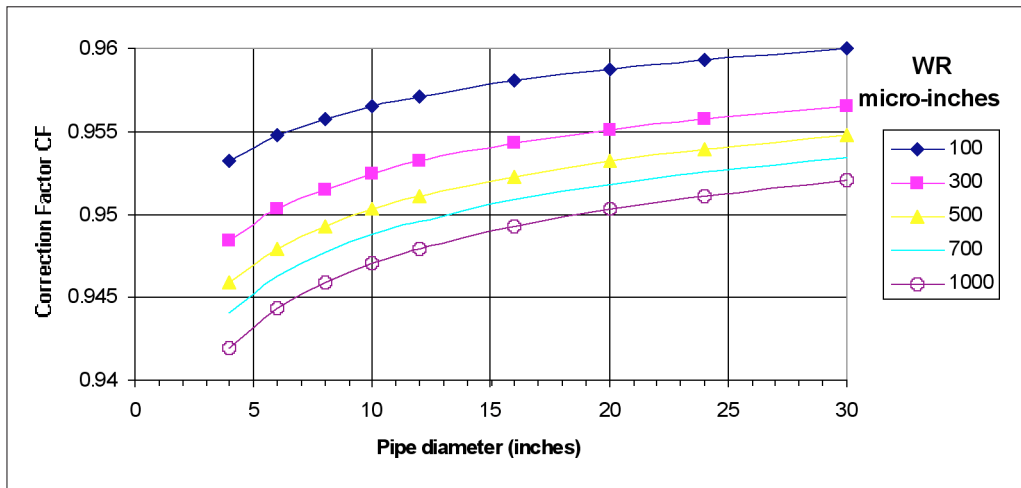


Figure 4. Variation of CF with pipe roughness and diameter.

Thus it is quite easy to produce 0.5 to 1% error with time as the pipe roughness changes, without any means of correction.

### 3. EFFECTS OF REYNOLDS NUMBER AND PIPE ROUGHNESS ON A FOUR-PATH ULTRASONIC METER

#### The Four-Path Ultrasonic Meter Geometry

An arrangement of four chordal paths proposed by British Gas is that shown in Figure 5.

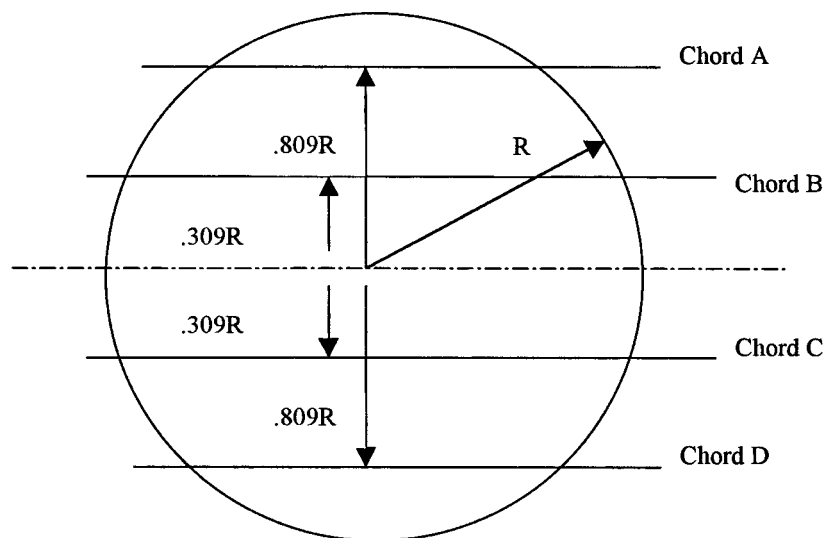


Figure 5. Ultrasonic multipath geometry proposed by British Gas.

A Gauss-Jacobi numerical integration [Ref.2] gives the average flow velocity  $V_{avg}$  over the area of the pipe from the weighted sum of the line averages along the chords  $V_i$

$$V_{avg} = \sum_{i=1}^{i=4} W_i V_i = 0.1382V_A + 0.3618V_B + 0.3618V_C + 0.1382V_D$$

where the weighting factors,  $W_i$ , are determined for the specific chord locations. Note that

$$\sum W_i = 1$$

It is significant that integration of a uniform velocity profile, using this method would give the correct answer. Another interpretation of the weighting factors  $W_i$  is the proportion of pipe area associated with each chord to obtain the flow, the sum of which must be 1 unity.

The average chord velocity  $V_i$  is obtained as shown in Figure 6.

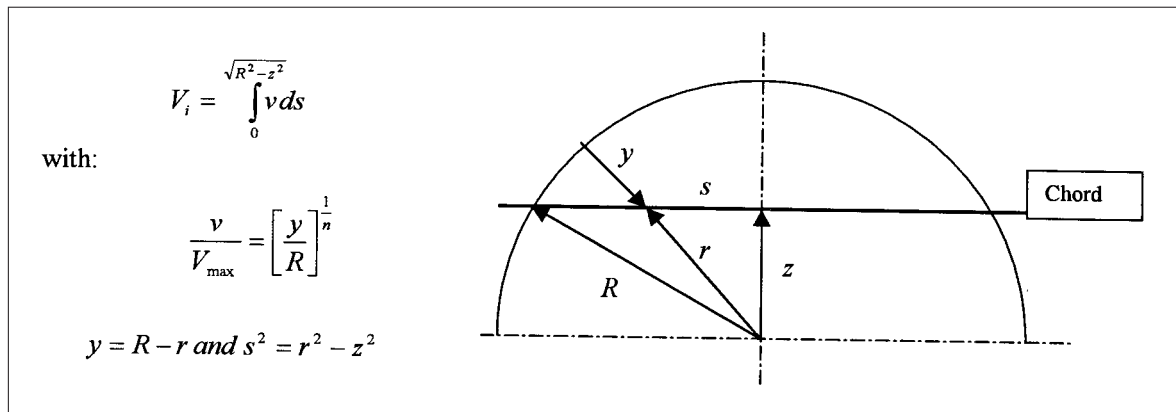


Figure 6. Evaluation of chordal integration.

This is integrated numerically by dividing the integration path  $s$  into 10 or more parts. Care is required with the segment next to the wall because of the very steep velocity gradient.

### Chordal Integration

Numerical integration of the chord velocities for the four-path configuration has been performed for a range of  $n$  in the power law distribution. A typical example for  $n = 7$  and  $n = 12$  is shown in Figure 7.

Note, these represent the same average flow with  $V_{avg} = 1$ , hence if the velocity increases in the center of the pipe it must decrease near the wall to maintain continuity. In this example the velocity on the centerline increases from 1.04 to 1.07, which is the error made by a meter using a single path through the centerline. However, with the four-path meter when the velocity on Chord-B increases, that on Chord-A decreases. The decrease on Chord-A is greater than the increase on Chord-B, but this is compensated for by the weighting factors to give virtually the same flow.

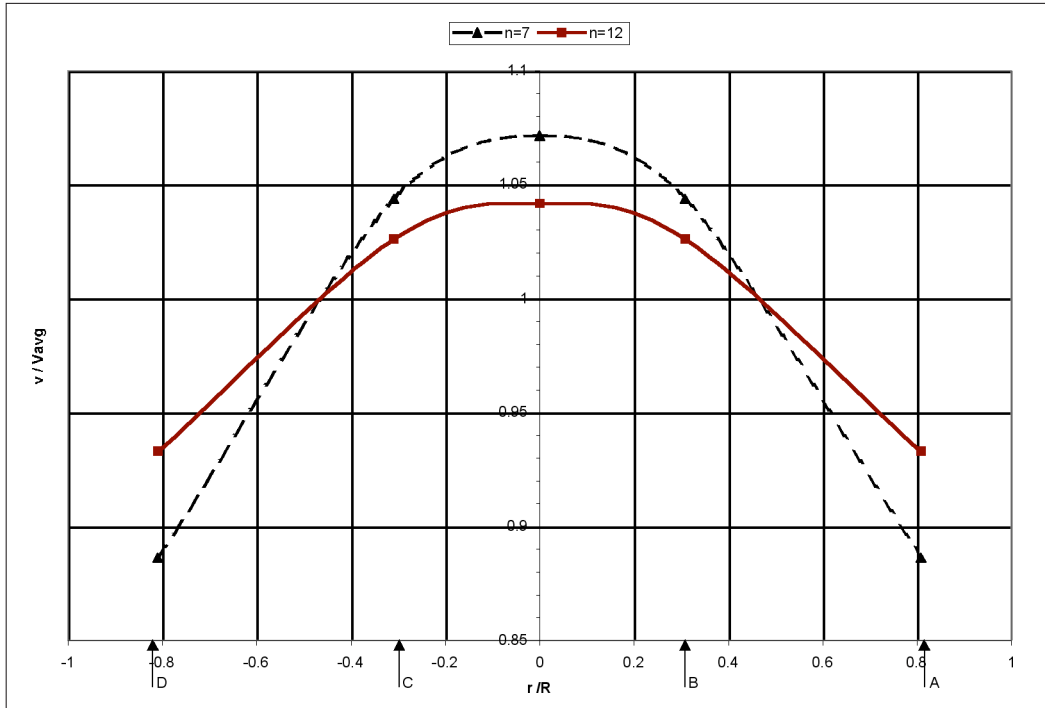


Figure 7. Velocity profile with four-path meter for two values of  $n$ .

The numerical integration process is shown in the table below:

$n$	$V_B, V_C$	$V_A, V_D$	$W_1 (V_B + V_C)$	$W_2 (V_A + V_D)$	$V_{avg}$	$V_{BC} / V_{AD}$
7	1.0437	0.8861	0.7552	0.2449	1.0002	1.1778
12	1.0260	0.9329	0.7424	0.2579	1.0003	1.0998

Furthermore there is information to show that the velocity profile has changed, by the ratio  $V_{BC}/V_{AD}$ , due to either Reynolds No or pipe roughness.

This process is repeated for values of  $n$  from 4 to 14, and the four-path meter (SeniorSonic) is compared to the single path through the centerline (JuniorSonic) with the result shown in Figure 8.

The four-path meter does an excellent job of integrating a power law profile, with a maximum error of 0.06% at  $n = 4$ , and from  $n = 5$  to 14 the error is reduced to 0.03%. Thus the meter should be immune to normal changes in Reynolds Number and pipe roughness, whereas the meter which depends on a single path through the center shows a 7% variation over the complete range.

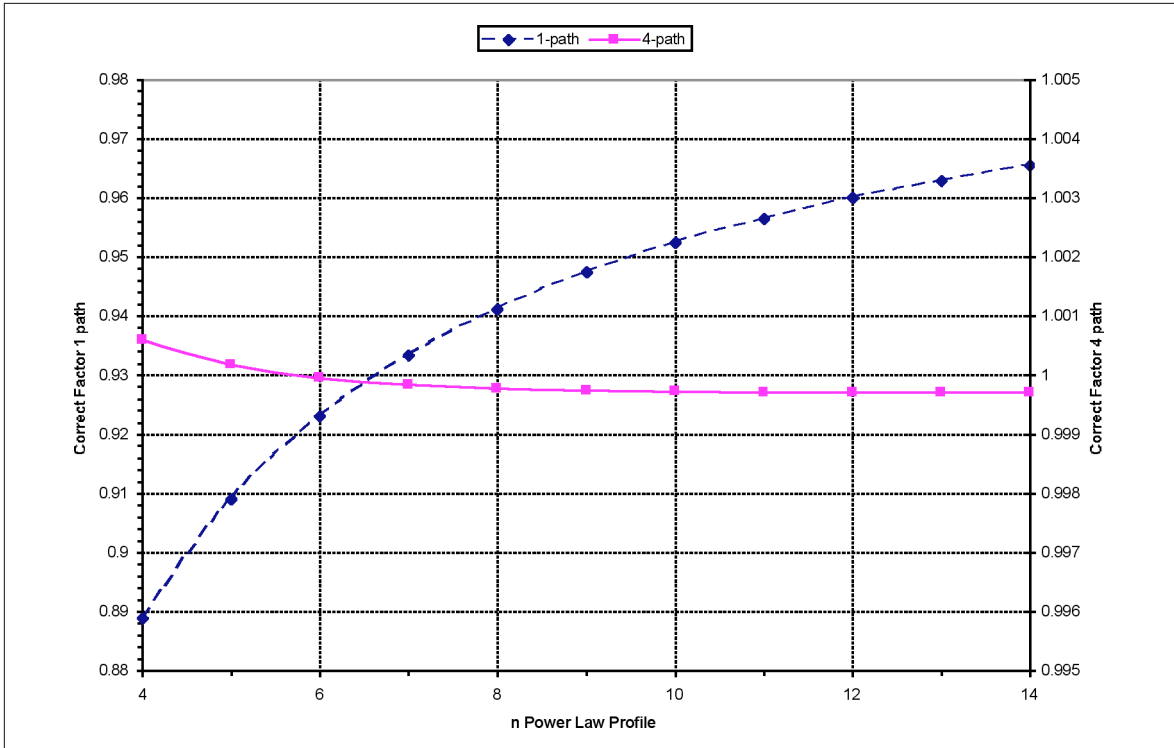


Figure 8. Effect of changing power-law profile on performance of centerline and Daniel four-path meters.

We can also make use of the ratio  $V_{BC}/V_{AD} = (V_B + V_C)/(V_A + V_D)$  to examine the velocity profile that exists in the pipe, and use the ratios  $V_B/V_C$  and  $V_A/V_D$  to check for symmetry. In reasonably well developed axi-symmetrical flow conditions, we would expect  $V_B/V_C = 1$ ,  $V_A/V_D = 1$ , and  $V_{BC}/V_{AD}$  to range from 1.10 to 1.18, as shown in Figure 9.

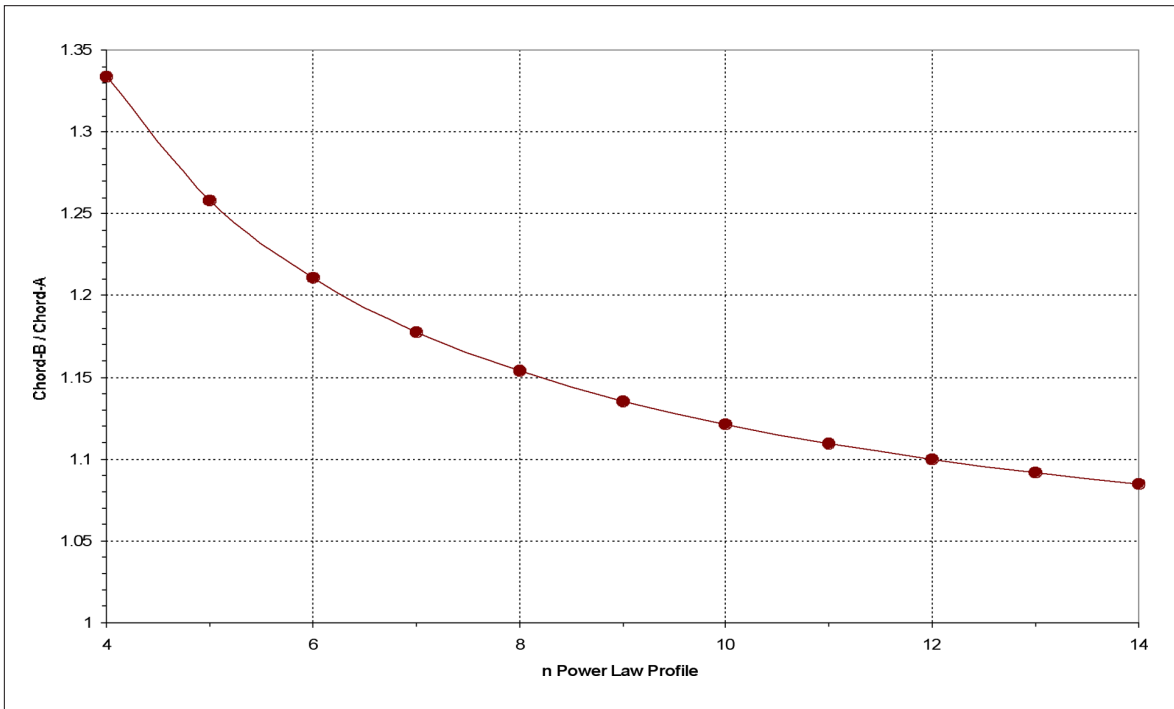


Figure 9. Variation of velocity ratio  $V_{BC}/V_{AD}$  with power law profile for the Daniel four-path meter.

## 4. THE EFFECT OF FLOW PROFILE ASYMMETRY ON SINGLE AND MULTI PATH ULTRASONIC METERS

### The profile

For this study, a mathematical model of the velocity profile downstream of a 90° elbow was used [Ref. 3]:

$$V(r, \theta) = \frac{2}{\pi^5} * r(1-r)^{1/4} * \theta^2(2\pi - \theta)^2 + (1-r)^{1/9}$$

In cylindrical coordinates,  $r$  is the radial position from 0 at the center to 1 at the meter wall, and  $q$  is the angle in radians. This profile is plotted as velocity contours in Figure 10.

Note that when  $r = 0$  (center),  $V = 1$ , and when  $r = 1$  (wall),  $V = 0$ . The maximum asymmetry occurs when  $q^2(2\pi - q)^2$  is a maximum i.e. when  $q = \pi$ .

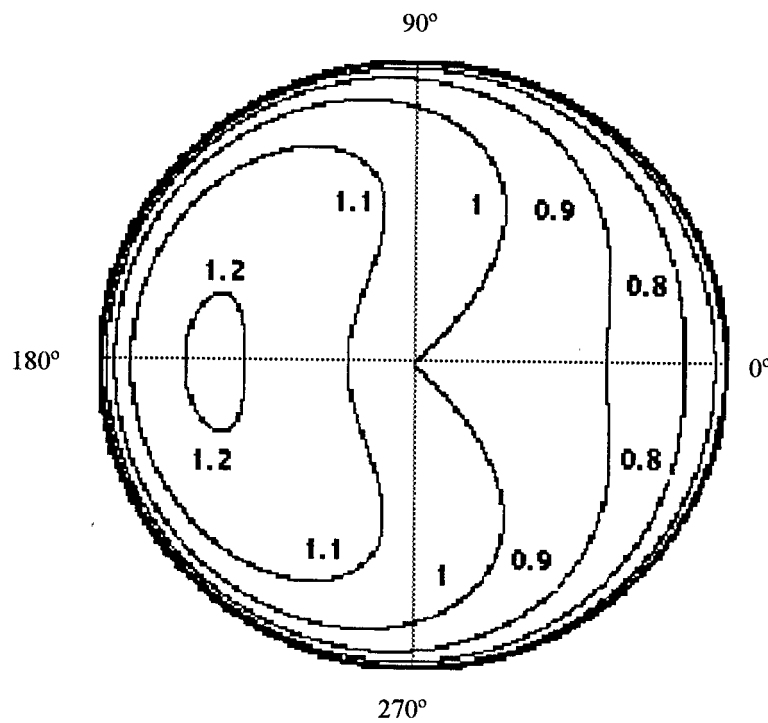


Figure 10. Mathematical model of velocity profile downstream of a single 90° elbow.

### Centerline Meters

For a single path through the centerline the results shown in Figure 11 are obtained, normalized for an average flow velocity = 1.

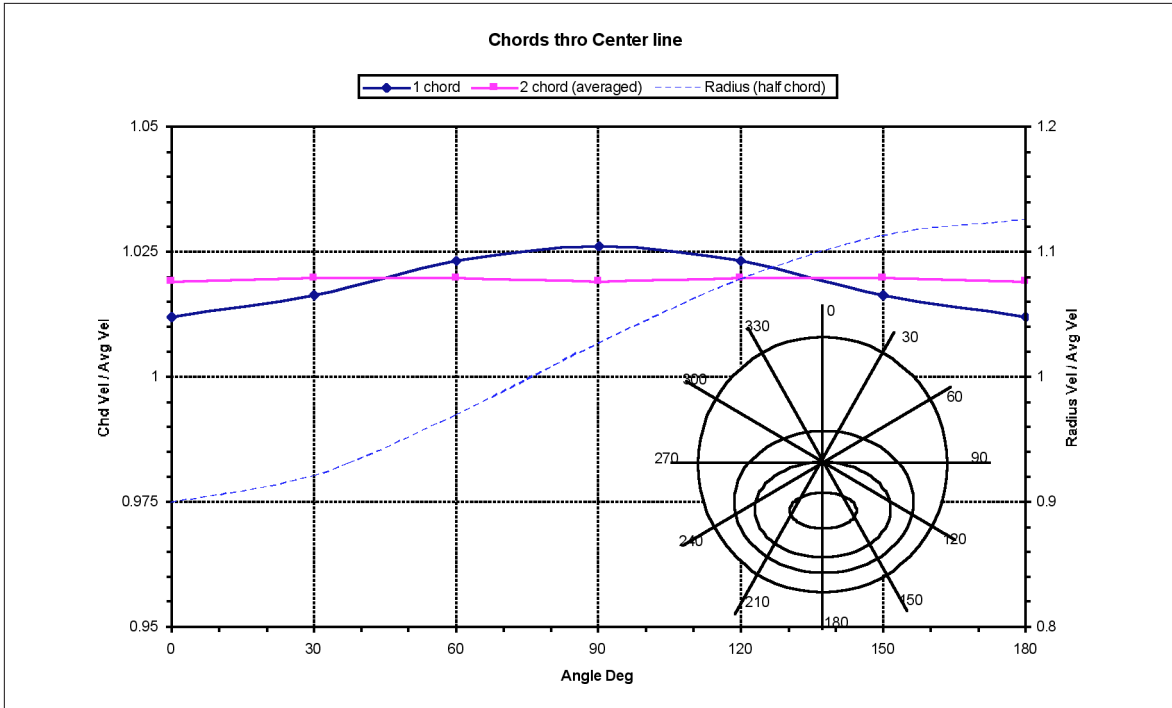


Figure 11. Velocities measured along centerline chords at various angles.

To give an idea of the asymmetry, the velocity which would be measured along a radius (half a chord) is shown by the broken line and second y-axis. The minimum velocity at  $0^\circ$  is 0.9 and the maximum at  $180^\circ$  is 1.125 i.e. a 25% variation.

The variation of velocity with the angular position ( $\theta$ ) of the diameter is much less: 1.012 at  $0^\circ$  and 1.026 at  $90^\circ$  or 1.4% and the actual value of the velocity is quite close the average flow velocity of 1. However, since it is normal practice to make a Reynolds number correction (CF) for a single path through the centerline as shown in Figure 1, with  $n = 9$  the power law velocity profile  $CF = 0.947$ . Thus the meter output would vary from 0.958 to 0.972, or a 3 – 4% error.

If two diameters are used at right angles to one another, made up from  $0^\circ$  and  $90^\circ$ ,  $30^\circ$  and  $120^\circ$ , etc., the output is virtually constant at 1.02 making the two path meter independent of angular position. Once again the Reynolds number correction will turn this +2% error into a –3% error and is not good in disturbed flows.

### Four-path SeniorSonic

Integrating along the chords of the four-path meter, located at +/- 0.309 R and +/- 0.809 R gives the results shown in Figure 12.

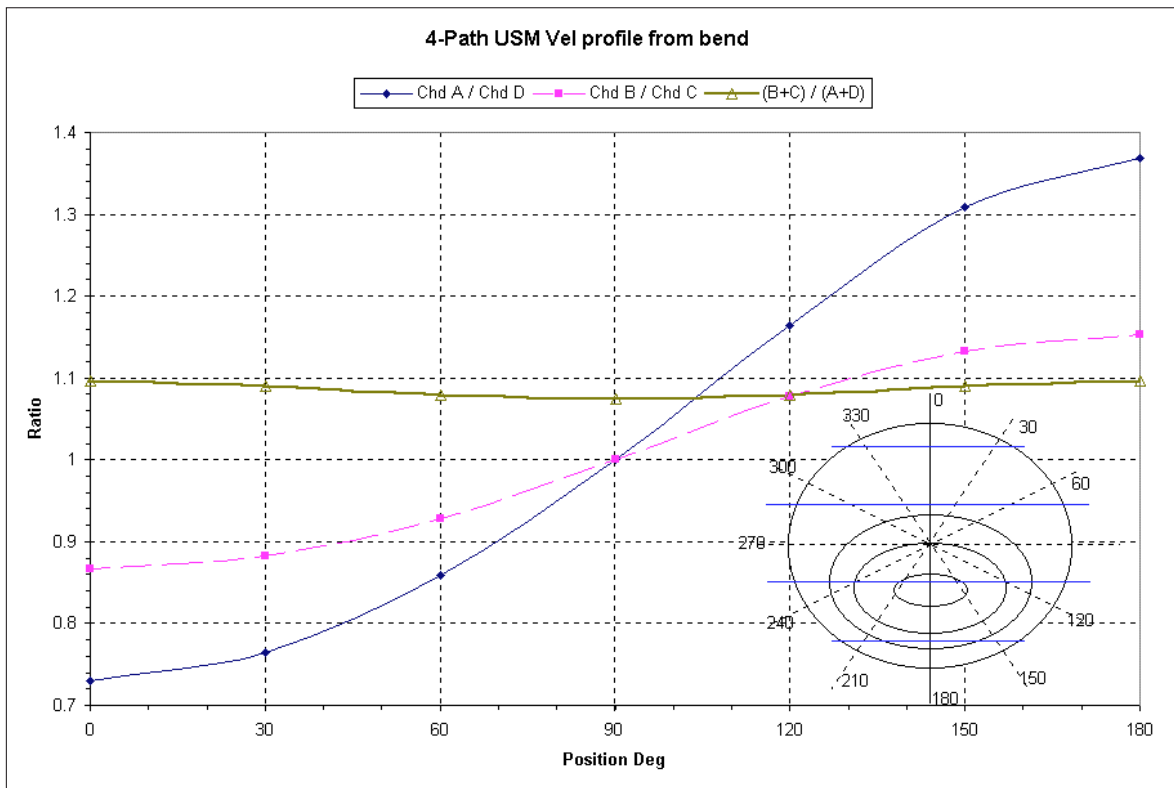


Figure 12. Chord measurements from four-path USM downstream from a bend.

The profile is not axi-symmetric, so the four-paths reflect the asymmetry in all cases except at the 90° position, where the paths and profile are symmetric about the 0° position. This is a mathematical profile which would never perfectly exist in practice, but which can be used to simplify integration.

The ratios of chord velocities can again be used as a measure of asymmetry as shown in Figure 13. In fully developed flow the velocities of the outer chords are 0.89 and the inner chords are 1.042, so  $V_A / V_D = V_B / V_C = 1$  and  $V_B / V_A = V_C / V_D = 1.042 / 0.89 = 1.171$

When the profile looks symmetrical at 90°,  $V_{BC} / V_{AD} = 1.075$  which is 10% off normal (1.171) and suggests that the profile is too flat.

The outer and inner chord velocities are shown in Figure 14, together with the results of the integration for the average flow velocity. The four-path integration technique does a very good job on this asymmetric profile, and is 0.2% high virtually independent of the angular orientation of the chords (shown on second Y axis).

The mean chord data gives  $V_{AD} = 0.94$  and  $V_{BC} = 1.03$ , which again appears more flat than the normal fully developed flow.

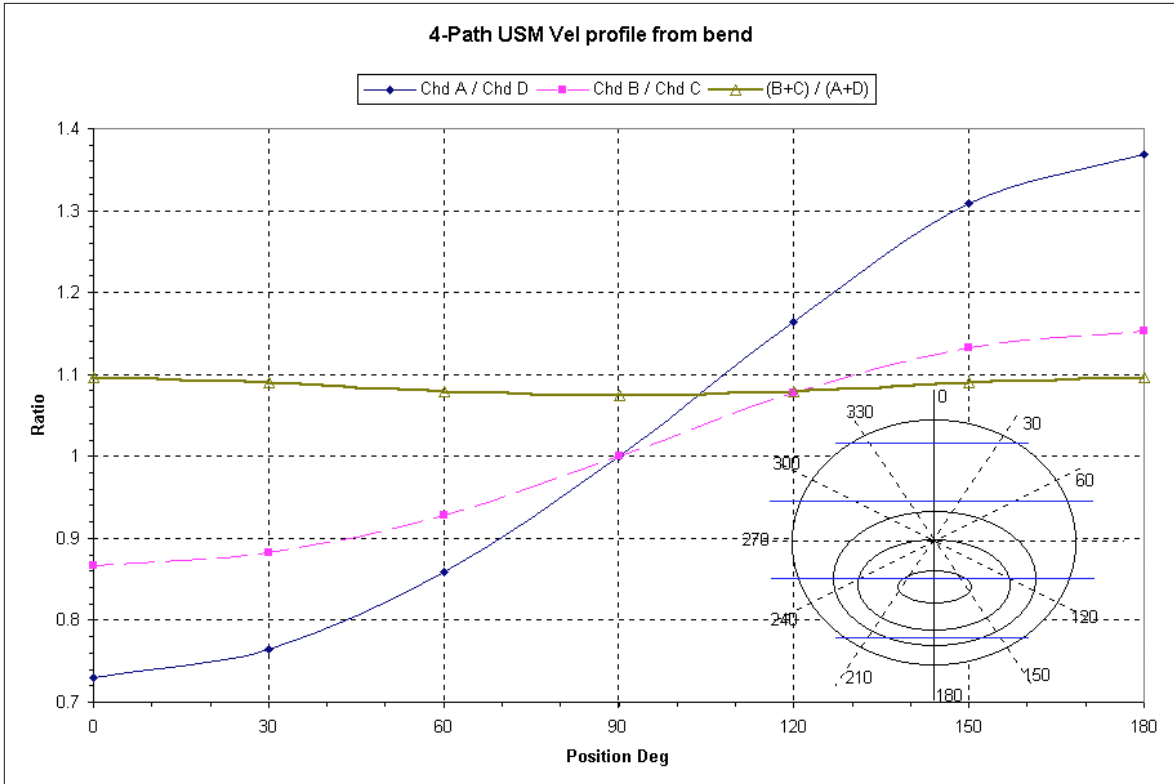


Figure 13. Velocity ratios from four-path ultrasonic meter downstream of a bend.

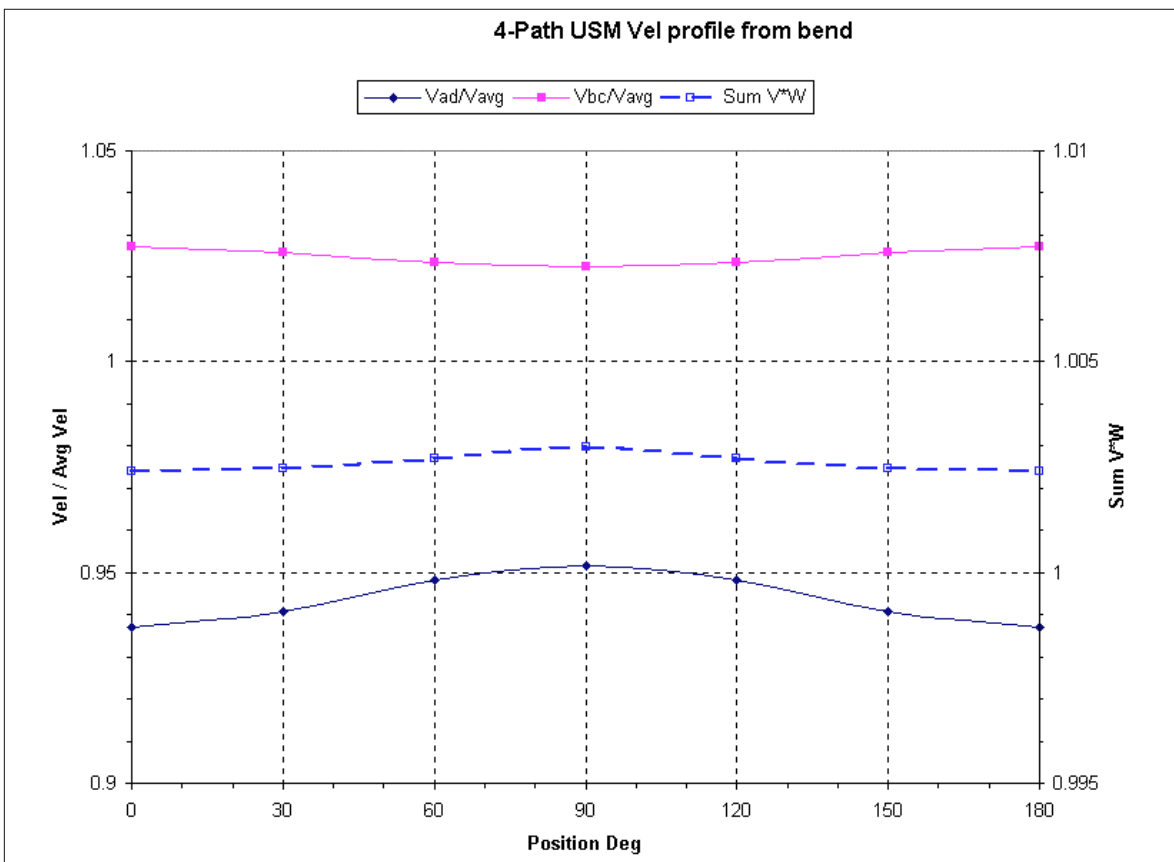


Figure 14. Inner and outer chord velocity contributions to the average flow velocity for the four-path ultrasonic meter downstream of a bend.

## 5. CONCLUSIONS

For centerline measurements in fully developed flow, corrections of 4 – 8% are necessary to correct for Reynolds number and roughness variations.  $Re$  variation can be corrected dynamically from knowledge of  $r$  and  $m$ , but variations in roughness can cause uncompensated errors of as much as 1%.

In asymmetric flow, variations of 1.5% can occur due to the orientation of the centerline chord relative to the asymmetry. An error of +1.5% will then become – 4% when the normal  $Re$  correction is applied. One can thus conclude that Reynolds number correction is in appropriate in disturbed flow, but only applies strictly to fully developed flow.

A flow conditioner might help improve the disturbed profile, but at the expense of additional pressure loss, cost, blockage and potential fouling. Furthermore, bi-directional flow would require two flow conditioners with separate forward and reverse calibrations.

Turning now to a four-path meter of the Daniel Senior Sonic type, in fully developed flow, corrections of only 0.06% account for all  $Re$  and roughness effects. In the asymmetric flow downstream of a single elbow, the integration error has been shown to be only 0.2%, irrespective of orientation. This is at least an order of magnitude less than the errors from a single path centerline meter.

Fixed upstream pipe-work would normally be expected to produce a fixed velocity profile, however with “T” pieces or headers the velocity profile can change with the proportion of flow in the respective branches. The four-path meter would detect and measure such changes through the velocity profile, while the integration technique would still give the correct flow rate. In fact four velocity measures of the profile are a very useful diagnostic tool provided by the meter.

The better accuracy and superior diagnostic ability of the four-path meter justify the claim that it is suitable for fiscal measurement, while the single path centerline meter is clearly not suitable.

A final interesting observation from the flow asymmetry work is that the velocity profile seen by the four chords is not unique for different orientations in the same flow. Hence it would be extremely difficult to devise a better integration technique (e.g. using variable weighing factors) that makes use of this velocity profile information. In fact it is obviously unnecessary, as the Gauss-Jacobi integration method works remarkably well.

## REFERENCES

1. “Boundary Layer Theory” by H. Schlichting, McGraw-Hill Book Co. 1960
2. ISO/TR 12765:1997(E), Measurement of Fluid Flow in Closed Conduits – Methods Using Transit Time Ultrasonic Flowmeters.
3. Franc, S., Heilmann, C. and Siekmann, H. E. “Point Velocity Method for Flow Rate Measurement in Asymmetric Pipe Flow” Flow Meas. Instrum. Vol. 7 No. 314 1996



# PROVING A FISCAL 5-PATH ULTRASONIC LIQUID METER WITH A SMALL VOLUME BALL PROVER. CAN IT BE DONE?

*Trond Folkestad, Norsk Hydro ASA*

---

## 1 INTRODUCTION

Norsk Hydro is installing its first fiscal liquid metering station based on Ultrasonic meters on the Oseberg Sør (South) platform comprising two multi-path Ultrasonic liquid flow meters in series with an Unidirectional small volume ball prover. The Ultrasonic liquid flow meters are 8" Krohne 5-path Altsonic V meters while the 12" Unidirectional ball prover is a Kongsberg Offshore design.

During flow testing of the metering system the required repeatability during proving could not be achieved. The repeatability during proving varied between more than ten times the requirement in the regulation from the Norwegian Petroleum Directorate (NPD) to just within the requirement. Most of the time varying between three to six times the requirement.

This paper will share the experience gained during flow testing the metering system for four months in Brevik, Norway. The paper will conclude with a recommendation for better test set-up and system design when using this type of Ultrasonic liquid flow meters with a small volume ball prover.

## 2 BACKGROUND

The Oseberg Sør platform in the North Sea, in production in the year 2000, will be a first stage separation platform. Second and third stage separation will be done at the Oseberg Field Centre 13 km away. The stabilised oil will be sent to shore in the pipeline to the Sture oil terminal in Norway, see Fig 1 and 2.

With maximum water content in the crude oil of 5 % by volume, Norsk Hydro decided to use liquid ultrasonic flow meters to measure this unstabilised crude oil, after gaining acceptance by the NPD.

Since there is little prior experience with proving ultrasonic liquid meters the metering system is a new design adapted to the limited space on the platform.



Fig 1, Location of the Oseberg Area

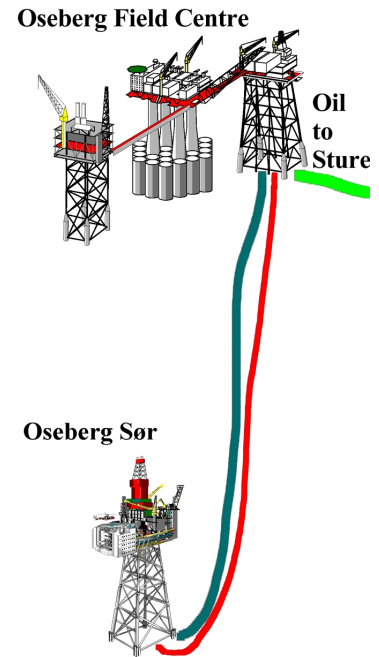


Fig 2, The Oseberg og Sør platform.

### 3 MEASUREMENT SYSTEM

#### 3.1 Calibrating the Ultrasonic liquid flow meter

The 5-path Ultrasonic liquid flow meters were calibrated using a water tower at Krohne Altometer in Sliedrecht, Holland. The meters achieved results well within the NPD linearity requirements (Flow range 10:1  $\pm 0.25\%$ , flow range 5:1  $\pm 0.15\%$ ) and satisfied the repeatability requirement as well ( $\pm 0.020\%$ ), see Fig 3.

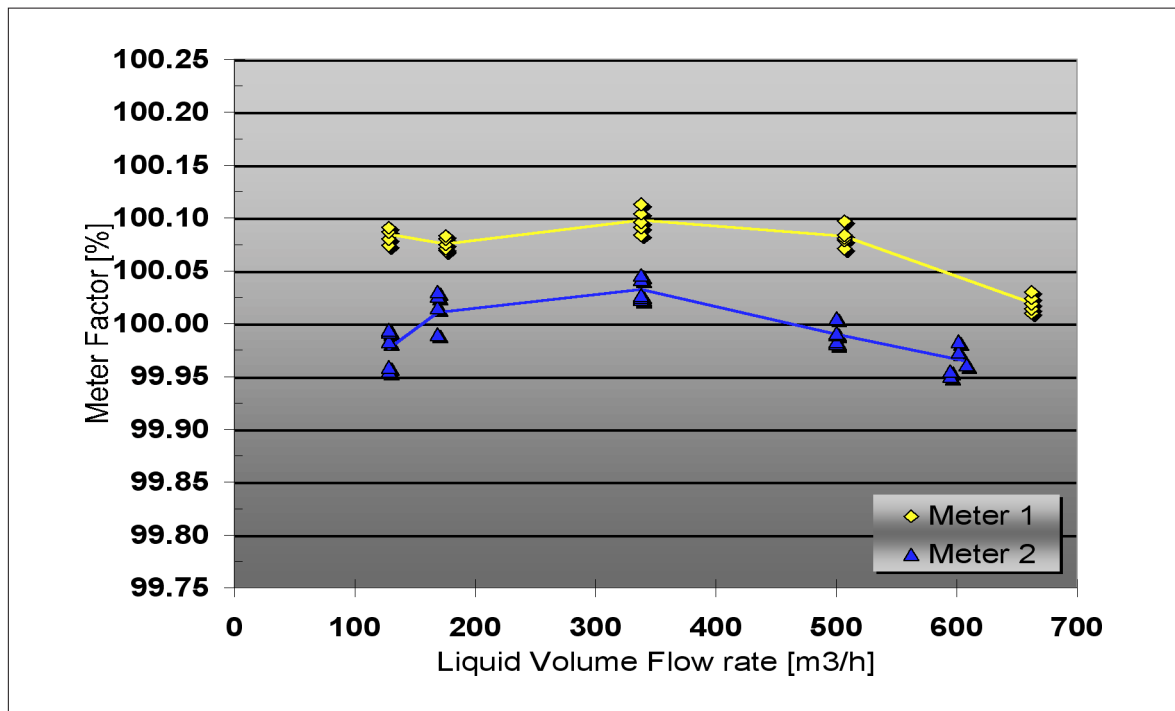


Fig 3 Calibration results, 5-path Ultrasonic liquid flow meters, with water. Meter 1 adjusted by - 0.058% after calibration.

#### 3.2 System design

The metering system consists of two 5-path Ultrasonic liquid flow meters in series with a Unidirectional small volume ball prover, see Fig 4. 10D in front of the first ultrasonic meter is a flow conditioner and there is 5D between the two ultrasonic meters.

There are four volumes in the prover varying from 592 litres to 630 litres. The number of pulses from the ultrasonic meters during one proving trial is from 3150 to 3355 pulses, requiring pulse interpolation during proving.

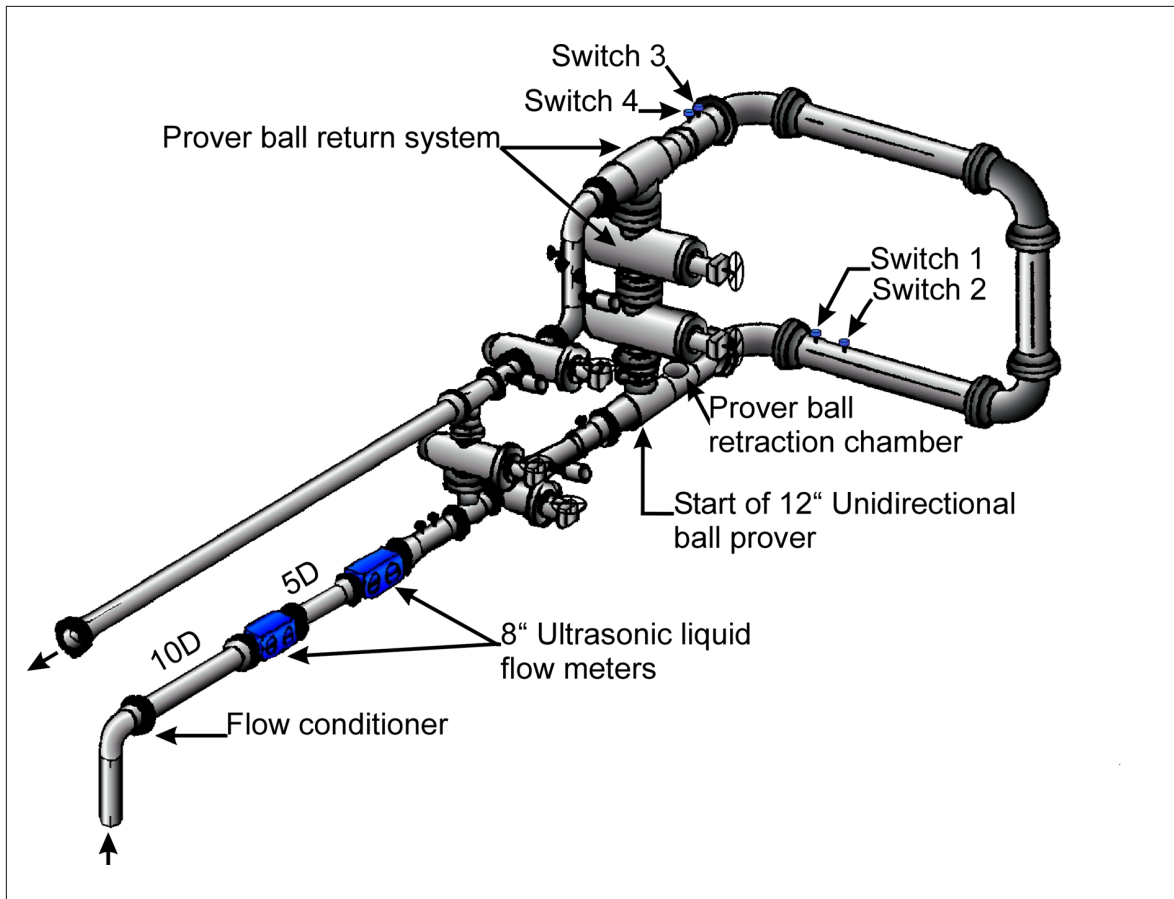


Fig 4 Layout metering system.

## 4 FLOW TESTS WITH POOR REPEATABILITY

Kongsberg Offshore started flow testing of the metering system in Brevik, Norway, in late November 1998. The repeatability results achieved during the initial test were surprisingly poor and no valid meter factor could be established within the NPD requirement.

Some errors were corrected without improving the repeatability results in any significant way. Krohne Altometer was also involved without finding any apparent reason for the poor repeatability results. Tests continued until February 1999, trying different ways to improve repeatability, without success.

According to the NPD regulation a valid meter factor is the average meter factor from a sequence of five consecutive proving trials when these five meter factors lie within a band of 0.050% of the average meter factor. If this is not true after five proving trials up to a total of ten proving trial can be made, always using the last five meter factors to calculate a valid meter factor. If no valid meter factor can be established after ten proving trials, a new proving sequence must be started.

Typical meter factors from single proving trials showing the large spread and consequently poor repeatability compared to the NPD requirement, are given in Fig 5 and 6 for both low and high flow rates.

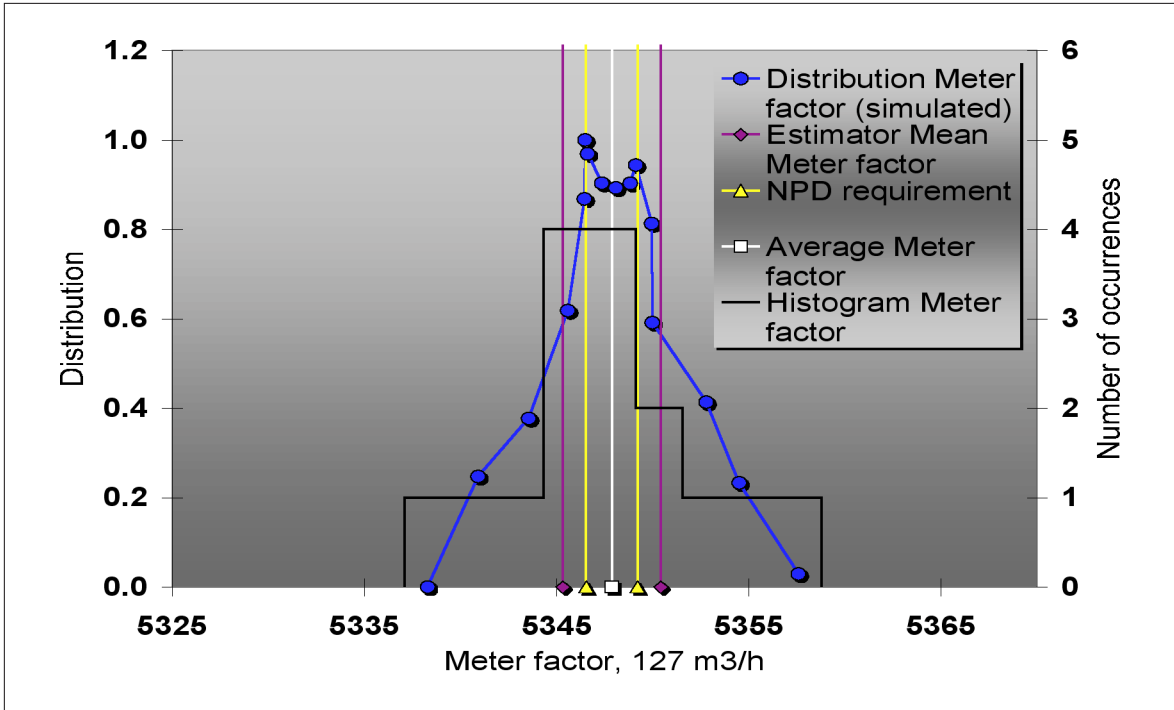


Fig 5 Typical proving trial results at low flow rate. The repeatability of the Estimator for the Mean meter factor is calculated at 95% confidence level.

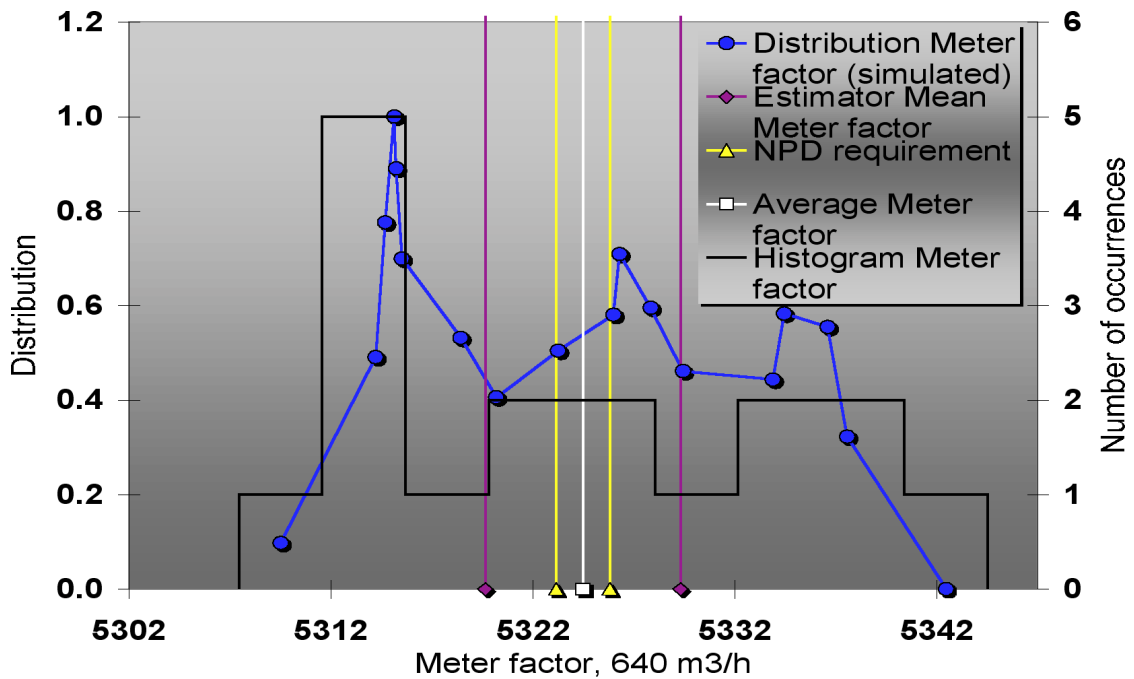


Fig 6 Typical proving trial result at high flow rate. The repeatability of the Estimator for the Mean meter factor is calculated at 95% confidence level.

The relative repeatability varies from 1.6 to 10.3 times the NPD requirement. Typical variation in Meter factor during several proving sequences is given in Fig 7 and 8.

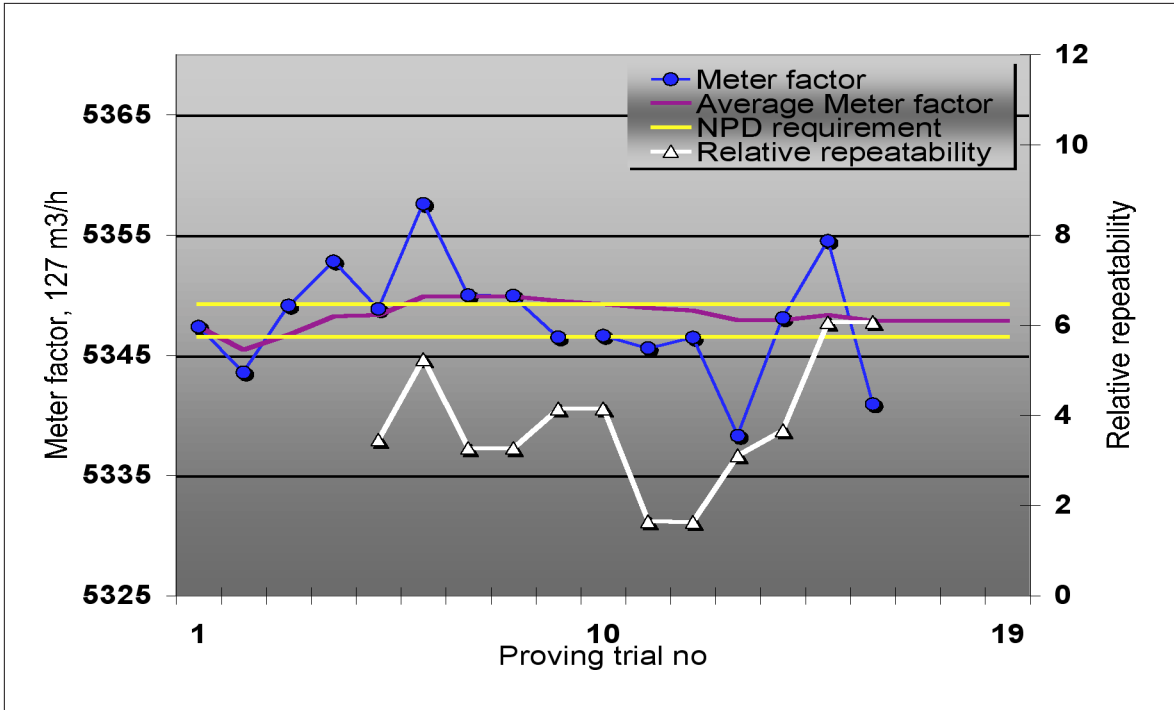


Fig 7 Typical variation in proving trial results at low flow rate.

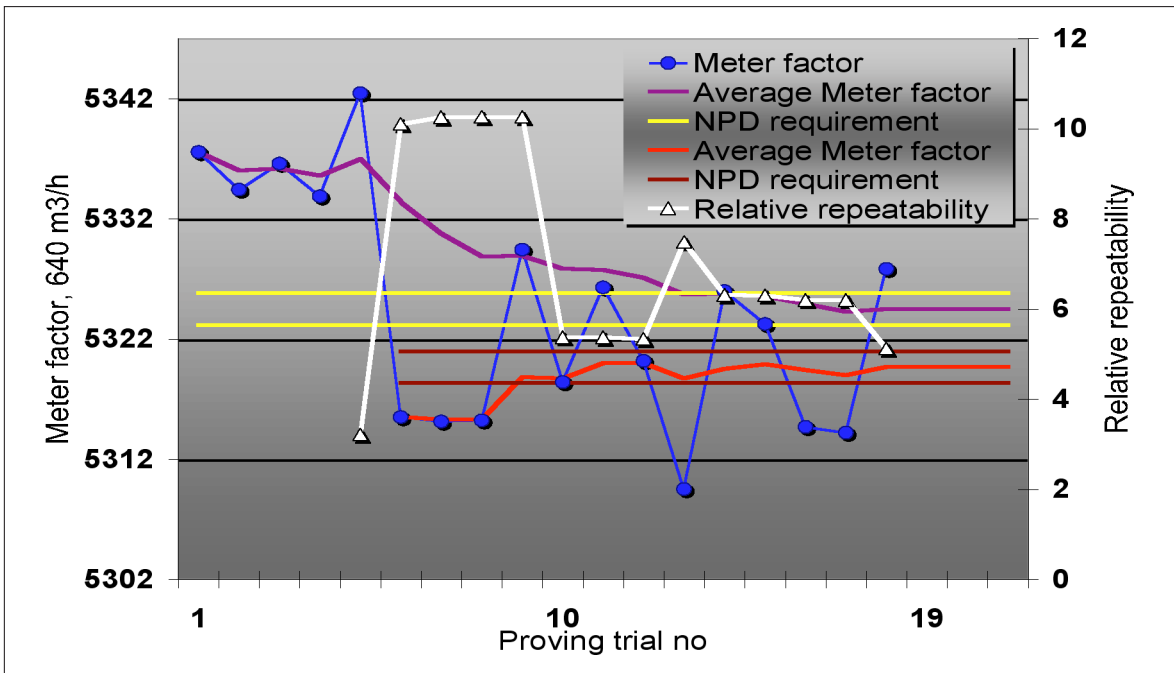


Fig 8 Typical variation in proving trial results at high flow rate.

In Fig 8, the average meter factor is also calculated when discarding the five first proving trials, giving a significant shift in average meter factor.

The conclusion so far was that the small volume prover was not able to prove the ultrasonic meters within NPD requirements and that the system should be accepted as is. No fault could be found in either the prover system or the ultrasonic meters.

Norsk Hydro could not accept this conclusion, stating that a reason had to be found for the poor repeatability during proving. Norsk Hydro decided to use more resources to analyse the problem and to continue with the flow testing in Brevik.

## 5 PROBLEM ANALYSIS

There are mainly three sources of error when proving with poor repeatability. The pulse interpolation system can be faulty, the pulses coming from the ultrasonic meters can be unstable or the flow rate can be unstable. The two first sources of error were checked out and the metering system found to work properly. That left unstable flow rate.

The time series from the ultrasonic meter was analysed and it was discovered as expected that the time series revealed pulsation in the signal, see Fig 9 and 10. The pulsation looks to be periodic and with a peak amplitude of 2 - 3% of the average flow rate. This is a large pulsation amplitude compared to the NPD repeatability requirement.

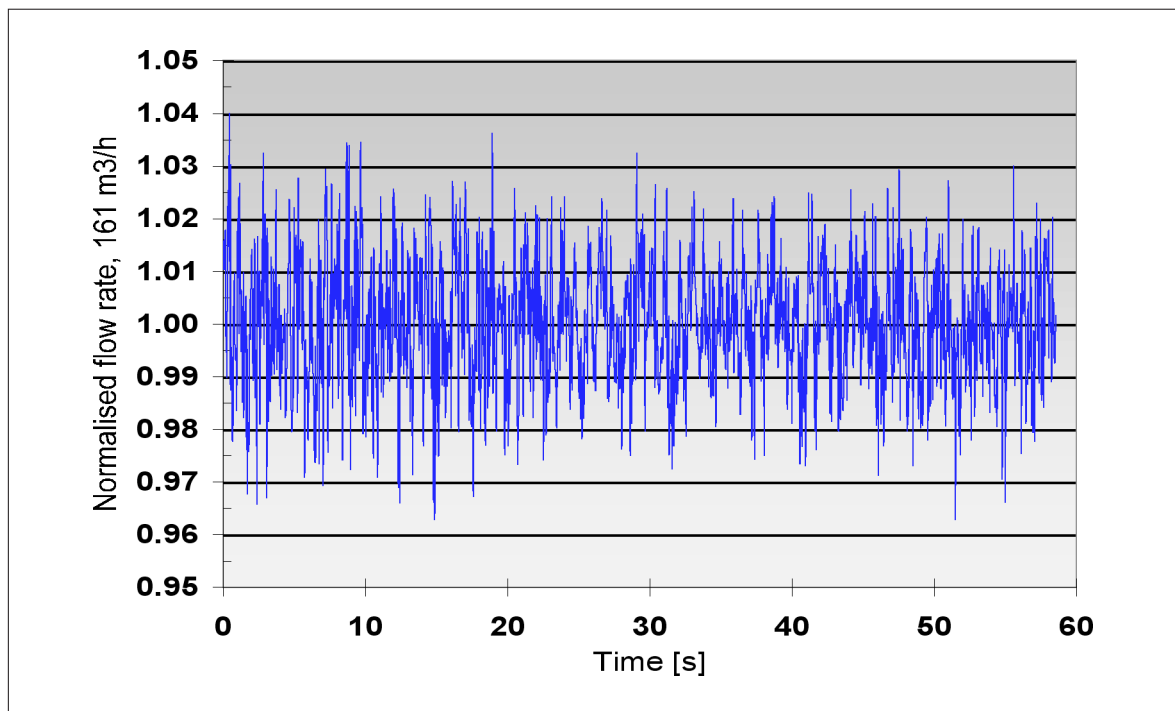


*Fig 9 Typical time series at low flow rate show fluctuating flow rate.*

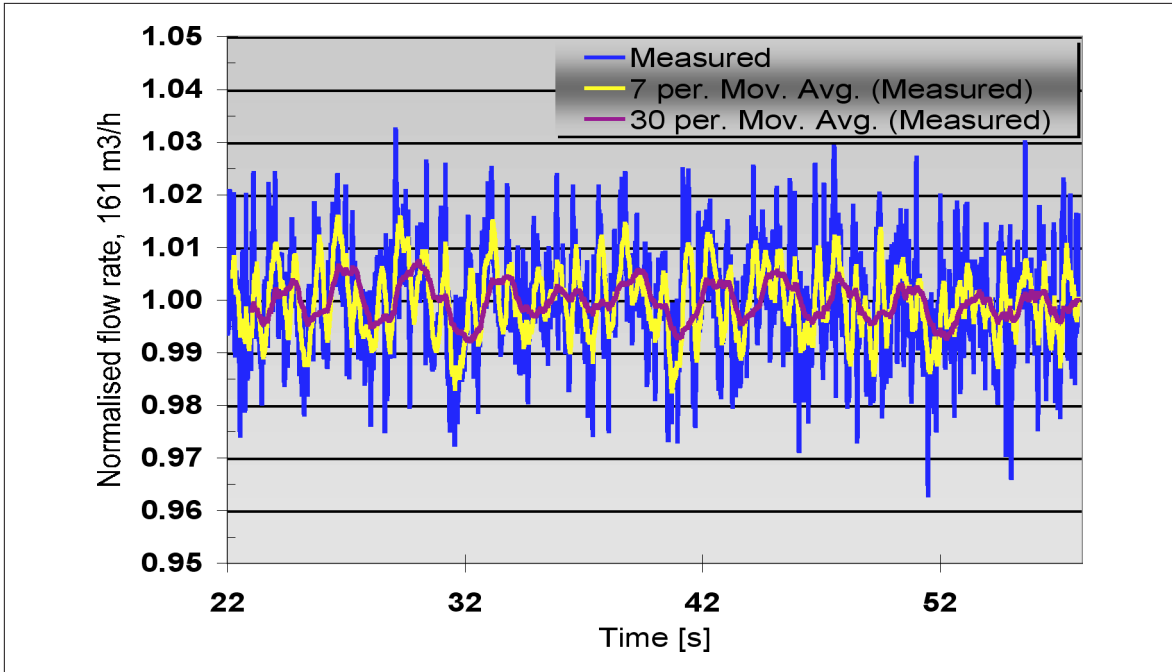


Fig 10 Typical time series at low flow rate indicates periodic pulsation with large amplitude.

The frequencies in the identified periodic pulsation look like 0.36 Hz and 1.3 Hz.

### 5.1 FFT reveals Pulsating flow

By performing a Fast Fourier Transform on the time series in Fig 9, the frequency components in the pulsation at low flow rate could be determined from the power spectrum, see Fig 11.

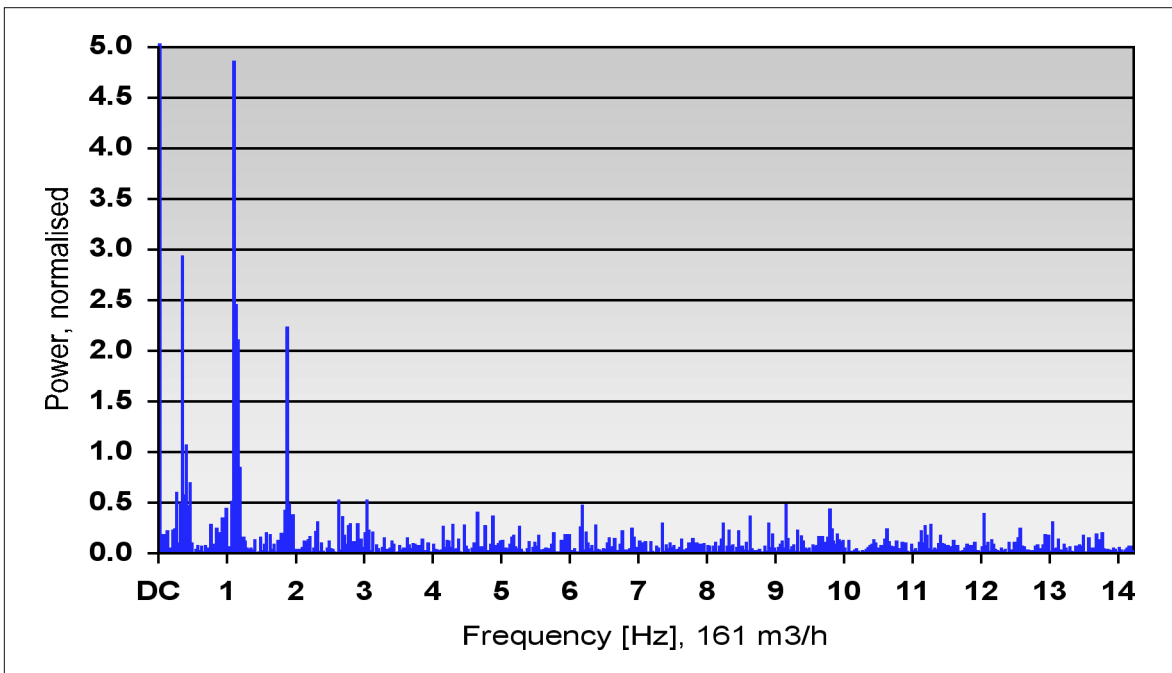


Fig 11 FFT on time series identifies pulsation frequencies at low flow rate.

For the low flow rate case, the centre frequencies of the three dominating frequency peaks and the cumulative peak amplitudes of these pulsations were calculated to be:

Table 1 Pulsation frequencies at low flow rate, 161 m<sup>3</sup>/h.

Pulsation frequency no.	1	2	3
Frequency, $f_i$	0.33Hz	1.09Hz	1.87Hz
Peak amplitude, $x_i$	0.53%	0.70%	0.44%

For the high flow rate case, see Fig 12, the centre frequencies of the four dominating frequency peaks and the cumulative peak amplitudes of these pulsations were calculated to be:

Table 2 Pulsation frequencies at high flow rate, 627 m<sup>3</sup>/h.

Pulsation frequency no.	1	2	3	4
Frequency, $f_i$	0.14Hz	0.64Hz	1.42Hz	2.37Hz
Peak amplitude, $x_i$	0.22%	0.32%	0.22%	0.26%

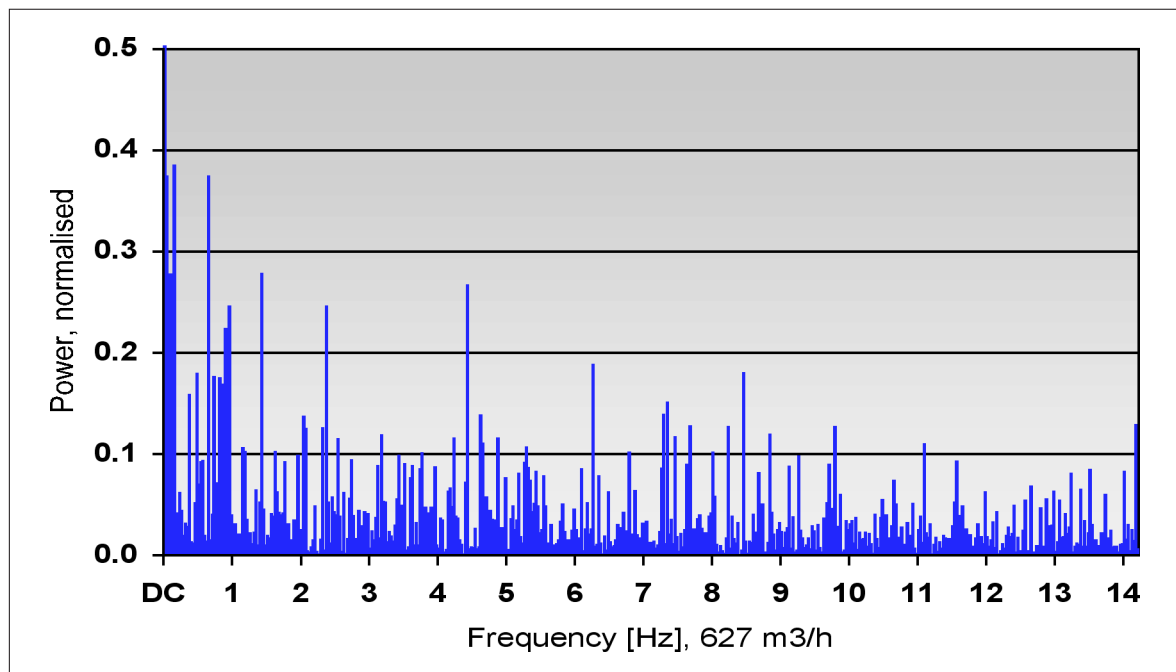


Fig 12 FFT on time series identifies pulsation frequencies at high flow rate.

Now, the questions remained, were these pulsation frequencies due to the flow or due to some inherent problem in the ultrasonic meters and could these pulsation frequencies explain the poor repeatability?

## 5.2 Simulations of proving results

To answer these questions, I simulated a proving trial with pulsating flow using the predominant frequencies with amplitudes as found from the time series. Finding the maximum and minimum meter factors, from Equation 1, the worst case repeatability for the meter factors could be calculated for each flow rate.

$$\text{Meter factor}_n = \frac{Q \cdot P_{\max}}{Fr_{\max} \cdot PrVol} \cdot \int_0^L \left[ 1 + \sum_{i=1}^k x_i \cdot \sin(2\pi f_i (t + \phi_i(n))) \right] dt \quad [\text{pulses/m}^3] \quad (1)$$

where

- Q = Flow rate in m<sup>3</sup>/hr.
- P<sub>max</sub> = Maximum pulses pr second from the ultrasonic meter.
- Fr<sub>max</sub> = Maximum flow rate in m<sup>3</sup>/hr corresponding to Pmax.
- PrVol = Prover volume in m<sup>3</sup> at standard conditions.
- L = Duration of one proving trial in seconds.
- k = Number of pulsating frequencies used in the simulation.
- φ<sub>i</sub>(n) = Phase shift as a function of n.

The simulations assumed that the ultrasonic meter was truly measuring the flow variations and that the prover was almost unaffected by the same flow variations. These simulations revealed that the poor repeatability results could be explained to a large extent by the pulsating flow found in the time series. See Fig 13, where the meter factor in Equation 1 is plotted as a function of n.

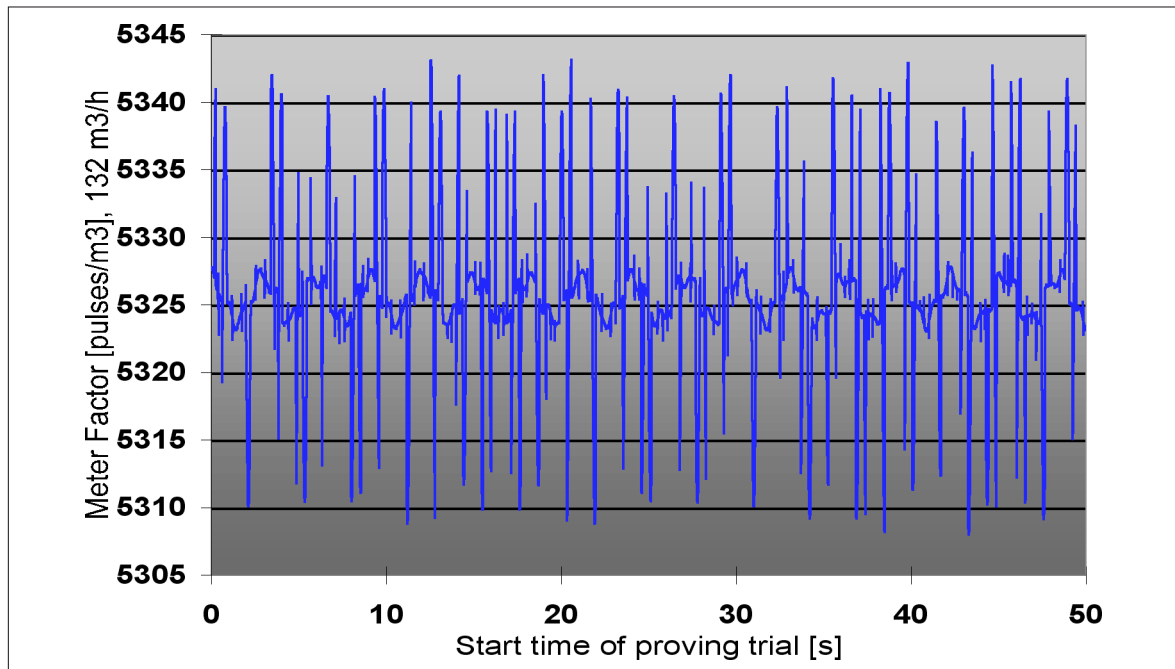


Fig 13 Simulated meter factors during proving with pulsating flow, low flow rate.

The worst-case repeatability found from the simulations varied from 0.3% to 0.8% for low flow rates and from 0.25% to 0.4% for high flow rates. This is from 5 to 16 times the NPD requirement.

The reason for this effect is that the periods of the pulsation frequencies are very small non-integer multiples of the time between the switches for one proving trial. At low flow rates the periods of the dominating pulsation frequencies are from 0.54 to 3.0 seconds while the time between the switches vary from 11 to 17.6 seconds. At high flow rates the periods of the dominating pulsation frequencies are from 0.42 to 7.1 seconds while the time between switches vary from 3.3 to 4.4 seconds.

For simplicity's sake, let us consider what happens in a flow pulsating with a single frequency, 0.38Hz. For such a flow, the worst-case shift from "true" average flow rate occurs when the period of the pulsation frequency is 0.5 times the time between the switches. The second worst-case shift is when the period of the pulsation frequency is 1.5 times the time between the switches. In Fig 14 is indicated that when the fluctuation in flow is asymmetric over time round the "true" average flow, during one proving trial, this causes a shift in the average flow rate and thus in the meter factor. Assuming the prover ball reacts to the "true" average flow rate. The size of the shift depends on the phase of the fluctuation at the start of proving and can be zero. This is why repeatability is sporadically within the NPD requirement.

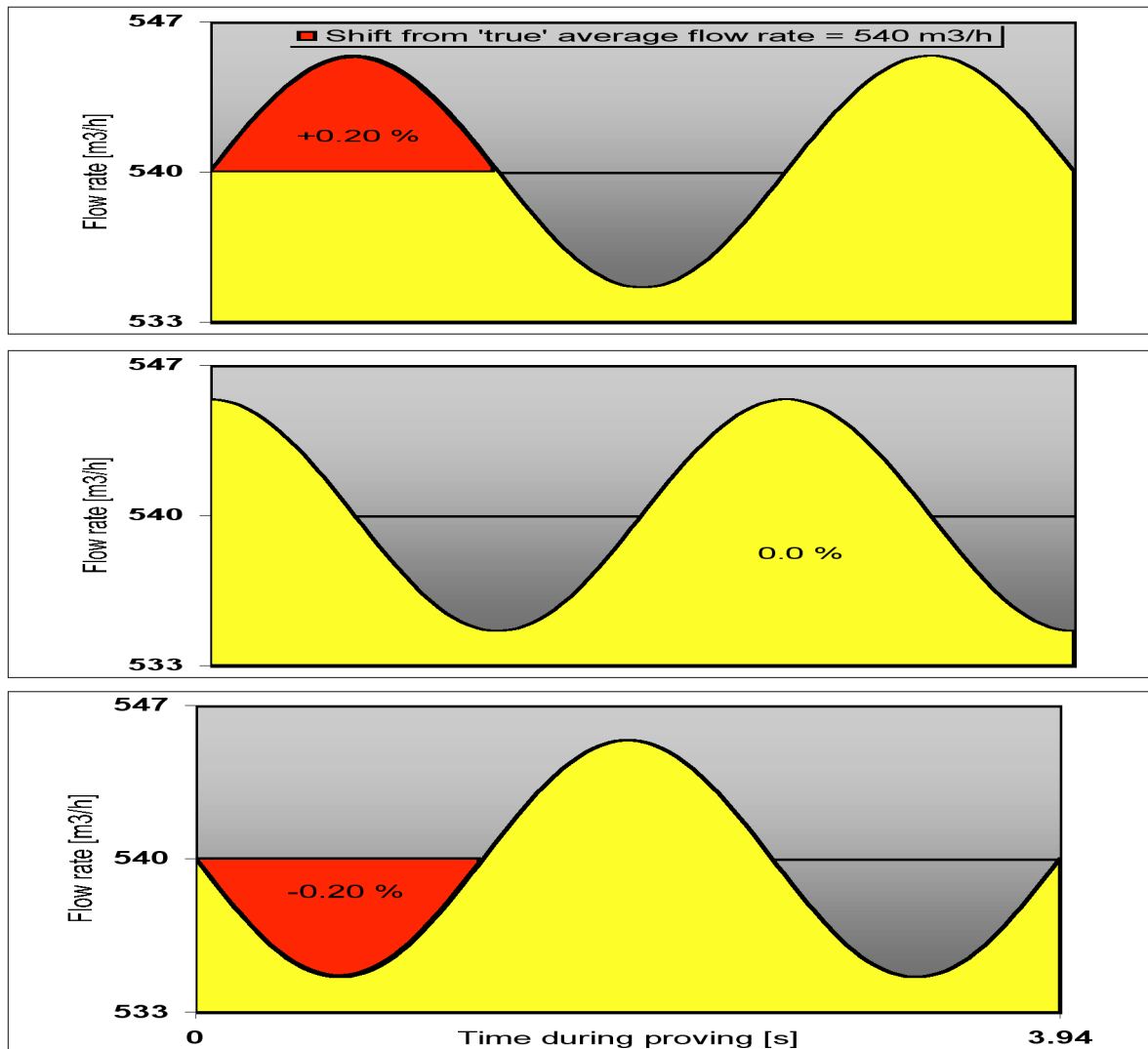


Fig 14 Simulated second worst-case shifts from "true" average flow rate due to pulsating flow at 0.38Hz, during one proving trial of 3.94 seconds.

In addition to the pulsating flow rate, the reduction and fluctuation in flow rate caused by the prover ball dropping down and travelling through bends, may also affect the proving result, but probably in a minor way compared to the pulsating flow.

What causes the flow fluctuations and what can we do to reduce or eliminate them?

### 5.3 Improvements to test loop

Looking at the test loop, flexible hoses were replaced by pipe or reinforced flexible hoses. This gave some improvement to the repeatability and some proving sequences at low flow were performed within the NPD requirement, see Fig 22, red dot. However, proving results were still not consistently within the NPD requirement, compare Fig 5, 6, 7 and 8 with Fig 20, 21, 22 and 23. FFT analysis revealed that there had been a slight reduction in the peak amplitudes of the dominating pulsation frequencies, thus corroborating the theory so far.

### 5.4 Test with turbine meter

To eliminate any doubt that the prover was actually functioning properly it was decided to install a turbine meter in place of the second ultrasonic meter. Several proving sequences were performed for various flow rates within the NPD requirements, see Fig 15 and 16.

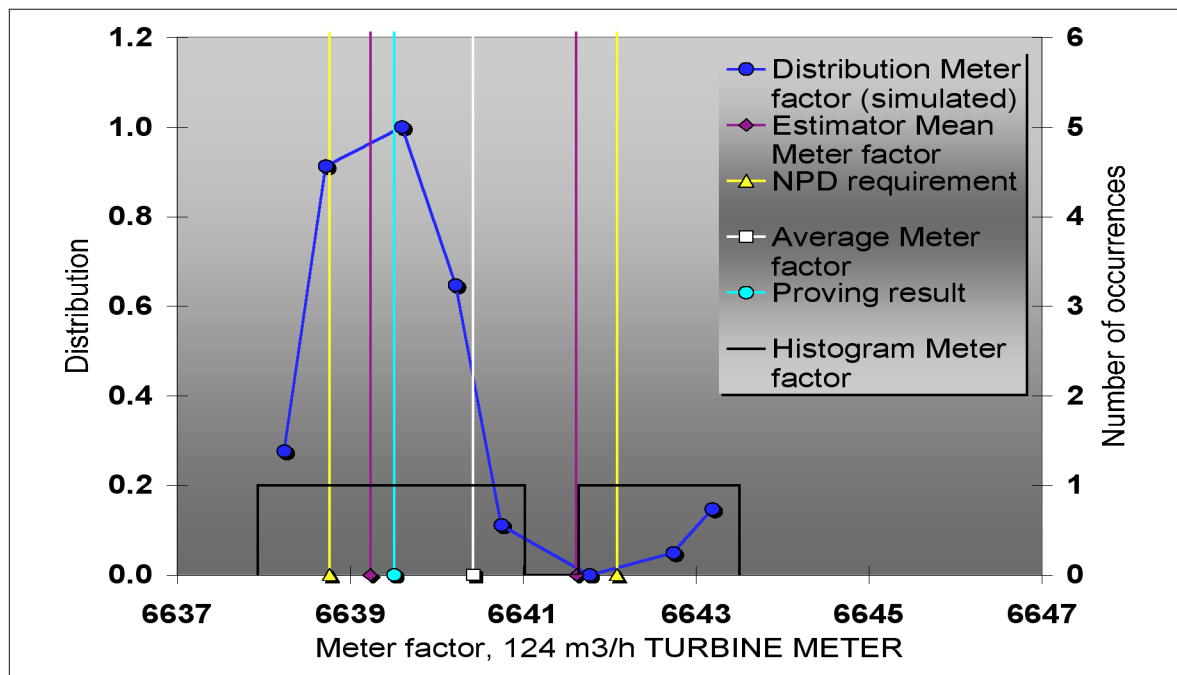


Fig 15 Typical proving trial results at low flow rate for turbine meter. The repeatability of the Estimator for the Mean meter factor is calculated at 95% confidence level.

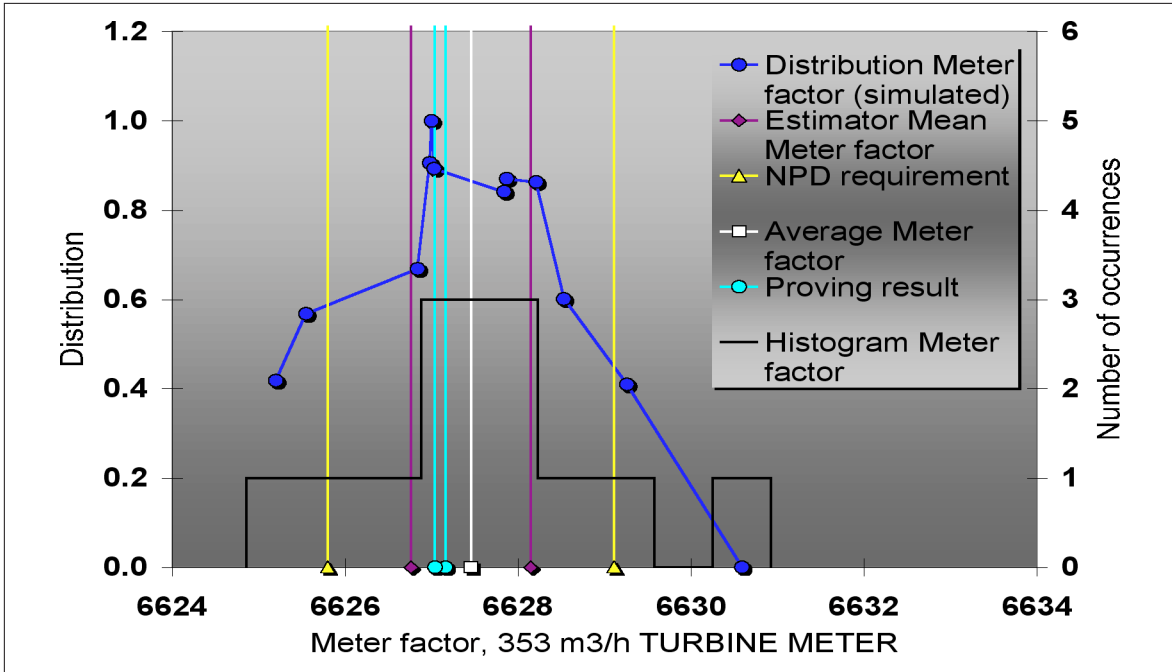


Fig 16 Typical proving trial results at medium flow rate for turbine meter. The repeatability of the Estimator for the Mean meter factor is calculated at 95% confidence level.

However, overall variation in meter factor of 0.081% indicated that the turbine meter also reacted to the pulsation in the flow, see Fig 17 and 18. As can be seen from comparison of the ultrasonic and turbine meter, displayed by the database computer in the metering system, see Fig 19. We can also see that during proving there is a significant drop in prover outlet pressure.

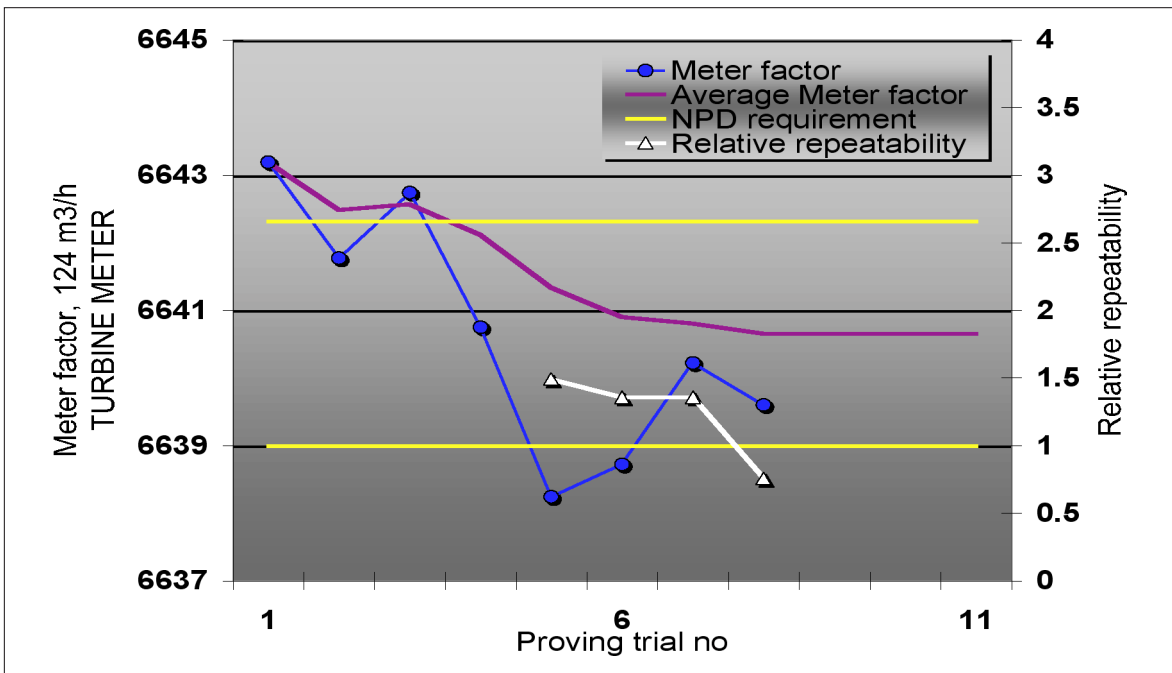


Fig 17 Typical variation in proving trial results at low flow rate for turbine meter.

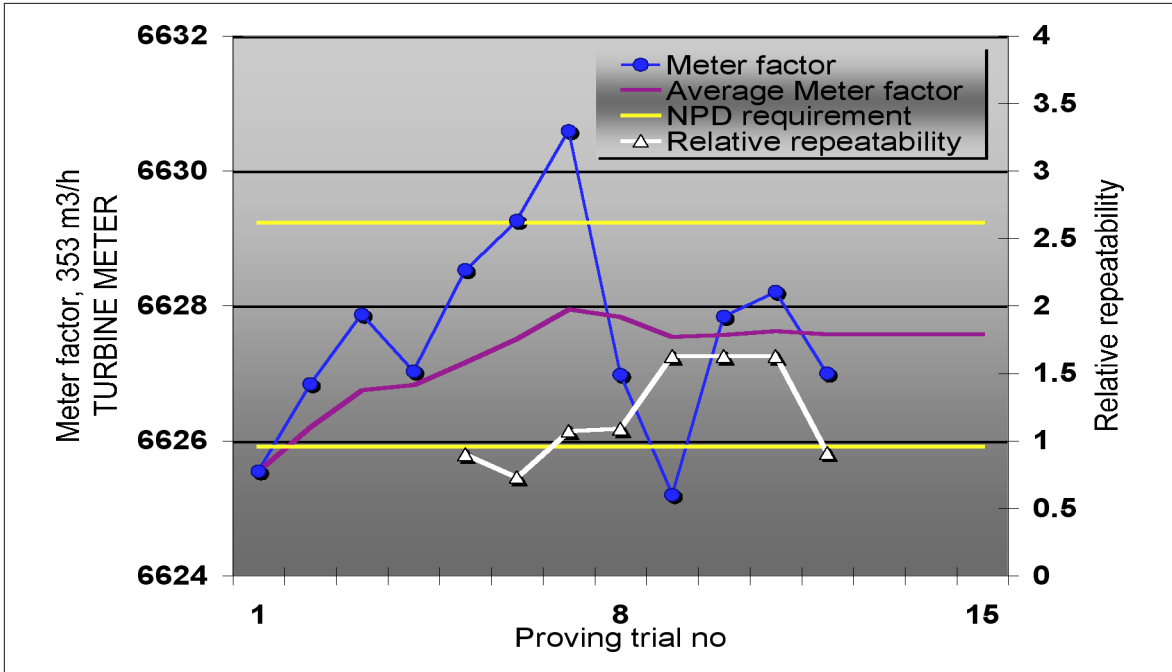


Fig 18 Typical variation in proving trial results at medium flow rate for turbine meter.

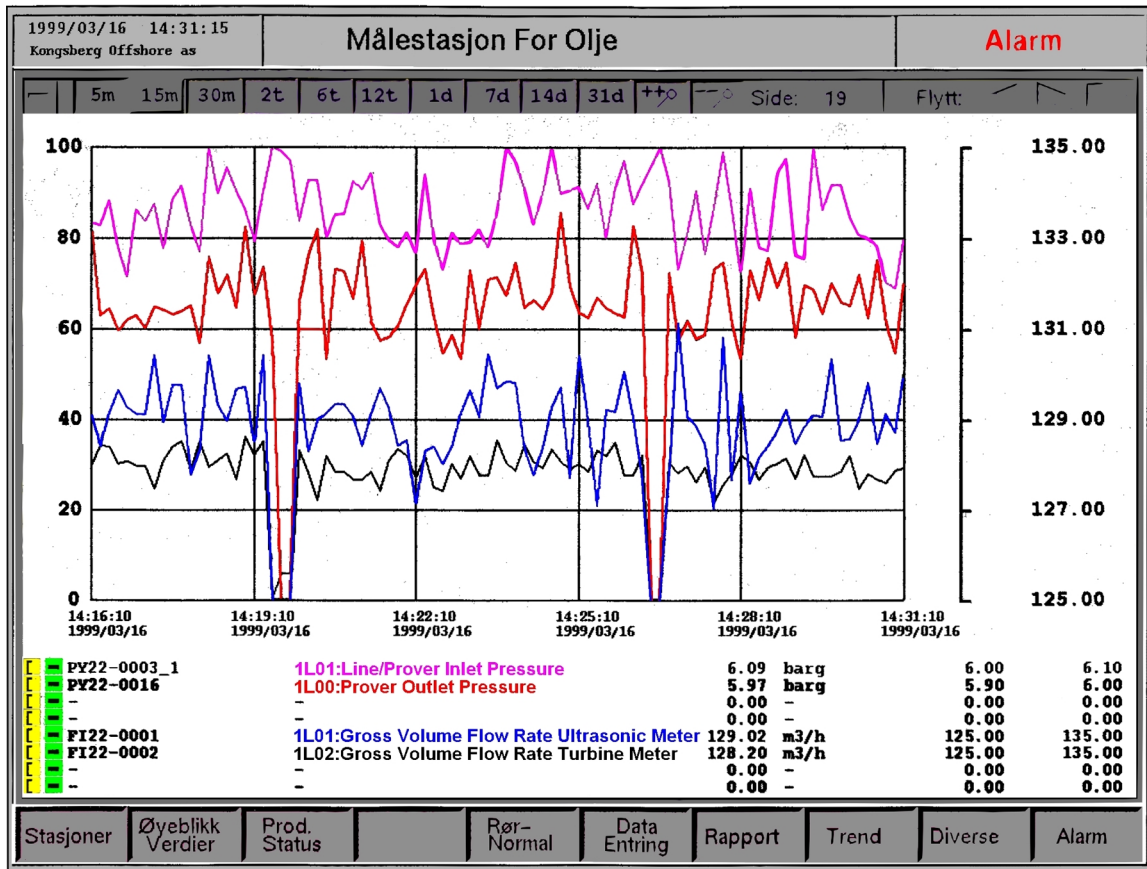


Fig 19 Trend display showing that the turbine meter and the ultrasonic meter reacts differently to the pulsating flow.

### 5.5 Probable cause of poor repeatability

The pulsation was finally determined to come from cavitation in the pumps in the flow loop. By using flow control valves to try to reduce cavitation, some improvement was achieved. However, we still could not achieve proving results for all flow rates consistently within the NPD requirement. There seemed to be no way that the test facility in Brevik could be sufficiently improved, in a short time, to give stable enough flow. It was therefore decided, in agreement with the NPD, to end the flow tests at Brevik and to prepare new flow tests on the Oseberg Sør platform during commissioning, in the year 2000. As preparation for the flow test a study to determine methods to achieve improved repeatability was started.

## 6 HOW TO ACHIEVE IMPROVED REPEATABILITY

There seem to be three ways to reduce the problem of pulsating flow and poor repeatability. One way is to improve design so that pulsating flow is reduced or eliminated. The second way is to use statistical methods and base the proving sequence on more than five consecutive proving trials and the third way is to make the ultrasonic meter behave more like a turbine meter.

### 6.1 Mechanical design

The installation of the metering system on the Oseberg Sør platform will have improved flow conditions due to more rigid and stable upstream flow from large pumps followed by a static mixer. This will possibly sufficiently reduce or eliminate the pulsating flow. Problem solved. However, this is not certain, so the other two ways of reducing the problem must also be considered.

### 6.2 Statistical evaluation of meter factors

Using enough proving trials to calculate the average meter factor, will give a representative average meter factor, when the flow is not shifting too much (normal production). How many proving trials is needed and how long will it take to prove the two ultrasonic meters? Using 15 to 20 proving trials will give a stable average meter factor for all flow rates, see Fig 20, 21, 22 and 23.

An estimator for the Mean meter factor,  $\bar{X}$ , is given by Equation 2. Assuming that the  $n$  meter factors,  $X$ , follow a normal distribution with standard deviation,  $s$ , and average,  $\bar{X}$ , the estimator for the Mean meter factor will follow a Student-t distribution with  $(n-1)$  degrees of freedom.

$$\bar{X} - t_{\frac{\alpha}{2}} \frac{s}{\sqrt{n}} < \bar{X} < \bar{X} + t_{\frac{\alpha}{2}} \frac{s}{\sqrt{n}} \quad (2)$$

The repeatability of the estimator for the Mean meter factor,  $\sigma$ , in percent is then found to be

$$\sigma = 2 \cdot t_{\frac{\alpha}{2}} \frac{s}{\bar{X} \sqrt{n}} \quad [\%] \quad (3)$$

The repeatability of the estimator for the Mean meter factor is calculated at 95% confidence level,  $\alpha$ , and is not within the NPD repeatability requirement at any flow rate, with  $n$  less than 25. The repeatability of the estimator for the Mean meter factor will fall within the NPD repeatability requirement, when  $n$  is large or when the flow is more stable. If  $n$  then is for example 30, the time needed to prove two ultrasonic meters will be more than 7 hours which is far too long.

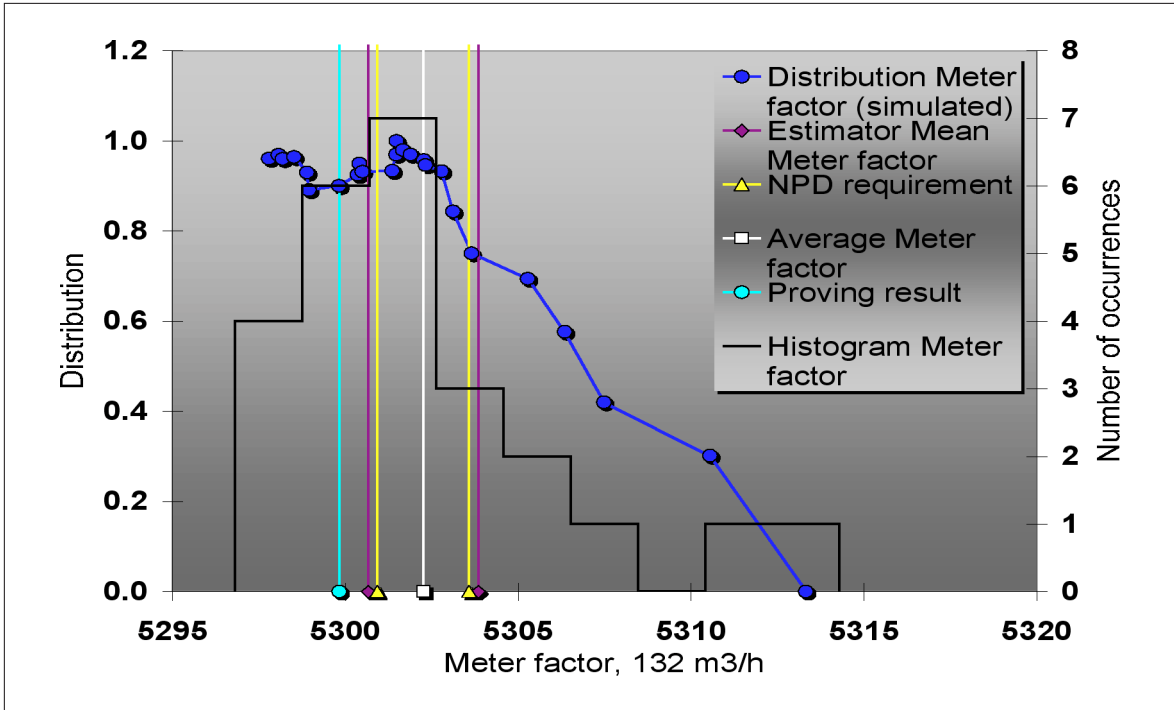


Fig 20 Typical proving trial result at high flow rate. The repeatability of the Estimator for the Mean meter factor is calculated at 95% confidence level.

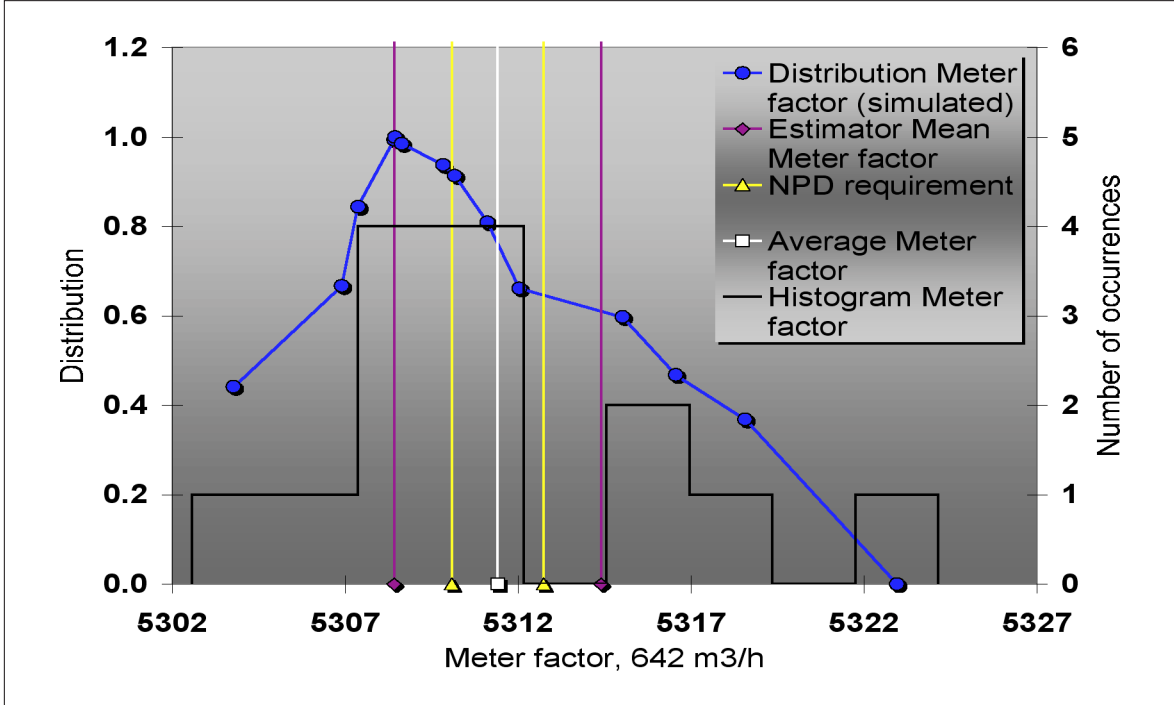


Fig 21 Typical proving trial result at high flow rate. The repeatability of the Estimator for the Mean meter factor is calculated at 95% confidence level.

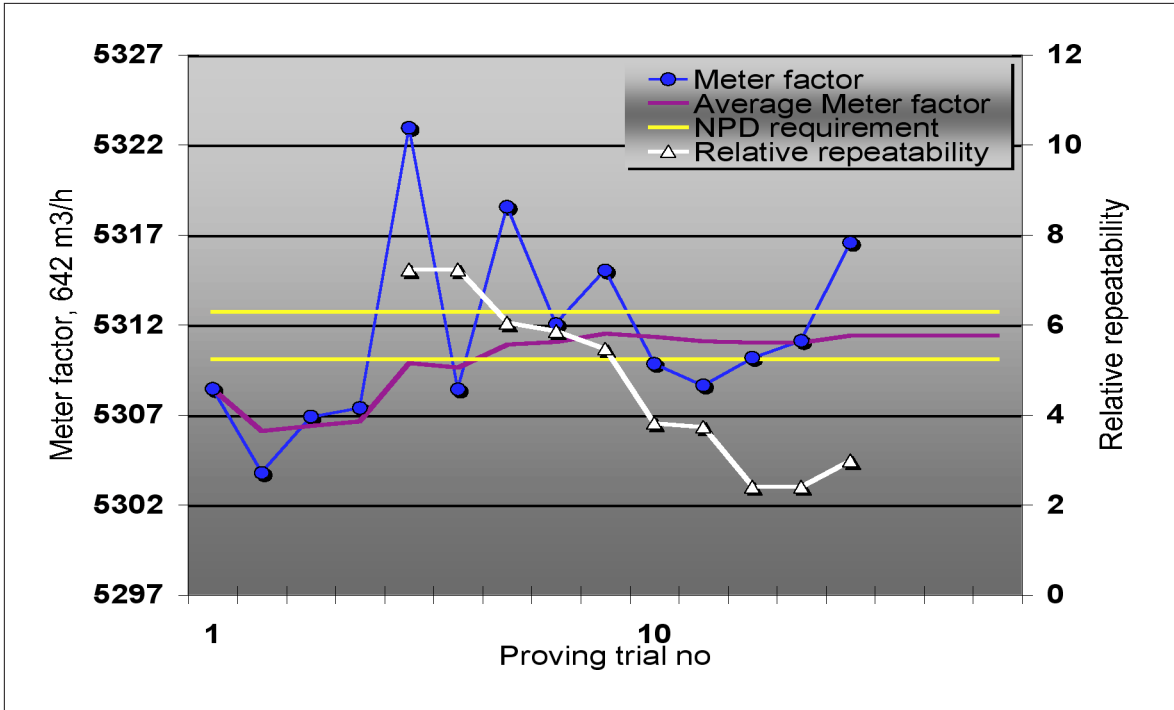


Fig 22 Typical variation in proving trial results at low flow rate.

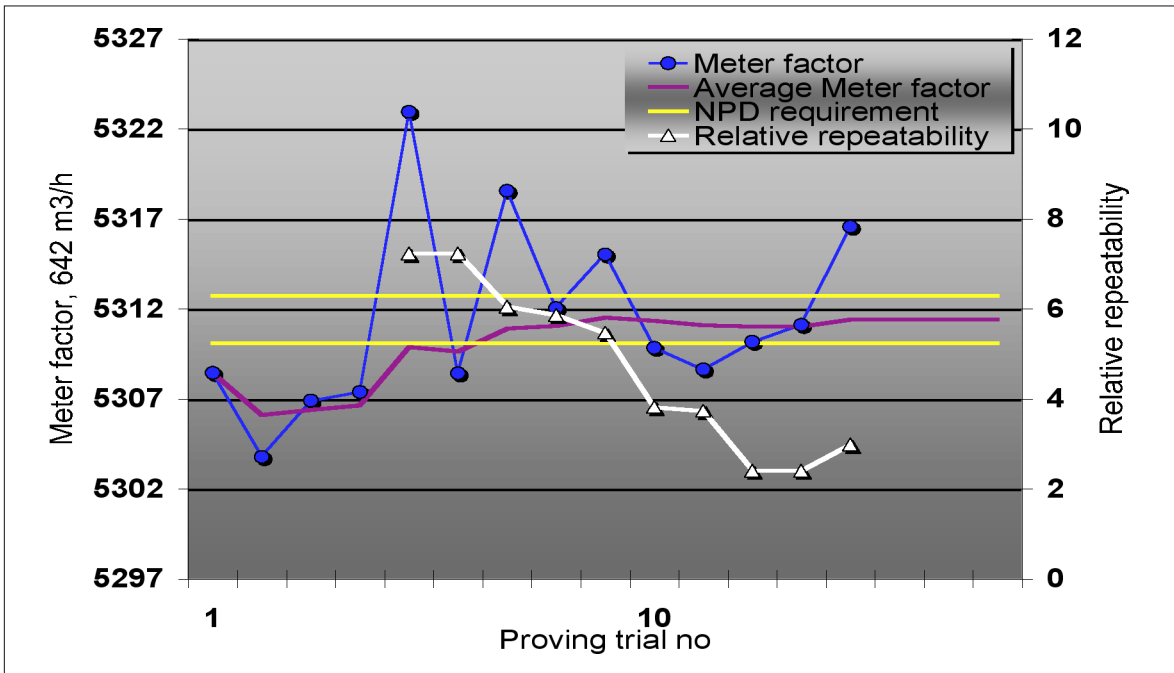


Fig 23 Typical variation in proving trial results at high flow rate.

The red dot in Fig 22 indicates that five consecutive proving trials lie within the NPD requirement. However, using these five meter factors to calculate the average meter factor will give a low meter factor, see Fig 20, not representative for all the data in Fig 20 and 22. Since it is just thanks to a random event that the NPD requirement was satisfied, this indicates a weakness in the current method for accepting new meter factors.

My proposed statistical method for accepting and calculating average meter factors is based on all meter factors being equally correct. The average meter factor is calculated using all consecutive meter factors from the start of the proving sequence as in Fig 22 and 23. The criterion for convergence of the average meter factor should be at least one-tenth the NPD repeatability requirement ( $\pm 0.0025\%$  change from the previous average value). At least five and maybe maximum twenty proving trials should be performed.

The proving data from Brevik indicates that stable enough average meter factors can be reached after 5 to 16 proving trials with this method, for all test series and flow rates.

To reduce random spurious convergence of the average meter factor and avoid accepting a new meter factor before the average meter factor has reached a sufficiently stable value, a two step convergence criterion is proposed. The two step criterion for convergence of the average meter factor should be at least one-fifth and one-tenth the NPD repeatability requirement (first  $\pm 0.0050\%$  change from the previous average value, then the next average value must change less than  $\pm 0.0025\%$  from the previous average value). This is a more robust method.

Using this method, convergence of the average meter factor could not be reached for some of the flow rates in Brevik, even after more than twenty proving trials. Convergence of the average meter factor was normally reached after 8 to 15 proving trials with this method and will be reached after five proving trials for more stable flow conditions, just like the current method accepted by the NPD.

Under more stable conditions the repeatability of the estimator for the Mean meter factor in Equation 3, could be used as a criterion, but it will require more proving trials than the proposed statistical methods described above.

The current method of using five consecutive proving trials within a sequence of ten, discarding as much as 50% of the values before calculating the average meter factor, is not a good method in a statistical sense. Completely valid meter factors are not used in calculating the average, not only outliers are discarded. When you have large fluctuations in flow rate, you need more values to calculate a good average than with stable conditions. This is not possible with the current method which requires very stable proving conditions to work properly.

### **6.3 Filtering meter response**

By making the ultrasonic meter respond to flow more like a turbine meter, some of the inherent advantages of using ultrasonic meters are lost. This is therefore the least preferred way of reducing the problem with pulsating flow and poor repeatability.

Many time series were logged by Krohne Altometer in Brevik, see Fig 24 for a typical time series during proving.

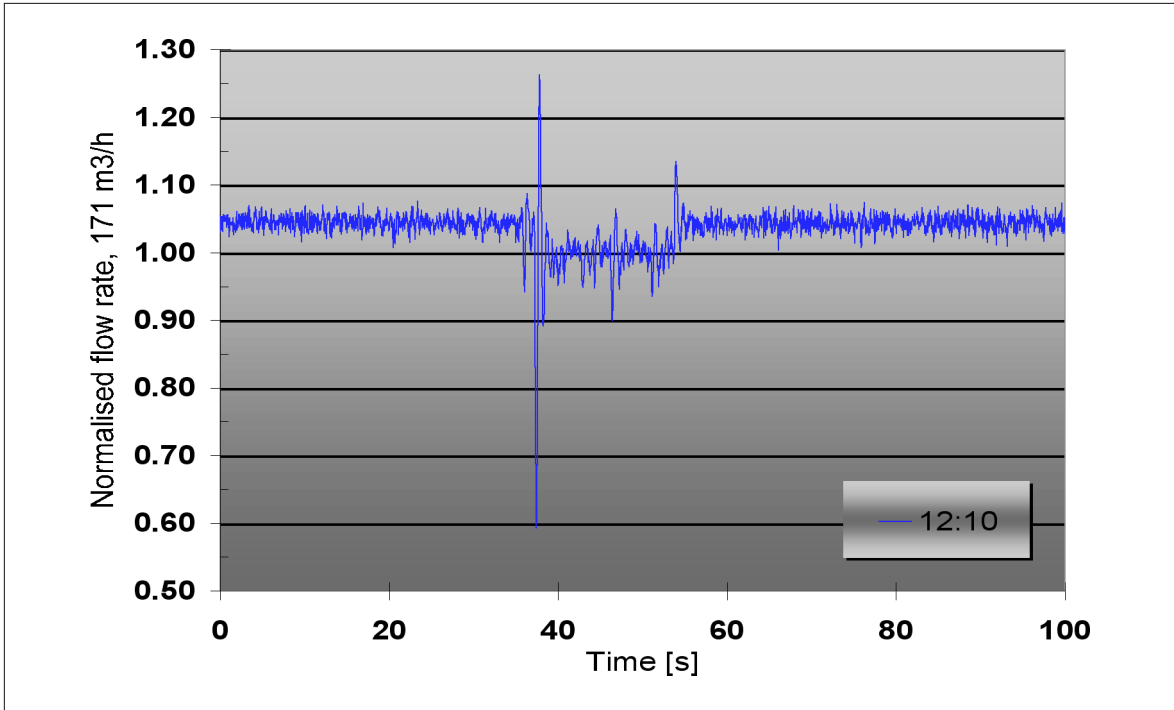


Fig 24 Typical time series during proving.

By calculating the volume of various portions of the prover and by using the relationship in Equation 4, the position of various events are identified in the time series, see Fig 25. Two reference positions are used—the ball drops down and the second bend.

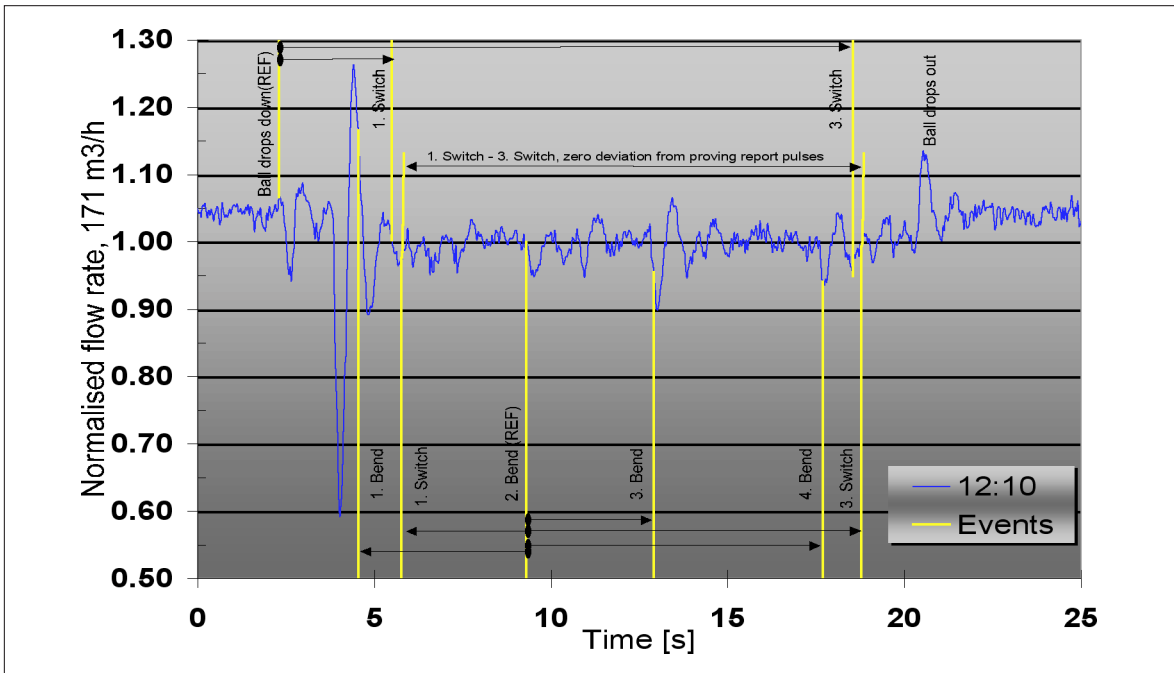


Fig 25 Typical time series during proving identifying the various events during proving.

The effect of various methods of changing the performance of the ultrasonic meter, like filtering time series, should therefore be readily verifiable. —Not so. It turned out after much deliberation that the timestamp on the time series and the timestamp on the proving reports from Brevik were not synchronised, so this had to be sorted out first.

The position in the proving trial of the first switch,  $D$ , can be determined in each time series from the integral in Equation 4. When this integral of the number of pulses from the ultrasonic meter during the proving trial, equals the number of pulses read from the proving report, the starting value  $d=D$ . So when  $d=D$  the Deviation( $d$ ) is zero and we know which part of the time series is the proving trial, corresponding to a known meter factor. By filtering the time series and integrating over the proving trial again, new meter factors can be calculated for the same time series. By using five consecutive proving trials the repeatability for the new average meter factor can be calculated and compared to the NPD requirement.

$$\text{Deviation}(d) = \int_d^{d+L} \text{Pulses from USM}(t) dt - \text{Proving report pulses} \quad [\text{pulses}] \quad (4)$$

where

$$L = 3600 \cdot \text{Pr Vol} \cdot C_{\text{PSP}} \cdot C_{\text{TSP}} / Q_{\text{Proving report}} \quad [\text{seconds}]$$

In Fig 26 is given a graphical illustration of Deviation( $d$ ) when stepping through all values of  $d$ . All time series have been aligned according to the position of the second bend. So ideally, the function Deviation( $d$ ) should be zero for the same value of  $d$  for all time series. This was not the case. After much analysis and number crunching I found that only by shifting the time stamps 20 minutes could the requirement that the Deviation( $d$ ) in Equation 4 should be zero, be reasonably satisfied simultaneously for all time series, at both low and high flow rates.

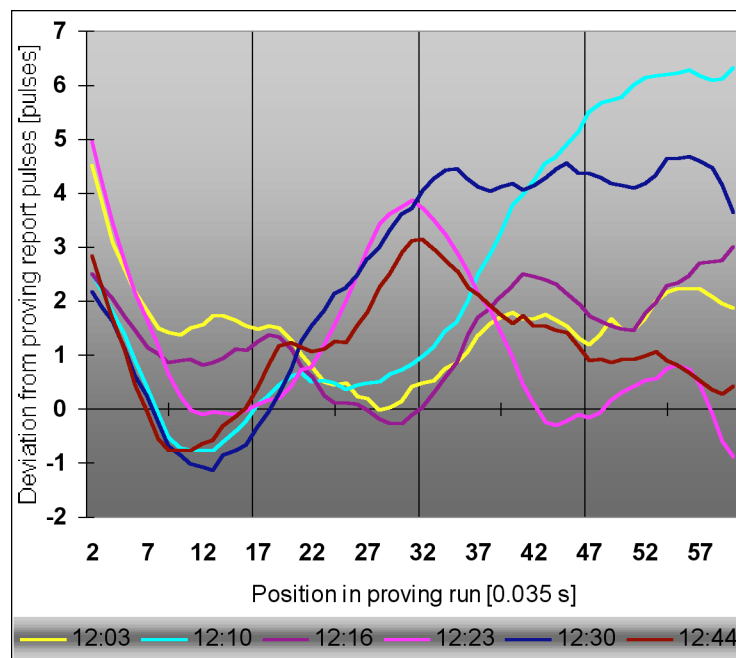


Figure 26 Deviation( $d$ ) for various time series

The duration of the proving trial, L, is calculated from the data in the proving report, see Fig 27 for the proving report used for these analysis.

1999/03/11 12:39 Oseberg Sør - Oljemålestasjon KOS FCM 212																
USM KALIBRERING OG KORREKSJONSFAKTORER side 1 av 2																
Volum i bruk.....: A (1-3)					Status: AVBRUTT											
Rørnormal Volum Sm3: 0.617910					USM Nr: 1											
Forsøk Nr.	Antall Pulser	Linje Temp grdc	Linje Trykk barg	Rørnorm Temp grdc	Rørnorm Trykk barg	Std. Tetthet kg/Sm3	Volum Strøm m3/h	Meter K-faktor P/m3	KOS Time	Krohne Time						
1	3284.4	30.70	5.92	30.67	5.57	800.00	171.30	5312.37	11:43	12:03						
2	3286.5	30.82	5.92	30.79	5.56	800.00	170.64	5315.68	11:50	12:10						
3	3284.7	30.94	5.91	30.91	5.60	800.00	171.20	5312.75	11:57	12:16						
4	3282.4	31.06	5.91	31.02	5.59	800.00	170.24	5309.00	12:04	12:23						
5	3282.0	31.16	5.92	31.15	5.65	800.00	171.38	5308.41	12:11	12:30						
6	3283.2	31.29	5.90	31.26	5.55	800.00	171.26	5310.33	12:18	-----						
7	3283.9	31.41	5.90	31.39	5.59	800.00	171.42	5311.40	12:25	12:44						
8	3286.5	31.54	5.92	31.51	5.60	800.00	171.11	5315.55	12:32	-----						
9	###	###	###	###	###	###	###	###	12:39	-----						
10	###	###	###	###	###	###	###	###	-----	-----						
Gj.snitt Siste 5									3283.6	31.29	5.91	31.27	5.59	800.00	171.08	5310.94
Forsøk Repeterbarhet: 0.134									K-faktor i bruk: ###							
									Differanse.....: ###							
Forsøk Nr.	CPSP	CTSP	CPLP	CTLP												
1	1.0000447	1.0005250	1.0005420	0.9848999												
2	1.0000447	1.0005289	1.0005421	0.9847872												
3	1.0000450	1.0005331	1.0005462	0.9846669												
4	1.0000449	1.0005368	1.0005453	0.9845606												
5	1.0000454	1.0005409	1.0005520	0.9844396												
6	1.0000446	1.0005449	1.0005426	0.9843264												
7	1.0000449	1.0005490	1.0005465	0.9842073												
8	1.0000450	1.0005529	1.0005481	0.9840931												
9	###	###	###	###												
10	###	###	###	###												
Gj.snitt siste 5 forsøk				CPSP	CTSP	CPLP	CTLP									
				1.0000449	1.0005449	1.0005469	0.9843254									
1999/03/11 12:39 Oseberg Sør - Oljemålestasjon KOS FCM 212																
USM KALIBRERING OG KORREKSJONSFAKTORER Side 2 av 2																
Forsøk Nr.	CPSM	CTSM	CPLM	CTLM												
1	1.0000000	1.0000000	1.0005765	0.9848772												
2	1.0000000	1.0000000	1.0005771	0.9847522												
3	1.0000000	1.0000000	1.0005766	0.9846365												
4	1.0000000	1.0000000	1.0005773	0.9845268												
5	1.0000000	1.0000000	1.0005785	0.9844272												
6	1.0000000	1.0000000	1.0005769	0.9843038												
7	1.0000000	1.0000000	1.0005773	0.9841817												
8	1.0000000	1.0000000	1.0005796	0.9840610												
9	###	###	###	###												
10	###	###	###	###												
Gj.snitt siste 5 forsøk				CPSM	CTSM	CPLM	CTLM									
				1.0000000	1.0000000	1.0005779	0.9843001									

Fig 27 Proving report used during analysis of time series.

The new meter factors after filtering can be calculated from Equation 5.

$$\text{Meter factor} = \frac{\text{Pulses from USM} \cdot C_{TLM} \cdot C_{PLM}}{\text{Pr Vol} \cdot C_{TSP} \cdot C_{PSP} \cdot C_{TLP} \cdot C_{PLP}} \quad \left[ \text{pulses/m}^3 \right] \quad (5)$$

By applying various filtering techniques, the repeatability during proving can be improved as in Fig 28.

There can however just as easily be introduced a systematic offset in the meter factor as a result of filtering, if one does not for example consider carefully the effect the reduction in flow rate during proving have on the outcome of the filtering (step response and transient response). One must also consider that filtering will be active during normal measurement.

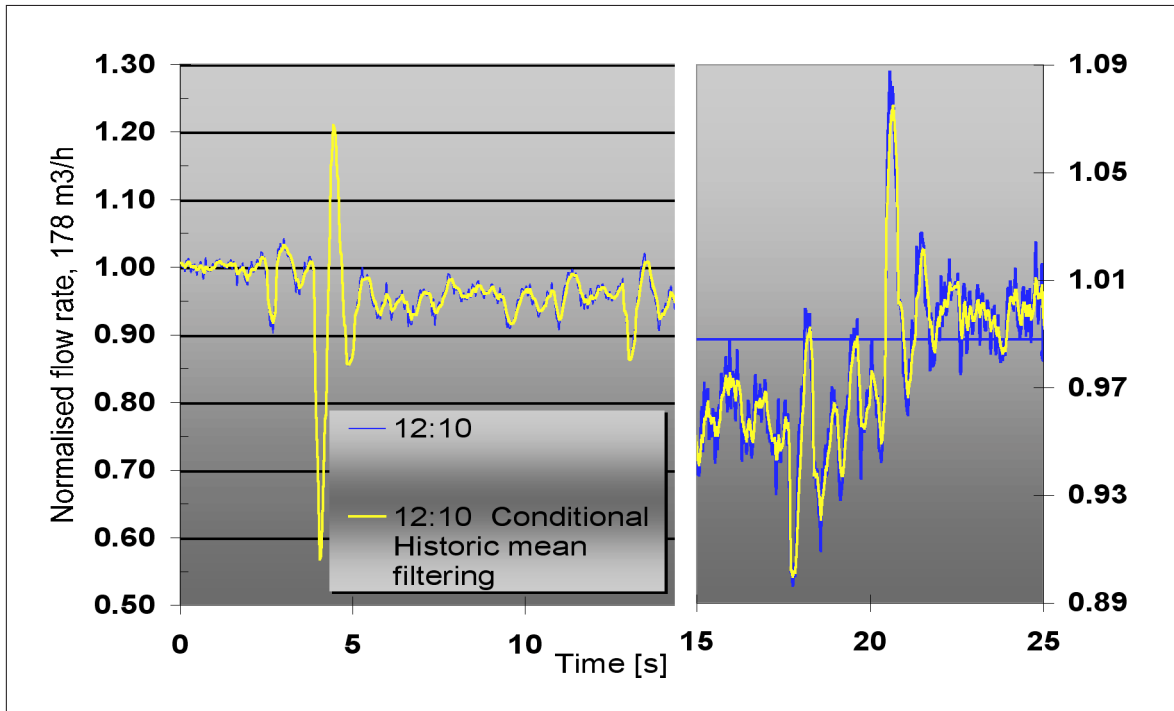


Fig 28 Unfiltered and filtered time series improving repeatability but possibly reducing accuracy. Blown up section show good transient response to large fluctuation in flow.

From Fig 24 and 25, we can see that the prover ball influences the flow rate during proving, especially when passing through bends. The fluctuation in flow this causes is still in effect when the detector switches are passed.

If we assume that a turbine meter will respond to the flow seen in Fig 24 with a low pass filter response, it is probable that although a turbine meter could be proven within the NPD requirements in Brevik, each meter factor achieved were consistently larger than it should be. The described effects will result in a slightly higher average flow rate during proving (slow step response) when a simple low pass filter is applied to the flow seen in Fig 24. The realisation that you can have good repeatability without good accuracy seems to be true in this case.

A conditional historic mean filter is used in Fig 28. The condition is that if the current measured flow rate varies from the previously determined flow rate by more than  $\pm 4\%$ , then the measured flow rate is used, else the historic mean filtered flow rate is used, with 39% weight to the last measured flow rate. This conditional filter gives both good step and transient response.

Using this simple filter the repeatability is improved from 0.140% to 0.101% for the proving trial in time series 12:03 to 12:30. Other filtering methods can improve this further. Using a simple historic mean filter, however, the repeatability gets worse!

So filtering the time series can just as easily worsen the repeatability as improve it, therefore one has to be careful which filtering method is used.

Why then did a turbine meter have better and not worse repeatability in Brevik? This is probably due to the different ways in which the ultrasonic meter, the turbine meter and the prover ball reacts to pulsating flow. The output from the ultrasonic meter is directly proportional to the changes in flow rate, having no mechanical part affected by the flow and thus having a very good step and transient response. The turbine meter on the other hand, being a mechanical device, probably reacts more to the changes in kinetic energy in the flow than the changes in flow rate and thus having a slower step and transient response. The prover ball probably reacts solely to the changes in kinetic energy in the flow, since the flow has to perform work on the prover ball overcoming friction and changes in inertia when passing bends.

For very stable flow conditions, the outcome will be the same for all three, but with severely pulsating flow, this is not the case. Making the ultrasonic meter behave more like a turbine meter (if someone should wish that), can therefore probably not be achieved by filtering the time series alone. One must also take into account the changes in kinetic energy in the flow which is the way in which the reference i.e. the prover ball sees the pulsating flow, see Fig 29.

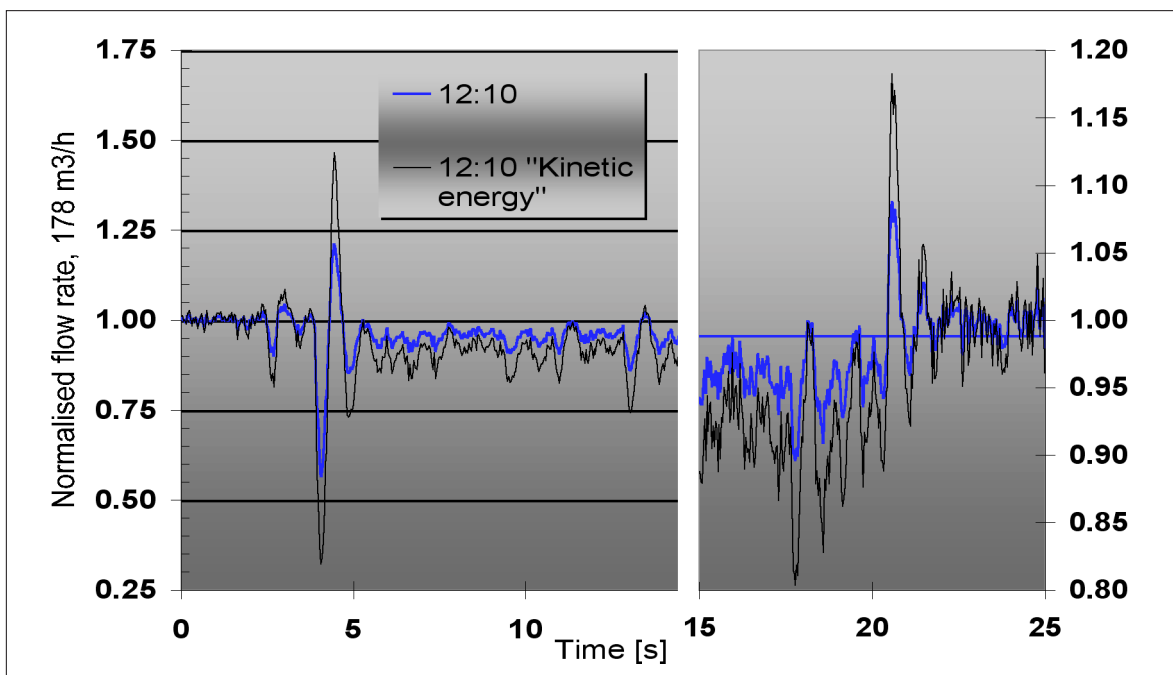


Fig 29 Unfiltered "kinetic energy" time series, possibly the way the prover ball sees the pulsating flow. Blown up section show that "kinetic energy" is more symmetrical in amplitude than the flow rate.

The best solution to poor repeatability of course is to have stable flow conditions and to make the metering system as insensitive to pulsating flow as possible.

## 7 CONCLUSION

The small volume ball prover is designed according to relevant standards and it performs as expected.

The 5-path ultrasonic liquid flow meters operate with good accuracy and stability and measure any fluctuation in flow below 14 Hz.

Pulsating flow with dominating low frequency components is the main cause of the poor repeatability during proving in Brevik. The reason for this is that one period of the pulsating frequencies are a small non-integer multiple of the proving time and the pulsation amplitudes are high. Higher frequency pulsations have no significant effect on repeatability.

To avoid cavitation in pumps during testing the liquid reservoir should be large and split between inlet and return volumes to avoid amplifying pulsations. One should also give the pumps as much head as possible. Low frequency pulsation should of course be avoided.

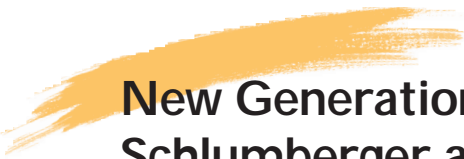
Upstream bends in the prover should be kept as far away from the detector switches as possible. The run-up length before the first detector switch should be as long as possible.

This type of Ultrasonic liquid flow meter is now recommended for use in fiscal liquid metering systems operated by Norsk Hydro.

We are convinced that proving a fiscal 5-path ultrasonic liquid meter with a small volume ball prover can be done, but final proof can only be given in the year 2000 during the final flow test.

## ACKNOWLEDGEMENT

I would like to thank Kongsberg Offshore and Krohne Altometer for providing the data from their respective parts of the metering system and for their participation in the analysis of the same data.



# New Generation Multiphase Flowmeters from Schlumberger and Framo Engineering AS

*Authors (alphabetized)*

*I. Atkinson, Schlumberger Cambridge Research (Cambridge, UK)*

*M. Berard, Schlumberger Riboud Product Center Clamart, France)*

*B-V Hanssen, 3-Phase Measurements AS (Bergen, Norway)*

*G. Ségéral, Schlumberger Riboud Product Center (Clamart, France)*

---

## Abstract

The cooperation between Schlumberger and Framo Engineering has resulted in a significant step forward in multiphase flow metering. This paper describes a new instrument, called **VenturiX**, which will be implemented in two new products: **PhaseTester**, dedicated to Periodic Testing services, and **PhaseWatcher**, dedicated to Permanent Monitoring applications.

The **VenturiX** is a compact instrument consisting of a venturi and a dual energy composition meter located at the Venturi throat and interrogated at high rate. The meter response is flow regime independent so no upstream flow conditioning is needed. It has been extensively tested over the last three years in several flow loops and in real field conditions. The results of these tests are reviewed.

## 1 Introduction

At the beginning of 1997, Framo Engineering AS and Schlumberger recognized that, although they were concerned by different applications - permanent monitoring for Framo, periodic testing for Schlumberger - they had reached similar conclusions and were developing similar technologies to meter multiphase flows. They decided to join forces in order to produce innovative solutions in this domain. A joint Technology and Marketing Center, called 3-Phase Measurements AS, was created at Bergen (Norway) where Framo Engineering AS is based, and staffed with personnel seconded by both companies.

This cooperation gave birth to a common three-phase meter called **VenturiX**. Three experimental prototypes have been built so far and extensively tested in several flow loops and against test separators in field conditions. A Pilot Series is being manufactured.

The **VenturiX** design is particularly compact, a mandatory requirement for periodic testing applications: it simply combines a venturi and a dual energy composition meter located at the venturi throat. The key feature is that the composition meter is scanned at high rate. The **VenturiX** response is particularly robust (independent of inlet flow regime), the most challenging requirement for multiphase flow meters, so no upstream flow conditioning is needed.

The **VenturiX** will be implemented in two products dedicated to different applications: **PhaseTester**, for periodic testing services, and **PhaseWatcher**, for permanent monitoring sub sea and topside.

This paper is aimed at explaining why the compact combination of a venturi and a dual energy composition meter is insensitive to flow-regimes, hence especially suitable for multiphase flow metering. It will also review the test campaigns carried out over the last three years covering a wide variety of flow conditions, in order to fine tune, step by step, the **VenturiX** interpretation model and make it flow regime independent.

## 2 History of the concept

In 1989, Framo Engineering AS started developing a multiphase flowmeter for Permanent Monitoring applications, sub sea and topside. The priority was to overcome what is now recognized as the most difficult challenge in multiphase flow metering to get a robust instrument that could be installed on any well whatever the flow conditions. This is why the meter was built around a straightforward concept backed up by well-proven technologies: a multiphase flow mixer aimed at damping the slugs and homogenizing the flow, a venturi and a dual energy composition meter. Framo commercialized their first meter in 1994. Since that time, 37 meters have been sold.

In 1990, Schlumberger started a program, first at Schlumberger Cambridge Research then at Schlumberger Riboud Product Center, aimed at producing a multiphase flowmeter for periodic testing applications. The objective was to replace the traditional well test separator. The two main motivations were to save costs and to improve data quality. Since the meter is required to travel from well to well, the critical design criterion were a compact design and a robust answer.

Schlumberger's multiphase program met early with failures from which important lessons were drawn.

A first instrument, called GVXM, was designed in 1994. The meter was intended to measure only the liquid and gas rates (the water cut was obtained from a liquid sample). It used a redundant combination of sensors: a Gradio-manometer, a Venturi and a velocity measurement based on Cross-Correlation between differential pressure sensors.

Two prototypes were extensively tested, first at Elf Pecorade and Agip Trecate flow loops, then against a test separator in the Middle East over a period of six months in real periodic testing conditions. Compared with the encouraging flow loop tests, the results of the field test were frustrating: 75 % of the liquid rates were within the 5 % targeted accuracy, but some liquid rates were out by 20 % or more; 80 % of the gas rates were within the 10 % targeted accuracy, but some gas rates were out by 30 % or more.

It was recognized that the GVXM interpretation model is flow regime dependent. It was discovered that the cross-correlation is an ambiguous velocity measurement, not resulting in the same answer in bubbly flows and in slug flows. For similar reasons, the interpretation of the gradio-manometer, in terms of effluent density, is questionable at high Gas Volume Fraction.

The GVXM project was closed at the end of 1996.

### 3 The VenturiX key concepts

Having spent a lot of time and money, Schlumberger had developed a few strong convictions.

- 1 Flow rates must be evaluated in terms of mass (which are conservative), not in terms of volumes (which are not)
- 2 To be compact, a multiphase flowmeter must accommodate any flow regime without the help of any upstream mixing device.
- 3 To accommodate slug flows, the composition meter needs to be interrogated at high rate.
- 4 A Venturi is an efficient flow conditioner.
- 5 The pressure drop across a venturi can be interpreted in terms of total mass flow rate, provided the fluid density is evaluated at the throat.
- 6 At the throat of a venturi, the slip law is flow regime independent because it is dictated by stringent fluid dynamic equations.
- 7 Any three phase composition meter must combine two different measurements. In this regard, a dual energy composition meter has a formidable advantage. Both measurements are performed at the same time and at the same place: both sense the same flow.

At this stage, it became clear that Schlumberger and Framo Engineering AS had selected the same well proven technologies - a venturi and a dual energy composition meter - but were using different strategies to deal with unsteady flows. It was acknowledged that Schlumberger's approach was attractive, because it was opening the door to a significantly more compact design. It was also recognized that the robustness of the **VenturiX** had to be checked against a wide variety of flow regimes. The test program needed to include well controlled environments, such as flow loops, where fluid properties and reference rates are indisputable, and also test separators in real field conditions where environmental parameters are usually not controlled.

## 4 Flow loop tests

Over the last three years, the **VenturiX** underwent six flow loop campaigns in five different sites totaling over 1,400 flow periods with different fluids, different line pressures and variable flow regimes. As summarized in the table below, each campaign was an opportunity to test the model against different environmental parameters and to refine it. Since the **VenturiX** stores raw data, a Schlumberger requirement, each model upgrade has been checked against the whole set of available data.

Date	site	flow periods	Issues
Q1 1997	SRPC (France)	200+	Venturi pressure-drop model and slip-law Quite steady flows. Line pressure up to 4 bars
Q2 1997	NEL (Scotland)	160	Unsteady flows. Line pressure up to 4 bars Fast processing of the Composition Meter
Q4 1997	Framo (Norway)	40	Line pressure up to 10 bars
Q1 1998	IFP (France)	210	Line pressure up to 30 bars Fluid Property Model
Q4 1998	CEPRO (Venezuela)	250	<b>Oil viscosity up to 2300 cPo</b>
Q2 1999	NEL (Scotland)	500	Multiflow II JIP. The ultimate qualification

The results of all of these tests using the latest version of the interpretation model are shown in the attached figures.

## 5 Field Tests against Test Separators

In Q4 1998, two additional prototypes were built and sent to the Field where they were evaluated in series with a test separator in typical Periodic Testing conditions. The results of three campaigns have been analyzed so far. The conditions are summarized in the table below. Two more campaigns were begun in Q3 1999, in Nigeria and in Venezuela.

Campaign	# 1	# 2	# 3	#4	#5	#6
Date	Dec 98	Jan 99	May 99	June 99	Aug 99	Sept 99
# of flow periods	38	38	27	22	10	2
# of wells tested	8	5	7	1	6	1
Line pres. (psia)	260-1200	150-1380	100-140	1000-1200	40-120	190
GVF (%)	60-90	60-98	70-97	92-94	0-90	93
<b>Oil visc. (cPo)</b>	< 15	< 15	<b>100-2000</b>		<b>140-620</b>	<b>200</b>
Liq. rate (blpd)	2500-11000	900-4800	500-1750	2200-6600	1000-6000	500-600
Gas rate (MMscfd)	2-8	0.8-10	0.3-1.5	13-46	0-0.1	0.3-0.5

The main results are shown on the following figures.

On Figure 7, the **VenturiX** liquid flow rate is plotted against the separator.

On Figure 8, the **VenturiX** gas flow rate is plotted against the separator.

On Figure 9, the error on the water/liquid ratio is plotted against the gas volume fraction at line conditions. (Note that the targeted accuracy is 5% absolute up to 90% GVF).

## 6 Design Specifications

The following specifications apply to a 4” **PhaseTester** (skid-mounted, portable module for periodic testing).

Design Specifications	
Weight	1,500 kg
Size	1.5 x 1.6 x 1.7 m
Power consumption	50 W
Chemical source activity	100 mCi
Hazardous area	Zone 1
Ingress protection	IP67
Line pressure rating	5,000 psi
Line temperature rating	-20 +150°C
Ambient temperature	-20 +85°C

Max. of	Maximum Design uncertainty (up to 90% GVF)		
	Liquid Rate	Gas Rate	Water/Liquid Ratio
	5% of reading	10% of reading	5% absolute
	2.5% of full scale	5% of full scale	
Full scale	155 m <sup>3</sup> /h	800 m <sup>3</sup> /h	100%

## 6 Conclusions

The **VenturiX** is an innovative multiphase flow meter designed initially by Schlumberger to replace conventional test separators in periodic testing operations. It has been jointly industrialized by Schlumberger and Framo Engineering AS, benefiting from Framo’s expertise in fluid process and sub sea installations, as well as from Schlumberger’s expertise in instrumentation and well testing.

The **VenturiX** is based on reliable and well-proven technologies. Venturi’s and nuclear densitometers have been used by the oil industry for a long time. It is compact because it does not require the help of any upstream flow-conditioning device. It accommodates unsteady flows because the Composition Meter is scanned at high rate. Its response is flow regime independent because gas/liquid flows are severely constrained while passing through a convergence.

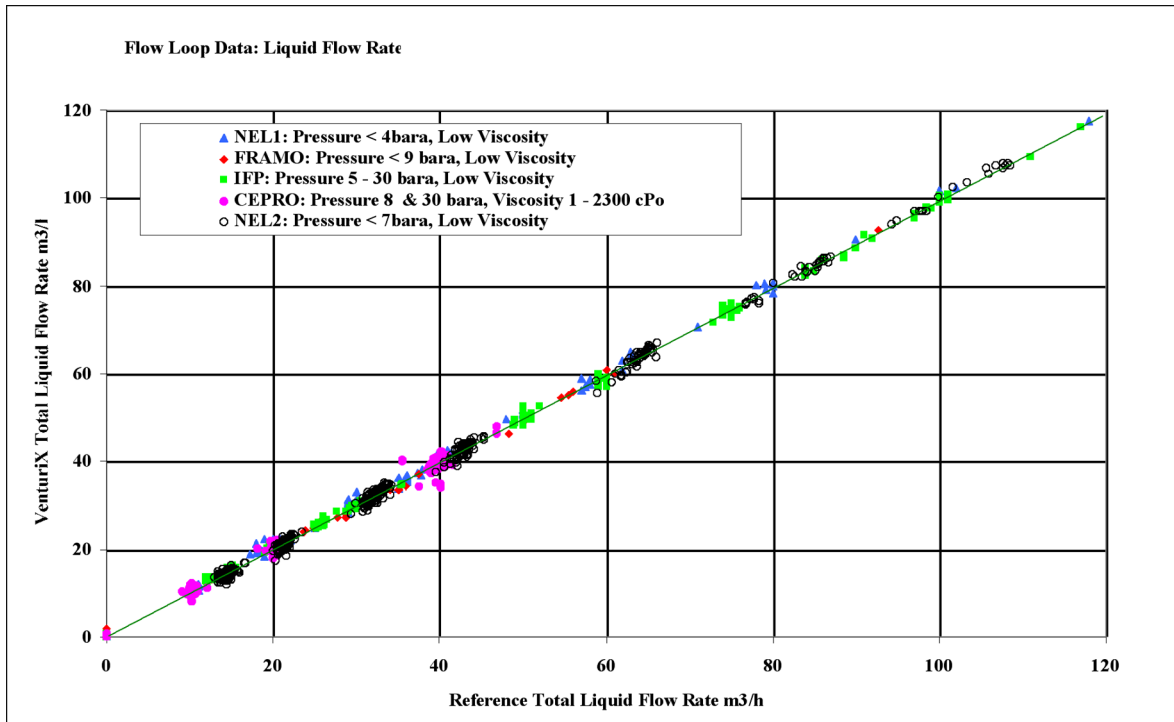
The robustness of the **VenturiX** interpretation model has been carefully checked over the last three years in a large variety of flow conditions in several flow loops and in real field conditions.

The **VenturiX** technology is being currently implemented in two products that will be available to the oil industry in a near future:

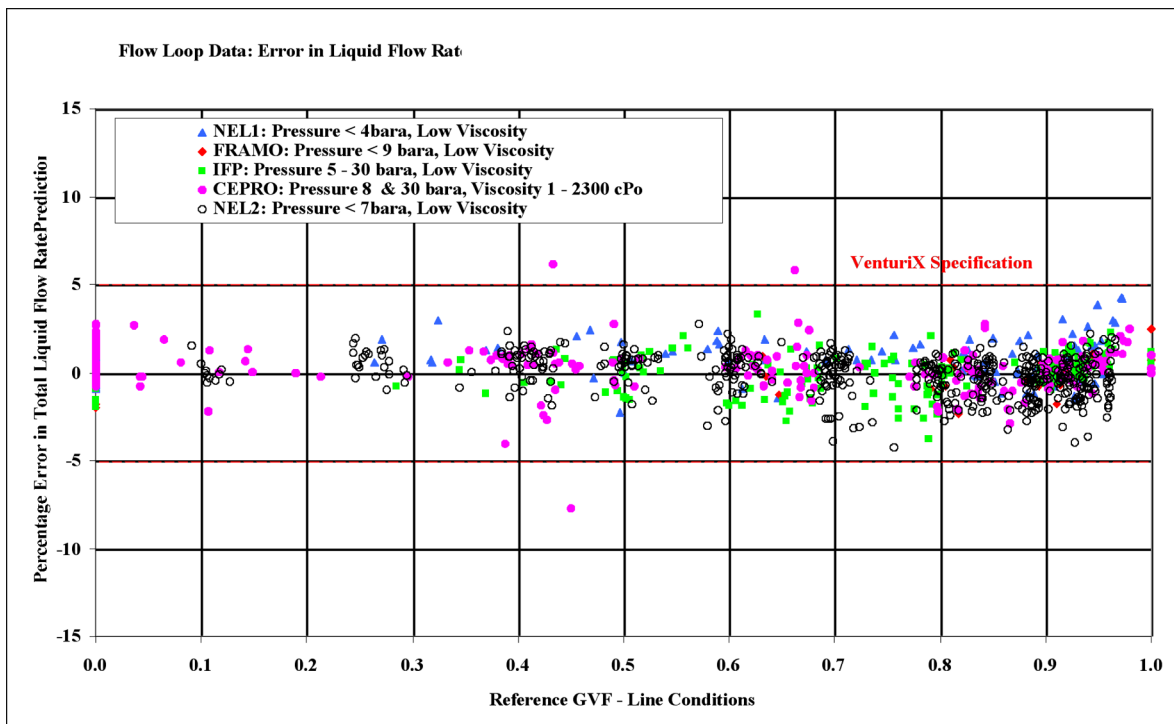
**PhaseTester** for Periodic testing applications

**PhaseWatcher** for Permanent monitoring applications

## VenturiX Flow-loop data

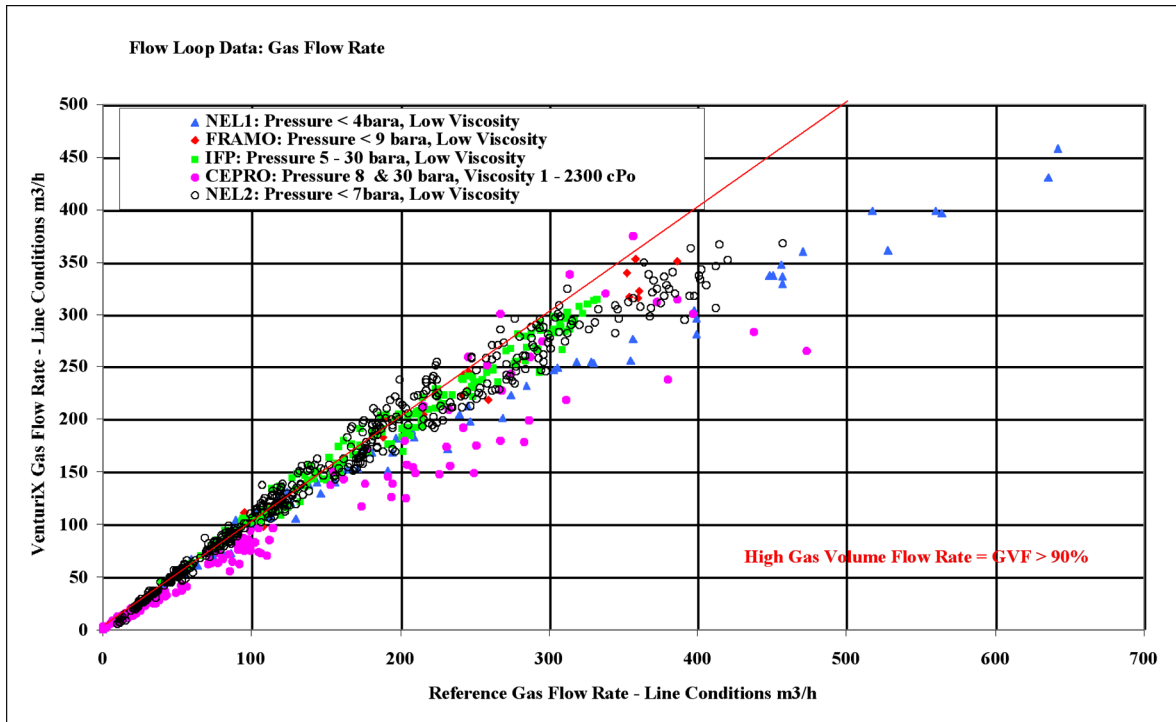


Predicted Liquid versus reference liquid (at line conditions) Fig. 1

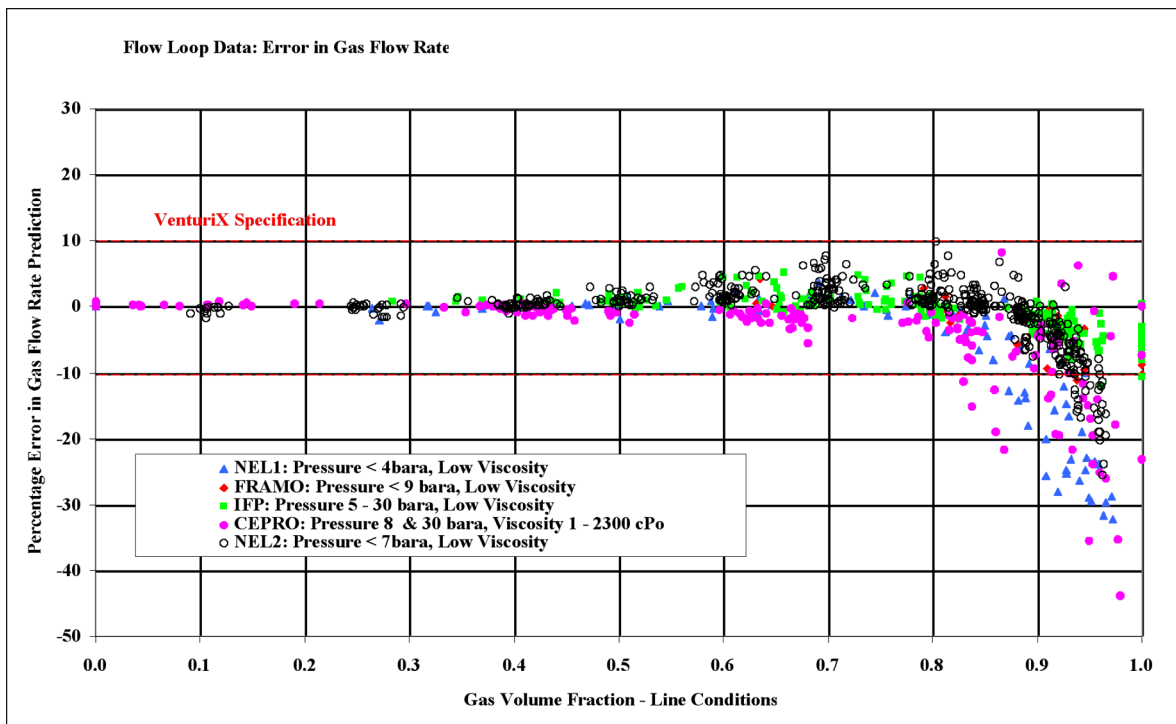


Liquid percentage error (at line conditions) Fig. 2

## VenturiX Flow-loop data

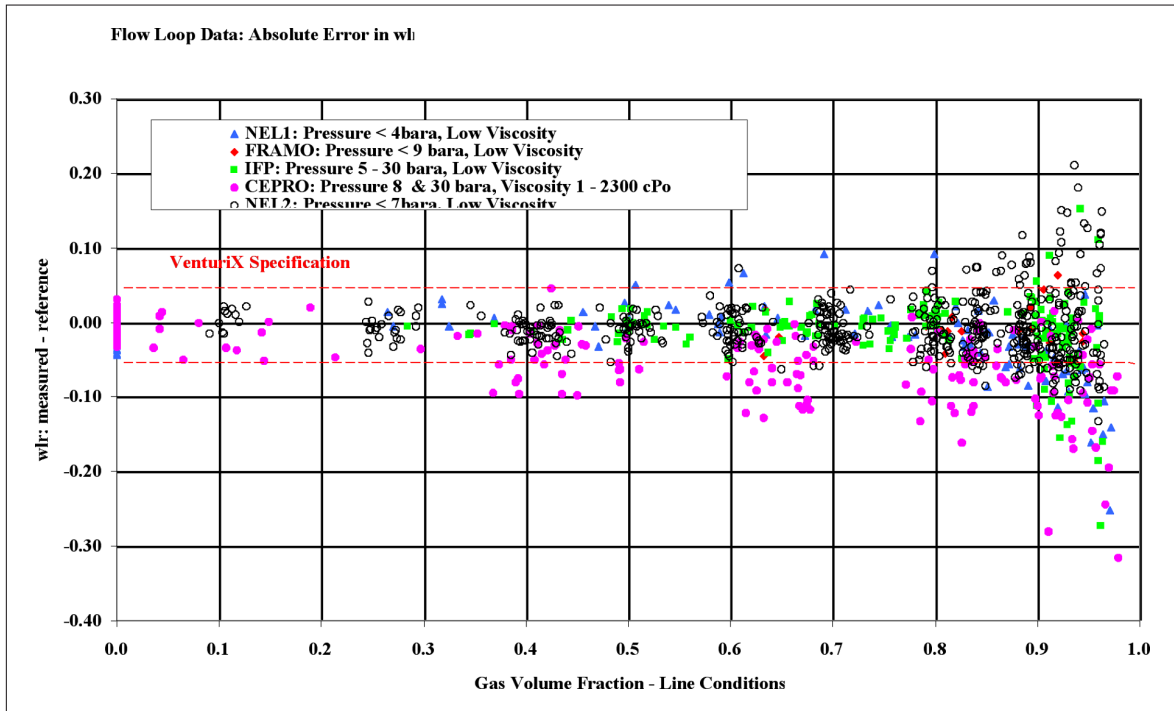


Predicted Gas versus reference gas (at line conditions) Fig. 3

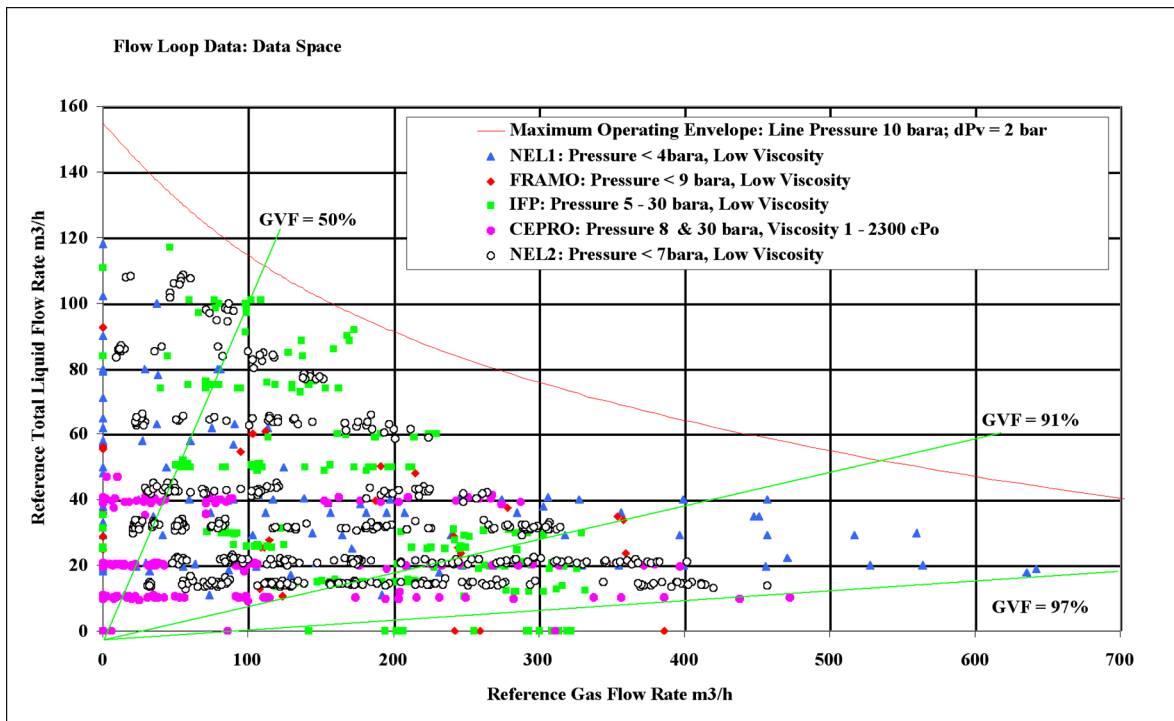


Gas percentage error (at line conditions) Fig. 4

# VenturiX Flow-loop data

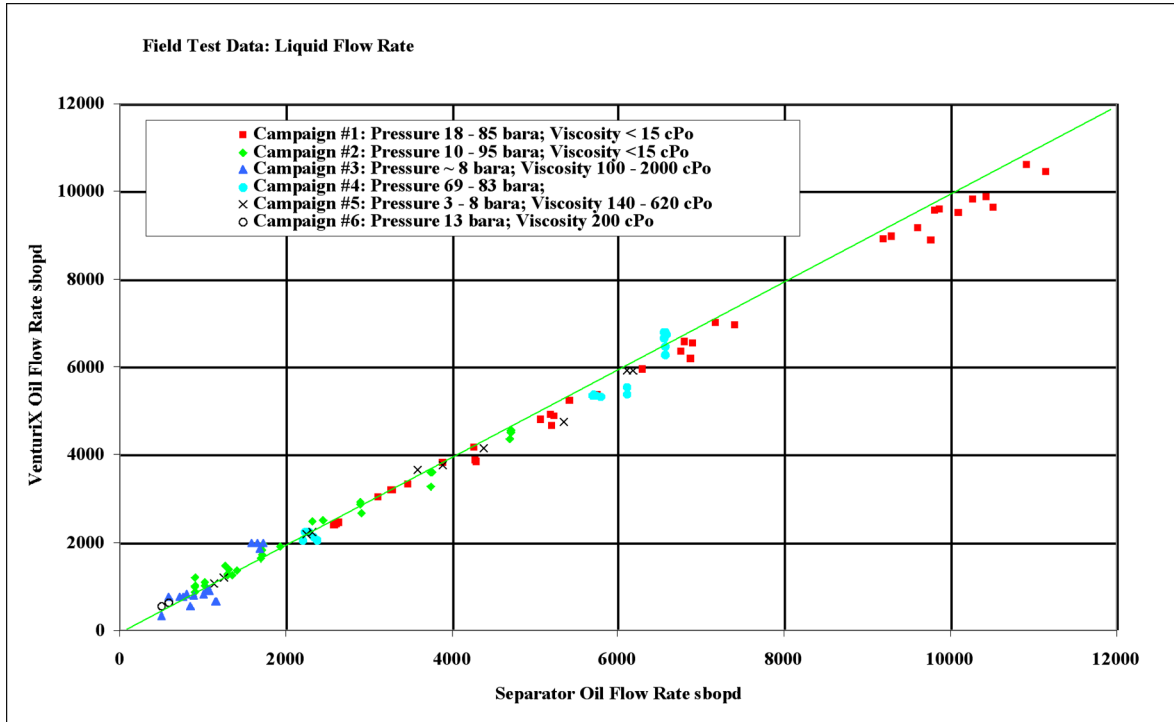


Water Liquid Ratio absolute error Fig. 5

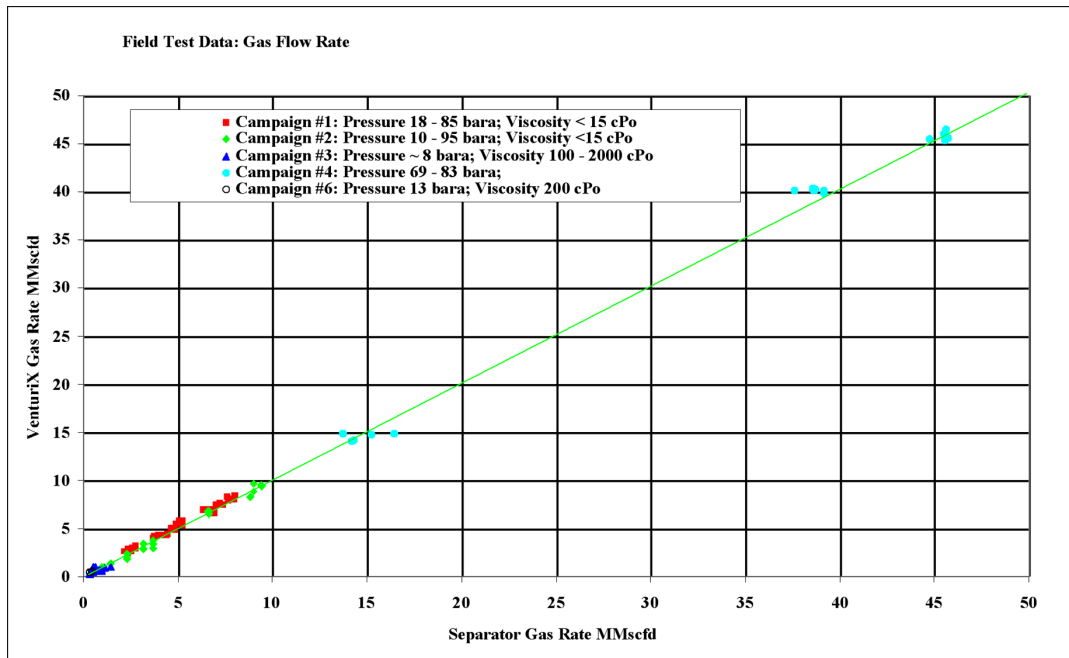


Gas-Liquid test matrix (at line conditions) Fig. 6

## Field Tests against Test Separators

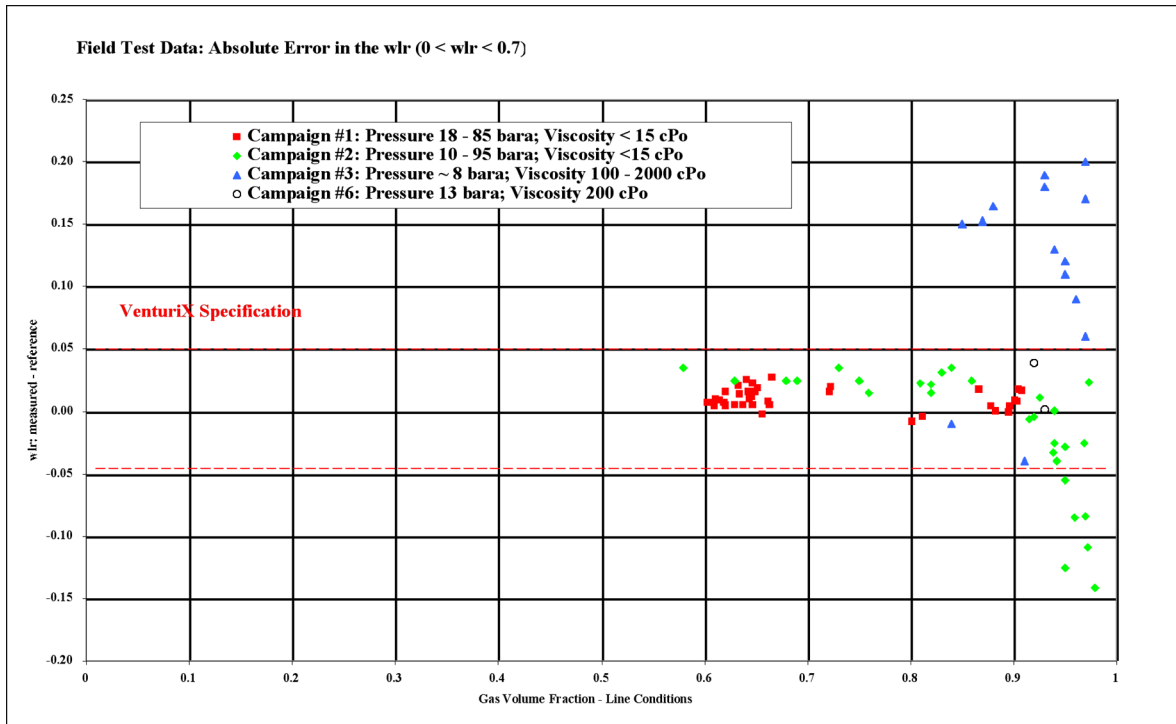


Predicted Liquid versus separator liquid (standard conditions) Fig. 7



Predicted gas versus Separator gas (standard conditions) Fig. 8

## Field Tests against Test Separators



Predicted WLR versus separator or sample Fig. 9



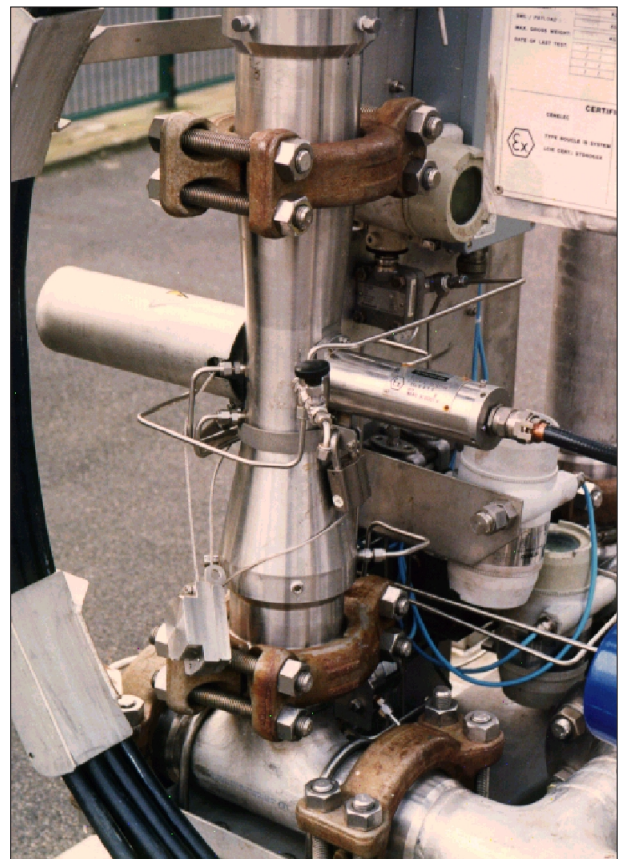
Field test picture Fig. 10

## VenturiX Prototypes 1, 2 & 3 (1440 psi)

*Skid assembly*



*Measuring Section*



**VenturiX Commercial Version (5000 psi)**





# A HIGH-ACCURACY, CALIBRATION-FREE MULTIPHASE METER

*G.J. Miller, C.J. Alexander, F. Lynch, D.J. Thompson  
Daniel (Europe) Ltd.*

*W. Letton  
Daniel Measurement and Control*

*A.M. Scheers  
Shell International E & P*

---

## INTRODUCTION

The need for accurate and reliable measurement of three-phase flow streams is well documented. To this end Daniel have developed a high-accuracy multiphase flowmeter “MEGRA” based on the sound measurement principle of (multiple energy) gamma ray absorption. The ultimate aim of such technology is to replace the measurement function of the traditional test separator with a cheaper, lower-maintenance and calibration-free alternative. At present, due to its high-accuracy water-cut (WC) and real-time performance, MEGRA has also been utilised for well management programs downstream of traditional test separators.

The flow-rates of the individual water, oil and gas phases are derived from a measurement of the bulk flow through an annular Venturi, combined with phase fraction information deduced from the absorption of gamma-rays within the multiphase fluid. The gamma-ray technique has the advantage over other multiphase metering methods in that it is applicable over the full range of water-cuts from 0 – 100% and does not depend upon the nature of the emulsion present.

This paper outlines the basic principles behind the multiphase flow measurement and highlights some of the advantages of the present technology. The use of relatively low-energy gamma-ray emissions and high-resolution solid-state detectors lends an enhanced sensitivity to the measurement. Consequently, water-cuts and gas volume fractions can be determined to high accuracy (< 2%) in relatively short measurement times (~ seconds).

A significant issue with commercially available multiphase meters is how well they cope with variations in their operational environment. Of particular interest is the sensitivity of a meter to changes in the salinity of the produced water, since not only is it a common occurrence, but one with potentially debilitating effects on most meters. The MEGRA multiphase meter has the potential to sense and compensate for such salinity changes. Furthermore, the method can be extended to achieve calibration-free operation in the field, with only a factory characterisation required.

It is generally accepted that multiphase meters face one of their severest tests in high gas volume fraction (GVF) applications, where the process flow may be less homogeneous and differences can arise between the liquid and gas phase velocities. Traditionally, operation under these conditions has been attempted through the use of mixing elements that somehow aim to homogenise the flow, via the measurement of key process parameters at frequencies matching the time-scale of turbulences within the flow, by the incorporation of advanced flow models and slip corrections or by some combination of these techniques. Another approach, now practical through recent advances in compact separator technology, involves rough separation of the process flow into a (wet) gas and (gassy) liquid stream, which are in turn monitored by a conventional gas-sensor and multiphase meter respectively.

On a stand-alone basis MEGRA uses a combination of basic flow conditioning, fast sampling and correction algorithms for operation under high gas-content conditions. However, its superior performance within the lower part of the gas fraction envelope, also make it ideally suited for integration with modern compact separator technology or for extending the well-testing capacities of existing test separators. This paper focuses mainly on the latter operating region and presents the results from field trials completed to date, which demonstrate the quality of metering performance achieved under live operating conditions of this type.

## BASIC PRINCIPLES

### Bulk Flow-Rate Measurement

The basic mechanical arrangement of the Daniel MEGRA multiphase flowmeter is shown in Figure 1. The bulk flow-rate is measured by means of an annular Venturi device integrated into the meter-body, which produces a differential pressure,  $\Delta P$ . For the case of homogeneous flow, the total volume flow-rate of the mixture,  $Q_m$ , may be derived from the pressure drop across the Venturi and the mixture density,  $\rho_m$ , by:

$$Q_m = C \cdot \sqrt{\frac{\Delta P}{\rho_m}}$$

The constant,  $C$ , incorporates both geometrical terms and a standard coefficient of discharge. The mixture density is derived from the individual densities of the water, oil and gas components, weighted by their phase fractions as determined by the composition measurement.

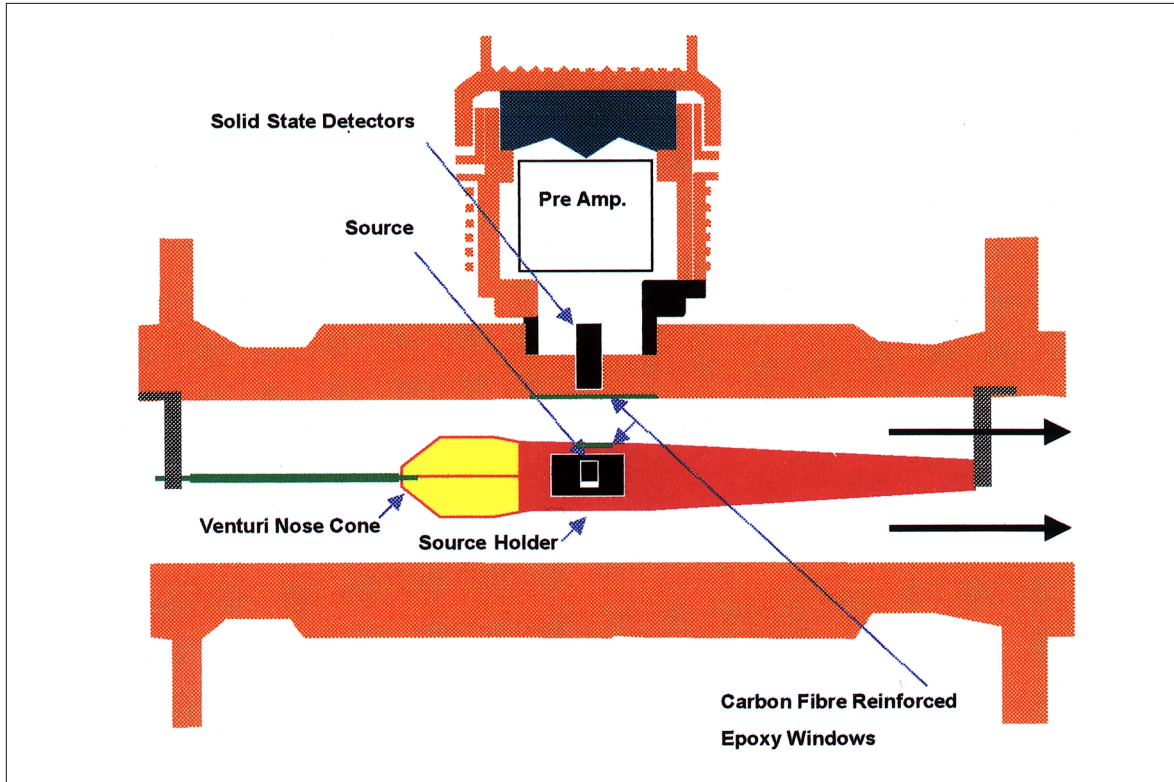


Figure 1: Schematic diagram of the Daniel MEGRA multiphase flowmeter, showing the concentric Venturi system used for bulk flow measurement and the radioactive source / detector arrangement from which phase fraction information is derived. The nose cone may be interchanged to alter the b-ratio.

The Venturi centre-body serves the secondary purpose of housing the radioactive source used in the gamma-ray absorption measurement. To ensure sufficient accuracy in the fraction measurement (following section), a fluid absorption path of  $\sim 20\text{mm}$  is required. With a standard Venturi arrangement, this would pose a severe limitation to the gross flow-rates achievable, but the concentric design allows the required path-length to be maintained for almost any cross sectional area of the fluid flow. In practice, the Venturi information can be replaced with that from any meter capable of measuring the total flow of the multiphase stream.

### Composition Measurement

Composition measurement by gamma-ray absorption is now a well-established technique in multiphase metering. Gamma rays produced by a collimated radioactive source, in this case housed in the centre of the meter, propagate through the multiphase fluid towards a gamma-ray detection device. As they pass through the fluid, they are attenuated to different degrees, depending upon the fractions of water, oil and gas present. Since evaluation of these fractions, ( $\alpha_w$ ,  $\alpha_o$  and  $\alpha_g$  respectively), corresponds to the determination of *two* unknowns (a constraint being that the phase fractions must add to unity), gamma-ray absorption must be measured at a minimum of *two* distinct energies. Mathematically the problem may be stated as follows. For a multiphase mixture, occupying a region of path-length  $D$ , the measured count-rate  $I_m$ , at a given energy  $E$ , is:

$$I_m(E) = I_v(E) \cdot \exp[-\mu_m(E) \cdot D] \quad \text{where} \quad \mu_m(E) = \alpha_w \mu_w(E) + \alpha_o \mu_o(E) + \alpha_g \mu_g(E)$$

Here,  $I_v(E)$  represents the empty pipe (vacuum) count rate at energy  $E$ , and the linear attenuation coefficients of the mixture (m) and pure phases (w, o, g) in obvious notation. By measuring at two distinct gamma-ray energies, where the absorption coefficients of the three phases are sufficiently different, a set of linearly independent equations is obtained which can be solved for two of the unknowns,  $\alpha_w$  and  $\alpha_o$  say. The remaining fraction,  $\alpha_g$ , is given by closure. The system of equations can be written in a convenient matrix notation:

$$\begin{bmatrix} \mu_m(E_1) \\ \mu_m(E_2) \\ 1 \end{bmatrix} = \begin{bmatrix} \mu_w(E_1) & \mu_o(E_1) & \mu_g(E_1) \\ \mu_w(E_2) & \mu_o(E_2) & \mu_g(E_2) \\ 1 & 1 & 1 \end{bmatrix} \cdot \begin{bmatrix} \alpha_w \\ \alpha_o \\ \alpha_g \end{bmatrix}$$

The elements of the  $[3 \times 3]$  matrix are obtained from a calibration process that involves filling the meter with samples of the pure fluids (water, oil and gas) in turn, or alternatively can be calculated from tabulated gamma-ray attenuation coefficients. This latter concept, which requires only a single empty-pipe count-rate measurement in the field, will be referred to as “calibration-free” operation.

The Daniel composition meter of Figure 1 uses an  $^{241}\text{Am}$  radioactive source, located at the centre of the metering stream, to provide gamma-rays of several energies up to 60 keV. The gamma-rays traverse a finite section of the process flow, where they are either absorbed by the fluid or are detected by a solid-state detector mounted on the exterior of the pipe. Due to the relatively low energy of the gamma-rays, the fluid path-length is restrained to around 20mm. To avoid the high gamma-ray losses that would otherwise occur on passage through the pipe walls, low-absorption Carbon Fibre Reinforced Epoxy windows are used to provide process isolation in the vicinity of the measurement path. Peltier-cooled solid state detectors provide sufficient energy resolution to distinguish the closely spaced lines of the Am-241 gamma-ray spectrum (Figure 2).

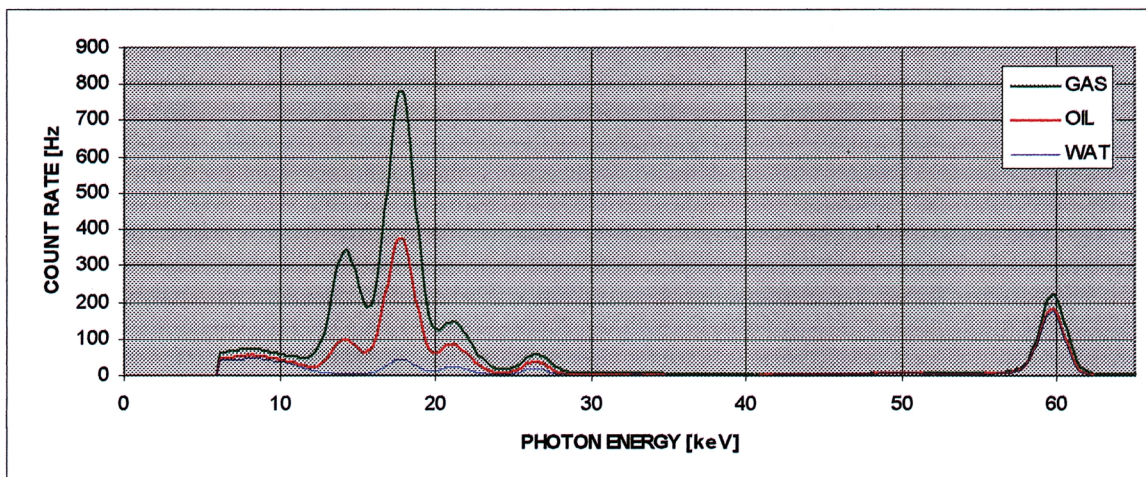


Figure 2: Typical gamma-ray energy spectra for the pure phases as measured by the solid-state detectors.

Measurement at two energies is a minimum requirement but in practice all gamma-ray lines of sufficient intensity (14, 18, 21, 26 and 60 keV in this case) are incorporated into the fraction calculation to improve the accuracy of the results.

With suitable optimisation [1,2] of the various design parameters (source energies, fluid path-lengths etc.), the MEGRA multiphase meter has proved capable of measuring phase fractions to an accuracy of better than 2% (absolute) over the full range of water-cuts and gas volume fraction, in measurement times of only seconds.

The MEGRA multiphase flowmeter has various advantages over competing technologies that also employ the gamma-ray absorption principle. The high contrast between water, oil and gas, at the lower energies employed here (Figure 2) contributes significantly to its water-cut measurement performance. Even at energies as low as 60 keV, the differential between oil and water is greatly reduced. At the higher energies commonly used in other multiphase meters (e.g. the 30 and 360 keV lines of Ba-133 and the 660 keV line of Cs-137) the contrast between oil and water becomes diminishingly small (Figure 3). Far longer counting times are then necessary to obtain the same statistical accuracy in the fraction measurement, and any inhomogeneity which occurs in the multiphase flow during this extended measurement period, will lead to an error in the derived fractions which must somehow be corrected for.

All technologies that incorporate radioactive sources must of course address the issue of radiation safety. The basic mechanical design of the MEGRA flowmeter, where the source is fully enclosed within the pipeline, has obvious security advantages. This arrangement also ensures that external radiation levels are negligibly small, since the stainless steel which forms the meter-body also provide adequate shielding for the relatively low energy emissions from the source. Another advantage of Am-241 is its comparatively long half-life (450 yrs compared to 10 yrs for Ba-133) which means that frequent replacement or adjustment of the source position to maintain the original reference count-rates, is unnecessary.

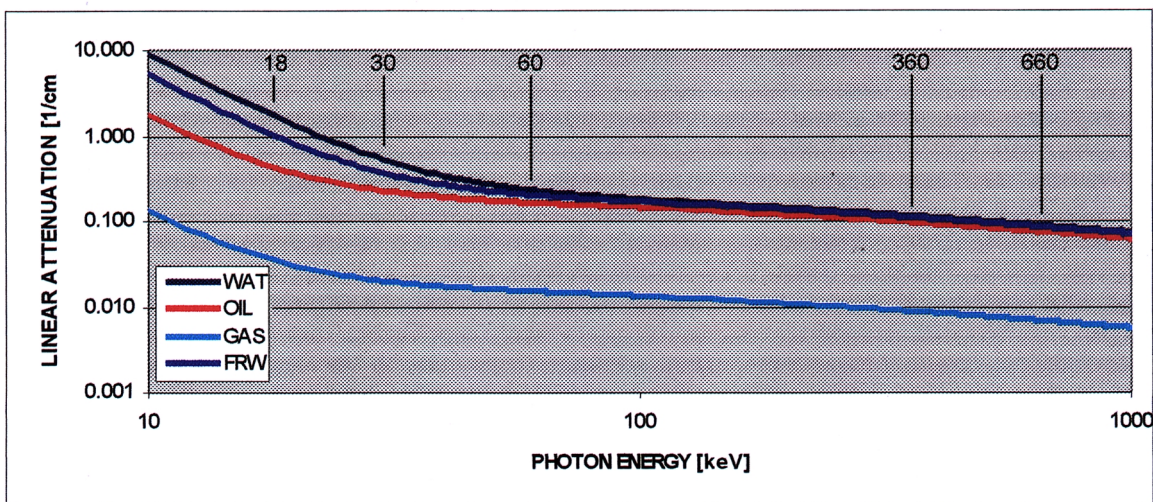


Figure 3: Photon linear attenuation coefficients for fresh and saline water ( $S = 100 \text{ kg/m}^3$ ), oil and gas. Also shown are the most common gamma-ray energies employed in commercial multiphase flowmeters.

## Salinity Evaluation

In practical multiphase metering applications there exists the possibility that the salinity of the production water will change with time, particularly in the case of water-injected reservoirs. For all multiphase flowmeters employing the gamma-ray absorption technique, such changes can lead to significant errors in the measured phase fractions if the reference count-rates (for 100% water) are not suitably corrected. In fact, most metering techniques (conductivity, microwave etc.) are similarly affected by changes in production water salinity.

As detailed above, a gamma-ray absorption measurement at *two* distinct energy levels provides sufficient information to evaluate *two* unknown parameters ( $\alpha_w$  and  $\alpha_o$  say), as required for complete phase fraction definition. However, with the present system, *three* (or more) gamma-ray energies can be resolved (Figure 2), which have sufficiently different responses to the individual fluid components (Figure 3) that a *third* unknown parameter, namely the salinity, can potentially be derived [2]. At the higher energies typically utilised by other manufacturers the contrast between the fluids is much reduced, rendering this technique somewhat impractical.

To include the salinity as a free parameter in the computation, the linear attenuation coefficient of the saline water is expanded in terms of the fresh water coefficient,  $\mu_f$ , and the salinity  $S$ .

$$\mu_w(E) = \mu_f(E) + K \cdot S$$

The dependence upon  $S$  is essentially linear, the constant  $K$  comprising the *mass* attenuation coefficients of the fresh water and the salt type, as well as a salt solubility factor. Increasing the number of energy levels to three, to allow for the extra degree of freedom, yields a system of equations that now forms a [4 × 4] matrix of a type similar to that derived earlier.

However, solution of this system of equations requires data of greater statistical accuracy than can be recorded during a typical measurement cycle of a few seconds. Fortunately, salinity changes in the field generally occur on a time scale far greater than this (months perhaps) and therefore it is possible to concatenate data from a large number of measurement cycles, over which the salinity may be assumed to remain constant. (The phase fractions may of course vary from cycle to cycle). As before, any information available from additional energy levels present (a 4<sup>th</sup> or 5<sup>th</sup> in this case) may be incorporated into the algorithm, with the effect of improving the overall accuracy of the result, or of reducing the necessary acquisition time. Figure 4 shows the computed salinity for a set of saline water reference fluids, derived with only a few minutes of accumulated data.

$$\begin{bmatrix} \mu_m(E_1) \\ \mu_m(E_2) \\ \mu_m(E_3) \\ 1 \end{bmatrix} = \begin{bmatrix} \mu_f(E_1) & \mu_o(E_1) & \mu_g(E_1) & K(E_1) \\ \mu_f(E_2) & \mu_o(E_2) & \mu_g(E_2) & K(E_2) \\ \mu_f(E_3) & \mu_o(E_3) & \mu_g(E_3) & K(E_3) \\ 1 & 1 & 1 & 0 \end{bmatrix} \cdot \begin{bmatrix} \alpha_w \\ \alpha_o \\ \alpha_g \\ \alpha_w \cdot S \end{bmatrix}$$

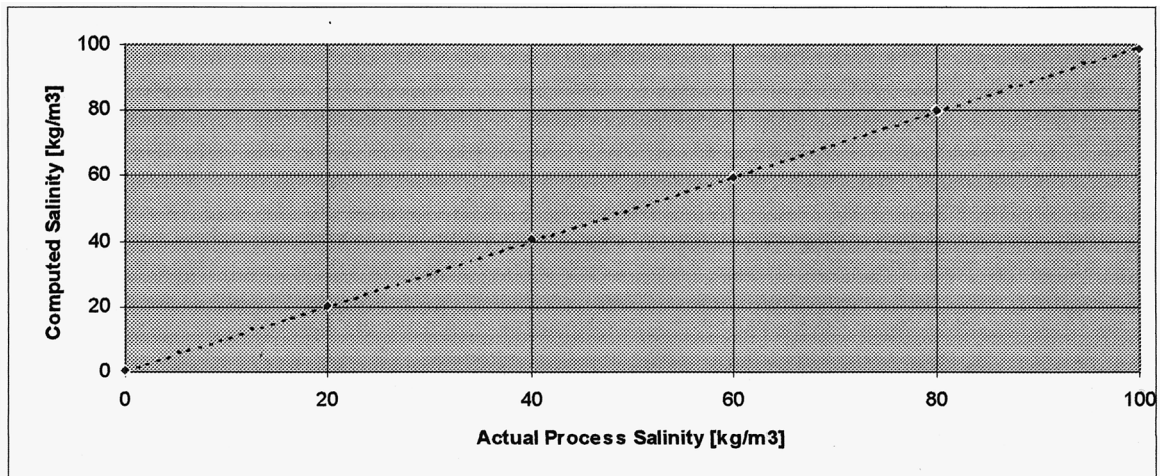


Figure 4: Water salinity as computed by MEGRA for a variety of saline reference solutions. At high water-cut, an accuracy of  $\pm 1$  kg/m<sup>3</sup> can be achieved with only a few minutes of accumulated data.

At lower water-cuts, longer accumulation times (stretching to several hours) are necessary to achieve the same accuracy in salinity. Fortunately, even in the worst case of injection-water breakthrough, the time scale for significant changes in the process water salinity is likely to be of the order of days.

### Calibration Free Operation

With suitable characterisation of the meter in the factory (in terms of its precise geometry, signal processing corrections etc.) it is possible to commission a meter in the field with only a single empty-pipe count-rate calibration as a reference point. Provided adequate information is available about the oil, water and gas components (from sampling and laboratory analysis for example) then the absorption characteristics of these pure phases can simply be entered as numerical coefficients. This in itself constitutes a major simplification to the installation and calibration procedure. With the added ability to determine water salinity dynamically (as described above), the calibration procedure can be simplified even further. Only the fresh water attenuation coefficients are then required and these are well established. The oil and gas characteristics (composition and density) must still be supplied, but small errors in these quantities are far less detrimental to the accuracy of the overall fraction calculation [3].

## PRACTICAL APPLICATIONS

Initial field applications of the MEGRA multiphase flowmeter were primarily on the gassy-liquid outlets of test-separators and in-line conditioning devices. To this end, static laboratory tests, which demonstrated a measurement accuracy of better than 2% over the full GVF and WC range, were extended to a series of flow-loop measurements that encompassed the operating envelopes of these initial applications.

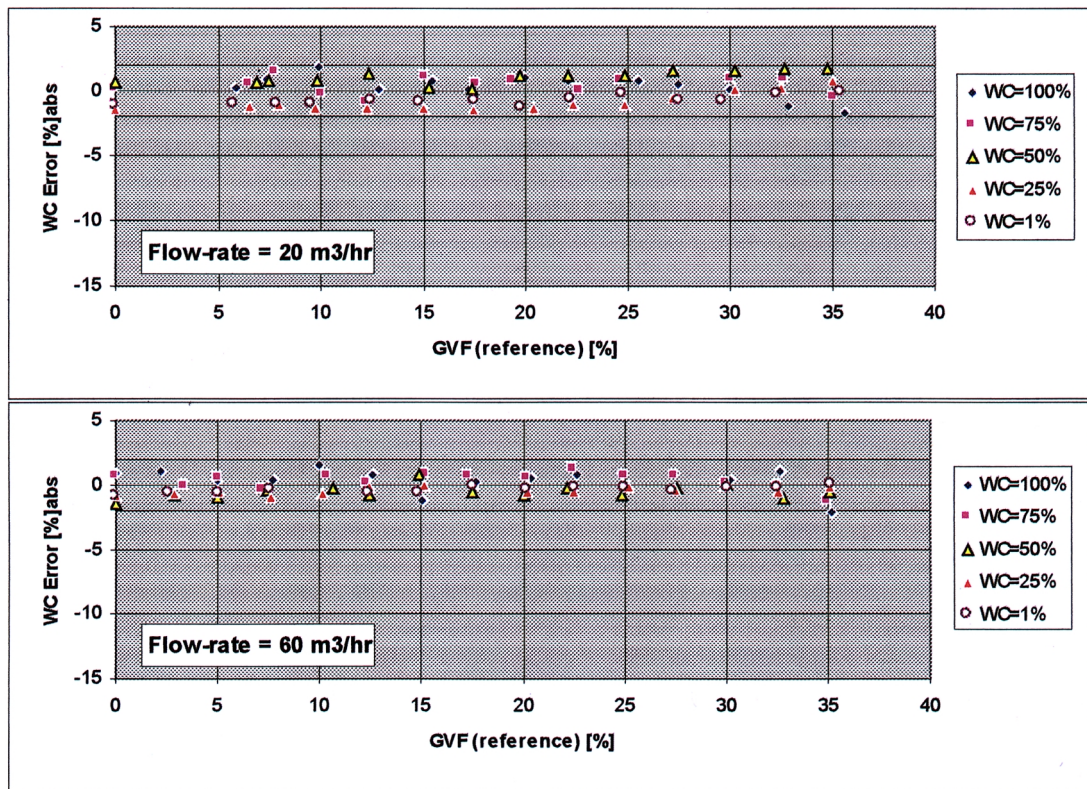


Figure 5: MEGRA Water-Cut error vs. Gas Volume Fraction at WCs from 1 to 100%. (From flow testing at Shell RTS's Donau flowloop, Rijswijk, The Netherlands).

Figure 5 shows the water-cut performance of the MEGRA multiphase flowmeter at two distinct liquid flow-rates. The data were recorded at Shell's Donau Flowloop in Rijswijk, The Netherlands. A water-cut accuracy of better than 2% (absolute) was maintained over the full WC range and up to GVF's of more than 35% - far in excess of the gas content specified for any of the initial field applications.

One advantage of MEGRA's high water-cut accuracy and fast time-response is aptly demonstrated by the results of extended field trials carried out at the onshore production site of NAM (Rotterdam) in The Netherlands. Traditionally net oil production was monitored at this site by bulk flow-rate measurements at the output of a test separator coupled with periodic sampling of the oil/water content of each reservoir stream. The results, however, were occasionally anomalous, particularly for some of the high water-producing wells. With a MEGRA multiphase flowmeter installed at the "liquid" output of the test separator, the reason for some of these discrepancies became clear. A rapid cyclic behaviour was evident in the water-cut of some streams (Figure 6), which had not been previously recognised [4]. To verify the integrity of the MEGRA data, a sequence of manual samples were gathered from the liquid outlet, at a period of about two minutes. As Figure 6 shows, the samples show excellent correlation with the synchronised MEGRA values. (The MEGRA cycle time was increased by a factor of ten for this test, simply to aid with time correlation of the data sets.

With the usual dwell time of just a few seconds, the water-cut oscillation in this well was observed to be even more pronounced). The cyclic behaviour has not been fully explained, but the disadvantage of estimating the water-cut of a well from process samples taken randomly in time is clearly demonstrated. The MEGRA multiphase flowmeter has now replaced periodic sampling as the primary source of WC information at this site, and due to the high-quality real-time data that it provides, forms an integral part of their reservoir management system.

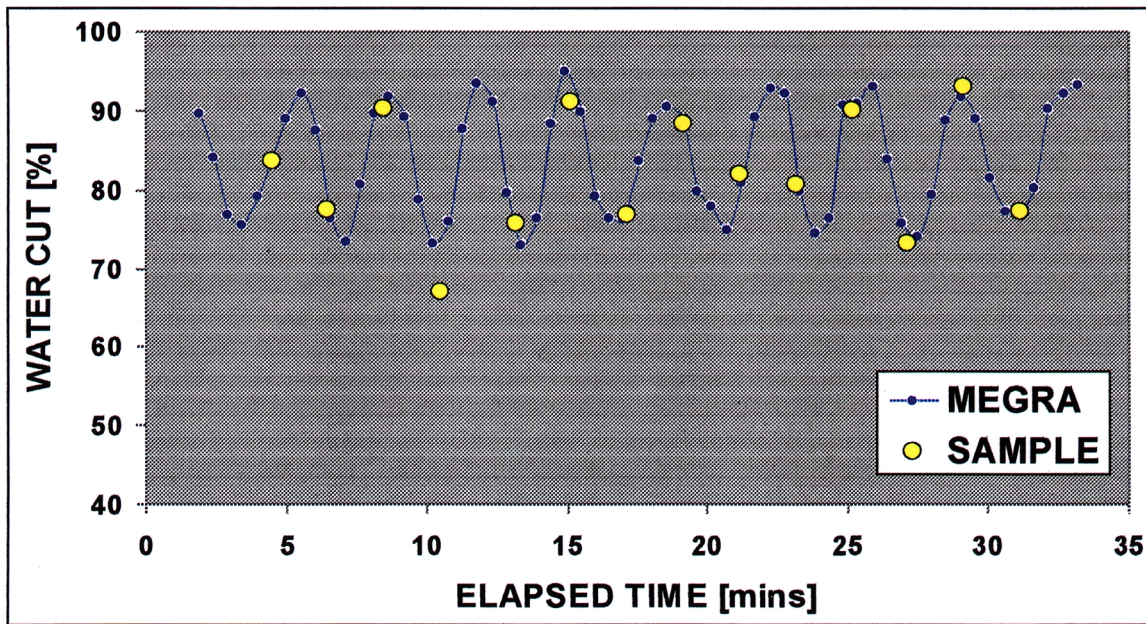


Figure 6: Water-cut data for the high WC well “RTD4” of NAM’s Rotterdam production site (The Netherlands) as measured by MEGRA and simultaneous local sampling.

A second series of field trials, commissioned by Shell BSP’s Production Systems Optimisation Team (Rasau Field, Brunei), compared the MEGRA’s metering performance directly to that of a high-accuracy Coriolis meter. The devices were mounted in series on the “liquid” output of the field’s test separator. The comparison highlighted some serious shortcomings in the water-cut accuracy of the “two-phase” meter in the presence of breakout gas, and once again provided detailed tracking of the multiphase stream’s real-time behaviour.

Figure 7 shows the results of a well test, with the test separator operated in “dump” mode [5]. Here the separator follows a fill and drain cycle, during which partial separation of the oil and water appears to occur. The resultant oscillations in the stream’s water-cut profile had not been previously recognised, but are clearly demonstrated by the MEGRA data. The results show that to obtain a representative WC under such conditions, well tests must be of sufficient duration to smooth out these variations. Furthermore, local sampling at a single point in time can not be regarded as a good indicator of the average WC of such a stream. Samples taken at the well-head on the other hand, where the liquid phases remained well-mixed, were in excellent agreement ( $\pm 2\%$ ) with the flow-weighted MEGRA WC values.

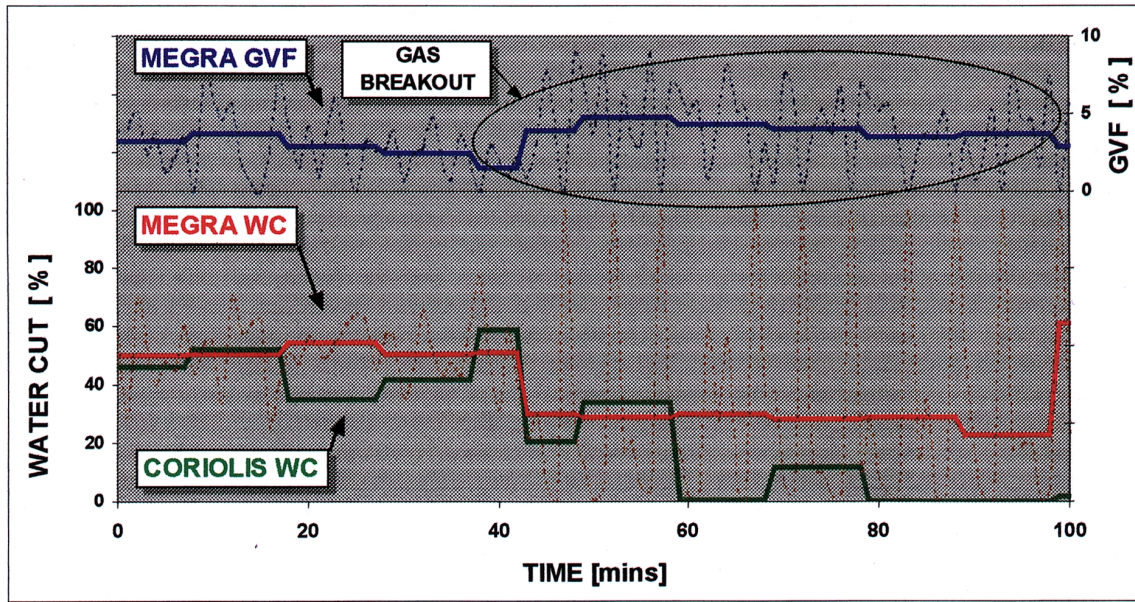


Figure 7: Multiphase flow composition as measured by MEGRA and Coriolis meters in series. The data [5] were gathered from the output stream of a test separator operated in “dump” mode (BSP, Rasau Field, Brunei). The upper section of the graph (right axis) shows the instantaneous (thin line) and averaged GVF (thick line) as measured by MEGRA. The lower section (left axis) shows the independent WC measurements of the two meters. The “real-time” MEGRA data is updated every few seconds. The averaged values, derived over the same integration period as the Coriolis meter, are for comparison only.

MEGRA shows that the gas content of the output stream varies from about 0 to 10% (Figure 7) and is strongly correlated with the presence of oil, as might be expected. In regions of high gas “breakout”, the Coriolis meter exhibits substantial errors. In the highlighted section the gas content exceeds 2% and the Coriolis WC reading deviates by as much as 70% from the MEGRA value. (The Coriolis meter is unable to distinguish between a reduction in fluid density due to increasing gas or decreasing water content).

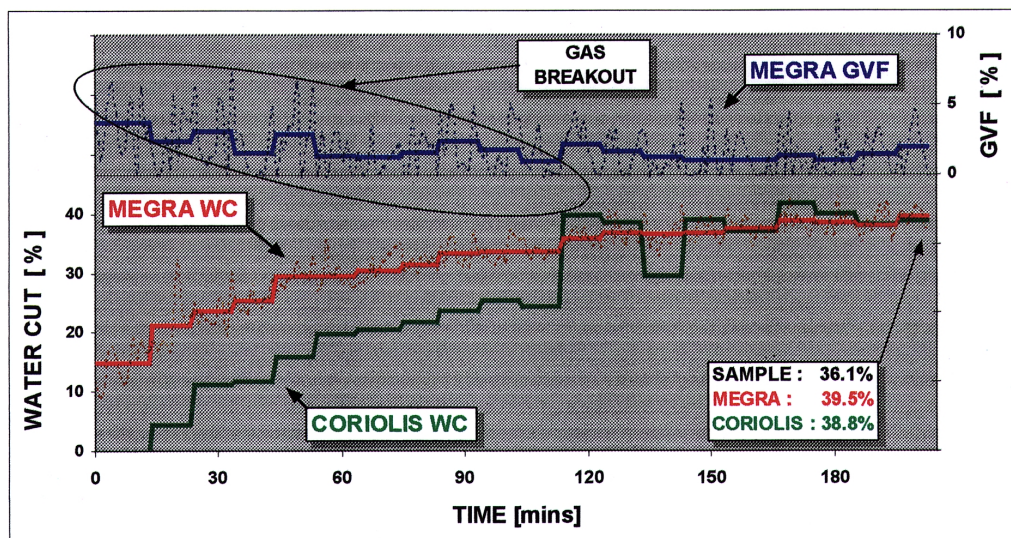


Figure 8: As for Figure 7, except in this case the test separator was operated in “continuous” mode.

Figure 8 shows a similar well-test, this time with the separator operated in “continuous” mode. A gradual rise in the water-cut is obvious as a new well is routed to the test separator. Fluctuations in the WC of the output stream, while finite, are much less pronounced in this case, and local samples are marginally more reliable. In regions of low gas content (less than 2%) the MEGRA and Coriolis water-cuts agree to within a few per-cent. Sampling estimates also lie in reasonable proximity. However, where the oil content of the stream is large (near the start of the test), so too is the associated gas breakout. Again this seriously hampers the WC performance of the two-phase meter. The MEGRA on the other hand is unaffected by the presence of the gas.

## SUMMARY AND CONCLUSIONS

A high-accuracy multiphase flowmeter, based on the gamma-ray absorption principle, has been developed, tested and is now commercially available. The use of relatively low-energy gamma-ray emissions, with respect to competitive multiphase meters, lends this technology an enhanced sensitivity to variations in the component phase fractions. Consequently, water-cuts and gas volume fractions can be measured to high accuracy in relatively short measurement times (seconds). A further advantage of this underlying sensitivity is that additional process parameters can potentially be derived, and a method of measuring changes in the process water salinity, which seriously affects most multiphase flow measurements, has been described and demonstrated. The ability to measure such changes provides a useful tool for reservoir monitoring and the detection of injection-water breakthrough etc.

In live applications the MEGRA multiphase flowmeter has proved to be dramatically superior to the traditional well-test methodology of bulk flow-rate measurement and periodic sampling. The hazards of the latter approach, when the process composition is rapidly varying have been highlighted. The advantages of employing a multiphase meter (over a conventional WC meter) in liquid streams where gas carry-under or breakout may potentially occur have also been demonstrated. The high quality of the real-time process data provided by MEGRA has already gained substantial interest for well-management purposes.

Overall, the ultimate aim of the MEGRA multiphase flowmeter – to replace the measurement function of the test separator – has been fulfilled. Equipment weight and space, as well as capital costs and maintenance are substantially lower. The improved accuracy in the phase fractions (from ~ 10% for the test separator to ~ 2% for MEGRA) and the associated reduction in well-test times and operator intervention also lead to markedly reduced operating costs.

## REFERENCES

1. Santen, H. van, Kolar, Z.I. And Scheers, A.M. (1995). Photon Energy Selection for Dual-energy Gamma and/or X-ray Absorption composition measurements in oil, water and gas mixtures. *Nucl. Geophys.* Vol. 9, No. 3: 193-202.
2. Scheers, A.M. and Slijkerman, W.F.J. (1996). Multiphase Flow Measurement using Multiple Energy Gamma Ray Absorption composition measurement. SPE 36593, Denver.
3. Scheers, A.M. (1998). Multiple Energy Gamma Ray Absorption (MEGRA) Techniques Applied to Multiphase Flow Metering. 4<sup>th</sup> International Conference on Multiphase Technology, London.
4. Hosper, F. (1998). Close-out Report on the Testing of the MEGRA Multiphase Flowmeter as installed on the RTD Test Separator. *Results reproduced by kind permission of Nederlandse Aardolie Maatschappij B.V., Schiedam.*
5. Production Systems Optimisation Team (1998). Comparitave Study of MEGRA meter and Coriolis meter for Water Cut Measurements. *Results reproduced by kind permission of Brunei Shell Petroleum.*



# Compact Cyclone Multiphase Meter (CCM) Discussion of Metering Principle, Slug Handling Capacities and Flow Measurement Results

*Arne Myrvang Gulbraar, Bjørn Christiansen, Dag Kvamsdal  
Kværner Process Systems a.s*

---

## **Abstract**

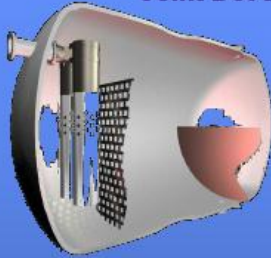
This paper presents the Compact Cyclone Multiphase (CCM) meter – the metering principle, slug handling capacities and flow measurement results. The CCM meter has previously been presented in various papers /1/-/4/. It is a “separation type multiphase meter” utilising cyclonic separation technology for compact separation of gas and liquid. After the gas/liquid separation, gas and liquid is measured individually by conventional single phase instruments before the phases are re-mixed for further multiphase transport.

# Background

Oil&Gas

## KPS Gas/Liquid Cyclone Products

Joint Development with STATOIL



### ← Cyclonic Inlet Device (G-Sep™ CCI)

- u Debottlenecking device
- u New separators can be smaller
- u Reduced chemical consumption

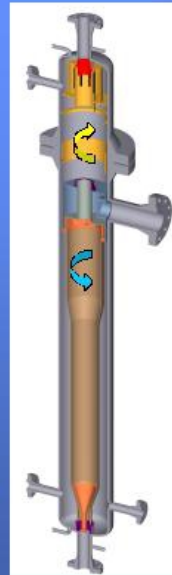
### Compact Cyclonic Degasser (G-Sep™ CCD) →

- u Replacement for 2 phase separators
- u Integral scrubbing sections
- u Component in CYSEP - Compact Separation Skid



### ← Compact Cyclonic Multiphase Meter

- u A spin-off product from the above separation equipment development



Kværner Process Systems

KVÆRNER

Presented at H2P2009-02, Norway, 2009

# Background

Oil&Gas

## Multiphase Meter vs. Test Separator

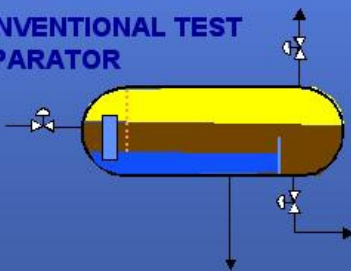
### Functions provided by the test separator

- Well testing
- Well clean-up
- Spare production capacity
- Test bed for new chemicals

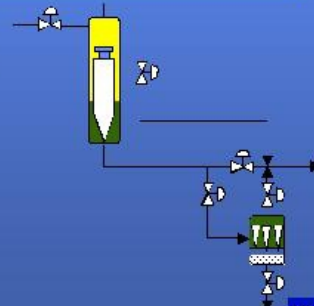
### Can the same functions be provided by the CCM ?

- Yes
- No (Yes by integrating sand cyclones)
- No
- No

### CONVENTIONAL TEST SEPARATOR



### CCM METER



Kværner Process Systems

KVÆRNER

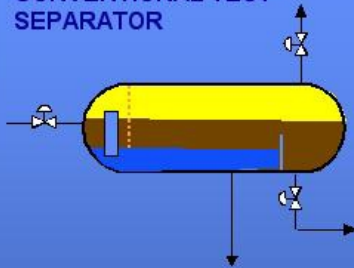
Presented at H2P2009-02, Norway, 2009

# Background

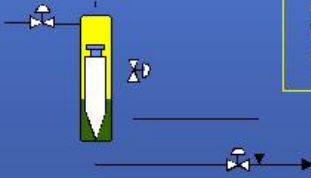
Oil&Gas

## Weight comparison: Replacing a test separator with a CCM

CONVENTIONAL TEST SEPARATOR



CCM METER



Design Capacity	100%	33% <sup>(1)</sup>
Liquid production rate [SM3/D]	10 000	3 300
Gas production rate [MSM3/D]	3.0	1.0
GOR [SM3/SM3]	300	300
Operating pressure [barg]	14	14
Temperature [°C]	80	80

Note 1) 33% case designed for well testing, not spare production capacity.

Weight comparison	TEST SEP.	CCM METER	% REDUCTION
Dry weight vessel [Tons]	26	4.4 (0.7)	83 (97)
Wet test weight vessel [Tons]	96	18 (2.1)	81 (98)
Operating weight vessel [Tons]	68	10 (1.3)	85 (98)

( ) - 33% of design capacity  
/4/

Kværner Process Systems

KVÆRNER

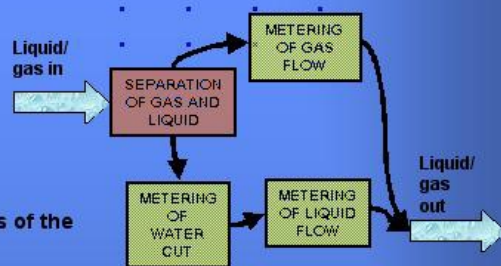
Presented at NBP2009-09, Norway, 2009

# Features & Benefits

Oil&Gas

## Separation - measuring - recombining

- High accuracy. Individual gas/liquid single phase meters are much more accurate than meters measuring both phases together
- Can meter single phase as well as multiphase:
  - Will measure either one of the phases regardless of the actual flow of the other phase
- Possibility for sampling of liquid and gas phase for analysis



## Off the shelf meters

- Calibration done at factory or in laboratory - no need for time consuming and inaccurate "field calibrations"
- Proven technology - high accuracy, tracability, repeatability and serviceability
- Proven, high and known durability of each individual meter



Kværner Process Systems

KVÆRNER

Presented at NBP2009-09, Norway, 2009

## Features & Benefits

Oil&Gas

### State of the art in compact separation

- u Cyclone principle for small footprint and minimum weight
- u 2 stages of cyclone separation yields high separation efficiency
  - Clean liquid phase [0 - 10 vol% of gas in the liquid ok for the CCM]
  - Clean gas phase [0 - 0,01 vol% of liquid in the gas ok for the CCM]
- u Unique combination of hydraulic design and control system makes it possible to achieve high separation performance even at severe slugging conditions.
- u Turndown of 100% with respect to separation (Gas Void Fraction can range from 0% to 100%).



Kværner Process Systems

KVÆRNER

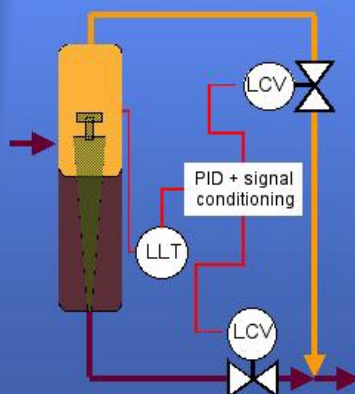
Presented at H2P2010-09, Norway, 2010

## Features & Benefits

Oil&Gas

### Control system and flow computer in one unit

- u Simple operation: Start, stop and reading of results.
- u EX rated for stand-alone installations in hazardous areas.
- u Graphical interface for reading of flow values and trends.
- u Connection to SCADA system through digital lines for accurate and reliable readings.



### Control system

- u One liquid level PID controller controls both valves for optimum turn-down (0-100% GVF) and minimal pressure loss. The signal is split using a very simple algorithm.



Kværner Process Systems

KVÆRNER

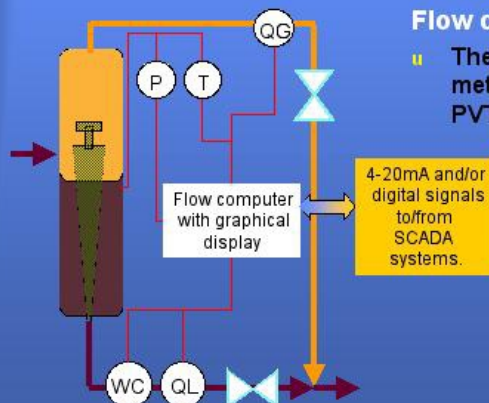
Presented at H2P2010-09, Norway, 2010

## Features & Benefits

Oil&Gas

### Control system and flow computer in one unit

- u Simple operation: Start, stop and reading of results.
- u EX rated for stand-alone installations in hazardous areas.
- u Graphical interface for reading of flow values and trends.
- u Connection to SCADA system through digital lines for accurate and reliable readings.



### Flow computer

- u The flow computer collects inputs from the meters and calculate oil, water and gas rates. PVT data can be used for high accuracy.



Kvaerner Process Systems

KVÆRNER

Presented at H2P2010-02, Norway, 2010

## Applications

Oil&Gas

- u **Used as an ordinary multiphase meter the CCM can be installed at any location topside/land based and measure the flow.**
  - Any flow regime
  - Single phase as well as multiphase flow
  - Well testing/reservoir management
- u **It can be used for fast well testing on land or topside. Typically 4 hours per well (land based).**
- u **It can be used as a mobile test facility mounted on a truck.**

### Applications where the CCM has special advantages:

- u **High GVF applications** ⇒ *The small liquid fraction is measured separately*
- u **Low Oil fraction applications**
- u **In areas where on-site "field calibration facilities" are not available**
  - Use a CCM for "flow calibration" of in-line multiphase meters?
- u **Where multiphase separation & metering in combination is required**

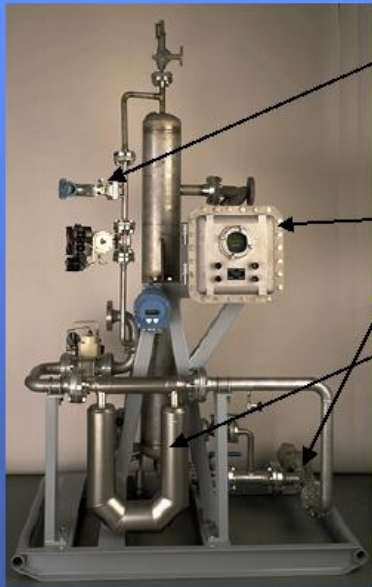
Kvaerner Process Systems

KVÆRNER

Presented at H2P2010-02, Norway, 2010

# CCM Metering Principle

Oil&Gas



## Instrumentation

- u **Gas flow meter**
  - f V-Cone, Annubar, Venturi or Orifice plate ... are options
- u **Microwave Full Range Water Cut Analyzer**  
Supplier: *Phase Dynamics Inc.*
  - Housing the CCM control system and overall flow computer
  - Kværner owns rights to sell PDI Water Cut Analyzers world wide outside the Americas
- u **Coriolis Liquid flow meter**
  - f Turbine, Venturi or PD ... are options
- u **Pressure: Absolute and differential**

➔ Factory/laboratory calibration of each individual instrument according to national standards, i.e. tracability.

Kværner Process Systems

KVÆRNER

Presented at H2P2010-02, Norway, 2010

# CCM Metering Principle

Oil&Gas

## Flow calculations, basics

- u  $Q_{gas} = Q_{gas, gas\ line} + Q_{gas, liq\ line}$
- u  $Q_{liq} = Q_{liq, liq\ line} + Q_{gas\ line}$
- u  $Q_{wtr} = Q_{wtr, liq\ line} + Q_{gas\ line}$
- u  $Q_{oil} = Q_{oil, liq\ line} + Q_{gas\ line}$

Flow calcs. are performed with PVT corrections

## Main flow calculations, from measurements

- u **Seen by the watercut meter:**

$$WC_T = \frac{Q_W}{Q_W + Q_O + Q_G} \quad \left[ WC = \frac{Q_W}{Q_W + Q_O} \right]$$

- u **Seen by the Coriolis meter**

$$Q_{TV} = \frac{m_T}{\rho_T}$$

$$Q_W = WC_T \cdot Q_{TV}$$

$$Q_O = (1 - WC_T - GVF_U) \cdot Q_{TV}$$

$$Q_{GU} = GVF_U \cdot Q_{TV}$$

$$GVF_U = \frac{\rho_T - WC_T \cdot \rho_W - (1 - WC_T) \rho_O}{\rho_G - \rho_O}$$

Kværner Process Systems

KVÆRNER

Presented at H2P2010-02, Norway, 2010

# CCM Metering Principle

Oil&Gas

## Utility System

- u **Control valves require:**
  - Pneumatic, Electrical or Hydraulic operation
- u **Power Supply required:**
  - 120 VAC, 230 VAC 50/60 Hz, or
  - 24 VDC
- u **Power consumption:**
  - Typically 100 Watts (higher if electrical control valves are used)

Kværner Process Systems

KVÆRNER

Presented at H2P2019-02, Norway, 2020

# CCM Performance

Oil&Gas

## Reference fluids

Crude/ Company ref.	Oil density [API]	Pressure [barg]	Temperature [°C]	Gas Void Fraction [%]
<b>Oseberg</b> Norsk Hydro	36	30-90	60-90	40-98
<b>Troll Oil</b> Norsk Hydro	25	23-35	60	30-98
<b>Grane</b> Norsk Hydro	19	10-20	60	40-97
<b>Ladybug</b> Texaco	32	15	40	40 -99
<b>Vic Bilh</b> Elf	23	15	60	< 80

- u Norsk Hydro : High Pressure Test Rig in Porsgrunn, Norway
- u Texaco : Humble Test Facility, Houston, US
- u Elf : Pou, France

Kværner Process Systems

KVÆRNER

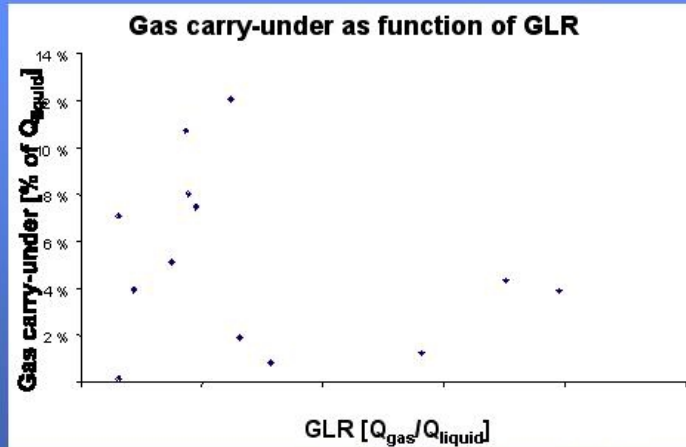
Presented at H2P2019-02, Norway, 2020

# CCM Performance

Oil&Gas

## Separation efficiency

u **Example 1: GRANE crude (API 19): Norsk Hydro Porsgrunn Test Facility**



u Note : There are some more gas carry-under than expected, this is due to (i) the viscous oil (ii) "early version separator internals" and (iii) the fact that the CCM meter are configured for higher flow. An increase in GLR gives better separation due to higher centrifugal forces. /1/

Kværner Process Systems

KVÆRNER

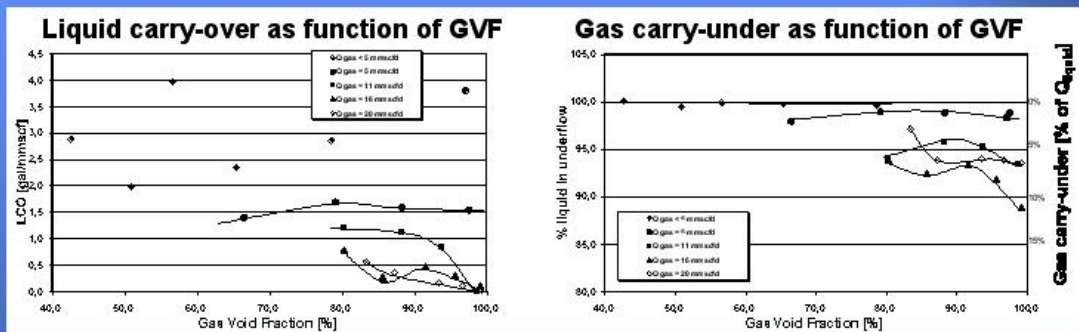
Presented at H2P2010-09, Norway, 2010

# CCM Performance

Oil&Gas

## Separation efficiency

u **Example 2: LADYBUG crude (API 32): Texaco Humble Test Facility**



u Note : Liquid carry-over measured from a reference gas scrubber downstream the gas outlet. Gas carry-under measured by a gamma densitometer on the liquid leg

Kværner Process Systems

KVÆRNER

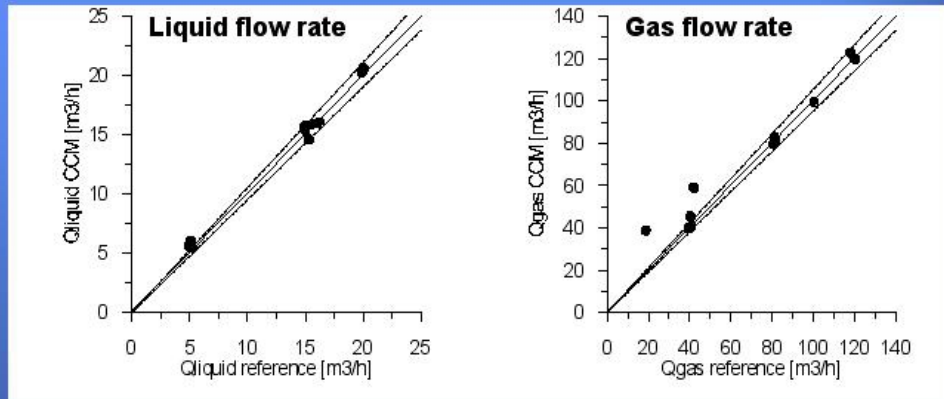
Presented at H2P2010-09, Norway, 2010

# CCM Performance

Oil&Gas

## Flow measurement results:

- u **Example 1: GRANE crude (API 19): Norsk Hydro Porsgrunn Test Facility**



- u Note : Liquid and gas flow as measured by the CCM meter and compared to the reference. The stapled lines are  $\pm 5\%$  lines. /1/

Kværner Process Systems

KVÆRNER

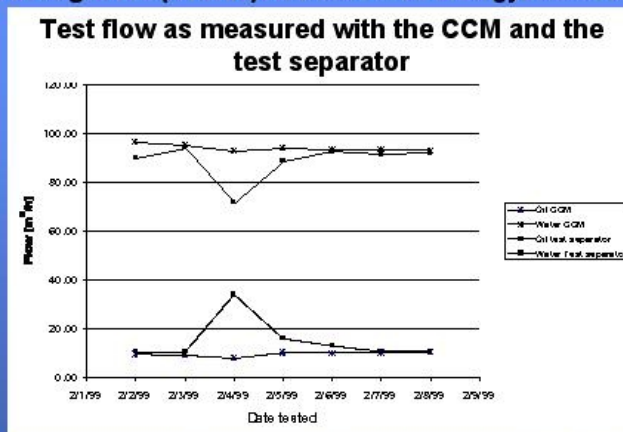
Presented at H2P'00-00, Norway, 2000

# CCM Performance

Oil&Gas

## Flow measurement results:

- u **Example 2: Everglades (API 15): Renaissance Energy, Canada**



- u Note : Tests run for 24 hour compared to the results from the test separator. At 2/4/99 additional gas from the fuel gas system was added. It is assumed that the increased gas flow damaged separation in the test separator, giving a high water carry-over into the oil outlet (i.e. increased oil flow and reduced water flow).

Kværner Process Systems

KVÆRNER

Presented at H2P'00-00, Norway, 2000

# CCM Performance

Oil&Gas

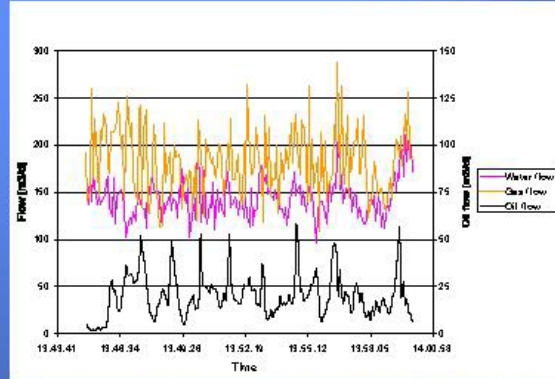
## Repeatability on a flowing well

- u What repeatability is achievable?
- u Conditions typical for land based wells with heavy oil shown in the graph
- u If the curve is fitted to a Normal distribution we find that for a 24 hour test the repeatability of the flow is:

$$Q_{oil} = 20.55 \text{ m}^3/\text{d} \pm 19.2\% (\pm 3\sigma)$$

$$Q_{water} = 143.6 \text{ m}^3/\text{d} \pm 4.4\% (\pm 3\sigma)$$

$$Q_{gas} = 182.2 \text{ m}^3/\text{d} \pm 6.0\% (\pm 3\sigma)$$



Gas and liquid flow variations measured at the tests at Everglades

- u Regardless of instrument this is the the flow of the well in a 24 hour period

Kværner Process Systems

KVÆRNER

Presented at H2P2010-02, Norway, 2010

# CCM Performance

Oil&Gas

## Slug handling capacities

### Experience from the field

- u No separation problems experienced

### Experience from test facilities like Norsk Hydro Porsgrunn and Texaco Humble

- u Slugging flow experienced especially on high watercut flow rates.
  - No separation problems experienced

### Experience from KPS in-house laboratory, Trondheim, Norway

- u Slug test of a 12" unit Degasser (Compact Gas/Liquid Cyclone Separator)
- u Purpose:
  - Test the Degasser's ability to handle slugs using normal control routines.
  - The slugs are artificially made using valves.

Kværner Process Systems

KVÆRNER

Presented at H2P2010-02, Norway, 2010

## Slug Test on 12" unit

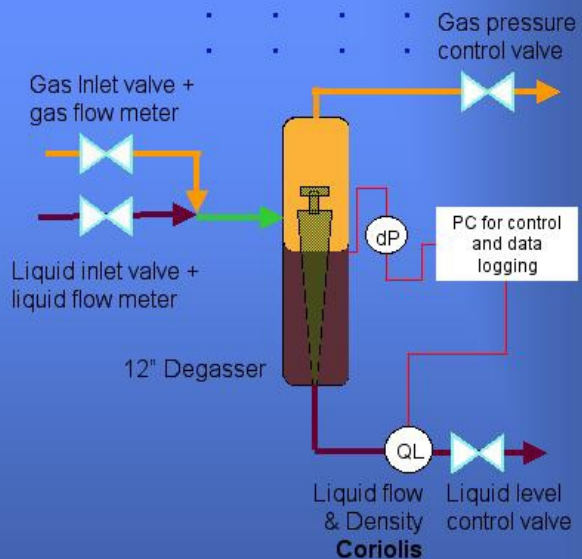
Oil&Gas

### Control

- u Level and gas pressure control of the Degasser.
- u Inlet valves control inlet flow, slug frequency and amplitude.

### Main measurements

- u Coriolis meter in liquid outlet for separated liquid density and flow.
- u Liquid carry-over by visual inspection
- u Flow (slugs) into the Degasser.



Kværner Process Systems

KVÆRNER

Presented at H2P2019-02, Norway, 2020

## Slug Test on 12" unit

Oil&Gas

### Summary of results

- u At low frequency the slugs are so long that the gas/liquid valves will go to fully closed positions and remain there for a while. This causes several things to happen:
  - Oil and water are separated in the annulus. The liquid density curves drops from 950 to 830 kg/m<sup>3</sup> because liquid goes from almost clean water to almost clean oil when level varies. No gas carry under is detected (visual inspection through transparent tubing) and no liquid carry over is detected.
  - Liquid flow coming out of the separator have twice the magnitude (peaks). This is because of the pressure caused by the gas slug entering the separator when the liquid valve is almost fully open and the gas valve is closed. The instantaneous excess gas will push the level down faster than the liquid valve initially can respond.
- u At higher frequencies the slugs are just “absorbed” by the Degasser. At lower frequencies the behavior will be like the 0.01 Hz or better. A continuous frequency of 0.01 Hz is the worst scenario for this separator, and not likely to occur in real installations).

Kværner Process Systems

KVÆRNER

Presented at H2P2019-02, Norway, 2020

## Slug Test on 12" unit

Oil&Gas

### Conclusions from the tests

- u The Degasser can handle slugs without effecting performance in any detectable degree, at least not in the laboratory
- u Faster reacting valves will reduce the largest total level variation and pressure variation.
- u Ordinary control valves were used in the experiments. The valve closure speed should be about the same or faster than the time it takes to empty the liquid in the vessel at fully open liquid valve.
- u If severe slugging is not anticipated, the speed of the valves are not important.

Kværner Process Systems

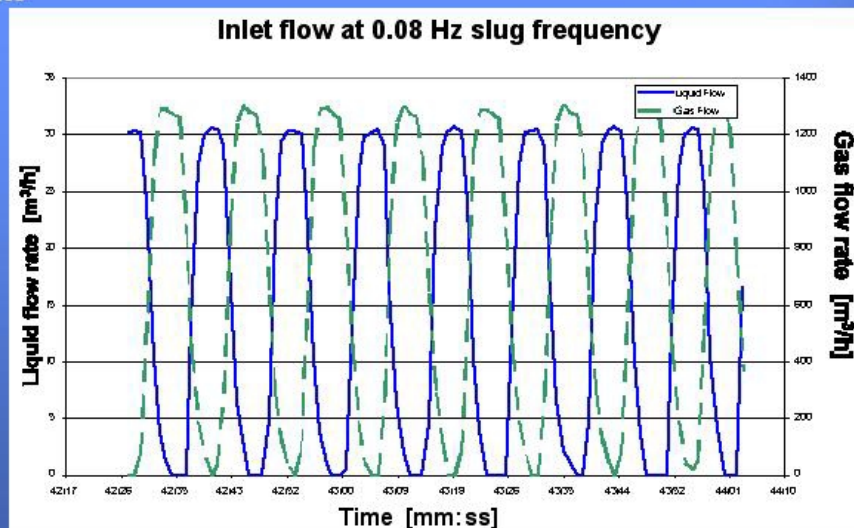
KVÆRNER

Presented at H2P2010-02, Norway, 2010

## Slug Test on 12" unit

Oil&Gas

### Results



Kværner Process Systems

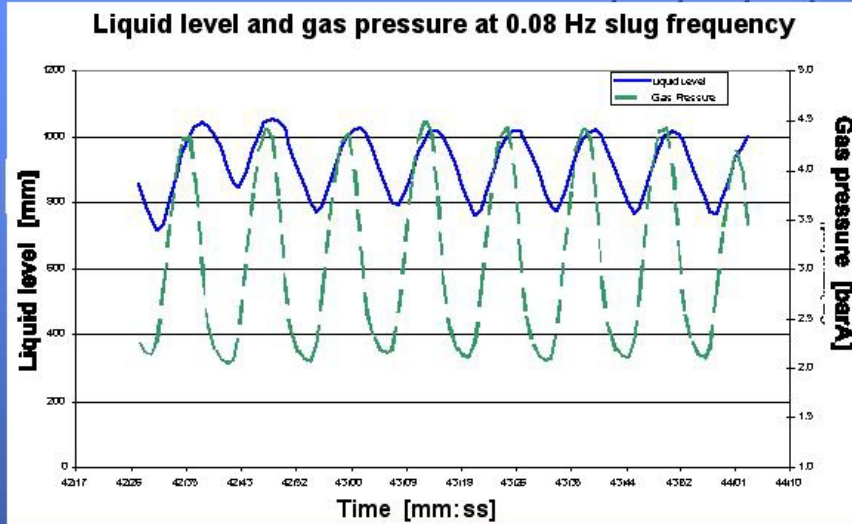
KVÆRNER

Presented at H2P2010-02, Norway, 2010

# Slug Test on 12" unit

Oil&Gas

## Results



Kværner Process Systems

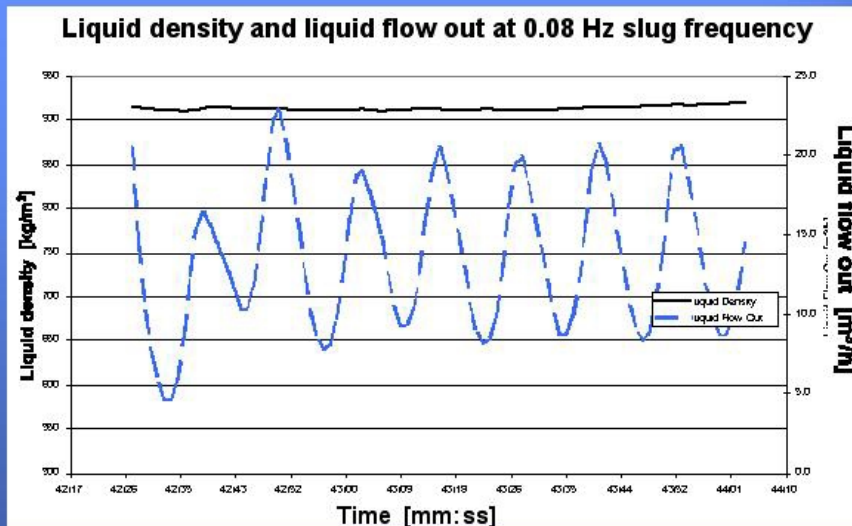
KVÆRNER

Presented at H2P2019-08, Norway, 1000

# Slug Test on 12" unit

Oil&Gas

## Results



Kværner Process Systems

KVÆRNER

Presented at H2P2019-08, Norway, 1000

## CCM Performance

Oil&Gas

### Other characteristics

#### u Pressure drop:

- Typically 1 bar (14,5 psi)

#### u Salinity dependencies:

- The PDI Water Cut meter will be affected through the calibration value for 100% water. The calibration data need to be adjusted accordingly.

- Currently the adjustment is manual
- The sensitivity is largest at small salt concentrations

- The Coriolis meter will be affected through the density calibration value for 100%water

#### u Viscosity dependencies:

- Moderate relationship between liquid viscosity and gas carry-under.

#### u Effects of transient flow on the individual flow measurements:

- Effects has not been separately identified, but not seen as critical since all flow meters use a very short time window to calculate the instant flow rates.

Kværner Process Systems

KVÆRNER

Presented at NBP&W-00, Norway, 1999

## CCM Meter - Highlights

Oil&Gas

### CCM - Compact Cyclone Multiphase meter "Separation type" multiphase meter

#### u The CCM meter is used to measure the flow rate of oil, water and gas

- Works on pure oil, pure water, pure gas and on any mixture of the phases.

#### u Compact skid includes:

- Compact Gas/Liquid separator
- Liquid/gas flow & WC measurements
- Re-mixing of the phases at skid outlet

#### u "Off the shelf" instruments are used

#### u Accurate flow measurements (i.e. single phase, gas and liquid)

#### u No need for on-site calibrations (i.e. factory calibration only)

#### u Easy maintenance (i.e. local)

#### u Regional fabrication by Kværner



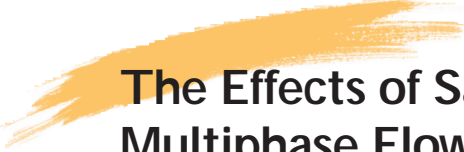
Kværner Process Systems

KVÆRNER

Presented at NBP&W-00, Norway, 1999

## References

- /1/ D Kvamsdal, B Christiansen, I Hjelkrem, «Operational experiences with a gas liquid cyclone», BHR, Multiphase technology, pp 101-117, Bannf, Canada, 1998
- /2/ B Scott, L Baker, B Svingen, «Well testing issues and a new comopact cyclone system», NSFMW, Gleneagles, Scotland, 1998
- /3/ S Davies, D Kvamsdal, I Hjelkrem, «Gas / Liquid Cyclonic Separators Used in a Separator Inlet Device and a Multiphase Metering System», International Technology Conference (JST), Algerie, 1998
- /4/ B Christiansen, «New, more cost-efficient process technology», Floating Production Systems (IRR), Oslo, Norway, 1999



# The Effects of Salinity Variation on Dual Energy Multiphase Flow Measurements and Mixmeter Homogeniser Performance in High Gas and High Viscosity Operation

*P. Harrison,  
Milverley Consultants Ltd, UK*

*S.J. Parry  
TH Huxley School of Environment, Earth Science and Engineering  
Imperial College, Silwood Park, Ascot, UK*

*G.L. Shires  
Department of Chemical Engineering & Chemical Technology  
Imperial College, London, UK*

---

It is a continuing concern of those involved with multiphase flow meters using dual energy X-ray/gamma phase fraction measurement that changes in the properties of the fluids being measured will cause errors. Density changes are accommodated through known PVT relations but changes in the chemical composition of the flowing fluids must be corrected for if errors are to be avoided. While significant changes in overall hydrocarbon composition are not usually encountered, salinity of the water fraction can vary over time for some wells and this changes not only the physical density but also the mass absorption of the water. In the first part of this paper the effects of fluid property changes on dual energy measurements are discussed in relation to the energy levels most commonly used for measurement.

The second part of the paper presents recent results from the Mixmeter homogeniser which continues to demonstrate excellent characteristics as a differential pressure meter in multiphase flow. Data for high gas fraction operation is presented together with work using high viscosity emulsions.

## 1. INTRODUCTION

Following the successful completion of the MIXMETER development project and the transfer of the technology to Jiskoot Autocontrol Ltd., study of the performance of the two key components of MIXMETER has continued.

Essentially MIXMETER consists of a specially developed homogeniser together with a dual energy densitometer (Figure 1). The homogeniser has a very stable differential pressure characteristic. This allows it to provide reliable multiphase velocity information over a wide range of flow conditions in addition to giving homogeneous downstream conditions for the X-ray/gamma dual energy densitometer. The dual energy instrument is also unusual in using a single beam and single source (Cs 137) to providing both energies for the measurement (32keV and 661keV).

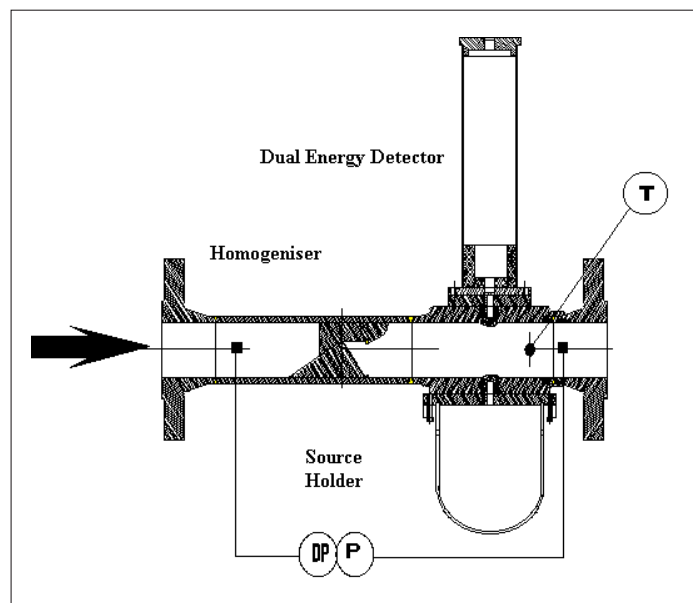


Figure 1: Mechanical Layout of MIXMETER

In relation to the dual energy system work has focussed on the sensitivity of the instrument and in particular changes in its performance which result from changes in fluid properties.

With regard to the homogeniser a detailed study of the NEL Multiflow test results has enabled a more sophisticated DP characteristic to be derived to extend the range of operation. Further, work at the Texaco facility at Humble has confirmed the ability of the device to provide reliable differential pressure velocity data when operating with high viscosity emulsions.

## 2. SENSITIVITY

### 2.1 Introduction

Dual energy phase fraction instruments can only provide accurate fraction measurements if the absorption of the individual fractions is known. The measurement parameter used for calibration is the absorption ratio which is the product of the density, the atomic mass absorption and the beam length (pipe diameter). If absorption ratio values change then measurement errors will occur. The atomic mass absorption is dependent on the atomic composition of the phase. Fortunately the overall composition of the hydrocarbon is not likely to change and density variations are taken account of through PVT corrections. Also, in many applications, the composition of the produced water is either unlikely to change or it is possible to take occasional samples for analysis. However there are applications where sampling is not convenient and where water composition may change dramatically; eg where water injection is used or where water driven downhole pumps are installed. Such changes are particularly significant as the atomic mass absorption changes (eg due to addition/subtraction of sodium, potassium, calcium, chlorine atoms etc.) as well as the physical density.

To allow investigation of uncorrected changes in fluid composition a computer model of a full multiphase matrix has been used together with absorption ratios from laboratory measurements.

### 2.2 Salinity Variations

The effect of a change in salinity will be most apparent in the water cut measurement. An increase in salinity will increase the water absorption and will result in a perceived increase in water cut. Liquid fraction will increase slightly and oil fraction will decrease. A reduction in salinity will have the opposite effect and these changes will alter the measured oil flowrate by an amount which will depend on the original water cut and GVF.

The sensitivity depends on the energies used in the dual energy instrument and in addition to the 32keV and 661keV pair from Cs 137 used in MIXMETER, absorption measurements were been made for 59keV (Am 241 or W x-ray) and 80keV (Ba 133 or Pb x-ray).

Figures 2 and 3 show the effect on water cut for salinity changes from a base level of 50g/l for a 32keV/661keV dual energy combination and for a 59keV/661keV combination.

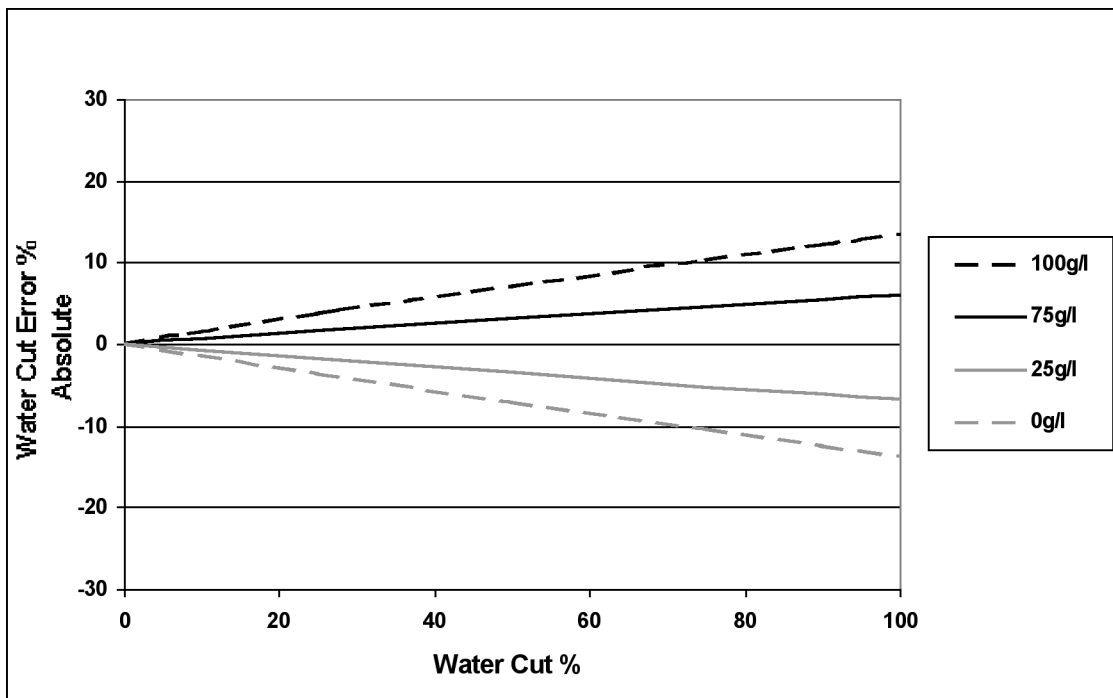


Figure 2: Water Cut Error due to Salinity Changes from 50g/l 32keV/661keV Dual Energy Gamma

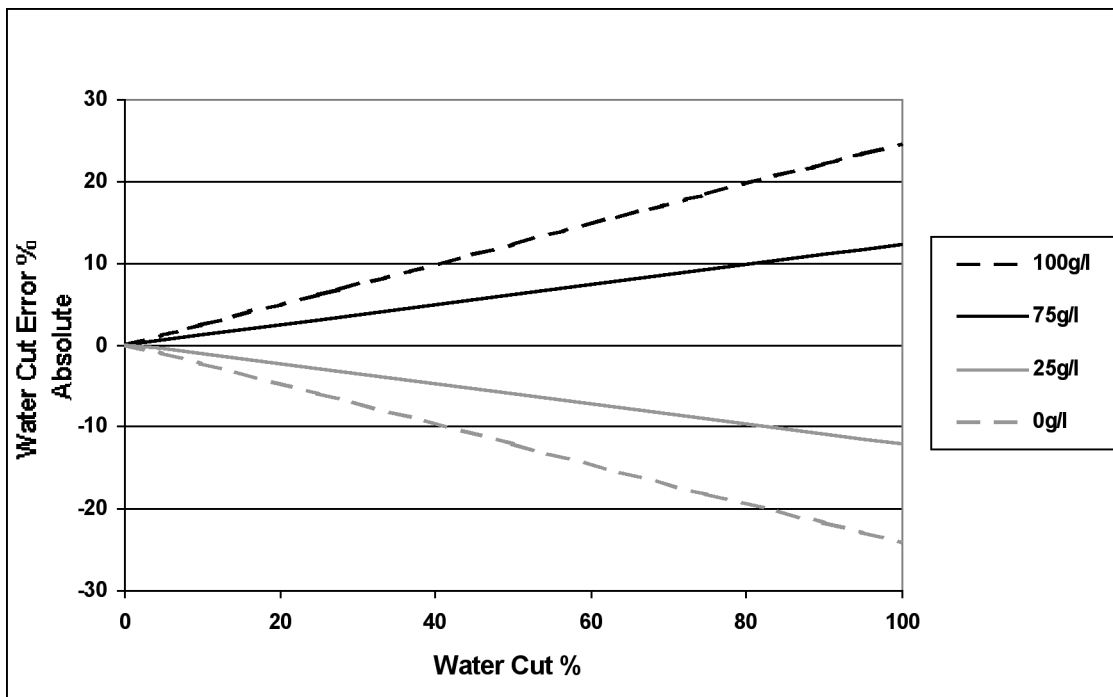


Figure 3: Water Cut Error due to Salinity Changes from 50g/l 59keV/661keV Dual Energy Gamma

It should be noted immediately that large changes in salinity have been used to produce the errors shown. Calibration errors will normally be less than 1g/l and will have a very small effect.

The effect is linear with respect both to initial water cut and to the change in salinity.

It can be seen that the 59/661keV combination appears to be more sensitive to salinity changes than the 32/661keV combination.

A third combination of energies commonly used in dual energy work is 30/350keV from Ba 133. As absorption under these conditions is very similar for all energies above 100keV this combination will respond in a similar manner to the 32/661keV combination.

The magnitude of the errors also depends on the density of the oil phase. The absorption ratio for a light oil (800kg/m<sup>3</sup>) has been used to generate the figures above. If a heavier oil is present (900kg/m<sup>3</sup>) the errors reduce by a factor of approximately 1.15.

The effect of the changes in salinity on the oil fraction and hence the final oil flowrate will depend on the water cut and the GVF. Figures 4 and 5 show the absolute oil fraction errors resulting from the 50g/l to 100g/l salinity changes shown in Figures 4 and 5.

The errors shown are absolute and, as may be expected, the errors in oil fraction become greater as water cut increases and as GVF decreases. However, once again, a large increase in salinity (50g/l – 100g/l) has been used to generate these changes.

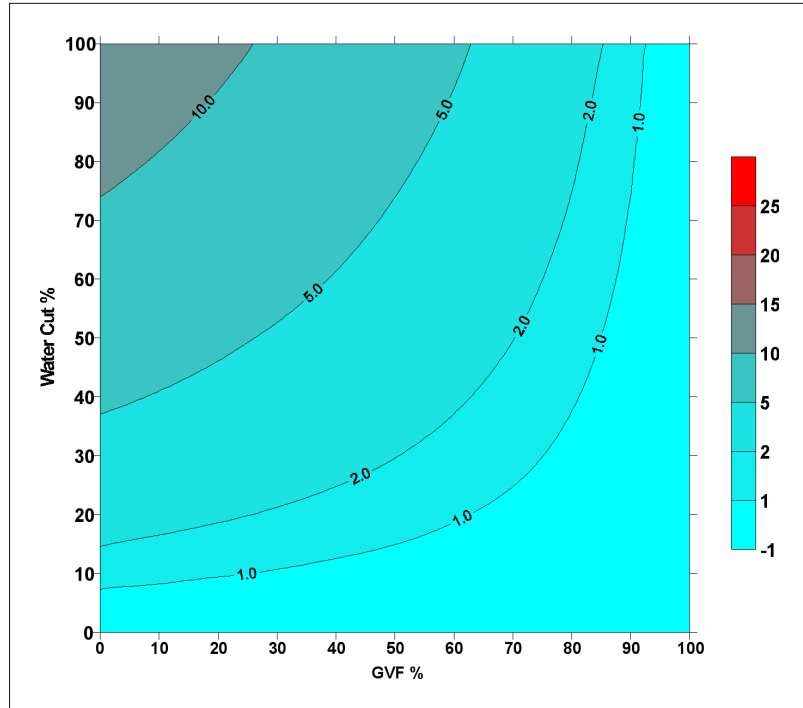


Figure 4: Absolute Oil Fraction Error due to Salinity Change from 50g/l to 100g/l  
32keV/661keV Dual Energy Gamma

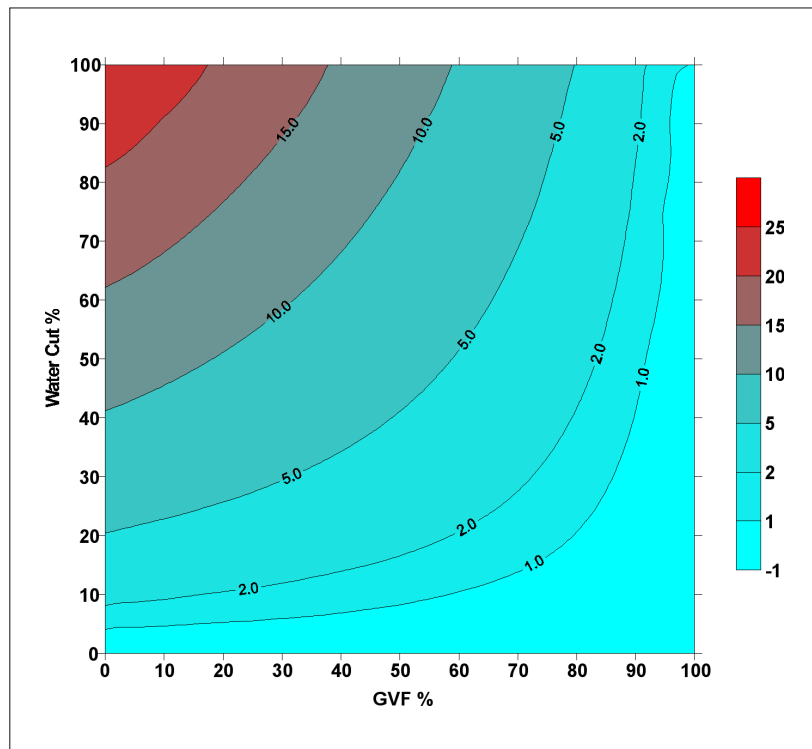


Figure 5: Absolute Oil Fraction Error due to Salinity Change from 50g/l to 100g/l  
59keV/661keV Dual Energy Gamma

The reasons for these performance differences become apparent when the responses of the energy level pairs to oil/water/gas mixture are considered. The following Figures 6 and 7 show graphically how the responses interact. Figure 6 is for 32/661keV combination. The hatched lines show the 661keV energy absorption ratio for the full range of phase combinations and the plain lines show the 32keV absorption ratios. The resolution of the measurement depends upon the angle of intersection of the two sets of response lines and the precision depends on the range of the absorption ratios.

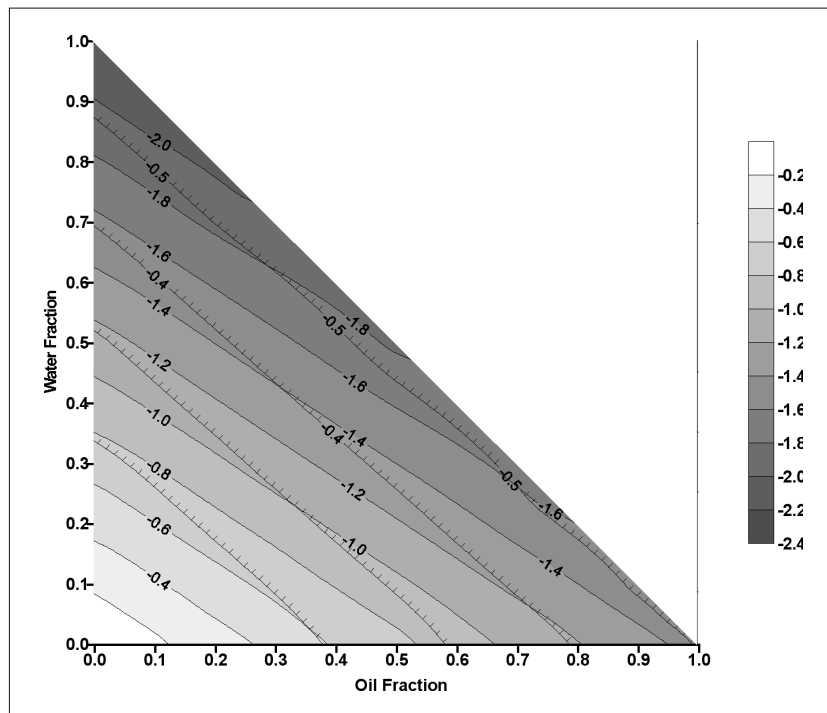


Figure 6: 32keV/661keV Dual Energy Response

Figure 7 shows the same plot for the 59/661keV energy combination. It is clear when comparing the two figures that the angle of intersection of the absorption lines is less for the 59/661 combination and also that the range of 59keV absorption ratio is less than for the 32keV. The 32keV/661keV combination offers better resolution and precision than the 59/661 keV energy pair.

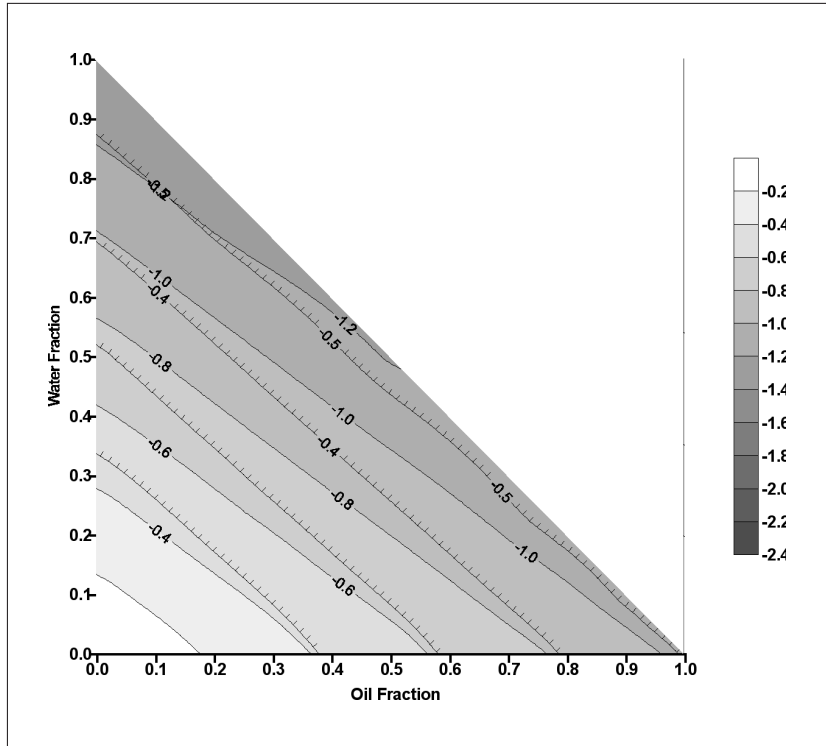


Figure 7: 59keV/661keV Dual Energy Response

### 2.3 Oil Density Variations

As noted in 2.1 above uncorrected variations or errors in oil density have a much smaller effect on dual energy measurements. Figure 8 shows the oil fraction error resulting from an uncorrected 5% increase in oil density imposed on a system with 50g/l salinity. Errors shown below are absolute oil fraction errors. These errors increase exactly in step with increasing oil fraction such that the relative error is constant at 5%. That is to say that an error in oil density calibration or an uncorrected change in oil density due perhaps to PVT error will be reflected in an almost exactly similar error in the oil measurement.

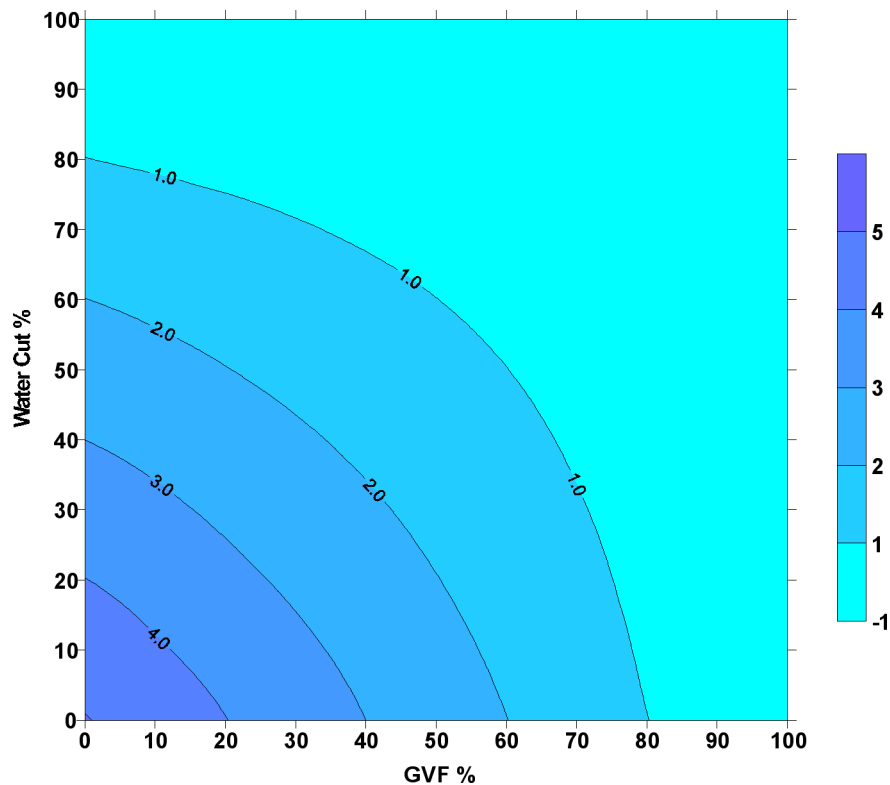


Figure 8: Absolute Oil Fraction Error due to Oil Density Change from 800kg/m<sup>3</sup> to 840kg/m<sup>3</sup>  
32keV/661keV Dual Energy Gamma

## 2.4 Conclusions

The work briefly described above shows some examples of how the effects of individual and combined uncorrected errors in calibration of dual energy instruments can be modelled and studied. By using data for intended applications field behaviour of the instrument under ‘upset’ conditions can be predicted.

Errors of this type will be systematic and will add to any random errors which may be present.

As noted from earlier work the small errors in oil density which may arise from PVT calculations will have a relatively small effect on the instrument. Also, small changes in salinity do not lead to large errors in absolute water cut. However the errors are systematic and where the salinity change and water cuts are high the effect on oil rate will be severe.

There are however a number of quite simple safeguards. The most obvious of these is the stability of the liquid fraction or GVF measurement. In the most extreme case of salinity change noted above (50g/l to 100g/l) the GVF error moved by less than 1% relative. Any rapid step changes in salinity such as injection breakthrough will therefore be apparent as a large swing between oil and water flows with total liquids staying the same. Basic trending enables this type of occurrence to be flagged easily. As a consequence of the same GVF stability, in situations where water cut is high increased salinity will rapidly lead to negative oil fractions being noted by the instrument, again indicating a change in fluid properties and a need to recalibrate.

### 3. SALINITY MEASUREMENT

#### 3.1 Introduction

Ideally an on line measurement of salinity is required in order to allow automatic correction for any changes. The addition of more instruments is not desirable and a solution where the existing dual energy system can be enhanced to include the additional measurement seems most attractive.

In simple terms the current systems with two energies allow three fractions or components in the pipe to be measured: two directly and the third by difference. A third energy will allow the additional salinity measurement to be made.

This idea is not new and is a simple extension of the dual energy method. A discussion of the principle was given by Scheers Ref (2). However practical implementation is difficult due to the need to obtain three energies of radiation of the correct levels to provide discrimination and of sufficient intensity to allow penetration of the fluid to be measured. The three energies of Am 241: 18, 26 and 60keV proposed in Ref (2) work well but the penetrating power of the two lower energies restricts application to very short path lengths and low liquid fractions.

#### 3.2 Test Work

During the last few months work has been carried out using an additional 59keV energy peak added to the 32keV and 661keV peaks used in MIXMETER. The following Figure 9 shows that this is about the ideal triple energy system to use with the salinity calibration lines for the three energies evenly spaced. Previous tests with a 75keV peak proved unsuccessful as the response of this higher energy peak was too similar to that of the 661keV peak.

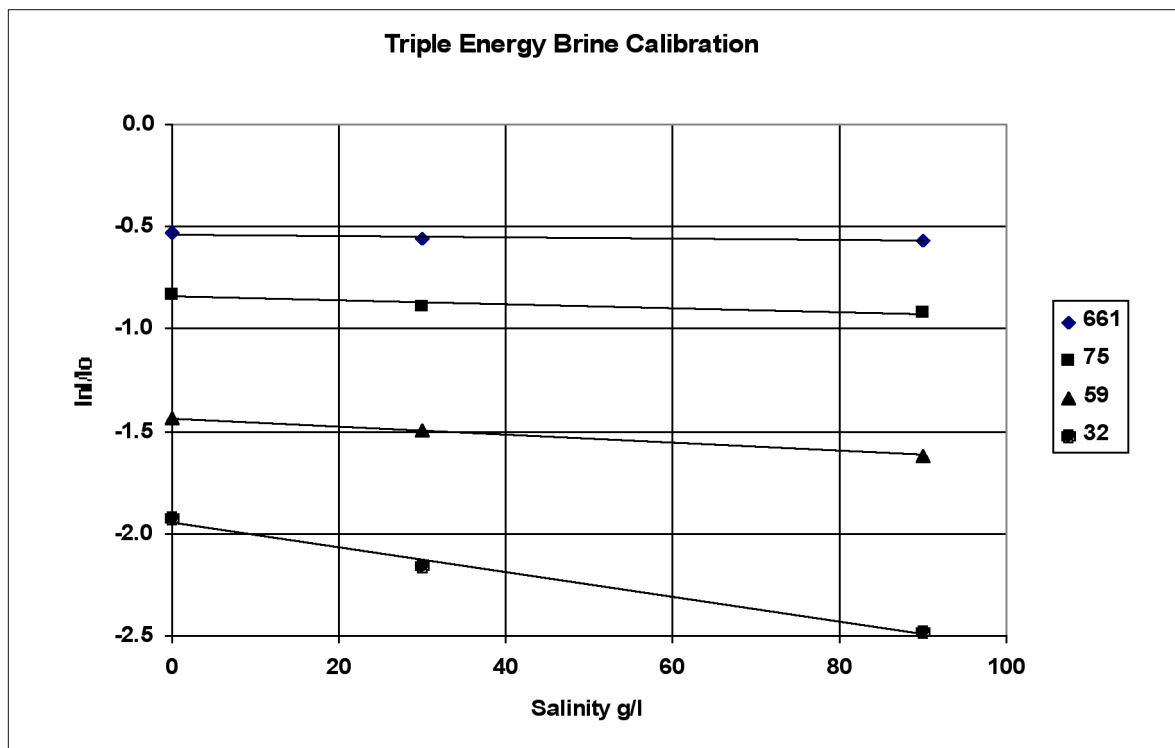


Figure 9: Brine Calibration, 661, 75, 59 and 32keV X-rays

Even with this ‘optimum’ combination it is very difficult to obtain consistent salinity measurements due to the need for extremely high precision for the measurement and calibration data. This can be appreciated by referring back to Figures 6 and 7 and considering the difficulties in working with the 32 and 59keV absorption grids. The MIXMETER system normally operates with measurement and calibration uncertainties to around 0.1% whereas to work with three energies and over a range of GVF’s and water cuts a further order of magnitude of precision is needed. It seems most unlikely that this can ever be achieved when the various sources of uncertainty are considered. However the opportunity remains to detect salinity changes when significant quantities of water are present and this will be pursued.

## 4. HOMOGENISER PERFORMANCE

### 4.1 Differential Pressure Velocity Measurement

The performance of the mixer as a multiphase differential pressure meter is crucial to the operation of MIXMETER and the unique ability of the device to maintain the same calibration characteristic over a wide range of liquid fractions was discussed in a previous paper (Ref 1).

The relationship used is

$$\Delta p = k U^2 \varepsilon_L \quad (1)$$

Where  $U$  is the total superficial velocity,  $k$  the resistance factor of the mixer and  $\varepsilon_L$  is the total liquid fraction in the homogenised region ( $\varepsilon_L = \varepsilon_O + \varepsilon_W$ ).

$\varepsilon_O$  and  $\varepsilon_W$  are the (measured) phase fractions in the homogenised region downstream of the mixer.

1

This relationship approximates the homogenous model where  $\rho_G \ll \rho_O$  or  $\rho_W$  and  $\rho_W \approx \rho_O$  but has been found to be more accurate as liquid properties vary. Indications are that density and viscosity effects offset each other.

Clearly the relationship will break down at some point as  $\varepsilon_L$  approaches zero in high gas and, generally, high velocity situations.

Limitations of available test rigs resulted in earlier work with the 4” meter being restricted to a maximum velocity of around 10m/s. Also, little work had been carried out at liquid fractions less than 10%. The claimed operating range of MIXMETER was therefore quoted as being within these limits. However the NEL Multiflow tests using a 3” meter allowed collection of a considerable amount of data at higher velocities and at lower liquid fractions and it was hoped that the results would allow some extension of the operating range of the meter.

Figure 10 shows the velocity characteristic of the 4” meter as determined at NEL and Treocate. The mixer differential pressure is plotted against the square of rig total superficial velocity multiplied by the liquid fraction (see equation 1).

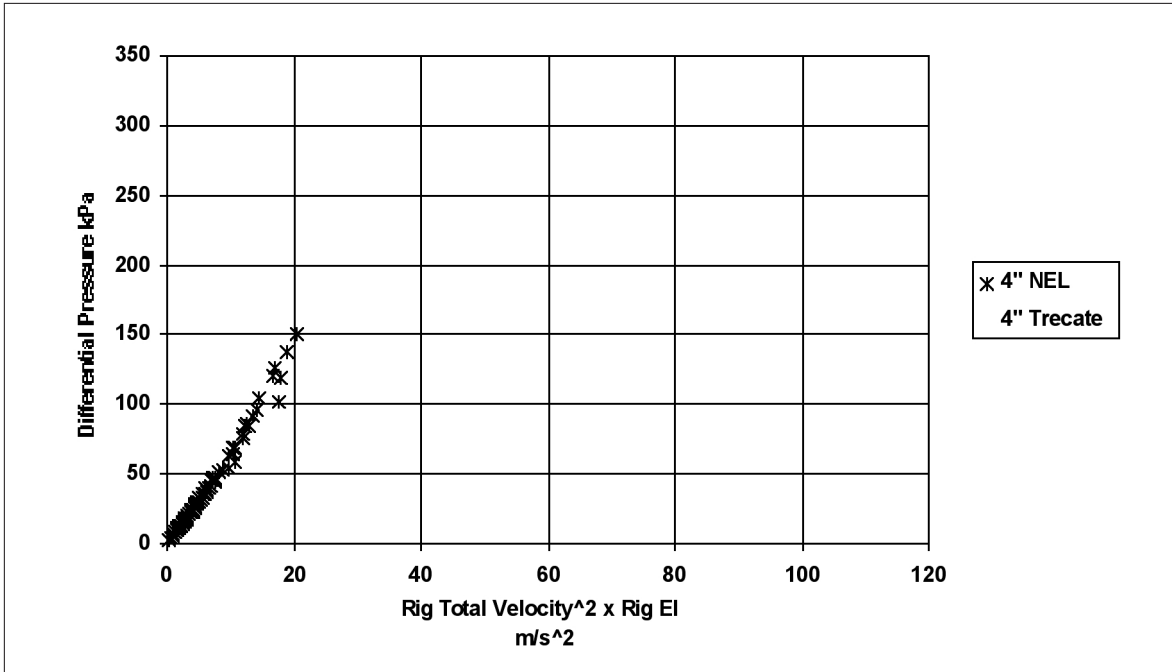


Figure 10: 4" Meter Differential Pressure Characteristic

Data is plotted on the same scale as later figures to allow comparison.

A similar plot for the 3" meter from Matrix 1 of the Multiflow tests is shown in Figure 11. A simple straight line calibration for the 4" meter is also shown for comparison.

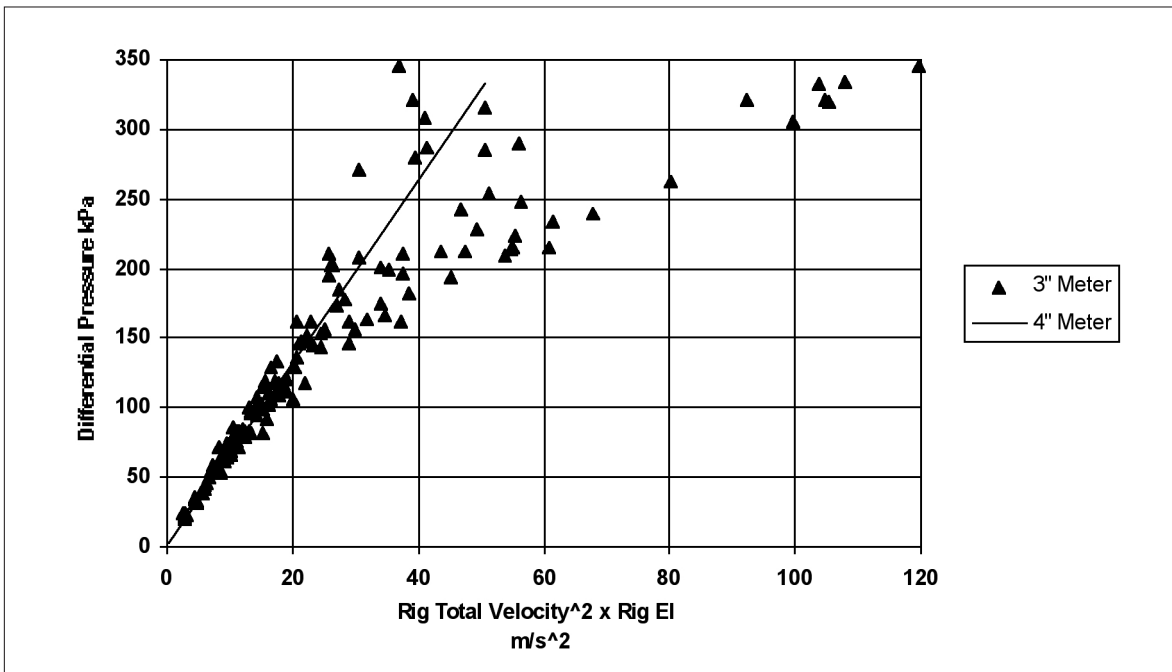


Figure 11: 3" Meter Differential Pressure Characteristic

The scattering as the velocity term increases does not look encouraging. However the data falls into groups based on liquid fraction allowing Figure 12 to be plotted to provide a basic family of calibration curves.

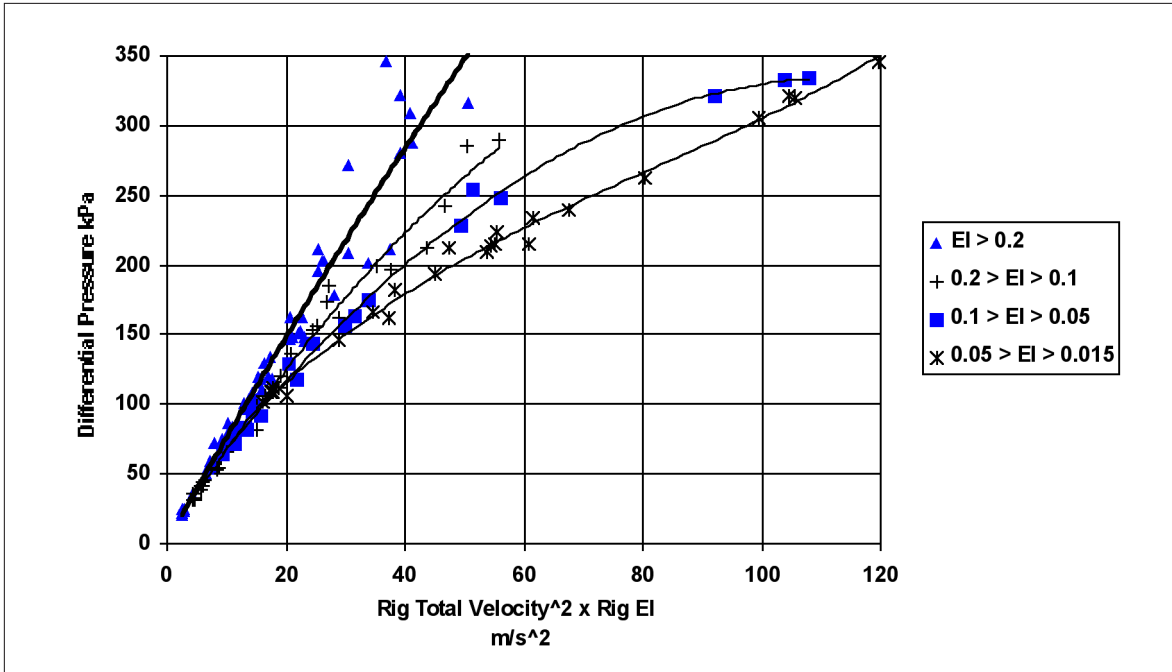


Figure 12: 3'' Meter Differential Pressure Characteristic:  $0.015 < El < 1.0$

Figure 12 above shows that a reasonable characteristic can be derived even for liquid fractions down to below 2%. However it becomes increasingly difficult for the gamma instrument to determine liquid fraction at these levels.

Selecting those test points with liquid fractions above 5% and by applying the above calibrations velocity measurements are obtained as shown in Figure 13.

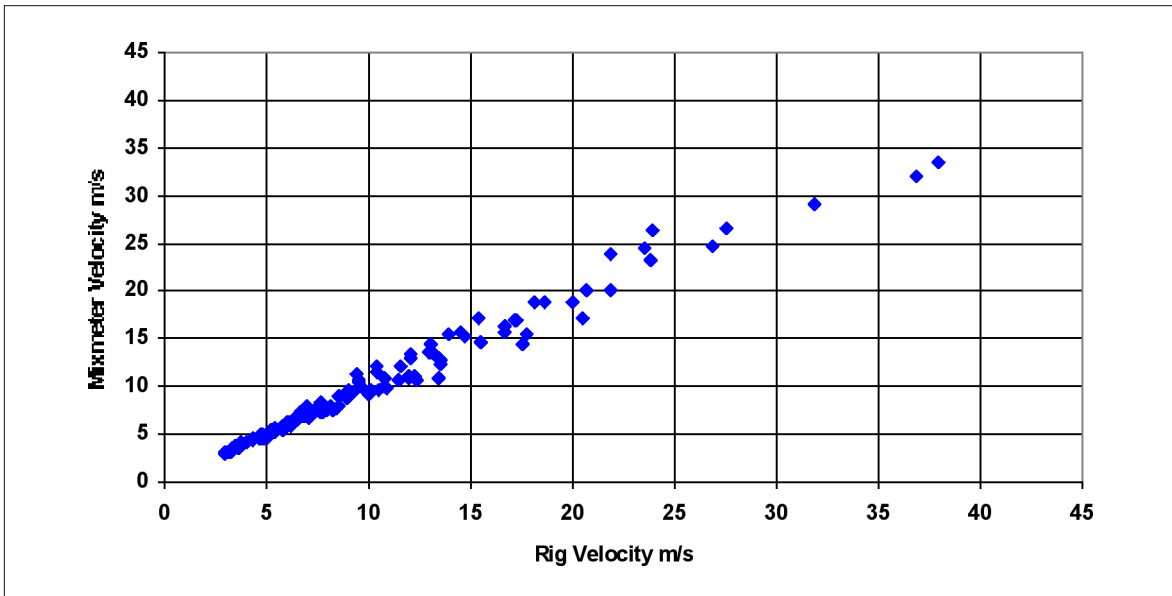


Figure 13: 3'' Meter Total Velocity Measurements for Liquid Fractions above 5% NEL Multiflow Matrix 1

Figure 13 suggests that even with the increasing uncertainty of liquid fraction measurement at very low fractions MIXMETER can perform adequately at velocities up to 20m/s and with gas fractions up to 95%.

### Enhanced Overall Performance

By using the improved DP calibration liquid and gas flowrate errors for the full NEL Multiflow Matrix 1 test range are as shown in Figs 14 and 15.

Errors are presented in the form of contour plots which allow the error to be plotted against two other variables, in this case reference water cut and GVF. This type of plot was used by the NEL Multiflow JIP and is very helpful in allowing three variables to be viewed together. However these plots can also be very misleading as the software extrapolates outside the data points. In this case there are almost no points below 25% GVF and the entire left hand quarter of the plot is therefore fabricated. It is seen as essential in using this type of plot that the data points are mapped onto the plot as has been done here so that the extent of the data can also be seen.

Liquid rates ranged from 3l/s to 23l/s and gas rates were between 5l/s and 75l/s.

For velocities up to 20m/s and GVF's up to 95% RMS error for liquid flowrate was just over 5% and for gas flowrate was 8.4%.

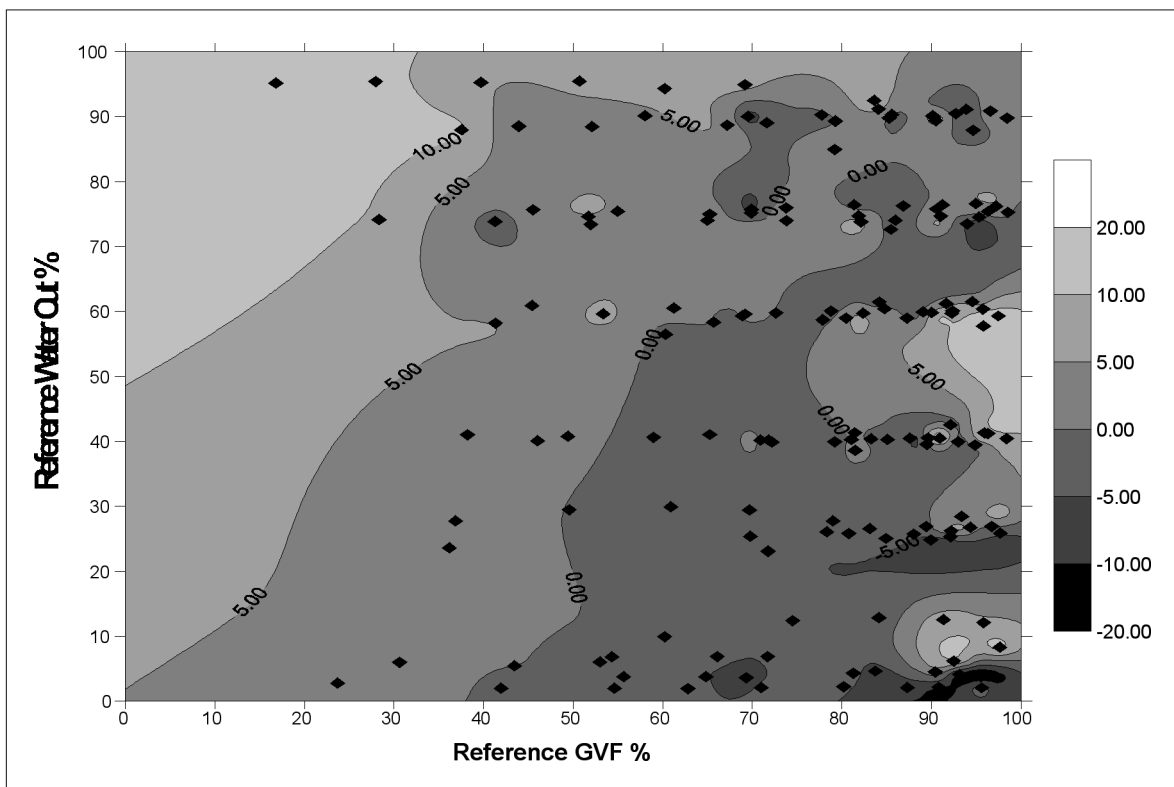


Figure 14: 3" Meter Liquid Flowrate Error vs Rig Water Cut and GVF

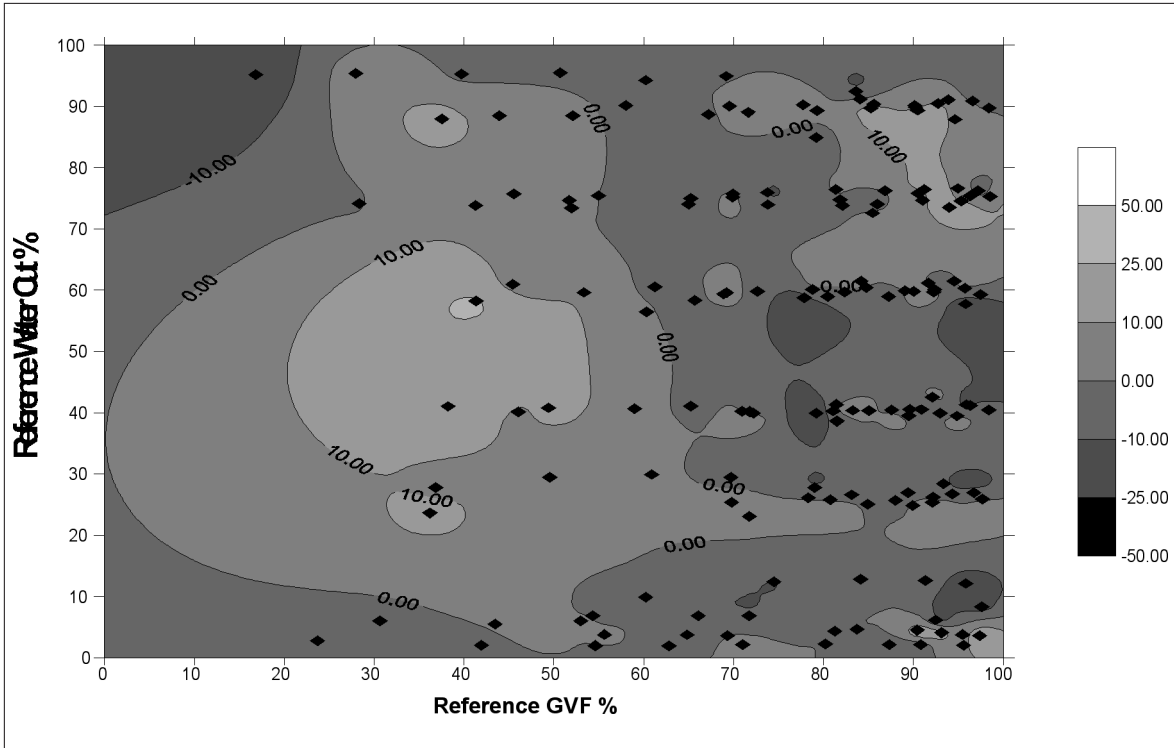


Figure 15: 3" Meter Gas Flowrate Error vs Rig Water Cut and Rig GVF

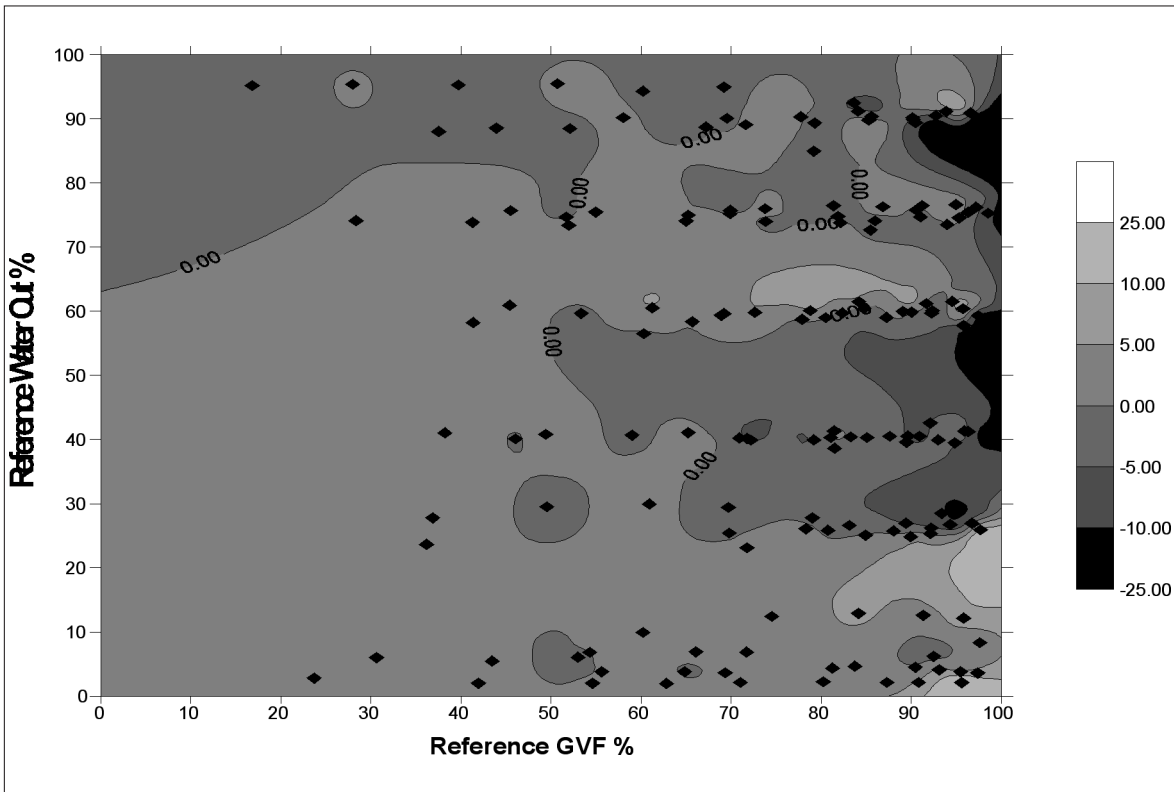


Figure 16: Absolute Water Cut Error vs Rig Gas Fraction

Within the operating range noted above RMS absolute water cut error is 4%. This increases to 5% when only results with gas fractions over 80% are considered and to 6.2% for all results with over 90% gas fraction (ie 90% -95% gas).

## 4.2 Viscous Crude Tests

Late in 1998 the 3" Production Prototype meter was taken to the Texaco Flow Facility at Humble in Texas for tests with a heavy, viscous crude oil. For comparison these tests were followed by a second series using a much lighter crude corresponding closely to the oils used at NEL.

The heavy crude has an API gravity of 19 and density during the tests was typically 915 kg/m<sup>3</sup>. The oil forms viscous emulsion with water. At typical test temperatures, around 35degC, dead oil viscosity was approximately 300Cp rising to approximately 1300Cp at 50% water cut. Methane gas (typical density 8kg/m<sup>3</sup> at test conditions) and a brine containing 26g/l of salts were used. 22 test points were run with water cut varying from 6% to 99% and liquid fraction from 0.03 to 0.90.

The lighter crude has an API gravity of 32 and typical density during the tests was 820kg/m<sup>3</sup>. Viscosity is estimated at around 4Cp. The gas used for the tests was a field gas (typical density 11kg/m<sup>3</sup> under test conditions) and a brine solution containing 96g/l of salts was used for the associated water. 50 test points were run with water cut varying from 5% to 90% and liquid fraction from 0.03 to 0.90.

It had been hoped to run at higher pressures but tests were limited to around 12bar downstream of the mixer.

### Results

Differential Pressure: The differential pressure characteristic for both crudes for liquid fractions above 0.2 is shown in Figure 17. It can be seen that there is very little difference between the two sets of data. Maximum velocity was limited by the rig and few points were run below a liquid fraction of 0.2. However these are plotted in Figure 18 and it can be seen that the trend for both crudes is moved to the right in the same way as the low liquid fraction results for the NEL tests discussed in Section 3.0 above.

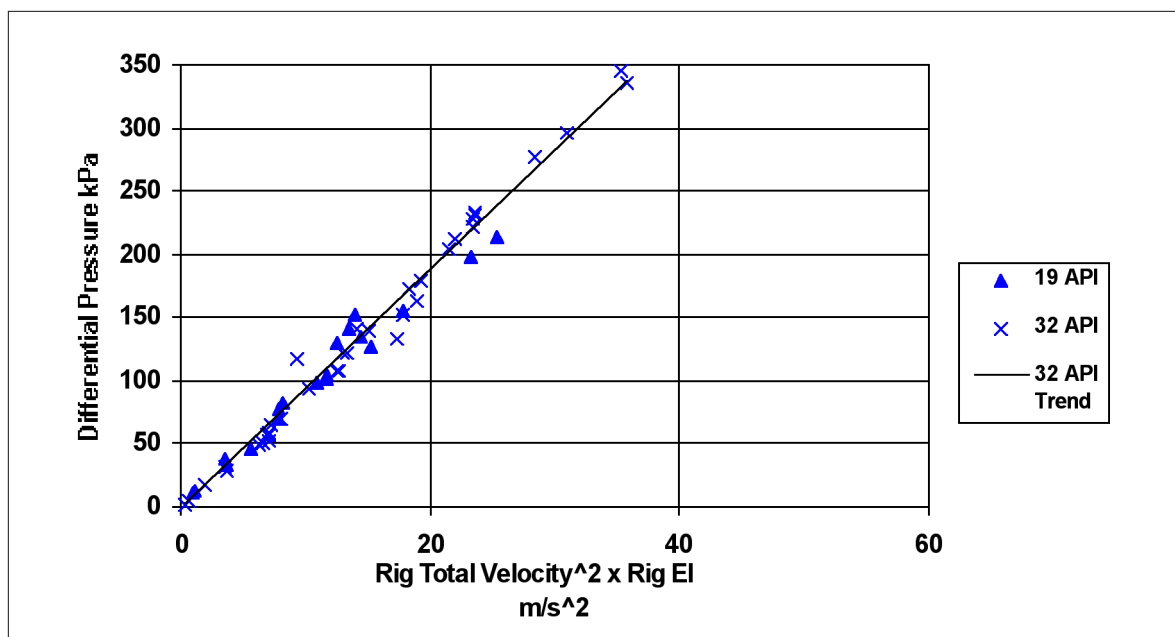


Figure 17: Differential Pressure Characteristic Humble Tests

El > 0.2

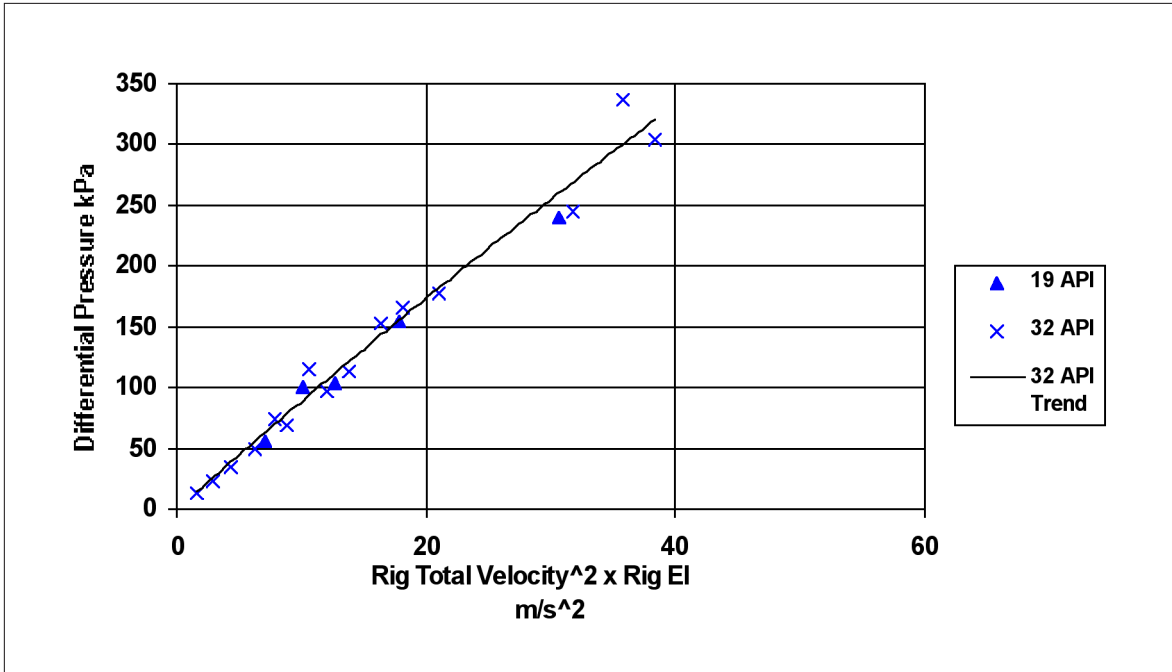


Figure 18: Differential Pressure Characteristic Humble Tests  $El < 0.2$

### 4.3 Conclusions

Detailed analysis of the NEL Multiflow data suggests that use of a more sophisticated calibration for the homogeniser differential pressure will allow operation at total superficial velocities up to 20m/s and liquid fractions as low as 5% with no significant increase in errors.

The NEL tests provided very difficult conditions for MIXMETER due to the low pressure regime and the emphasis in the test matrix on high gas fractions. However results were very satisfactory with RMS errors for the main matrix based on original meter operating limits of 5.1% for liquid rate, 7.3 % for gas rate and 3.4% for absolute water cut.

It also seems clear from the test performed at Humble that the differential pressure characteristic is not sensitive even to fairly large changes in viscosity and density.

Full results are not presented here but as might be anticipated there were no problems with the dual energy measurements when using the heavy crude and the instrument functioned normally even when the line contents were transformed to a stiff 'mousse' at the end of a full day of circulation.

## 7.0 FINAL CONCLUSIONS

Systematic errors in dual energy gamma phase fraction instruments which can arise due to calibration errors or changes in fluid properties during operation can be predicted readily using a simple model together with absorption data for fluids which can be taken from laboratory measurements or calculated from chemical composition data.

For a 'typical' set of oil, gas and water properties errors in oil density lead to relative errors in oil fraction and flowrate of a similar size. eg a 5% increase in oil density will result in a 5% relative increase in measured oil fraction.

An error of this magnitude is unlikely and the instruments are generally very tolerant to anticipated errors in hydrocarbon properties.

Large changes in salinity can cause significant water cut errors to occur where water cuts are high. However the nature of these errors is such that GVF remains essentially constant so that it is possible to identify changes of this type through standard trending of the instrument output.

Use of a third energy to measure salinity offers a simple and direct method to avoid errors due to salinity changes. However, even using the best spread of energy levels within the range which is practical for normal pipe diameters the measurement is too sensitive to be of practical use. The method may be feasible if lower energies are used with small diameter lines or when liquid fractions are low. However, for applications where salinity is expected to vary and where sampling is not an option an alternative method of monitoring the water quality may be needed.

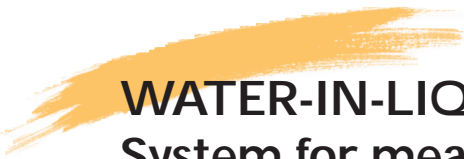
Data from the NEL Multiflow tests has enabled the MIXMETER homogeniser DP characteristic to be extended such that the operating range of the meter is now up to 20m/s and 95% gas fraction.

The mixer characteristic could be extended beyond 95% gas fraction but it becomes more difficult for the dual energy instrument to measure liquid fraction under these conditions.

Tests with a heavy crude forming a viscous emulsion have demonstrated that the homogeniser maintains its characteristic under these adverse conditions.

## References:

- (1) Hewitt, G.F., Harrison, P.S., Parry, S.J. & Shires, G.L. (1997) “The ‘MIXMETER’ flowmeter: Another Step Towards Routine Multiphase Flow Measurement?” Multiphase ’97, Cannes
- (2) Scheers, A.M. (1998) “Multiple Energy Gamma Ray Absorption (MEGRA) Techniques Applied to Multiphase Flow Metering” 4th International Conference on Multiphase Technology, London
- (3) Hewitt, G.F., Harrison, P.S., Parry, S.J. & Shires, G.L. (1995) “Development and Testing of the Mixmeter Multiphase Flowmeter” North Sea Flow Measurement Workshop, Lillehammer



# WATER-IN-LIQUID PROBE

## System for measuring Water-in-Liquid Ratio at low and high gas volume fractions

*Christian Dreyer Skre, M.Sc.  
Christian Michelsen Research AS*

---

### 1. ABSTRACT

A prototype dielectric on-line monitor for measurement of water cut in multiphase petroleum flow has been built. The system is a low cost and robust system capable of measuring 0-100% water cut at 3% uncertainty. The system has been tested successfully at gas volume fractions (GVF) ranging from 0% to 93%. The monitor is designed with a view to installation topside, subsea or downhole.

The measurement concept is based on dielectric measurements of the liquid in the flow at high frequency using an open ended coaxial probe. The method utilises the complex permittivity of the fluid to calculate the water cut. The instrument consists of the dielectric sensor installed in the pipe wall, an electronic unit for measuring the complex reflection coefficient and a PC for control, signal analysis, calculation of water cut and data presentation. The sensor facilitates easy installation, e.g. similar to a pressure transducer.

### 2. INTRODUCTION

The water production from oil producing reservoirs will normally increase during depletion. This has focused effort on the measurement of water both in the reservoir and at the surface. There are several meters on the market measuring the water-in-liquid ratio (WLR) of an oil/water mixture. Many of these are excellent instruments. However, they are all intended for liquid flow, only. A common feature is that they are based on measurement of the dielectric constant of the total pipe volume, either at high frequencies (microwaves) or at lower frequencies (capacitance/conductance). When gas is present in the flow these meters naturally suffer from high uncertainties. However, for wells with high gas contents, such as gas lifted wells and condensate wells, there is at present no automatic on-line technique available on the market. The solution has therefore been sampling followed by analysis of the liquid, which is not very practical and not at all suited for subsea or downhole applications. A novel technology for this application should therefore operate at the high void fractions (up to 98%) as well as at the lower range down to 0%.

Multi-phase meters are certainly able to measure the water-in-liquid ratio in a multi-phase flow. However, these are not low-cost instruments and the likelihood that one is installed at every single well on e.g. a manifold is generally low. In addition, the uncertainty of the water-in-liquid ratio measurement tends to increase as the GVF becomes high. This is mainly due to the fact that multi-phase meters are designed for measuring all three phases covering all practical combinations of phase fractions, i.e. they employ sensors with equal sensitivity over the whole cross-section of the pipeline.

### 3. MEASUREMENT SYSTEM AND EXPERIMENTAL ROUTINES

A high frequency electromagnetic wave is transmitted through an open-ended coaxial probe into the liquid film, which is located at the inner wall of the pipeline as shown in Figure 1.

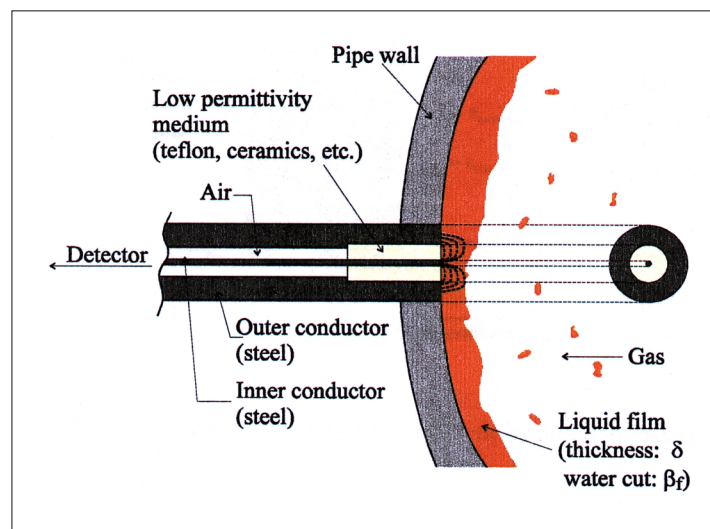


Figure 1 Open-ended coaxial probe for measurement of the relative permittivity of liquid films in multiphase flow. The mixture is assumed to consist of an oil-water liquid film, and a gas core behind the liquid. The water volume fraction of the liquid film is denoted as the water in liquid ratio,  $\beta_f$ , the film thickness has been given the symbol  $\delta$  and the permittivity of the liquid bulk.

At the probe-liquid interface some of the electromagnetic energy is reflected. The reflected signal is dependent on the permittivity of the medium in front of the probe. The complex reflection coefficient,  $\Gamma_R$ , at the end of a coaxial probe depends on the complex permittivity,  $\epsilon^*$ , of the medium the probe is in contact with:

$$\Gamma_R = \frac{1 - j\omega Z_0 C(\epsilon^*)}{1 + j\omega Z_0 C(\epsilon^*)} \quad (1)$$

where  $Z_0$  is the characteristic impedance of the probe,  $\omega$  is the angular frequency,  $\omega = 2\pi f$  where  $f$  is the frequency, and  $C(\epsilon^*)$  is the fringe capacitance of the probe.

From a microwave measurement of the reflection coefficient, the relative permittivity of the medium can be determined.

At high GVFs the flow regime will approach an annular distribution, and a dielectric measurement of the liquid must therefore be performed near the pipe wall. Thus, the measurement system is based on an open-ended coaxial probe designed with a short penetration depth and installed in the pipe wall to be able to measure only on the liquid film. By this arrangement a three-phase problem can be reduced to a two-phase measurement. By proper signal analysis, the system can handle gas bubbles and thin liquid films. The sensor will facilitate easy installation, e.g. similar to a pressure transducer.

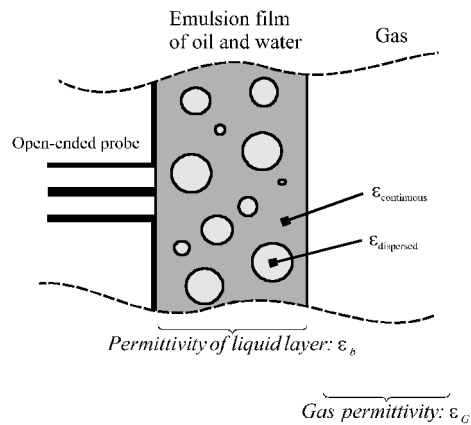


*Figure 2 Schematic illustration of the permittivity measurement by an open-ended coaxial probe*

The laboratory measurement system (Figure 3) consists of a microwave reflectometer controlled by a personal computer and a sensor. The sensor, an open-ended coaxial-probe, is mounted in the pipe wall of the multiphase flow line, and the reflectometer measures the reflection coefficient from the probe. The permittivity of the liquid film is then calculated from the reflection coefficient.

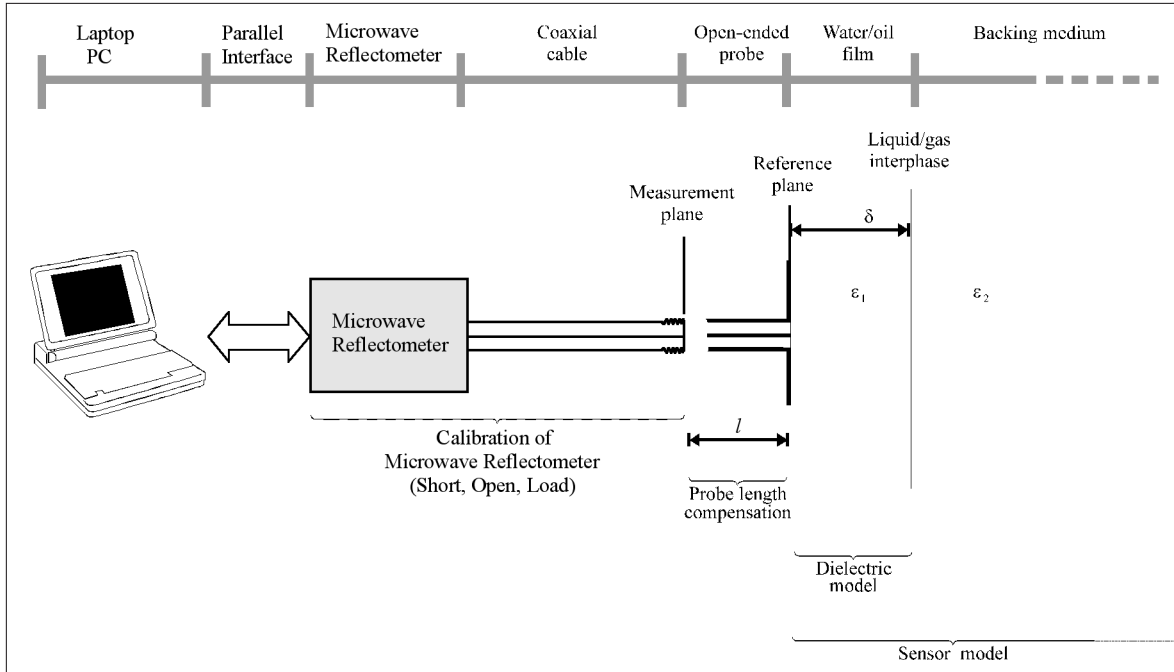


Figure 3 Measurement procedure and sketch of the overall measurement system ( $\epsilon_1 = \epsilon^*$  and  $\epsilon_2 = \epsilon_G$ ).  $l$  in the figure is the physical length of the open-ended probe, and it can be related to the electrical length of the probe as follows:  $l_e = \sqrt{\epsilon_{\text{coax}}} \cdot l$  where  $\epsilon_{\text{coax}}$  is the permittivity of the medium between the inner and outer conductor of the probe.

In determining the WLR of the oil-water emulsion film in front of the open-ended probe, the overall calibration must take the following parts into account:

- *Calibration of the reflectometer.* This must be performed to define the end of the coaxial cable as the measurement plane.
- *Probe length compensation.* This compensates for the physical length and the impedance mismatch of the probe.
- *Sensor model* which relates the reflection coefficients at the end of the probe, the reference plane, to the permittivity of the liquid film, 1.
- *Dielectric model* for calculating the water in liquid ratio of the liquid film on the basis of the permittivity of the film and the known permittivities of oil and water. Both analytical and chemometric models are developed (cf. Section 4).

Tests of the laboratory prototype system have been performed at the CMR multiphase flow loop, and the tests aim at evaluating the feasibility of this method for water in liquid ratio measurement in a multiphase flow.

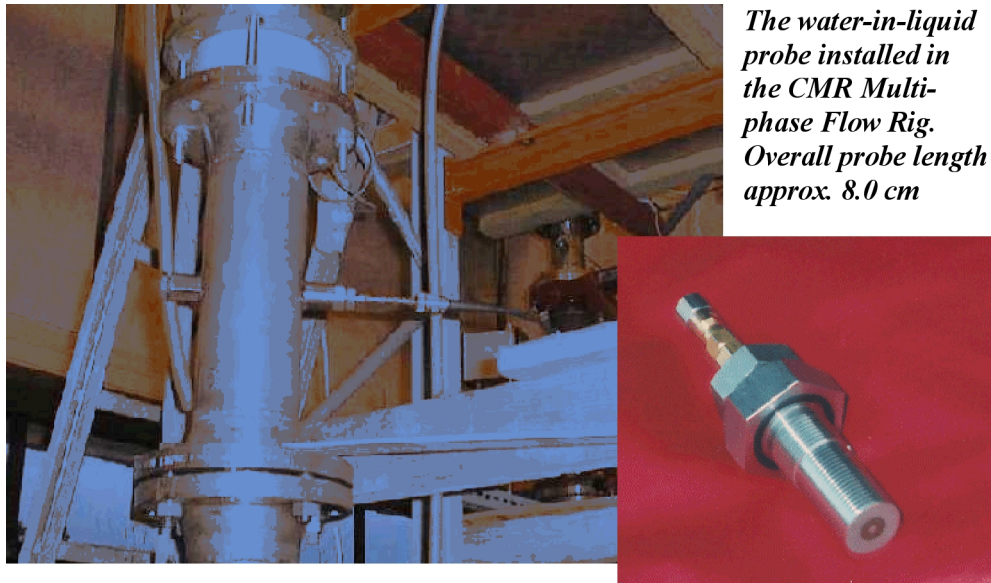


Figure 4 The sensor installation in vertical upward flow.

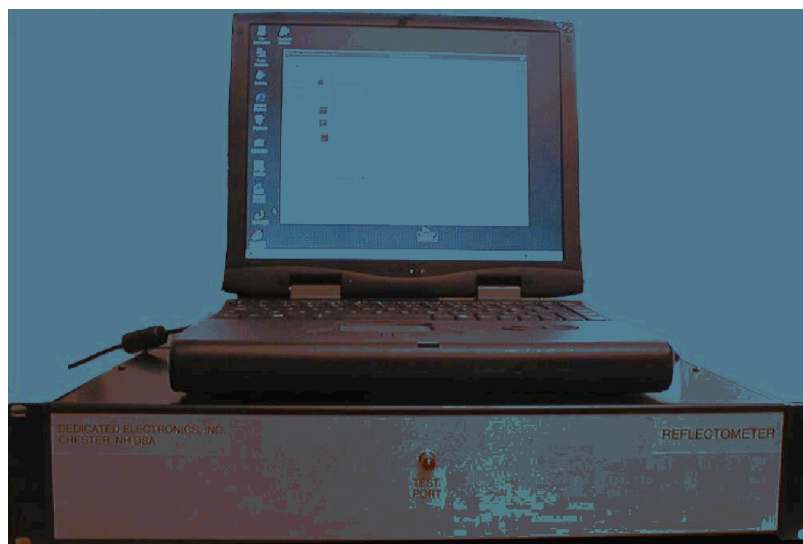


Figure 5 The prototype WLR system, including a dedicated microwave electronics unit, and a portable PC which is used to control the microwave electronics and the data collection and processing.

### 3.1 The CMR multiphase test facility

The test facility consists of a 4” diameter flow loop, a 3 m<sup>3</sup> separator tank, a 7.5 kW centrifugal pump and reference instrumentation for determination of phase fractions, flow rates, flow pressures and temperatures as schematically shown in Figure 6. The flow constituents are Fina Auto-diesel, salted tap water and compressed air.

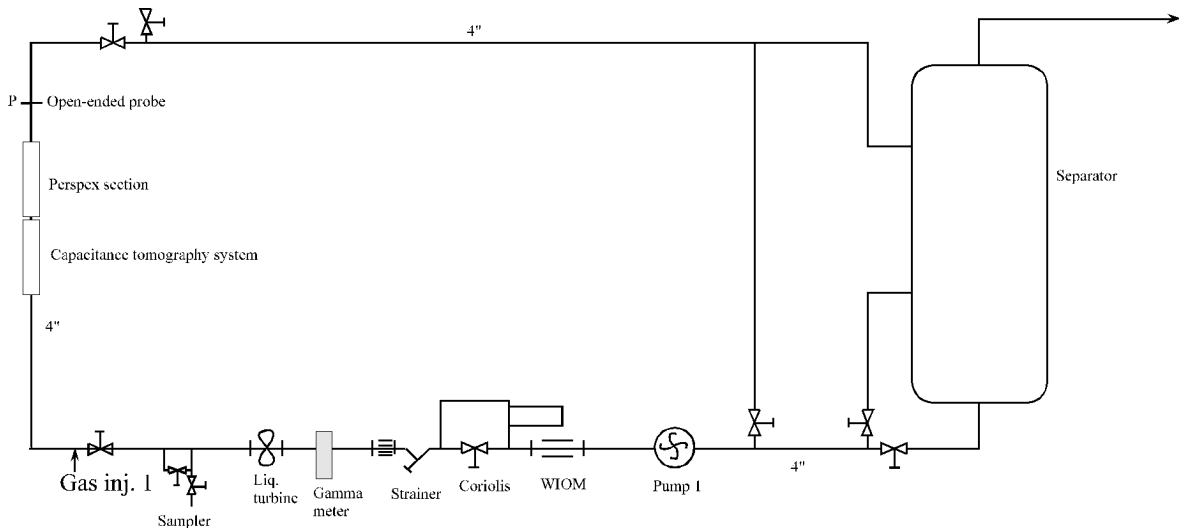


Figure 6 The CMR multiphase flow facility

The separator contains 1 m<sup>3</sup> of oil and 1 m<sup>3</sup> of water. These are separated by gravity and are fed into the loop through separate legs with a throttle valve at each leg to adjust the water in liquid ratio. Downstream of a water-oil mixing junction (T-piece), the liquid enters the centrifugal pump. The pump is, together with a downstream Daniel 4" liquid turbine meter, part of an electronic control loop connected to an automatic flow controller in the control room. This control loop is used to set the liquid flow rate to a chosen pre-defined value.

The water in liquid ratio is measured by means of a Fluenta WIOM 300 installed downstream of the centrifugal pump. The WIOM gives feedback to the throttle valves via a second automatic flow controller in the control room. By this control loop the water in liquid ratio can also be fixed at a chosen set point.

In water continuous flow the reference water in liquid ratio is determined by means of the Coriolis meter and a Krohne gamma densitometer. The Coriolis and the gamma meter measure the density of the oil-water mixture passing through the meters.

The density of oil (diesel) and (saline) water are known and the reference water in liquid ratio can then be calculated as:

$$WLR_{ref} = \frac{\rho_{Coriolis} - \rho_O}{\rho_W - \rho_O} \cdot 100\% \quad (2)$$

where  $\rho_{Coriolis}$  is the density measured by the Coriolis meter,  $\rho_O$  is the density of the oil and  $\rho_W$  is the density of the saline water. A similar expression is used to calculate the WLR from the oil/water density measured by the Krohne gamma densitometer. The average value of the WLRs determined from the Coriolis and the Krohne meter was used as the reference WLR in water continuous flow.

The air from the compressor is stored in a separate tank at a constant pressure of 10 barA. It is supplied to the test facility through a needle valve after being measured by a 1.5” orifice plate meter. There is also a control loop for the gas valve, but the flow controller is normally run in manual mode in order to decrease the response time of the adjustment of the gas injected into the loop. In this project multiphase flow at high gas fractions are emphasised. With regard to this a V-cone meter has been installed in addition to the orifice meter, for measurement of high gas flow rates<sup>1</sup>. The V-cone meter is mounted as part of a new supply line for injection of gas into the flow loop.

The gas is injected at the point denoted as gas injection point 1, see Figure 6

The multiphase flow passes through the vertical test section, enters a horizontal return pipe-line and flows back to the separator. The gas is vented out to open air from the separator.

### 3.2 Reference measurements

The reference liquid flow rate measurement is provided by the Daniel 4» turbine meter which has a calibrated measurement range of 19.3-284 m<sup>3</sup>/h. The nominal relative uncertainty in single phase water flow is 0.25%. At lower flow rates a 1.5” Micro Motion coriolis meter is used as a reference instrument. This meter has a nominal relative uncertainty of 0.2%. Since a mixture of oil and water is used the real uncertainty has been estimated by a comparison between the readings of the turbine meter, the coriolis meter and a Venturi meter. A conservative uncertainty of 2.0% is therefore used for the liquid flow rate (QLiq).

The reference gas flow rate is measured by a 1.5» orifice plate meter or a 1.5» V.cone flow meter depending on the flow rate of gas injected. Since the pressure at the gas flow meter location differs from the pressure at the point of measurement, the actual flow rate (QGas.Ref) can be calculated by the following relationship:

$$Q_{Gas.Ref} = Q_{Gas} \cdot \frac{P_{Gas}}{P_{Flow}} \quad (3)$$

The effect of changes in temperature is neglected because of the short distance between injection point and the test section. The differential pressure across the orifice plate is measured by a 0-300 mbar dP-transmitter. The uncertainty of the Orifice meter is 2.8% of full scale which is 120 Sm<sup>3</sup>/h. The uncertainty of the V-cone meter is 1.0% of measured value at flow rates 60-230 Sm<sup>3</sup>/h, and 2.0% at flow rates 230-750 Sm<sup>3</sup>/h. The absolute pressure at the gas meter location ( $P_{Gas}$ ) is measured by a 0-10 bar transmitter with an uncertainty of 0.05 bar. The pressure in the test section ( $P_{Flow}$ ) is measured by a 0-2.5 bar transmitter with an uncertainty of 0.0125 bar. It is mounted diametrically opposite to the open-ended probe, see Figure 6.

<sup>1</sup> The operating range of the orifice meter is 0-120 Sm<sup>3</sup>/h, while that of the V-cone meter is nominally 60-750 Sm<sup>3</sup>/h. In practice, due to gas delivery restrictions and pressure losses the maximum amount of gas which can be injected into the loop is about 350 Sm<sup>3</sup>/h.

The uncertainty of the water in liquid ratio ( $\beta_f$ ) measured by the Fluenta WIOM 300, is 1.0% absolute. This is established through calibration vs. samples of the liquid flow.

Comparative tests of water in liquid ratio determined by the Coriolis meter and samples taken in the liquid metering run indicate an uncertainty of  $\pm 2\%$  absolute.

The reference gas volume fraction is calculated using the following equation:

$$\alpha_v (\%) = \frac{Q_{Gas}}{Q_{Gas} + Q_{Liq}} \cdot 100 \% \quad (4)$$

Using Eq. (4), the uncertainty of the reference gas volume fraction is expressed by:

$$\alpha_v (\%) = \frac{Q_{Gas}}{Q_{Gas} + Q_{Liq}} \cdot 100 \% \quad (5)$$

After differentiating, inserting the uncertainties and manipulating the expression, we end up with a nominal uncertainty of<sup>2</sup>:

$$\alpha_v (\%) = \frac{Q_{Gas}}{Q_{Gas} + Q_{Liq}} \cdot 100 \% \quad (6)$$

which is an absolute uncertainty.

It is important to note that the gas volume fraction given by Eq. (4) is the “no-slip” gas fraction, i.e. it equals the local gas area fraction only when there is zero slip between the gas and the liquid phases. This is not the case since the gas flows faster than the liquid in the vertical upward flow considered here. Hence, the reference gas volume fraction generally differs from the local gas phase fraction.

In a summary, all the uncertainties are listed in Table 1 below where the relative uncertainty indicates percentage of indicated value, while the absolute uncertainties are related to full scale, i.e. 100%.

---

<sup>2</sup> The calculation presented here is for the case of a gas flow rate giving a total relative uncertainty of less than 5%.

Parameter	Symbol	Uncertainty (Type)
Liquid flow rate	$Q_{liq}$	2.0% (Relative)
Gas flow rate	$Q_{gas}$ turn down (1:4): flow rates < 30 Sm <sup>3</sup> /h:	3.0-5% (Relative) > 5% (Relative)
Gas volume fraction (GVF) <sup>3</sup>	$\alpha_V$	2.0% (Absolute)
Water-in-liquid-ratio (WLR)	$\beta_f$	1.0% (Absolute) in W/O <sup>4</sup> 2.0% (Absolute) in O/W

Table 1 Uncertainties of the reference measurements.

## 4. RESULTS

The system has been continuously tested throughout the development period. The system has also been used for acquiring data in connection to the multivariate analysis to develop the chemometric models<sup>5</sup>. Thus the performance of the system is constantly under evaluation. At the time of printing, a more thorough performance test is on going.

The performance tests show that so far the system is capable of handling all types of multiphase flow regimes generated in vertical upwards flow from 0 to 100% WLR and 0 to 90% gas volume fraction using only one, non-intrusive sensor.

Measurement results are given in Figure 7 and Figure 8 on the two next pages.

In Figure 7, a test of the analytical models used in the system. For GVF's below 80% the average deviation from reference WLR is 1.3%, the maximum deviation is 5.3%. The average deviation from reference WLR, all test point included, is 2.1 %, the maximum deviation 11.4 %. In this test the WLR varied from 0 to 100 % and the GVF from 0 to 93%.

Figure 8 shows the test of the chemometric models with new data, the average deviation from reference WLR is 0.9 %, the maximum deviation 3.8 %. In this test the WLR varied from 0 to 100 % and the GVF from 0 to 82%.

<sup>3</sup> This uncertainty estimate refers to the "no-slip" gas fraction where there is zero slip between the gas and the liquid phases. Generally the reference gas volume fraction differs from the local gas phase fraction.

<sup>4</sup> W/O denotes oil continuous flow while O/W denotes water continuous flow.

<sup>5</sup> Chemometrics is the branch of the multivariate methods, which is adopted by chemists. The methods are powerful statistical techniques for extracting relevant information that exists in any interaction effects that are present between two or more variables.

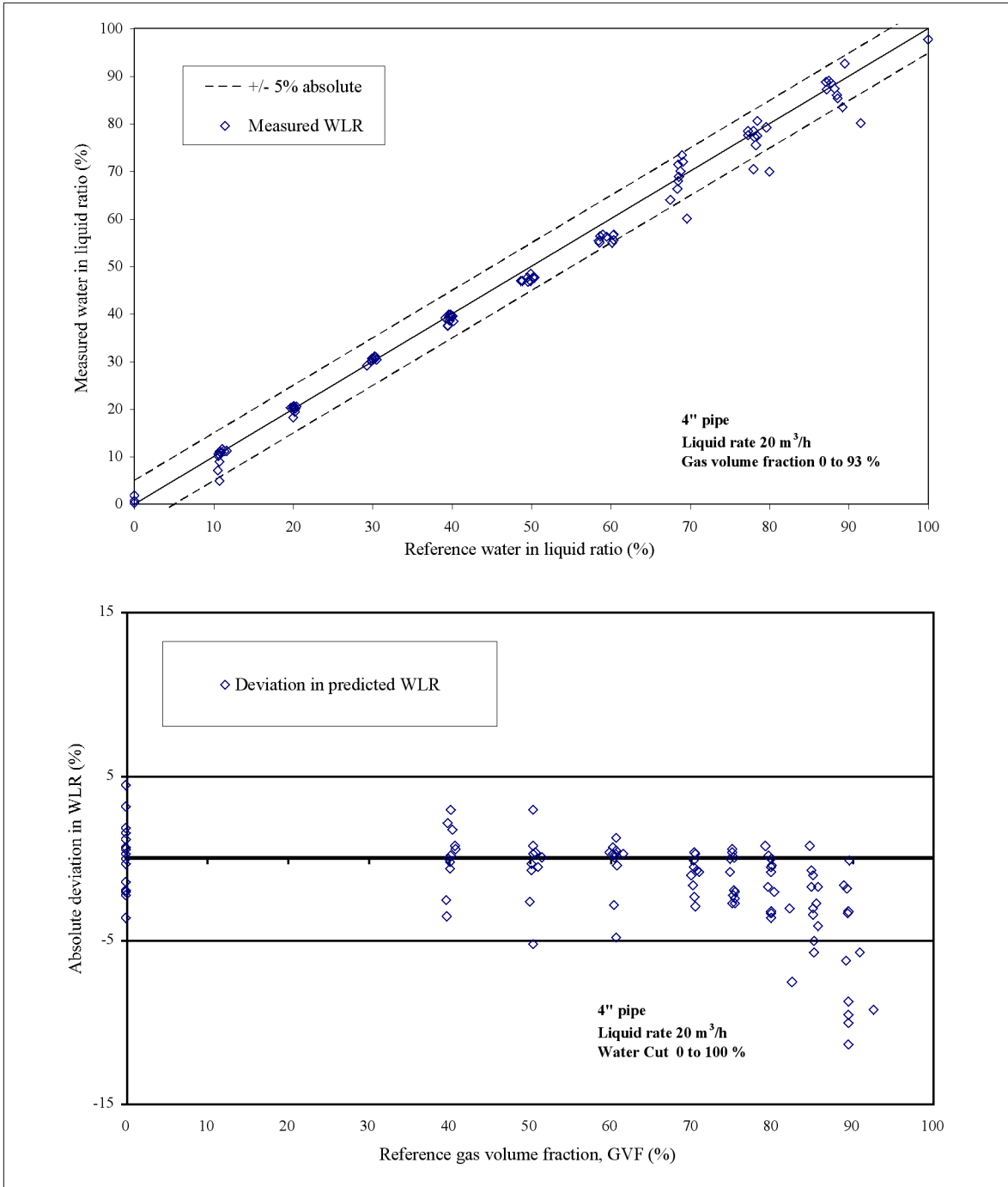


Figure 7 The figure show a test of the analytical models used in the system. For GVF's below 80% the average deviation from reference WLR is 1.3%, the maximum deviation is 5.3%. The average deviation from reference WLR, all test points included, is 2.1 %, the maximum deviation 11.4 %. In this test the WLR varied from 0 to 100 % and the GVF from 0 to 93%.

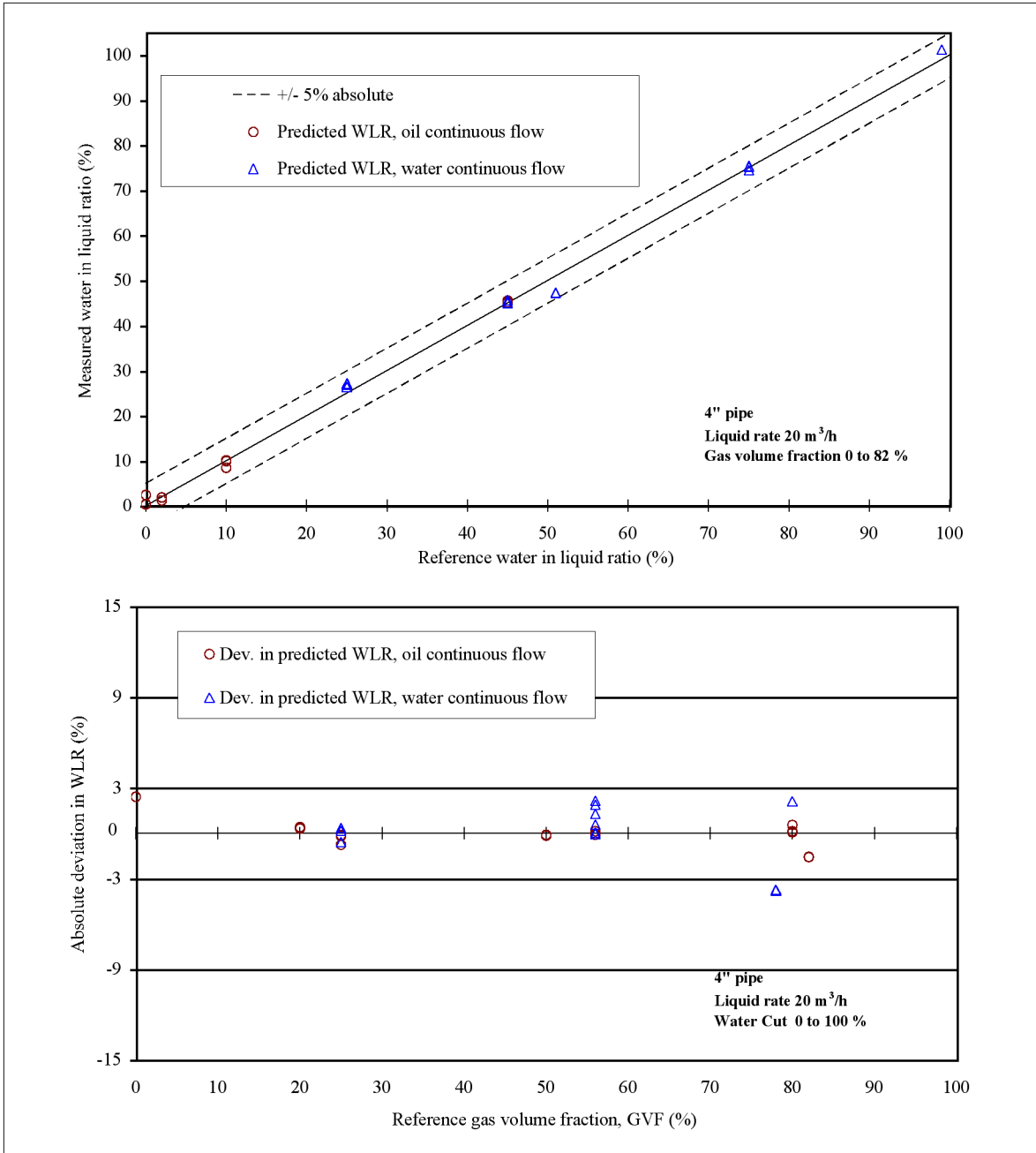


Figure 8 In a test of the chemometric models, the average deviation from reference WLR is 0.9 %, the maximum deviation 3.8 %. In this test the WLR varied from 0 to 100 % and the GVF from 0 to 82%.

## 5. LIQUID SAMPLING OF THE CORE AND THE FILM

This section presents the results of a preliminary experimental investigation into the Water-in-Liquid Ratio (WLR) of the core and the film of an oil-water-air flow in the annular-mist regime.

### 5.1 Introduction

In annular-mist flow, the proposed water cut monitor provides an estimate of the Water-in-Liquid Ratio (WLR) for the liquid film only. In order to estimate the overall WLR for an annular-mist flow, it is necessary to relate the WLR in the liquid film, as measured by the water cut monitor, to the WLR of the liquid conveyed as droplets in the gas core. Accordingly, a sampling device was designed and constructed which allows samples of liquid to be taken from the core and film of an annular-mist flow. The sampling device was mounted at the top of the vertical working section of the flow loop at CMR in which oil-water-air flows in the annular-mist regime can be established.

A series of experiments were carried out to obtain liquid samples from the core and film at the following flow conditions:

1. The total liquid flow rate into the working section was maintained at a constant value of 10 m<sup>3</sup>/h.
2. The air flow rate was set at 350 m<sup>3</sup>/h.
3. The water-in-liquid ratio  $\beta_{f\_Ref}$  of the liquid entering the working section, prior to the point at which the air was injected, was varied in the range 20% to 90%.

At each flow condition the flow was allowed to stabilise prior to samples being taken. Independent measurements indicated that the overall gas volume fraction was always approximately equal to 96%. Images obtained, where possible, using a capacitance tomography system showed that for this value of gas volume fraction the flow was always in the annular-mist regime.

### 5.2 Experimental set-up

In the vertical test section shown in Figure 6, the probe pipe section was replaced by an identical pipe section containing the core and the film sampling devices. A schematic of the sampling section is shown in Figure 9.

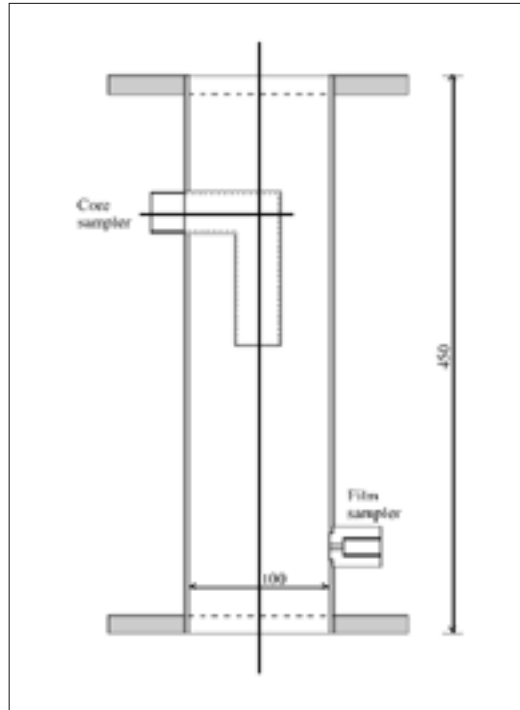


Figure 9 Schematic of the sampling section

### 5.3 Results of Sampling

At each of the flow conditions described above, liquid samples of approximately one litre in volume were bled into sampling vessels from both the core and the film. Any air that entered the sampling vessels was vented to atmosphere. In order to minimise any disturbance to the liquid film, the rate at which liquid was bled from the film was always less than 0.5% of the total liquid flow rate. Following collection of the samples, the oil and water were allowed to separate out in the sampling vessels under the influence of gravity. The water-in-liquid ratios  $\beta_{f\_Core}$  and  $\beta_{f\_Film}$ , for the liquid in the core and film respectively, were then obtained by measuring the oil and water levels in the appropriate sampling vessels.

In Figure 10,  $\beta_{f\_Core}$  and  $\beta_{f\_Film}$  are plotted against  $\beta_{f\_Ref}$ . It is clear from Figure 10 that the values of  $\beta_{f\_Core}$  and  $\beta_{f\_Film}$  are always very close to the value of  $\beta_{f\_Ref}$ .

Figure 11 shows a plot of  $\beta_{f\_Core}$  minus  $\beta_{f\_Film}$  versus  $\beta_{f\_Ref}$  for all of the flow conditions investigated. It is clear from Figure 11 that the value of  $\beta_{f\_Core}$  is always within 2% of the value of  $\beta_{f\_Film}$ . This result is very encouraging because it implies that the WLR in the film and in the core are approximately the same, which in turn implies that a good estimate for the overall WLR for an annular-mist flow can be obtained by measuring the WLR in the liquid film alone. Further work should be carried out to confirm that this result is valid for a wider range of flow conditions.

Note that results obtained by Zabara et al. [5] suggest that, under many conditions, the majority of liquid in a vertically upward, cocurrent annular-mist flow is conveyed in the film rather than in the gas core. Consequently, measurement of the WLR in the film might be expected to give a value representative of the overall WLR even if flow conditions are encountered where there is a difference in the values of  $\beta_{f\_Core}$  and  $\beta_{f\_Film}$ .

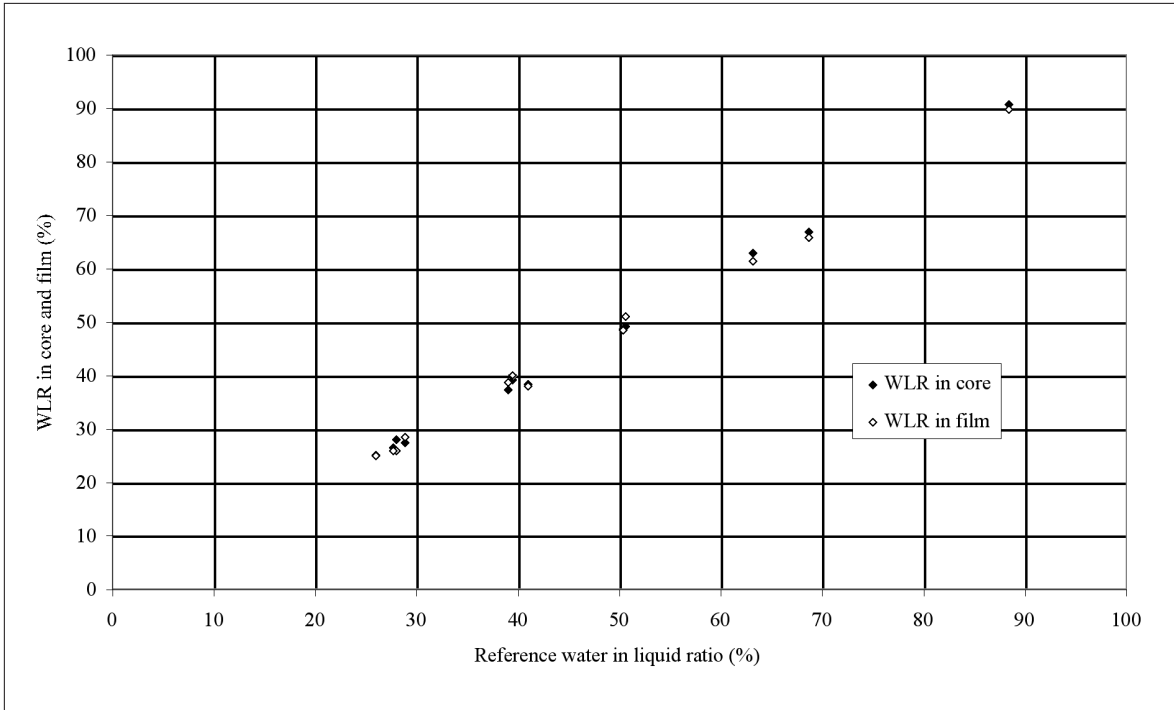


Figure 10 Water in liquid ratio determined by sampling of the core and the film, respectively, plotted versus the reference water in liquid ratio determined by sampling of the liquid phase. The water is saline water of conductivity 9.05 S/m.

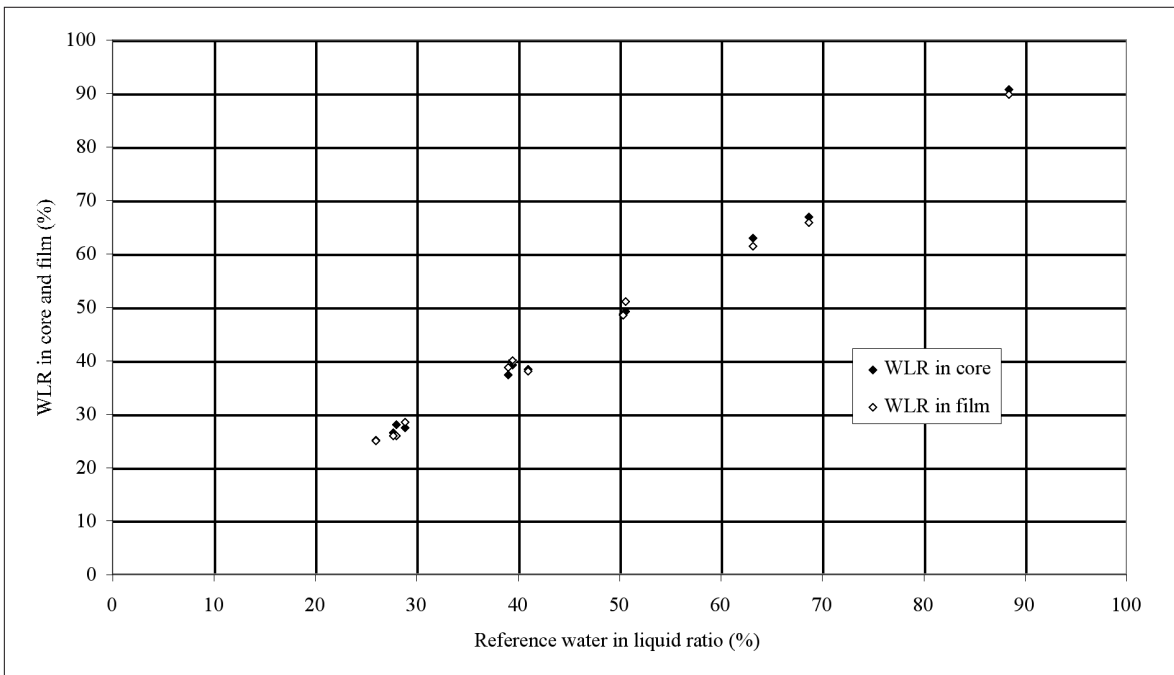


Figure 11 Absolute deviation in the water in liquid ratio between the samples of the core and the film plotted versus the reference water in liquid ratio determined by sampling of the liquid phase. The water is saline water of conductivity 9.05 S/m.

## 6. DISCUSSION AND CONCLUSION

A prototype WLR probe measurement system has been tested by mounting a probe in the pipe wall in contact with the fluid at the CMR multiphase test facility. The results show that an open-ended coaxial probe can be used for on-line measurement of the water in liquid ratio in a multiphase flow and that it is sufficiently accurate across a wide range of gas-liquid ratios in vertical oil-water-gas pipe flows. The results from the tests are promising, and the feasibility of the technique has been proved. Because of the simplicity of the probe this makes it a very powerful tool for monitoring of oil-water-gas processes.

The following main conclusions can be drawn for most of the test points in the range 0-100% water in liquid ratio:

- 1 In oil/water flow with no gas the water in liquid ratio is measured well within  $\pm 5\%$  absolute deviation compared to the reference.
- 2 The water in liquid ratio can be measured within  $\pm 5\%$  absolute deviation compared to the reference for gas fractions in the range 0-85% using analytical permittivity models.
- 3 For gas fractions higher than 85% the uncertainty increases, and is also dependent on whether the flow is oil- or water-continuous. For gas fractions in the range 85-95%, the water in liquid ratio is measured within  $\pm 10\%$  absolute deviation in oil-continuous flow, and  $\pm 12\%$  absolute deviation in water-continuous flow. At all test conditions good repeatability of the measurements were found.
- 4 In general, and particularly at gas volume fractions higher than 85%, the measured water in liquid ratios are underestimated compared to the reference water in liquid ratio when using analytical models. The main reason for this is the presence of gas in the film in front of the probe, or the appearance of a film thickness lower than the sensitivity depth of the probe at very high gas volume fractions.
- 5 With the chemometric models the uncertainty can be narrowed in to 3% absolute for GVF's from 0 to 82%. The tendency to underestimate the WLR is not seen here.
- 6 At the operating frequency in question, it has been found that the measured water in liquid ratios are not significantly affected by the increased water salinity as long as the conductivity of the water is known. The permittivity of the water, for the dielectric model, can then be determined.

In addition the following can be stated:

- 7 A preliminary experimental investigation into the WLR of the core and the film of an oil-water-air flow in the annular-mist regime implies that the WLR in the film and in the core are approximately the same. This in turn implies that a good estimate for the overall WLR can be obtained by measuring the WLR in the liquid film alone. Further work should be carried out to confirm that this result is valid for a wider range of flow conditions.

## 7. ACKNOWLEDGEMENTS

The development work performed to build the WLR-probe measurement system is a team effort constituting scientists who are currently or have been working at Christian Michelsen Research AS, Dept. of Industrial Instrumentation. Academic spin off from the development work has been 3 Ph. D. theses and 2 M.Sc. theses.

The development has been supported continuously by British Petroleum (now BP Amoco) and the Norwegian Research Council since the first project was initiated in 1996.

## 8. FURTHER WORK

CMR is currently moving on with the building of an industrial prototype, which is going to be tested at a field location next year. Also, projects for building of subsea and downhole versions are started. A main task in the latter two projects is the development of state of the art miniature microwave- and detector electronics (ASIC design) in co-operation with University of Bergen, Department of Physics. A successful development of miniaturised electronics will render possible a very compact sensor/detector unit for installation in almost any process topside, subsea or downhole.

The development of a subsea WLR probe system is currently supported by the Norwegian Research Council and Kongsberg Offshore AS (KOS)

## 9. REFERENCES

- [1] **Hilland, Jannicke**, *On-line Quality Determination of Petroleum Fluids by means of Dielectric Spectroscopy and Chemometric Modelling*. Thesis submitted for the degree of Dr. Scient. University of Bergen (1997) CMR-97-F10033. (CMR-Confidential)
- [2] **Midttveit Ø., Aspelund A., Skre C. D.**, *The CMR multiphase flow test facility: System description, Reference measurement system, Test fluids*. CMR Work Note (1998)
- [3] **Aksland Ove**, *Vasskuttmåling i fleirfasestraum ved hjelp av open ende koaksial probe*, Cand. Scient thesis, Departement of Physics, University of Bergen, Norway (1998), (CMR, Confidential)
- [4] **Midttveit Ø., Tjomsland T., Aspelund A., Lucas G.**, *Water Cut Monitor for Multiphase flow of High Gas Content. Pre-project: Flow test of high frequency open-ended probe, and liquid sampling*, CMR-96-F10024, Christian Michelsen Research AS, Bergen, Norway (1996), (CMR Confidential)
- [5] **Zabaras, G., Dukler, A. E., and Moalem-Maron, D.** *Vertical Upward Cocurrent Gas-Liquid Annular Flow*. AIChE Journal Vol.32, No. 5, May 1986.



# FUNCTIONAL ENHANCEMENTS WITHIN ULTRASONIC GAS FLOW MEASUREMENT

*Per Lunde, Christian Michelsen Research AS, Bergen, Norway.*

*Kjell-Eivind Frøysa, Christian Michelsen Research AS, Bergen, Norway.*

*John Bjørn Fossdal, Kongsberg Metering\*, Kongsberg, Norway.*

*Tom Heistad, Kongsberg Metering\*, Kongsberg, Norway.*

*\*) a business unit of Kongsberg Offshore a.s*

---

## SUMMARY

Results and progress from an ongoing R&D program related to the Kongsberg Metering MPU 1200 multipath ultrasonic gas flow meter are presented. The results are outcomes of an R&D Joint Industry Programme (JIP) conducted by Kongsberg Metering (KOS) in a cooperation with Christian Michelsen Research AS (CMR), Statoil, Norsk Hydro and Phillips Petroleum Company Norway, and supported by the Research Council of Norway. The JIP addresses three main topics: (1) calculation of gas density from the measured sound velocity, (2) operation at complex installation conditions (with disturbed flow velocity profiles), and (3) measurement of wet gas.

## 1. INTRODUCTION

Multipath ultrasonic transit time meters for gas flow measurement (USM) have been developed to a stage where they can be considered as alternatives to the more conventional orifice plate and turbine meters for fiscal metering. As compared with more conventional meters, the USM technology offers significant advantages such as compactness, bi-directionality, short upstream and downstream requirements with respect to bends, no pressure loss, fast response, and large turn-down ratio (1:50). Measurement possibilities are provided which have not been available earlier, such as process monitoring (e.g. pulsating flow, gas quality), and self-checking capabilities. The first generation of ultrasonic meters have been on the market for about 5-10 years, and have demonstrated their capability to provide metering accuracy within national regulation requirements. In appropriate applications, multipath ultrasonic meters offer cost benefits. Although there still remains some hesitation in applying the technology for fiscal and sales gas metering until wider experience has been obtained, and industry standards have been established [1], [2], USM technology is increasingly gaining acceptance throughout the industry, and is today in use in gas metering stations onshore and offshore.

In addition to work related to the accuracy and robustness of such meters for fiscal metering applications (flow velocity metering) [2], there is currently an interest in exploiting the potentials of such meters for additional applications. From 1997 to 1999, an R&D Joint Industry Programme (JIP) is being conducted by Kongsberg Metering (KOS) in a cooperation with Christian Michelsen Research AS (CMR), Statoil, Norsk Hydro and the Research Council of Norway [3]. The JIP addresses three main topics: (1) calculation of gas density from the measured sound velocity, (2) operation at complex installation conditions (with disturbed, non-ideal flow velocity profiles), and (3) measurement of wet gas flow. In the wet gas project Phillips Petroleum Company Norway is also a partner. Results and progress from the ongoing R&D programme related to the KOS MPU 1200 multipath ultrasonic transit time gas flow meter<sup>1</sup> are presented in the following.

## 2. DENSITY METERING USING THE VELOCITY OF SOUND

In conventional ultrasonic gas flow metering, the USM measures the flow velocity. Through external input of the pressure (P), temperature (T) and compressibility factor (Z), the volume flow rate at standard reference conditions can be found. In order to measure the mass flow rate of gas, the density is measured externally typically either by a density meter or by gas chromatography. This conventional technique is illustrated in Fig. 1. In addition to the measurement of flow velocity and flow rate, the USM also gives a measurement of the velocity of sound in the gas. Traditionally, the measured velocity of sound has only been used for quality check of the meter. This has been done either by comparison of the measured velocity of sound of the various acoustic paths of the meter, or by comparison of the measured velocity of sound with an externally estimated velocity of sound (for example estimated from the output of a gas chromatograph).

---

<sup>1</sup> From October 1998, Kongsberg Metering's FMU 700 multipath ultrasonic transit time gas flow meter has been denoted MPU 1200.

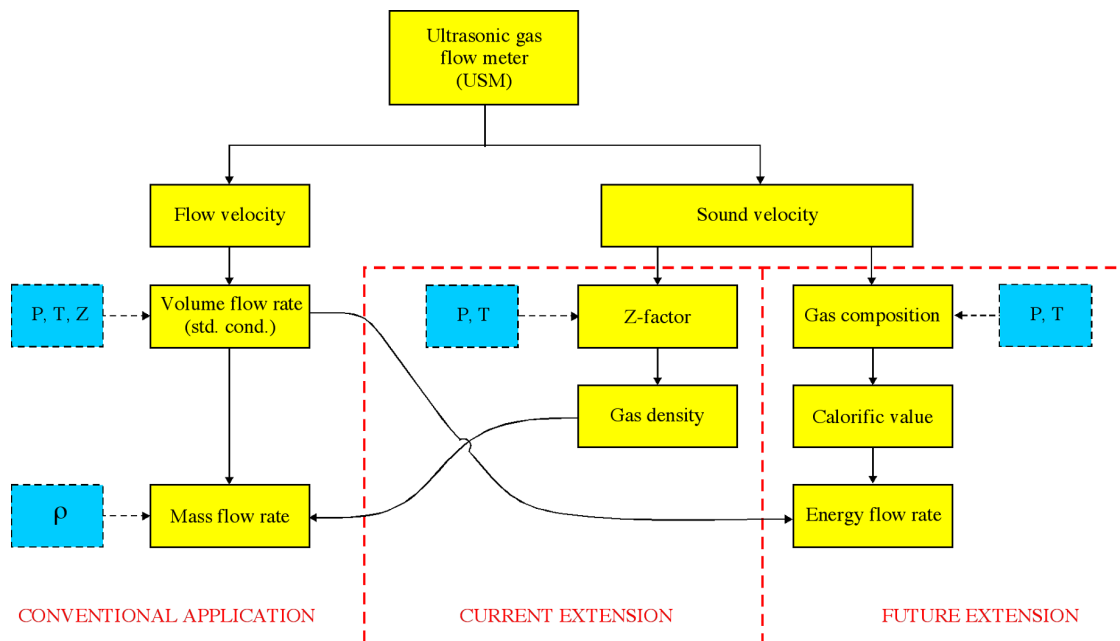


Fig. 1 Illustration of the principles of conventional USM flow metering and the current and future extensions of such metering.

In 1995, Sakariassen [4] described a method of calculating the velocity of sound based on a relationship between pressure, temperature and density. When the USM is installed close to a density meter, such a relation can be used as a quality check of the USM. The velocity of sound calculated from the density can be compared to the velocity of sound measured by the USM. If the deviation between these two estimates of the velocity of sound is too large, it may indicate that the USM may not be working properly.

In his 1995 paper, Sakariassen also hints at finding the relationship to calculate density from the velocity of sound. Such a method will mean that the mass flow rate through a USM can be measured without any external density metering.

Watson [5] and Beecroft [6] have reported attempts to establish such algorithms for calculating the density from the velocity of sound. Watson reports that an algorithm for estimation of density from velocity of sound has been established for gases with methane content greater than 80 %. This algorithm requires the input of an approximate gas composition. Beecroft reports a work based on empirical data from the Trent and Tyne fields, where USMs have been installed and where the density has been measured externally. In his paper, Beecroft states that "currently, knowledge of the gas composition is required to allow an accurate calculation of density, and is likely to remain that way for the foreseeable future".

In parallel to the works reported by Watson and Beecroft, the present JIP has addressed establishing of algorithms for estimating the density from the velocity of sound and the velocity of sound from the density [7]. Such methods may make the USM into a mass flow meter, possibly at a reduced accuracy as compared to the conventional way of measuring the mass flow. This is illustrated as the current extension in Fig 1. The work has been based on an equation of state, and the theoretical relations between the gas compositions, pressure,

temperature and the velocity of sound of natural gas. In addition, general knowledge on natural gas compositions has been used. An uncertainty analysis has been carried out for the established algorithm. In addition, experimental work has been performed to analyze and improve the velocity of sound measurement in the USM. Finally, the established algorithm has been tested experimentally in an explicit flow test. This work is described in the following.

## 2.1 Model description

A theoretical model for calculating the density from the velocity of sound for a natural gas has been established. The model uses the AGA-8-94 equation of state [8] but is not dependent on this equation of state. A possible future change of equation of state in the theoretical model can be done with just minor model development. At present, the theoretical model requires the following input:

- Pressure at line conditions (external measurement).
- Temperature at line conditions (external measurement).
- Velocity of sound at line conditions (USM measurement).
- Molar fractions of N<sub>2</sub>, CO<sub>2</sub>, H<sub>2</sub>O and H<sub>2</sub>S (external measurement / estimate).

Generally, this information is not sufficient to identify the density uniquely. Therefore, assumptions have to be made in order to pick out the "correct" density for a given set of input parameters. These assumptions are related to the likelihood of appearance of the various gas components. For example: consider the following two natural gases: (1) 95 % methane and 5 % propane; (2): 80 % methane, 10 % ethane, 5 % propane and 5 % higher hydrocarbons. Both gases contain 5 % propane, but the second gas is much more likely to appear in practice than the first gas. From such general guidelines, the "correct" density is chosen.

There are, however, cases where a heavy and a light gas have the same velocity of sound, and where the general guidelines referred to above, give no information on which of these two gases that should be chosen. This can typically be the case for the combination of elevated pressures (typically above 100 bar) and low temperatures (typically below 10 °C). In order to reduce such potential problems, the user can specify an interval in which the molar weight of the gas will lie.

The theoretical model can be implemented in an ultrasonic flow meter without any hardware changes. Thus, update of existing flow meters is possible.

In addition to the model for density estimation mentioned above, a model for estimation of the velocity of sound has been established, using the same input as the density model (except that input velocity of sound is replaced by input density). As mentioned above, such a model is to be applied for quality check of a USM that already is installed close to a density meter. Like the model for estimation of density, this model uses the AGA-8-94 equation of state. Also the same guidelines for the gas components are used in the two models. In the model for estimation of the velocity of sound, however, there is no need for specification of an interval for the molar weight of the gas.

## 2.2 Sensitivity analysis

The input values of pressure, temperature, velocity of sound and molar fraction of  $N_2$ ,  $CO_2$ ,  $H_2O$  and  $H_2S$  to the model of estimation of the density of a natural gas, are associated with input uncertainties. In addition, the guidelines for the gas components in the determination of the "correct" density (described above) are associated with uncertainties that are gas dependent. A sensitivity analysis has been carried out to study the influence of these input uncertainties on the uncertainty of the estimated density [9].

Generally, the uncertainty of the estimated density due to uncertainties in the input parameters will vary with pressure and temperature, and also to some extent with the type of natural gas. As an example, results from an uncertainty analysis based on a typical Åsgard gas composition will be referred. This gas is quite typical with respect to uncertainties in the input parameters, and generality should therefore be assured. The temperature range that has been considered in this uncertainty analysis is  $-10\text{ }^\circ\text{C}$  to  $70\text{ }^\circ\text{C}$ . The pressure range is 10 bar to 200 bar.

A standard uncertainty of 0.5 % in the input  $N_2$  component (which means that for example 1% is used instead of 0.5 %) will for pressures below 100 bar contribute (isolated) with a standard uncertainty in the density of less than 0.2 %, and in most cases much less than 0.2 %. For pressures above 100 bar, one can expect large standard uncertainty in the density (typically 1 % or larger) for temperatures below  $25\text{ }^\circ\text{C}$ , while at higher temperatures, the standard uncertainty will typically be less than 0.2 %. The standard uncertainty of the input  $CO_2$  component contributes almost exactly in the same way as the standard uncertainty of the input  $N_2$  component.

A standard uncertainty of 0.5 m/s in the measured velocity of sound will contribute (isolated) with 0.4 % or less to the standard uncertainty of the density. Application of an uncertainty model (VESUM) for measurement of the velocity of sound by a USM, indicates that a standard uncertainty at this level, or better, is within reach, especially at dimensions of 12" and larger [10].

The pressure and temperature uncertainties will in practice contribute less to the uncertainty in density than the uncertainty in the inert gas compositions and the velocity of sound do. The uncertainty analysis indicates that the velocity of sound measurement must be relatively good (standard uncertainty of about 0.5 m/s or less), in order to provide a relatively accurate density estimation. The uncertainty of the  $N_2$  and  $CO_2$  content indicates that in practice, a good density estimate can be obtained if the content of  $N_2$  and  $CO_2$  does not vary more than some tenths of a percent. At Åsgard, for example, the  $N_2$  fraction is about 0.7 %. Then variations from say 0.5 % to 0.9 % can be tolerated without updating the input molar fraction of  $N_2$ . Similar tolerances exist for  $CO_2$ ,  $H_2O$  and  $H_2S$ .

In addition to the uncertainties of the input parameters to the algorithm, the guidelines for the gas components in determining the "correct" density will introduce uncertainties that are gas dependent. For the Åsgard field this standard uncertainty is quite small, below 0.1 % except for the region where the pressure is above 120 bar and the temperature is below  $20\text{ }^\circ\text{C}$ . For other fields, this uncertainty contribution can typically be some tenths of a percent. An evaluation of this uncertainty contribution is possible before installation at a specific gas field. With stable  $N_2$  and  $CO_2$  content, and with a good velocity of sound measurement, it

should for many gas fields be possible to obtain the density with a relative expanded uncertainty of about 0.5 % or less (95 % confidence interval). Other gas fields will give a larger uncertainty. Therefore, in most cases an expanded uncertainty of 0.5 – 1 % or better should be within reach.

### **2.3 Flow testing and results**

The two algorithms for calculating the density from the velocity of sound, and the velocity of sound from the density, have been implemented in a 6" MPU 1200, and a flow test at Statoil's K-Lab was carried out in April 1999 to test the algorithms. The reference density at K-Lab was calculated from the output of a gas chromatograph. The input N<sub>2</sub> and CO<sub>2</sub> values to the algorithms are taken from the same gas chromatograph. At K-Lab, only one gas composition was available. This gas composition is (by chance) relatively well suited for the general guidelines for the gas components in the determination of the "correct" density, but not perfect in this respect. In order to test the algorithm at various densities, two temperatures (about 30 °C and 50 °C) and two pressures (about 30 bar and 80 bar) were used. For each of the four P, T – combinations, the flow velocities 5 m/s, 10 m/s and 20 m/s were tested in order to demonstrate flow independence of the algorithms as implemented in the USM. The results from the K-Lab test are shown in Fig. 2, where the deviation between the density as calculated from the measured velocity of sound and the reference density is shown for each P, T, v combination. Typically, in this test, the density has been measured by the USM to within ±0.1 % of the reference density.

### **2.4 Perspectives (planned work)**

In future this work is planned to be extended in two ways:

As stated in Section 2.2, the algorithms do not work properly on all gas compositions, due to the guidelines for the gas components in the determination of the "correct" density. More robustness is planned to be built in here, especially in cases where some rough knowledge on the gas composition is available.

In previous work at CMR, it has been demonstrated that the calorific value can be found from the velocity of sound and additional measurements. It is planned to design an algorithm well suited for USMs based on these results. This may give possibilities to also measure the energy flow rate using USM, as illustrated as a future extension in Fig. 1.

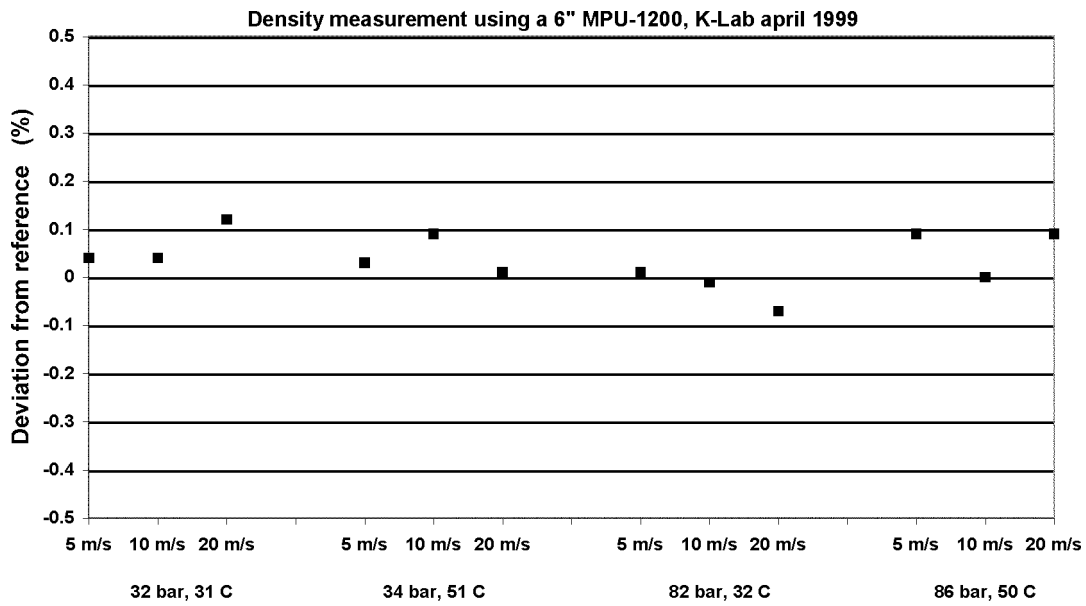


Fig. 2 Results from the online test of the density algorithm at K-Lab using a 6" MPU 1200.

### 3. INSTALLATION EFFECTS

In compact metering stations, with the flow meter possibly installed close to bend configurations, the flow profile can be quite complex, with an asymmetric axial flow profile, and also significant asymmetric transversal flow components. In the present JIP, the performance of the MPU 1200 ultrasonic meter has been studied at a wide range of complex flow profiles, both numerically calculated (CFD) and experimentally established (flow tests). These results have been used to improve the meter's integration of the flow velocity over the pipe cross section, to obtain improved measurement accuracy for meters installed close to bends. Results from the testing of an improved MPU 1200 integration algorithm are presented.

As a background, in order to describe the problem of non-ideal flow, consider a single acoustic path (non-bouncing) with interrogation length  $L_i$  and an angle  $\phi_i$  to the axial direction. First, if the average flow velocity along acoustic path no.  $i$  is purely axial with value  $\bar{v}_{i,A}$ , the upstream and downstream transit times can, to the lowest approximation in the Mach number, be written as

$$t_{1i} = \frac{L_i}{c - \bar{v}_{i,A} \cos \phi_i}; \quad t_{2i} = \frac{L_i}{c + \bar{v}_{i,A} \cos \phi_i} \quad (1)$$

where  $c$  is the velocity of sound. The average axial flow velocity along acoustic path no.  $i$  can be found as

$$\bar{v}_{i,A} = \frac{L_i (t_{1i} - t_{2i})}{2t_{1i}t_{2i} \cos \phi_i} \quad (2)$$

which is the formula (or a variant of the formula) used for calculating the average axial flow velocity along the acoustic path. However, when an average transversal flow component along the acoustic path,  $\bar{v}_{i,T}$ , is present (see Fig. 3), the transit times are changed to

$$t_{1i} = \frac{L_i}{c - \bar{v}_{i,A} \cos \phi_i - \bar{v}_{i,T} \sin \phi_i}; \quad t_{2i} = \frac{L_i}{c + \bar{v}_{i,A} \cos \phi_i + \bar{v}_{i,T} \sin \phi_i} \quad (3)$$

and the estimated flow velocity will be

$$\bar{v}_{i,A} + \bar{v}_{i,T} \tan \phi_i = \frac{L_i(t_{1i} - t_{2i})}{2t_{1i}t_{2i} \cos \phi_i} \quad (4)$$

Thus, transversal flow components will influence on the measured flow velocity along a single path. If not eliminated or corrected for, these contributions give measurement errors.

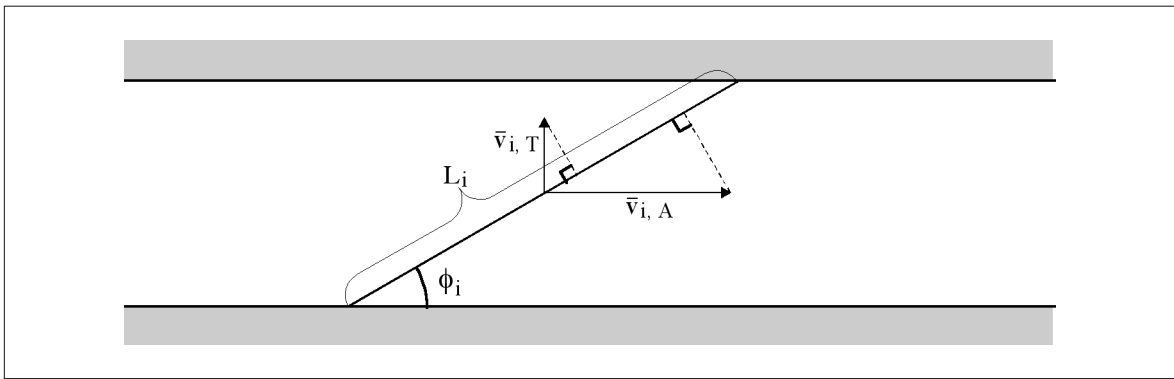


Fig. 3 The influence of axial and transversal flow components on a single acoustic path illustrated by decomposition of the flow velocities along the acoustic path.

In a multipath USM, the measured flow velocities from the individual acoustic paths are combined to obtain an average axial flow velocity over the pipe cross section. This process is denoted the integration method for the specific USM. A good integration formula should fulfil two requirements:

- Integrate the axial flow velocity to a sufficiently high accuracy.
- Eliminate as good as possible the influence of the transversal flow components.

Transversal flow components will occur especially when the USM is installed downstream bends and other obstructions of the pipe flow. It is expected that downstream a double bend out of plane, the transversal flow regime is typically a swirl, while downstream a single bend, a cross flow is typically established, see Fig. 4. As demonstrated above, such transversal flow components can contribute to the flow measurement performed by each acoustic path. There are examples from installations downstream double bends out of plane where the transversal flow components can be 10 % of the axial flow component, or larger. In order to handle such transversal flow components, a USM needs to compensate for the appearance of such components, either by measuring the transversal component or by indirect compensation. Such indirect compensation can for example be that symmetric cross flow will be automatically compensated for through the geometrical configuration of the acoustic paths (contribution to one acoustic path is equal in magnitude but of opposite sign of the contribution to an other acoustic path). Thus, a careful design can in some cases cause the

effect of the transversal flow components to cancel between the various acoustic paths. However, in practice, the transverse flow components often will neither be a symmetric swirl nor a symmetric cross flow, but instead some kind of an asymmetric variant of either swirl or cross flow, or something in between.

In the JIP, a review of the integration method used in a 6-path USM has been performed after gaining experimental experience (flow testing) of this type of meter for about 4 years. The work has led to a further optimization of the integration method used in the meter, based among other on the set of experimental flow test data, and thus to an improved performance of the meter.

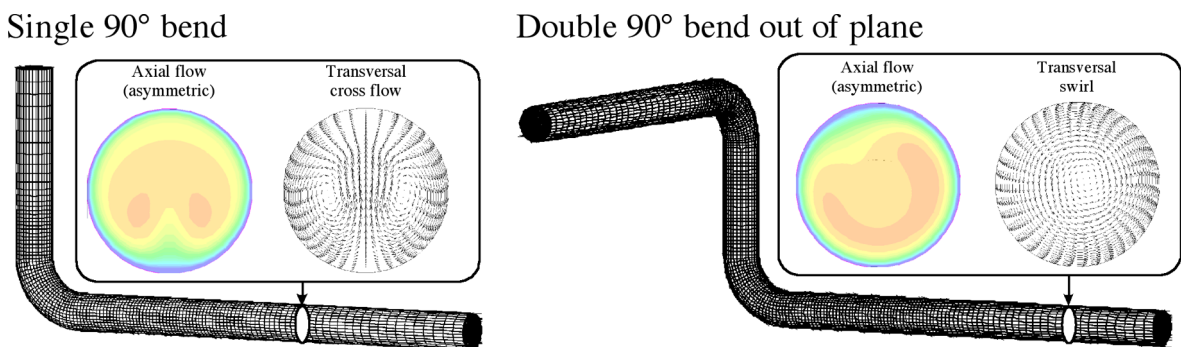


Fig. 4 Illustration (CFD calculations) of typical cross flow (left pipe configuration) and swirl (right pipe configuration) flow regimes.

### 3.1 Experimental input (flow testing)

From the first tests in 1995 [11], the 6-path USMs have been flow tested at various flow laboratories. In the study presented here, a selected set of experimental data, gathered in the period 1995 to 1998, has been used as a basis. These include the following installations:

- Baseline tests with 40 to 100 diameters straight pipe upstream the USM.
- Baseline tests with flow conditioners upstream the USM.
- Installation tests with a single 90° bend upstream the USM.
- Installation tests with a double 90° bend out of plane upstream the USM.
- Installation tests with a U-bend upstream the USM.

The experimental input data used in the present study come from flow tests at

- Statoil's K-Lab, Norway
- Ruhrgas' Lintorf HP test facility, Germany
- Gasunie's Bernoulli Laboratory, Westerbork, The Netherlands
- Southwest Research Institute, Texas, USA
- Offshore installation at Oseberg, Norway

The experimental data set from these flow tests constitutes the major basis for the integration model development which is done under the present project. In addition, complementary results using computer simulations have been used to some extent. The computer simulations are discussed below.

### 3.2 Modelling

As stated above, a good integration method must integrate the axial flow profile sufficiently well, in addition to reduce the influence of the transversal flow components as much as possible. The axial flow profile integration used up to now in the 6-path USM is based on a well established mathematical / numerical algorithm, and has demonstrated to integrate well both symmetric and asymmetric axial flow profiles. In the modification work, it has therefore been essential that in the case of no transversal flow components in the pipe, the modified integration method should give the same answer as the method currently implemented in the USM.

In order to obtain an improved cancellation of the transversal flow components, knowledge on the asymmetry in these components has to be established. This knowledge on asymmetric transversal flow components has been established through careful studies of the experimental data available from flow tests. In addition, two simulation tools developed at CMR have been used. First, the computational fluid dynamics (CFD) code MUSIC is used to simulate the pipe flow through and downstream various bend configurations. Thereafter, an updated draft version of the USM uncertainty model GARUSO has been used to calculate the flow velocity estimated by each acoustic path in a USM, and the contribution to these flow velocities from the axial and the transversal flow components in the pipe flow. Thereafter, the average axial flow velocity as estimated by the USM is compared to a reference value that is also calculated by the program. In this way, a numerical "flow test laboratory" has been established.

The CFD flow simulations have been carried out for the following 4 types of pipe geometry:

- Single 90° bend.
- Double 90° bend out of plane, no separation between the bends.
- Double 90° bend out of plane, 3 inner diameters separation between the bends.
- Double 90° bend out of plane, 10 inner diameters separation between the bends.

For each of the geometries, three different inlet flow conditions have been chosen for the pipe work in the CFD simulations. This has been done because in practice, the inlet conditions on a bend configuration may be far from an ideal, fully developed turbulent axial flow profile with no transversal flow components. By using several inlet flow conditions, the robustness of USMs against such variations in inlet conditions can to some extent be studied.

For the single bend conditions, the following three inlet flow conditions have been used:

- Fully developed symmetrical axial flow profile (power law profile) with no transversal flow components.
- Fully developed symmetrical axial flow profile (power law profile) with a superposed symmetric swirl, and a maximum transversal flow component of about 5 % of the axial flow component.
- Fully developed symmetrical axial flow profile with a superposed cross flow.

For each of the double bend out of plane geometries, the following three inlet flow conditions have been used:

- Fully developed symmetrical axial flow profile (power law profile) with no transversal flow components.

- Fully developed symmetrical axial flow profile with a superposed symmetric swirl, with a maximum transversal flow component of about 10 % of the axial flow components. Rotation of swirl in positive and negative direction.

In addition, each of these flow simulations has been carried out at the two Reynolds numbers 105 and 107. This gives a total of 24 different flow situations that have been analyzed. For each of these 24 cases, virtual USMs with various acoustic path configurations have been "installed" 5 D, 10 D, 15 D and 20 D downstream the bends. The flow velocity estimated by each acoustic path in a USM, and the contribution to these flow velocities from the axial and the transversal flow components in the pipe flow, are then calculated. At every (virtual) USM installation point, the USM has been rotated from 0° to 360° in steps of 5° in order to see the influence of various orientations of the meter.

### 3.3 Integration method

By analyzing the experimental (flow testing) and numerical (simulation) data, some candidate models for the asymmetry in the transversal flow components have been established. These asymmetry models lead to candidate integration models for obtaining the average axial flow velocity from the flow velocities estimated by each acoustic path. The candidate integration models use the same input as previous models (i.e. the measured flow velocity at each of the 6 acoustic paths). This means that no hardware changes are necessary, and therefore also updating of existing 6-path USMs to the new models is possible. The integration of the axial flow profile (symmetric or asymmetric) is performed exactly as earlier. This means that the new candidate integration models should provide improved results in installation tests, while the baseline test results should remain about unchanged, when compared to the existing integration method in the 6 path USM. In the present paper, results using one of these candidate integration models will be shown. The integration model to be implemented in the MPU 1200 is to be chosen in the near future.

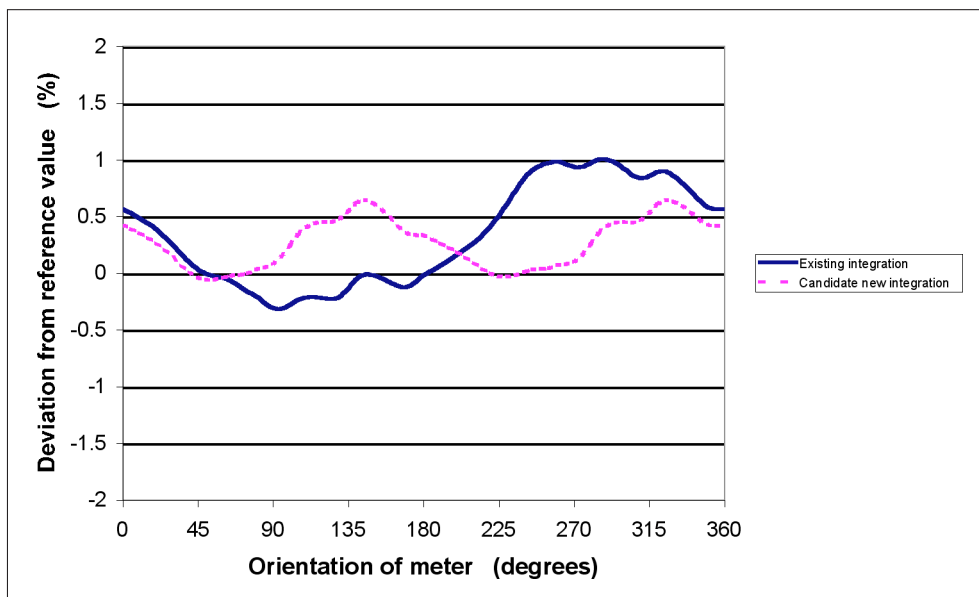


Fig. 5 Example of calculated deviation from reference (simulation results) for a 6-path USM using the existing and the candidate new integration method. In this example, the USM is "installed" 10D downstream a double bend out of plane with 3D separation between the bends and a rotational inlet flow on the bends. Results for various orientations (rotations) of the USM are shown.

As an example of the existing and the candidate new integration method, a GARUSO simulation based on MUSIC CFD input is shown in Fig. 5. Here the deviation between the USM output and the reference flow velocity is calculated for various orientations of the meter spool in the pipe, when the USM is rotated from 0° to 360°. The installation is 10D downstream a double bend out of plane with 3D separation between the bends, and with a rotational inlet flow to the bends. It is seen that the candidate new integration model will reduce the span of the deviation over the various orientations of the meter from about 1.3 % for the existing model to about 0.7 % for the candidate new model. In this context it should be noted that all USMs show some dependency of the orientation of the meter. This has been demonstrated experimentally in flow tests of various meter types (4 - path, 5 - path and 6 - path meters), see e.g. [12], [13]. Such orientation effects should be reduced as much as possible.

### 3.4 Flow testing and results

The new candidate integration method has been developed based on experimental data from pre-1999 flow tests and CFD data. The method is then tested in two new flow tests as part of a verification. The first test is designed especially for the integration method project. In this test, a 6" MPU 1200 was used. The test was carried out at Statoil's K-Lab in June 99. The second test was carried out by Southwest Research Institute (SWRI) and Gas Research Institute (GRI) on a 12" MPU 1200 in August 99. This test was part of a larger test where three commercially available USMs were tested [12], [13]. The 12" MPU 1200 was equipped with the old integration method. In both tests, the candidate new integration method was tested through postprocessing of the experimental data.



*Fig. 6 Installation of a 6" MPU 1200 at Statoil's K-Lab 10D downstream a single 90° bend. A flow conditioner is mounted in the read flange upstream the single bend. Photograph provided by Statoil K-Lab.*

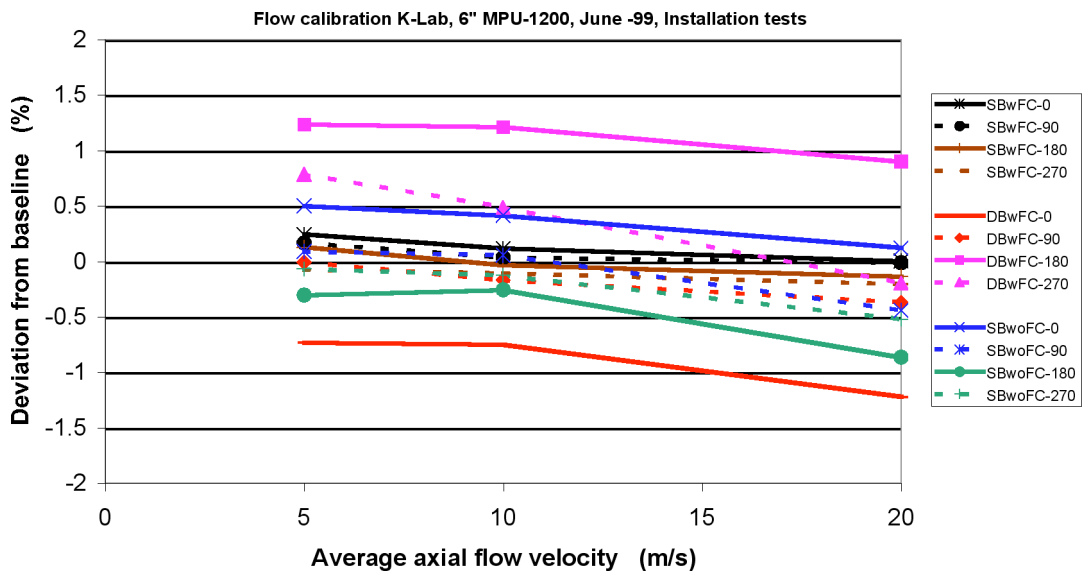


Fig. 7 The deviation from baseline tests for installation tests of a 6" MPU 1200 at K-Lab in June 1999 using the existing integration method of the meter. Legend text: SBwFC: MPU 1200 installed 10D downstream a single bend with K-Lab flow conditioner installed upstream the bend. DBwFC: MPU 1200 installed 10D downstream a double bend out of plane with K-Lab flow conditioner installed upstream the bends. SBwoFC: MPU 1200 installed 10D downstream a single bend with no flow conditioner installed upstream the bend. 0, 90, 180 and 270 refer to orientation (rotation) of the meter in degrees relative to a normal installation of the meter with the electronics on top of the meter.

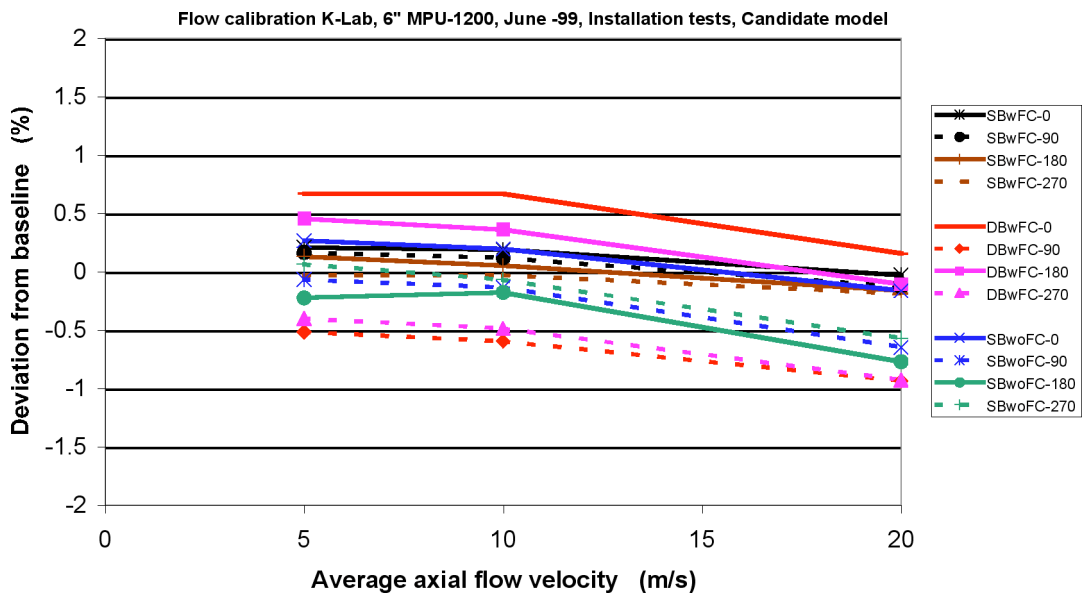


Fig. 8 Same as Fig. 7, except that the candidate new integration method has been used instead of the existing integration method of the MPU 1200.

At Statoil's K-Lab, 4 types of installations were tested:

- Baseline tests with the USM located about 40 D downstream a K-Lab flow conditioner.
- Installation tests 10D downstream a single 90° bend. A K-Lab flow conditioner was installed upstream the bend.
- Installation tests 10D downstream a double 90° bend out of plane. A K-Lab flow conditioner was installed upstream the bends.
- Installation tests 10D downstream a single 90° bend. No flow conditioner was installed.

For each of these 4 installations, the meter was tested in 4 different orientations (0°, 90°, 180° and 270° rotation) of the meter, relative to the normal installation orientation (with the electronics at the top of the meter). Three flow velocities, 5 m/s, 10 m/s and 20 m/s, were used in each installation test.

Upstream the single or double bend in the installation tests, there are several other bends, as can be seen on Fig. 6. Therefore, the inlet flow profile on the single or double bend can be quite complex. Therefore, a flow conditioner was installed upstream the single / double bend. This was done to ensure that the measured installation effects on the USM were due to the bend configuration in question. In addition, single bend tests were also carried out without a flow conditioner upstream the bend, in order to investigate effects of various inlet flow conditions. The average flow velocities measured by the 6 acoustic paths demonstrate that the inlet flow profile on the single bend may be an important parameter when flow calibrations take place.

In Figs 7 and 8, the deviation from baseline measurements has been shown for the installation tests. This presentation form has been chosen because the deviation from baseline demonstrates the influence of the bend configuration as compared to a baseline condition. Results using both the existing MPU 1200 integration method and the candidate new integration method are shown. It can be seen that the spread of the results is larger for the existing method than for the candidate new model.

At SWRI, a 12" MPU 1200 was tested in the following installations:

- Baseline tests 100D downstream a single 90° bend, without flow conditioner between the bend and the meter.
- Installation tests 10D and 20D downstream a single 90° bend, with no flow conditioner between the bend and the meter.
- Installation tests 10D and 20D downstream a double 90° bend out of plane, with no flow conditioner between the bends and the meter.
- Installation tests 10D and 20D downstream a double 90° bend in plane, with no flow conditioner between the bends and the meter.
- Baseline tests and installation tests with flow conditioners (of various types) between the bend and the meter.

For each installation test, the meter has been tested with two orientations (0° and 90° rotation). Upstream the bends, a Gallagher flow conditioner has been installed [13]. The MPU 1200 was equipped with the existing integration method. The data from each acoustic path have, however, kindly been made available to the present project by T. Grimley, SWRI, enabling testing of the candidate new integration model through postprocessing. In Fig. 9, the deviation from reference has been shown for the flow tests at SWRI (with the existing integration method), for all flow tests

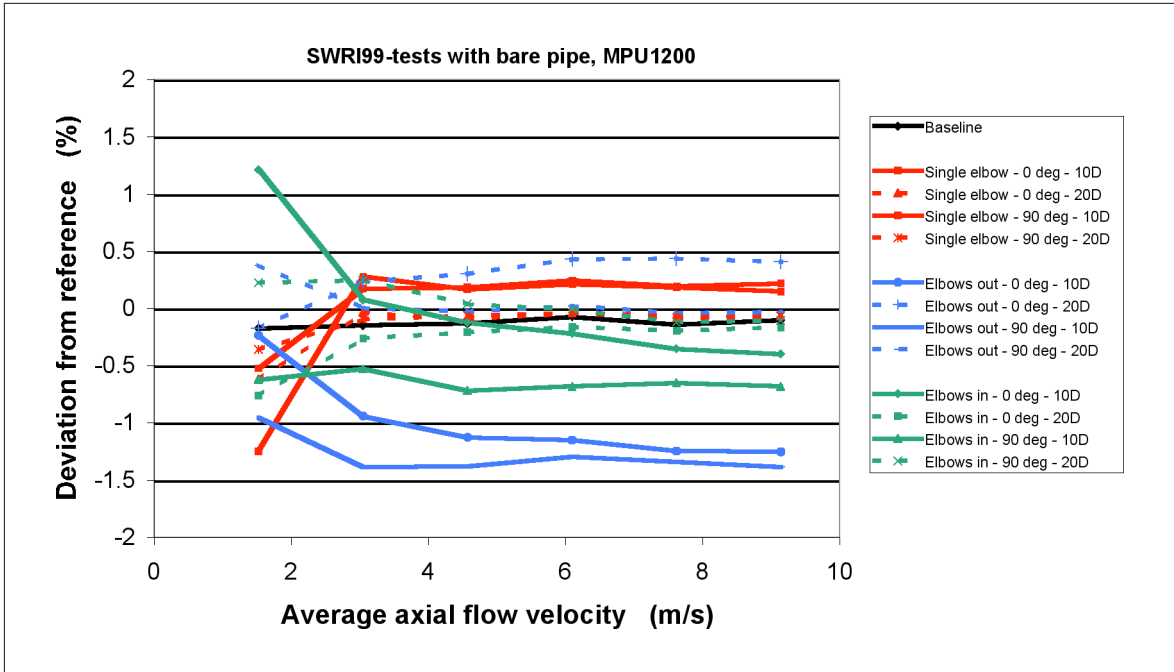


Fig. 9 The deviation from the reference measurement for a 12" MPU 1200 installed 10D and 20D downstream a single 90° bend (single elbow), a double 90° bend out of plane (elbows out) and a double 90° bend in plane (elbows in). Orientation of the meter is 0° and 90°. Existing integration formula used.

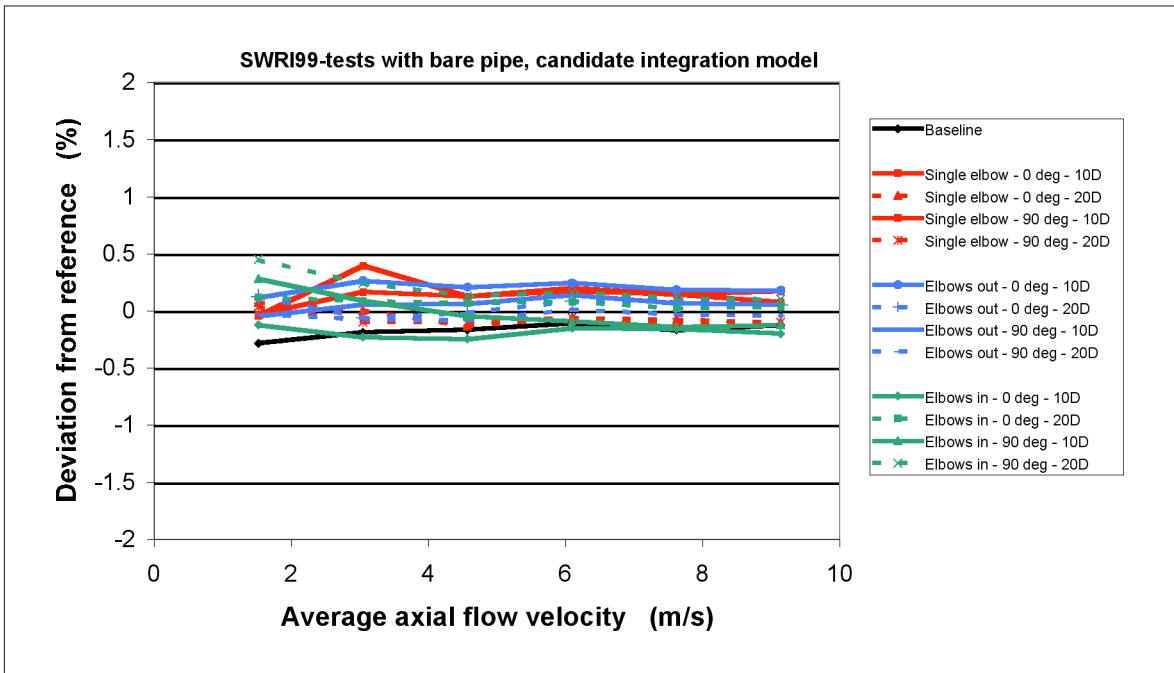


Fig. 10 Same as Fig. 9 except that the candidate new integration model is used through postprocessing of the experimental data (using the same data as used as basis for Fig. 9).

Table 1 Flow weighted mean error for installation tests of a 12" MPU 1200 at SWRI using bare tube or a flow conditioner (of various types) between the bend and the MPU 1200. Existing integration formula used. Table taken from [13].

	Single Elbow		Elbows Out		Elbows In	
	0	90	0	90	0	90
<b>Bare at 10D</b>	0.14	0.29	-1.02	-1.22	-0.18	-0.52
<b>Bare at 20D</b>	0.03	0.04	0.48	0.12	-0.10	0.10
<b>19 Tube</b>	0.33	0.42	0.09	-0.11	0.14	0.10
<b>Vortab</b>	0.05	0.02	-0.19	-0.19	-0.12	-0.09
<b>Nova 50E</b>	0.02	0.02	-0.42	-0.64	-0.18	-0.14
<b>Nova 50E @ 3D</b>	-0.05	0.15	-0.38	-0.69	-0.17	-0.16
<b>GFC</b>	0.24	0.15	-0.13	-0.11	0.06	0.08

Table 2 Same as Table 1 except that the candidate new integration model is used through postprocessing of the experimental data.

	Single Elbow		Elbows Out		Elbows In	
	0	90	0	90	0	90
<b>Bare at 10D</b>	0.29	0.30	0.35	0.22	-0.04	0.08
<b>Bare at 20D</b>	0.08	0.06	0.20	0.11	0.20	0.30
<b>19 Tube</b>	0.31	0.38	-0.13	0.10	0.13	0.10
<b>Vortab</b>	0.07	0.01	0.10	0.12	-0.08	-0.03
<b>Nova 50E</b>	0.01	-0.01	-0.27	-0.23	-0.24	-0.18
<b>Nova 50E @ 3D</b>	-0.02	0.15	-0.22	-0.23	-0.26	-0.24
<b>GFC</b>	0.25	0.14	-0.12	-0.09	0.04	0.08

Table 3 Same as Table 1 except that the candidate new integration model is used through postprocessing of the experimental data and that the numbers are relative to the reference meter at SWRI and not relative to the baseline tests.

	Single Elbow		Elbows Out		Elbows In	
	0	90	0	90	0	90
<b>Bare at 10D</b>	0.14	0.15	0.20	0.07	-0.19	-0.07
<b>Bare at 20D</b>	-0.08	-0.09	0.05	-0.04	0.05	0.15
<b>19 Tube</b>	0.15	0.21	-0.29	-0.06	-0.03	-0.06
<b>Vortab</b>	-0.15	-0.21	-0.13	-0.11	-0.30	-0.26
<b>Nova 50E</b>	0.03	0.01	-0.25	-0.21	-0.22	-0.16
<b>Nova 50E @ 3D</b>	0.16	0.33	-0.04	-0.05	-0.08	-0.06
<b>GFC</b>	0.15	0.04	-0.22	-0.18	-0.05	-0.01

without flow conditioner between the bend and the flow meter. It can be seen that there is a span of about 2 % between the various curves. In addition, the linearity of the individual curves is not good at low flow velocities. In Fig. 10, the similar deviation from reference has been shown when postprocessing the same data set using the new candidate integration method. It can be seen that all curves now are well within  $\pm 0.5$  % deviation from the reference meter. This indicates that the asymmetry model for the transversal flow components, which is a part of the candidate new integration model, represents a better performance of the MPU

1200 downstream bend configurations. It should be noted that the results from the K-Lab and the SWRI - tests have not been used in the development of the candidate integration method.

The results of the tests of the MPU 1200 meter have been summarized by Grimley [13] in Table 1. Each number in this table represents a flow weighted mean error for a specific installation of the meter with or without flow conditioner. The numbers are given relative to the baseline measurements. In Table 2, similar numbers are calculated for the candidate new integration model. It is seen that generally, the flow weighted mean errors are reduced. In Table 3, the flow weighted mean error is shown when compared to the reference measurements at SWRI (and not to the baseline measurements). It is seen that the highest deviation from reference is 0.33 %.

The flow tests at K-Lab of a 6" MPU 1200 and at SWRI of a 12" MPU 1200 have both shown that the MPU 1200 is less sensitive to installation effects with the candidate new integration method than with the existing integration method. At SWRI, the deviation from reference measurement in the installation tests was less than 0.5 % in all tests. At K-Lab, the deviation was larger. In both tests, the span in deviation between the various installation tests was reduced by using the candidate model instead of the existing integration model.

#### **4. METERING OF WET GAS**

As a part of the JIP, the MPU 1200 ultrasonic gas flow meter is being further developed to measure natural gas flow that contains liquid phase contaminants. These liquids contaminants may be either condensate, water, or chemical treatments injected into a pipeline. Up to 5% liquid (by rate, cf. Section 4.1) is often used as tentative maximum wetness figure for such wet gas flow. A 6" wet gas test meter using 3 acoustic paths has been developed by KOS and CMR and is currently being tested in wet gas flow. The first objective is to measure the gas volume flow rate, in spite of liquid contaminants being present, and without knowing the liquid volume fraction. Possibilities for measurement of the liquid volume fraction using ultrasonic techniques are also addressed in the project (but are not reported here). As a basis for the meter development, experimental and theoretical studies have been conducted, addressing (among others) (a) an uncertainty analysis of wet gas USMs, (b) the influence of wet gas (liquid droplets, liquid film, etc.) on the transmitted and scattered sound field (such as sound velocity, sound attenuation, scattering level, transducer directivity, etc.), and (c) chemical resistance of the transducers. Selected results from this ongoing work are presented in the following.

## 4.1 Uncertainty analysis

**Background.** For ultrasonic metering of the gas volume flow rate, a number of factors due to the liquid contaminants in the gas influence on the uncertainty budget of the ultrasonic meter, such as:

- (A) Uncertainty of the **gas area** ( $A_g$ ), i.e. the cross-sectional area occupied by the gas phase in the meter body. This is determined by the uncertainty of the liquid hold-up.
- (B) Possible build-up of liquid in the transducer ports, causing an acoustic bridge between the transducers and the steel meter body ("**cross-talk**"), dependent on the self-draining capacity of the transducer ports. An increased level of ultrasound propagating in the meter body acts as noise, causing a reduced signal-to-noise ratio (SNR), which contributes to increase the uncertainty of the transit time determination (relative to in dry gas).
- (C) Reduced signal level relative to the dry case, due to **excess sound attenuation** caused by (i) liquid droplets in the wet gas, and (ii) liquid present on the transducer faces. This results in a lower signal-to-noise ratio (SNR), which contributes to increase the uncertainty of the transit time determination (relative to in dry gas).
- (D) **Liquid present on the transducer faces**, which causes a shift in the measured transit times. Such liquid may also influence on the transducer directivity and thus the acoustic diffraction correction, causing a larger uncertainty of the transit time determination (relative to in dry gas).
- (E) **Path failure** due to possible flooding of the transducers (due to liquid slugs, high liquid volume fraction in horizontal stratified flow, etc.). A single path failure with subsequent meter recovery may not be dramatic, but a failure of all paths will be more serious.

These effects cause additional uncertainty due to wet gas, relative to the uncertainty of the USM in dry gas.

**Uncertainty model.** In the "GERG project on ultrasonic flow meters" (1995-98) [2], a theoretical uncertainty model for multipath ultrasonic metering of dry gas has been developed, and implemented in a PC program, GARUSO Version 1.0 [14]. The procedure used for evaluating and expressing uncertainties is the procedure recommended by ISO in the "Guide" [15]. The uncertainty model takes into account an extensive set of factors that may contribute to the uncertainty of the ultrasonic measurement, such as the standard uncertainties of gas parameters, geometry parameters, a number of contributions to the measured transit times, and the integration technique. For more details, cf. refs. [14], [2].

Under the present project, the GARUSO uncertainty model has been extended to account for wet gas effects, where the "wet gas contributions" (A)-(D) addressed above have been modelled and built into the uncertainty model, in addition to the "dry gas contributions" referred to above.

It should be mentioned that the uncertainty model takes as a starting point that the meter does function and operate in the wet gas flow, i.e. that acoustic signals are detected on all paths (although the model accounts for low signal-to-noise ratio, SNR). Path failures due to flooding (point (E) above) are not accounted for in the uncertainty model. In practice, path failures may be treated in the meter e.g. by extrapolation procedures based on history and profile information.

**Wet gas metering, functional relationship.** In a dry gas situation, the average axial gas flow velocity over the pipe's cross-section (at pipe flow conditions),  $\bar{v}_g$ , and the axial gas volume flow rate (at pipe flow conditions),  $q_g^A$ , are given as

$$\bar{v}_g = \sum_{i=1}^N w_i \bar{v}_i, \quad (5)$$

$$q_g^A = \bar{v}_g A \quad (6)$$

respectively. Here,  $\bar{v}_i$  is the average axial gas flow velocity along the  $i$ th acoustic path, given by Eq. (2), and  $w_i$  is the integration weight factor of the  $i$ th path.  $N$  is the number of acoustic paths, and  $A$  is the pipe's inner cross-sectional area.

In a wet gas situation, the axial volume flow rate of the gas phase (at pipe flow conditions) is given as

$$q_g = \bar{v}_g A_g \quad (7)$$

where

$$A = A_g + A_l \quad (8)$$

and  $A_g$  and  $A_l$  are the portions of the pipe's cross sectional area which are occupied by the gas and liquid phases, respectively. In wet gas flow, the meter's integration method is here assumed to be the same as in dry gas. The volume flow rate measured by the USM is then

$$q_g^A = \bar{v}_g A = \bar{v}_g (A_g + A_l) = q_g \left( 1 + \frac{A_l}{A_g} \right) \approx q_g (1 + \phi_V), \quad \text{for } \phi_V \ll 1 \quad (9)$$

so that

$$q_g \cup q_g^A (1 - \phi_V) \quad (10)$$

Eq. (10) is the expression used in the USM to calculate the gas volume flow rate in wet gas from the measured transit times.

Here,  $\phi_V$  is the liquid volume fraction, which for a relatively homogeneous multiphase mixture (over the volume  $V$  inside the meter body) is approximately equal to the liquid hold-up, i.e.

$$\phi_V \approx \frac{V_l}{V_g + V_l} \cup \frac{A_l}{A_g + A_l} \approx \text{liquid hold-up}, \quad (11)$$

which is small in wet gas (i.e.  $\phi_V \ll 1$ ).  $V_g$  and  $V_l$  are the volumes which are occupied by the gas and liquid phases (at pipe flow conditions), respectively, in the volume  $V = V_g + V_l$  inside the meter body.

To avoid confusion, it should be noted that the "liquid volume fraction"  $\phi_V$  as defined here, is in general not equal to the "liquid rate fraction",  $\phi_q$ , defined as

$$\phi_q = \frac{q_l}{q_g + q_l} \quad (12)$$

where  $q_g$  and  $q_l$  are the volume flow rates of the gas and liquid phases (at pipe flow conditions), respectively.  $\phi_q$  is a quantity which is usually measured in connection with testing of multiphase flow meters (measured e.g. at the gas and liquid injection pipes, or after separation), and is sometimes (misleadingly) referred to as the "liquid volume fraction". The frequently used tentative maximum wetness figure of "5 % liquid" in wet gas flow usually refers to  $\phi_q$ , i.e.  $\phi_q < 0.05$ .

The two-way relationships between the  $\phi_V$  and  $\phi_q$  are

$$\phi_V = \left[ I + \frac{\bar{v}_\ell}{\bar{v}_g} \left( \frac{I}{\phi_q} - I \right) \right]^{-1}, \quad \phi_q = \left[ I + \frac{\bar{v}_g}{\bar{v}_\ell} \left( \frac{I}{\phi_V} - I \right) \right]^{-1}. \quad (13)$$

where  $\bar{v}_\ell$  is the average axial liquid flow velocity over the pipe's cross-section (at pipe flow conditions). Two special cases may be of interest. For (the hypothetical) case of no slip,

( $\bar{v}_\ell = \bar{v}_g$ ), one has  $\phi_V = \phi_q$ . For wet gas one has  $\phi_q \ll 1$  (since  $\phi_q < 0.05$ ), giving  $\phi_q$  (since  $\bar{v}_g \geq \bar{v}_\ell$ ). In this case the relationships (13) reduce to

$$\phi_V \approx \frac{\bar{v}_g}{\bar{v}_\ell} \phi_q \quad (14)$$

**Uncertainty analysis.** From Eq. (10), the relative expanded uncertainty of the gas volume flow rate,  $q_g$ , becomes

$\phi_V$  is thus in general larger than  $\phi_q$ , and may exceed 5 %. Since the slip ratio  $\bar{v}_g/\bar{v}_\ell$  is usually unknown,  $\phi_V$  can not easily be determined from  $\phi_q$ , but may have to be measured separately.

$$E_q = k \sqrt{(E_q^A)^2 + u^2(\hat{\phi}_V)} = k \sqrt{E_m^2 + E_I^2 + u^2(\hat{\phi}_V)} \quad (15)$$

Here,  $k$  is the coverage factor ( $k = 2$  for a 95 % confidence interval),  $E_q^A$  is the relative combined standard uncertainty of the estimate  $\hat{q}_g^A$ ,  $E_m$  is the relative combined standard "path uncertainty" of  $\hat{q}_g^A$  (accounting for propagation of standard uncertainties of the geometry parameters and transit time contributions),  $E_I$  is the relative combined standard "integration uncertainty" of  $\hat{q}_g^A$ , and  $u(\hat{\phi}_V)$  is the standard uncertainty of the estimate  $\hat{\phi}_V$  (representing the uncertainty in the measurement of  $A_x$  due to the uncertainty of the liquid volume fraction estimate).

Relatively comprehensive expressions for  $E_m$  and  $E_I$  are given in ref. [14] (derived for dry gas), and will not be repeated here. The same expressions can also be applied to the wet gas case. In case of wet gas, however,  $E_m$  becomes larger than in dry gas (especially at low flow velocities), as described in the following for the "wet gas contributions" (A)-(D) discussed above.

Possible increased cross-talk due to liquid build-up in the transducer ports (cf. (B)), contributes in  $E_q$  (15) through  $E_m$  (reduced SNR). Increased signal attenuation due to (i) liquid droplets in the gas, and (ii) liquid present on the transducer faces (cf. (C)) also contributes through  $E_m$  (reduced SNR). Shift in measured transit times and changed diffraction correction due to liquid present on the transducer fronts (cf. (D)) contribute through  $E_m$  as well. The uncertainty of the gas area  $A_g$  (cf. (A)) contributes through the term  $u(\phi_V)$ . Due to space limitations, the details of this analysis will not be given here.

Results. Fig. 11 shows an example of a calculated relative expanded uncertainty,  $E_q$ , for a multi-path USM, plotted as a function of the average axial gas flow velocity. The three different curves (a), (b) and (c) are explained in the figure text. The figure demonstrates some characteristic and important results predicted by the uncertainty model, for the "excess uncertainty" due to wet gas relative to the "dry gas baseline uncertainty", (a) (which is taken to be a tentative but typical example).

The "wet gas contributions" (B) and (C) to the USM uncertainty seem to be most influential at low gas flow velocities, below about 5 m/s, cf. curve (b). The reason is that these contributions essentially cause a reduced signal-to-noise ratio SNR, where the noise is here modelled as incoherent (a random effect). Random effects do not cancel in the transit time difference,  $t_{1i} - t_{2i}$

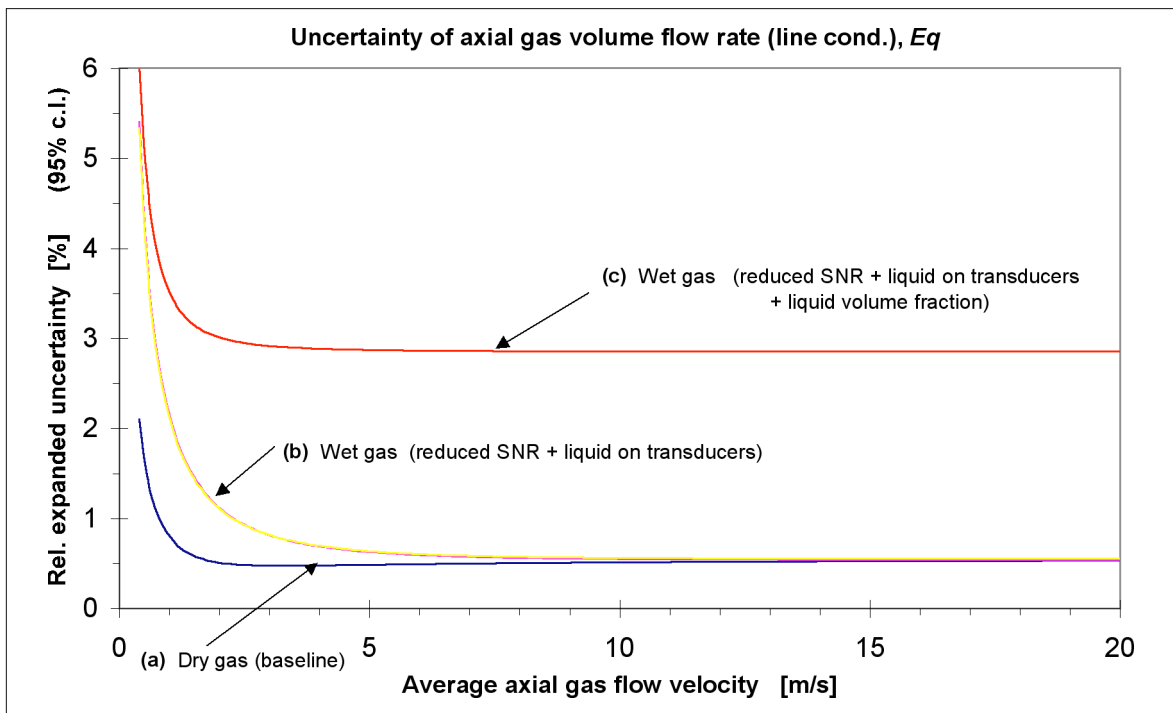


Fig. 11 Example of calculated relative expanded uncertainty,  $E_q$ , for a multipath USM, calculated using the GARUSO uncertainty model. (a) Dry gas operation (baseline example); (b) Wet gas operation (effects of increased cross-talk and sound attenuation (reduced SNR), and a 0.5 mm liquid "film" on the transducer faces); (c) Same as (b), but with additional uncertainty due to the unknown liquid volume fraction  $f_V$  (assumed here to lie in the range 0-5 %). A "blind wetness correction" approach (using  $f_V = 2.5$  %) is used.

of Eq. (2), and therefore become increasingly important at low flow velocities. (In the present example the SNR is taken to be 40 dB in dry gas, and 10 dB in wet gas, corresponding to extra transit time (standard) uncertainties of 11 ns and 360 ns, respectively.)

With respect to the "wet gas contribution" (D), a 0.5 mm liquid "film" at the transducer faces has been considered in the present example. The influence on the detected transit time is here (somewhat simplified) modelled as a systematic effect, which to a large degree is cancelled in the meter (cf. Eq. (2)). The contribution to the USM uncertainty due to a 0.5 mm liquid film is thus relatively small in the present model, of the order of 0.1 %.

The "wet gas contribution" (A),  $u(\hat{\phi}_V)$ , is invariant to the flow velocity, and as long as this uncertainty contribution is larger than  $\sqrt{E_m^2 + E_t^2}$  (which may often be the case), it contributes essentially as a constant shift of the uncertainty curve, except at the very low gas flow velocities. In the present example, the liquid volume fraction  $\phi_V$  is not known, but is assumed to be in the range 0-5 %, and a "blind" estimate  $\hat{\phi} = 2.5$  % has been used ("blind wetness correction")<sup>2</sup>. The standard uncertainty of the liquid volume fraction is thus taken as  $u(\hat{\phi}) = 2.5\% / \sqrt{3} = 1.4\%$ .

A key result from this uncertainty investigation is the following: If the liquid volume fraction is known to be less than 5 % (for instance), a relative expanded uncertainty at a level of 3 % should be a relevant perspective for USMs, by using the "blind wetness correction" approach (i.e. without knowing the actual liquid volume fraction). If the liquid volume fraction was known to be less than 1% (for instance), the relative expanded uncertainty in wet gas would be significantly lower (the uncertainty model predicts 0.8 % if the corresponding "dry gas baseline relative expanded uncertainty" was 0.5 %).

If a better estimate for the liquid volume fraction was available than in the "blind wetness correction" approach used above, the expanded uncertainty of the gas volume flow rate could be correspondingly reduced. Such results provide interesting perspectives and potentials for the use of USM in wet gas applications.

## 4.2 Influence of wet gas on sound velocity and attenuation

**Background and motivation.** Liquid contaminants in the gas may influence significantly on the sound propagating through the gas/liquid medium. Such effects are

- Scattering of ultrasound due to liquid droplets in the flow (gas-liquid aerosol, or mist),
- Increased sound attenuation (excess attenuation), due to sound scattering in the mist flow, and by liquid present on (flowing over) the transducer faces,
- Lowering of the sound velocity, due to sound scattering in the mist flow.

<sup>2</sup> By "blind wetness correction" it is here meant that in lack of knowledge (measurement) of the liquid volume fraction  $\phi$ , but by a tentative knowledge of the maximum value for  $\phi_V$ , one takes the mid value in the  $\phi_V$  interval as the estimate of  $\phi_V$ . The standard uncertainty of this estimate is then calculated using a type B evaluation of uncertainty, and assuming a rectangular probability distribution for the variation of  $\phi_V$  in the  $\phi_V$  interval [ISO, 1995].

These effects are dependent on a number of parameters, such as pressure, temperature, volume fraction, droplet size distribution, gas/liquid quality, flow velocity and the USM signal frequency. Pressures up to 200 bar and temperatures in the range from -20 to 100 °C (or more) may be relevant. The liquid volume fraction may exceed 5% (cf. Section 4.1). Very limited information about typical droplet size distributions in real wet gas flow is available; - here the range 0.5 - 1000  $\mu\text{m}$  has been considered. (For application at separator outlets with demister filters, more narrow ranges may be relevant.) Signal frequencies between 100 and 200 kHz are relevant for USMs.

The investigation of these effects, and their influence on USM operation, is of interest for several reasons. Increased sound attenuation is important for USM operation, since it leads to a reduced signal-to-noise ratio (SNR), which again causes larger transit time uncertainty, and thus larger USM uncertainty. In dramatic cases, it may cause loss of acoustic path(s). A changed sound velocity, however, is not dramatic for traditional USM operation, since USMs are practically insensitive to changes in the sound velocity. On the other hand, changes in sound attenuation, sound velocity and the scattering level, - and the variation of such changes from path to path, may provide useful information about the wet gas medium. A parameter which is of particular interest in this context is the liquid volume fraction,  $\phi_V$ . If online estimation of  $\phi_V$  were available, that would provide possibilities to reduce the uncertainty in wet gas metering, as discussed in Section 4.1.

**Basic approach.** In the present section, selected attempts to investigate such influences of wet gas on the sound propagation are reported. An approach is used where one seeks improved physical insight into the mechanisms causing the effects discussed above. A combination of theoretical modelling and laboratory experiments is used for this purpose. In the laboratory experiments one seeks to test and verify candidate theoretical models. A sufficiently proven model can be used to investigate the effects of parameters such as pressure, temperature, gas/liquid quality, signal frequency, liquid volume fraction, droplet diameter, etc., on the sound propagation through the wet gas medium.

Here, the discussion is confined to the investigation of changes in sound attenuation and sound velocity due to gas-liquid aerosol (mist). Influences on the level of scattered ultrasound in gas-liquid aerosol are not discussed here.

**Modelling.** From the general literature on sound propagation in emulsions (liquid droplets mixed in another liquid) and gas-liquid aerosols (liquid droplets in gas), many candidate models for changes in sound velocity and attenuation in such two-phase media are available. A number of relevant models have been implemented, compared and evaluated with respect to sound propagation in gas-liquid aerosols, including effective medium models, coupled-phase models and multiple scattering models [16], [17]. These are sound propagation models used in other areas (media) and applications, which to varying extent have been verified within those areas. However, the present application of ultrasonic wet gas metering represents a new area for such models (with respect to frequency range, pressure range, temperature range, liquid volume fraction range, gas/liquid types), and the validity and applicability of the models within this area is not established. For the gas/liquid aerosols in question for wet gas metering, there is observed a significant deviation in results using the various types of models [17].

In the present paper, results using the Waterman-Truett multiple scattering model with Allegra-Hawley scattering coefficients are shown [18], [19]. This model takes into account the thermal and viscous boundary layer effects close to the droplet surface (inside and outside of the droplet), the generation of sound waves inside and outside of the droplets, and higher order oscillation modes (monopole, dipole, quadropole, etc.). The model is potentially applicable at all frequencies of relevance, from very long to very short acoustic wavelengths relative to the droplet diameter. This includes droplet resonances appearing when the acoustic wavelength is of the order of the droplet diameter.

**Experiments.** In the laboratory experiments reported here, an aerosol (mist) of olive oil in air, at 1 atm. and room temperature (23 °C), has been used for comparison with the Waterman-Truett multiple scattering model. The mist is generated using a TSI 9306 aerosol generator. The theory predicts increasing attenuation and increasing change in sound velocity for the small droplets (with largest attenuation for 0.1-1.0 mm droplets, and largest sound velocity changes for sub-mm droplets). For model testing it might then at first glance seem favourable to use droplets in the 0.1-1.0 mm range, in order to obtain larger measurable effects for the changes in sound attenuation and velocity. However, the very small droplets carry a very small portion of the total volume, so the liquid volume fraction would then be very low (sub-ppm), and the effects also relatively small. Hence, the effects of liquid droplets with a size distribution in the range of a few mm have been investigated here.

A Malvern Spraytec RTS 5000 laser diffraction system has been used for the reference measurements of droplet size distribution and liquid volume fraction  $\phi_V$ . The Sauter mean diameter of the size distribution used here is approximately 2 mm, and the liquid volume fraction,  $\phi_V$ , is approximately 9 ppm.

Olive oil is used to reduce evaporation effects, which for the droplet sizes in question would be significant if another liquid such as e.g. water was used. The theory indicates that the results do not vary much with liquid type, so the use of olive oil for model testing should be relevant. (Similar experiments with other liquid types such as water and Exxsol D100 have also been made, but are not reported here.)

Changes in temperature and the relative humidity (RH) were monitored during the acoustic measurements, and used to correct the measurements in the aerosol (since temperature and RH also influences on the sound attenuation and velocity).

**Results.** Fig. 12 shows a comparison of experimental results (markers) and modelling results (curves) for the change in sound velocity (upper plot) and the increased sound attenuation (lower plot) caused by liquid droplets in the olive-oil-in-air aerosol, plotted as a function of the liquid volume fraction,  $\phi_V$  (up to 100 ppm = 0.01 %). The changes are shown relative to the corresponding dry gas case (air), at the same pressure, temperature, and relative humidity (RH). Three measurement series are shown, nos. 1, 2 and 3, taken over a period of more than a year. The most recent series, no. 3, is believed to be the most accurate of these, since better temperature and relative humidity measurements were available for this series, enabling a better correction for temperature and RH effects. Theoretical predictions are given for droplet diameters 0.5, 1, 2, 5, 10 and 50  $\mu\text{m}$ .

For the excess sound attenuation, the agreement between the experimental results and the theory is considered to be relatively good, especially for the Series 3 measurements, which fall almost exactly on the 2 mm curve predicted by the theory. The series 1 and 2 measurements are also relatively close to the theoretical prediction, but fall more in-between the 1 and 2 mm curves. Note the increased sound attenuation which is predicted by the theory for large liquid volume fractions, and for small droplets. (For even smaller droplets than about 0.1 - 1.0 mm, the attenuation will decrease.)

With respect to sound velocity effects, precision measurement is more demanding than for the sound attenuation, due to a relatively small change in sound velocity which is observed for the liquid volume fraction and droplet sizes investigated here (which of course is an interesting result in itself). However, a reduction of the sound velocity due to the liquid droplets is measured in most cases, although the spread in measurement data is significant. In average, the series 3 data fall relatively close to the 2 mm curve. Note the increased reduction in sound velocity which is predicted by the theory for large liquid volume fractions, and for small droplets.

In Fig. 13, the Waterman-Truell model has been used to investigate the effect of increased gas pressure on the sound propagation in mist. The pressure is raised to 50 bar, while the temperature is kept constant (23 °C, as in Fig. 12). The fluids have been changed, from olive-oil-droplets-in-air to Exxsol-D80-droplets-in-methane (which is more relevant for wet gas applications). This is done since the theory predicts (not shown here) that the effect of pressure on sound attenuation and velocity is considerably larger than the temperature and fluid type effects. Droplet diameters in the range 1 - 1000 nm are simulated. Note that in Fig. 13 liquid volume fractions up to 10 % = 100000 ppm are shown, to cover a larger range than in Fig. 12. As a consequence, significantly larger scales are used in Fig. 13 for the predicted changes of sound velocity and attenuation.

A comparison of Figs. 12 and 13 reveals that the theoretical model predicts a dramatic influence of gas pressure on the excess sound attenuation and on the change in sound velocity of the gas-liquid aerosol. Increasing pressure reduces the excess attenuation and the change in sound velocity, due to reduced characteristic acoustic impedance between the gas and the liquid droplets at elevated pressures. Very large effects are predicted in some parameter ranges. For example,

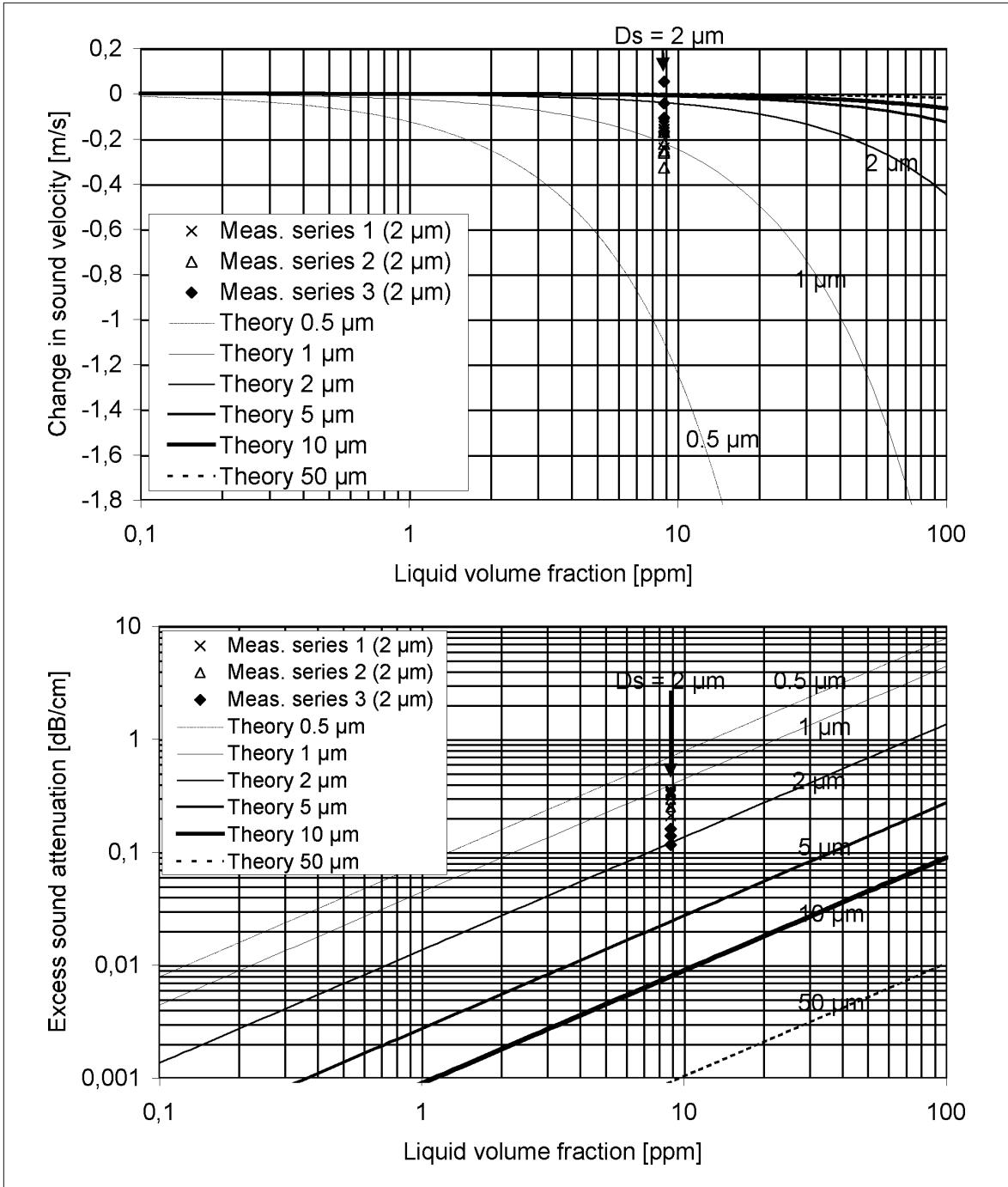


Fig. 12 Comparison of experimental results (markers) and modelling results (curves) for the change in sound velocity and attenuation caused by the liquid droplets in a gas-liquid aerosol, plotted as a function of the liquid volume fraction,  $\phi_v$ . Static laboratory measurements with mist of 2 mm diameter droplets of olive oil in air, at 1 atm. and 23 °C.

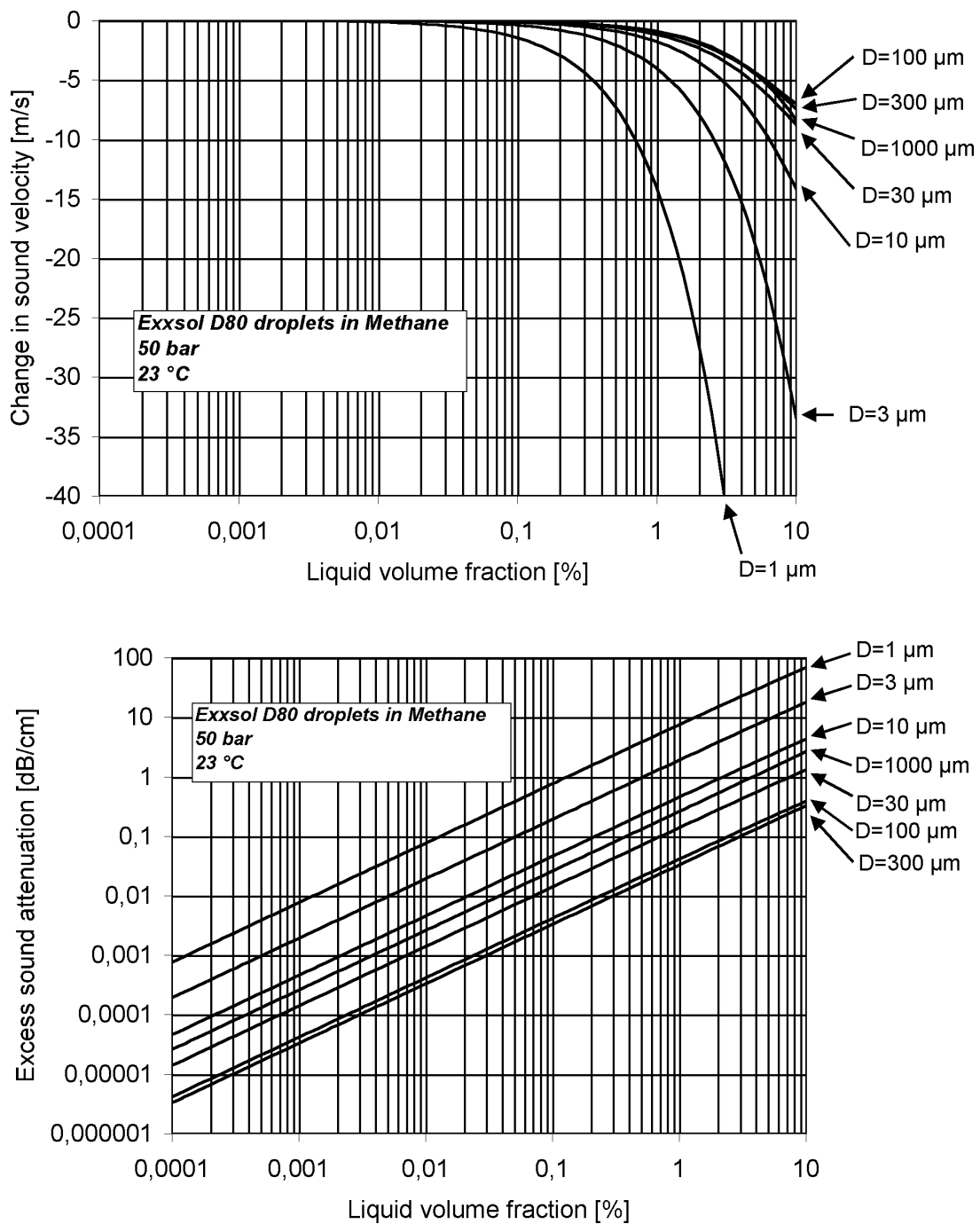


Fig. 13 Predicted change in sound velocity and attenuation using the Waterman and Truell multiple scattering model. Mist of Exxsol D80 droplets in methane, at 50 bar and 23 °C.

the excess attenuation of a 10 ppm (0.001 %) and 1 mm diameter aerosol at 1 atm. is predicted to be about 0.45 dB/cm, or 45 dB/m, which is relatively large (cf. Fig 12). At 50 bar, the excess attenuation of this aerosol is predicted to be about 0.01 dB/cm, or 1 dB/m, which is negligible. Such results have significant consequences for operation of USMs in wet gas mist flow. As mentioned above, the influence of the gas/liquid qualities and the temperature are predicted to be negligible in comparison.

It is interesting to note from these simulation results that small droplets, in the range below 1 mm, which "carry" a low liquid volume fraction, are predicted to cause the largest change in sound velocity, and the largest sound attenuation. Large droplets "carry" a higher liquid volume fraction, but are predicted to cause the least change in sound velocity, and the lowest sound attenuation.

It should be noted that the measurements shown here are results from an ongoing project, and represent preliminary results. Experimental testing and verification of theoretical models for sound attenuation and velocity in gas-liquid aerosols is indeed a challenging work, due to the relatively small effects one experiences in the parameter ranges where controlled measurements can be set up at a reasonable cost. In other parameter ranges, where the effects are larger and potentially more easily measured, experiments under controlled conditions are far more difficult to set up.

So far one may conclude that the experimental results are in fair agreement with the candidate theoretical model for sound attenuation and velocity which is investigated and used here, and support this theory. However, more measurement data points (over a larger range of liquid volume fraction, droplet diameter, pressure, temperature, etc.) are necessary to conclude on the validity of the theory.

#### **4.3 Hardware development and flow testing**

A 6" wet gas test meter using 3 acoustic paths has been developed by Kongsberg Metering and CMR, and is currently being tested in wet gas flow (natural gas and Stoddard solvent) at CEESI in Colorado, USA. Preliminary test data were obtained shortly before the deadline of this paper. The results are encouraging, but are insufficient for presentation at the time of writing. The first objective is to measure the gas volume flow rate, in spite of liquid contaminants being present, and without knowing the liquid volume fraction. Possibilities for measurement of the liquid volume fraction using ultrasonic techniques are also addressed in the project.

## **5. CONCLUSIONS**

Results and progress from an ongoing R&D program related to the Kongsberg Metering MPU 1200 multipath ultrasonic gas flow meter have been presented. Three main topics are addressed: (1) calculation of gas density from the measured sound velocity, (2) operation at complex installation conditions (with disturbed flow velocity profiles), and (3) measurement of wet gas.

An algorithm for calculation of the gas density on basis of the sound velocity measurement output from the USM, and additional measurements of pressure and temperature, has been developed and implemented in a 6" MPU 1200. The method has been tested at Statoil's flow laboratory K-Lab, Norway (April 1999), with deviation from the reference density measurements of typically  $\pm 0.1$  %. A sensitivity analysis of the method has been carried out, indicating that more generally, the relative expanded uncertainty of the current ultrasonic density measurement method may be expected to lie in the 0.5-1 % range (within a 95 % conf. interval). However, solutions are identified which in the future may further improve this uncertainty number.

An improved integration algorithm for more robust and accurate operation of the MPU 1200 at complex installation conditions has been developed, and is to be implemented in the meter. The improvements involve only software changes in the USM, so that existing meter installations can be easily upgraded. The method has been flow tested (by post-processing) for a 6" meter (June 1999) at K-Lab, Norway, and for a 12" meter on recent (August 1999) flow test data provided by Southwest Research Institute, Texas. Significant reductions of the meter uncertainty are demonstrated in both tests, including improved robustness with respect to relevant bend configurations.

Work is underway to upgrade the MPU 1200 technology for measurement of natural gas flow that contains liquid phase contaminants (wet gas). A 3-path 6" test meter is currently being flow tested in wet natural gas at CEESI, Colorado. The GARUSO uncertainty model for ultrasonic gas meters has been further developed and used to account for wet gas effects. The influence of wet gas (liquid droplets, liquid film, etc.) on sound transmission and scattering is investigated through experimental and modelling work. Changes in sound attenuation, sound velocity and the scattering level, - and the variation of such changes from path to path, are parameters of interest for design and operation of USMs in wet gas, and may potentially provide useful information about the wet gas medium.

## **ACKNOWLEDGEMENTS**

The authors wish to thank T. A. Grimley, Southwest Research Institute, Texas, and the Gas Research Institute, Chicago, for giving permission to use the experimental flow test data shown in Table 1 and Fig. 9, which were originally used as a basis for ref. [13]. Also they gave permission to use new (CMR - processed) results in Table 2 and 3, and Fig. 10, based on these experimental flow test data.

In addition to the authors, Andrew C. Baker, Hilde Furset, Atle A. Johannessen, Øyvind Nesse, Tore Tjomsland, Frode Johnsen and Anders Hallanger, CMR, have contributed to the work presented here.

The work has been carried out in a Joint Industry Programme between Christian Michelsen Research, Kongsberg Metering, Statoil, Norsk Hydro and Phillips Petroleum Company Norway, and has been supported by The Research Council of Norway.

## REFERENCES

- [1] **AGA-9:** "Measurement of gas by multipath ultrasonic meters". Transmission Measurement Committee, Report no. 9, American Gas Association (A.G.A.) (June 1998).
- [2] **Wild, K.:** "A European collaboration to evaluate the application of multi-path ultrasonic gas flow meters", In: Proc. of 4<sup>th</sup> International Symposium on Fluid Flow Measurement, Denver, Colorado, USA, June 28-30, 1999.
- [3] **Kristensen, B. D., Lofseik, C. and Frøysa, K.-E.:** "An overview of projects related to the KOS FMU 700 6 path ultrasonic gas flow meter", A.G.A.-98 Operations Conference, Seattle, Washington, May 17-19, 1998.
- [4] **Sakariassen, R.:** "Why we use ultrasonic gas flow meters", Proc. of the 13<sup>th</sup> North Sea Flow Measurement Workshop, Lillehammer, Norway, 1995
- [5] **Watson, J.:** "A review of important gas flow measurement parameters", Practical Developments in Gas Flow Metering. One Day Seminar – 7 April 1998, National Engineering Laboratory, East Kilbride, UK.
- [6] **Beecroft, D.:** "Is a wet gas (multiphase) mass flow meter just a pipe dream?", Proc. of the 16<sup>th</sup> North Sea Flow Measurement Workshop, Gleneagles Hotel, Perthshire, Scotland, 26-29 October 1998.
- [7] **Tjomsland, T. and Frøysa, K.-E.:** "Calculation of natural gas density from sound velocity. Description of theory and algorithms implemented in the DeCa code," CMR report no. CMR-97-F10015, Christian Michelsen Research AS, Bergen (June 1997). (Confidential.)
- [8] **Starling, K. E. and Savidge, J.:** "Compressibility factors of natural gas and other related hydrocarbon gases", A.G.A. Transmission Measurement Committee, Report No. 8 (AGA-8-94); American Gas Association; 2nd ed., November 1992; 2nd printing (July 1994).
- [9] **Frøysa, K.-E., Furset, H. and Baker, A. C.:** "Density and ultrasonic velocity calculations for natural gas. Sensitivity analysis of DeCa," CMR report no. CMR-98-F10002, Christian Michelsen Research AS, Bergen (December 1998). (Confidential.)
- [10] **Frøysa, K.-E. and Lunde, P.:** "VESUM - Version 1.0. Uncertainty model for velocity of sound measurements for the 6-path FMU 700 ultrasonic gas flow meter," CMR report no. CMR-98-F10001, Christian Michelsen Research AS, Bergen (December 1998). (Confidential.)
- [11] **Lygre, A., Johannessen, A. A., Dykesteen, E. and Norheim, R.:** "Performance test of a 6 path USM", Proc. of the 13<sup>th</sup> North Sea Flow Measurement Workshop, Lillehammer, Norway, 1995.

- [12] **Grimley, T. A.:** "12 inch ultrasonic meter verification testing at the MRF ", Proc. of the 4<sup>th</sup> International Symposium on Fluid Flow Measurement, Denver, Colorado, USA, June 28-30, 1999.
- [13] **Grimley, T.:** "Recent 12-inch ultrasonic meter testing at the MRF", Presented to the A.G.A. Gas Measurement Research Council, Seattle, Washington, September 14, 1999.
- [14] **Lunde, P., Frøysa, K.-E. and Vestrheim, M.:** "GARUSO - Version 1.0. Uncertainty model for multipath ultrasonic transit time gas flow meters". CMR Report No. CMR-97-F10014, Christian Michelsen Research AS, Bergen (August 1997).
- [15] **ISO,** "Guide to the expression of uncertainty in measurement. First edition". International Organization for Standardization, Genève, Switzerland (1995)
- [16] **Lunde, P., Frøysa, K.-E., Nesse, Ø., Vestrheim, M. and Midttveit, M.:** "Wet gas flow metering. Ultrasonic transit time methods. Basic Studies". CMR Report No. CMR-96-F10029, Christian Michelsen Research AS, Bergen (December 1996). (Confidential.)
- [17] **Frøysa, K.-E. and Lunde, P.:** "Comparison of simulation models for ultrasonic propagation in wet gas", In: Proc. of 22nd Scandinavian Symposium on Physical Acoustics, Ustaoset, 31 January - 3 February 1999, edited by U. K. Kristiansen, Scientific / Technical Report No. 429904, Norwegian University of Science and Technology, Dept. of Telecommunications, Acoustics (May 1999), pp. 11-12.
- [18] **Waterman, P. C. and Truell, R.:** "Multiple scattering of waves," J. Math. Phys. 2, 512-537 (1961).
- [19] **Allegra, J. R. and Hawley, S. A.:** "Attenuation of Sound in Suspensions and Emulsions: Theory and Experiments", J. Acoust. Soc. Am. 51, 1545-1564 (1972).



# INVESTIGATIONS REGARDING INSTALLATION EFFECTS FOR SMALL ULTRASONIC GAS FLOW METERING PACKAGES

*Geeuwke de Boer , Instromet Ultrasonics, Dordrecht, The Netherlands.  
Martin Kurth, Instromet International, Essen, Belgium.*

---

## 1. ABSTRACT

Ultrasonic gas flow meters for custody transfer measurement (accuracy better than 0.5%) have gained a rapid and increasing acceptance over the last few years. The most common applications are gas transmission and underground gas storage (UGS), due to the typical benefits of ultrasonic flow meters, such as no pressure drop, large turn down ratio and the bi-directional capability. Generally, this used to concentrate on the larger sized meters and installations (typically 10” and higher). An important contribution for the acceptance was the research regarding installation effects, which as a consequence, had mainly been focused on larger sized meters.

Based on trade-offs between the purchase price of an ultrasonic meter, operating costs, and total capital expenditure for a gas flow metering installation, it is anticipated that in the near future ultrasonic gas flow meters will also become a viable alternative for an increasing number of applications in smaller sized systems. The market has shown a specific interest in a package consisting of an ultrasonic meter and a flow conditioner. Also when a back-up meter or check meter is required a combination of an ultrasonic meter and a turbine meter would be an economical solution.

Therefore it was considered to be of interest to initiate a research project dedicated to installation effects and the effects of various flow conditioners, for a smaller size ultrasonic gas flow meter (6”), in particular in a package including a flow conditioner or a turbine meter. Results will be presented of a series of tests with different upstream conditions, performed at the “HDV Lintorf” test facility owned by Ruhrgas AG. Due to the fact that not all tests have been finished at the time of writing of this paper, the results are not yet complete and only the first sets of results will be presented in this paper.

As typical applications for smaller sized meters are found in stations measuring the gas flow from a high pressure transmission line to a lower pressure distribution network or to a large industrial consumer, solutions are suggested to avoid the potential ultrasonic noise problem due to pressure reduction by means of optimising station design for use of an ultrasonic gas flow meter.

## 2. INTRODUCTION

Prior to the introduction of high accuracy ultrasonic gas flow meters for custody transfer, between 1991 and 1994, Instromet carried out investigations of the behaviour of large size (20") USFM's using the high pressure test installation at Westerbork (NL). Between 1994 and 1995 Instromet also participated in a Joint Industrial Project (team members: Gas de France (F), Gasunie (NL), Ruhrgas (D), Instromet) for evaluation of a 12" UFM [Ref.1]. Many other investigations followed, mainly in US, Canada and Europe. In 1997 the Dutch Gasunie presented their long time experience at their border stations at the North Sea Work Shop (NSWS) [Ref.2].

Following the research in the application of large sized meters, ultrasonic gas flow meters for custody transfer measurement (accuracy better than 0.5%) have gained a rapid and increasing acceptance over the last few years. The most common applications are gas transmission and underground gas storage (UGS) because of the typical benefits of ultrasonic flow meters, such as no pressure drop, large turn down ratio and the bi-directional capability.

Currently, in gas flow applications in smaller line sizes (4" – 8") often orifices or turbine meters are found. Measuring with orifices has a long tradition but is limited in accuracy and rangeability and at high operating (maintenance, recompression) costs. It has to be recognised that, currently, in clean gas applications, a good quality turbine meter offers excellent accuracy for a reasonable price, however it is a mechanical device having moving parts that are subject to wear. Considering this, it is anticipated that in the near future ultrasonic gas flow meters will become a viable alternative for an increasing number of applications in smaller sized systems. In particular, an ultrasonic meter will pay off in small sized metering systems having specific requirements such as:

- Compact dimensions (limited straight upstream pipe length) and minimum weight
- Measuring gas which is not very clean
- Minimum maintenance (unmanned offshore installations)
- Reduced operating costs
- Bi-directional capability and low pressure drop
- Dual (redundant) measurement

In order to support the application of ultrasonic gas flow meters in smaller line sizes, Instromet decided in 1999 to start further research into the performance of smaller sizes of USFM's, by means of testing a 6" 3-path meter at the Ruhrgas AG research test facility in Lintorf (D). The objective was to investigate the effects due to velocity profiles resulting from different upstream conditions as well as effects of flow conditioners. Test conditions included fully developed turbulent flow profile (40 D straight upstream pipe as a minimum), downstream of a single bend and downstream of double bends out of plane, at various distances (10 D and 13 D), according to ISO 9951, tests with various models of the Spearman flow conditioner and tests downstream of a turbine meter.

### 2.1. Dual (redundant) metering applications.

Because of the interest in dual (redundant) metering in certain application areas, the test program included the evaluation of a package consisting of an ultrasonic meter and a turbine meter, although this may not be the most relevant for the North Sea area. and for offsho-

re applications. The objective was to investigate a package of an ultrasonic meter and a turbine that was expected to be the optimum combination. The assumption was that a turbine meter in front of an ultrasonic meter can act as sort of flow conditioner. It will definitely not be an ideal flow conditioner, meaning that the effect of the turbine meter with regard to the USM has to be accounted for. As long as the effect is stable and the whole package is calibrated to start with, this should be an option.

## **2.2. Application of flow conditioners.**

Specifically of interest for the North Sea area and for offshore applications is compact sized and minimum weight metering packages being either a single meter or a meter with flow conditioning devices. Regarding flow conditioners, an important feature of ultrasonic meters is the lack of an obstruction in the line and, as a consequence zero pressure drop. Therefore from the beginning, Instromet has not been very enthusiastic about the application of flow conditioners since it would give away these features. However in the market for smaller sized meters the zero pressure drop feature is not as important as it is for the large sized meters. As a consequence the market has shown an interest in using flow conditioners expecting improved accuracy or benefits in installations, for example shorter length of straight upstream piping.

Ideally a flow conditioner should help to restore – in the shortest possible pipe length - a distorted flow profile to the “natural” flow profile, being the fully developed turbulent flow profile, the shape of this profile is dependant of the actual Reynolds number and local wall roughness. This would ensure that a gas flow meter will not behave differently due to the presence of the flow conditioner nor that the position of the meter relative to the flow conditioner is critical.

However, immediately downstream of the flow conditioner the profile is even more distorted because of the presence of the flow conditioner itself, so it takes some length of pipe before this restoring of the flow profile becomes effective. Therefore, also a target was to evaluate possible concepts with a flow conditioner and the effectiveness of such, and investigate the effects due to velocity profiles under different upstream conditions: a fully developed turbulent flow profile (53D straight upstream pipe), downstream of a single bend and downstream of a double bend (out of plane), at 10D and 13D distance, with just an ultrasonic meter as well as including a flow conditioner. It should be noted that currently available flow conditioners have been designed to be used with orifice meters or turbine meters, none has been optimised for ultrasonic meters.

## **2.3. Design concepts with respect to ultrasonic noise.**

Having refined the technical possibilities of the UFM itself, there must be an assurance that the UFM will not be disturbed by ultrasonic noise generated by regulator valves. In take off stations where the pressure difference from the transmission line (50 – 85bar/ 700 – 1200psi) to the distribution line (15 – 40bar/ 200 – 550psi) can rise up to 70bar/ 1000psi, certain precautions have to be taken. Instromet has developed different type of silencers, which can be incorporated into the design of the measurement station to ensure the correct operation of the UFM. So in order to benefit to a maximum from the features of an ultrasonic gas flow meter, traditional station design concepts should not be used but instead some new design concepts should be adopted.

### 3. TEST METERS AND TEST FACILITY

The actual meter under test was a 6"/ DN150 ANSI#600 ultrasonic gas flow meter according to the 3-path Q.Sonic design. The main characteristics of this ultrasonic meter are summarised in the table below.

Model	Q.Sonic-3	
Paths	3	
AGA-9 compliant	Yes	
Accuracy	Better than 0.7%, after dry calibration	
Nominal diameter	DN150	6"
Inner diameter	154mm	6 1/16
Qmax	1600 m3/hr	55,000 ft3/hr
Qmin	80 m3/hr	2900 ft3/hr
Length of the meter	750mm	30"

For all tests the pressure tap was made on the UFM body and the temperature measuring point was directly downstream of the meter.

The turbine meter used upstream of the UFM was an Instromet meter type SMRI-X4X with built in flow conditioner allowing an upstream length of 2D only according to ISO 9951. The size was DN150/ 6" G650 rating. The length of this turbine meter is 3 diameters.

The tests are performed at the "HDV Lintorf", a test facility owned by Ruhrgas A.G., in Germany. A schematic drawing of this test facility is presented in figure 2. Figure 1 is a picture presenting a part of the test facility. 5 orifice metering runs, nominal diameter 8 inch, in parallel are used as references, each individually calibrated (traceable to the water test facility in Delft (NL)). The table below summarises the main characteristics of the test facility.

HDV Lintorf	min		max	
Flow range (actual)	100 m <sup>3</sup> /h	3,500 ft <sup>3</sup> /h	10000 m <sup>3</sup> /h	350,000 ft <sup>3</sup> /h
Pressure range	10 bar	140 psi	45 bar	650 psi
Temperature range	5 °C	41 °F	28 °C	83 °F
Medium	Natural gas			
References	5 orifice plates, $\beta = 0.66, 0.66, 0.44, 0.44, 0.23$			
Uncertainty	0.3 %			

## 4. TEST PROGRAMME

The first part of the test programme was performed from May 6, 1999 to June 21, 1999.

As a start a baseline calibration is performed. It assumed that using long (at least 40 diameters) straight upstream piping will result in a fully developed turbulent flow profile at the location of the ultrasonic meter. The turbine meter is installed 3D downstream of the ultrasonic meter, this test is considered to be the baseline for the turbine meter as well (ref. FIG. 5.).

In the same configuration some variations of flow conditioners, based on the Spearman design, are tested. The flow conditioners are installed at a distance of 5D or 13 D upstream of the ultrasonic meter (ref. FIG. 6.). The effect of the turbine meter regarding the flow profile is investigated by moving the turbine meter to a position immediately upstream of the ultrasonic meter (ref. FIG. 7.).

After this the ultrasonic meter is moved to a location 10 D and 13 D downstream of a 90 degree elbow. In this position the ultrasonic meter is calibrated with and without a flow conditioner. The turbine meter is again in a position 3 D downstream of the ultrasonic meter (ref. FIG. 8, 9.).

Next the turbine meter is moved to a position 3 D downstream from the elbow. The ultrasonic meter is installed immediately downstream of the turbine meter, so effectively 6 D downstream of the elbow (ref. FIG. 10.).

The following test is with two elbows out of plane. The same procedure as before is repeated, first the ultrasonic meter 10 D and 13 D downstream of the disturbance, then with a flow conditioner 5 D before the meter and 5 D from the disturbance. The turbine meter location is with these tests again 3 D downstream of the ultrasonic meter (ref. FIG. 11, 12.). Then the turbine meter is moved to a position 3 D downstream from the double elbow out of plane. The ultrasonic meter is installed immediately downstream of the turbine meter, so effectively 6 D downstream of the double elbow out of plane (ref. FIG. 13.).

A repeat of the straight pipe configuration concludes the first part of the test program.

The test program was continued from September 20, 1999 with some more calibrations in the straight pipe configuration, first a repeat of the test with undisturbed flow, followed by some more tests with flow conditioner variations (ref. FIG. 5., FIG. 14. and FIG. 6.). With the ultrasonic meter immediately after the turbine meter a test was done simulating a turbine meter, suffering from wear (high bearing resistance) (ref. FIG. 7.).

The tests of the first series are summarised in the following table, reference is made to the figure numbers with the drawings that represent the different piping arrangements.

Upstream configuration.	distance	flow cond	distance	first meter in line	distance	second meter in line	NR	FIG
straight pipe			53D	UFM	3D	TRM	1	5
straight pipe	48D	#5A	5D	UFM	3D	TRM	2	6
straight pipe	40D	#5A	13D	UFM	3D	TRM	3	6
straight pipe	48D	#7B	5D	UFM	3D	TRM	4	6
straight pipe	48D	#6B	5D	UFM	3D	TRM	5	6
straight pipe			53D	TRM	0D	UFM	7	7
straight pipe			53D	TRM	0D	UFM	8	7
single bend			10D	UFM	3D	TRM	9	8
single bend			13D	UFM	3D	TRM	10	8
single bend	5D	#5A	5D	UFM	3D	TRM	12	9
single bend			3D	TRM	0D	UFM	13	10
double bend			10D	UFM	3D	TRM	14	11
double bend			13D	UFM	3D	TRM	15	11
double bend	5D	#5A	5D	UFM	3D	TRM	16	12
double bend			3D	TRM	0D	UFM	17	13
straight pipe			44D	UFM	3D	TRM	18	5

The following table summarises the tests done after the work was continued.

Upstream configuration.	distance	flow cond	Distance	first meter in line	distance	second meter in line	NR	FIG
straight pipe			44D	UFM	3D	TRM	19	5
straight pipe		#5	40D	UFM	3D	TRM	20	14
straight pipe		#7C	5D	UFM	3D	TRM	21	6
straight pipe		#6C	5D	UFM	3D	TRM	22	6
straight pipe			44D	TRM	0D	UFM	23	7
straight pipe turbine meter with friction			44D	TRM	0D	UFM	24	7

## 5. BASE LINE TEST CALIBRATIONS

Figure 15. presents a graph of the results of the calibrations with long straight upstream piping, being numbers 1, 18 and 19 from the tables before, identified as “basis 1”, “basis end” and “basis repeat”. Between “basis 1” and “basis end” there is a small shift, “basis repeat” is in close agreement with “basis end”. The results are presented relative to a baseline, being the average error curve that is calculated from “basis1” and “basis end”. All the following results are as well presented as deviations relative to the same baseline

## 6. TEST RESULTS WITH FLOW CONDITIONER

The flow conditioner used in these tests is a perforated plate according to the “Spearman” design, in particular, the mark IV model having 4 holes in the center of the plate. This flow conditioner was selected because of the fact that the published test results look promising and the design may be used without paying royalties or licence fee’s. The design parameters such as the pitch circles and hole diameters are all defined relative to the inner diameter of the pipe. In order to be flexible and to have the possibility to investigate the sensitivity to mismatching the flow conditioner design to the pipe schedule (inner diameter), 3 different variations were manufactured, according to inner pipe diameters of 146 mm, 150 mm and 154 mm. The variations are identified as #5, #6 and #7. Later-on an attempt is made to tune the original designs by making some modifications, identified by appending the capital A, B etc. to the identification.

It is recognised that in order to obtain a reasonable performance, a perforated plate type flow conditioner requires some distance (3D to 5D) between the source of the profile distortion and the plate and as well some distance (5D to 10D) between the flow meter and the perforated plate.

Taking this into account, the “ideal” flow conditioner should not introduce a deviation compared to the baseline calibration of the flow meter, not have an effect that is dependant of the distance between the flow meter and the flow conditioner and not have an effect that is velocity dependant.

The results of the calibrations with long straight upstream pipe are presented in the graph in Fig. 16. The best performing flow conditioner is #5, although at 5D distance the meter error curve is shifted by about 0.5 %, reducing to 0.4% and 0.2 % with longer distance (13D and 40D). However it is questionable whether the 0.2% deviation should be considered to have any significance.

The graph in Fig. 17. shows the results of the calibrations in ideal flow conditions and in distorted flow. The graph compares the results with flow conditioner #5, for long straight upstream pipe, downstream of an 90 degree elbow and downstream of double elbows out of plane, identified as “#5 5D”, “90 10D #5 5D”, and “RK 10D #5 5D”. The flow conditioner is positioned for all the three graphs 5D upstream of the ultrasonic meter, in case of distorted flow at 5 D distance from the source of the distortion.

It appears that this flow conditioner performs reasonable well to reduce the effects of distorted flow profiles when measuring the gas flow with the ultrasonic meter, provided that the meter is calibrated with this flow conditioner.

## 7. TEST RESULTS WITH TURBINE METER IN FRONT

In order to evaluate the practical and economical use, an Instromet turbine meter with a patented built-in flow conditioner, which allows upstream length of 2D only, was installed in the test-line flange to flange immediately upstream of the UFM. The benefits can be expected to be:

1. Shorter measurement sections (3D upstream pipe, 3D turbine meter, 5D UFM, 2D downstream pipe = 13D total length),
2. The turbine can act as sort of flow conditioner,
3. The turbine meter can be used as a silencer for ultrasonic noise generated by an upstream regulator and
4. There is a double custody transfer measurement with different measuring principles.

Figure 18. shows the results with the turbine meter immediately upstream of the ultrasonic meter, with long straight pipe upstream, downstream from an elbow and downstream from two elbows out of plane. The fact that the ultrasonic meter worked as well as it did, in the severely distorted and turbulent flow profile immediately downstream of the turbine, was better than expected. Compared to the error curve for the straight pipe situation, the errors for distorted flow profiles change by about 0.3 to 0.4 %. It should be reminded that the ultrasonic meter is located only 6 D downstream of the source of the flow profile distortion. As all the error curves show a shift relative to the base line (ultrasonic meter alone in ideal flow conditions) for initial high-pressure calibration it is recommended to have both meters calibrated together.

As a spin-off the UFM could be used for diagnostics to detect any wear resulting in higher friction of the turbine. It is expected that this is possible by measuring the swirl angle of the velocity profile behind the turbine meter. This angle is going to change during wear-off. Separate from this, the flow as measured by the turbine meter and the ultrasonic meter can be compared. Figure 19. presents the results of a test comparing the turbine meter error and the ultrasonic meter error in normal conditions and in a condition where a large friction in the turbine meter is simulated. For this purpose the mechanical index of the turbine meter is removed in order to have access to the magnetic coupling in the transmission that drives the counter. The magnetic coupling is “braked” by applying a reverse momentum to the maximum possible value, which means just avoiding that the magnetic coupling gets disengaged (jumps from pole to pole). In order to prevent damage to the turbine meter this test was performed for lower flow rates only. It appears that the error curve of the turbine meter changes drastically in negative direction, whereas the error of the ultrasonic meter changes to a lesser extent in positive direction. The possibility to measure and trend this difference and capability of our ultrasonic meter to detect and measure the swirl of the flowing gas are subject to further investigations. The aim is to design and implement a concept offering extended features for detecting and diagnosing measuring problems and correct or compensate for the possible errors.

## 8. TEST RESULTS WITH ULTRASONIC METER (alone)

Figure 20. presents a graph showing the performance of the ultrasonic meter under the same conditions as before but without any upstream flow conditioning or turbine meter in front. The graph shows the change in error curves of the ultrasonic meter compared to the baseline calibration for the following situations: 10 D and 13 D downstream of a single elbow (identified as 90 10 D and 90 13 D) and downstream of two elbows out of plane (identified as RK 10 D and RK 13 D). The large deviation observed for one condition at the lowest flow rate is questionable, it has to be verified whether this a reliable data point.

With 10D straight upstream pipe length and without any flow conditioner the meter shows acceptable results with deviations to undisturbed conditions better than  $\pm 0.3\%$  (ISO 9951 tolerance) in a 10:1 measuring range.

## 9. STATION DESIGN

The pressure in gas transmission lines is usually between 50 – 85bar (700 – 1,200psi) and between 15 - 40bar (200 – 550psi) in the gas distribution net. The pressure reduction by regulators and control valves generates very high levels of sound from the audible up to ultrasonic frequency range. If the acoustic energy that is generated is in the same frequency band as where the meter operates, there is a likelihood of interference with the measuring signals of an ultrasonic gas flow meter. If the noise level is too high corrective measures have to be taken to attenuate the noise level. Bends, tees, filters, turbine meters or heat exchangers all have a reducing effect on the noise that reaches the ultrasonic gas flow meter.

Instromet has developed a mathematical model to predict the emission levels of the ultrasonic noise related to the process conditions and as well as the effect of the piping configuration. Using this model for an existing or a planned installation, an assessment can be made regarding the performance of the ultrasonic meter: will it work properly or is there a chance to have problems.

As a rule of thumb for estimating the attenuation of ultrasonic noise in components of an installation, the following table can be used:

Straight pipe	0 dB	filter	15 dB
90° bend	5 dB	Heat exchanger	30 dB
Tee	10dB	T (“noise catcher”)	16 dB
Turbine meter	15 dB	Instromet silencer	12 dB
Natural dry gas, ANSI 600#			

The station design using an UFM is different from, for instance, turbine meter stations where usually the meter is placed downstream of the regulator. In the case of the UFM the meter has to be isolated from the valve in terms of ultrasonic sound. A heat exchanger is an excellent silencer with an attenuation of approximately 30dB. The additional 2 bends results in 10dB damping. Using 2 tees instead of the bends would improve another 10dB and would result in totally 50dB - enough for most applications.

The 2 other examples shown on the next page, use 2 Instromet T-noise-catchers and either a turbine meter or a silencer element. The regulator is upstream. Typically the ultrasonic noise of a regulator on the upstream side is twice that one downstream. Therefore the preferred location of the regulator is downstream of the UFM.

## CONCLUSIONS

1. The basic test of a 6" sized Q.Sonic has confirmed that the design complies with AGA-9 for smaller sizes and is within the ISO 9951 tolerance of  $<\pm 0.3\%$ , for the installation conditions presented in this report and with 10 straight upstream pipe length.
2. Using a flow conditioner will provide acceptable results but the meter and the flow conditioner should be calibrated and used as a package.
3. Using a turbine meter in front of the UFM with flange to flange, the UFM complies with AGA-9 under the upstream conditions according to ISO 9951 and within the tolerance ISO 9951 (0.33%)
4. Using a double Tee with Instromet designed silencer and a turbine meter or perforated plate type silencer (Instromet make) upstream, the ultrasonic flow meter can handle a large pressure drop, the operating limits can be calculated using Instromets' USFM station design software.

## References

- [1] F.Vulovic, Gas de France – B.Harbrink, Ruhrgas – K.van Bloemendaal, Gasunie NSWS 1995, paper 18 "Test Results Q.Sonic"
- [2] G.Sloet and G.de Nobel, Gasunie, NSWS 1997, paper 14 "Experience with UFM at the Gasunie export stations"
- [3] ISO 9951 / Measurement of gas flow in closed conduits – turbine meters, 1993
- [4] J.Lansing and G.de Boer, Instromet, AGA Operations Conference, May 17-19, 1998 "Benefits of dry calibrating UFM"
- [5] J.Lansing, Instromet, 4<sup>th</sup> International Symposium on Fluid Flow Measurement, Denver, Colorado – June 30, 1999, "Benefits of dry calibrating UFM"



FIG. 1. Part of "HDV Lintorf" Testfacility

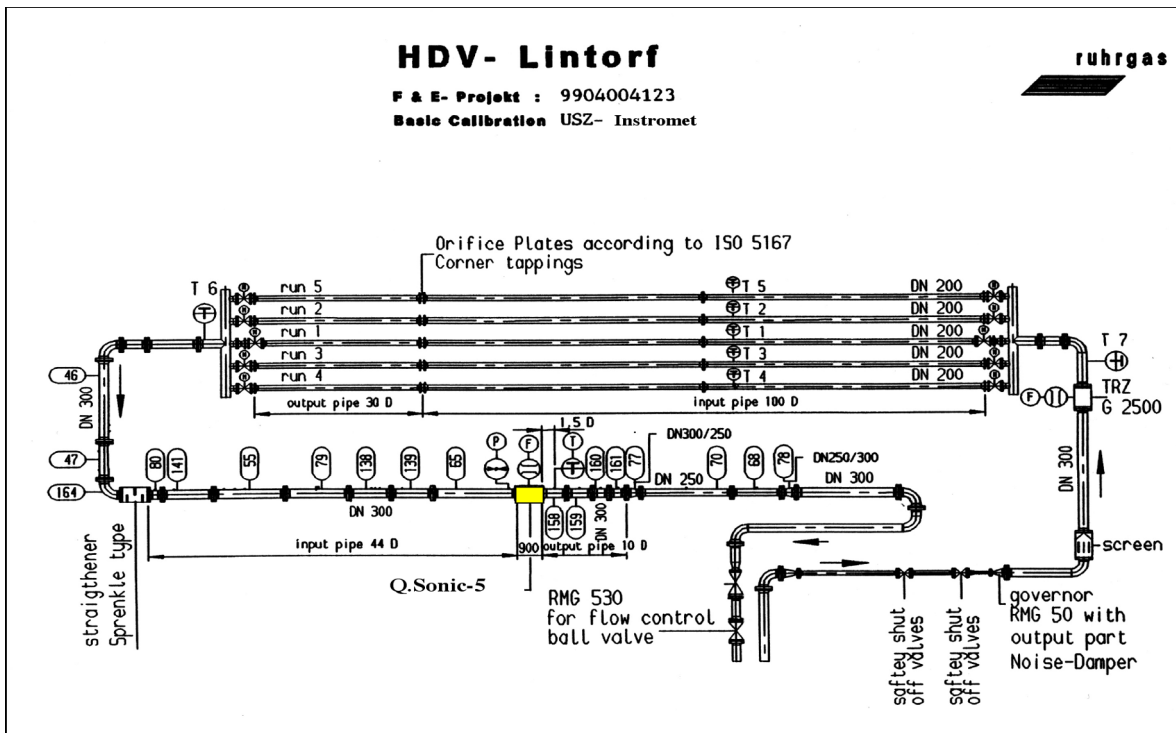
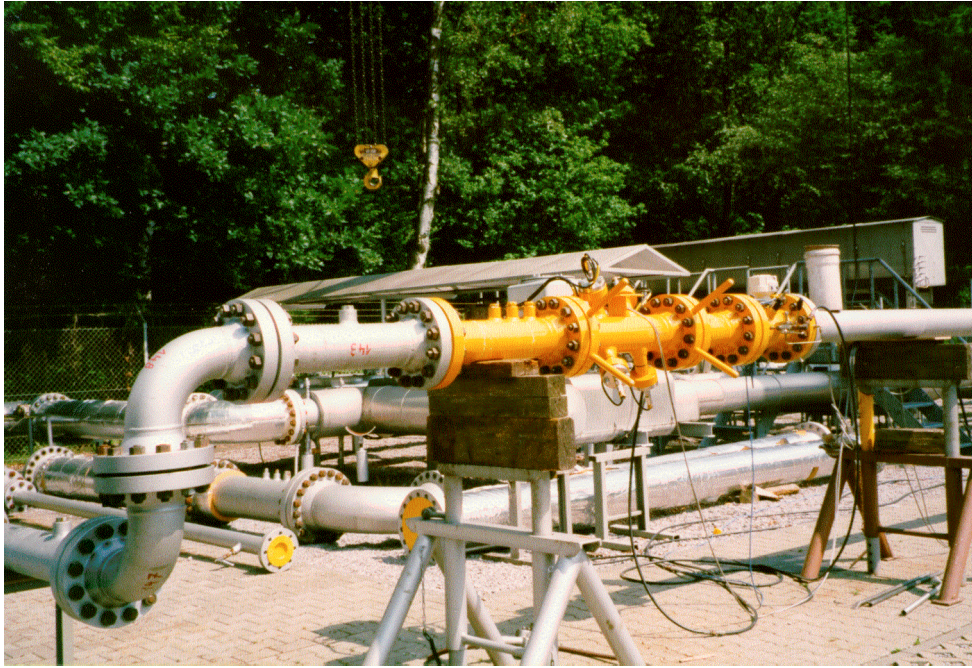


FIG. 2 Schematic diagram "HDV Lintorf"



*FIG. 3. Piping configuration for double elbows out of plane.*



*FIG. 4. Piping configuration with turbine meter upstream of ultrasonic meter*

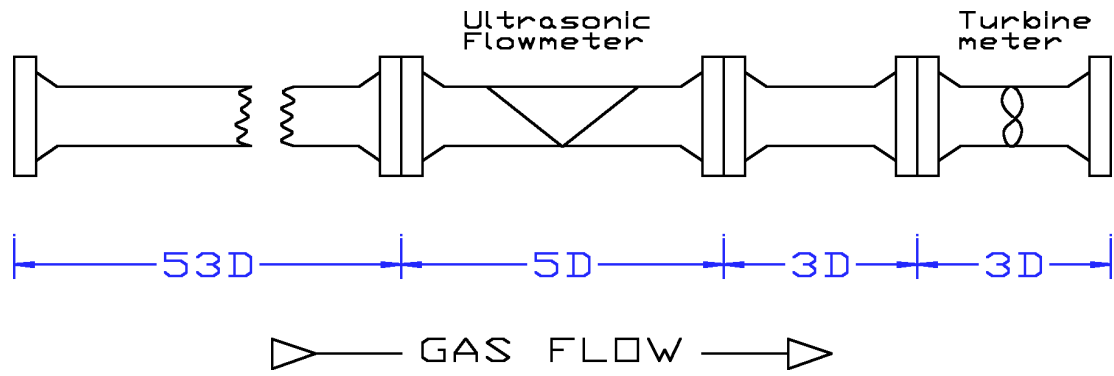


FIG. 5.

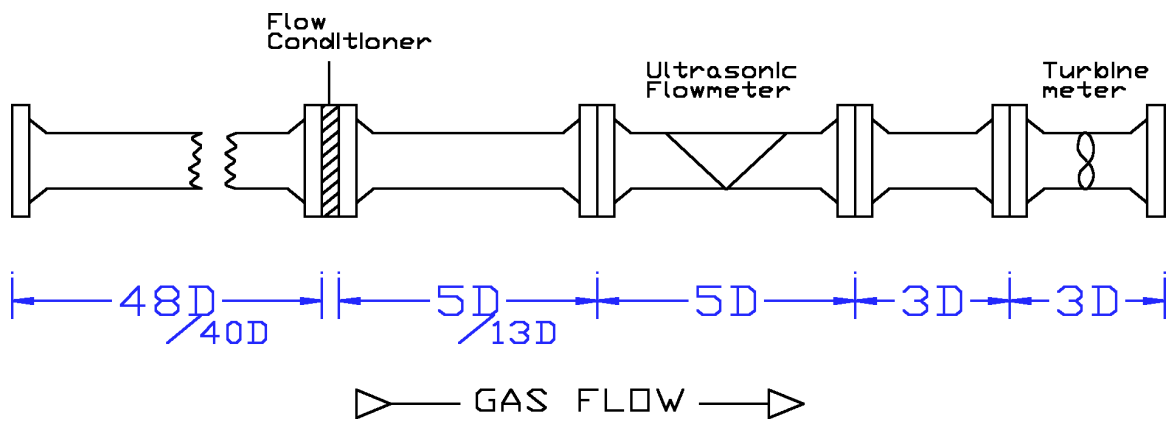


FIG. 6.

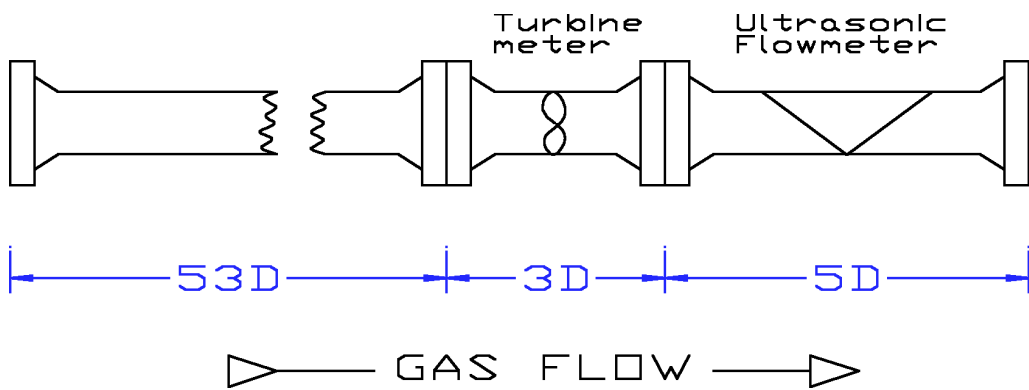


FIG. 7.

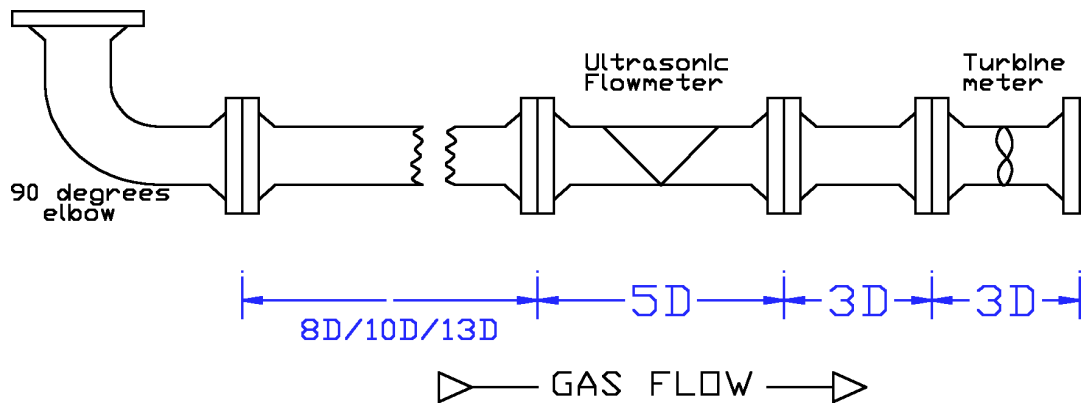


FIG. 8.

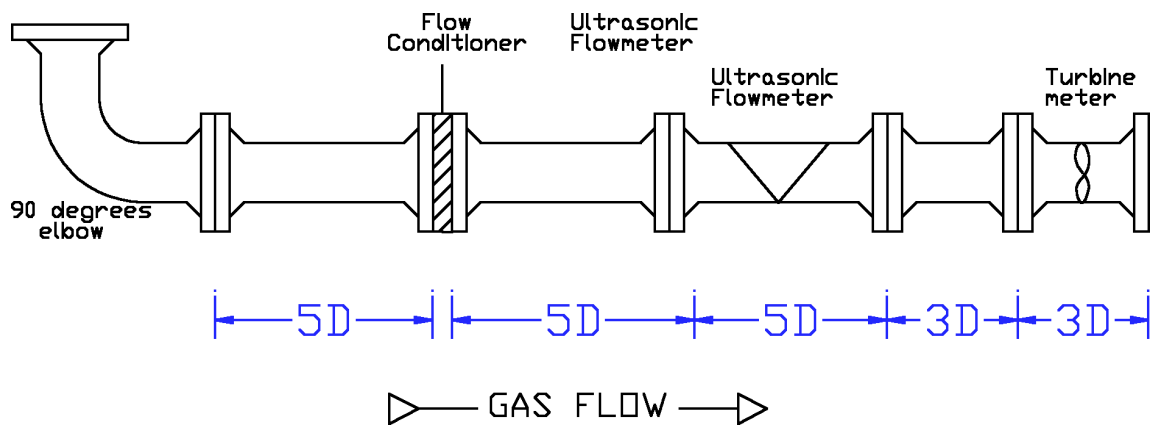


FIG. 9.

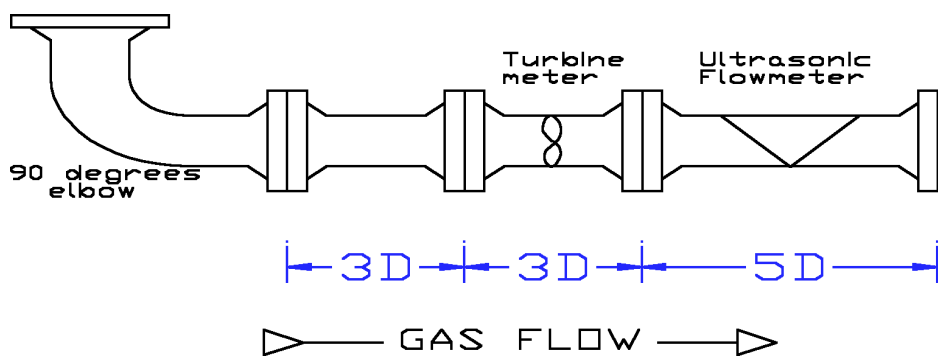


FIG. 10.

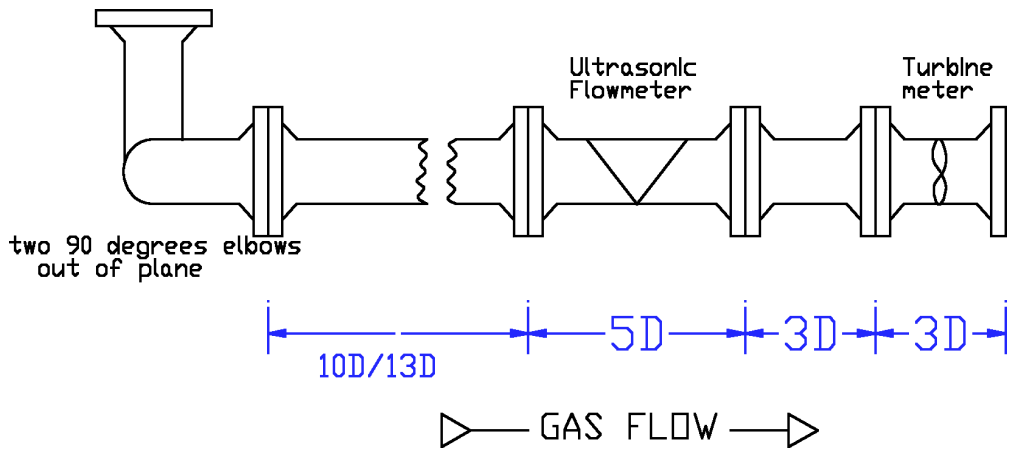


FIG. 11.

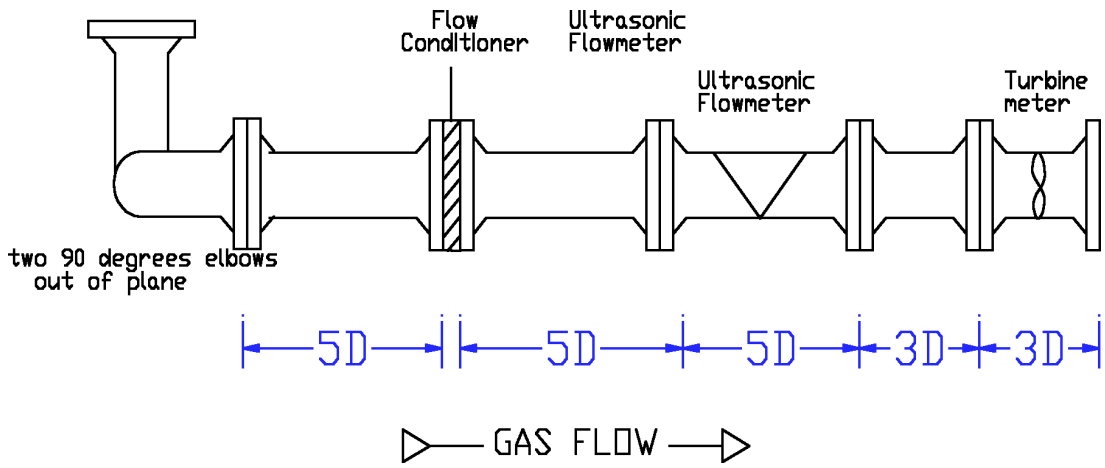


FIG. 12

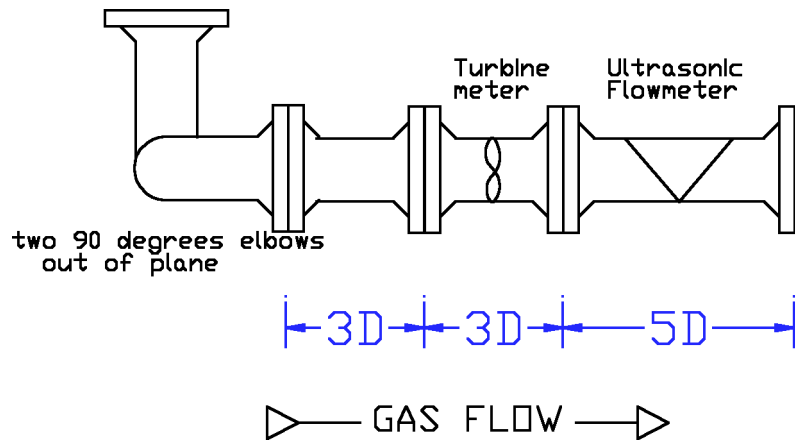


FIG. 13.

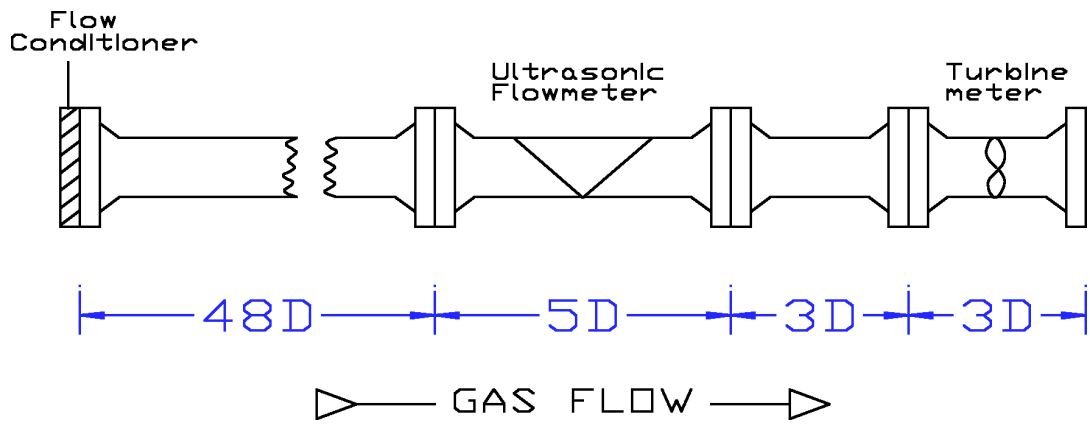


FIG. 14.

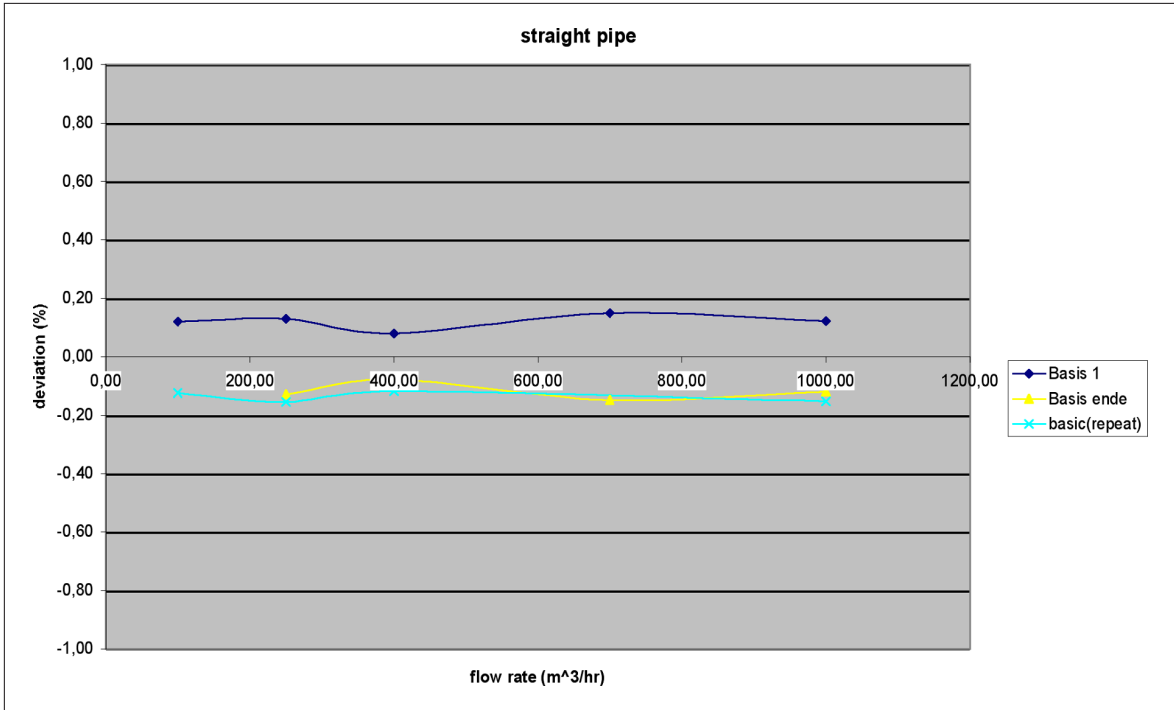


FIG. 15. Base line calibration (straight pipe) test results

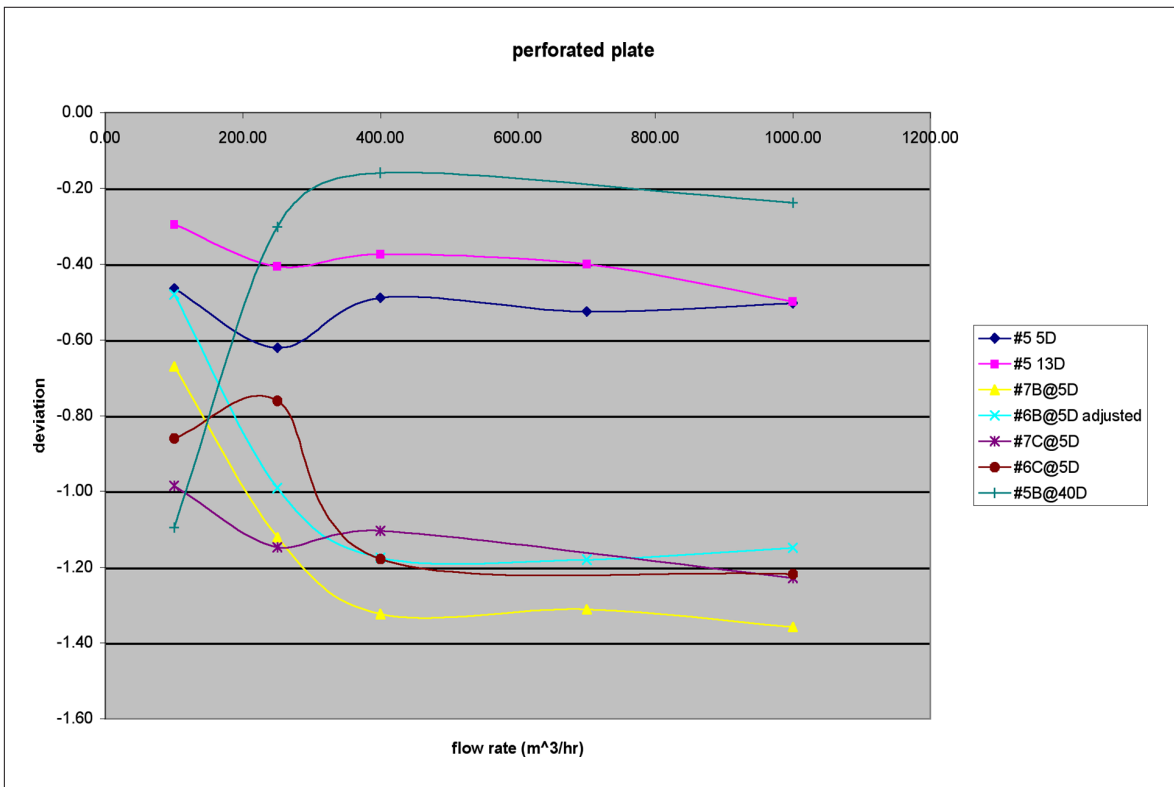


FIG. 16. Test results with flow conditioners in straight pipe configurations.

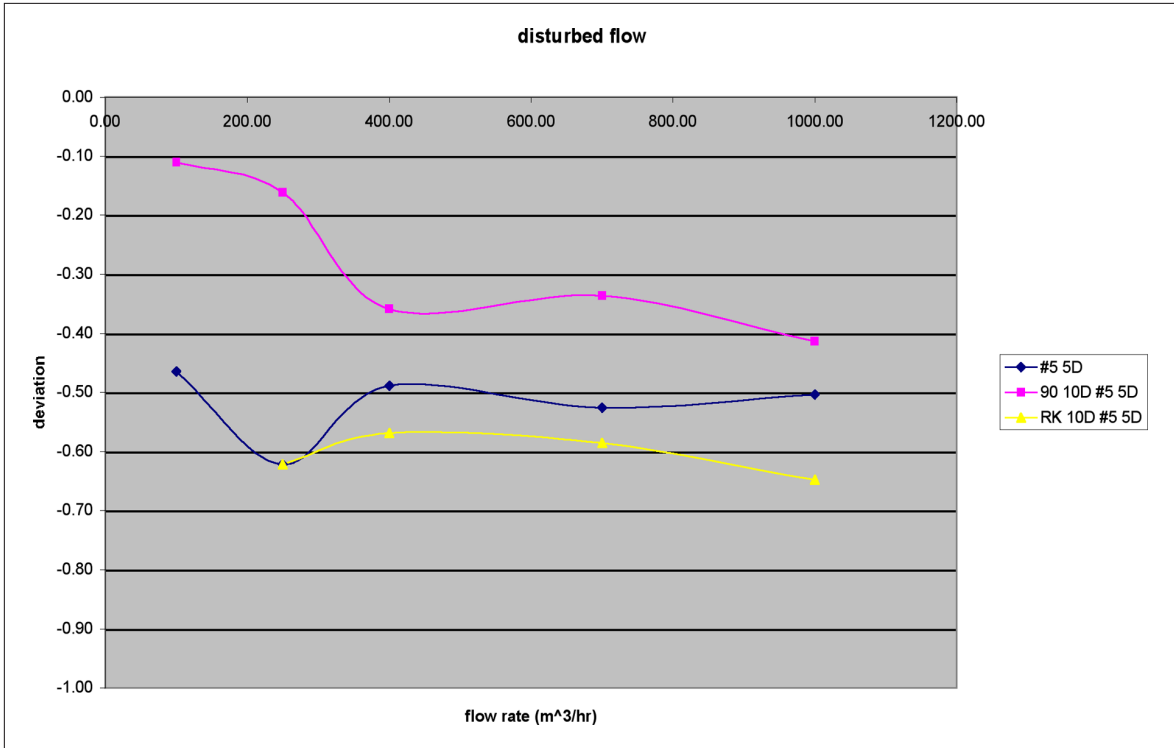


FIG. 17. Test results with flow conditioner in straight pipe, downstream from elbow and downstream of double elbows out of plane.

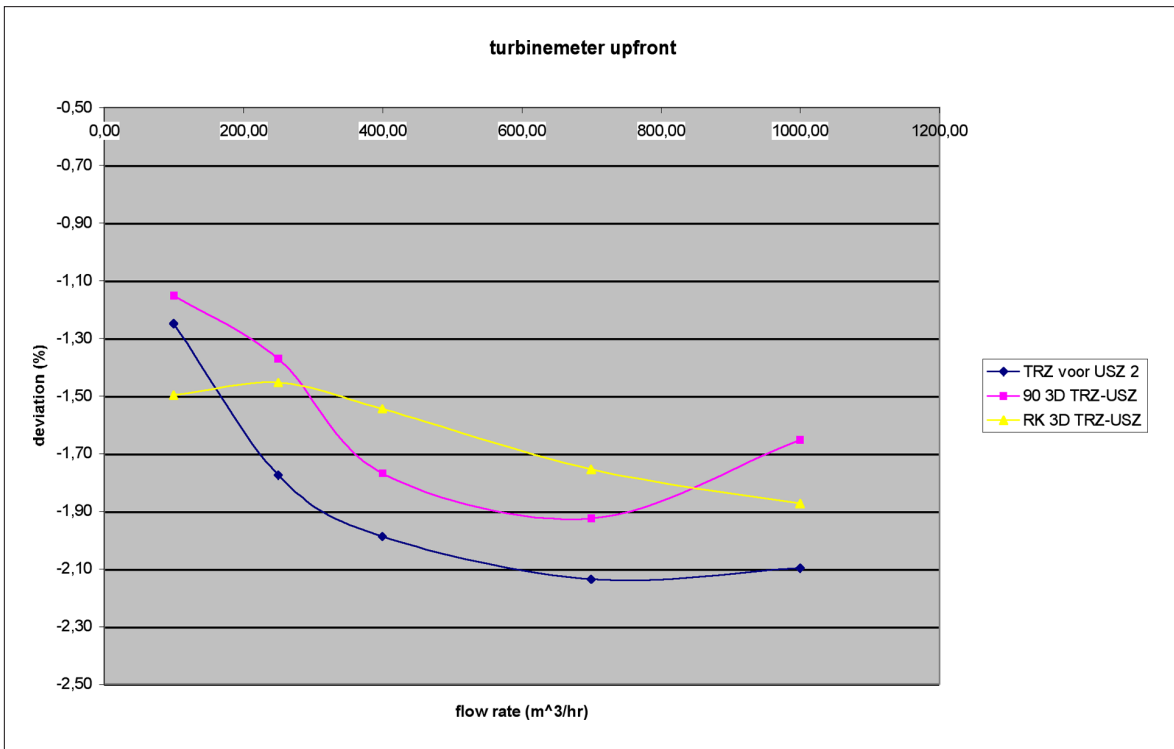


FIG. 18. Test results with turbine meter upstream of ultrasonic meter, in straight pipe downstream of single elbow and downstream of double elbows out of plane.

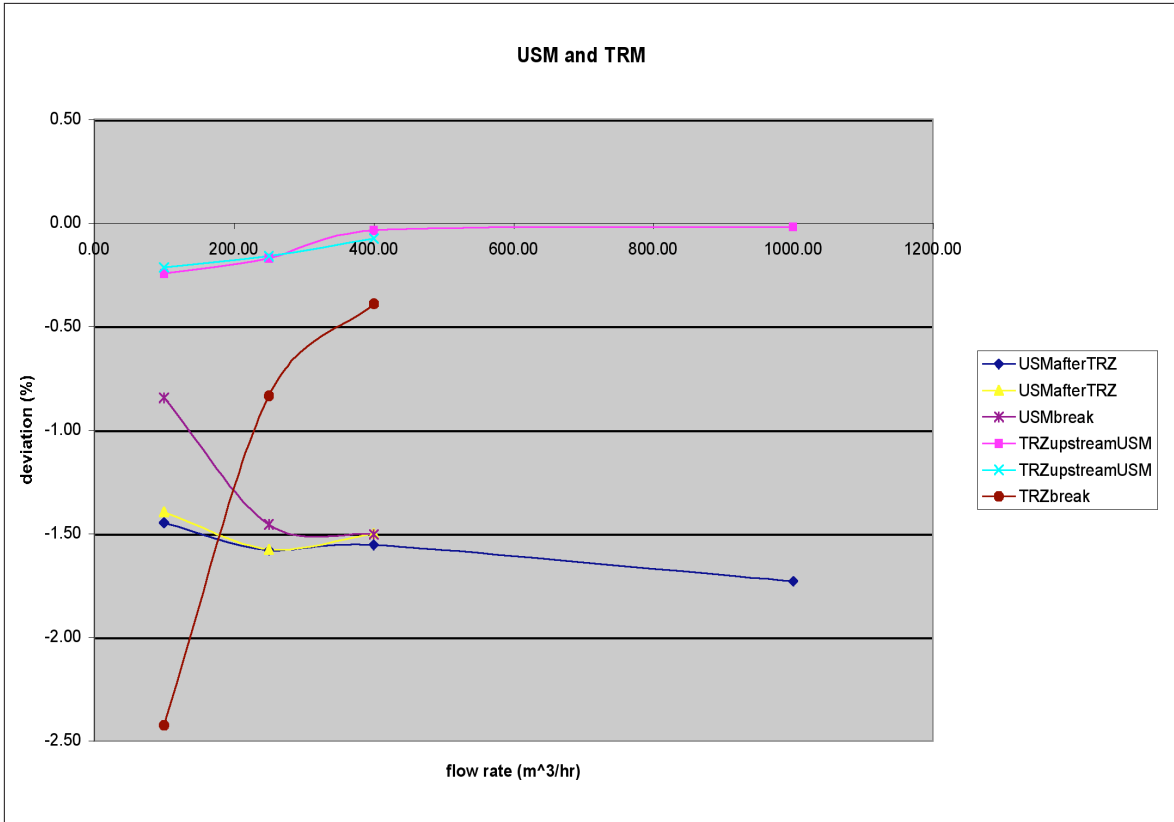


FIG. 19. Test results with turbine meter upstream of ultrasonic meter, normal and simulated friction in turbine meter.

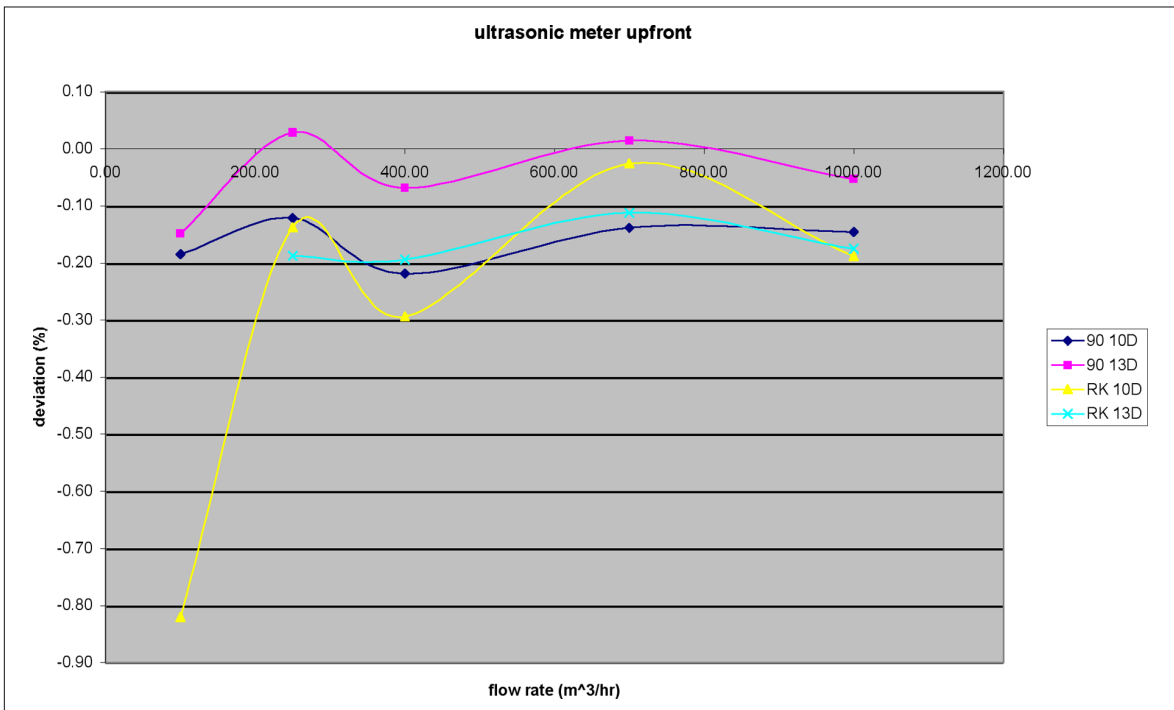


FIG. 20. Test results for ultrasonic meter in distorted flow profiles, downstream of single elbow and double elbows out of plane

# M&R station with UFM

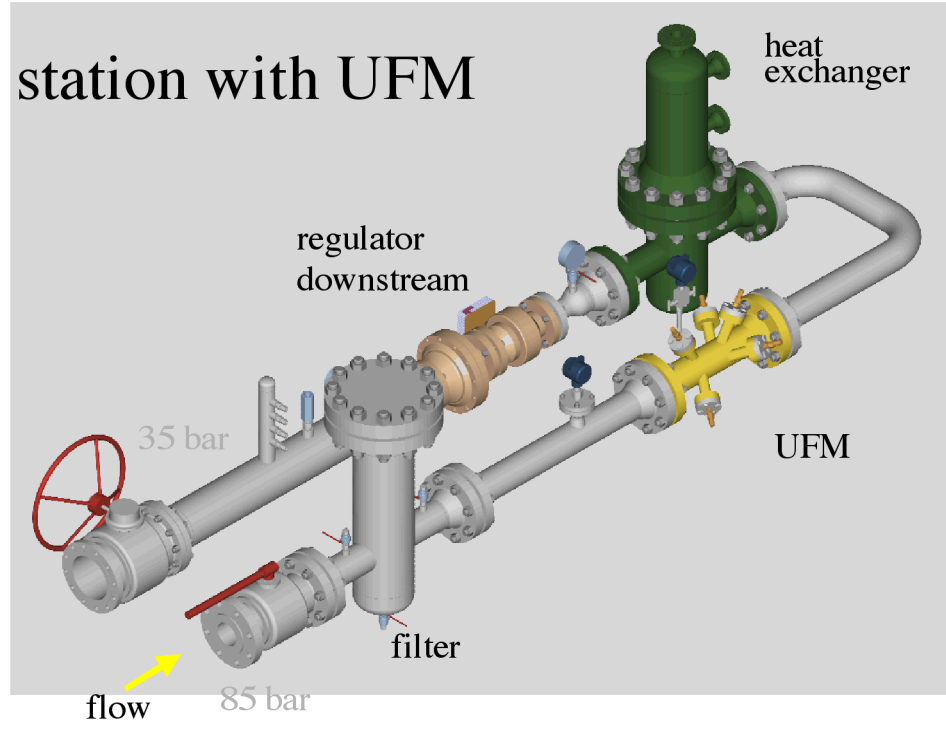


FIG. 21. Metering station with ultrasonic flow meter.

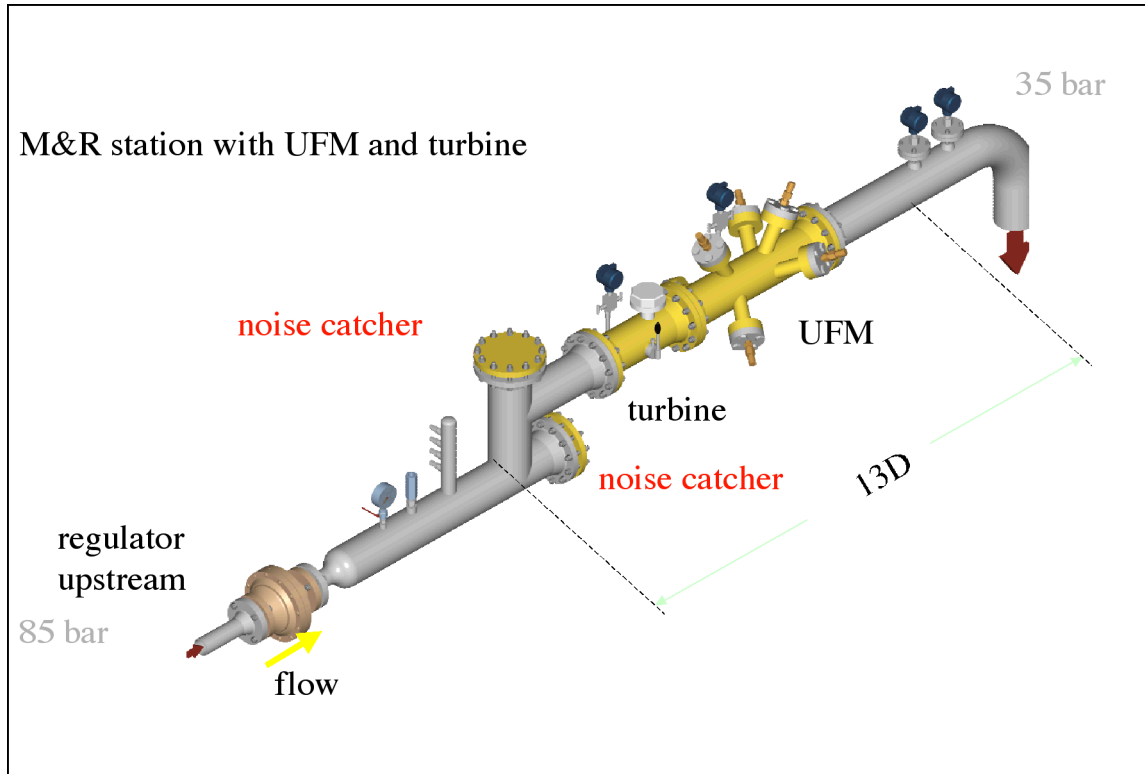


FIG. 22. Ultrasonic metering run with Tee's to attenuate noise from regulator valve

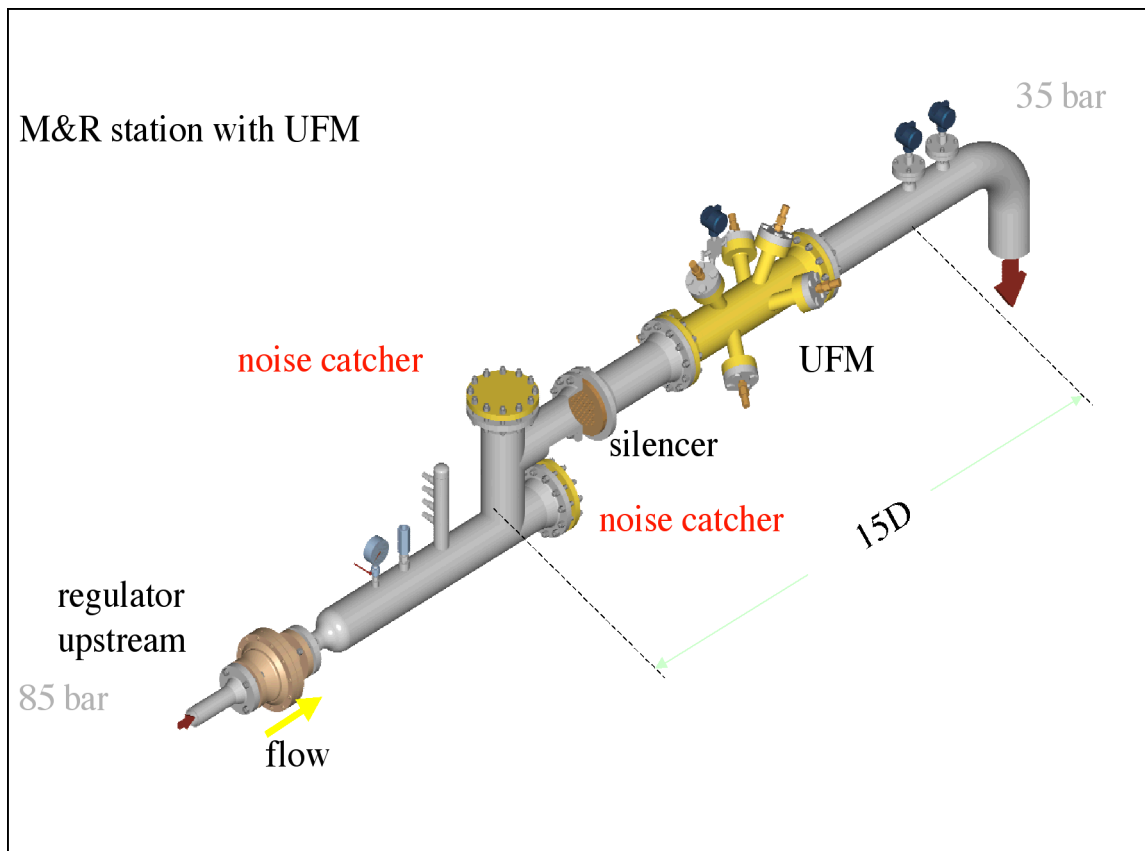


FIG. 23. Ultrasonic metering run with silencer to attenuate noise from regulator valve.

# Aspects of bi-directional fiscal metering by means of ultrasonic meters

*G.H. Sloet*  
*NV Nederlandse Gasunie*

---

## Introduction

N.V. Nederlandse Gasunie is the major gas transmission company in the Netherlands. In 1998 the company sold 79.8 billion m<sup>3</sup> natural gas. From this amount of gas 43.4 billion m<sup>3</sup> was sold in the domestic market and 36.4 billion m<sup>3</sup> was exported to other European countries.

To deliver the gas to its customers Gasunie operates an extensive gas transmission grid, with 11389 kilometres of transmission lines, 8 compressor stations, 75 regulator stations, 15 export stations and 1114 city gate stations in the domestic market.

Starting in 2001, Russian gas will flow via Poland and Germany to the Netherlands. The gas will enter the Dutch transmission system at the existing Oude Statenzijl export station in the northern part of the country.

Importing gas via a station that has been designed as an export station is a new phenomenon for Gasunie and a redesign of the existing station is necessary. Gasunie Research was approached with the instruction to work out and test a proposal for a bi-directional flow measurement concept based on ultrasonic gas meters. In this paper an overview of the work executed so far will be presented, together with results of experimental work that has been done at Gasunie's high pressure, high flow Bernoulli laboratory at Westerbork, the Netherlands.

## Flow measurement at export measurement stations

Due to the stringent requirements in terms of availability and uncertainty of the measurement, at Gasunie's major export stations, the gas flow measurement is implemented as a complete double system. Not only the flow meters, but also the temperature and pressure sensors and flow computers are doubled and in the number of meter runs always a spare run is included, which can take over from one of the regular meter runs in case of failure. Results of research work on the design of the export stations have been published in [1], [2] and [3].

At the Oude Statenzijl station the meter runs are equipped with a turbine meter, which is considered as primary meter, and an ultrasonic flow meter, which is used as backup meter. A typical layout of such a meter run is shown in Figure 1.

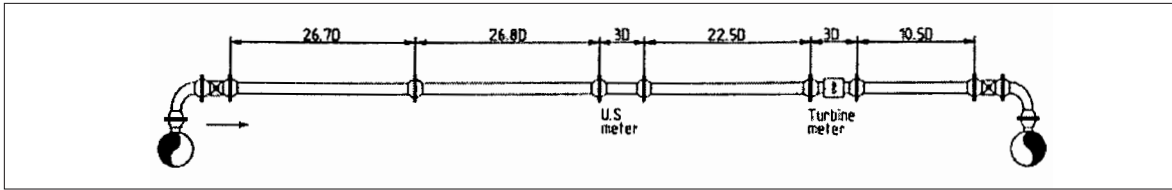


Figure 1 - Layout of a typical meter run

Upstream of the ultrasonic meter a Laws flow conditioner is installed to remove the flow disturbances coming from the underground header and riser, which in fact form a double bend out of plane. The results of the flow measurement by the turbine and ultrasonic meter are continuously compared by means of an on-line comparison technique, based on hourly averages. Results of this comparison have been reported before in [].

## Approaches for a bi-directional flow measurement

As a first stage in the project alternative approaches for a bi-directional measurement were considered: duplication of the total measuring station, switching of meter runs so that the gas always flows in the same direction through the metering section and use of full bi-directional meter runs. From an economical point of view the third alternative is the most favourable one. No extra piping and valves are needed, no extra station space is required and when the direction of the flow changes no switching actions have to be executed.

Focus was given to the design of a meter run equipped with meters that can be used bi-directionally. Taking into account the required uncertainty and availability of the flow measurement only one candidate meter, the multi-path ultrasonic flow meter, could meet these requirements. Standard turbine meters, although certain manufacturers claim that they can be used in a reversed flow without damage, were not considered as an alternative of full value.

## A bi-directional meter run with ultrasonic meters

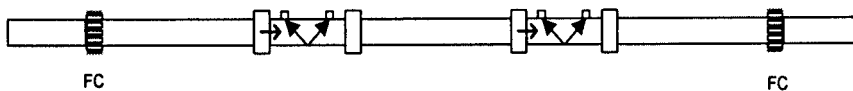


Figure 2 - Schematic design of a bi-directional meter run

After the selection of the measurement principle the stringent availability requirement lead to the decision that two ultrasonic meters in one run were required. The requirement to use the bi-directional meter run in an existing export measuring station restricted the available length for the meter run. The bi-directional nature of the meter run lead almost automatically to a symmetric design as in Figure 2. The gas flows from the header via a riser pipe through a 90 degree elbow and a ball valve into the actual meter run. To eliminate flow disturbances caused by the header - elbow combinations, which form double bends out of plane, flow conditioners are required at both sides of the meter run.

Now the questions arises where to install the meters? A first intuitive approach is to situate the ultrasonic meters are far away as possible from each other to avoid acoustic influences from one meter to the other (Figure 3) ; an alternative, however, is to place the meters as

close as possible to each other (Figure 4). Now the meter manufacturer will be able to predict the paths of the ultrasonic beams and advise how the meters should be positioned to avoid that an ultrasonic beam from one meter interferes with the transducers of the other meter. The first approach brings the ultrasonic meter relatively close to the flow conditioner due to the restricted length of the meter run, imposed by the station layout. In both cases a temperature transmitter has to be situated upstream of one of the meters, depending on the direction of the flow.

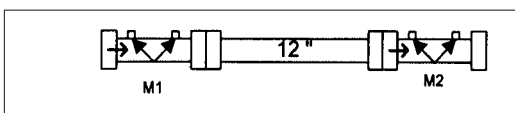


Figure 3 - Meters apart

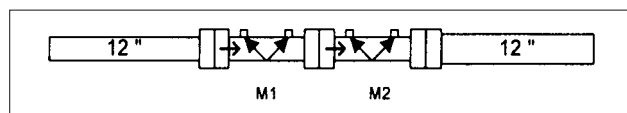


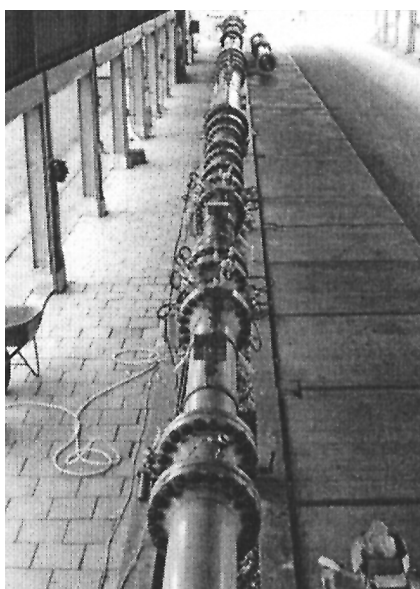
Figure 4 - Meters adjacent

Both possible alternatives resulted in a number of questions, for which the answers were not clear beforehand:

- What is the mutual acoustic influence of two ultrasonic meters in one meter run?
- What is the effect of a temperature transducer upstream, relatively close to an ultrasonic meter?
- What is the effect of a nearby flow conditioner on an ultrasonic meter?
- Are calibration curves for a bi-directional meter calibrated in both directions comparable?

In order to find answers to these questions a set of experiments at Gasunie's Bernoulli flow laboratory at Westerbork were conducted. In the next section a selection from the measurements, giving a representative overview, is presented.

## Experimental results



### Equipment

In the experiments two 12" Q.sonic 5 ultrasonic meters, made available by Instromet Ultrasonics, were used. The pulse outputs of the meters were connected to the data-acquisition system of the Bernoulli system to be able to compare the readings of the meters to the flow indicated by the reference meters of the laboratory. Uniform, Instromet's diagnostic software package for ultrasonic meters, was used to monitor the performance of the ultrasonic meters during the experiments. Standard, calibrated, pressure and temperature sensors from the laboratory were used in the experiments. Existing flanged piping was used to form the different straight pipe lengths that were required in the experiments.

### Acoustic influence

Figure 6 shows one of the configurations that has been used to determine the effect of the upstream meter on the behaviour of the downstream meter. The results obtained with this configuration are shown in Figure 7.

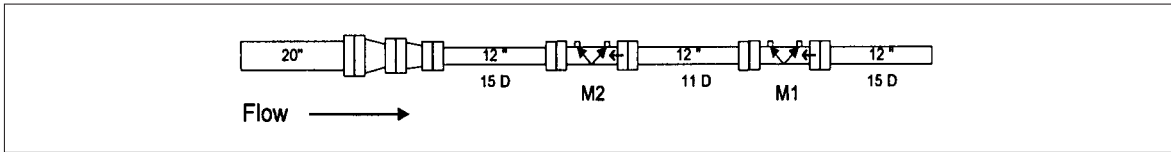


Figure 6

At a distance of 11 pipe diameters no influence from the upstream meter on the downstream meter can be seen. Also the performance of the individual paths of the downstream meter, read out by the Uniform software, was not affected. The spread of the results at the lower flow rates is a phenomena that is likely to be caused by a line pack effect in the installation. For these experiments, where a large pipe section had to be installed, the large meter run of the installation had to be used. This meter run is normally not used for 12 “ meters.

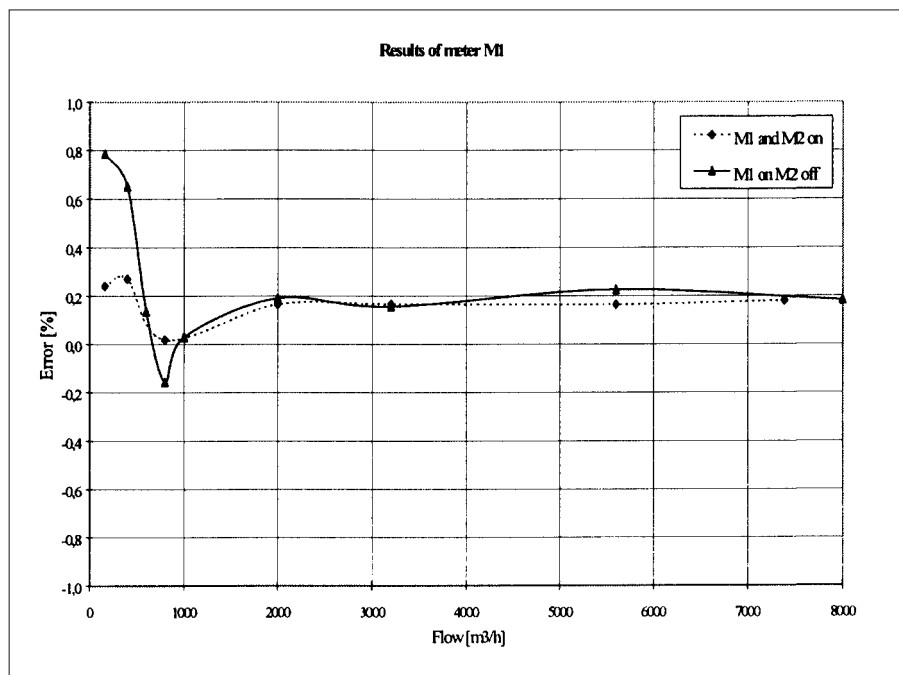


Figure 7 - Results interference at distance

With two meters adjacent to each other a similar experiment was carried out. The set up from Figure 8 was used for the measurements. After the measurement one of the meters was rotated one bolt position (12°) and the measurement was repeated. The results are shown in Figure 9.

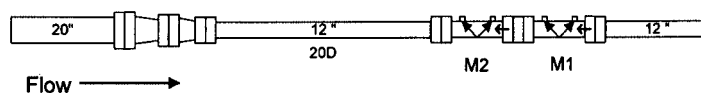


Figure 8

Due to flow limitations on the day of the second set of measurements no higher flow than 3200 m<sup>3</sup>/h was possible. There seems to be an influence of meter 2 on meter 1 when meter two is rotated. This means that the position of the meters is very critical when both meters are very close to each other. A slight rotation may influence the performance of the meters, indicating that the ultrasonic signal from the meter upstream is picked up by the downstream meter.

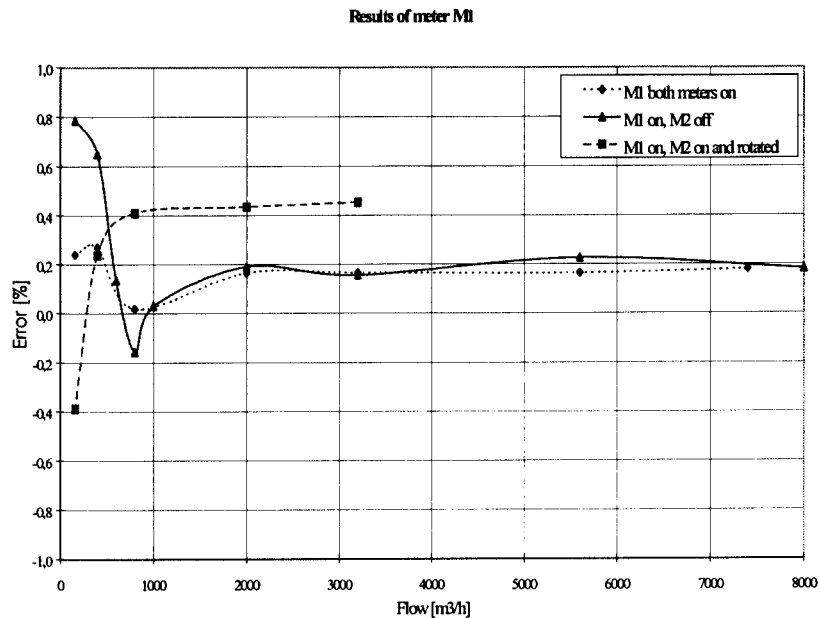


Figure 9 - Results adjacent meters

*Temperature transducers upstream*

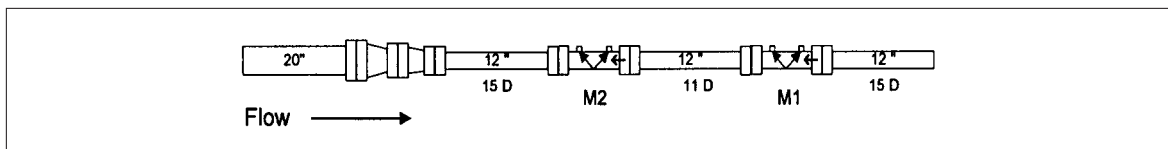
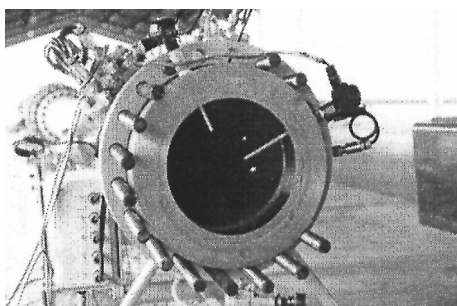


Figure 10

The configuration from Figure 10 was used to investigate the effect of Pt 100's mounted in front of one of the meters. In Figure 11 a photograph of the Pt 100's used can be found.



As can be seen in Figure 12 the Pt 100's mounted in front of the first meter change the curve of the first meter at higher flow rates. The curve of the second meter, which is further away from the disturbance, is not affected. In field practice the effect of Pt's will be more severe as Gasunie is using pocket mounted temperature transducers with a larger diameter than the Pt 100's used in these experiments.

Figure 11- Pt's in front of the meter

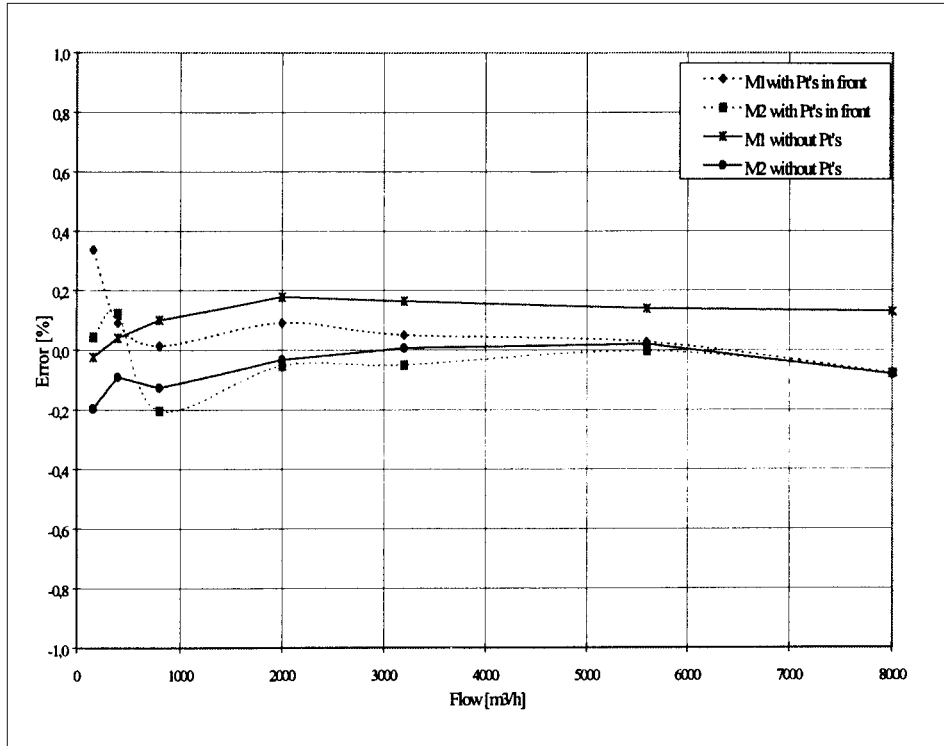


Figure 12 - Effect of Pt's upstream

### Influence of nearby flow conditioners

In the meter runs of the Gasunie export stations currently Laws flow conditioners [], from the type shown in Figure 13, are used. This was the reason that for the experiments with flow conditioners this type of flow conditioner was selected.

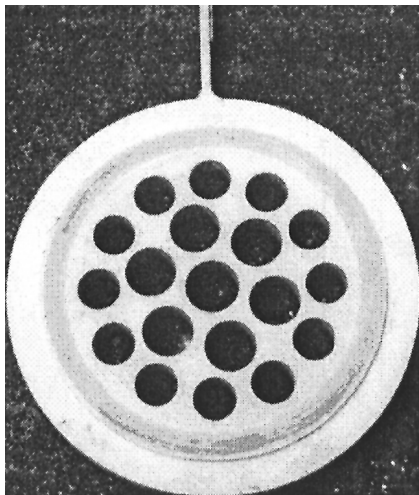


Figure 13 - Laws plate

To investigate what the effect of distance of a Laws flow conditioner to the ultrasonic meter a series of calibrations with the flow conditioner at different distances from the meter has been done. As flow disturbance a pipe diameter reduction from 20 " to 12" was used. From flow profile measurements it is known that reducers lead to a very flat profile, causing misreading of meters. In Figure 14 the results of these calibrations are shown.

Calibration results with the flow conditioner at 20D, 13.5D and 10D are lying close together and taking the repeatability of the test installation and line pack effects at low flow rates into account one may state that these results are comparable. The graph of the experiment with the flow conditioner at 5D, however, deviates. This leads to the conclusion that a Laws flow conditioner at 5D is too close to the meter and that it is advisable to have at least 10D between flow conditioner and ultrasonic meter.

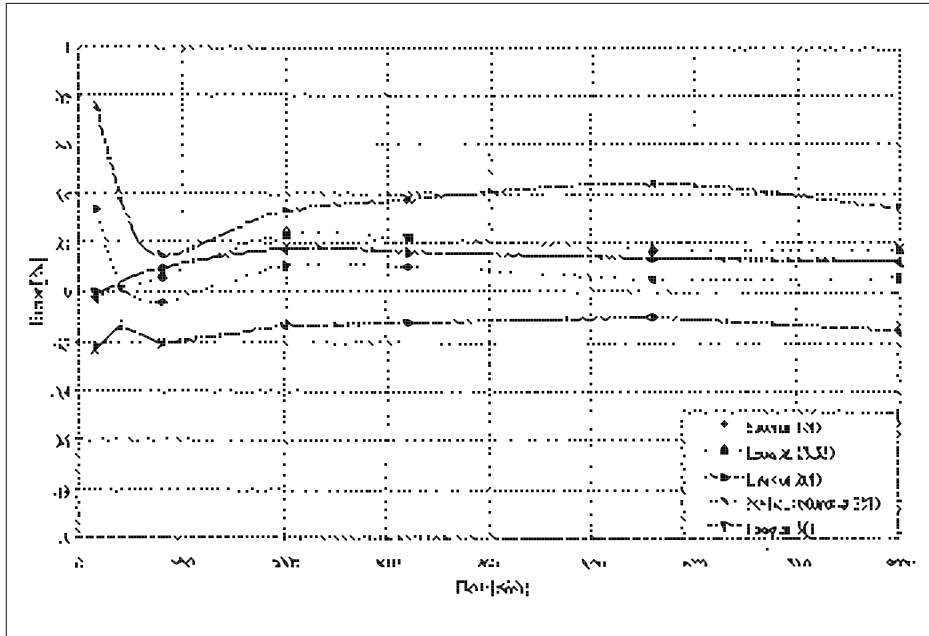


Figure 14 - Influence of flow conditioner

**Calibrations in both directions**

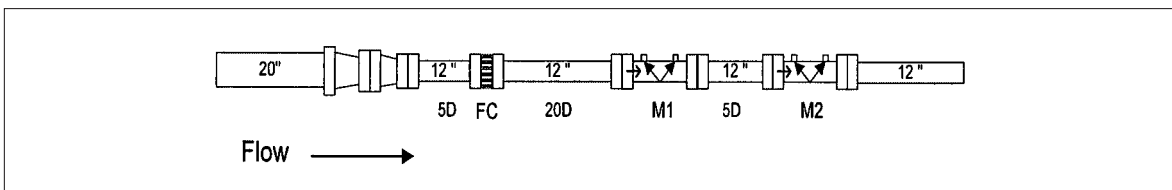


Figure 15

With a flow conditioner at 20 D in front of the meter as shown in Figure 15 two calibrations were performed.

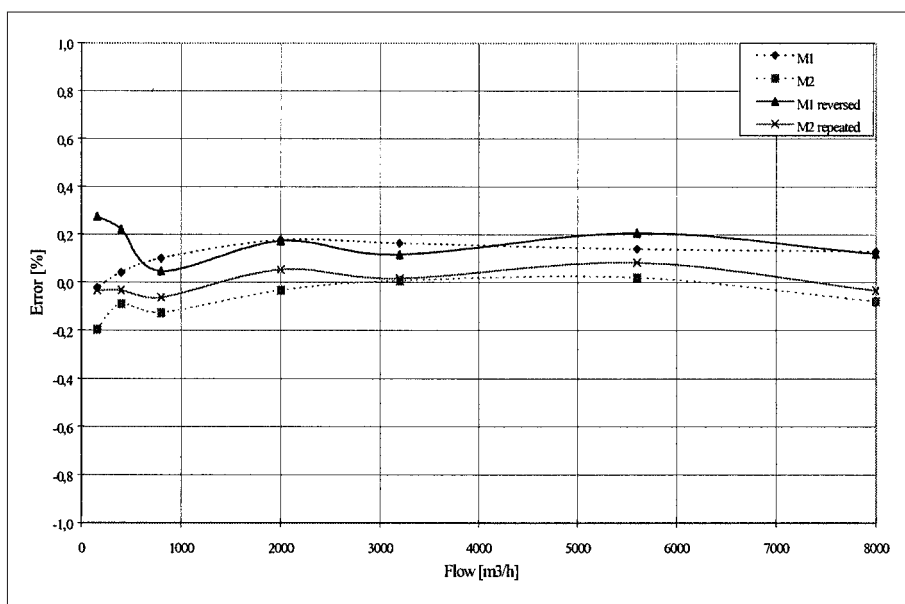


Figure 16 - Calibration in both flow directions

After the first calibration the first meter was taken out of the meter run and mounted facing the reverse direction. The results of this experiment are shown in Figure 16. As might be expected from the concept of the ultrasonic meter, no significant differences between the two calibration curves of meter 1, have been found. As explained earlier results at lower flow rates show more variance due to a line pack effect in the test installation.

**Overall test of the concept**

With the set up from Figure 17 a calibration was done to test a complete meter run. The results are given in Figure 18.

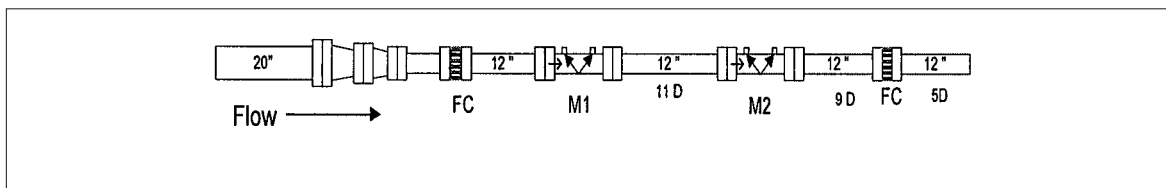


Figure 17

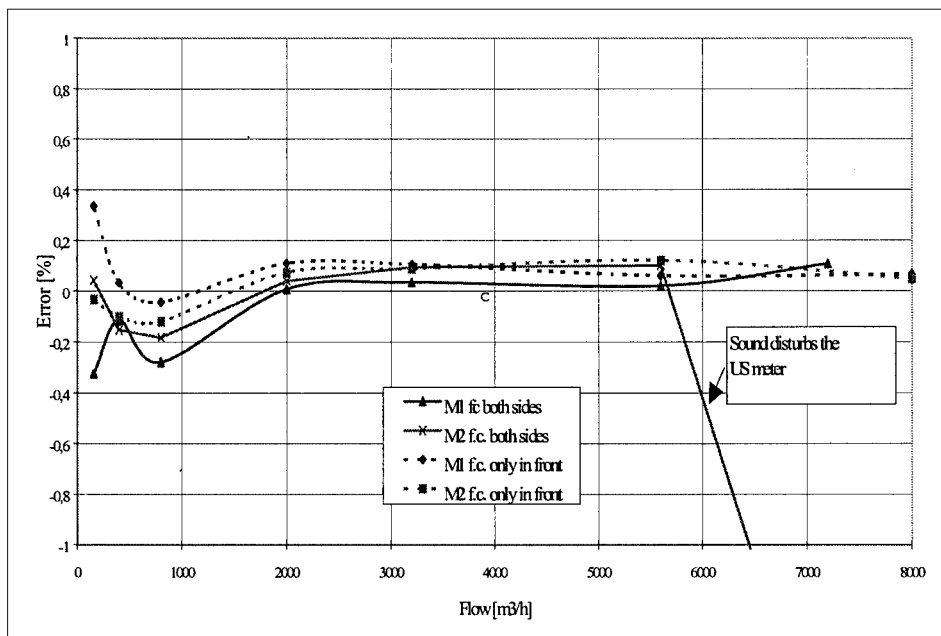
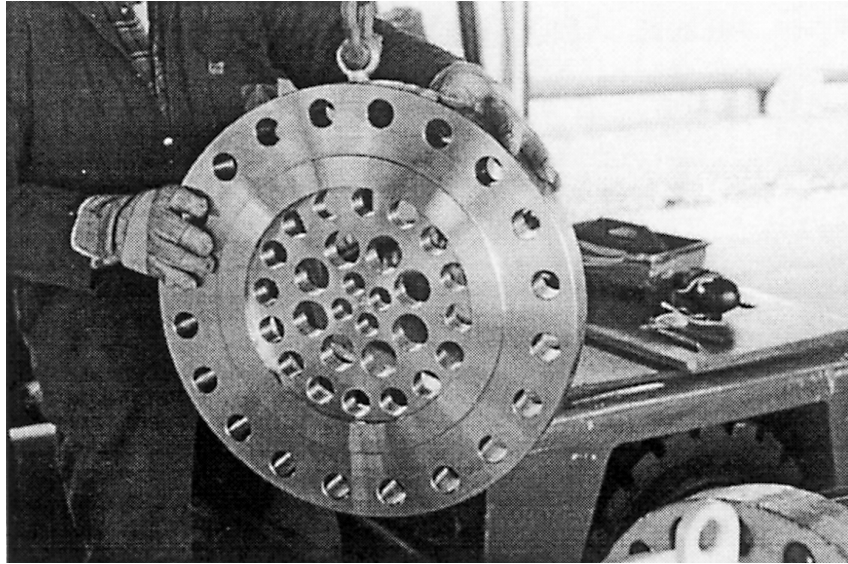


Figure 18 - Results overall test

Although in the experiments with one flow conditioner in the test line a slight whispering, coming from the flow conditioner, was heard it came as a complete surprise that with the above set up at high flow rate the whole meter run was producing a deafening sound. At a distance of one meter from the pipe wall a sound level of 105 dBa was measured. From the fact that one of the meters malfunctioned at higher flow rates it may be concluded that the sound produced is not limited to the audible range. The test was repeated with the flow conditioner reversed to investigate whether the chamfered rim of the holes, which were in the first experiment at the downstream side of the second plate, would influence the sound production. No significant difference with the first experiment was found

Another test that has been done with two different types of flow conditioners. Upstream the Laws plate was mounted. Downstream a Spearman [] flow conditioner, shown in Figure 19, was used to find out if different designs, using different sizes of holes would eliminate the sound. This attempt was unsuccessful. Only a minor difference in sound level was measured. Due to the limited time available for the experiments at the test installation it was decided to spend more time on this phenomena at a later time.



*Figure 19 - Spearman flow conditioner*

## Conclusions

Ultrasonic gas flow meters are by design bi-directional meters, which is confirmed by the calibration curves recorded in both flow directions, which lay in a relative narrow band. Flow disturbances relatively short in front of the meter, for example caused by temperature transducers or flow conditioners, may disturb the functioning of the meter, leading to mis-reading.

Two ultrasonic meters mounted at a distance of 10D do not mutually influence each other. A minimum distance has not been determined in this project. When two meters are mounted adjacent, influences may be found depending on the relative position of the meters.

A combination of two plate-type flow conditioners in one meter run, although mounted at a relatively large distance, may lead to a high level sound production in the meter run. The produced sound exceeds not only the acceptable level for audible sound, but may also lead to a malfunctioning of the meter at high flow rates. This means that the tested design, with two plate type flow conditioners, can not be used in the current form for export stations. Alternative designs for the meter runs will have to be considered.



# HOW TO OPTIMISE ALLOCATION SYSTEMS BY USING MONTE-CARLO SIMULATION

*L. Coughlan, Shell UK Exploration & Production*

*M. Basil, Flow Ltd, Presenter*

*P. Cox, Flow Ltd*

---

## 1 Introduction

The present low Oil price is forcing all petrochemical operating companies to actively review and reduce expenditure whilst maintaining or increasing production, ensuring a healthy return on investment for the shareholders. This has generated the need for new and innovative approaches in the way we manage our business. By forming a common interest group between operating service companies ideas can be developed with more focus and put into practice quicker. The authors having formed such an alliance would like to demonstrate that, by application of system models utilising Monte Carlo Simulation (MCS), how the operator can focus his limited resources and budget in the areas of greatest sensitivity and where the biggest benefit can be gained.

This type of model is equally applicable to both old and new systems. By assessment of the impact of each node within a system, against the output requirements using the MCS modelling techniques, the importance and impact of each node can be established. For existing systems this allows the user to define whether the present operating conditions meet the applicable agreements: and if optimisation in areas can be made whilst still remaining within the terms of the relevant agreements. For new green field developments the uncertainty can quickly be determined, establishing the limits which can be achieved and hence equipment required. The biggest benefit is for new projects over existing facilities, the allocation possibilities can be tested and the best method found not only in exposure but also cost.

Combining the benefits of applying new technology and optimising the use of the available facilities can easily be determined at project definition stage. Making presentation to all concerned parties simple and clear; and decisions can consequently be made faster.

The application of MCS techniques and the availability of powerful desktop computers are the key elements to the underlying simplicity and reliability of this approach. Enabling the determination of the propagation of uncertainties of most simple and complex measurement systems including many which cannot be found readily by conventional analytical means.

A detailed description of the MCS technique as applied to uncertainty determination can be found in the paper “Uncertainty of Complex Systems by Monte-Carlo Simulation” [1].

## 2 APPLICATION POSSIBILITIES

When a new measurement station is built, an uncertainty calculation of the system should be carried out. These figures are intended to show any associated parties the systems maximum potential exposure at any given time, the limits of this figure are usually quoted in any legal agreement. If the new measurement point is entering an existing pipeline system then it will be expected to meet the same level of uncertainty budget as the other entrants into the system (this may be negotiable).

The initial intention of the MCS model was to ascertain the uncertainties of such a system. During the development of the model other uses started to materialise; and as more individuals interfaced with the product the application possibilities increased. Aspects of not just uncertainty percentages but actual production allocation and determination became viable, mis-measurement determination, facilities optimisation (enabling resource application to areas of greatest exposure) and future prospect potential determination. This type of model is now being taken forward with the intention of becoming a full operational tool. By taking the concept further, has allowed a full pipeline system model to be developed giving a higher level overview of exposure for all partners.

The conceptual stage of a project, looking at existing facilities and new tie back wells can be reduced. By quickly determining the best overall usage of the existing facilities against the available and proposed flow regimes under the conditions prevailing or envisaged. Thus making the determination of whether it's a viable proposal or not at an earlier stage, or in fact that by changing the present regime of operating scenarios other previously discarded ventures may now be viable.

### 2.1 Uncertainty Model

#### Propagation of Uncertainties

Input distributions may be normal, uniform, triangular, skewed, or any shape that reflects the nature of the measurement being assessed (see appendix 1 for examples). Using conventional analytical techniques [2], [3], the various distributions are handled in the same manner, consequently the resultant “Root Sum Square” (RSS) solution will give a “Normal” distribution regardless of the input type. The output distribution can also be in error depending on the input shapes, skewed from the actual true mean with no indication of or ability to calculate the offset value. Combination of distributions that are not symmetrical, or are poorly defined, to find system uncertainty is difficult to achieve using analytical mathematics and this problem is not confined to measurement uncertainty [4].

By utilising the MCS technique to combine distribution curves, the type of input will be reflected in the resultant output distribution, the correct propagation of distribution is carried forward (both in terms of returning actual means and uncertainty distributions). The example in figure 1 shows the combination of normal and triangular distributions, giving values for both conventional and MCS resultants.

### Skewed Triangular, Normal and Combined Distribution

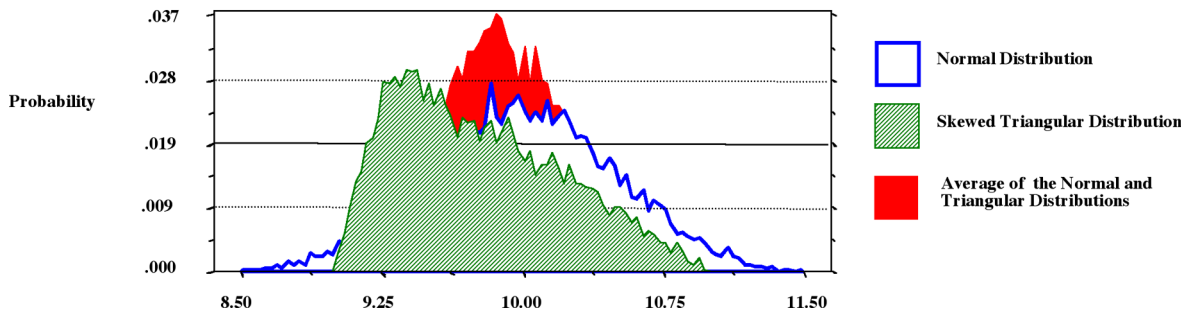


Figure 1

- A “Normal” distribution is generated with a mean of 10 with 95% confidence limits of +/- 10%
- A “Skewed “Triangular” distribution is generated with a mean of 10 skewed to 9.3 with limits of +/-10% giving a mean of 9.77
- These distributions are averaged giving a “Gamma” distribution with a mean of 9.89. This is compared with the average of 10 if the means are found without knowledge of the distribution thus demonstrating how a systematic bias error may arise.

Comparison of Distribution Means	Conventional	Monte Carlo	Discrepancy
Triangular Distribution	10.00	9.77	0.23
Normal Distribution	10.00	10.00	0.00
Mean of the Average (Gamma Distribution) of Normal and Triangular Means	10.00	9.89	0.11

## Building a System Model - Stage 1

The model is made up from various macro modules. These are joined together to form an interactive system, which is easy to manipulate by the user, whilst not compromising integrity. Taking each step at a time, we start the building of the model by looking at an individual stream on a measurement system. The user interface package is in pictorial format, allowing simple manipulation or data entry and even more importantly easy access to the results. The model is made up from a mixture of visual basic macros, excel sheets and incorporates MCS modules. The beauty of this build up approach is the fact it doesn't matter what type of system is being analysed, orifice, ultrasonic, turbine etc. or even a mixture of all types can be accommodated.

The system inputs can be any of or a combination of the following; constant values, variables dependant on process conditions or results of calculations. The model is built to be generic for any particular type of device, the variants of input types e.g. density measured or calculated, can be selected by software switches. The model has the ability to handle snapshots of live values or user entered values.

Modelling an orifice system (see Fig 2) Visual basic modules handle the conventional processing of AGA8 line density and ISO5167 (DP uncertainty determination) inputs and results. Pressure and Temperature sensitivities are handled via an Excel spreadsheet and outputs from these are fed into various MCS modules. In turn the results are fed through to final computation via more visual basic modules (ISO5167, ISO6976 and AGA8) giving values for Mass, Volume and energy (both quantity and uncertainty).

The distribution of the orifice meter stream mass, volume and energy flow rate found from the model in figure 2 yields a mean and uncertainty that agrees well with conventional methods when all uncertainty sources are considered. However by looking at the distribution and by comparing the mean with the true calculated value a small bias is observed. This is due to the non-linearity resulting from the square root of the density and differential pressure within the ISO5167 calculation. The bias, which is insignificant for a single stream, compounds as streams are combined leading to a larger system bias, overlooked by conventional uncertainty methods.

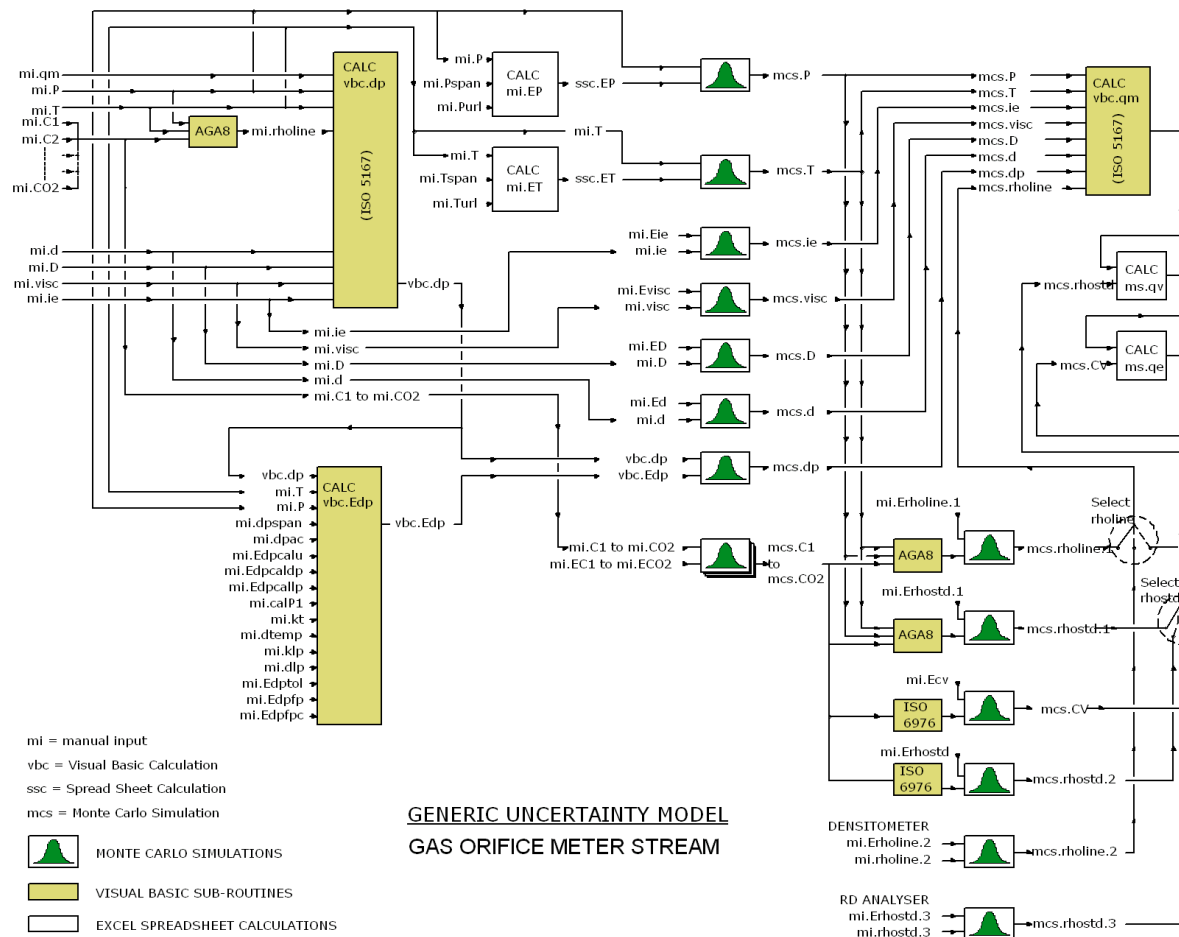


Figure 2

## Building a System Model - Stage 2

Taking the single stream into the measurement station scenario, by the addition of extra streams (duplicate macro of first stream) a measurement station can be developed (see Fig 3).

**Note:** care must be taken with the common equipment, effects should not be calculated twice, the application should be selectable via software switches. The program should also give warning as to possible duplication of effects.

Also the model will negate the requirement for duplication of input variables. Again the system will be presented in pictorial format, showing the necessary intermediate values as well as the final summated outputs.

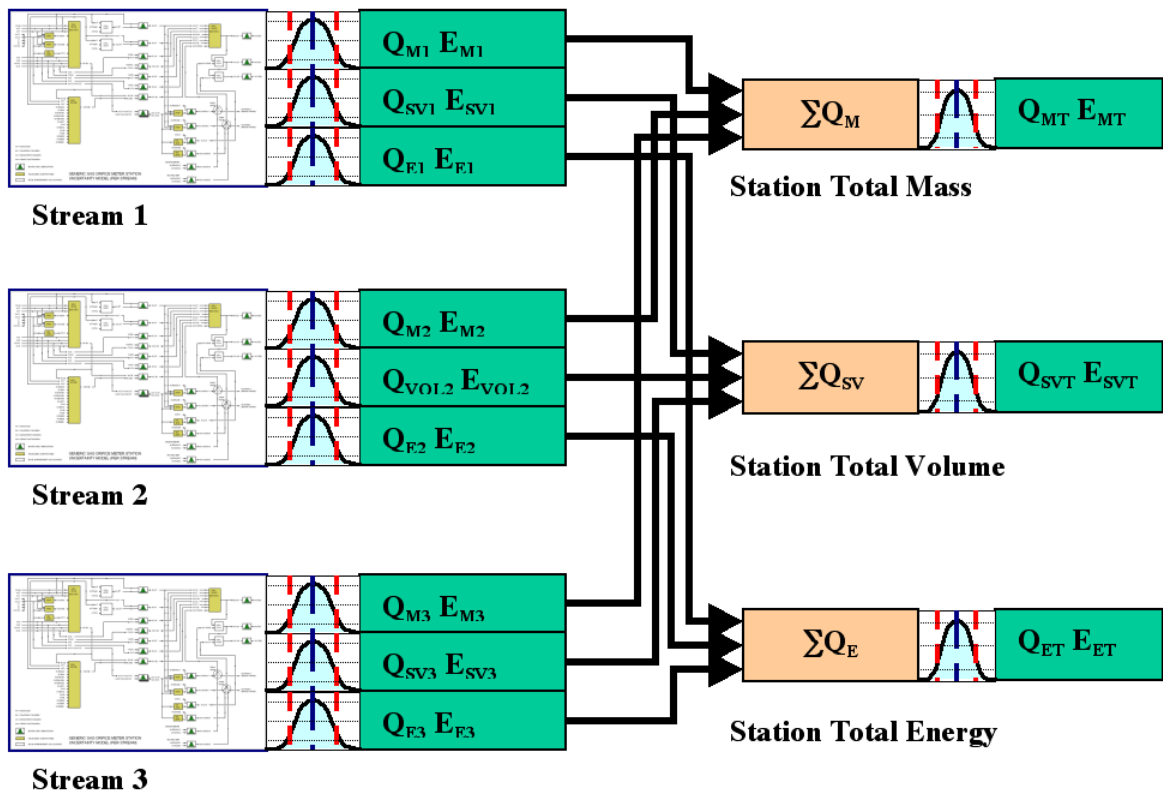
This gives the user his exposure, not only as a percentage of uncertainty, but also in actual value of output. The model can be used in cases of equipment failure to quickly identify the impact, and be used as a calculation basis for any mis-measurements required. The main exposure is to ensure that the agreement clauses for system uncertainty are being met, and if required to form the basis of a dispensation to allow continued operation based on exposure during equipment failures.

The simulated stream measurements are applied randomly to the model to give a set of flow rates with normal distribution. The total flow rate is found from the mean of the distribution and the uncertainty with a 95% confidence level found from twice the standard deviation. Between 20,000 and 100,000 simulation runs may be required to give a good definition to the resultant distribution, a rule of thumb is that as the number of input variables increases, so does the required number of runs – ratio of 1: 1000. Whilst this sounds onerous it will take less than a few minutes to complete, using modern powerful desk top computers and software packages.

The example in figure 3 shows three identical orifice meter streams. The discharge coefficient uncertainty and expansion factor uncertainty, which are common to all streams at the same flow rate, are combined with the individual stream uncertainties. With conventional methods this is found from the RSS of the uncertainties whereas with MCS methods the uncertainty distributions are summed and the uncertainty is found from the mean and 95% confidence limits of the resulting distribution.

When the uncertainty results are compared the MCS uncertainty is found to be less than the RSS uncertainty, which is due to the combination of the slight bias in each stream distribution. When the true result is compared to the MCS distribution mean the bias observed is greater than the bias observed for a single stream but is nevertheless small. The RSS method of combining uncertainties overestimates the system uncertainty and does not identify the system bias and strictly speaking is invalid for propagating uncertainties with an inherent bias.

Figure 3



*Station Model*

- Mass Uncertainty
- Volume Uncertainty
- Energy Uncertainty

## Building a System Model - Stage 3

The previous stage developed a measurement station. If this station were part of a bigger picture, a plant or multi-user pipeline, it would have an impact on the resultant output values. The export station of the system will determine the size of the pot (or pie) while the input systems will determine the share of the pot (or pie). If we refer to each measurement station as a nodal point within an overall system the model can then take its third step. A system model built up of all the nodal points, again in an overall pictorial image allowing the system manager the values at each point and the associated uncertainties. This means a decision affecting the system can be made based on sound information, allowing for optimal usage of system resources and giving knowledge of key areas of impact.

As the system grows the simulation run time will increase, however this can be negated by increasing processing capacity.

The building blocks can be utilised for the development of any type of system arrangement. An allocation system, looking at the terminal and field meters, can give by difference determinations of unmeasured inputs in terms of value and uncertainty (see Fig 4). Pipeline models, for use with multiple partner systems, can give each individual quantity, exposure and tax liability (see Fig 5). Being user configurable any combination of stations is possible giving any output requirement.

## Allocation / Reservoir Management

Once the model has been tested, the input values can be tied to live data sources. Simulation must be run in batches, giving the user the required data for production totals and consequent Gas / Oil ratios, daily or as frequently as hourly. The possibility exists to build up a case history, utilising well tests, compositional analysis, production parameters and choke positions to generate figures whilst the measurement equipment is unavailable on any particular inlet separator.

Field A Separator Meter

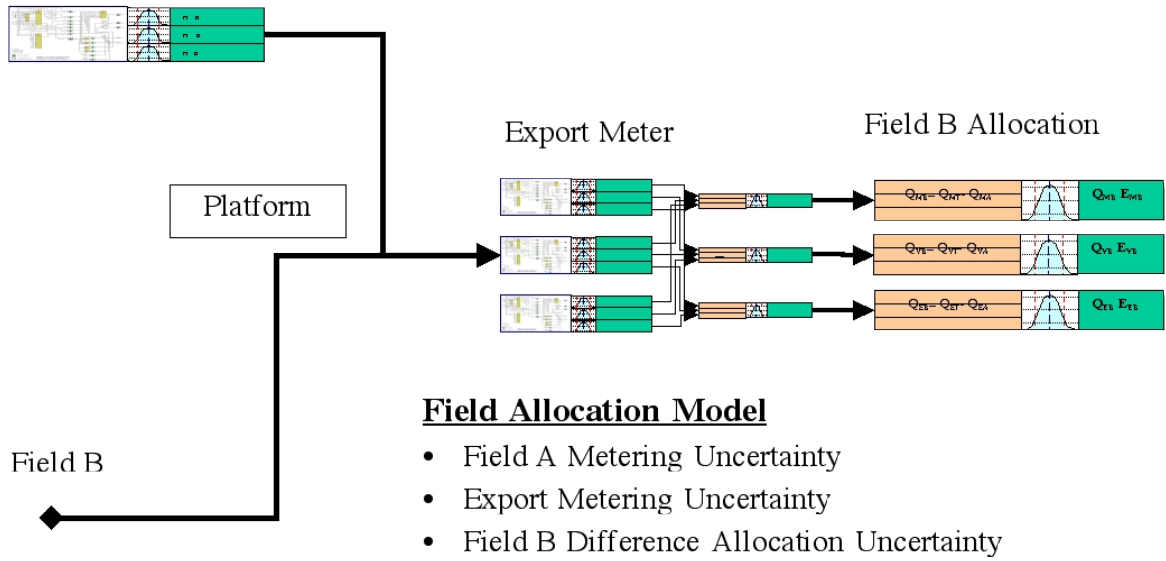


Figure 4

Field A Separator Meter

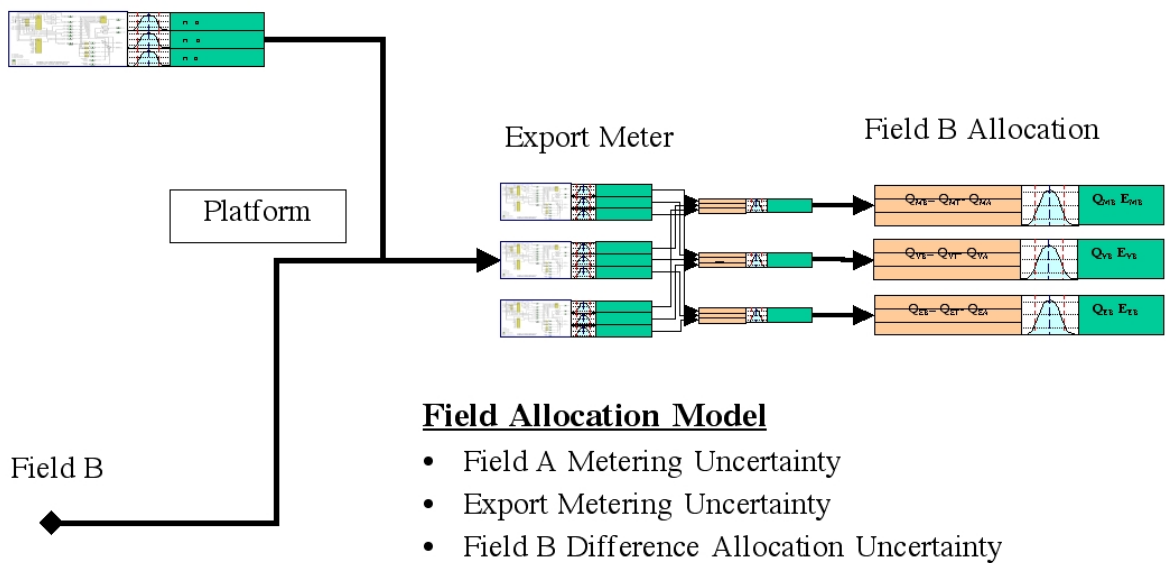


Figure 5

## Benefits for Project Work

The model approach gives two main benefits for any project group; firstly it can provide the necessary station or system uncertainties at hand over to operations and secondly it allows the project team to quickly quantify the various options available to them in terms of meeting the agreement or system operator stipulated limits.

By utilisation of a derived system model of a facility, the inputs to the various separators can easily be manipulated. The life cycle of wells can mean, where once a separator was fully utilised it may now have the potential for another stream due to the decline in the existing well. This gives the potential for the processing of new fields across existing facilities, however it can be difficult getting funds if the potential financial expenditure is not kept to the minimum. In manipulating the various options, gaining answers on quantities and uncertainties, the project team can quickly identify the preferred options and equipment needed. Also the model will give necessary data for presentation of the viable case based on best utilisation of existing facilities. This gives the potential for previously shelved projects to be revisited, and by correct manipulation of equipment made viable.

## 3.0 CONCLUSIONS

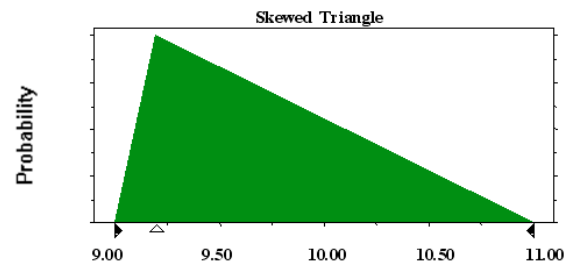
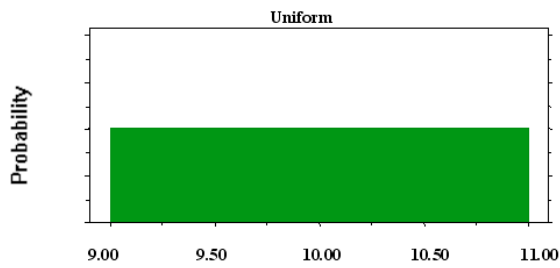
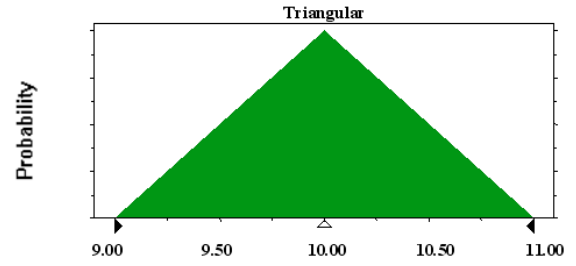
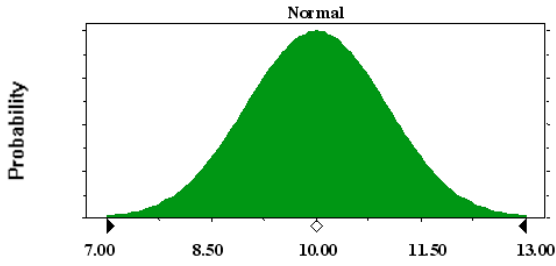
- Forming an alliance between operators and service companies ensures a product is developed faster with the necessary interface and output requirements needed to be utilised by industry.
- The standard static statement of uncertainty value produced as part of the project groups hand over package, has been superseded with a dynamic easily updated figure which can be used by the operations to optimise system management and identify areas with the greatest exposure for effective resource utilisation.
- System allocation and measurement spot checks can be run quickly providing the required information to enable fast determination of value for accounting purposes.
- Project groups can quickly identify the best utilisation of existing facilities when accommodating new field developments. Both in terms of flow and uncertainty for both the installation and also potentially the system to which it enters.

## REFERENCES

- [1] Basil, M. and Jamieson, A. W. (1998). Uncertainty of Complex Systems by Monte Carlo Simulation, North Sea Flow Measurement Workshop, Gleneagles, 26 – 29 October 1998
- [2] British Standards Institution (BSI), Guide to the expression of uncertainty in measurement, PD6461: Part 3: 1995.
- [3] International Organization for Standardization (ISO): Measurement of fluid flow – Evaluation of uncertainties, ISO5168TR: 1998.
- [4] Mooney C. Z., Monte Carlo Simulation, Quantitative Applications in the Social Sciences Series, Sage Publications Inc, 1997.

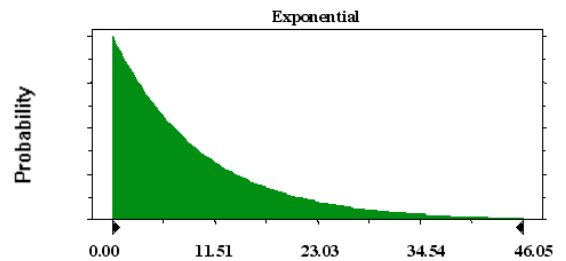
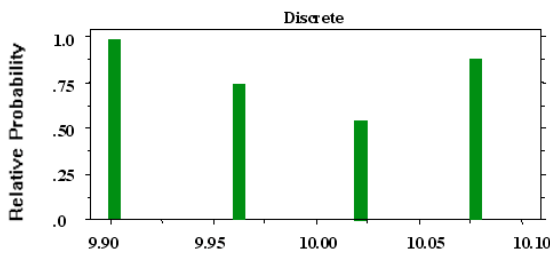
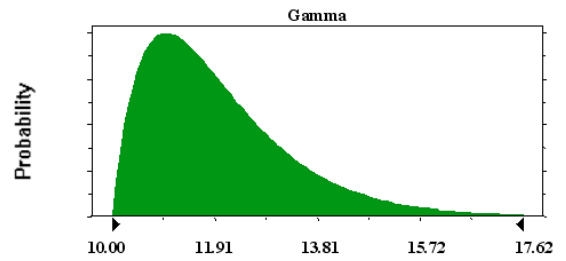
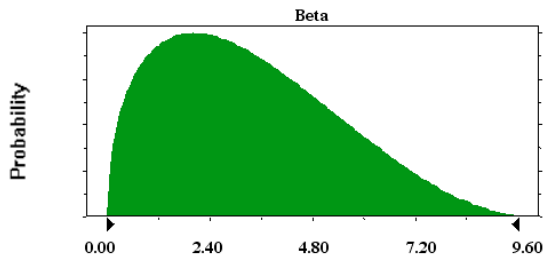
## APPENDIX 1A

### Typical Randomly Generated Input Distributions



## APPENDIX 1B

### Asymmetric Randomly Generated Input Distributions

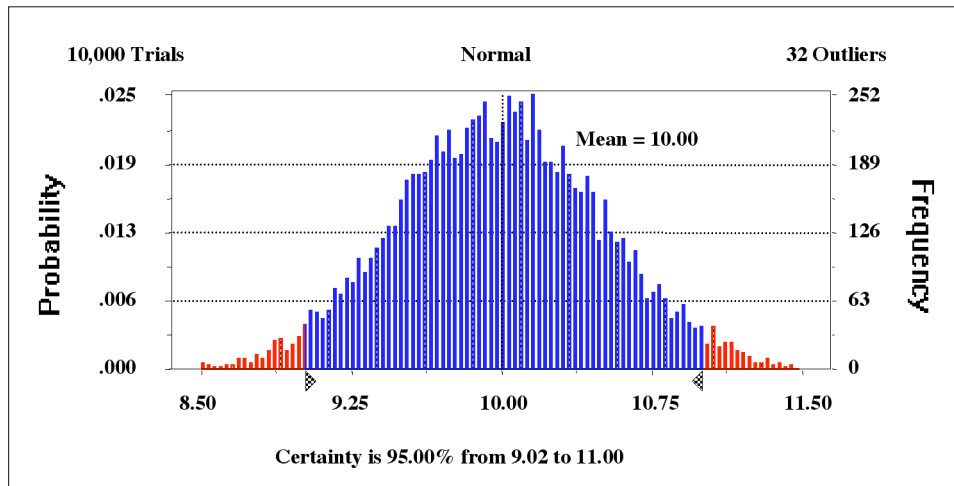


## APPENDIX 2A

### A Typical Normally Distributed Output

Outputs within the 95% confidence limits shown with arrows. The uncertainty is defined as the 95% confidence limits that are at 2 (1.96) standard deviations limits.

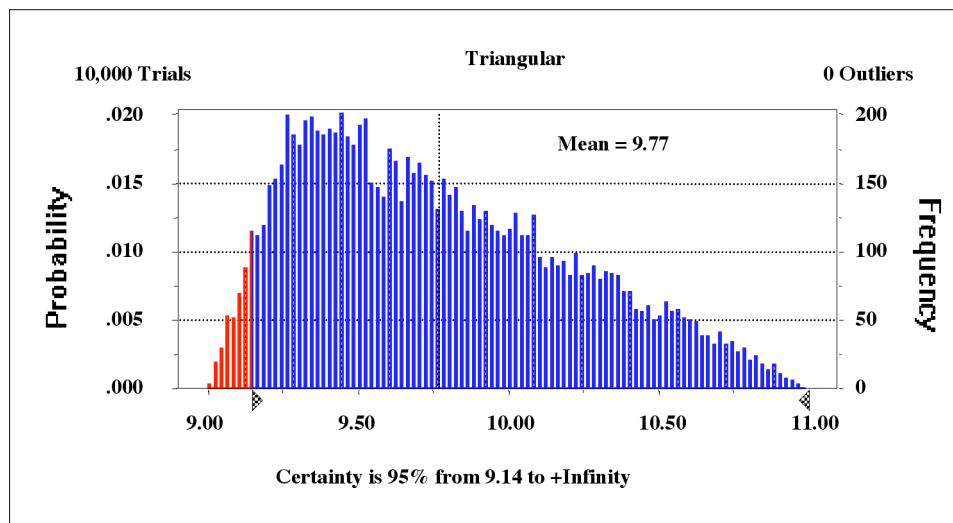
10,000 trials shown would be needed for a large model and for more presentable results.



## APPENDIX 2B

### Output of a Triangular Distribution

The result is offset from the correct mean of 10 by -0.23 with the 95% confidence limits only the left hand side.

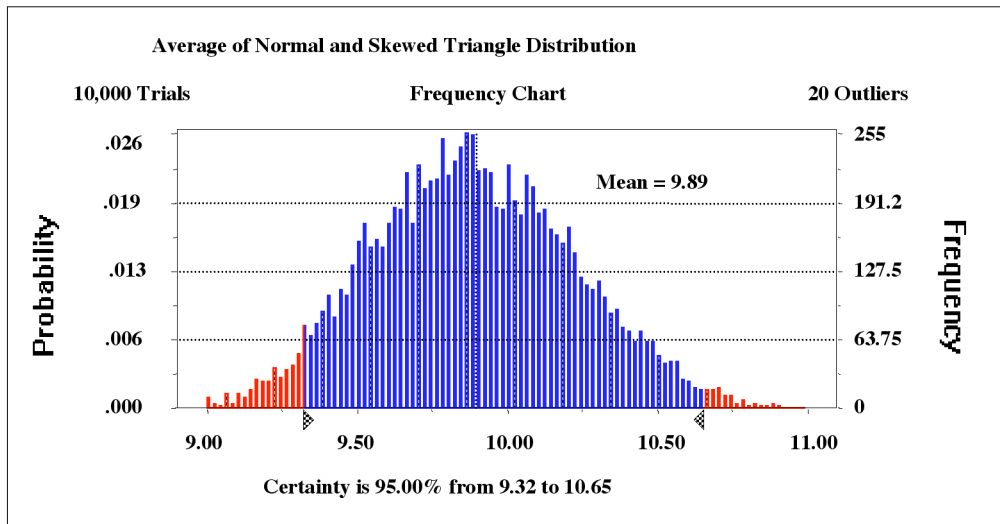


## APPENDIX 2C

### *Output of the Average of a Normal Distribution and a Triangular Distribution*

Outliers show the results that are out with limits for the dataset

95% confidence limits (shown as certainty limits) to illustrate bias





# PRESENTATION OF THE HANDBOOK OF UNCERTAINTY CALCULATIONS - FISCAL METERING STATIONS

*Eivind O. Dahl and Ronny Albrechtsen*  
*Christian Michelsen Research AS*

---

## 1. ABSTRACT

A new *Handbook* [1] for uncertainty calculations on fiscal metering stations is presented. The *Handbook* has been developed by Christian Michelsen Research AS (CMR) on behalf of the Norwegian Society for Oil and Gas Measurement (NFOGM) and the Norwegian Petroleum Directorate (NPD).

The aim of the *Handbook* is to secure a more uniform uncertainty evaluation of fiscal metering stations. The *Handbook* provides a practical introduction to uncertainty calculations based on the principles and terminology defined by the ISO-publication Guide to the expression of uncertainty in measurement [2]. Furthermore, the *Handbook* contains a comprehensive evaluation of two specific fiscal oil and gas metering stations. The uncertainty calculations are implemented in two software programs that are described and included as a part of the *Handbook*.

## 2. INTRODUCTION

### 2. Uncertainty in measurement

The fiscal measurement of oil and gas in the North Sea must be in accordance with NPD regulation [3]. This requires that an uncertainty analysis of a fiscal metering system must be performed according to “recognised standards”.

In practise, different methods for evaluation of measurement uncertainties are used. In 1995 the International Organisation for Standardisation (ISO) published the Guide to the expression of uncertainty in measurement [2]. The document is commonly referred to as the Guide. The overall objective of the Guide has been to establish an internationally accepted method for estimating measurement uncertainty, and to provide guidelines for the calculation procedure and the reporting of the results. In addition, the Guide has introduced some new terms and suppressed some traditional terminology to standardise the concepts so that “everyone speaks the same language” and agrees on how uncertainties should be quantified.

It should be noted that the Guide at present is an ISO recommendation and not a standard. However, the standard published in 1997 by the European co-operation for Accreditation of Laboratories (EAL) [4], is in conformity with the Guide. Previously, ISO 5168 [5] - [6] has been used for reference when calculating uncertainties on gas metering stations, and the principles have also to some extent been applied in uncertainty calculations on oil metering stations. However, ISO-5168 and the ISO-Guide are based on significant different views on measurement uncertainty [7], and ISO-5168 was revised and reduced to a technical report in April 1999 [8].

The Guide comprises a theoretical and a mathematical approach to the field of uncertainty calculations, and it provides detailed procedures for performing uncertainty calculations in general. The *Handbook*, however, provides a more practical approach to the field of uncertainty calculations, where the principles of the Guide are applied to an oil- and a gas fiscal metering station. The intention is further to simplify, and to some extent standardise, the uncertainty evaluation of fiscal oil and gas metering stations.

## 2.2 The Handbook

In 1994 the Norwegian Society for Oil and Gas Measurement (NFOGM) initiated the establishment of a workgroup with the scope of work: “Uncertainty calculations of flow measurements in the oil and gas industry”. Based on the previous work at CMR on uncertainty calculations [9]-[13], the workgroup invited CMR to propose a project for completion of the work. In 1997 CMR therefore proposed a project for developing a *Handbook* for uncertainty calculations of fiscal metering stations. The project was initiated and financially supported by NFOGM and NPD in 1998.

The *Handbook* includes uncertainty calculations and analysis of the two fiscal metering stations. This analysis reveals the uncertainties that must be included in the calculations and which are negligible. Two programs have been developed in Microsoft Excel 97 for performing uncertainty calculations on these two metering stations. The programs are part of the *Handbook*, which also serves as a user manual.

The functional relationships and measurement procedures used in fiscal metering stations to calculate the standard volume flow rate (oil) or the mass flow rate (gas) are vital for the uncertainty evaluation. Thus, the necessary functional relationships and procedures are described and outlined along with references in the *Handbook*. The *Handbook* may therefore to some extent serve as a measurement *Handbook* for fiscal metering stations. The *Handbook* is separated in two parts; one part covers the uncertainty calculations and evaluation, and a second part contains the user manuals for the software programs.

By practical use of the *Handbook*, the reader should have gained sufficient knowledge about uncertainty analysis to secure proper application of, and to fully exploit, the calculation programs. The user should then also be able to perform similar uncertainty evaluations on other kinds of instrument and measurement systems.

A reference group comprising six metering specialists has reviewed the *Handbook* and the calculation programs in order to secure the quality of the final product

### 3. UNCERTAINTY ANALYSIS

#### 3.1 Scope of work

The fiscal metering stations evaluated in the *Handbook* are intended to be typical, and consist of equipment most widely used in the North Sea. The equipment of the metering stations evaluated is listed in Table 1 and Table 2. The fiscal oil metering station is based on turbine meter measurements and pipe proving, and is based on use of *K-factor* and volume correction factors in determination of the standard volume flow rate. The fiscal gas metering station is based on orifice plate measurements, and includes an on-line (by-pass) installation of the density transducer with optional correction of density from by-pass conditions to line conditions.

Table 1 Equipment list for the evaluated fiscal oil metering station.

Measurement	Instrument
Volume flow rate	Turbine Meter / Pipe Prover (general type)
Temperature	Rosemount 3144 Temperature Transmitter Class A (EN 60751) Temperature Element
Static Pressure	Rosemount 3051P Pressure Transmitter
Density	Solatron Model 7835 Liquid Density Transducer

Table 2 Equipment list for the evaluated fiscal gas metering station.

Measurement	Instrument
Mass flow rate	Orifice Meter (general type)
Temperature	Rosemount 3144 Temperature Transmitter Class A (EN 60751) Temperature Element
Differential Pressure	Rosemount 3051P Differential Pressure Transmitter
Static Pressure	Rosemount 3051P Pressure Transmitter
Density	Solatron Model 7812 Gas Density Transducer

In section 3.3 a sample of an uncertainty analysis of the Solatron 7835 Liquid Density Transducer is shown, while the *Handbook* covers the other transducers.

#### 3.2 Calculation and evaluation

The Guide [2] procedure for calculating and evaluating uncertainties has been applied consistently throughout the *Handbook*. The Guide procedure includes establishment of the equations for mathematically combining the standard uncertainties based on the functional relationship between the measurand and the input quantities. This means that the sensitivity of the quantity in question with respect to the different input measurements can be taken into account through calculated sensitivity coefficients. The Guide offers a universal method for uncertainty analysis where the standard uncertainties are transferable. This means that the result of an uncertainty calculation can be used directly in a subsequent uncertainty evaluation, which makes the measurements taken at different times and at different places comparable.

The *Handbook* contains complete calculations of the uncertainties of the different primary variables, such as temperature, absolute pressure, differential pressure and density. The primary variables, with their calculated uncertainties, are further used with the functional relationships and measurement procedures of the metering stations to calculate the combined uncertainties of the flow rates. The functional relationships and measurement procedures, which are described in the *Handbook*, are according to measurement standards, such as [14]-[23]. Thus, the *Handbook* may to some extent be used as a guide for fiscal metering stations.

Based on the algorithms and measurement procedures defined in the standards, uncertainty budgets have been established. Uncertainty budgets provide means for evaluating the uncertainties of the input quantities, as well as evaluating their influence on the combined uncertainties of the calculated results.

### **3.3 Example of uncertainty analysis**

An example of uncertainty analysis of the liquid density measured by the Solatron 7835 Liquid Density Transducer [24] is given in Section 3.3.1. The measured liquid density is pressure and temperature corrected according to specific algorithms, which are outlined in the Appendix. In this example the density meter is mounted on-line (in a by-pass), downstream the turbine meter. The by-pass installation would normally require a separate correction for the pressure and temperature deviations between the by-pass and line conditions. This installation effect is described in Section 3.3.2.

#### **3.3.1 Liquid density transducer uncertainty**

To calculate the uncertainty of the measured density, the functional relationships for both the primary density measurement and the pressure and temperature corrections are required. Furthermore, the model uncertainties that are attached to the corrections themselves must also be included, since they are not ideal corrections but e.g. derived from experimental tests. The functional relationships and the correction procedures for the Solatron 7835 Liquid Density Transducer are briefly described in the Appendix, while the *Handbook* [1] treats the subject in fully details.

An uncertainty budget for the density transducer can be established using the procedure of the Guide. The uncertainty budget is very useful when comparing the magnitude of the different uncertainty contributions, and it may reveal if some of the uncertainties can be neglected in order to simplify the uncertainty calculations. Such a sample uncertainty budget for the liquid density measurement is shown in Table 3.3. This uncertainty budget is only briefly described here, while the *Handbook* [1] presents detailed uncertainty budgets for all the transducers in the oil and gas metering stations as specified by Table 1 and Table 2.

The combined standard uncertainty  $u_c(\rho)$  of the measurand (liquid density) equals the positive square root of the combined standard variance. Standard uncertainty is the uncertainty of a result of a measurement expressed as one standard deviation. The combined standard variance  $u_c^2(\rho)$  is calculated as follows<sup>1</sup>:

$$u_c^2(\rho) = \sum_i (S_i^2 \cdot u_i^2) \quad (1)$$

where

- $S_i$  - sensitivity coefficient of input quantity i
- $u_i$  - standard uncertainty of the input quantity i

The sensitivity coefficients are obtained from the partial derivatives of the functional relationship with respect to the different input quantities of interest (e.g., temperature and pressure). An example of how to calculate the sensitivity coefficients is illustrated in the Appendix.

Input quantities that contribute to the combined standard uncertainty of the liquid density are given in Table 3.3 along with sample values.

The transducer uncertainty<sup>2</sup> and the uncertainties due to stability<sup>3</sup> and repeatability are given in the technical manual for the liquid density transducer [24].

The measured density is pressure and temperature corrected according to the algorithms given in the technical manual (cf. Appendix). The uncertainties of the pressure and temperature measurements (P, T) must therefore also be included in the calculation of the combined uncertainty. In the Appendix the expressions for the sensitivity coefficients are derived based on the correction algorithms.

The pressure and temperature correction procedure is empirical and not ideal. An imperfect correction introduces an extra uncertainty (model uncertainty) that must be included in the uncertainty budget. Hence, the uncertainties of the pressure and temperature corrections are included in Table 3.3 as “temperature effect” and “pressure effect”. These model uncertainties are given in the technical manual for the liquid density transducer.

The expanded uncertainty  $U(\rho)$  of the final density estimate,  $\rho$ , can be evaluated by multiplying the combined standard uncertainty by a coverage factor,  $k$ , on the basis of the level of confidence required for the interval  $r \pm U(\rho)$ . Assuming a normal distribution of  $\rho$ , and requiring a level of confidence close to 95%, yields  $k_{95} = 1.96$  <sup>a</sup> 2.0. Thus, the expanded uncertainty at 95% confidence level<sup>4</sup> is given by

$$U(\rho) = k_{95} \cdot u_c(\rho) \quad (2)$$

---

<sup>1</sup> If, however, some of the input quantities are correlated then covariance terms have to be included in Eq., see the Guide [2] or the Handbook [1] for fully details.

<sup>2</sup> The uncertainty due to the transducer includes calibration reference uncertainty

<sup>3</sup> The uncertainty due to stability is based on a yearly calibration interval and represents the drift (increasin /decreasing offset) in the readings with time.

<sup>4</sup> A confidence level of 95% corresponds to two standard deviations.

**Table 3.3 Sample uncertainty budget for the Solatron 7835 Liquid Density Transducer.**

Measurand: Liquid Density			Value at operating condition: 776 kg/m <sup>3</sup>		
Input quantity	Estimate	Standard Uncertainty	Sensitivity Coefficient	Standard Variance	Expanded Uncertainty (k <sub>95</sub> = 2)
Transducer	-	0.0750 kg/m <sup>3</sup>	1	5.625·10 <sup>-3</sup>	
Stability	-	0.0750 kg/m <sup>3</sup>	1	5.625·10 <sup>-3</sup>	
Repeatability	-	0.0100 kg/m <sup>3</sup>	1	1.0·10 <sup>-4</sup>	
Temperature effect	-	0.11250 kg/m <sup>3</sup>	1	1.266·10 <sup>-2</sup>	
Pressure effect	-	0.03030 kg/m <sup>3</sup>	1	9.181·10 <sup>-4</sup>	
<i>T</i>	65 °C	0.056 °C	0.01580 kg/m <sup>3</sup> /°C	7.83·10 <sup>-7</sup>	
<i>P</i>	20.2 barg	0.08 bar	0.0101 kg/m <sup>3</sup> /bar	6.53·10 <sup>-7</sup>	
Combined variance			u <sub>c</sub> <sup>2</sup> (ρ)	0.02493	<b>U(ρ)</b>
Combined standard uncertainty:			u <sub>c</sub> (ρ)	0.158 kg/m <sup>3</sup>	<b>0.32 kg/m<sup>3</sup></b>

It is evident from Table 3.3 that the pressure and temperature measurements (P, T) have negligible influence on the combined uncertainty compared to the other contributors. However, the uncertainty of the temperature correction (Temperature effect) is the largest contributor and it is actually larger than the uncertainty of the transducer itself. Thus, the uncertainty due to the temperature correction cannot be neglected from the uncertainty budget.

### 3.3.2 Installation effects

If the liquid density transducer is mounted in a by-pass loop (on-line measurements), a pressure and temperature deviation between the line and by-pass loop will occur. This effect must be included in the combined uncertainty of the liquid density measurement.

The IP Petroleum Measurement Manual, Part VII, Density [21] gives guidelines for on-line installations of liquid density meters. Maximum pressure and temperature deviations for different HC liquids, that will cause a change in liquid density of 0.03% are given in the IP manual. For stabilised crude oil of 850 kg/m<sup>3</sup>, the maximum differences in pressure and temperature are 4 bar and 0.4°C respectively [21], and these maximum deviations will each cause a change in the liquid density of 0.03%. The temperature and pressure coefficients of the quoted crude oil are 0.0007 g/ml/°C and 0.00007 g/ml/bar, respectively. The coefficients may change with operating conditions, and the uncertainties are in this case assumed to have a rectangular distribution rather than a normal distribution<sup>5</sup>. The uncertainties caused by P and T deviations are not considered to be purely random, but will also contain systematic effects. Ideally the systematic effect should be corrected for, but in practise they may be hard to evaluate and quantify.

<sup>5</sup> The pressure gradient is expected to be negative, while the sign of the temperature gradient depends on the ambient temperature. It is therefore assumed that the quoted uncertainty of 0.03% of reading represents endpoints of a uniform or rectangular probability distribution of the density. The standard uncertainty due to P and T deviations can then be computed as (0.0003/√3) or rather than (0.0003/k<sub>95</sub>) or for a normal (Gaussian) distribution. Assuming a rectangular distribution gives a conservative estimate, which represents the “worst case” scenario.

For this sample calculation, these coefficients are used for the liquid density of 776 kg/m<sup>3</sup>, even if they are only valid for a crude oil with density equal to 850kg/m<sup>3</sup>. In a real case, however, one must document the real deviation in temperature and pressure caused by the by-pass installation at the actual operating conditions, and further how this influence the liquid density measurement. I.e., the values of the temperature and pressure coefficients should be determined for the specific oil.

Table 3.4 Sample uncertainty budget for the Solatron 7835 Liquid Density Transducer including the uncertainty due to 4 bar pressure and 0.4°C temperature differences between the line and by-pass loop.

Measurand: Liquid Density			Value at operating condition: 776 kg/m <sup>3</sup>			
Input quantity	Estimate	Standard Uncertainty	Sensitivity Coefficient	Standard Variance	Expanded Uncertainty (k <sub>95</sub> = 2)	
Transducer	-	0.0750 kg/m <sup>3</sup>	1	5.625·10 <sup>-3</sup>		
Stability	-	0.0750 kg/m <sup>3</sup>	1	5.625·10 <sup>-3</sup>		
Repeatability	-	0.0100 kg/m <sup>3</sup>	1	1.0·10 <sup>-4</sup>		
Temperature effect	-	0.11250 kg/m <sup>3</sup>	1	1.266·10 <sup>-2</sup>		
Pressure effect	-	0.03030 kg/m <sup>3</sup>	1	9.181·10 <sup>-4</sup>		
<i>T</i>	65 °C	0.056 °C	0.01580 kg/m <sup>3</sup> /°C	7.83·10 <sup>-7</sup>		
<i>P</i>	20.2 barg	0.08 bar	0.0101 kg/m <sup>3</sup> /bar	6.53·10 <sup>-7</sup>		
Temperature deviation	0.4°C	0.1344 kg/m <sup>3</sup>	1	1.807·10 <sup>-2</sup>		
Pressure deviation	4 bar	0.1344 kg/m <sup>3</sup>	1	1.807·10 <sup>-2</sup>		
Combined variance			$u_c^2(\rho)$	0.06107		$U(\rho)$
Combined standard uncertainty:			$u_c(\rho)$	0.247 kg/m <sup>3</sup>		<b>0.49 kg/m<sup>3</sup></b>

From the uncertainty budget in Table 3.4 it can be inferred that the installation effects (the pressure and temperature deviations between line and by-pass) are the main uncertainty contributors. It is here demonstrated that the uncertainties due to the by-pass installation give a significant contribution to the combined uncertainty of the liquid density measurement, and must therefore be evaluated carefully.

### 3.4 Documentation

The *Handbook* briefly describes the documentation requirements regarding uncertainty calculations. According to the ISO-Guide [2], Chapter 7, all the information necessary for a re-evaluation of the measurement should be available to others who may need it.

This puts strong requirements on the documentation of the uncertainty evaluation and analysis. This means that it must be verified that the functional relationships applied in the evaluation in the *Handbook*, equals the functional relationships actually implemented for the transducer or metering station in question.

Furthermore, documentation in form of uncertainty budgets (with background documentation of the algorithms and input quantities) like the ones presented in the *Handbook*, are suggested as a clear and straightforward way to present uncertainty calculations. These kinds of uncertainty budgets also provide powerful means for evaluation of the influence of different input quantities on the combined uncertainty.

## 4. THE EMU-99 SOFTWARE TOOLS

Based on the conclusions from the calculations and evaluations in the *Handbook*, two Excel programs have been developed for performing uncertainty evaluations of the fiscal oil and gas metering stations. The programs, which also are parts of the *Handbook*, are made in Microsoft Excel 97 and are used as normal workbooks in Excel.

The EMU-99 (Evaluation of Metering Uncertainties) programs may as well be applied to other instruments than listed in Table 1 and Table 2. However, the user must then evaluate and verify that the type of uncertainty specifications and the functional relationships incorporated in the EMU-programs are valid for the alternative instrument. Furthermore, the user must verify that the evaluations and conclusions made in the *Handbook* regarding the instrument in question are also applicable to the alternative instrument. If the above requirements are verified and documented, the user may change the default uncertainty values and confidence levels in the programs according to the data sheets of the alternative transmitters in order to calculate the uncertainty of the metering station for alternative instrumentation.

The programs contain only the input quantities found to be significant regarding the uncertainty calculation, thus minimising the amount of data needed and simplifying the calculations. The user may easily change input quantities, such as the operating conditions of the metering stations, in order to simulate the influence of changes in input quantities on various combined uncertainties of the metering stations that the programs calculate and display.

### 4.1 Output from the program

The outputs from the program may be used as supplement to the documentation of the uncertainty calculations, and as means for analysing the influence of different operating conditions on the combined uncertainty of the metering station. This may be well suited for people working with the design of new metering stations, and for renewal and re-evaluation of older metering stations.

The input data to the programs must be properly documented, and the functional relationships and default values implemented in the program must also be verified.

One of the output features is a graph presenting the combined relative expanded uncertainty of e.g. the mass flow rate of the gas metering station (or the standard volume flow rate of the oil metering station).

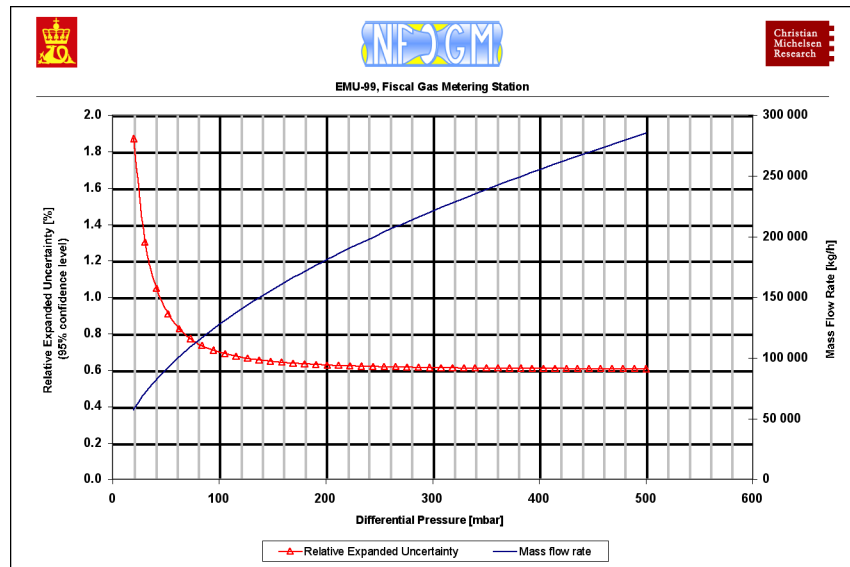


Figure 4.1 Typical output from the EMU-99, Fiscal Gas Metering Station, program presenting the relative combined expanded uncertainty and the standard mass flow rate vs. the differential pressure across the orifice.

Furthermore, a simple uncertainty summary report is generated by the program, which presents the most relevant information from the uncertainty calculation. The display of the uncertainty summary report is shown in Figure 4.2, and this may e.g. be used when varying some of the input quantities to study their influence on the combined uncertainty of the flow rate (in this case the mass flow rate).

	Unit	Value	Standard Uncertainty	Relative Expanded Uncertainty
Temperature	°C	50	0,056	0,23 %
Pressure <sup>1</sup>	barg	103,5	0,080	0,16 %
Differential Pressure	mbar	450	0,469	0,22 %
Orifice diameter	m	2,6631E-01	9,3245E-05	0,07 %
Pipe diameter	m	4,4455E-01	8,8909E-04	0,40 %
Density <sup>2</sup>	kg/m <sup>3</sup>	50,00	0,127	0,51 %
Diameter Ratio, β	-	0,5991	0,0012	0,41 %
Discharge Coefficient, C	-	0,60286	1,5071E-03	0,50 %
Expansibility Factor, z <sup>2</sup>	-	0,998339	0,000086	0,02 %
Orifice Plate buckling	kg/s	-	0,0000	0,00 %
Correlation term	kg/s	0,000820396	-	-
Differential Pressure	450	mbar	-	-
Mass Flow Rate	<b>276 722,24</b>	kg/h	-	-
Standard Uncertainty	<b>823,41</b>	kg/h	-	-
Relative Expanded Uncertainty (95% conf. level)	<b>0,61</b>	%	-	-

<sup>1</sup> Static pressure measured at ...: Upstream ...tapping

<sup>2</sup> Expansibility factor referred to: Upstream ...tapping

\*The density is corrected for installation effects

Figure 4.2 The uncertainty summary report display from the EMU-99, Fiscal Gas Metering Station program.

## 5 CONCLUSION AND FURTHER WORK

The major intention of the *Handbook* is to simplify, and to some extent standardise, the calculation of uncertainties of fiscal metering stations.

The *Handbook* may also be basis for courses on uncertainty calculations and lectures on uncertainty calculations and evaluations. It may even be used as a metering *Handbook* for oil and gas fiscal metering stations, while it covers the functional relationships and gives a brief overview of the instrumentation of such metering stations.

Further extension of the *Handbook* to also cover parallel metering runs, gas chromatography, ultrasonic metering stations and other transducers for measurement of primary variables like temperature, density and pressure are desirable. However, first the *Handbook* will be published and feedback based on practical use of the *Handbook* will be collected. A future revision is meant to include updates based on this feedback in addition to other possible extensions.

## 6. REFERENCES

- [1] Dahl E O, Nilsson J, Albrechtsen R, *Handbook of uncertainty calculations – Fiscal metering stations*, Christian Michelsen Research AS (CMR), Norwegian Society for Oil and Gas Measurement (NFOGM), Norwegian Petroleum Directorate (NPD), published by NFOGM, ISBN 82-91341-28-1.
- [2] ISO (International Organisation for Standardisation) (1995): Guide to the expression of uncertainty in measurement. On behalf of BIPM, IEC, IFCC, ISO, IUPAC, IUPAP, OIML. ISBN 92-67-10188-9.
- [3] Norwegian Petroleum Directorate (1997): Regulations relating to fiscal measurement of oil and gas in petroleum activities. ISBN 82-7257-522-1.
- [4] EAL-R2 (European Cooperation for Accreditation of Laboratories) (1997): Expression of the uncertainty of measurement in calibration. Edition 1. April 1997.
- [5] ISO 5168 (1978), Measurement of fluid flow – Estimation of uncertainty of a flow rate measurement, International Organisation for Standardisation, 1978.
- [6] ISO/DIS 5168 (1989), Measurement of fluid flow – Estimation of uncertainty of a flow rate measurement, International Organisation for Standardisation, 1989, revision of ISO 5168 (1978).
- [7] Grinten, Jos G.M. van der, Recent developments in the uncertainty analysis of flow measurement processes, NMi Certin B.V., The Netherlands, Paper 11, Paper presented at the North Sea Flow Measurement Workshop, Kristiansand, Norway, 27-30. October 1997.

- [8] ISO-TR 5168 (1999), Measurement of fluid flow – Estimation of uncertainty of a flow rate measurement, International Organisation for Standardisation, 1989, revision of ISO/DIS 5168 (1989).
- [9] Midttveit Ø. and Nilsson J. (1997): A practical example of uncertainty calculations for a metering station - conventional and new methods. Paper 12, Paper presented at the North Sea Flow Measurement Workshop, Kristiansand, Norway, 27-30. October 1997. Ref. no. CMR-97-A10025.
- [10] Dahl E.O. and Nilsson J., A work note on uncertainty calculations – conventional and new methods, Fiscal gas metering station, CMR-98-F10027, (CMR Confidential).
- [11] Dahl E.O. and Nilsson J., A work note on uncertainty calculations – conventional and new methods, Fiscal oil metering station, CMR-98-F10028, (CMR Confidential).
- [12] Lunde P., Frøysa K.-E., and Vestrheim M., Garuso – Version 1.0, Uncertainty model for the multipath ultrasonic transit time gas flow meters, CMR-97-A10014.
- [13] Midttveit Ø., Nilsson J., Johannessen A.A., Villanger Ø. and Albrechtsen, R., Cost effective allocation – Functional specification of the AMC-program, CMR-99-F10019, (CMR Confidential).
- [14] ISO (International Organisation for Standardisation), Measurement of fluid flow by means of pressure differential devices, ISO-5167-1:1995.
- [15] ISO (International Organisation for Standardisation), Measurement of fluid flow by means of pressure differential devices. Part1: Orifice plates, nozzles and venturi tubes inserted in circular cross-section conduits running full, ISO-5167-1:1995/AM1:1998.
- [16] ISO (International Organisation for Standardisation) (1999), Natural Gas – Measurement of properties. Part 1: Volumetric properties: density, pressure, temperature and compression factor, ISO CD 15970 – Rev April 1999.
- [17] European Norm, Industrial Platinum Resistance Thermometer Sensors, EN-60751, 1995.
- [18] Bureau International Des Poids et Mesures, Techniques for Approximating the International Temperature Scale of 1990, pp. 134-144, 1997, ISBN 92-822-2110-5.
- [19] API Manual of Petroleum Measurement Standards (1980): Chapter 11 Physical Properties Data, Chapter 1 Volume Correction Factors.
- [20] API Manual of Petroleum Measurement Standards (1987): Chapter 12 Calculation of Petroleum Quantities, Chapter 2 Calculation of Liquid Petroleum Quantities Measured by Turbine or Displacement Meters.

- [21] The Institute of Petroleum, Petroleum Measurement Manual, Part VII Density, Section 2, Continuous Density Measurement, Nov. 1983.
- [22] NORSOK standard, I-SR-105, Fiscal measurement systems for hydrocarbon liquid, Rev. 2, June 1998.
- [23] NORSOK standard, I-SR-104, Fiscal measurement systems for hydrocarbon gas, Rev. 2, June 1998.
- [24] Solatron 7835 Technical Manual, Part No.: 7835 5001, October 1994.

## Appendix

This appendix contains the functional relationships on which the uncertainty budgets in Table 3.3 are based. For even more detailed coverage of the calculation and evaluation, please refer to the “*Handbook of uncertainty calculations – fiscal metering stations*” [1]

**Table A.1 The values used in the sample calculation in Table 3.3.**

Parameter	Value
Uncorrected line density	776 kg/m <sup>3</sup>
Time between calibrations	12 months
Operating temperature	65 °C
Calibration temperature	15 °C
Operating pressure	20.2 barg
Calibration pressure	1.01325 bara
Calibration constant, $K_0$	$-1.19136 \cdot 10^3$
Calibration constant, $K_1$	$-2.65568 \cdot 10^{-1}$
Calibration constant, $K_2$	$1.23906 \cdot 10^{-3}$
Calibration constant, $K_{18}$	$-1.394 \cdot 10^{-5}$
Calibration constant, $K_{19}$	$9.234 \cdot 10^{-3}$
Calibration constant, $K_{20A}$	$4.466 \cdot 10^{-9}$
Calibration constant, $K_{20B}$	$-1.213 \cdot 10^{-6}$
Calibration constant, $K_{21A}$	$6.046 \cdot 10^{-2}$
Calibration constant, $K_{21B}$	$-1.641 \cdot 10^{-3}$

The uncertainties in the data sheet for the Solatron 7835 Liquid Density Transducer [24] are given at 95% confidence level. The Solatron 7835 Liquid Density Transducer is based on the vibrating cylinder principle, where the output is a periodic time of the vibrations. This periodic time is then related to the density according to:

$$D = K_0 + K_1 \cdot \tau + K_2 \cdot \tau^2 \quad (3)$$

where

- $D$  - uncorrected density [kg/m<sup>3</sup>]
- $K_0$  - constant from the calibration certificate
- $K_1$  - constant from the calibration certificate
- $K_2$  - constant from the calibration certificate
- $t$  - periodic time [ms]

The calibration constants,  $K_0$ ,  $K_1$  and  $K_2$ , are determined at a given calibration temperature (normally 20 °C) and pressure (normally 1.01325 bara).

If the transducer operates at temperatures other than the calibration temperature, a correction of the calculated density must be made for optimal performance. The temperature correction is performed according to:

$$D_T = D \cdot (1 + K_{18} \cdot (T - T_{cal})) + K_{19} \cdot (T - T_{cal}) \quad (4)$$

where

- $D_T$  - temperature corrected density [kg/m<sup>3</sup>]
- $D$  - uncorrected density [kg/m<sup>3</sup>] from Eqn. 3.
- $K_{18}$  - constant from the calibration certificate
- $K_{19}$  - constant from the calibration certificate
- $T$  - operating temperature [°C]
- $T_{cal}$  - calibration temperature [°C]

If the transducer operates at pressures other than the calibration pressure, a second correction for pressure must also be applied, and this correction is performed according to:

$$D_{PT} = D_T \cdot (1 + K_{20} \cdot (P - P_{cal})) + K_{21} \cdot (P - P_{cal}) \quad (5)$$

where

- $D_{PT}$  - pressure (and temperature) corrected density [kg/m<sup>3</sup>]
- $D_T$  - temperature corrected density [kg/m<sup>3</sup>] from Eqn. 4.
- $K_{20}$  - constant from the calibration certificate
- $K_{21}$  - constant from the calibration certificate
- $P$  - operating pressure [bar]
- $P_{cal}$  - calibration pressure [bar]

The constants,  $K_{20}$  and  $K_{21}$ , are given as a function of the line pressure and the calibration pressure:

$$\begin{aligned} K_{20} &= K_{20A} + K_{20B} \cdot (P - P_{cal}) \\ K_{21} &= K_{21A} + K_{21B} \cdot (P - P_{cal}) \end{aligned} \quad (6)$$

where

$K_{20A}$  - constant from the calibration certificate  
 $K_{20B}$  - constant from the calibration certificate  
 $K_{21A}$  - constant from the calibration certificate  
 $K_{21B}$  - constant from the calibration certificate

The functional relationships to be applied are given in Eqn. 4, 5 and 6. The functional relationship for temperature and pressure corrected density then becomes:

$$D_{PT} = \left\{ K_0 + K_1 \cdot \tau + K_2 \cdot \tau^2 \cdot (1 + K_{18} \cdot (T - T_{cal})) + K_{19} \cdot (T - T_{cal}) \right\} \cdot (1 + K_{20} \cdot (P - P_{cal})) + K_{21} \cdot (P - P_{cal}) \quad (7)$$

The sensitivity of the temperature and pressure corrected density, with respect to the temperature and pressure respectively, can then be found by partial differentiating Eqn. 7.

$$S_{D_{PT}-T} = \frac{\partial D_{PT}}{\partial T} \quad (8)$$

$$S_{D_{PT}-P} = \frac{\partial D_{PT}}{\partial P} \quad (9)$$

The changes between line and calibration temperature and pressure used in the calculations are 45°C and 20.2 bar, respectively.



# SQUARE ROOT ERROR AND IMPULSE LINE PULSATION AT CATS. TERMINAL MIDDLESBROUGH, UK

*Mike Donoghue & Martin Crane*

---

## 1. Introduction

The Central Area Transmission System (CATS) is a natural gas gathering system based in the central area of the North Sea. A riser platform and 255 miles of pipeline, including six subsea tie-in points, supplies gas to the Teesside based terminal that is situated on the North East coast of the United Kingdom. BP Amoco operates the system on behalf of CATS co-venturers which consists of the following companies BG International, BP Amoco, Amerada Hess, Phillips, TotalFina, and Agip

Current fields which flow gas through the CATS system include both BP Amoco operated and third party operated fields and are as follows:.

Everest	BP Amoco Operated
Lomond	BP Amoco Operated
J-Block	Phillips Operated
Armada	BG Operated
Erskine	Texaco operated
ETAP	BP Amoco Operated
Banff	Conoco Operated
Andrew	BP Amoco Operated

# CATS Pipeline Schematic

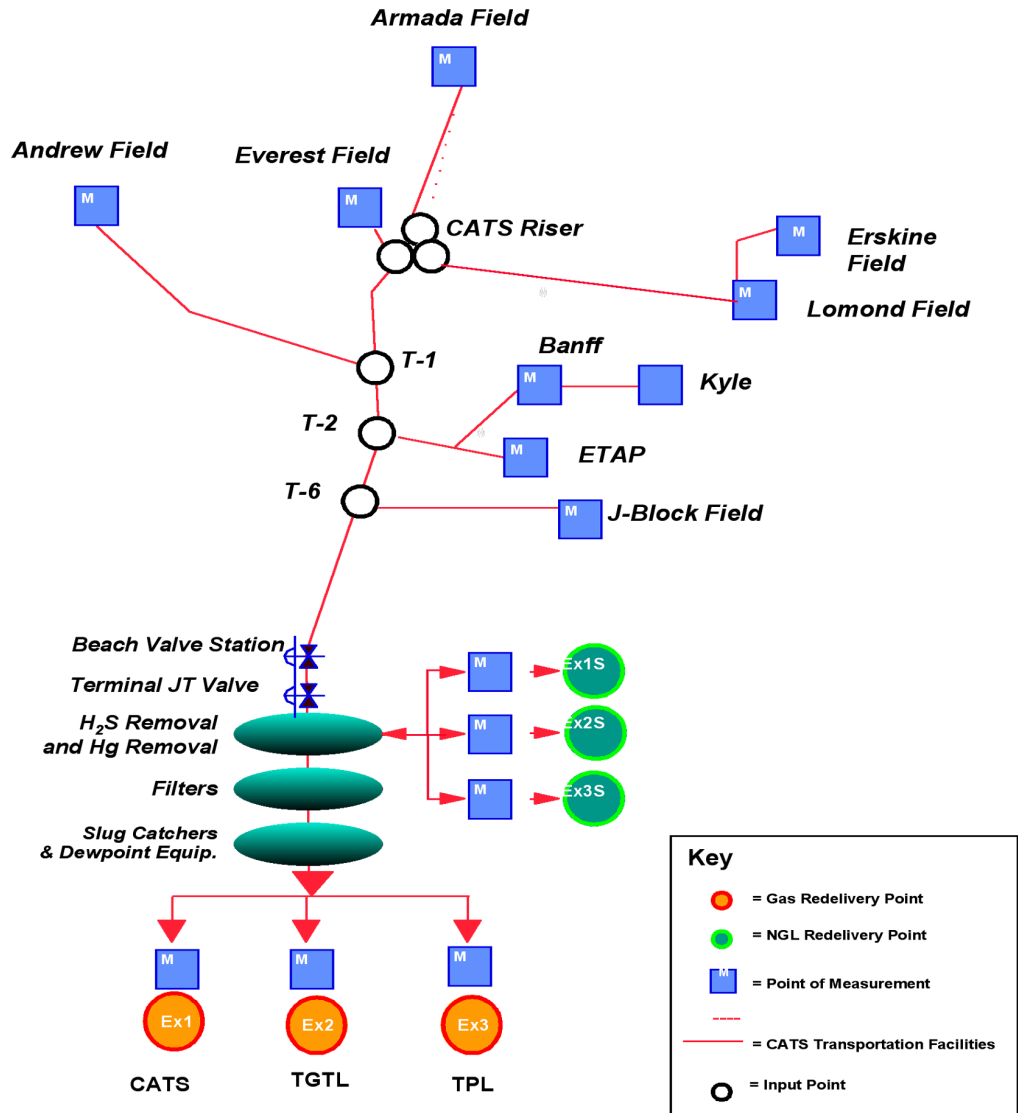


Fig 1

During 1996 the CATS terminal was expanded in order to transport gas from the ETAP, Armada and Erskine fields and redelivery this gas into Transco's National Transmission System (NTS). This expansion included the installation of Hydrogen Sulphide treatment vessels, a new re-delivery metering facility (EX1) for the pipeline, two 600mmsfc/day gas processing trains and an export metering facility (P1NTS) in order to measurement the inputs into the NTS. This expansion took the throughput of the CATS system from 0.65 BCF/day to 1.6 BCF/day

Each of the CATS gas processing trains is a typical fractional unit with depropanisation, debutoniastion and C5+ liquid streams. A schematic for these trains as been provided in Fig 2 After the initial low temperature separation and stabilisation Nuovo Pignone reciprocating compressors are used to compress the stabilised gas off take back up to the required export pressure.

The new EX1 and PINTS metering system were designed in accordance with current established metering standards and comprise of five 16in orifice plate runs for both systems as shown in FIG3. Each metering stream has both upstream and downstream isolation valves and a stream switching valve situated downstream of the orifice plate carrier. In operation it is this switching valve which is opened or closed in order to bring the associated stream on or off-line.

The metering header design and pipework immediately upstream from the metering system had been considered, in terms of flow profile and characteristics, in order to deliver the required accuracy and uncertainty performance. However no detailed modelling was deemed necessary in order to ascertain the effects of possible pulsation caused through the configuration of pipework or the reciprocating compressors.

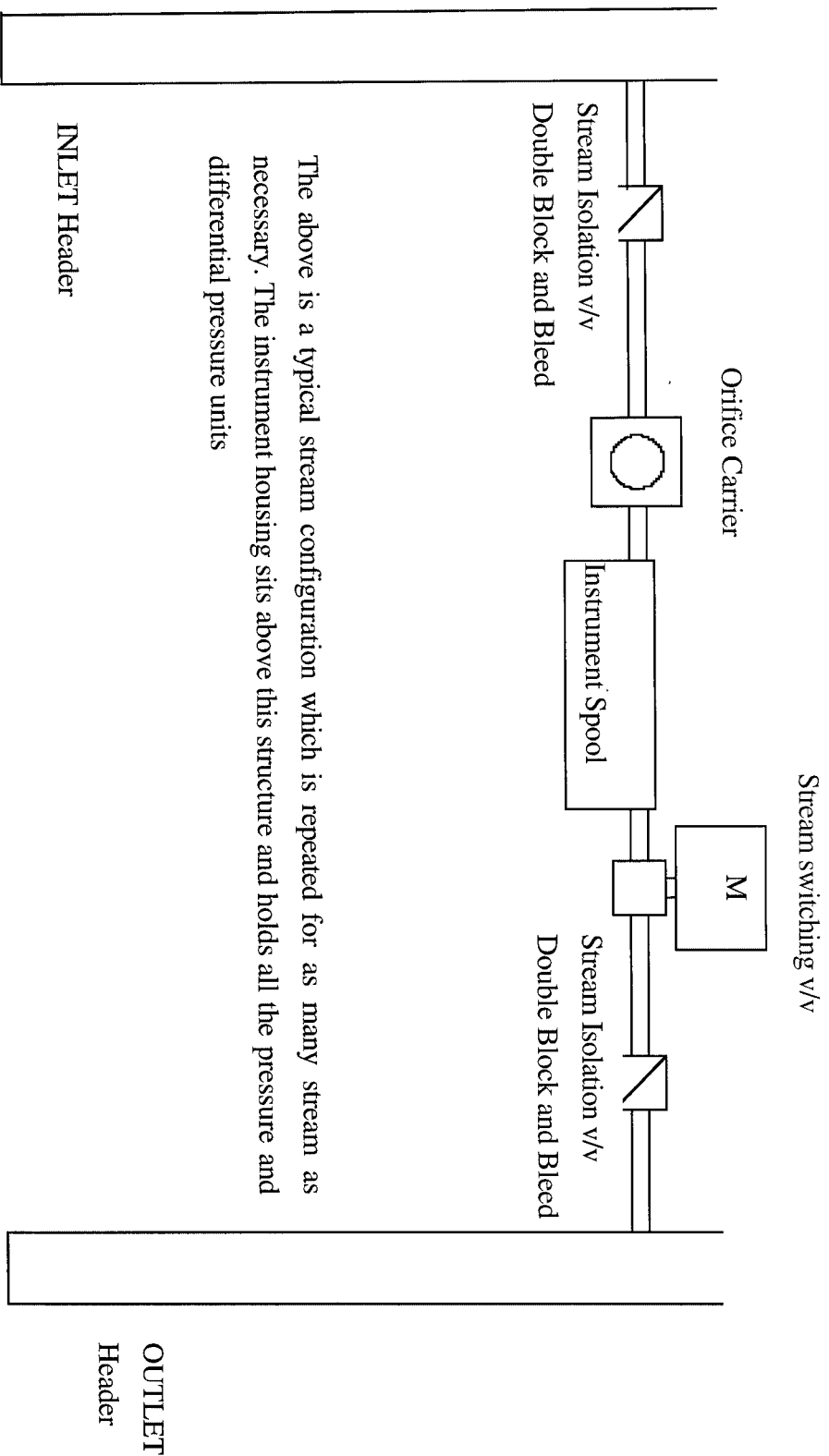
In the final commissioning phase of both EX1 and PINTS, very small fluctuating differential pressure measurements (DP's) were noticed on metering runs that were off-line. Concerns were raised with regard to these low differential pressures and the effect they may be having on flow measurement.

Fluctuating DP's caused by pulsation are know to cause errors associated with the square root error (SRE) of differential transmitters and through this then affect the overall uncertainty of the measurement system. CATS decided that the effect of the above factors needed to be evaluated in order to demonstrate the measurement system met its design parameters.

It is this investigation into the cause of these small DP's that this paper outlines both in terms of the methodology and techniques used to ascertain the possible effect of pulsation on flow measurement with particular reference to (SRE).

The investigation would eventually prove that no effects on the measurement values were being recorded, on any of the measurement systems at the CATS terminal. Both the newly installed skids, being EX1 and P1NTS as well as the original EX2 and EX3 skids were covered by the testing program and shown to be accurate at all rates in accordance with both the standard industry guidance and the CATS Measurement Manual (CMM).





The above is a typical stream configuration which is repeated for as many stream as necessary. The instrument housing sits above this structure and holds all the pressure and differential pressure units

Fig 2

## 2. Initial Symptoms

During the early stages of start-up both the EX1 and P1NTS metering systems were flowing at low rates of approx. 70 mmscf/day. At these conditions no symptoms were evident which would suggest possible future measurement problems. However on increasing flow rates fluctuating DP's were observed, in the range of 0.5 to 0.8 KPa, on meter tubes which were selected to standby mode (i.e. the stream switching valve closed, upstream and downstream isolation valves opened).

Initial thoughts were that there was a problem with achieving valve integrity on stream switching valves. Venting the body cavity on the stream switching valves to flare and monitoring for any pressure increase quickly disproved this.

Flowing several periods of monitoring and trending these low DP's against plant operations, thoughts turned to the belief that a possible cause could be pulsation generated by the reciprocating compressors. CATS were aware through Amoco's measurement network that work had been completed in the USA on this issue and decided to ask for assistance from the measurement network. From these discussions concerns were raised with reference to the level of Square Root Error (SRE). It was important to prove that any such error induced into the SRE caused by any pulsation was below the 0.5 limit set out in the CMM, with reference to the potential affect on the performance of measurement systems at the CATS Terminal.

In conclusion to the above observations and discussions it was decided that three elements would require to be determined, pulsation, the differential pressure readings observed on the closed in meter tubes and ultimately the effect on the SRE.

At this point CATS requested the mechanical and fluids engineering division of Southwest Research Institute (SwRI) to investigate pulsation effects and fluctuating differential pressure readings on off line meter tubes.

## 3. Procedure

Detailed tests were conducted on the first three streams of the CATS plant sales gas meters, P1NTS, and the pipeline redelivery meters, EX1. The remaining streams were not commissioned at the time of the tests due to the low throughput requirement of the system and consequently they did not form part of the testing program

The original re-delivery meters were also tested although no symptoms of the fluctuating differential pressure readings seen on EX1 and P1NTS had been observed at these stations.

The purpose of the tests was to evaluate whether the DP's seen at the measurement stations were a direct result of pulsation effects and attempt to locate the source of any such pulsation. In order to achieve this accurate measurement of the fluctuating DP's would be required. The frequency and amplitude of pulsation in the meter runs and the instrumentation impulse lines were also evaluated in order that the full effect on SRE could be determined.

A total of 16 tests were performed in the field investigation and the test configurations are outlined in Appendix 1 Table of Results.

The investigation was conducted by obtaining two types of measurements: differential pressure and pulsation (dynamic pressure). Two differential pressure measurements were made one with the measurement units mounted as close to the orifice as practical and then secondly at the far end of the instrument impulse lines. The first measurements allowing the SRE level to be determined from the dynamic variations (fluctuations) close to the orifice fitting. The dynamic amplification and distortion of the orifice signal, caused by the impulse line length and configuration, were then determined from the second measurements taken at the location of the system DP transmitters.

Pulsation data was collected using high frequency piezoelectric dynamic pressure transducers. These were connected to pressure tapings in the meter tube piping in a few cases and on the ends of the impulse lines during other tests. The pulsation measurements provide additional information about the conditions at the end of the impulse lines and are used to confirm the differential pressure measurements.

A number of the tests were designed specifically to prove or disprove particular aspects of the pulsation behaviour.

- Test 1 Base line readings taken for each stream.
- Test 2 The meter tube on which differential pressure was being measured was shut down to determine the effect of eliminating flow on the differential pulsation.
- Test 3 Base line readings taken for the next set of tests.
- Test 4 The flow rate on the meters being tested was reduced by opening the previously shut off stream. The impulse line pulsation on the shut off run increased when the upstream manual valve was opened prior to the downstream automatic valve being opened.
- Test 5 Base line readings taken for the next set of tests.
- Test 6 A different meter run was shut off to confirm the effect of eliminating the flow rate on pulsation.
- Tests 7-10 Conducted at the higher pressure inlet gas, EX1, meters.
- Test 9 Flow rate in the monitored stream was increased, by closing the valves on one of the other steams.
- Test 10 The previously closed meter run was opened and the monitored stream was closed and data was measured with no flow.
- Test 11 A brief test conducted on two of the impulse lines on the EX2/3 meters and no changes in operating conditions were made.
- Tests 12-16 Conducted on NTS Sales Gas Meters to determine the effect of the over head (OH) compressors and other changes. During the first 4 of these tests, 12 through 15, the flow was through meter runs 1 and 2 only. During Test 13 the OH compressors were shut off and it was determined that the low level, approximately 6 Hertz (Hz) pulsation was present even when the compressors were not operating. Tests 14 and 15 involved an exchange of transducer locations to measure any impulse line shift or change in the average differential pressure. During the final test, No. 16, the third meter run was opened to flow to confirm the effect of reducing flow rate in the monitored stream.

## 4. Results

### **Square Root Error Results**

Unfiltered SRE levels are the worst case scenario and often include pulsation frequency peaks. These were seen at the orifice, however, with the filtering mechanisms used both by the transmitters and flow computers these are not included in the actual SRE value recorded. The unfiltered SRE levels measured at orifices during each of the tests are shown in the Appendix 1 Table of Results.

Inappropriate pulsation peaks can be identified on a case by case basis and filtered where the difference is important. For example, as the meter run was being shut down during Test 2, an SRE of 1.05 percent was recorded. However, because of a local impulse line frequency, this unfiltered SRE is larger than the filtered or corrected SRE for Test 2, which was 0.26 percent. SRE levels are larger at low flow rates when the average differential pressure is low. The largest SRE seen during Test 2 occurred when the differential pressure was 10 KPa. The NTS meters at CATS are not operated at differential pressures below this level. At a normal flow rate of 25 KPa, the corresponding SRE would be approximately 0.25 percent unfiltered and less than 0.1 percent if properly filtered.

SRE levels at the NTS Sales Gas Meters and the other meters tested are also reported in Appendix 1 Table of Results. They are approximately 0.25 percent or less when filtered. At normal flow rates that result in differential pressures of 12.5 KPa or more, the worse case SRE is expected to be less than 0.25 percent in all cases and significantly less under most standard operating conditions.

### **Pulsation Frequency and Amplitude Results**

In addition to the square root error levels, differential pressure amplitude and dynamic pressure data were recorded during each test to determine the frequencies and amplitude of the pulsation within the meter runs and the impulse lines. The significant pulsation frequency and amplitudes are presented in Appendix 1 Table of Results for each test. In addition a sample of frequency spectrum sheets for Tests 1 through 16 are presented in Appendix 2.

As shown in the results table, when differential pressure was measured close to the orifice, there was typically a low level pulsation of 1 KPa at a frequency of 6 to 9Hz with frequencies of 6.5 to 7.0 Hz being the most common centre frequency (see Tests 1 through 4). The orifice differential pressures close to the meter also contained larger amplitude, higher frequency component around 69 to 70 Hz. The amplitude of this differential pulsation ranged from 1KPa to over 15 KPa. The differential pulsation near the orifice also contained intermediate frequencies, such as 42 and 56Hz, at lower amplitudes, as shown in the Appendix 1 Table of Results.

The source of the 6 to 7 Hz pulsation's were found to be in the meter run piping but at a low level less than 1.5 KPa, as shown by several measurements. The amplitude of the low frequency pulsation in the meter run piping and in the impulse line close to the orifice are essentially the same, less than 1 KPa.

On the other hand, the amplitude of the 6 to 7Hz differential pressure measured at the transmitter end of the impulse lines is much larger, and ranged from 1 KPa to 20 KPa. The reason for the increase in amplitude of this low frequency pulsation is the fact that the impulse lines have an acoustic resonance at or near this approximate 7 Hz excitation. The resonance of the impulse line is produced by the tubing stub length, which connects the transmitters to the orifice. The source of the pulsation excitation is external to the impulse lines and is thought to be from some small disturbance in the gas plant piping.

The amplitude of the low frequency (approximately 6 to 7 Hz) pulsation at the transmitters is the cause of the fluctuating differential pressure readings in the metering system flow computer. From these measurements assurance was drawn that there was no dynamic variation in flow rate or a significant measurement error, which corresponds to the observed variation in differential pressure.

Early in the testing, the source of the low level 6 to 7 Hz excitations was thought to be the OH compressors, which have a fundamental operating speed of 6.67 Hz (400rpm). This was disproved with respect to both the variations in the observed frequency up to 9.0 Hz, and the results obtained from test 13. During test 13 the OH compressors were shut off for a short period however the 6 to 7 Hz pulsation remained in the meter run piping this demonstrates that the compressors were not the source of the low frequency pulsation.

The source of this pulsation is thought most likely to be from some form of vortex shedding or Strouhal frequency at a piping branch, pressure vessel entrance or others obstacles within the piping configuration of the plant. Although an effort was made to find the exact source of this pulsation, it was not located. It was demonstrated that the 6 to 7Hz excitations are produced upstream of the NTS meter runs by stopping flow in the meter run, this was achieved by alternately closing the downstream & upstream valves. The 6 to 7Hz pulsation's remained in the piping and impulse lines with the downstream valve closed but when the upstream valve was closed the impulse line resonance disappeared. Because of the low level of this excitation, locating the source would most likely be of little value, as it would not be easy to filter or to eliminate at source.

The cause of the higher frequency pulsation, typically 69 to 70 Hz, seen in the differential pressure measurements close to the orifice, was also demonstrated to be an acoustic resonance. Because the dynamic differential pressure transducer could not be placed directly at the orifice, connection was made via a small length of impulse line between the orifice meter pipe wall and the transducer. The acoustic resonance of the length of piping used with high pressure gas is approximately 70 Hz. Therefore it was deduced that this frequency is a resultant of the measurements made and not a component in the meter run piping or at the end of the impulse lines where the transmitters are located.

Differential and piping pulsation were measured on Stream 3 at the EX1 inlet gas meters during Tests 7 through 10. The results here were similar to the results at the NTS meters. The low frequency 7 to 9 Hz pulsation was observed at a large amplitude at the transmitter end of the impulse line, and the 6 to 7 Hz excitation frequency was observed at a low level of approximately 0.7 KPa in the meter run piping. The higher frequency pulsation in the differential pressure measurements close to the orifice were somewhat different and show intermediate frequencies, such as 42Hz, as well as the 69 to 70Hz, at lower amplitudes. These differences are most likely due to the difference in the speed of sound and the operating conditions for the higher pressure inlet gas.

## 5. Conclusions

The following conclusions are based on the results of the data observed and recorded at the CATS terminal and the subsequent analysis of acoustic responses of the orifice impulse lines

1. Unfiltered SRE levels gave the worst case values and often included pulsation frequency peaks. These do not effect the measurement transmitter, and therefore, should not be included in the actual SRE value
2. Low amplitudes pulsation is present at the P1NTS and the EX1 orifice meters and causes Square Root Errors of 0.25 percent or less in all normal flow conditions. The contractual limit for SRE as specified in the CATS Transport Allocation Agreement is 0.5%.
3. Flow rates that result in differential pressures of less than 10 KPa cause an increased SRE.
4. The differential pressures as measured contain a low amplitude pulsation of approx. 0.7 KPa at 6 to 7Hz and a higher amplitude of pulsation at a higher frequency around 69 to 70 Hz.
5. The cause of the high frequency pulsation 69 to 70 Hz is an acoustic resonance within the temporary connection line used.
6. Tests demonstrate that the reciprocating compressors at the CATS terminal are not the source of the low frequency pulsation.
7. Sources of excitation energy, such as turbulent flow, control valves and vortex shedding, piping configuration are attributed as the cause of the pulsation levels.
8. Differing levels of low amplitude pulsation can be observed across each of the meter tubes when in standby mode
9. The values of differential pressure used by the stream flow computers are subject in the first instance to a sampling/damping rate of 0.5 seconds by the DP transmitters. The flow computers with cycle times of approximately 3 seconds then average this signal hence the unfiltered SRE seen at the orifice do not affect the actual measurements taken at the DP Transmitters
10. Data from the tests prove that SRE at all of the orifice meters at CATS are low and for all normal operating conditions can be ignored.
11. The effects of pulsation at the EX1 meters are similar to the NTS results in terms of low levels in the meter run piping and significant amplification in the impulse lines.
12. No indication of pulsation induced error could be seen on the original Ex2 / Ex3 skids

## 6. Follow up Actions and Recommendations

1. Metering stations should incorporate automatic stream switching configured to maintain differential pressures above a value determined from analysis, thus would reducing SRE to a minimum level. This is a standard feature of the CATS measurement systems, station average DP's are used in conjunction with switching limits of 12.5 to 15 KPa causing meter tubes to close down before SRE levels becomes noticeable.
2. The operator should have the function to select the order of meter tube operation. This can be used to ensure the optimum use of the facility in terms of preferentially selecting the tubes least affected by pulsation. This is a standard feature of the CATS metering measurement systems.
3. Impulse lines should be kept to the minimum practicable length and if possible close coupled to the orifice boxes. It is recognised that close coupling raises differing problems with reference to calibration facilities. The CATS preferred design is for the instrument house to be placed across the meter tubes in order to provide high static calibration facility inside a temperature controlled environment. Within this enclosure impulse lines are kept to the minimum practical length.
4. A facility to obtain both dynamic pressure (pulsation) measurements and SRE effects on differential pressures should be included in the design and fabrication of the metering system. The CATS CMM lays out this requirement for all the measurement systems used within the CATS system. It does not however stipulate that measurements be taken to prove SRE levels
5. A review of possible pulsation effects on metering stations should be carried out as soon as operational constraints allow. Thus allowing the operator to obtain an understanding of each meter tubes flow characteristic and achieve optimum performance.
6. Design consideration should be given to possible pulsation issues when orifice meters are to be used in a fiscal application. Consideration should be given to the piping configuration used, in an attempt to remove or reduce areas that give raise to vortex shedding, failing this thought could be given to some form of acoustic damping.

## Appendix 1

Test No.	Location	Meter Tubes Exporting	Data Type	Frequency (Hz)	SRE Unfiltered (%)	Amplitude (KPa)
1	NTS-1 Orifice	1, 2 & 3	Differential	6.0 to 7.0 69 to 70	0.15	0.62 to 1.2 3.5 to 5.2
2	NTS-1 Orifice	2 & 3	Differential	6.0 to 7.0 57 to 72.5	1.05(filtered 0.26)	0.5 to 1.1 0.2 to 3.7
3	NTS-3 Orifice	2 & 3	Differential	6.0 to 7.0 65 to 67	0.15	0.5 to 1.0 8.5 to 10.0
4	NTS-3 Orifice  NTS-1 Impulse Line NTS-1 Upstream. NTS-1 Downstream	1, 2 & 3	Differential  Differential Pulsation Pulsation	6.0 to 7.0  65 to 67  6.0 to 6.5 6.1 to 7.0 14	0.68 (filtered 0.01)	0.5 to 1.2  3.2 to 16  6.0 to 22 0.28 to 1.4 0.97

5	NTS-3 Orifice	1,2 & 3	Differential	67	0.44(filtered 0.01)	8.5	
	NTS-2 Impulse line						7.0
	NTS-1 Upstream.						7.0
	NTS-1 Downstream						7.0
6	NTS-3 Orifice	1,2 & 3	Differential	to 7.5	0.22	0.06 to 1.2	
	NTS-3 Impulse Line			67			to 4.4
	EX1-3 Impulse Line			7.0			1.4 to 4.4
7	EX1-3 Impulse Line	1&2	Differential	7.0 to 9.0	---	0.7 to 5.0	
	EX1-3 Orifice			42			0.01
8	EX1-3 Impulse Line	1,2 & 3	Differential	to 8.5		to 3.5	

9	EX1-3 Orifice EX1-3 Impulse Line EX1-3 Upstream. EX1-3 Downstream	2 & 3	Differential Differential Pulsation Pulsation	42 to 9.5 to 7.0 6.0 to 7.0	0.01	to 0.7 to 11.2 0.7 0.7 to 1.4
10	EX1-3 Orifice (with/Flow) EX1-3 Orifice (without Flow) EX1-3 Impulse Line (with Flow) EX1-3 Impulse Line (without Flow) EX1-3 Upstream. EX1-3 Downstream	1 & 2	Differential  Differential  Pulsation Pulsation	25,42,55  25,42,55  7,5,25  7,5,25  5,15,25 11	--	to 2.2 to 0.2 3.0 to 5.2  0.7 0.7 to 1.4

11	EX2/3-1 Impulse Line EX2/3-2 Impulse Line	1,2 & 3	Differential Differential	11 to 12.5 11 to 12.5	---	to 4.7 0.7 to 1.1
12	NTS- 1 Orifice NTS-1 Impulse Line	1 & 2	Differential Differential	6.9 to 7.0 6.0 to 6.5	0.01	to 2.2 2.7 to 13.2
13	NTS- 1 Orifice NTS-1 Impulse Line NTS-3 Impulse Line HP NTS-3 Impulse Line LP NTS-1 Upstream	1 & 2	Differential Differential Pulsation Pulsation Pulsation	6.9 to 7.0 6.0 to 7.0 7.0 6.0 to 7.0	0.02	to 2.0 to 15 to 6.9 to 6.2 0.3 to 0.7
14	NTS- 1 Orifice NTS-1 Impulse Line NTS-3 Impulse Line HP NTS-3 Impulse Line LP NTS-1 Upstream	1 & 2	Differential Differential Pulsation Pulsation Pulsation	6.9 to 7.1.5 to 6.5 6.0 to 7.0 to 7.0 6.0 to 7.0	0.01	to 1.9 to 16.2 to 6.2 to 11.7 0.3 to 1.0

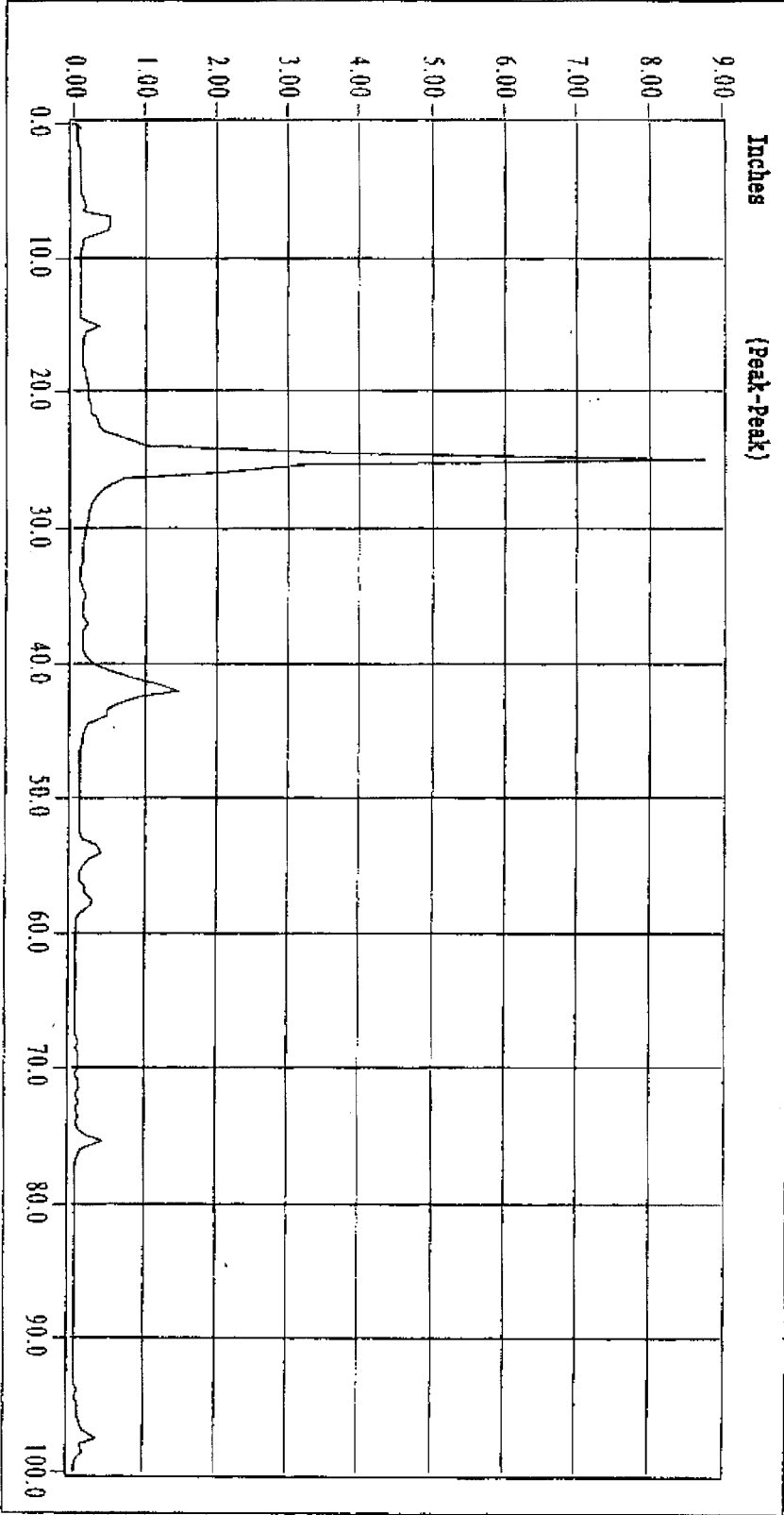
15	NTS- 1 Impulse Line	1 & 2	Differential	to 6.5	0.02	to 17.4
	NTS-1 Orifice		Differential	to 71.5		to 3.2
	NTS-3 Impulse Line HP		Pulsation	6.5		to 8.3
	NTS-3 Impulse Line LP		Pulsation	to 7.5		to 7.6
	NTS-1 Upstream		Pulsation	6.0 to 7.5		0.3 to 0.7
16	NTS- 1 Impulse Line	1 & 2	Differential	6.0	0.07	to 12.4
	NTS-1 Orifice		Differential	69 to 69.5		to 2.2
	NTS-3 Impulse Line HP		Pulsation	7.0		to 9.0
	NTS-3 Impulse Line LP		Pulsation	to 7.5		4.1 to 15.9
	NTS-1 Upstream		Pulsation	6.0 to 7.0		0.3 to 0.7

Appendix 2

152758.DAQ

spectrum

SRE DP1



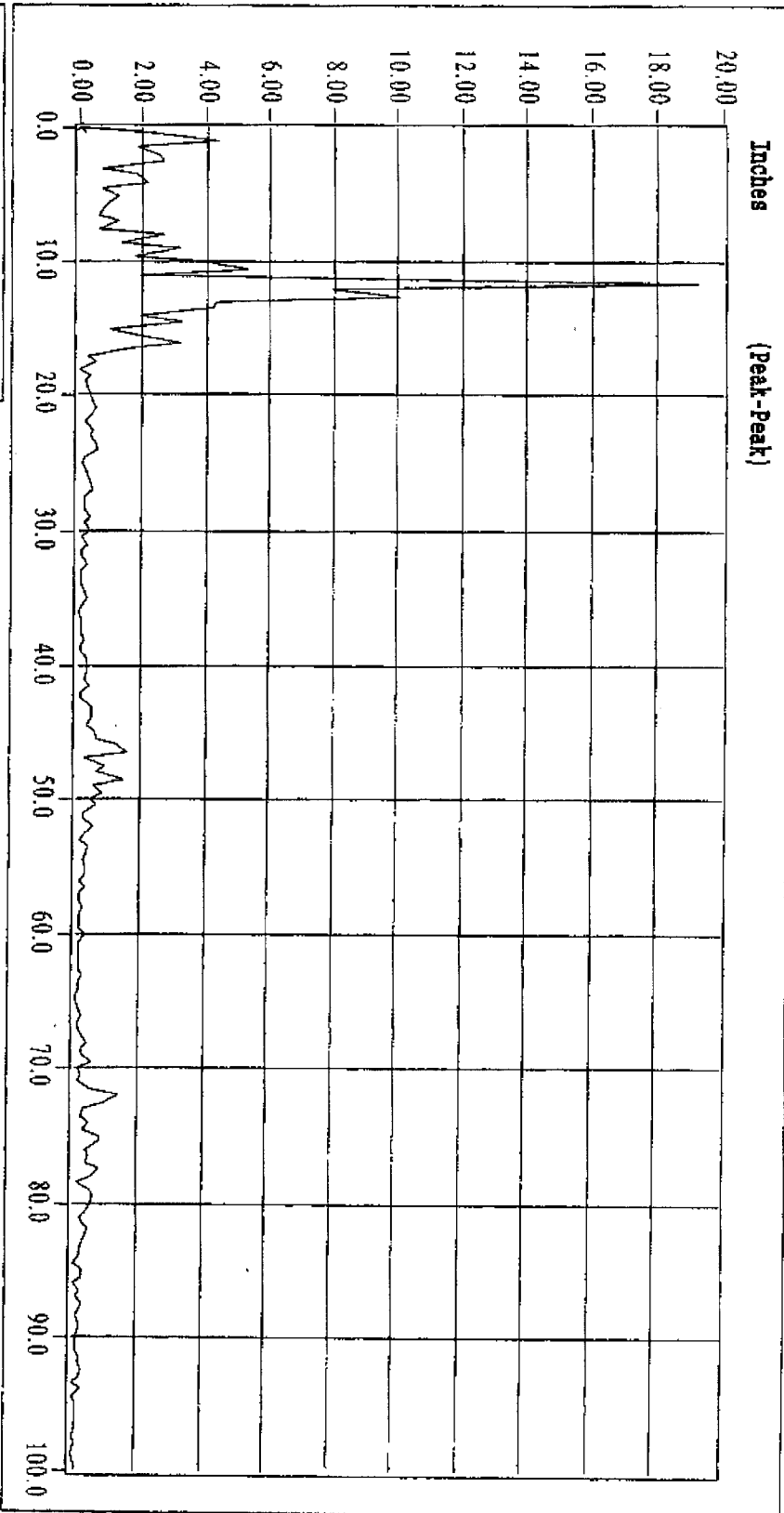
4/29/98 3:27:20 PM

test10

180445.DAQ

spectrum

SRE DP1



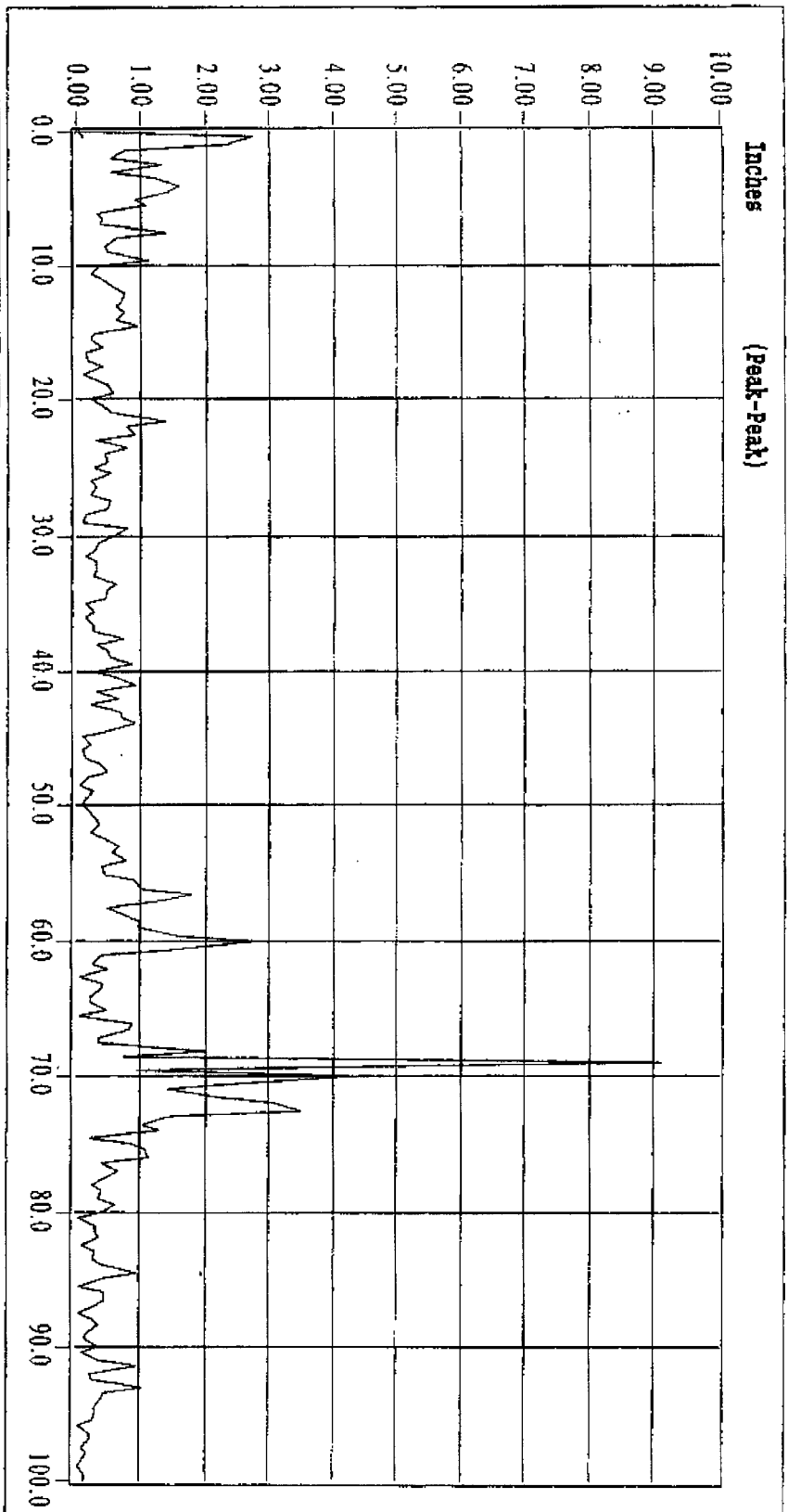
4/29/98 6:04:44 PM

test 11

091732.DAQ

spectrum

SRE DP1

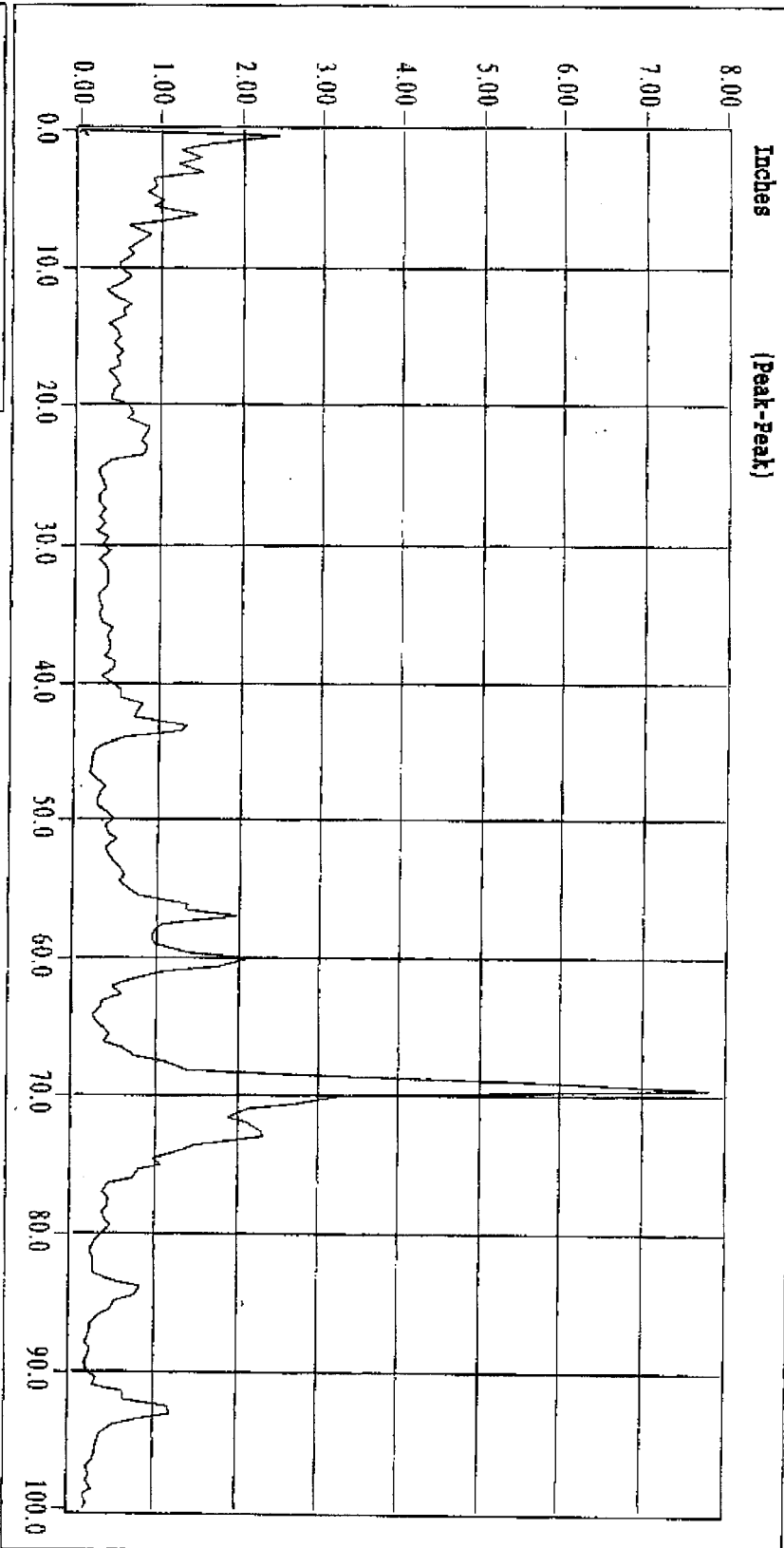


4/30/98 9:17:30 AM

094557.DAQ

spectrum

SR8 DP1



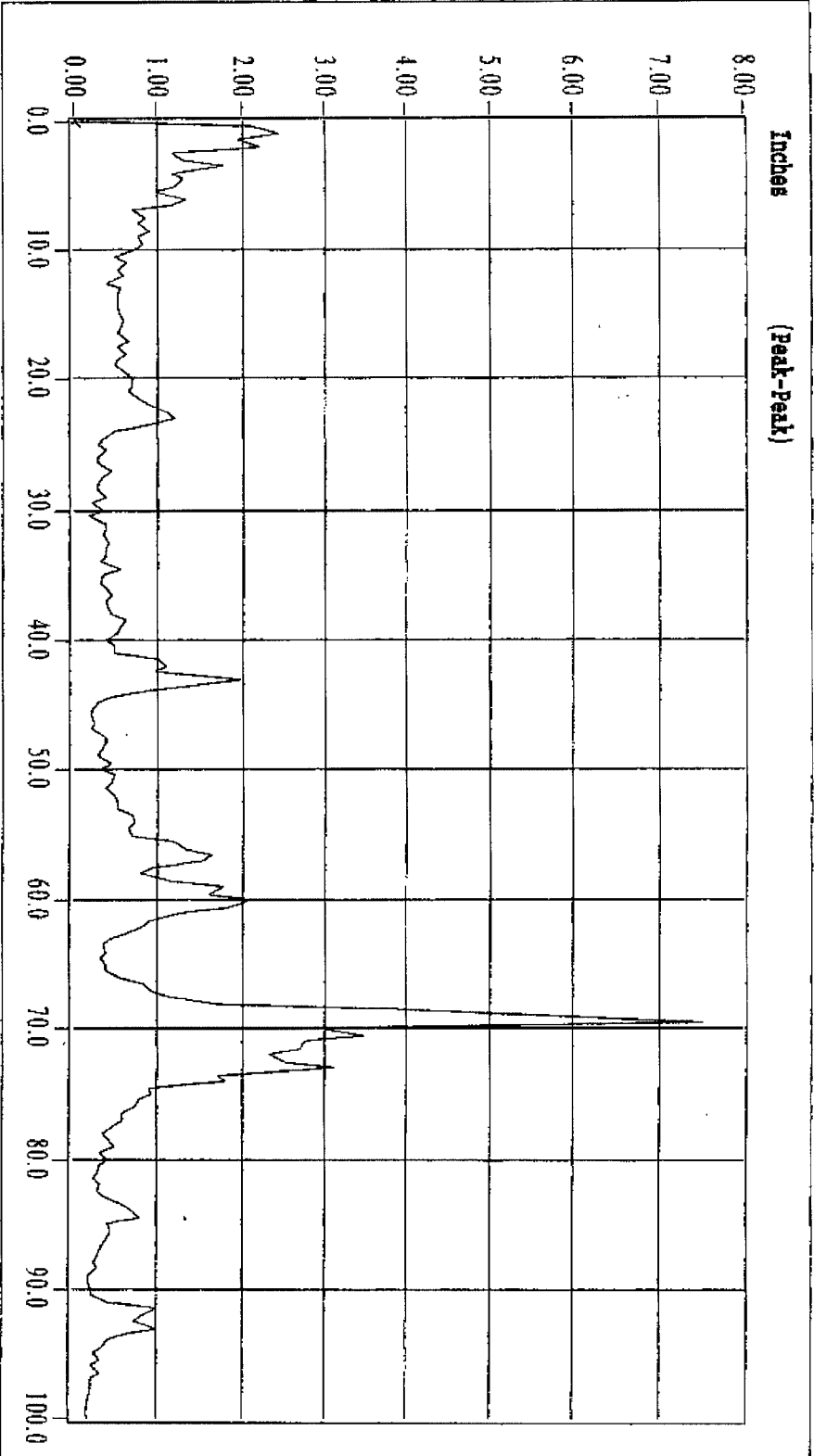
4/30/98 9:45:34 AM

test13

103407.DAQ

Spectrum

SRE DP1



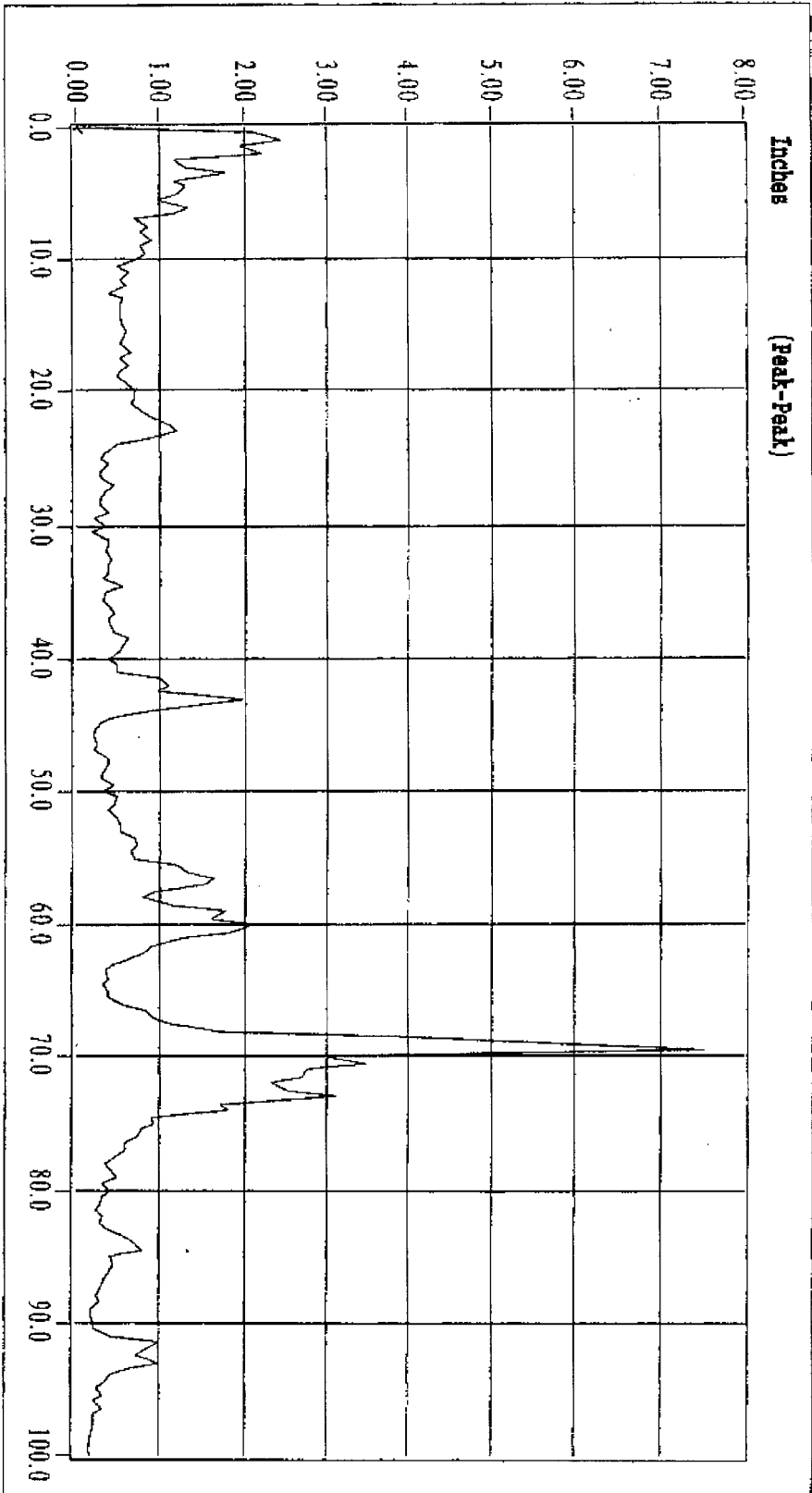
4/30/98 10:33:45 AM

test14

103407.DAQ

spectrum

SRE DP1



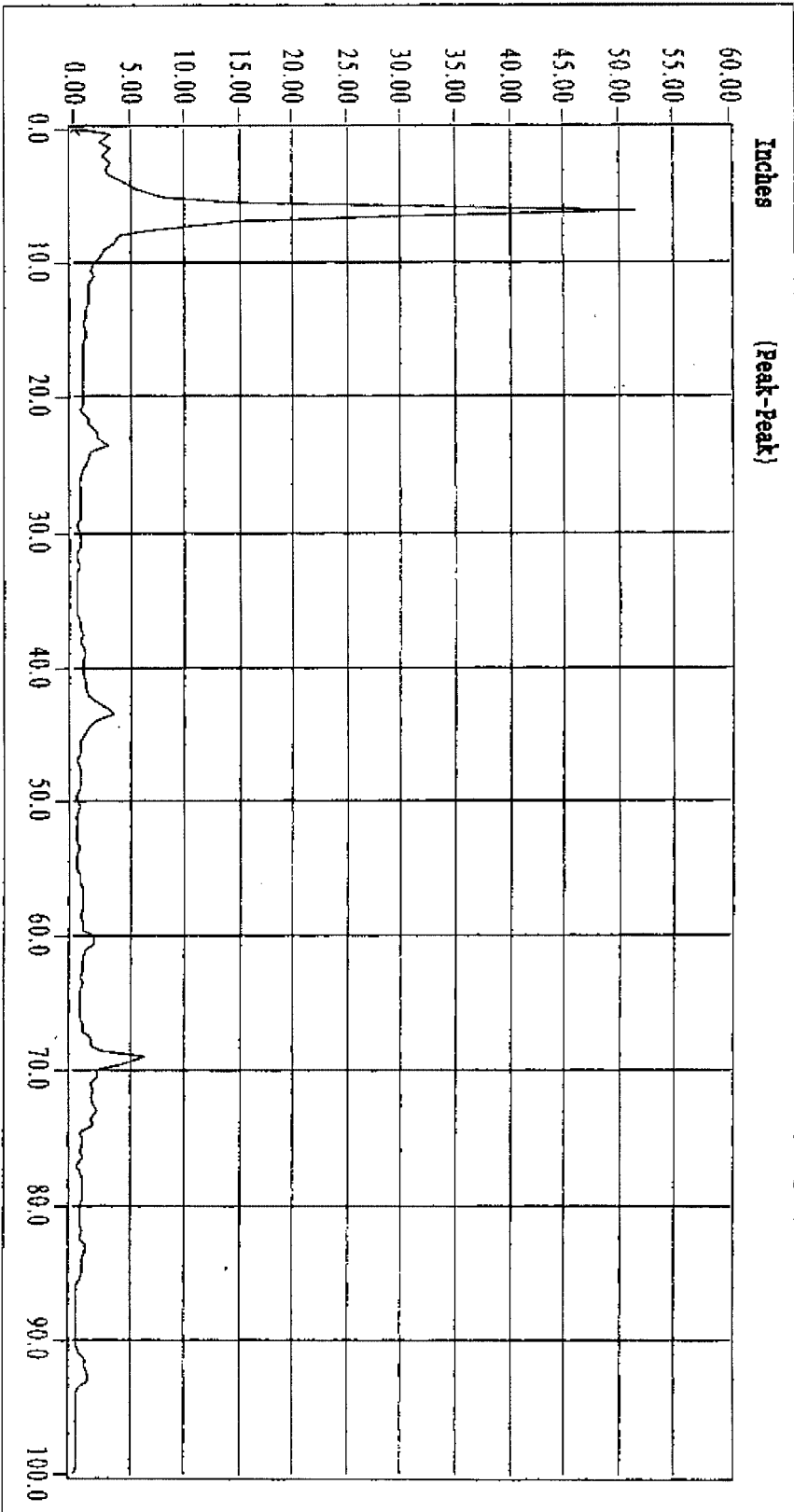
4/30/98 10:33:45 AM

test15

111935.DAQ

spectrum

SRE DP1

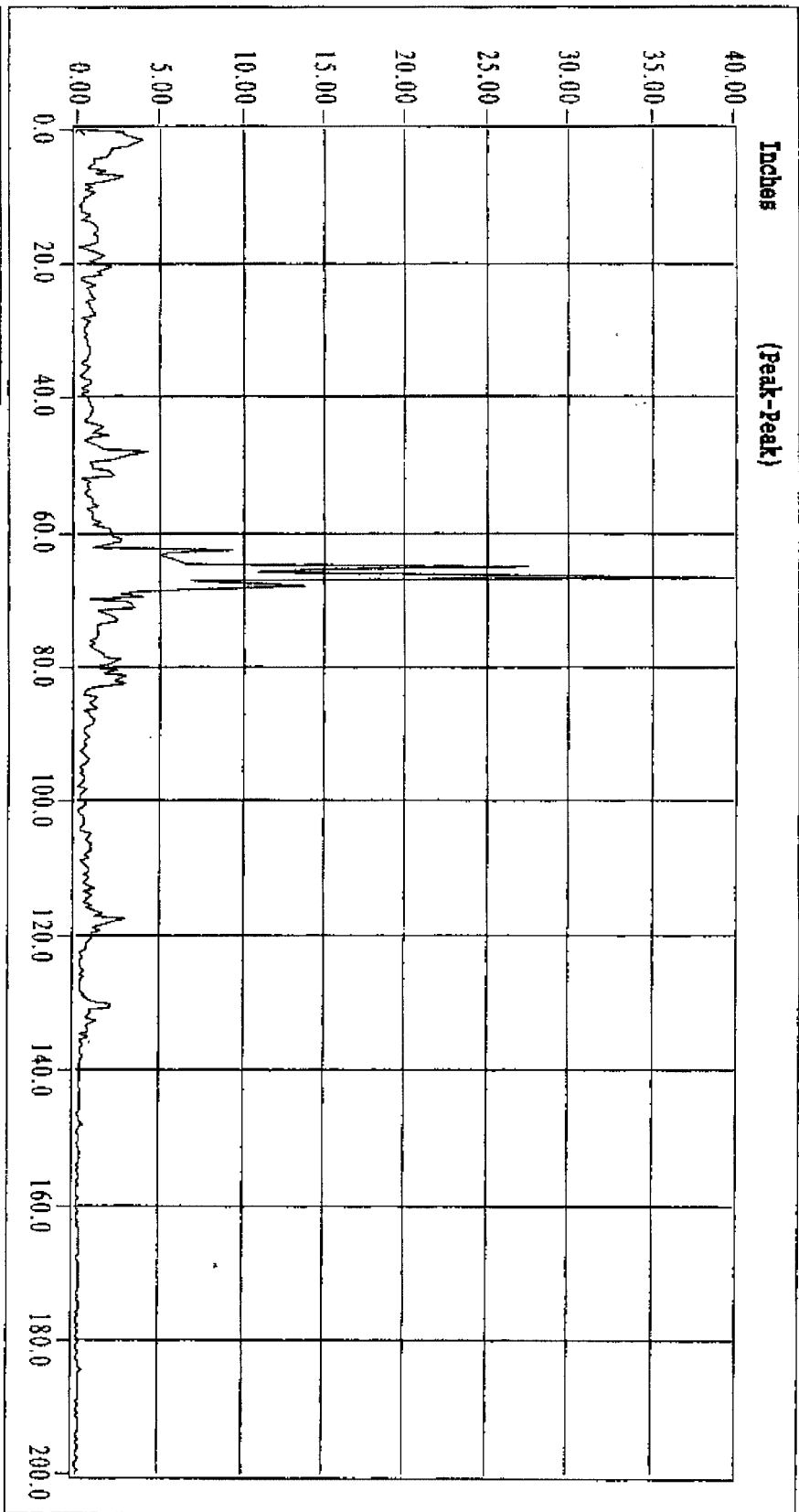


4/30/98 11:19:13 AM

142030.DAQ

spectrum

SRE DP1

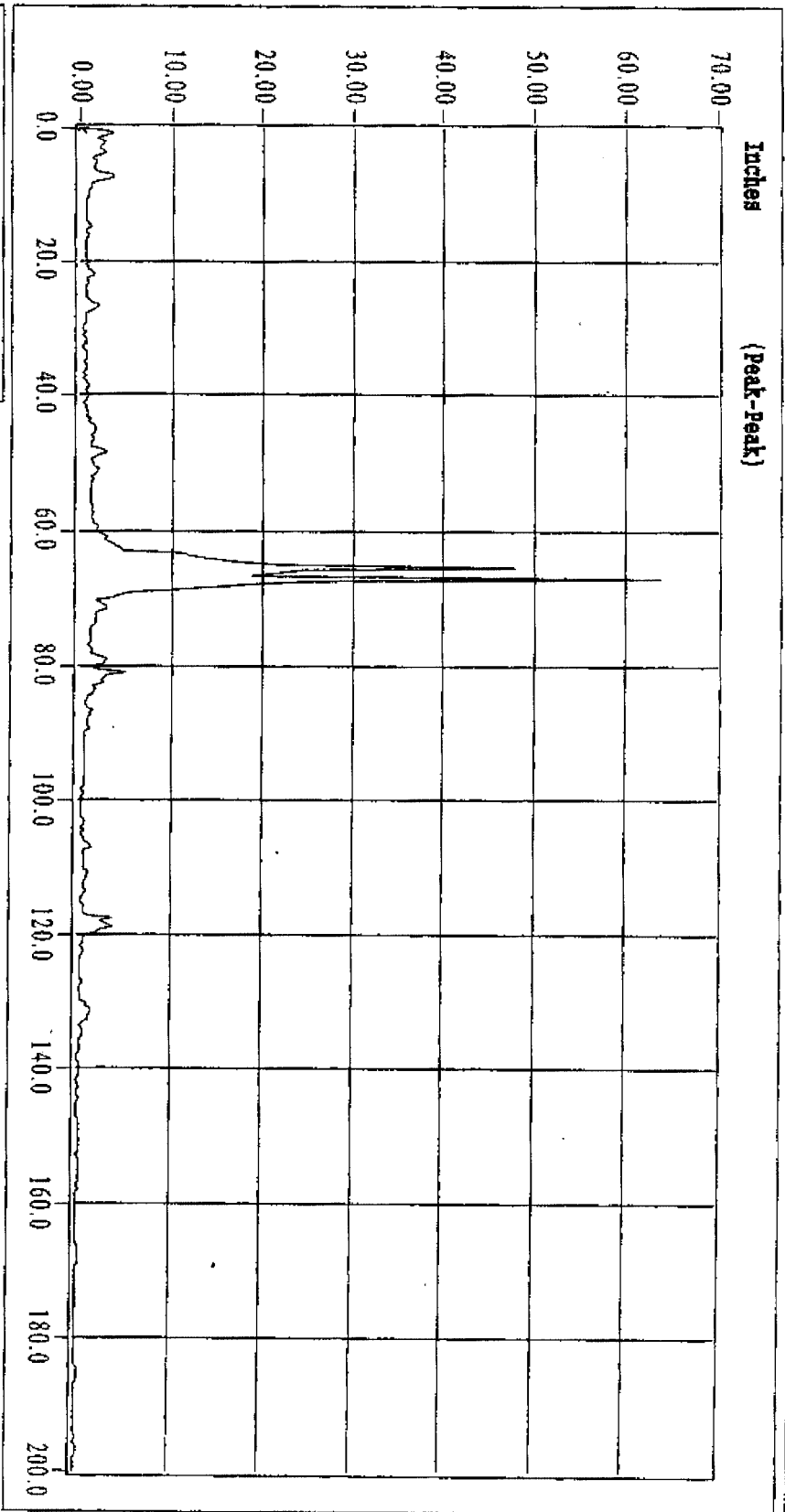


4/28/98 2:20:13 PM

165942.DAQ

PK Spectrum

SRE DP1



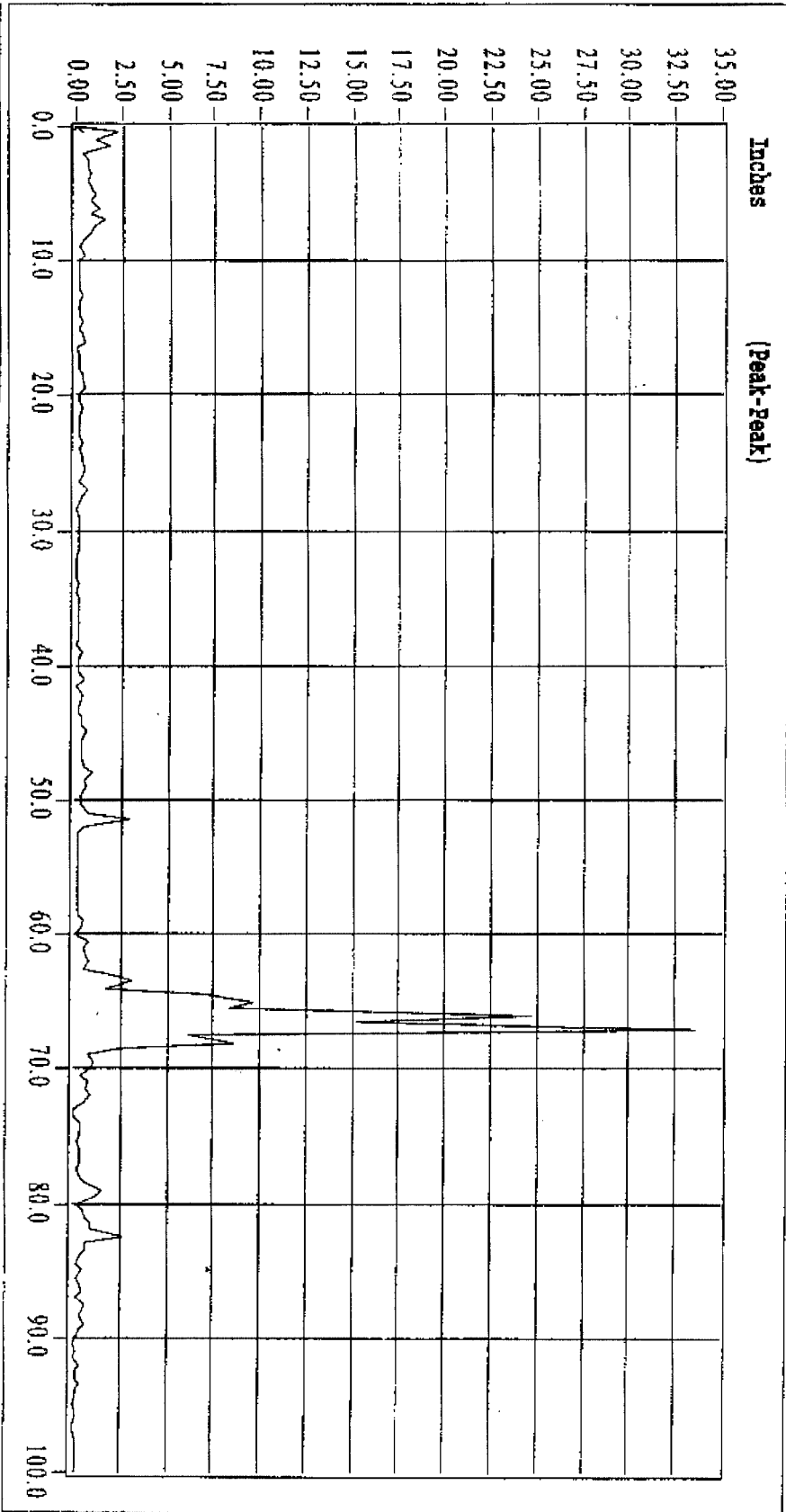
4/28/98 4:59:05 PM

test4

174315.DAQ

spectrum

SRE DP1



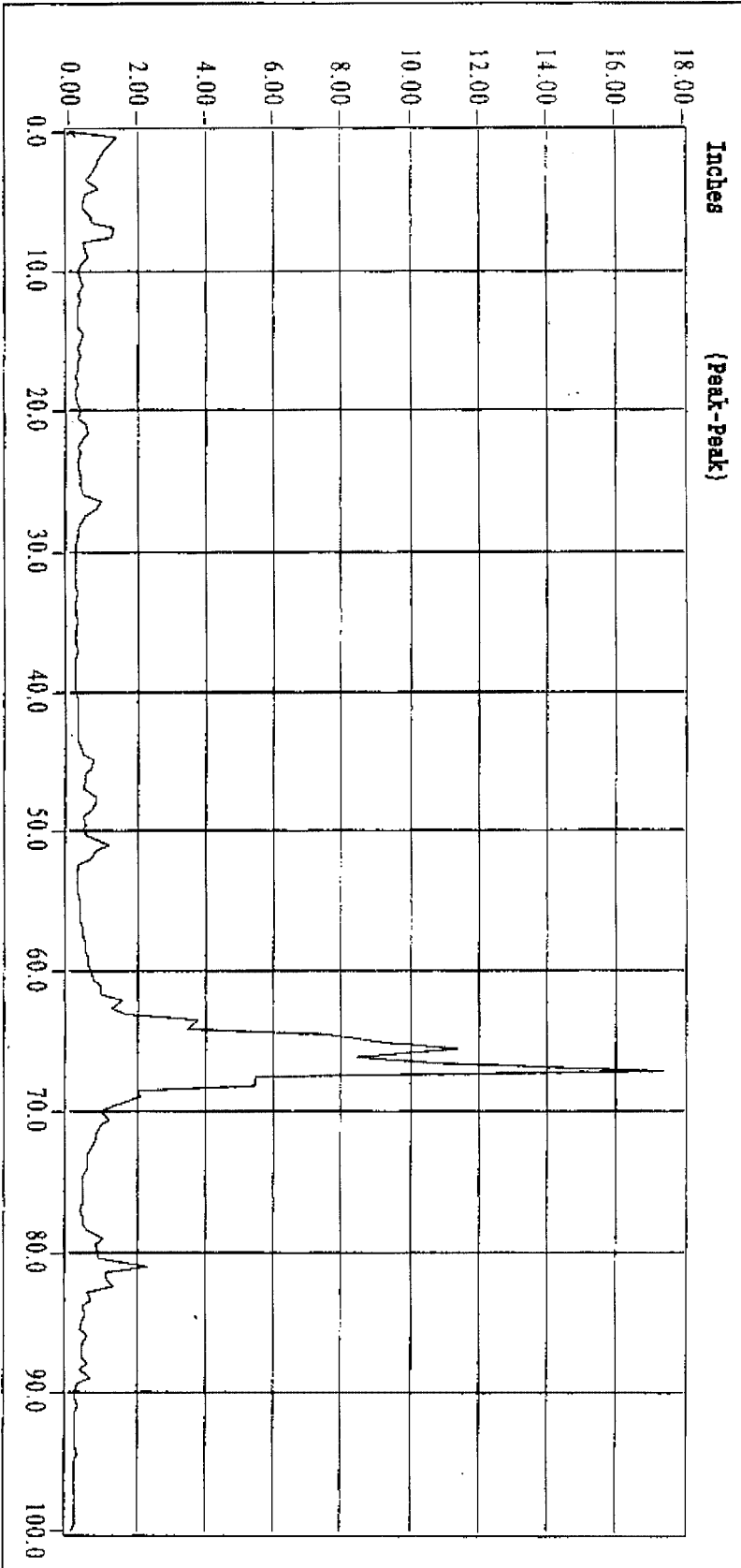
4/28/98 5:43:13 PM

test5

192324.DAQ

spectrum

SRE DP1

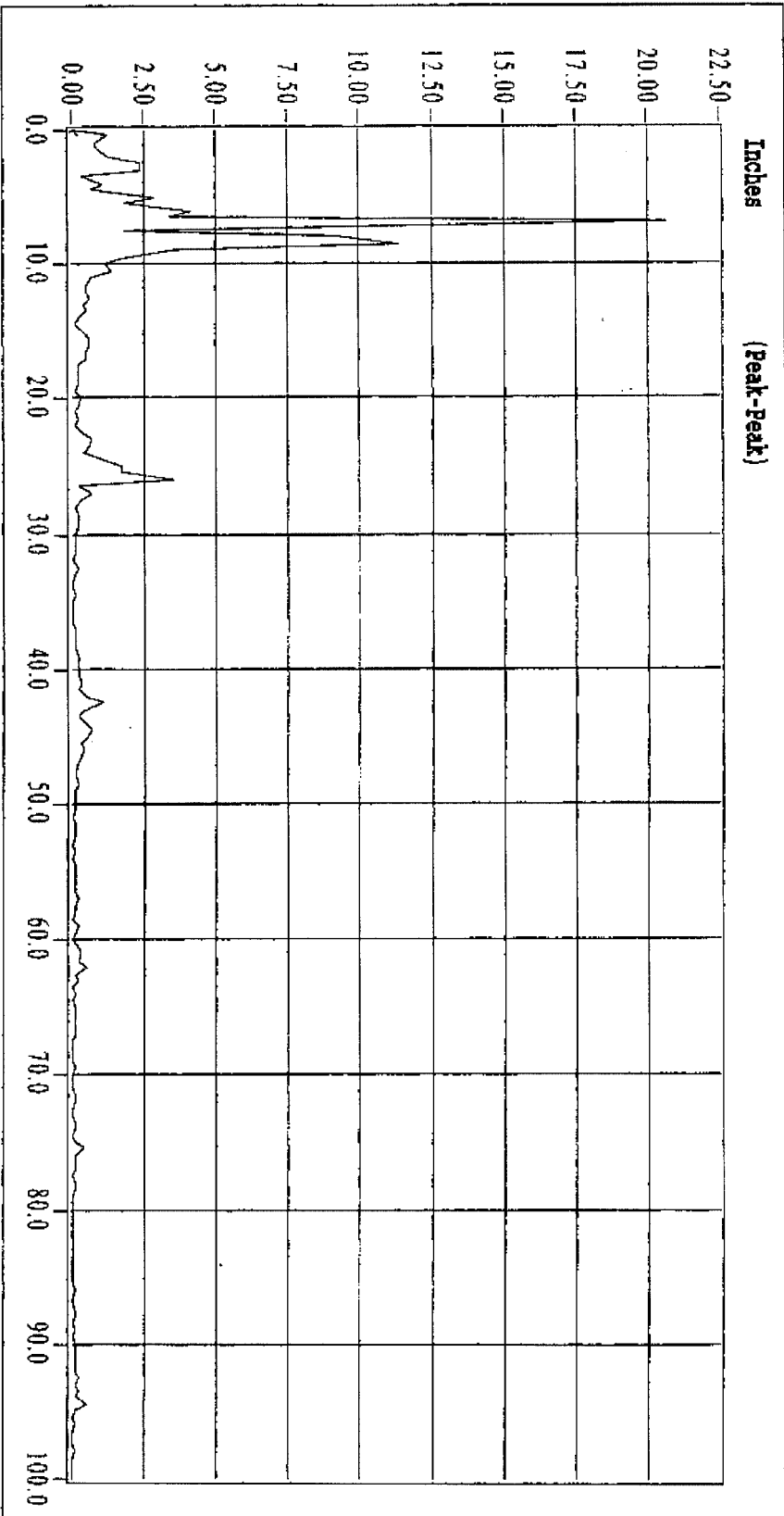


4/28/98 7:23:18 PM

117714.DAQ

spectrum

SRE DP2

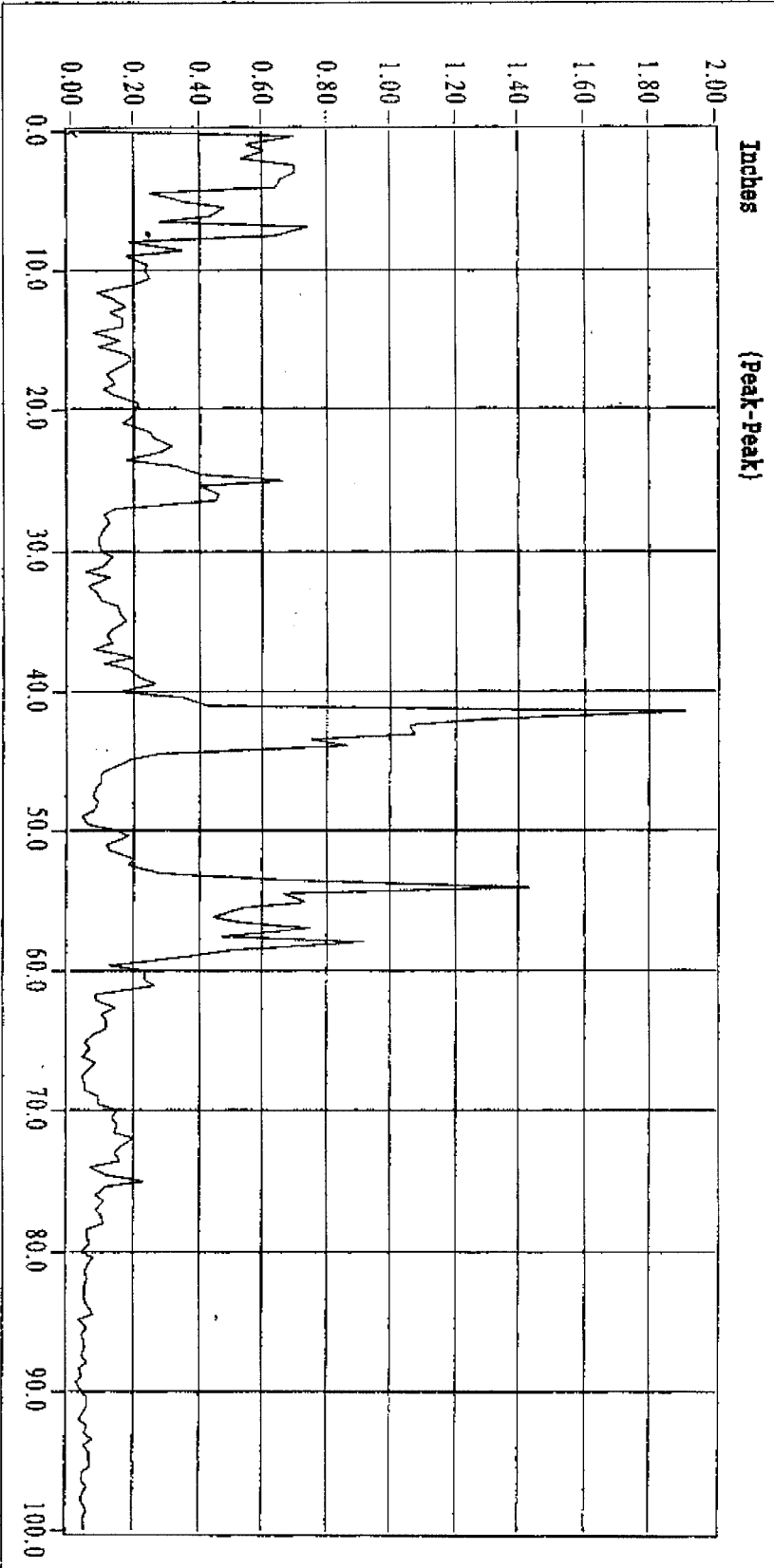


4/29/98 11:16:04 AM

140817.DAQ

spectrum

SRE DP1

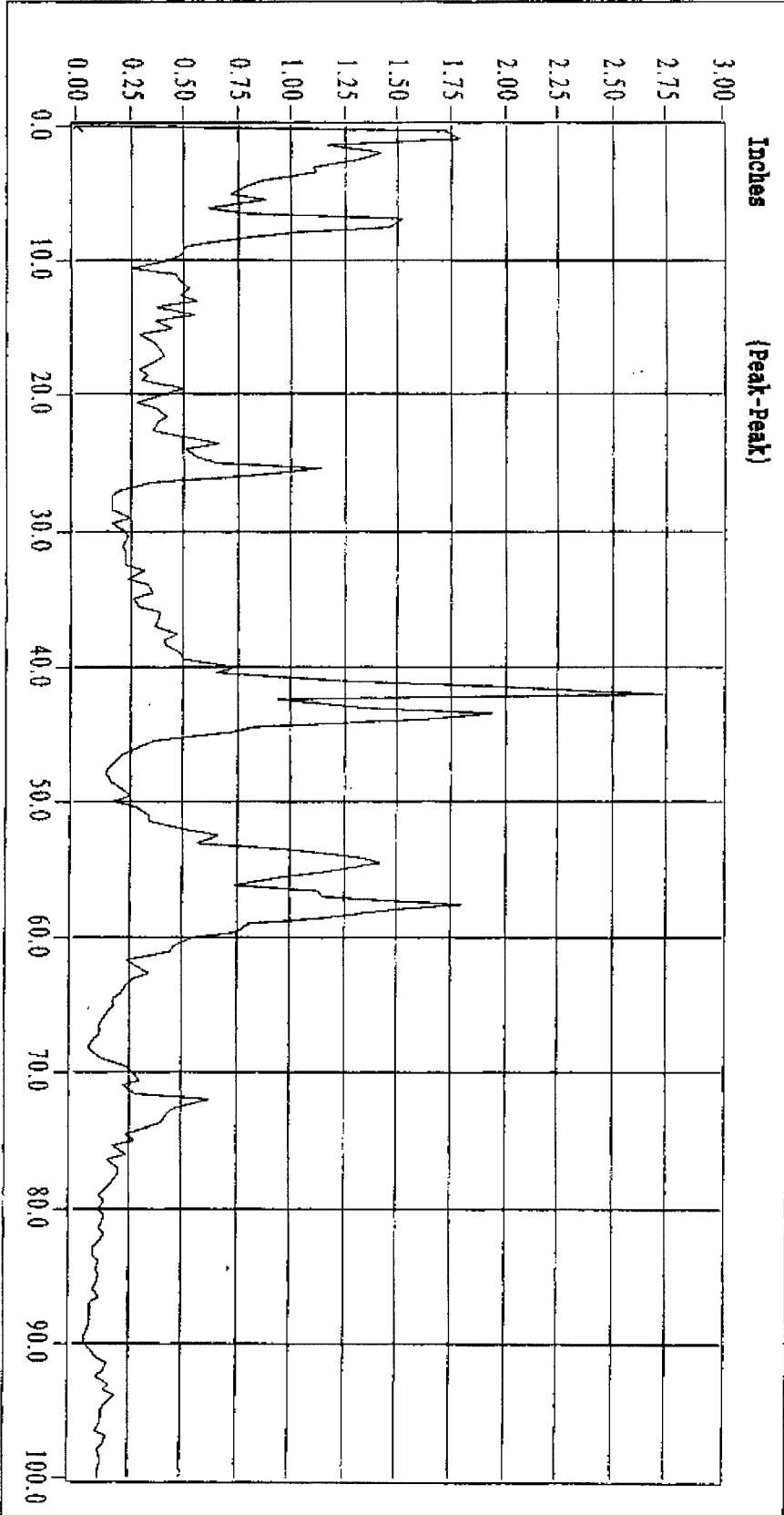


4/29/98 2:07:23 PM

150119.DAQ

spectrum

SRE DP1



4/29/98 3:00:42 PM

test9

## Acknowledgements

CATS Terminal would like to thank the following contributions to this paper

Mr Alan J Nicholl      Shail Ltd

Mr R.J. McKee        South Western Research Institute

Dr R.J.W. Peters      Daniel Industries



# MULTIPHASE MEASUREMENT SYSTEM WITH FULLY REDUNDANT MEASUREMENTS TO IMPROVE ACCURACY AND SIMPLIFY MAINTENANCE

*Arnstein Wee, Roxar ASA*

---

## 1. Abstract

Multiphase flow meters have been accepted and used by the industry for reservoir management and production allocation for several years. Multiphase metering is a fairly new technology that is an attractive alternative to test separators due to reduced field development and maintenance costs in addition to “real time” information as opposed to long term averages. However, multiphase metering technology is not yet very well understood by all field-operators, which makes it more challenging to verify correct operation and further to detect and isolate failures compared to conventional test separators. Traditionally, three phase “measurements” has been performed by separating the flow and measuring at single-phase conditions. Single-phase measurements are well understood by the industry and although the measurement uncertainties of a test separator in many cases are underestimated due to the operational limitations and maintenance requirements, operators normally have procedures and skilled personnel to ensure reliable measurements.

Multiphase measurement differs from a traditional single-phase measurement system by simultaneously performing multiple measurements to measure multiple flow rates. Since the final results are based on a combination of several measurements, any error in just one of the measurements may affect one, several or all the derived flow rates. This aspect of multiphase metering adds to the complexity of deriving simple procedures for maintenance and proving of a multiphase flow meter. Consequently, operators are reluctant to remove the test separator as a proving mechanism to fully take advantage of the cost benefit by using multiphase flow meter. This paper describes a system that can justify omitting the test separator as a proving mechanism by adding two independent and redundant systems to a standard MFI MultiPhase Meter. The system is an integrated part of the MFI MultiPhase Management System (MMS) and enables operators to extend savings in investment and operating expenditures gained from multiphase metering technology.

## 2. System Components

The system consist of the following main components:

- 1) MFI MultiPhase Composition Meter\*
- 2) MFI MultiPhase Cross-Correlation Velocity Meter. \*
- 3) Venturi Velocity Meter.
- 4) Dual Temperature, Pressure and delta Pressure transmitters.
- 5) PVT Module.
- 6) MultiPhase Management System (MMS)

\*) Integrated part of a standard MFI MultiPhase Meter.

### 2.1. Composition Meter

The composition and cross correlation sensor (MFI MultiPhase Meter Sensor) is a compact, straight spool piece with no moving parts and no significant pressure drop. A four-inch sensor, as shown in figure 1 below, is less than 700 mm long.

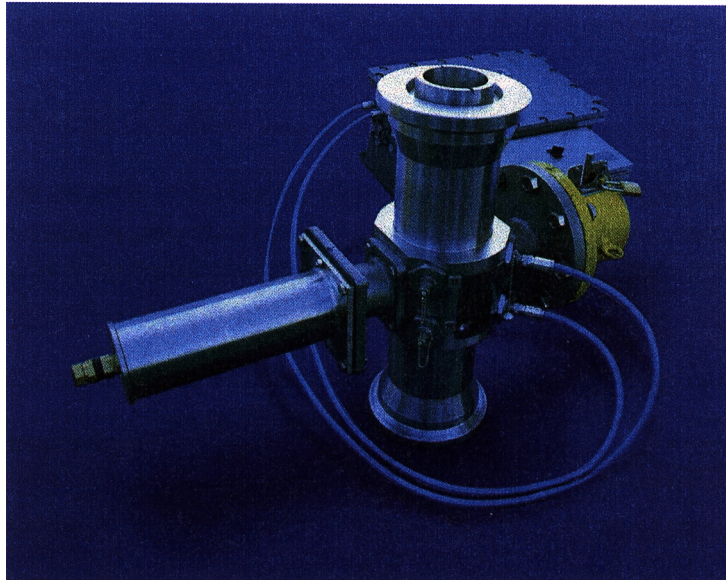


*Fig. 1 - 4" MFI MultiPhase Meter. The sensor is a compact, straight spool piece with no moving parts and no pressure drop. A four inch sensor is less than 700 mm long and used to measure the composition and velocity by cross-correlation.*

Measurement of the multiphase composition is based on measurement of dielectric constant of the multiphase mixture using a patented microwave technique together with measurement of gamma ray absorption based on a standard single energy gamma ray densitometer. These two measurements together with the sensor area provide three equations sufficient to calculate the oil, water and gas fraction as listed below.

Unknowns: % Oil, % Water and % Gas in the cross section of the pipe.

Equations:

$$(1) \sum (\Phi_{oil} + \Phi_{water} + \Phi_{gas}) = 100\%$$

$$(2) \Phi_{oil} \times \rho_{oil} + \Phi_{water} \times \rho_{water} + \Phi_{gas} \times \rho_{gas} = \rho_{measured}$$

$$(3) \Phi_{oil} + \Phi_{water} + \Phi_{gas} = f(\Phi_{oil}, \Phi_{water}, \Phi_{gas}, \epsilon_{oil}, \epsilon_{water}, \epsilon_{gas}, \epsilon_{measured})$$

Where:

$\Phi$  = Volume Fraction

$\rho$  = Density at line conditions.

$\epsilon$  = Dielectric constant at line conditions.

As shown in equation three, the composition meter must be calibrated with the dielectric constant of oil, water and gas. The dielectric constant of water is a complex variable of the form:

$$\epsilon_{water} = \epsilon' + j\epsilon''$$

Where:

$$\epsilon' = f(\text{Temperature})$$

$$\epsilon'' = f(\text{Conductivity})$$

Consequently, in order to calibrate the composition with the dielectric constant for water, only the water conductivity is required as calibration input. Alternatively, the meter itself can be filled with produced water and used to measure the water conductivity.

Most other multiphase meters require that the sensor must be filled with oil and gas in order to calibrate the composition measurement. The MFI Multi-Phase Meter, on the other hand, does not have this requirement due to the well-defined correlation between hydrocarbon density and dielectric constant as shown in figure 2 below.

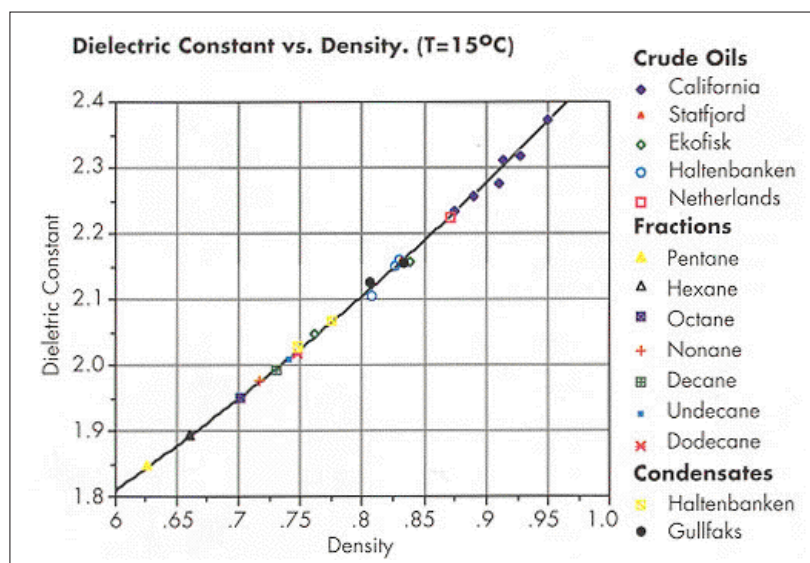


Figure 2: Relationship between hydrocarbon density and dielectric constant at microwave frequencies.

This correlation is only valid for microwave frequencies and can not be used for low frequency measurements such as capacitance and inductance. In addition, Roxar has patented this relationship in connection with hydrocarbon measurements.

## 2.2. Cross Correlation Velocity Meter

Roxar has in qualification tests at Porsgrunn (7 international oil companies), Gannet (Shell), Humble (Texaco), Trecate (Agip) and Pecorade (ELF) shown that the volumetric MFI Cross Correlation velocity meter and mass based Venturi velocity meter have almost equal performance. The MFI Cross-Correlation velocity meter is in addition the only meter of its kind being able to cross correlate on fine bubble flow and mist/gas flow.

The Cross-Correlation velocity meter uses two identical microwave sensors (such as used in the composition sensor) separated by a known distance in the pipe to measure velocity. By statistically comparing measurements from the upstream sensor with those of the downstream sensor using cross-correlation methods, one can determine the mean transit time for the mixture to move between the sensors. The sensor spacing and the measured transit time give velocity.

The sensitivity of the Cross-Correlation Meter is unparalleled and the MFI Cross-Correlation Meter works for all flow regimes including fine bubble flow. Furthermore, Roxar has broad experience with Cross-Correlation on different process conditions ranging from a few bars and slugging conditions to several hundred bars and stable flow. Our experience is ranging from low-pressure conditions where the variation in the signal is several thousand percent, to very high-pressure conditions, where the variation is less than 0.01%. Figure 3 to figure 6 show two examples of cross-correlation data at two different flow regimes plotted at the same scale. Figure 3 is an example of bubble flow conditions. Although the amplitude is small, there is a clear correlation between the signals giving the corresponding cross correlation peak of figure 4.

At slugging flow conditions, as shown in figure 5, the amplitude variation is much greater since the variation in the flow is greater. From cross-correlation data in figure 5 it is possible to see three gas slugs, several large gas bubbles and many small bubbles giving a corresponding cross-correlation peak as in figure 6. The information contained in the signals also provides useful information regarding the slip between liquid and gas. Roxar has developed a slip flow model to determine the gas and liquid velocities respectively from the measured velocity. Among other inputs, this model uses the statistical data from the composition and the velocity meter. These two velocities are combined with the readings from the composition meter to obtain the actual oil, water and gas flow rates. The Cross-Correlation Meter has a number of advantages compared to other multiphase velocity meters (including Venturi Tubes):

- Turn-down ratio of up to 35:1
- No moving parts
- None intrusive
- High sensitivity
- It also functions with zero water cut and fine bubble flow such as might be present during early production, liquid slugs in long pipelines or high pressure applications
- No differential pressure taps and tubing that can foul, partially fill or leak, or dP transmitters that can drift
- Easily used in high pressure systems without sacrificing accuracy

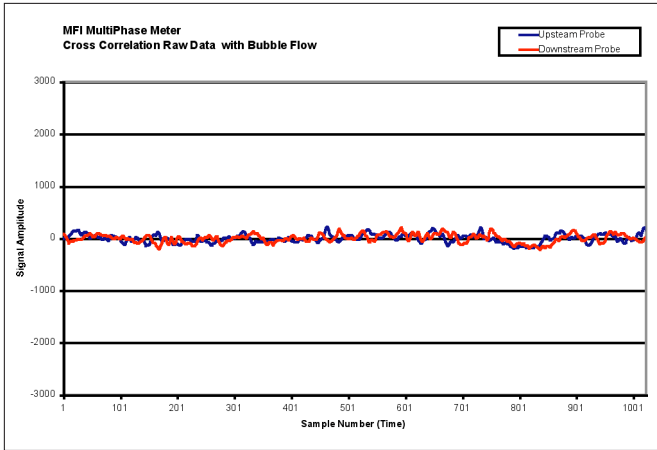


Figure 3:  
This is an example of bubble flow conditions. Although the amplitude is small, there is a clear correlation between the signals.

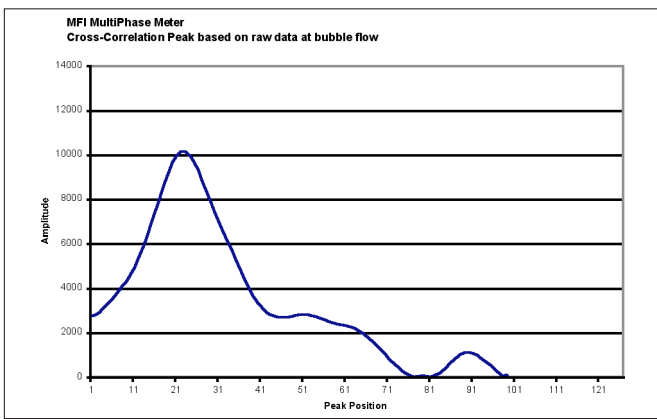


Figure 4:  
Corresponding cross correlation peak for bubble flow.

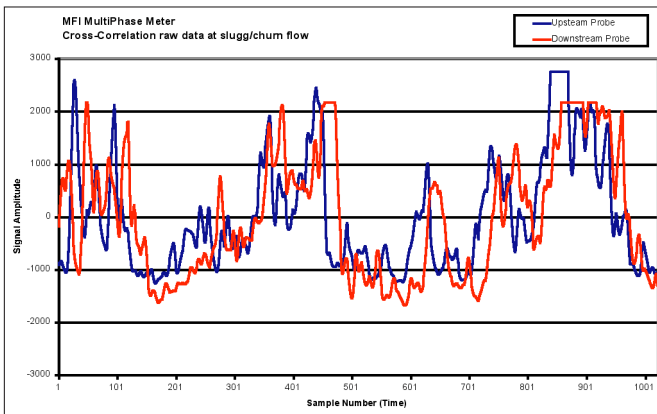


Figure 5:  
Cross correlation data at slug/churn flow. The amplitude variation is much greater compared to figure 3 since the variation in the flow is larger. From cross-correlation data it is possible to see three gas slugs, several large gas bubbles and many small bubbles.

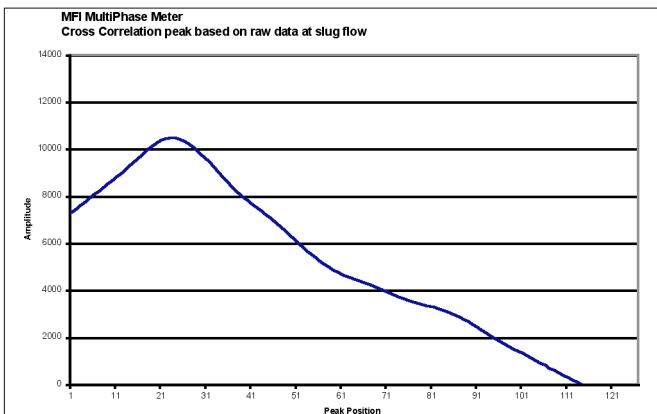


Figure 6:  
Corresponding cross correlation peak for slug/churn flow.

### 2.3. Venturi Velocity Meter

The venturi velocity meter is essentially measuring the mass flow of the multiphase mixture. Combining the total mass flow measurement from the venturi meter with the composition measurement provides a measurement of the volumetric flow rates comparable towards the Cross Correlation velocity meter.

### 2.4. PVT Module

The PVT module calculates the oil and gas densities in addition to the gas oil ratio (GOR) at any given temperature. Entering the mole fraction, mole weight and density of the hydrocarbon fractions of the well enable configuration of the PVT module. The PVT module can be used to calculate the oil and gas density and GOR at any pressure and temperature. Consequently, the module serves multiple purposes such as calibration values for oil and gas density for the MultiPhase Meter and conversion to other temperature and pressure conditions such as standard or “test-separator” conditions.

In addition, the PVT module provides a redundant “measurement” of the GOR. The multiphase meter is measuring the GOR, which is derived based on a combination of the oil and gas density calibration from the PVT module, measured, GVF and velocities.

The PVT module can also be used to alter the expected hydrocarbon fraction (mole weight, density and fraction of components) based on a known oil and gas density and GOR. This function can be used to “calibrate” the PVT composition towards measurements from a test separator, or as a part of an iteration process between the PVT module and the MFI MultiPhase Meter.

### 2.5. MultiPhase Management System

The MFI MultiPhase Management System (MMS) is the overall system for managing one or several MFI MultiPhase Meters. The MMS is implemented on standard PC-based software and hardware, and will for the user be seen as a windows based, easy to use graphical Man Machine Interface. From the graphical user interface of the MMS the multiphase meters can be configured, calibrated, diagnosed and operated.

In addition, the large amount of information available from the multiphase meter is stored in a standard SQL database. The use of a standard SQL database for data storage results in significantly easier data utilisation and distribution. Connected to a remote accessible network, the data from the multiphase meter can be on-line processed and analysed from locations far away from the meter itself.

- PVT package for conversion of flow rates to user specified pressure and temperature conditions, and automatic density calibration
- Preventive maintenance routines to verify operation and measurement with redundant transmitters and measurement principles.
- Independent Software package for remote use of the data available from the SQL Database (trending, pre-defined reports, etc)
- Simulation package for re-calculation of the logged raw data.
- Well Management Module for data logistics and analyse.

A block diagram of the MMS modular system is shown in figure 7.

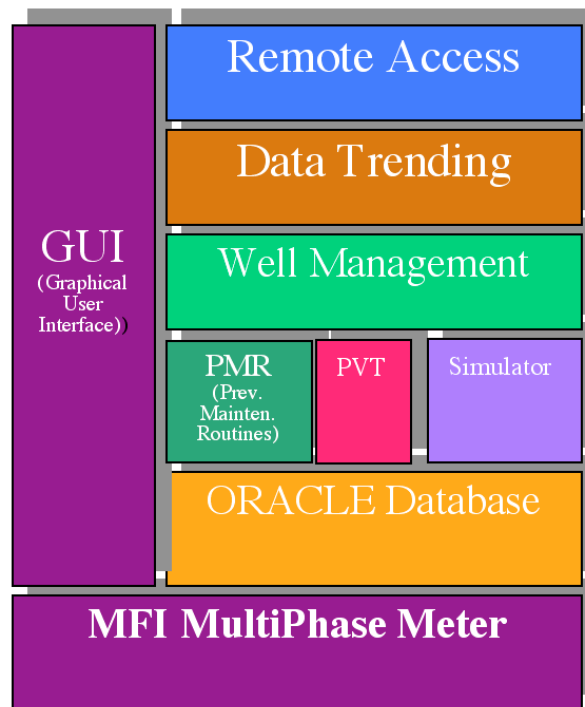


Figure 7: MultiPhase Management System (MMS). A modular program to fully take advantage of the abilities within multiphase measurements.

### 3. System Description

#### 3.1. System Overview

Normally, metering equipment are at regular intervals taken out of service and send to a laboratory for calibration and maintenance. Alternatively, calibration can be carried out on the site using a proving system following a regular calibration schedule. In both cases, calibration and maintenance is both costly and time consuming and in most cases calibration and maintenance are carried out on instruments that are fully within its specification. As a consequence, it is becoming more common to use dual redundant system such that calibration and maintenance only are performed if the two measurements differ by a predefined amount.

A similar methodology called PMR (Preventive Maintenance Routines) has been adopted to the MFI MultiPhase Meter based on redundant measurements from “well known” measurements principles.

The MFI MultiPhase Meter has in several independent qualifications tests shown a very good match between the Cross-Correlation and venturi velocity meter over the entire operating envelope of the meter. The Cross-Correlation velocity meter is a volumetric measurement principle whereas the venturi velocity meter is based on mass flow. Combining the two measurements give redundancy and a means to improve the accuracy of the overall velocity measurement. The composition measurement (GVF and watercut) is based on measurement of dielectric constant (microwave measurement) and density (gamma radiation



The MFI multiphase meter measures the oil, water and gas mass flow rates at actual conditions. In order to do so, it needs to be calibrated with the oil, water and gas density together with the water conductivity. Any error in the oil or gas density calibration values will typically affect the measured gas to oil ratio while the measured hydrocarbon mass flow rate remains almost unaffected. The reason for this is the MFI patented “AutoZero” correlation between dielectric constant and density for hydrocarbon as shown in figure 2. This effect is demonstrated in simulations of three cases as shown in figure 8-13 below. For each case a variation of  $\pm 10\%$  of the oil and gas density is introduced and the relative change in the oil, gas, water and hydrocarbon mass flow rate is shown in the graphs.

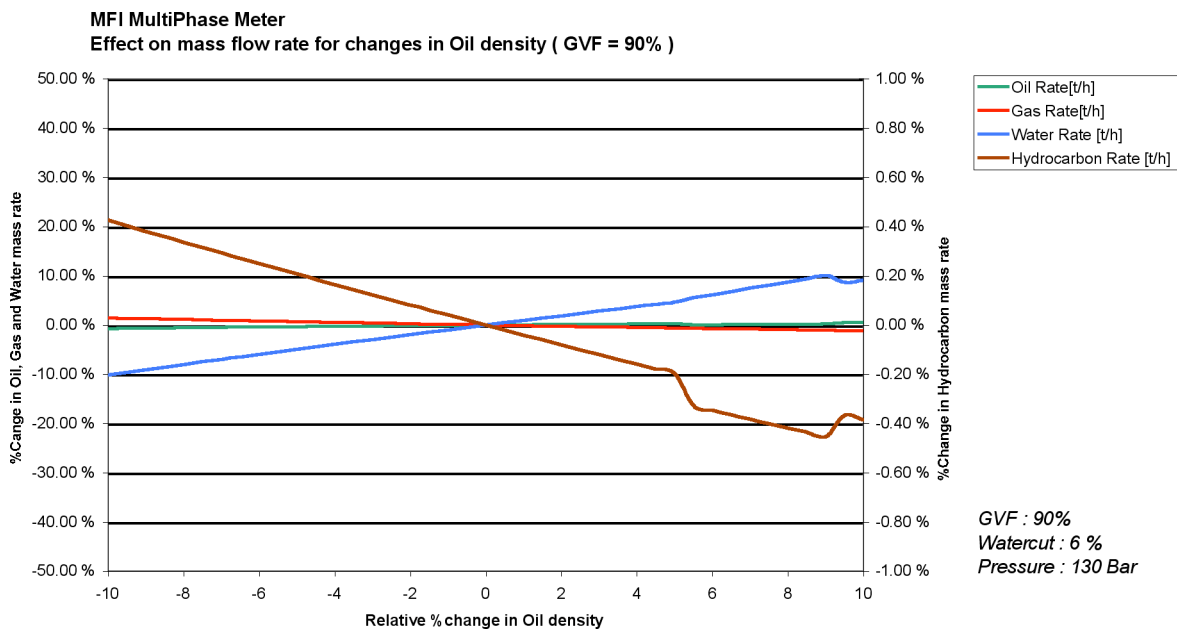


Figure 8: Effect on mass flow rates as a function of calibration value for oil density.

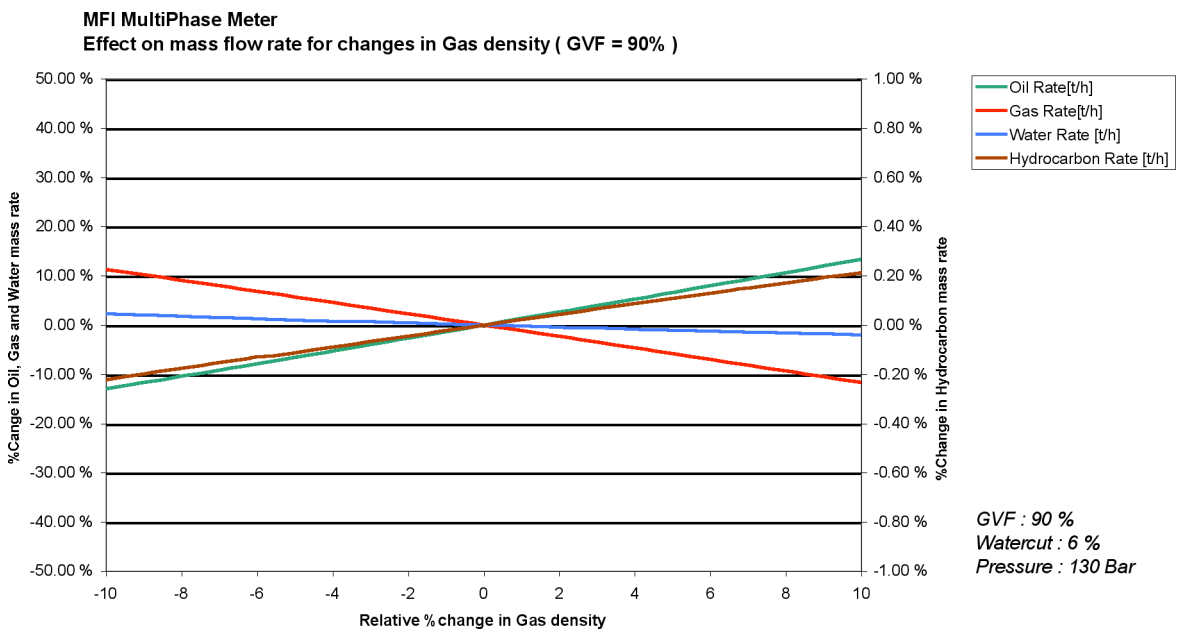


Figure 9: Effect on mass flow rates as a function of calibration value for gas density.

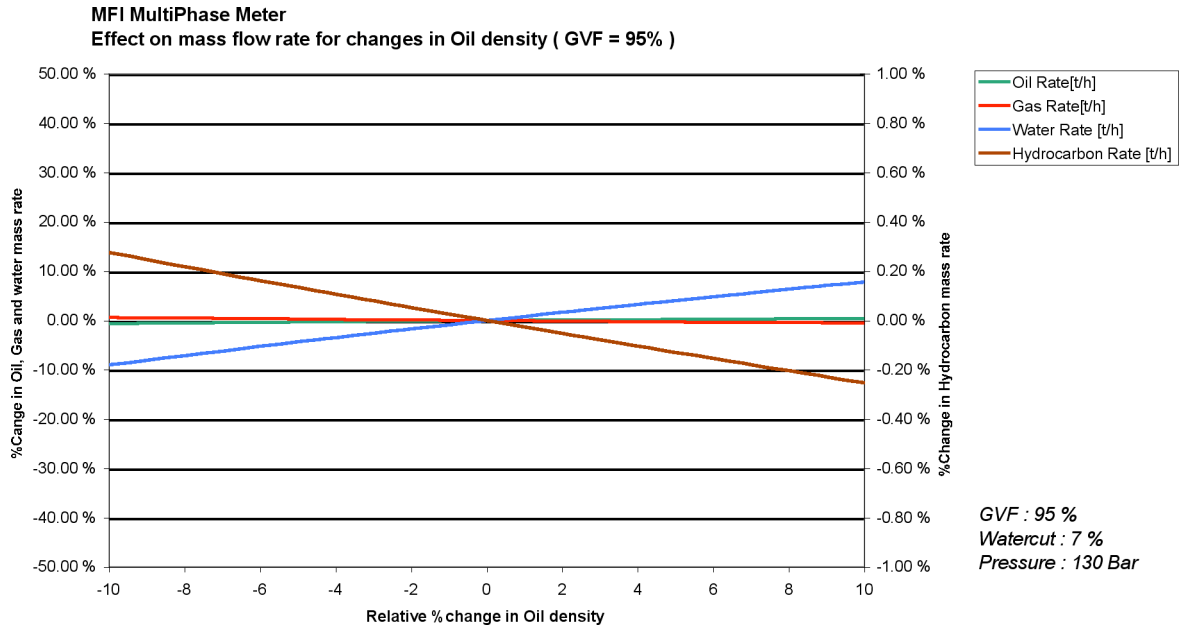


Figure 10: Effect on mass flow rates as a function of calibration value for oil density.

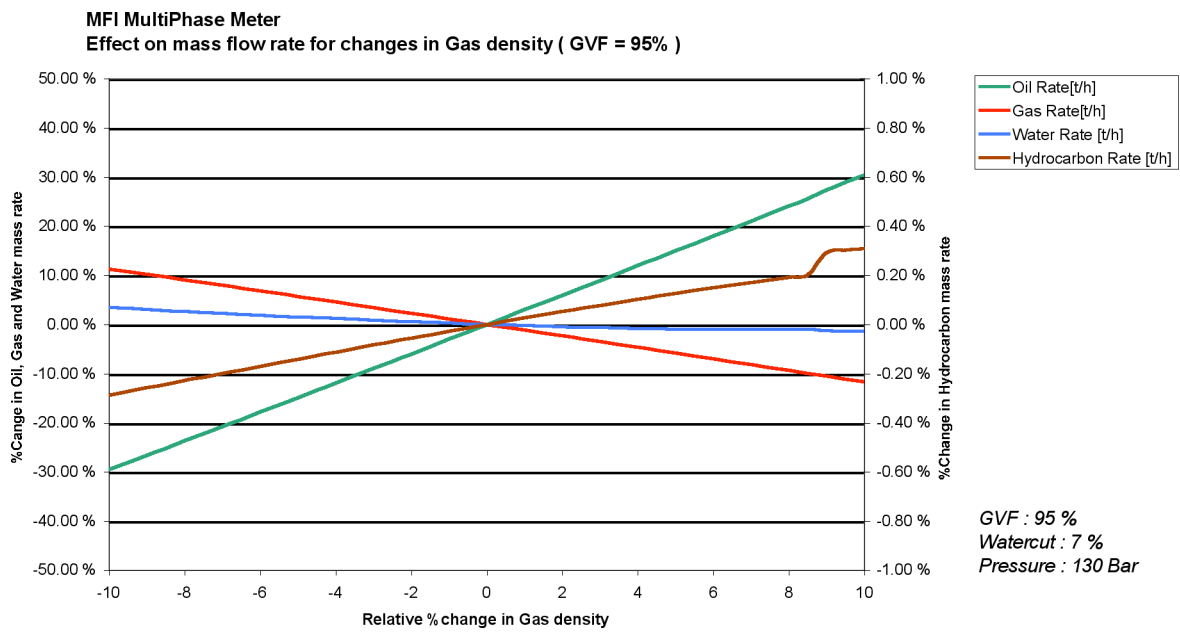


Figure 11: Effect on mass flow rates as a function of calibration value for gas density.

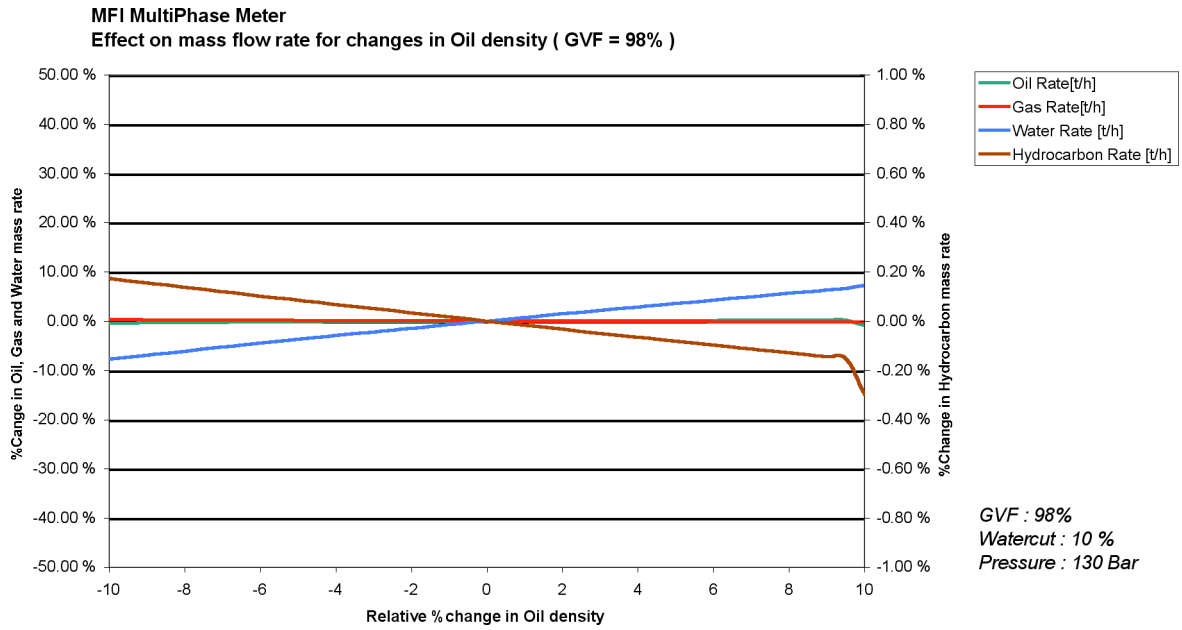


Figure 12: Effect on mass flow rates as a function of calibration value for oil density

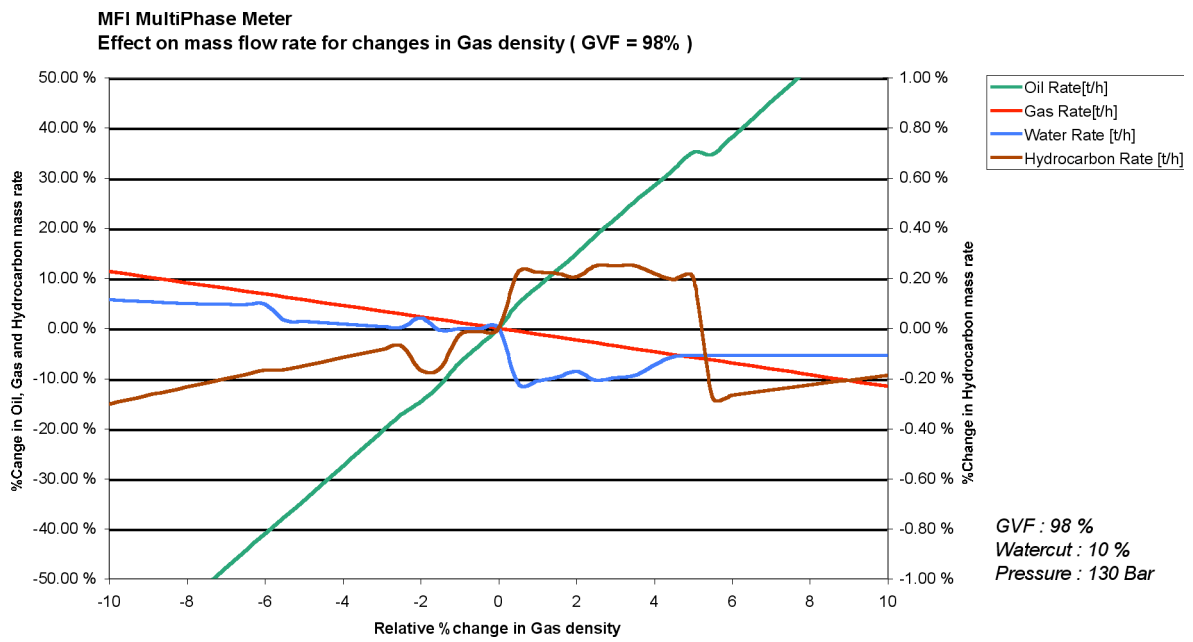


Figure 13: Effect of mass flow rates as a function of calibration value for gas density.

The effect on the measurements for all the above listed cases are summarized in the table below:

Composition		Relative Change[%]		Measurement effect[%]			
GVF	Watercut	Density Oil	Density Gas	Oil	Water	Gas	Hydr. Carb.
90 %	6 %	10 %	0 %	0.6 %	0.6 %	9.0 %	<b>0.28 %</b>
90 %	6 %	0 %	10 %	20.5 %	3.5 %	11.5 %	<b>0.30 %</b>
95 %	7 %	10 %	0 %	0.7 %	10.0 %	1.5 %	<b>0.40 %</b>
95 %	7 %	0 %	10 %	13.5 %	2.2 %	11.5 %	<b>0.22 %</b>
98 %	10 %	10 %	0 %	0.9 %	7.2 %	0.3 %	<b>0.30 %</b>
98 %	10 %	0 %	10 %	68.0 %	5.7 %	11.6 %	<b>0.30 %</b>

As seen from the graphs, the hydrocarbon mass flow rate is far less sensitive to errors in the hydrocarbon density calibration values compared towards the oil and gas flow rate. E.g., whereas the relative error on the oil mass flow rate may be as great as 60-70 % in the event of a 10% change in oil and gas density calibration values, the relative error on the hydrocarbon mass flow rate is within 0.4%. This feature is due to the well-defined and “proprietary” correlation between hydrocarbon density and dielectric constant for dielectric measurements in the microwave frequency region.

#### 4. Case Study

Discrepancies in the measurement system can be detected comparing the redundant measurement variables. Any difference between redundant measurement beyond predefined limits may originate from failures in the measurement system, changes in the well properties such as a compositional change of the hydrocarbon fraction, water salinity changes or internal deposits such as wax or scale in the multiphase sensor. Any discrepancy in the measurement system can be detected and isolated by monitoring the following variables over time:

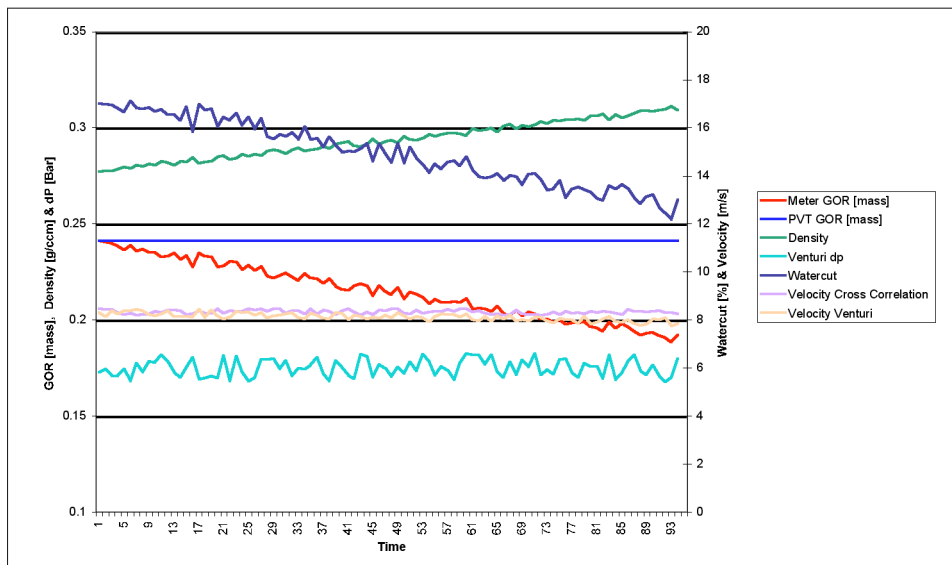
- a) Measured Mass GOR (Meter GOR).
- b) GOR from PVT module (PVT GOR)
- c) Measured density.
- d) Measured Watercut
- e) Measured venturi delta pressure.
- f) Velocity based on Cross-Correlation
- g) Velocity based on Venturi

System alarms would typically be generated based on a discrepancy between measured GOR and PVT GOR, Cross-Correlation velocity and Venturi Velocity and finally redundant temperature, pressure and delta pressure transmitters. To identify the origin for the discrepancy, it is required to analyze the trend in the measurement data to identify potential problems.

The following examples demonstrate how failure situations can be detected and analyzed. The plots are based on simulation of raw data using the MFI simulation module. Any measurement error has gradually been introduced such that at time equals 1, no error has been introduced and at time equals 100, maximum error has been introduced. The following “failure” situations has been simulated:

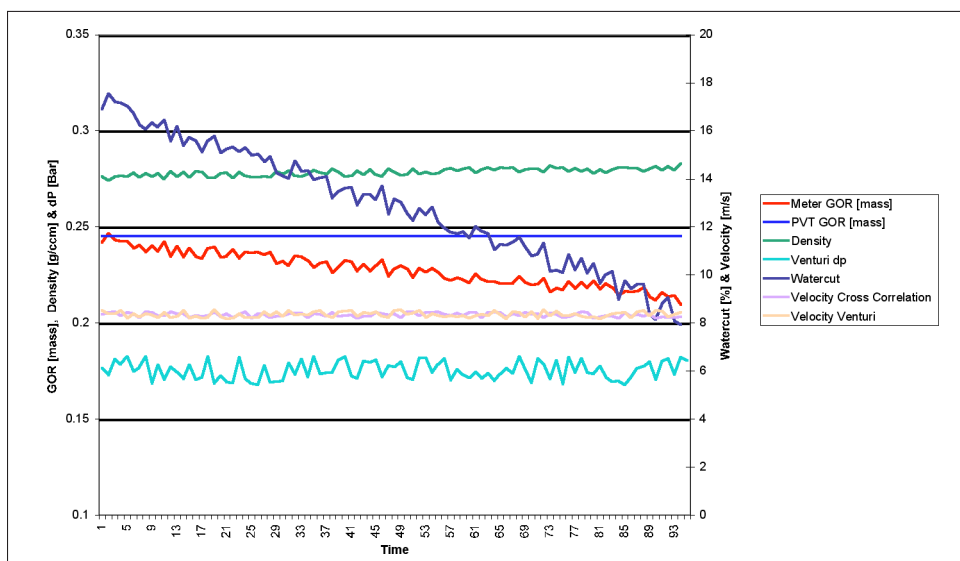
- 1) Error in density measurement.
- 2) Error in watercut measurement.
- 3) Compositional change of well fluids.
- 4) Error in venturi delta pressure measurement.
- 5) Internal deposits such as scale and Wax.

#### 4.1. Error in Measured Density



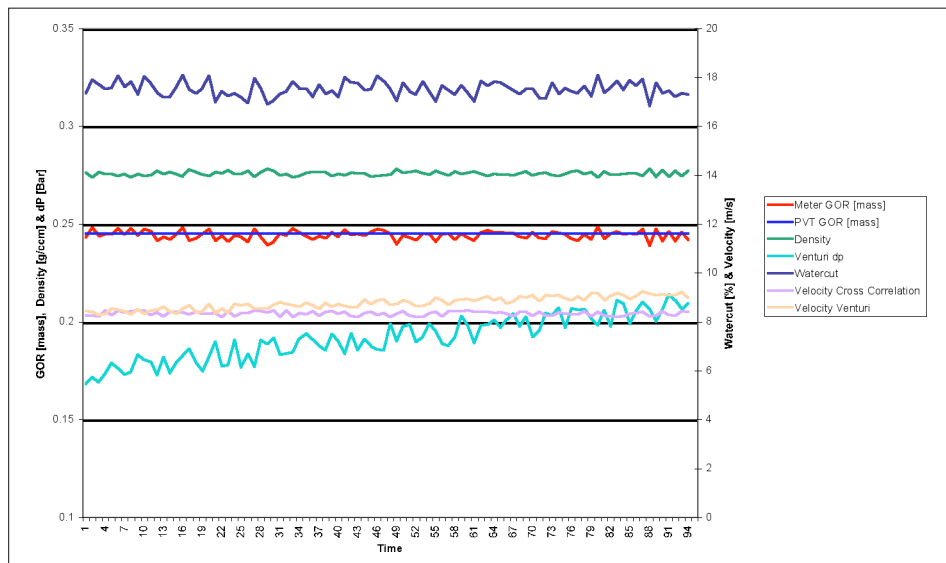
In the event of an error in the gamma densitometer, there will be an effect on the measured density. Since the measured density is wrong, it would affect the measured watercut, measured GOR (Meter GOR) and eventually the volumetric velocity from the venturi.

#### 4.2. Error in Measured Watercut



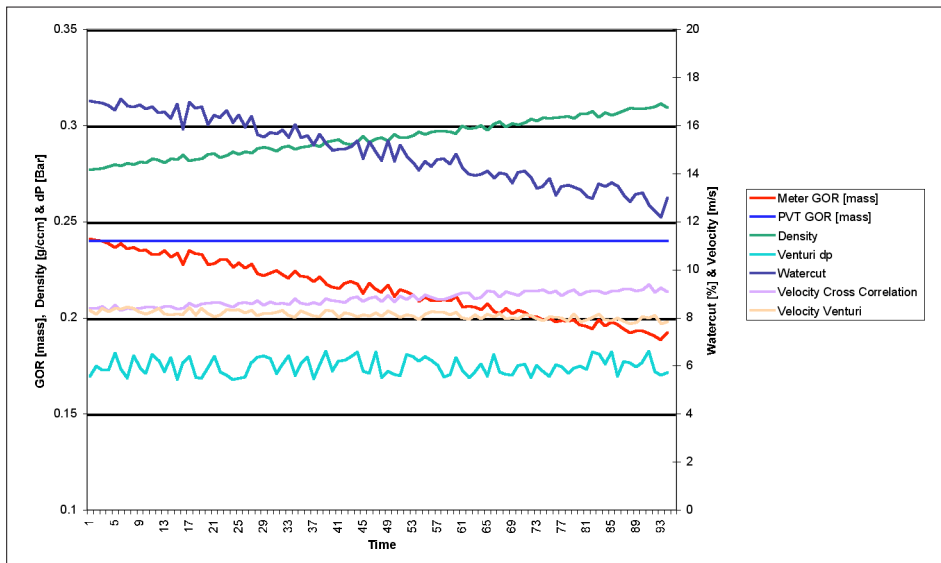
Any failure in the watercut measurement will most easily be detected by comparing the GOR based on the PVT module (PVT GOR) and the measured GOR (Meter GOR). In watercontinuous flow, a similar behavior could be an indication of a salinity change in the produced water such as at water break through in the reservoir. However, the GOR of the meter may also change due to a compositional change of the well such as a gas break-through. Therefore it may be required to verify the watercut measurement by either a sample from the well stream or by inspection of a long-term trend of the watercut in order to assess the cause for discrepancy on mass GOR.

### 4.3. Error in PVT Module Composition



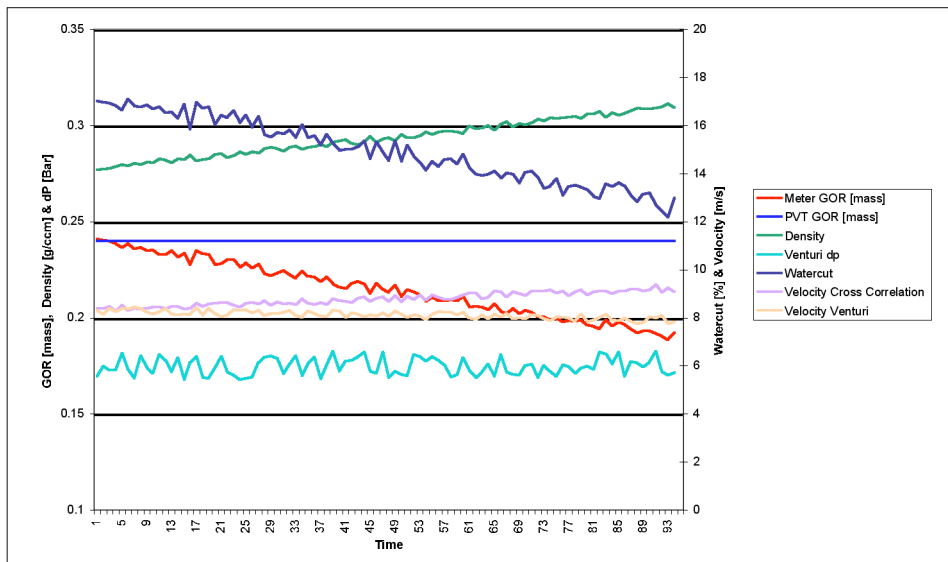
Gas break-through of the well would typical affect the composition of the hydrocarbon fraction. A compositional change of the well would most easily be detected by comparing the GOR of the meter and the PVT module. As shown above, a compositional change of the well would typical affect the mass GOR of the meter while the other measurements would be less influenced. Since the PVT module is unaware of the change in well composition, it will remain unchanged. To investigate the possibility for a well compositional change, the PVT module can be used to estimate the new well composition based on the measurements from the MFI MultiPhase Meter. An iteration process between the PVT module and the meter will then be initiated and continue until the GOR from the PVT module matches the GOR from the meter. The outcome of this iteration process would be the new hydrocarbon well composition.

#### 4.4. Error in Venturi Delta Pressure Measurement



Deviation between the velocity measured by the venturi meter and the Cross-Correlation is an indication of an error either in the venturi meter, Cross-Correlation meter or density measurement. Since the GOR of the PVT module matches the GOR of the meter, the density measurement is most likely correct and hence indicating an error in the venturi velocity measurement. For this particular situation, there is most likely an error on the delta pressure drop across the venturi since it is not following the same trend as for the stable readings from the Cross-Correlation measurement.

#### 4.5. Internal deposits such as Scale or Wax



Tests performed by Statoil and Rogaland Research Center has shown that the MFI MultiPhase Meter is able to measure with severe amount of scale on the inside of the sensor. However, scale and wax would affect the calibration of the meter. Above is a typical behavior of the meter in the event of scale or wax. The behavior of the venturi in the event of scale and wax is uncertain and for this particular example it is assumed to remain unaffected. In fact, the venturi may give an output velocity of zero due to plugging of delta pressure tapings, or give a very high velocity due to reduced beta ratio. However, since the behavior of the cross correlation meter is well defined whereas the venturi is uncertain, they would most likely not give the same result as demonstrated by this example.

A typical indication of scale or wax is increased density together with decreased watercut. As a result, the GOR measured by the meter would not match the GOR from the PVT module. In addition, the velocity measured by the Venturi would not match the velocity measured by the Cross-Correlation velocity meter for several reasons. First, reducing the area of the sensor would affect the calibration of the Cross-Correlation velocity meter such that it gives a too high velocity, and second, it would have an uncertain affect on the dP measurement and beta ratio of the venturi.

## 5. Summary

The cost benefit by using multiphase meters is according to oil field operators substantial compared towards conventional technology. MultiPhase meters have, over the past few years, shown to be reliable and give good and repeatable measurement. At present, one of the main challenges within the industry is to provide the required amount of understanding among end users related to working principles, limitations and maintenance requirements in addition to utilization of new opportunities based on real time measurements. Roxar has developed a new concept called MMS (MultiPhase Management System) to provide the end user with a tool for simplified calibration and maintenance based on Preventive Maintenance Routines (PMR) in addition to modular add-on functions to fully take advantage of large amount of “real-time” data stored in a database. The foundation for the PMR module is based on an extensive qualification program of independent velocity measurements, integration of a PVT package and the well-defined correlation between dielectric constant and density for hydrocarbon at microwave frequencies. The MMS system will be an attractive solution to manage well test and allocation data both in terms of investment and operation cost in addition to improved utilization of multiphase measurements to recover and produce more oil.



# Operational Experience with Multiphase Meters at Vigdis

By

*Odd-Petter Kalsaas, Fluenta AS, and Espen Egner, Saga Petroleum ASA*

---

## Introduction

Two identical 8» MPFM 1900 VI were delivered to the Vigdis Field Dev. project in January 1996. The meters are installed on the Snorre platform, one on each of the main flow lines from the Vigdis satellites, and were commissioned for use in October 1997.

Based on an unexpected shift in the calibration of the capacitance sensor, observed and corrected during commissioning, Fluenta recommended to Saga Petroleum that the two meters should be upgraded from ceramic liners to the new PEEK open electrode construction. Saga agreed to this recommendation, and the job was performed during a two week planned shutdown in May 1998.

The two multiphase meters were re-commissioned in first week of June '98. Further adjustments were done during the next months, in order to optimise the performance of the meters. MPFM measurements during a multirate test from all Vigdis wells are compared to test separator measurements in April 1999.

Comparison between the multiphase meters, and the downstream separator measurements, now shows stabile and repeatable measurements well within Fluenta uncertainty specifications.

This paper will report on the combined experiences of Saga Petroleum and Fluenta, both with respect to failure mode, repair, operational experience and the use of data.

## 2. The Fluenta MPFM 1900VI measurement technology

The Fluenta multiphase meters are specifically designed to handle the various, and often complex, flow regimes that must be expected, without introducing mixing or separation of the flow. This has been achieved by developing a unique method for interpretation of sensor signals, the Dual Velocity method. This method is capable of handling complex flow regimes, including severe slugging, inhomogeneous phase distribution and interphasial slip.

## 2.1. Measurement principle

The MPFM 1900VI measurement system consists of a capacitance sensor, an inductive sensor, a gamma densitometer, a venturimeter and a system computer. The mean dielectric constant of the flow is measured using a non-intrusive, surface plate, capacitance sensor. The mean density of the flow is measured using a clamp-on gamma densitometer. Together these two measurements provide the instantaneous composition of the flow at the measurement location. At high water cut, when water is the continuous liquid phase, the mixture conductivity is measured using an inductive type sensor. This then replaces the capacitance measurement in the composition calculation. Velocity of the flow is determined by cross-correlation between different electrode pairs in the capacitance sensor. A venturi meter extends the range of the multiphase meter to cover single phase liquid and annular flow, and add redundancy to the velocity measurement. By combining both the compositional and the velocity information of the flow, the actual flowrates of oil, gas and water are determined by mathematical models hosted in a PC system.

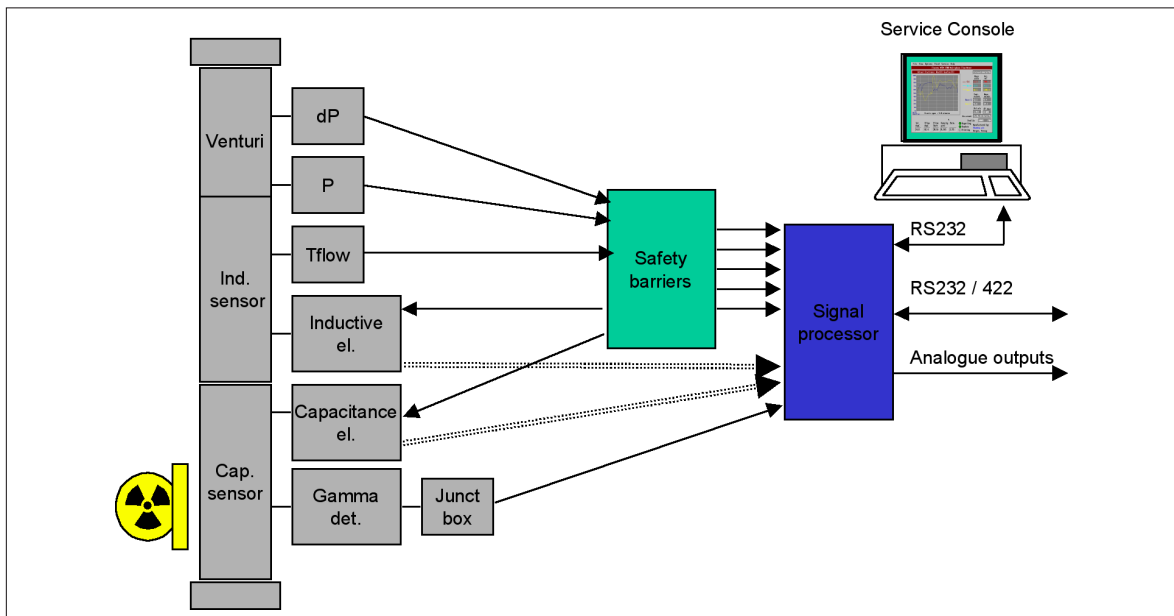


Figure 2.1 The Fluenta MPFM 1900VI; Block diagram

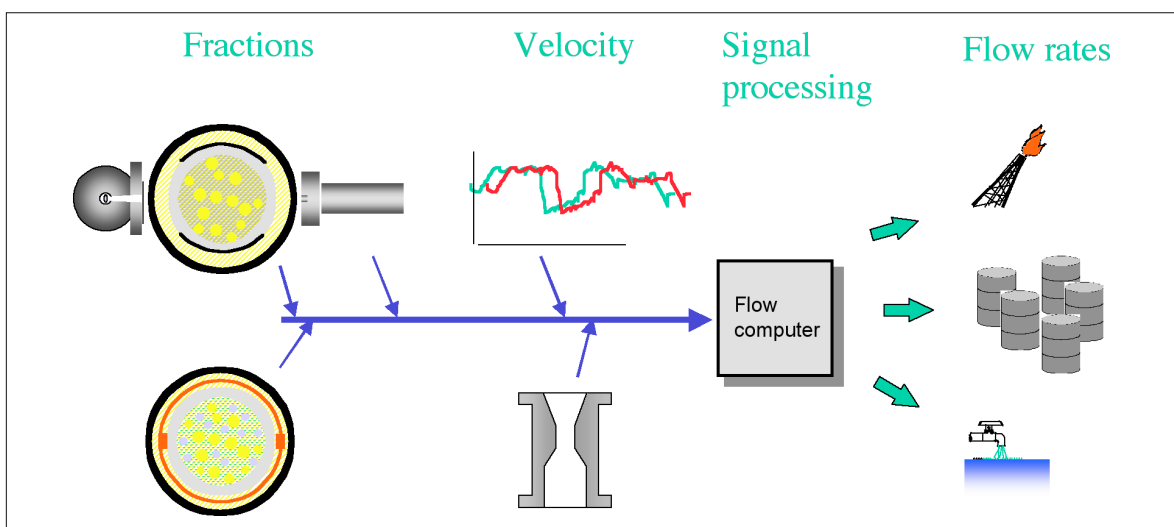


Figure 2.2 The Fluenta MPFM 1900VI; Measurement principle

## **2.2. The Dual Velocity method for handling of interphasial slip.**

The sensor system has been configured to measure the distribution of velocities present in the flow, and interphasial slip is directly measured and compensated for using the unique “Dual Velocity method”. This is achieved by measuring the two most predominant velocities in the multiphase velocity distribution; the velocity of the pseudo-homogenous dispersed phase, and the average velocity of larger gas bubbles.

By combining these velocities with measured cross-sectional area fractions of dispersed phase and “large bubbles”, flowrates of oil, gas and water can be calculated irrespective of flow regime (restricted to vertical upwards flow). In a somewhat simplified way, one can explain the Dual Velocity method to treat the flow as a “two-phase” mixture in terms of velocity: a pseudo-homogeneous mixture of oil, water and small gas bubbles; and a “free” phase consisting of larger gas bubbles travelling with an average velocity significantly higher than that of the “dispersed phase”.

The non-intrusive design, together with the Dual Velocity method for handling of phase slip, means the Fluenta multiphase meters do not require mixers to homogenise the flow, or separator to split the flow, before measurement. This gives the meter a wide operating range, which is not limited by the efficiency of the upstream flow conditioner or splitter. Interaction with the flow is kept to a minimum, avoiding pressure drop, erosion, or creation of emulsions that may otherwise seriously affect the downstream process.

## **2.3. Operational experience**

Fluenta has participated with good results in a number of independent tests, both in laboratory as well as in field, with its multiphase meters. Perhaps even more important is the extensive operational experience that has been accumulated since introduction of the multiphase fraction meter MPFM 900 in 1992. A total of 20 Fluenta multiphase meters are now in operation world wide. Reporting of test results and operational experiences from these various installations is not scope of this presentation, the reader is however referred to separate documentation, see reference list at the end of this paper.

As a brief summary, however, the referred tests and field installations conclude that the Fluenta multiphase meter provides data of a quality at least as good as a well managed test separator, that the availability of instantaneous data provides for improved well control, that the meter is easily maintained and operated, and that the failure rate is low.

Operational experience has however also shown that the liner technology previously used in the capacitance sensor has been a weak part of the system. The problem that has occurred in some applications has been related to stability and surface wetting of the ceramic liner. A new sensor construction, avoiding the previous liner technology, was introduced in 1997. This has been a success. The new capacitance sensor construction employs open electrodes embedded in PEEK (Polyetereterketone). The open electrode design increases sensitivity of the capacitance measurement, as the ceramic liner previously separating the electrodes from the bulk medium has been removed. But more important; the previous problem of water wetting of the liner surface is avoided. Not only is the liner removed, the PEEK insulator backing is also inherently hydrophobic. The first unit with the new sensor construction went into operation in August 1997. These installations have confirmed the expected good stability and sensitivity of the new design.

### 3. Field installation at Vigdis

Two identical 8" MPFM 1900 VI were delivered to the Vigdis Field Dev. Project in January 1996. The meters are installed on the Snorre platform, one on each of the main flow lines from the Vigdis satellite.

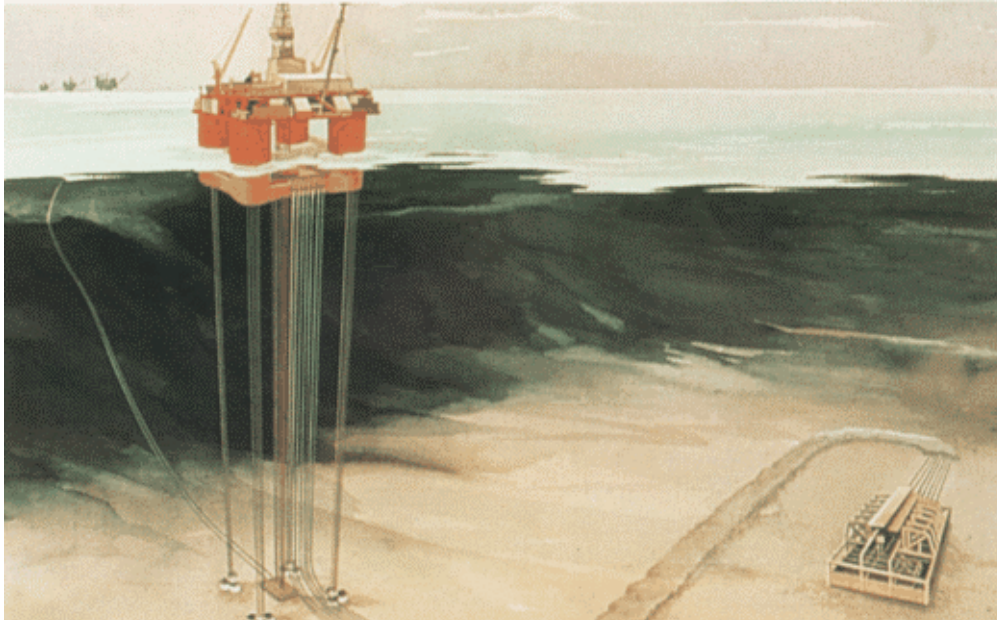


Figure 3.1 Snorre TLP

Reservoir oil is transported 6-7 km through two separate production lines from the Vigdis field to Snorre TLP, where the Vigdis process facilities are sited. The arrival temperature at Snorre TLP during normal production is 70°C. Normally three to four wells are produced through each of the production lines. A schematic drawing of the main Vigdis topside process is shown in Figure 3.2. The two 8" MPFM are marked with circles in the figure. All MPFM measurements are recalculated to standard conditions using PVT properties representing an approach to the Vigdis process.

#### 3.1. Purpose of Fluenta 8" MPFM at Vigdis

Testing of individual wells at Vigdis are performed using the test separator at Snorre TLP. One line may be lead to the test separator, while the other line is producing through the Vigdis process. With an increasing amount of wells producing to Snorre TLP, there is a need for alternatives to the traditional test separator control of individual wells. Fluenta 8" MPFM 1900 provide continuous measurements of each of the two production lines, so that observed variations in the Vigdis production may be tracked to the deviating line. Regardless of other activities at the Snorre TLP test separator, all wells at the deviating line may be tested individually, using the Fluenta 8" MPFM 1900. In addition, Idun measurement system is installed in each of the wells for allocation purposes. Fluenta 8" MPFM 1900 measurements on each of the production lines, were intended to be used as a continuous quality control and a quality improver for Idun.

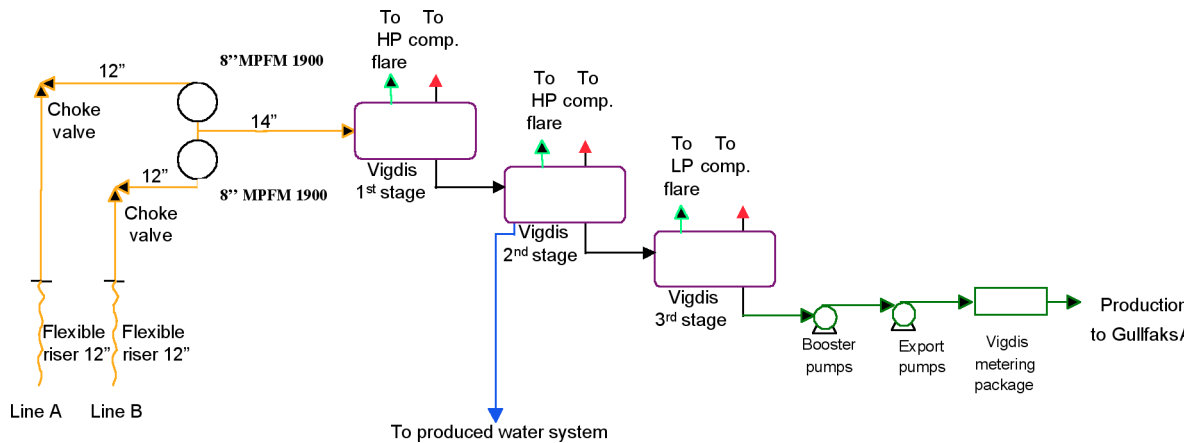


Figure 3.2 A schematic drawing of the main Vigdis topside process, including the placement of Fluenta 8" MPFM 1900.

### 3.2. Reference measurements

Reference measurements for each of the multiphase meters are achieved using the Snorre TLP test separator. There will be almost similar conditions at the 8" MPFM and the test separator during a separator test of Vigdis, and good reference measurements are expected. Results from a multirate test are presented in this paper.

Fiscal oil measurements at the Vigdis metering package before transportation to Gullfaks A, are used as continuous reference oil measurements to the sum of both MPFM. There is no gas injection at Vigdis, and the field contains highly undersaturated oil with a constant GOR. The fiscal oil measurements may therefore be used as reference measurements of gas. Water produced from 2<sup>nd</sup> stage separator plus the remaining water in oil at Gullfaks A are used as reference measurements for water. This is not a fiscal reference.

## 4. Operational experience of multiphase meters

The two multiphase meters were installed in the Vigdis modules during the first half of 1996, while the modules were still at the assembly site at Nymo. First oil was flowed through the meters in the early part of 1997, and commissioning by Fluenta was performed during 22 – 28 October 1997.

During commissioning, Fluenta noted that the flow rate through multiphase meter tagged #801 was well below the lower operating range for the meter. The flow rate through the meter tagged #806 was within the operating range, and the flow rate measurements were in agreement with separator measurements. It was further noted that the calibration of the capacitance sensor had shifted since the factory calibration. This was commented as unusual. No accurate comparison between multiphase meter readings and separator measurements were performed or available. Better PVT data for calculation to standard conditions would be required in order to deliver optimum performance from the meters.



*Figure 4.1  
One of the two multiphase meters installed at the Snorre TLP*

#### **4.1. Operational experience; October '97 – April '98**

Both meters have been operational the whole of this period. No operational problems have been reported, and no scheduled or unscheduled service has been performed. Data for direct calibration or comparison between multiphase meter readings and separator readings has not been available.

#### **4.2. Refurbishment of the internal sensor assembly**

Based on the observed and unexpected shift in the calibration of the capacitance sensor, Fluenta recommended to Saga Petroleum that the two meters should be refurbished. Saga agreed to this recommendation, and the job was performed during a two week planned shutdown in May 1998.

The work involved a complete upgrade of the sensor internals, replacing the previous liner technology with contact electrodes in a Peek insulator. The meters were back in the line within the scheduled shutdown period.

#### **4.3. Operational experience with the new sensor design**

The two multiphase meters were re-commissioned in first week of June '98. The measurements from meter #806 were in line with the separator readings, but no data for accurate comparison or calibration were available. It was observed that meter #801 was still operated well below the operating range of the meter.

In August 1998, Saga reported to Fluenta that water cut readings for meter #806 was in error. This had occurred as an additional well had been routed through the meter, and a flow rate dependence of the water cut was observed. Investigation of the problem showed that the open electrodes tended to pick up electrostatic noise generated within the flow itself (due to friction). In the previous sensor design this electrostatic noise was filtered by the capacitance of the liner. The solution was therefore to implement a similar filter function in the detector electronics. The sensor detector electronics was modified according to the above, and the flow rate dependence of the water cut disappeared.

Since then, no further operational problems have been observed and both meters have been in continuous operation with satisfying performance. Figure 4.2 shows the oil flow rates from the meters compared to the fiscal measurements in the beginning of February 1999. The readings from the meters were about 8% too low at the time.

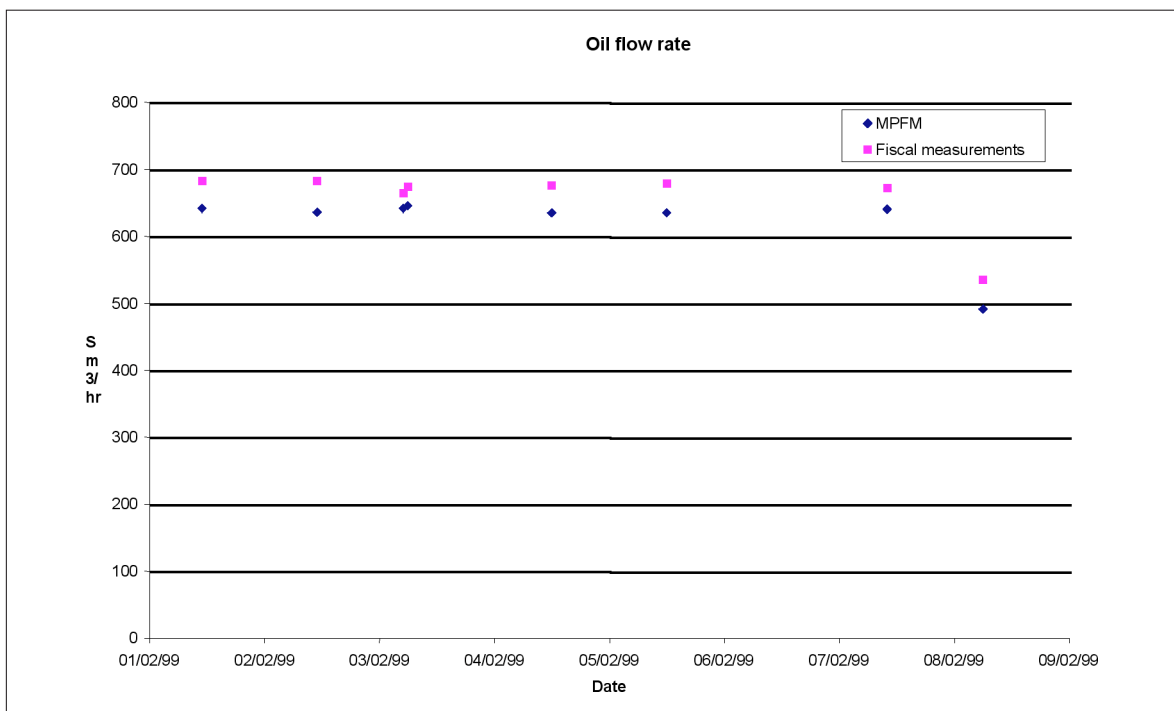


Figure 4.2 Oil flow rate from multiphase meters compared to fiscal measurements, February 1999

#### 4.4. A preliminary conclusion

The upgrade from the originally delivered sensor construction (ceramic liners), to the new open electrode design have proved successful. Measurements from the two meters show repeatable readings, in good agreement with process measurements and fiscal readings at the Snorre platform. The sum of the measured oil flow rate from the two multiphase meters do however show a systematic deviation of around -8% from the fiscal oil measurement. This is within Fluenta specification for a statically calibrated meter. By in-situ flow calibration, the systematic deviation can be further reduced.

At this stage, one could therefore have decided to implement a simple solution using meter factors to correct the deviation. The two Vigdis multiphase meters are normally operated within a fairly narrow operating range, which would have made this solution quite acceptable.

## 5. In-situ performance optimisation and evaluation

Saga wanted the meters to be capable of handling a large change of working point, e.g. variations that will occur when different well combinations are routed through the meters. In the beginning of 1999, Saga and Fluenta therefore started discussing how to narrow the gap between multiphase and fiscal measurement of oil, without using the simple approach of factor calibration. Although this approach would certainly have improved the results for this particular well combination, a larger change of working point would possibly require re-calibration.

The signal processing used in the Fluenta multiphase meters are based on a physical interpretation of the flow conditions inside the meter. Any change of these interpretation models should be generic, rather than specific for a particular installation. In order to avoid the simple factor calibration, the actual reason for the deviation would therefore have to be identified.

### 5.1. Density model improvements

Data from the multiphase meters were analysed, and it was found that the assumed density distribution within the dispersed part of the flow was too simple. While the implemented model assumed a homogeneous density distribution in the dispersed flow in between large gas bubbles, a more correct approach is to assume a higher concentration of gas towards the middle of the pipe also in the dispersed part of the flow. The meters at Vigdis are quite large (8" ID), which explains why the effect of a simple model for the density distribution is more pronounced here than for other installations.

A new improved algorithm was developed, assuming a higher density closer to the wall of the pipe than in the centre of it. This results in a lower gas fraction and hence a lower gas flow rate, in addition to a lower water cut. The measured oil flow rate will then increase. This new model is implemented as a general improvement of the flow models used in all Fluenta multiphase meters.

In March 1999 the new density distribution algorithm for the dispersed phase of the flow was implemented. Since no test separator was available at the time, the sum of the flow rates through the two meters were compared to the readings from the separators at stage 1, 2 and 3, and the fiscal oil flow rate measurements. The readings were stable and repeatable, within the uncertainty specifications for the meters. The water cut and the flow rate through the two meters are not same, so this test was a check of the sum of the flow rates and the average water cut calculated by the two meters. Error! Reference source not found. shows the flow rate through the meters compared to fiscal measurements in the beginning of April 1999. The readings from the meters are about 3% low. Compared to Figure 4.2 the deviation was reduced by 5% by using this improved algorithm.

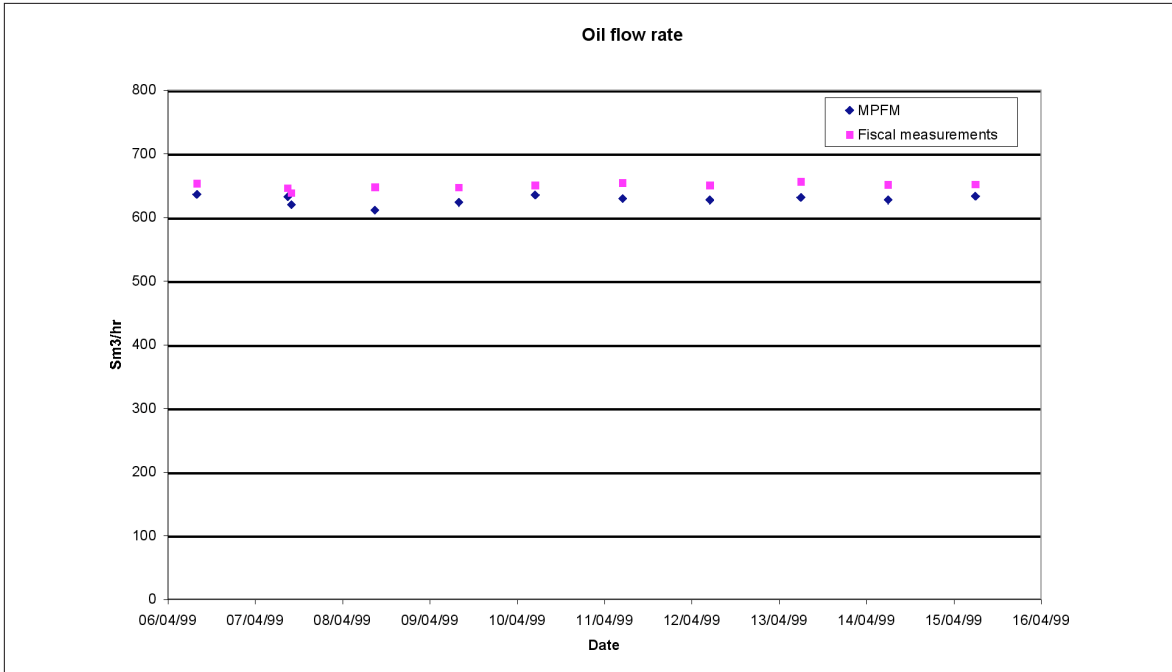


Figure 5.1 Oil flow rate from multiphase meters compared to fiscal measurements, April 1999

### 5.2. Multi rate test

In April 1999 a multi rate test of the Vigdis production wells was performed. Flow from different well combinations was sent through one of the multiphase meters at a time, to a test separator. This made it possible to test each meter with different flow rates and water cuts.

Figure 5.2. shows the liquid flow rate measured with meter #801. Except for the lowest flow rate, all points are within the +/- 7% uncertainty specification. The lowest flow rate has a deviation of 9%. At this point the meter is operating well below its specified operating range.

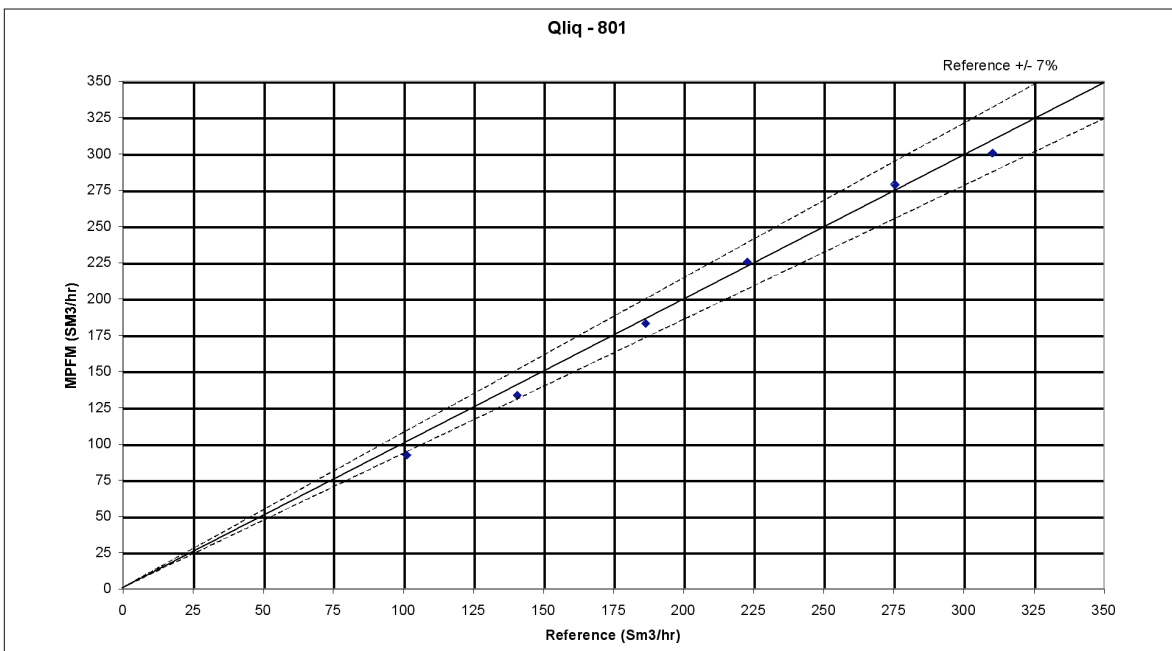


Figure 5.2 Liquid flow rate from meter #801. Water cuts were from 0% to 17% for these points. The water cut readings from the meter were from 0% to 6% (abs) too high.

The gas flow rate from meter #801 is shown in Error! Reference source not found.. All points are within the +/- 10% uncertainty specification. The lowest flow rate has the highest deviation. As with the liquid flow rate, the meter is here operating well below its specified operating range.

The offset in water cut reading is caused by non-calibrated capacitance electronics. The electronics were upgraded in flowing conditions, and the process schematic at Snorre will not allow static system calibration without shutting down the flow. Static calibration will be performed at first opportunity.

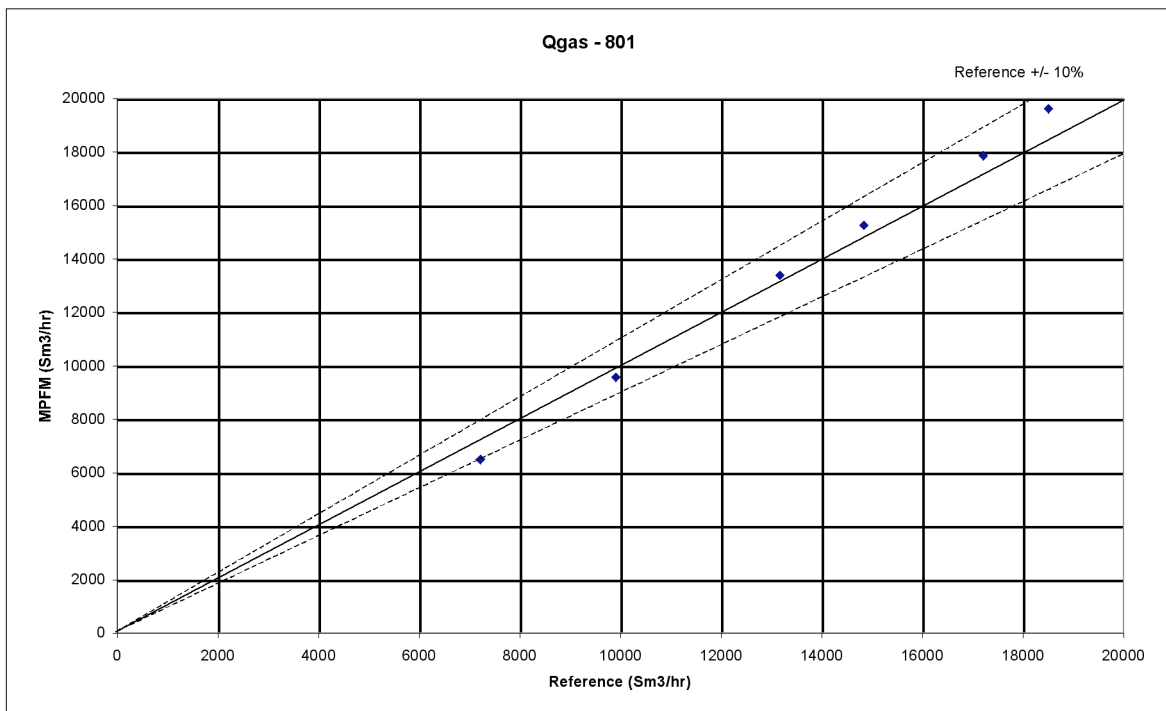


Figure 5.3 Gas flow rate from meter #801.

Figure 5.4 shows the liquid flow rate measured with meter #806. The curve shows that the deviation increases when the flow rate and the measured differential pressure drop. The reason for this is probably an offset in the dP transmitter. It was working in the lower 0.2% to 4% range for half of the testpoints.

Figure 5.5 shows the gas flow rate measured with meter #806. The curve shows that the deviation increases when the flow rate and the measured differential pressure drop, as happened with the liquid flow rate. The dP transmitter was working in the lower 0.2% to 4% range for half of the testpoints, as indicated on the figure.

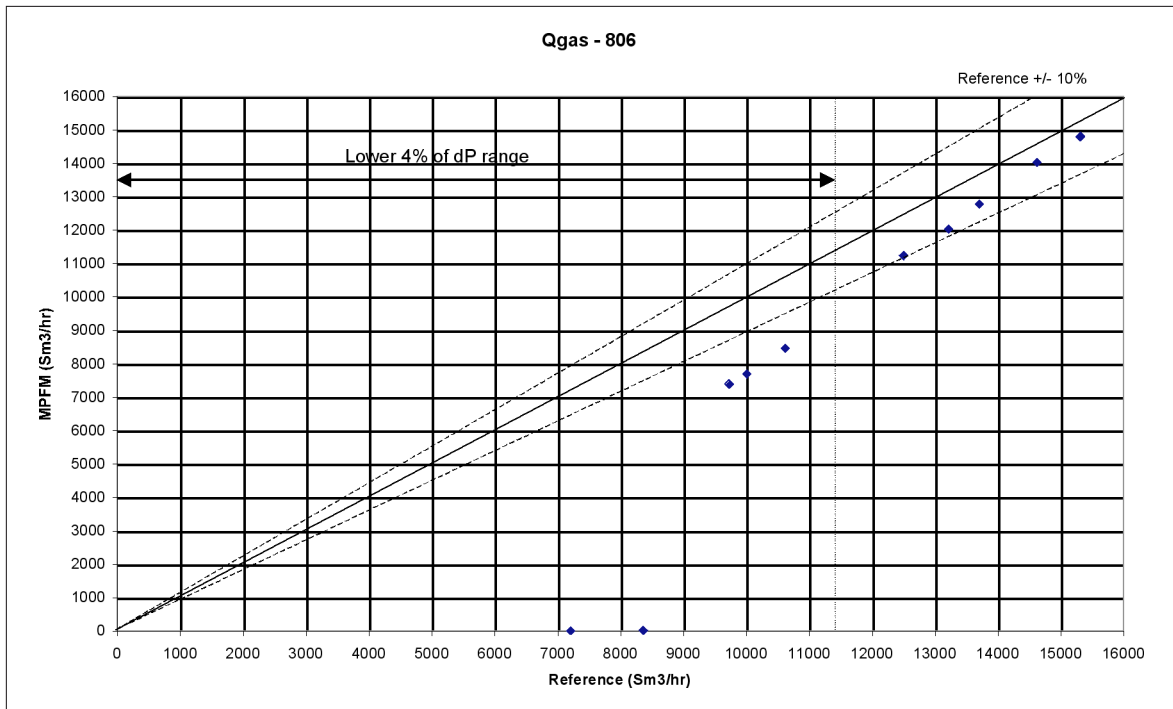


Figure 5.5 Gasflow rate from meter #806

### 5.3. dP model improvements

After the multirate test was finished, the results were analysed. It was observed that the dP transmitters over the venturi on the two meters gave different readings when the measured dP was in the lower 0.2% to 4% of the dP range. For these low rates the gas and liquid flow rate readings for meter #806 were too low. At higher flow rates a minor dP difference can be neglected, since the flow rate through the venturi is given by the square root of the dP value. Similar experience from other installations had already led to a new algorithm which calculates a dP offset based on the instantaneous mixture density. This offset correction is necessary since the venturi is vertically mounted, which causes the weight of the flow mixture inside the sensor to give a static contribution to the dP reading.

The distance between the two pressure outlets is a function of the meter ID, but is normally between 15 and 30 cm. When the differential pressure caused by the flow is in the lower 5% of the range of the cell, an offset of this size will give a significant contribution to the dP reading. This effect will increase with the distance between the pressure tappings, and will therefore increase proportionally with meter ID.

The new algorithm was implemented in meter #806 in August 1999. Different flow rates have been tested and the results are good. The dP readings from meter #801 are slightly higher than meter #806. It seems that the dP transmitter on meter #801 has a small offset which corresponds to the weight of the flow mixture inside the meter. Therefore the program in meter #801 will not be upgraded before more results are available from meter #806. Error! Reference source not found. shows the flow rate through the meters compared to fiscal measurements after the new dP offset algorithm was implemented. The deviations between the readings are within +/- 3%.

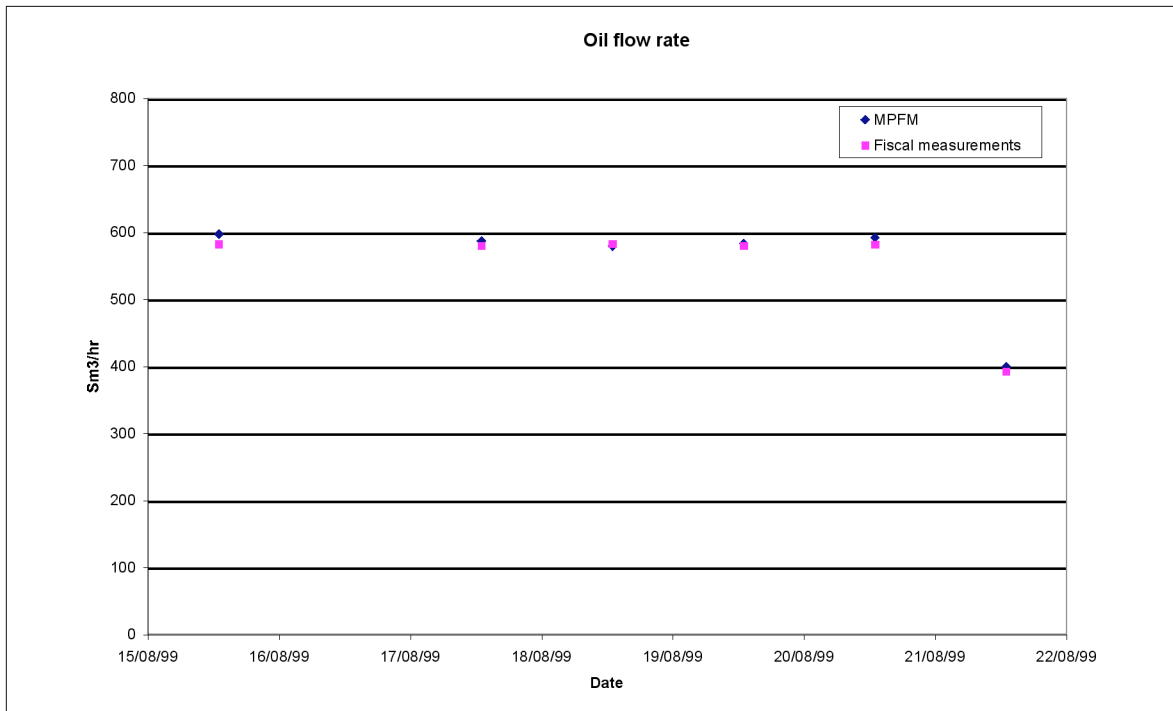


Figure 4.2 Oil flow rate from multiphase meters compared to fiscal measurements, August 1999

## 6. Summary and conclusion

Two Fluenta 8" MPFM 1900 VI multiphase meters are installed at the Snorre TLP, one in each of the production lines from Vigdis. There is no bypass facility installed, and in normal operation, there is also no possibility to individually check the meters towards a reference. This configuration does not easily accommodate performance monitoring, system modifications or calibration. Saga Petroleum and Fluenta have worked closely together to overcome this, and have arrived at a high quality multiphase measurement system for the Vigdis satellite.

A potential problem with the sensor liner technology was identified during commissioning of the meters, but was rectified during a planned shutdown six months after commissioning, before any serious malfunctioning had been experienced. Both meters were then upgraded with new sensor internals, with open electrode design. The refurbishment of the two meters performed in May 1998 made the readings from the meters repeatable, without any drifting. A filter function implemented in the detector electronics removed a flow rate dependence of the water cut which was observed in August 1998.

After this upgrade, the combined meter readings gave an oil flow rate of about 8% low compared to fiscal measurements. Data from the meters were analysed, and indicated that further improvements were possible. Saga and Fluenta agreed not to use meter factors in order to correct the observed deviation, but instead try to improve the signal interpretation models used in the meters. The first change was made to the density distribution model for the dispersed phase of the flow. The new algorithm reduced the deviation between the meters and the fiscal measurements from about 8% to 3%.

The multirate tests performed in April 1999 showed that most points were within the meter specification. In addition, it showed that the dP transmitters on the meters had different offset values. That gave too large flow rate deviations when the transmitters operated in the lower 0.2% to 4% range. A new dP offset algorithm was developed which compensates for the static contribution caused by the weight of the fluid between the dP tappings on the meter. This algorithm was implemented in August 1999. The oil flow rate deviations between the meters and the fiscal measurements have been within +/-3% since this upgrade.

Figure 6.1 gives an overview of the oil flow rate measurements since January 1999. It shows clearly how the deviations between meter readings and fiscal measurements have been reduced since the upgraded flow models were implemented.

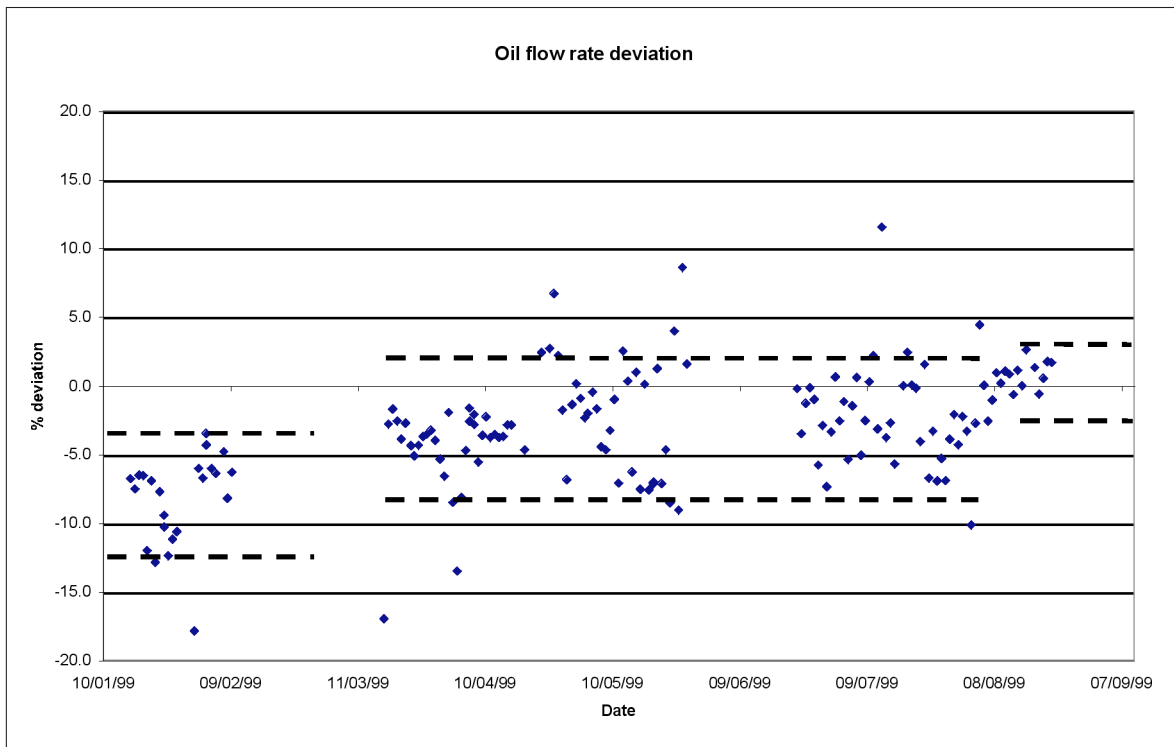


Figure 4.2 Deviation between oil flow rate readings from meters and fiscal measurements since January 1999

## References; Tests and Field applications of Fluenta Multiphase meters

1. NEL test report no. 187/95: NEL Multiflow Project – Characterisation of the performance of multiphase flowmeters for oil/water/gas measurement, January 1996
2. NEL test report no. 092/97: NEL Multiflow II Project – Characterisation of the performance of multiphase flowmeters – The challenge to acceptability, January 1998
3. NEL test report no. 111/97: Independent testing of Fluenta Multiphase Flowmeter for Seligi F, February 1998
4. Hydro Research Centre Porsgrunn test report no. 96S\_CJ5: The “Porsgrunn 2” test programme of multiphase flow meters, November 1996
5. The North Sea Flow Measurement Workshop 1995: “ The Norwegian test programme for qualification of multiphase meters”, Ole Økland and H. Berentsen, Statoil; G. Flakstad, Saga Petroleum; S. A. Kjølberg and H. Moestue, Norsk Hydro
6. SPE 36837 Multiphase Flow Meter Successfully Measures Three-Phase Flow at Extremely High Gas Volume Fractions - Gulf of Suez, Egypt, *B Leggett et. Al*
7. OTC 8506: “MMS 1200 - Cooperation on a Subsea Multiphase Meter Application”, *E.F. Caetano, J.A.S.F. Pinheiro, C.C. Moreira, PETROBRAS and L. Farestvedt, FLU-ENTA Inc*
8. OTC 8549: “The development and use of a subsea multiphase flowmeter on the South Scott Field”, *S. G. Slater, A. McK. Paterson, M. F. Marshall, Amerada Hess (UK) Ltd.*
9. 4<sup>th</sup> Annual International Conference, “The future of multiphase metering”; “Multiphase metering in Malaysia - Current and the future”, *Razali Ibrahim, Petronas Malaysia*
10. 4<sup>th</sup> Annual International Conference, “The future of multiphase metering”; “Multiphase metering developments in Brazil”, *Dr. R. Machado, Dr. E. Caetano, J.A. Pinheiro, Petrobras Brazil*
11. 5<sup>th</sup> Annual International Conference, “Field applications and new technologies for multiphase metering”; “Multiphase metering qualification process at Petrobras – Field application stage”, *Dr. R. Machado, Dr. E. Caetano, C. Kuchpil, C. B. Costa e Silva, M.J. Borges Filho, Petrobras R&D Center Brazil*
12. SPE 49118 Application of The First Multiphase Flow meter in The Gulf of Mexico, *Edward G. Stokes, Conoco Inc.; Dennis T. Perry, Petro Traces Inc.; Marschall H. Mitchell, Conoco Inc.; Martin Halvorsen, Fluenta a.s.*